The development of novel optical screening tests for the presumptive identification of New Psychoactive Substances (NPS) in seized illicit materials

Morgan Philp

A thesis submitted for the Degree of Doctor of Philosophy (Science)

University of Technology Sydney

July 2018

This page intentionally left blank

Certificate of original authorship

I certify that the work in this thesis has not previously been submitted for a degree nor has it been submitted as part of requirements for a degree except as part of the collaborative doctoral degree and/or fully acknowledged within the text.

I also certify that the thesis has been written by me. Any help that I have received in my research work and the preparation of the thesis itself has been acknowledged. In addition, I certify that all information sources and literature used are indicated in the thesis.

This research is supported by an Australian Government Research Training Program Scholarship.

Production Note:
Signature removed prior to publication.

25/07/2018

Morgan Philp

Date

Acknowledgements

This thesis could not have been completed without the support I received from many others in my work and personal life and I would like to take this opportunity to extend my gratitude to all those people here.

To my supervisor Shanlin, your calm, caring and generous nature always kept me level-headed. I value the trust you placed in me throughout my PhD from project direction to representing our research group overseas. Your continued encouragement and support did not go unnoticed and I have nothing but good memories of my time as your student and I will be forever grateful that I chose your Honours project in 2012 all those years ago.

To my co-supervisor Ron, the labs at UTS just would not be the same without you in them. Thank you for your ongoing encouragement and passion for seeing through all projects successfully. For a busy man, you always found time to check on my progress and share your chemical knowledge with me. I am very grateful to be one of the lucky ones who have you on their supervisory panel.

A special thank you to Shanlin's toxicology research group (past and present members) for your support and for providing some normality to this PhD lifestyle. Shout-out to Dan, my fellow NPS researcher who I have shared this journey with. We have come a long way since our first ANZFSS conference in Adelaide and you have made my time here considerably more enjoyable. I look forward to seeing your conference Vans once more.

To the number of desk buddies I had during my time at UTS, you have honestly all kept me sane throughout this process. Kia, Tanya and Mel (Friday night Dream Team) during the early days, and Alicia, Rolanda and Mac in the later half. Thank you for putting a smile on my face and breaking up my long hours in the lab.

To Scott, your ability to go from the comic of the group to offering trusted and meaningful advice whenever needed is incredible. These are your strengths and what makes you the great, young academic you have become. Thank you for sharing your PhD woes and providing a glimmer of hope for post-PhD normalcy.

I would like to thank my family and friends for putting up with me throughout this PhD and especially for their incredibly encouraging words prior to submission. I truly appreciate you all. To my mum, Terri, thank you for allowing our phone calls to be hijacked by me talking about polymers and for reading through thesis chapters in your spare time.

To Christian, there are so many things I am grateful of, but most importantly is your dedication to standing with me while I went on this PhD journey. Thank you for being there after late nights, long hours and failed experiments. Your genuine praise and recognition at each turn did not go unnoticed.

"[This PhD research] was the best of times, it was the worst of times…"

- Charles Dickens, Tale of Two Cities, 1859

Table of Contents

List of Figures

List of Tables

Abbreviations

^{13}C-NMR	carbon nuclear magnetic resonance
^{1}H-NMR	proton nuclear magnetic resonance
4-EMC	4-ethylmethcathinone
4-FMC	4-fluoromethcathinone
4-HMC	1-(4-hydroxyphenyl)-2-(methylamino)propan-1-one
4-MEC	4-methylethcathinone
4-MMC	4-methylmethcathinone
4-MPBP	1-(4-methylphenyl)-2-(pyrrolidin-1-yl)butan-1-one
4-MPPP	4-methylpyrrolidinopropiophenone
AC	alternating current
ACN	acetonitrile
amu	atomic mass unit
approx.	approximately
aq.	aqueous
atm	atmosphere
ATR	attenuated total reflectance
br.	broad
BuMgCl	butylmagnesium chloride
CAT	2-amino-1-phenylpropan-1-one
conc.	concentrated
d	doublet
DCM	dichloromethane
dd	doublet of doublet
dec.	decomposed
deform.	deformation
EI	electron ionisation
Et2O	diethyl ether
EthMgCl	ethylmagnesium chloride
FTIR	Fourier transform infrared
GC-MS	gas chromatography-mass spectrometry
h	hours
J	coupling constant

lit.	literature value
M	moles per litre
m	multiplet
m/z	mass to charge ratio
M+	molecular ion
MCAT	methcathinone
MDPBP	1-(2H-1,3-benzodioxol-5-yl)-2-(pyrrolidin-1-yl)butan-1-one
MDPBP	1-(2H-1,3-benzodioxol-5-yl)-2-(pyrrolidin-1-yl)butan-1-one
MDPV	3,4-methylenedioxypyrovalerone
MDPV	3,4-methylenedioxypyrovalerone
MeOH	methanol
min	minutes
MIP	molecularly imprinted polymer
MIPH	molecularly imprinted photonic hydrogels
MOMV	1-(4-methoxyphenyl)-2-(methylamino)pentan-1-one
mp	melting point
MW	molecular weight
NPS	new psychoactive substance
ø	diameter
oop	out of plane
PCC	pyridinium chlorochromate
PE	polyethylene
ppm	parts per million
ppt.	precipitate
PropMgCl	propylmagnesium chloride
PVAc	polyvinyl acetate
q	quartet
RBF	round bottom flask
Ref.	references
R_f	retardation factor
RT	room temperature
s	singlet
SN_2	one step nucleophilic substitution reaction
t	triplet
THF	tetrahydrofuran

TIC	total ion chromatogram
TLC	thin layer chromatography
TMS	tetramethylsilane
UCNP	upconversion nanoparticles
unk.	unknown
unsym.	unsymmetrical
UV-Vis	ultraviolet-visible
α-PVP	α-pyrrolidinopentiophenone
δ	chemical shift
λ	wavelength
$\bar{\nu}$	wavenumber

This page intentionally left blank

Abstract

The large and increasing number of illicit materials seized each year combined with the introduction of many new psychoactive substances (NPS) to the traditional drug market are concerning realities. The need for simple presumptive field tests able to accurately detect compounds such as synthetic cathinones with good sensitivity is apparent. Field testing is an important tool for law enforcement officers to obtain rapid feedback regarding an unknown substance while awaiting confirmatory analysis results often in a backlog.

Chemical reactions selective toward the synthetic cathinone molecular structure were investigated for their application as a receptor element in an optical screening test. Oximations, hydrazone formations, semicarbazide formations and metal complexation were examined with a number of cathinone analogues. As an alternative to chemical reactions, molecularly imprinted polymers (MIPs) selective toward synthetic cathinone compounds were prepared, optimised and tested for their selective binding ability.

The synthetic cathinone class of compounds failed to show significant reactivity with the reagents selected under a range of experimental conditions. However, their ability to actively reduce the cupric ion of a copper-neocuproine complex to afford a yellow-orange coloured product was observed. This colour test was optimised, validated and later improved upon to increase useability in the field as an optical screening test. The MIPs showed potential in selectively recognising the presence of the target cathinone molecule through binding studies performed, however, before the polymer can be used as a receptor, further optimisation is required.

The three receptors investigated provided different degrees of success. The chemical colour test was successfully developed into a protocol for application in field testing of cathinones; the MIPs showed some potential for further investigation and application in a different protocol for cathinone detection; and the use of chemical reactions for tagging purposes was not achieved due to the inherently unreactive carbonyl group of the cathinone molecular structure. Nonetheless, this research provided significant and useful chemical analysis of the synthetic cathinone class of NPS, while raising awareness of current deficiencies in the presumptive identification of NPS.

This page intentionally left blank

Chapter 1: Introduction

This page intentionally left blank

Chapter 1: Introduction

Summary

This chapter examines the emergence of the now well-known and ill-famed group of New Psychoactive Substances (NPS), with a particular focus on the synthetic cathinone compounds.

The bulk of this chapter provides an overview of current methods used in the detection and identification of illicit drugs in seized materials. The preliminary techniques that do not require extensive technical training and can be readily implemented in field-testing are the focal point, with an emphasis on chemical colour testing. Other portable spectroscopic techniques are also reviewed and the lack of reliable, simple and portable field testing methods are discussed.

The last part of this chapter reviews promising applications of chemical sensing technology for the detection of illicit drugs. Molecular recognition events and optical signal reporting are combined to produce self-reporting molecular sensing technologies.

Section 1.4 is taken from a first author publication in the Wiley journal, Drug Testing Analysis (see next page for details).

A review of chemical 'spot' tests: A presumptive illicit drug identification technique

Morgan Philp[1*] and Shanlin Fu[1]

[1] Centre for Forensic Science, University of Technology Sydney (UTS)

Philp M, Fu S. A review of chemical 'spot' tests: A presumptive illicit drug identification technique. *Drug Test Anal*. 2018;10:95–108. https://doi.org/10.1002/dta.2300

Statement of contributions of joint authorship

Morgan Philp: (candidate)
Writing and compilation of manuscript, including tables and figures

Shanlin Fu: (principal supervisor)
Editing and co-author of manuscript

Section 1.4, a large portion of this chapter, is taken from the above journal paper.

1.1 New Psychoactive Substances

New Psychoactive Substances (NPS) have been defined by the United Nations Office on Drugs and Crime (UNODC) as substances of abuse that are not controlled by the 1961 Single Convention on Narcotic Drugs or the 1971 Convention on Psychotropic Substances, but which pose a public health threat[1]. Referred to as 'legal highs', 'bath salts' and 'research chemicals' since their appearance on the illicit drug market, the worldwide proliferation of NPS became a phenomenon.

These synthesised substances are designed to mimic effects of known illicit drugs and have been categorised based on their chemical structures and effect. The main substance groups are synthetic cannabinoids, synthetic cathinones, ketamine, piperazines, phenethylamines, and plant-based substances[2].

1.1.1 Current situation

As of 2017, the *World Drug Report* showed there has been a total of 739 different NPS reported to the UNODC between 2009 and 2016[3]. However, it is not just the number of different compounds that are problematic but also the number of NPS seizures that are occurring worldwide, with over 20 tons being seized in 2015 alone[3].

The emergence of these compounds was accompanied with a number of challenges for law enforcement authorities, particularly in regards to the legislation that bound them, or lack thereof. However, in the last few years the NPS class of substances have become controlled in many jurisdictions[4].

The challenges of NPS are still apparent in hospital emergency admissions[5] or fatalities[6] and for researchers assessing the risk of harm[7] and developing new identification methods[8]. Dedicated prevention programs, early warning systems, committees and research groups have been established around the world.

1.1.2 Synthetic cathinones

Synthetic cathinones are one of the major classes of NPS with a structure based on that of an active ingredient in the khat (*Catha edulis*) plant, cathinone[9]. Khat is a flowering evergreen

shrub native to East Africa and the Arabian Peninsula whose leaves (see Figure 1-1) and stem tips have been chewed by locals for the euphoric and stimulant effects for centuries[10].

Figure 1-1. Fresh khat leaves (from Palmer, 2010)[11]

The earliest reported synthetic cathinone was methcathinone in Germany in 1928[12]. Since then, cathinones have been developed for both medicinal use and as substances of abuse. Bupropion is a cathinone that is used clinically, while methcathinone and pyrovalerone were originally intended for medicinal purposes, and are now used solely for recreational purposes [13].

During the mid-2000s these drugs became established on the illicit drug market sold legally under brand names such as Ivory Wave in order to circumvent controls. Reports have indicated China, India or Pakistan are responsible for supplying the drugs to Europe [14], where packaging for distribution via retail shops, internet sites (e.g. London Underground), the Dark Web (e.g. Silk Road) and independent dealers can take place [15].

1.1.2.1 *Chemistry and Structure*

Synthetic cathinones are a large family of beta-keto phenethylamine derivatives with the general structure provided in Figure 1-2. Substitutions made at the phenyl ring, alkyl side chain and amino group led to the formation of a large number of possible analogues. The UNODC have advised up to 140 synthetic cathinones have been reported from 2009-2016[3]. A list of common synthetic cathinones encountered is provided in Table 1-1.

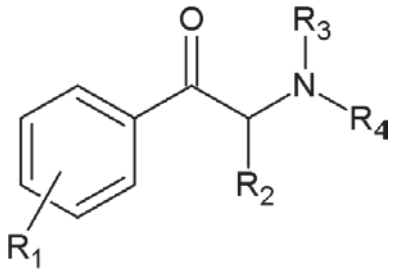

Figure 1-2. Generic structure of synthetic cathinone analogues showing the substitution possibilities that led to formation of a wide range of compounds

Table 1-1. The names and chemical structures of common synthetic cathinones showing the location of the substituentsto the benzene ring and amine group

Compound Name	**Common name**	**Chemical Structure**
2-(methylamino)-1-(4-methylphenyl)propan-1-one	4-methylmethcathinone (4-MMC)	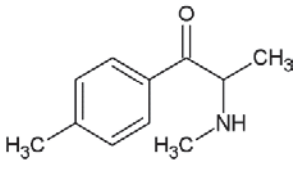
2-(methylamino)-1-phenylpropan-1-one	Methcathinone (MCAT)	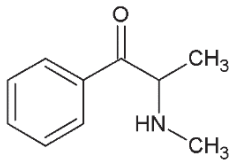
2-(ethylamino)-1-(4-methylphenyl)propan-1-one	4-methylethcathinone (4-MEC)	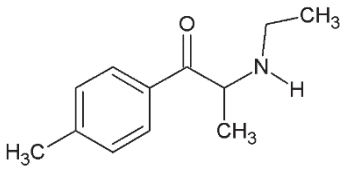
1-(4-fluorophenyl)-2-(methylamino)propan-1-one	4-fluoromethcathinone (4-FMC)	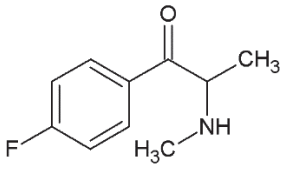

1-(1,3-benzodioxol-5-yl)-2-(methylamino)propan-1-one	methylone	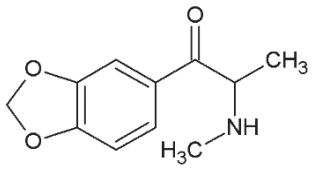
1-(1,3-benzodioxol-5-yl)-2-(methylamino)butan-1-one	butylone	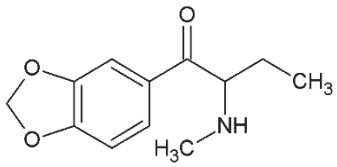
1-(1,3-benzodioxol-5-yl)-2-(methylamino)pentan-1-one	pentylone	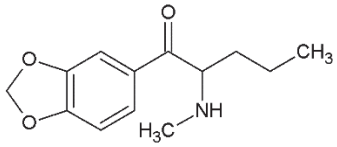
1-phenyl-2-(pyrrolidin-1-yl)pentan-1-one	α-pyrrolidinovalerophenone (α-PVP)	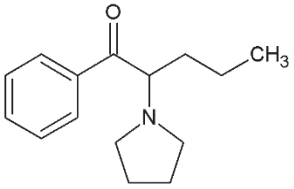
1-(4-methylphenyl)-2-(pyrrolidin-1-yl)pentan-1-one	pyrovalerone	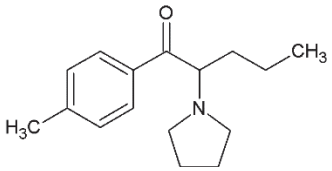
1-(2*H*-1,3-benzodioxol-5-yl)-2-(pyrrolidin-1-yl)pentan-1-one	3,4-methylenedioxypyrovalerone (MDPV)	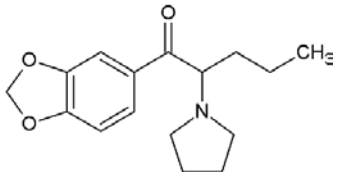

Although structurally similar to amphetamines, cathinones are chemically distinct due to the presence of the carbonyl functional group[16]. Studies have shown that in hydroxylic media,

cathinones undergo relatively rapid isomerisation and dimethyldiphenylpyrazine formation[17]. Several research groups have attempted to investigate chemical properties of the synthetic cathinones, including thermal degradation[18], stability in biological matrices[19, 20], derivatisation for GC-MS analysis[21], and derivatisation to make cathinone precursors[22].

1.1.2.2 *Analysis*

The method of choice to rapidly identify substituted cathinones in powders remains gas liquid chromatography connected to electron impact mass spectrometry (GC-MS)[23]. This is demonstrated by its use in the identification of pure synthetic cathinones following synthesis[24], and submitted unknown samples and products[25]. Sixteen compounds were able to be resolved particularly easily without derivatisation, and common adulterants: benzocaine, lidocaine and procaine were also resolved in the same method [8].

A number of different techniques have been used to characterise cathinones: a quick and versatile method using direct analysis in real time mass spectrometry (DART-MS)[26]; the ability to discriminate regioisomers using Raman spectroscopy[27]; detection of buphedrone in a case report using HPLC-DAD[28]; application of methods to the quantification of 28 cathinones and metabolites in urine by liquid chromatography-high resolution mass spectrometry (LC-HRMS)[29]; identification of seized materials employing NMR[30] and the identification and characterisation of a new compound, 3,4-methylenedioxy-N-benzyl cathinone (BMDP) found in new 'legal high' samples using liquid chromatography-high resolution quadrupole time-of-flight mass spectrometry (LC-QTOF-MS)[31].

1.2 Illicit drug identification techniques

The large and lucrative illicit drug market continues to grow each year as it adapts to a changing marketplace. On a global scale, the extent of drug supply and demand is indicated by the 2.4 million drug seizures made by law enforcement personnel annually[3]. Law enforcement personnel typically made these seizures at customs, national borders, and crime scenes, and consist of illicit drugs in transit as well as seizures from clandestine laboratories.

Unknown materials seized includes powders, compressed powders (blocks), capsules, tablets, liquids, solutions, suspensions, impregnations, resins, oils, tabs (blotter paper) and even plant material. National borders and customs encounter a large number of illicit drug concealments in attempts to smuggle contraband into areas for subsequent distribution. These concealments have included suitcases, impregnations, suspensions, body packs, internal concealments, and parcel post[32]. Across the globe, there has been a change in the supply and distribution of illicit substances. End-users are purchasing an increasing number of drugs on the Darknet and having them delivered via parcel post. Ecstasy-type substances, followed by hallucinogens (e.g. LSD), cannabis, cocaine and NPS are the most common purchases made via online marketplaces[33].

The most commonly seized drugs by number are cannabis, amphetamine-type stimulants, opioids and cocaine-related substances, respectively[3]. Comparatively, NPS were seized in much lower quantities. However, the growing number of NPS on the market is significant, with one new drug reported to the EU Early Warning System each week in 2016[34]. Although NPS are often transient to the drug market, 4-fluoroamphetamine, JWH-018, and mephedrone have showed a stable presence by remaining on the market since they first appeared in 2008[33]. Fentanyl and other synthetic opioid derivatives remain extremely dangerous public safety threats, particularly in the United States where 167 kg of illicit fentanyl was seized in 2015[35]. Other seized substances include tryptamines, anesthetics, steroids, benzodiazepines, and hallucinogens, all of which Australia saw record numbers of seizures in the last reported year[36].

The Scientific Working Group for the Analysis of Seized Drugs (SWGDRUG) provide recommendations for the minimum standards of identification of seized drugs and have divided analytical techniques into three categories (A, B, and C) based on their respective discriminating power (DP) [37]. Category C affords the least DP and includes colour tests, immunoassays, and ultraviolet spectroscopy. Category B techniques have a higher DP and include microcrystalline tests, thin layer chromatography (TLC) and microscopic and macroscopic examination (of cannabis only). Category A techniques afford the highest DP and include infrared and Raman spectroscopy.

Preliminary illicit drug identification procedures, employed by all law enforcement agencies encompass fast and portable techniques as a first response to identifying an unknown substance at the scene. These are critical stages in the investigation process as they determine the next tactical decision, such as search warrants, arrests, and bail applications. The most

ubiquitous and controversial presumptive screening test used by officers at a scene is the colour (spot) test. Chemical reagents incorporated into commercial test kits indicate if a particular drug may be present in a sample of the seized material by the presence of a specified colour change.

Technological improvements have led to an increase in portable spectroscopic instrumentation able to be employed in the field such as portable FTIR and Raman spectrometers. These techniques are being used alongside and often replacing, more traditional analyses such as TLC and chemical colour testing. Microcrystalline testing is no longer a common screening method for drugs of abuse, while physical examinations are routinely performed but rarely for identification purposes.

The analysis of seized materials includes the use of techniques considered pre-analytical. These techniques have a lower discriminating power but can be combined to afford effective determination of different drug classes at a much lower cost than confirmatory techniques [38].

1.3 Physical examination

Macroscopic features of illicit natural plant materials are rich in information and can largely assist in their identification. The most commonly examined plant material in forensic laboratories is *Cannabis sativa* which possesses longitudinal grooves along the stem, a palmate leaf structure, and coarsely serrated leaf margins[39]. The literature abounds with descriptions of the physical form of controlled plant materials such as coca leaf[40], kratom[41], *Salvia divinorum*[42] and khat[43], while the EMCDDA warns of mistakenly identifying psilocybin-containing mushrooms for non-psychoactive mushrooms in the wild[44]. Law enforcement personnel are trained to provide preliminary examinations of biological material so as to reduce the need for laboratory examinations.

Morphological features of natural materials, such as trichomes and cystolithic hairs, can also be studied under stereomicroscopes to distinguish samples. The combination of cystolithic hairs on the upper leaf surface and longer trichomes and sessile glands on the lower surface are unique to cannabis and allow for its identification[39]. Microscopic examination of kratom samples showed small hair-like fibers that were not consistent with those seen on marijuana and therefore provide an excellent physical differentiation[45].

Illicit synthetic substances are often non-descript and variable in appearance, and thus physical examination is not regarded as a reliable form of identification. Zhu *et al.* [46] reported on two seized samples of identical appearance: light yellow liquid in amber vials, and found them to be a mixture of piperazine analogs and a mixture of amphetamines, respectively.

The limited identification afforded by physical descriptors of illegal drug tablets or pills such as size, colour, shape, and imprint design are, however, particularly useful for users and harm reduction services as an easy way to recognize and create awareness of pills with dangerous adulterants or misrepresented drugs[47, 48]. A study of brand names associated with new psychoactive drugs revealed there were over 1000 brand names used to advertise NPSs online with a single brand name used to identify various NPS at different times[49]. Although not used in identification, these physical descriptors remain useful for intelligence purposes[50].

1.4 Chemical colour tests

Suspected illicit substances seized by police and customs officers at national and state borders are submitted for analysis to identify the drug present. This identification process typically follows a sequence of techniques designed to be cost and time efficient while providing reliable results. Qualitative presumptive analysis for drug samples indicates the presence or absence of a particular drug class using simple methods often amenable to portable field test kits.

Despite the low discriminating power, presumptive analysis of controlled substances is critical to investigation processes as it is often the first step in the identification and will determine the next tactical decision, such as search and arrest warrants[51]. The most commonly used presumptive screening tool is the colour (spot) test used by law enforcement in the field and technicians in a forensic laboratory. Chemical reagents are added to a small sample of the material and the colour changes are observed with the naked eye. Specified colour changes will indicate the presence of a particular drug. The lack of sample preparation required, ease of use, rapid results afforded, portability, and low cost make chemical colour tests an ideal presumptive identification. These attributes are especially useful considering the large numbers of samples received. Concerns regarding the selectivity of colour testing are apparent and have received attention via numerous media reports[52, 53]. In attempts to improve on the subjective nature of the test, colorimetric analysis has been incorporated into chemical colour testing[54] showing potential for semi-quantitative analysis[55]. The emergence of NPS,

often disguised as traditional recreational drugs, led to colour test validation studies to determine effectiveness and potential cross-reactivities of current test methods[56].

1.4.1 Historical overview

1.4.1.1 *Microchemistry*

Microchemistry began to establish itself in the early 19th century as a field of chemistry that required small amounts of material to develop either a change in colour, formation of precipitate or evolution of gas with specific compounds. Early discoveries included the blue colour reaction between starch and iodine[57] and various chemical reactions with poisons[58]. In the twentieth century, this field grew significantly as people soon realized the benefit of micromethods over macromethods due to their precision and rapidity[59]. A forefather of 'spot testing,' Fritz Feigl, produced important work during this period by introducing new methodologies for characterizing inorganic chemical species using organic reagents to create intensely coloured products, and also introducing the concepts of specificity, selectivity, and sensitivity[60-62].

1.4.1.2 *Drugs of abuse testing*

In the 19th century, colour and precipitation tests became essential in early forensic toxicology studies for the identification of plant alkaloids. A series of tests named after their chemist inventors appeared in the mid to late 1800s, including Dragendorff, Marquis, Mandelin, Mecke, and Froehde[63].

The discovery of new alkaloids combined with greater knowledge of their chemical structures led to the arrival of new colour tests in the following decades, including Chen's test for ephedrine[64] and Scott's test for cocaine[65]. The arrival of synthetic drugs of abuse saw further successful applications of these colour test methods, and in 1985, Jungreis detailed the necessity of spot testing for drug and poison detection in the growing area of narcotic abuse[66].

Clarke's Analysis of Drugs and Poisons[67], a reference text written by leading international scientists provides a wealth of information to forensic laboratories on methods of

identification, including colour tests. Recent decades have also seen the publication of government documents detailing drugs of abuse colour test standards[68], technical notes on colour testing[69], and methods for validating colour tests[37, 70].

1.4.2 Chemistry of common colour tests

A chemical reaction between the drug of interest and the test reagent(s) causes the observed colour change in chemical spot tests. Mechanistically, an electron transfer takes place between the drug molecule (or substructure thereof) and the chemical reagent to produce coloured metal complexes and charged organic species. An important aspect that has a considerable effect on the colour and intensity of the products is the pH of the test solution[71]. A list of the 15 most commonly used colour test reagents and target drug classes is provided in Table 1-1, while the chart in Figure 1-3 classifies these colour tests based on pH conditions and products formed. Colour tests can also be classified based on the drugs or substructures that react with the reagent.

Table 1-2. Colour test reagent compositions and targeted drugs for common colour spot tests used in illicit drug detection

Test reagent	**Composition**	**Targeted drugs**	**Ref.**
Chen-Kao [a, b]	Acetic acid solution (1% v/v) **(1)** Copper sulfate solution (1% w/v) **(2)** Sodium hydroxide solution (8% w/v) **(3)**	Ephedrine (and norephedrine)	[69, 72]
Dille-Koppanyi [a, b, c, d]	0.1 g cobalt(II) acetate tetrahydrate in 100 mL methanol with 0.2 mL glacial acetic acid **(1)** 5 mL isopropylamine in 95 mL methanol **(2)**	Barbiturates	[69, 73]
Duquenois-Levine [a, b, c, d]	2.5 mL acetaldehyde and 2 g vanillin to 100 mL ethanol (95% v/v) **(1)** Conc. hydrochloric acid **(2)** Chloroform **(3)**	Cannabinoids in cannabis	[69, 73, 74]
Ehrlich's [a, c]	1 g *p*-dimethylaminobenzaldehyde in	Ergot alkaloids and LSD	[69]

	10 mL methanol, then add 10 mL conc. *o*-phosphoric acid **(1)**		
Fast Blue B [d]	Fast Blue B salt (diazotized o-dianisidine, 1% w/v) **(1)**	Cannabinoids in cannabis	[75]
Ferric chloride [a, b]	8.25 g ferric chloride hexahydrate in 100 mL distilled water **(1)**	Phenols	[73]
Froehde [a, b]	0.5 g molybdic acid in 100 mL hot conc. sulphuric acid **(1)**	Range of aromatic compounds	[76]
Liebermann's [a, b]	1 g sodium/potassium nitrite in 10 mL conc. sulphuric acid **(1)**	Phenols and substituted benzene rings	[73, 77, 78]
Mandelin's [a, b]	1 g ammonium vanadate in 1.5 mL water, diluted to 100 mL with conc. sulphuric acid **(1)**	Amphetamines and anti-depressants	[69, 73]
Marquis [a, b, c, d]	1 mL formaldehyde (40% v/v) in 100 mL conc. sulphuric acid **(1)**	Broad spectrum test: mostly opium alkaloids and amphetamines	[69, 73]
Mecke [a, b]	1 g selenious acid in 100 mL conc. sulphuric acid **(1)**	Opium alkaloids	[69, 73]
Scott's [a, b, d]	Cobalt thiocyanate (2% w/v) diluted 1:1 with glycerine **(1)** Conc. hydrochloric acid **(2)** Chloroform **(3)**	Cocaine (and methadone)	[69, 73, 79]
Simon's [b, c, d]	2 mL acetaldehyde in 100 mL sodium nitroprusside solution (1% w/v) **(1)** Sodium carbonate solution (2% w/v) **(2)**	Distinguishes primary and secondary amines	[69, 73]
Zimmerman [a, b, c,]	2,4-dinitrobenzene (1% w/v) in methanol **(1)** Potassium hydroxide (15% w/v) **(2)**	Benzodiazepine derivatives and synthetic cathinones	[69, 80]
Zwikker [b, c, d]	0.5 g copper(II) sulfate pentahydrate in 100 mL distilled water **(1)** 5 mL pyridine to 95 mL chloroform **(2)**	Barbiturates	[76]

[a] contains corrosive chemicals

[b] contains flammable chemicals

[c] contains toxic chemicals

[d] contains suspected/possible carcinogenic chemicals

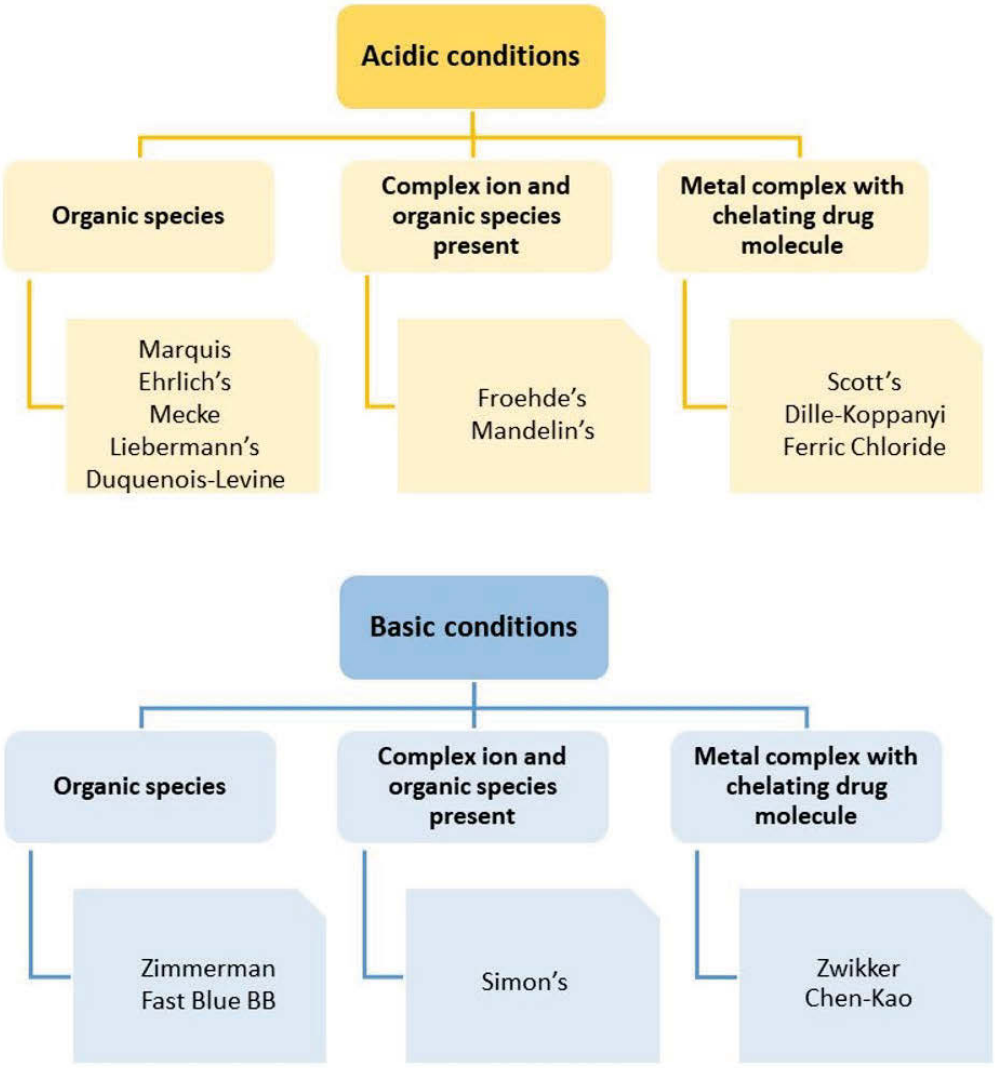

Figure 1-3. Classification of 15 common colour test reagents categorised by the pH of the test solution and the type of coloured product formed.

1.4.2.1 *General screening reagents*

These test reagents produce colour changes with many drug classes. The Marquis reagent is the most frequently used colour test for screening unknown substances and is the first to be performed in test sequences[81]. Originally developed for the detection of morphine and other alkaloids via a red-violet colour change[82], it has since found excellent use as a general screening test for many synthetic drugs. For example, orange-brown, black and olive-green colour changes with amphetamine HCl, 3,4-methylenedioxyamphetamine HCl, and 3,4-dimethoxymethamphetamine HCl, respectively[83]. However, other compounds have also

been found to react with Marquis, including aspirin and sugar[83]. In a German report on the chemistry of colour tests, Kovar[69] showed the purple coloured product with opium alkaloids is an oxonium-carbenium salt, while amphetamine reacts with only one molecule of formaldehyde to form an orange carbenium ion product (see Figure 1-4).

Compared to Marquis, the Liebermann's reagent is mentioned significantly less in the literature. Widdop[73] describes the many colours seen with Liebermann's, while other reports show its use in the detection of methcathinone analogs[84] and synthetic cannabinoids containing an indole structure[85]. A critical investigation into the chemical reaction of the Liebermann colour test showed the mechanism occurring with phenols[77]. The nitrous acid reagent produces carbocations and N-nitrosamines with primary and secondary amines, respectively (see Figure 1-4). The substituents present on the benzene ring will affect the colour observed, and occasionally it is necessary to heat the test at 100 °C to see the result[73].

Transition metal complexes are highly coloured compounds that change colour upon a change in oxidation state and have therefore been found very useful as reagents in colour tests. Colour tests based on reduction-oxidation reactions often involve transition metals in their highest valence state dissolved in sulphuric acid[86]. The ammonium vanadate reagent in the general screening Mandelin's test is present as vanadium(V), reduced to vanadium(IV) in the presence of alkaloid compounds such as cocaine, codeine, and heroin producing orange, olive and brown colours, respectively[87] (see Figure 1-4). The mechanisms of these reactions with drugs of abuse have not been investigated, and it is unknown if the coloured complex ion product contains drug molecules acting as ligands. The molybdic acid reagent in Froehde's test also undergoes a redox reaction with molybdenum(VI) reducing to molybdenum(II) in the presence of aromatic compounds (see Figure 1-4). Wongwiechintana *et al.*[86] used X-ray Diffraction (XRD) to determine the structure of the purple product with morphine and found a ring rearrangement followed by dehydration produced a hydroxyquinone system on the aromatic morphine ring. This work demonstrated the Molybdenum complex was not responsible for the reaction colour change.

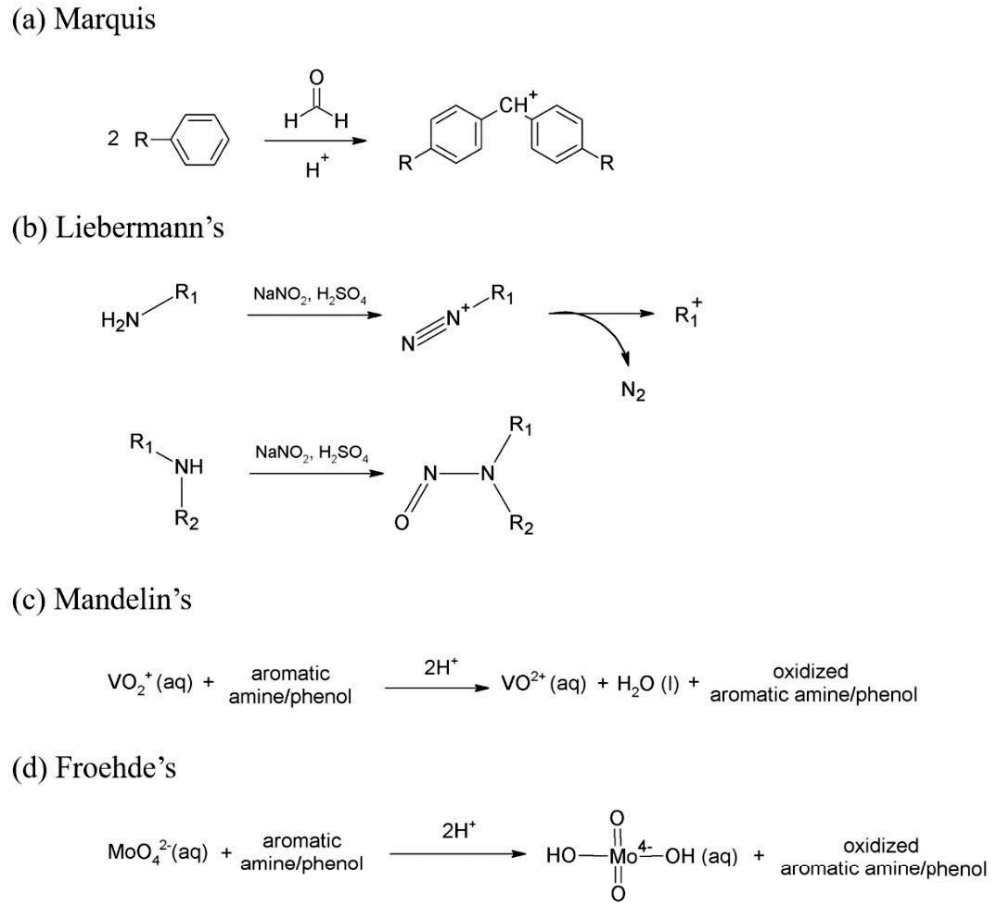

Figure 1-4. Chemical reactions of common colour tests that are selective toward a range of drug classes and used in general screening methods. Marquis reagent (a); Liebermann's reagent (b); Mandelin's reagent (c); and Froehde's reagent (d).

1.4.2.2 *Functional group selective*

Colour tests can react with a certain functional group present in the compound and are therefore appropriate for detection within a range of drug classes. Sodium nitroprusside is a chemical reagent that has previously been described for its ability to detect methyl ketones and aldehydes[88]. Modification of the test method to include acetaldehyde changed the target class of compounds to secondary amines and thus made the method useful in presumptive testing of many illicit compounds[89], particularly methamphetamine and 3,4-methylenedioxymethamphetamine (MDMA). The newly named Simon's test affords a blue coloured product as the result of an iron complex, named the Simon-Awe complex[69] (see Figure 1-5).

References to the Zimmerman reagent from the 1950s and 1960s relate to the detection of steroidal compounds[90, 91] wherein the colour development is due to a reaction occurring at the carbonyl and adjacent methylene group. However, in a report from the UNODC, the Zimmerman reagent was recommended for synthetic cathinone detection[80]. Kovar[69] also describes the use of this reagent for benzodiazepine detection through the creation of a Meisenheimer complex (see Figure 1-5).

A simple functional group identification test for the presence of phenols is the ferric chloride reagent. The structure of the resulting purple coloured product is due to the iron(III)-phenol complex (see Figure 1-5). The importance of the acidity of the test solution[92], as well as solvent and added base[93], has been described. The coloured reaction with a cutting agent, baking soda, has also been reported[76].

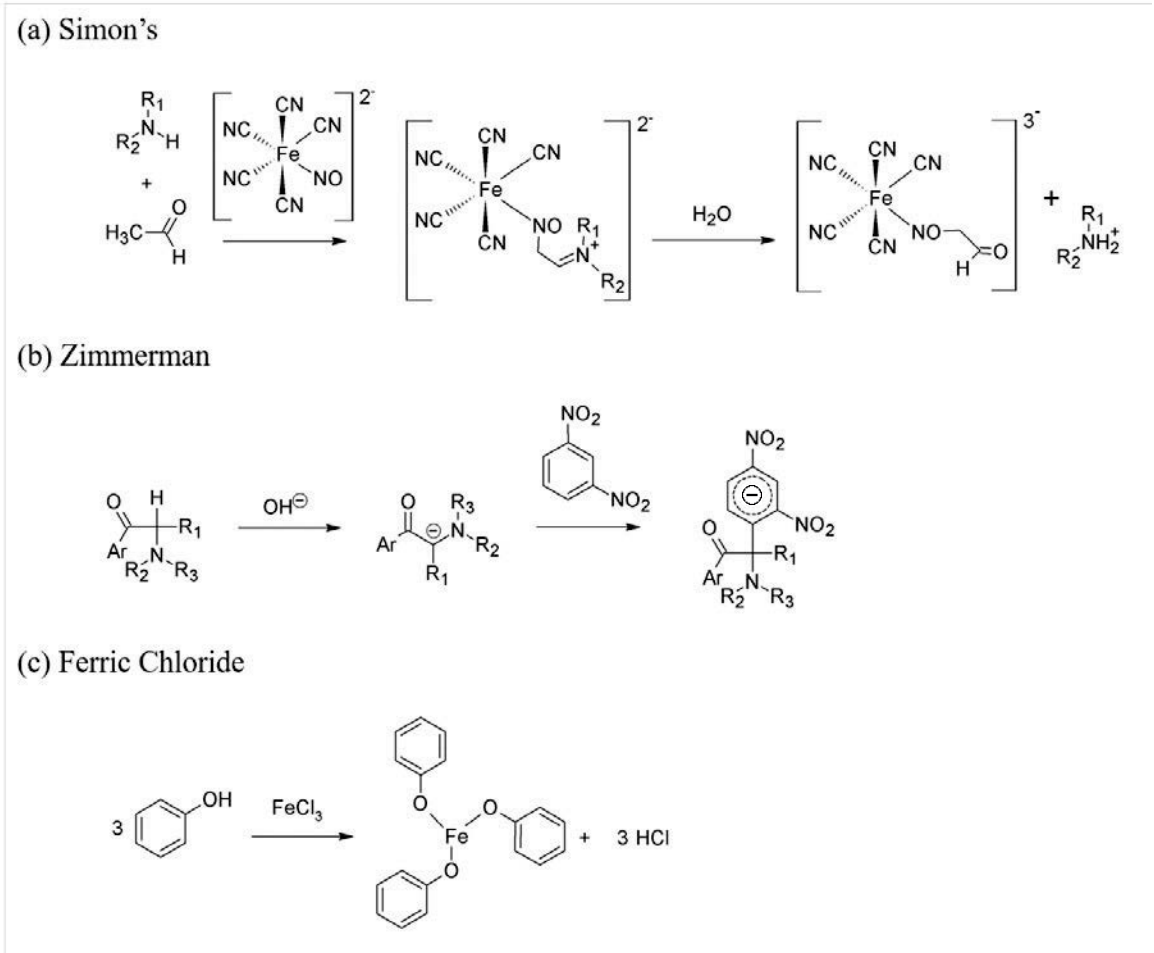

Figure 1-5. Chemical reactions of common colour spot tests that are selective toward certain functional groups. Simon's reagent for secondary amines (a); Zimmerman reagent for β-amino ketones (b); and ferric chloride reagent for phenols (c).

1.4.3 Drug class selective

Many colour tests are highly specific toward a certain drug class or group based on molecular structure and functional groups present. The Duquenois-Levine (D-L) test for cannabis requires the formation of a purple product and the transfer of that product into the chloroform layer for a positive result[71]. Many researchers have reported the exact mechanism occurring as unknown[94]. However, more recently, Liquid Chromatography-Triple Quadrupole Mass Spectrometry (LC-MS/MS) and Atmospheric Pressure Ionization-High Resolution Time-of-Flight Mass Spectrometry (API-HRTOFMS) were used to ascertain the chromophore structure[95] (see Figure 1-6). Rubiano *et al.*[96] also looked into detail at the D-L reaction to provide a better understanding of the mechanism. He found that activating substituents on the benzene ring resulted in positive colour changes. The targeted drug class for D-L can be ambiguous as to which cannabinoids are detected, with the literature describing its use for cannabis only[73, 97, 98] and marijuana and hashish, inclusively[85].

Opium alkaloids will react with the Mecke reagent via rearrangement and oxidation in the presence of selenious acid[69] (see Figure 1-6). Despite the toxic and corrosive nature of these reagents, they are still frequently employed and more recently show value in distinguishing heroin from fentanyl[99].

The cobalt thiocyanate test for cocaine is one of the less understood test reagents, and its mechanism is not amply described in the literature. Although unable to isolate the coloured complex, Oguri *et al.*[100] proposed an octahedral structure for the cocaine-cobalt(II) thiocyanate complex with two thiocyanate ligands and two *bis* chelating cocaine ligands, based on a stoichiometric study. Another study by Haddoub *et al.*[79] revisited the use of cobalt thiocyanate for the detection of cocaine by applying the reagent to a TLC plate and proposed a hexacoordinated cobalt(II) complex with one *bis* chelating cocaine molecule, three water molecules, and one isothiocyanate ligand (see Figure 1-6). Scott modified the cobalt thiocyanate test to differentiate between the cocaine free base and cocaine hydrochloride[65].

Cobalt is also present in the Dille Koppanyi reagent for barbiturates which produces a purple cobalt complex, stabilized by isopropylamine molecules[69] (see Figure 1-6). The purple colour change observed with copper sulfate, and sodium hydroxide solutions as described by Chen and Kao is a test for ephedrine and pseudoephedrine[64]. The proposed structure is a copper chelate complex with ephedrine molecules as bidentate ligands, linked via vicinal amino and hydroxyl groups[69](see Figure 1-7). Although often described as a test for secondary amines,

Toole *et al.* demonstrated the lack of reaction with secondary amine methcathinone analogs[84].

Ehrlich's reagent has been used for over 100 years for detection of indoles, specifically those present in lysergic acid diethylamide (LSD) and other ergot alkaloids. Kovar[69] described the 2:1 ratio of indole to *p*-dimethylaminobenzaldehyde (p-DMAB) in the final coloured product (see Figure 1-7), however Lamb *et al.[101]* determined the reaction takes place at the beta position of the indole.

Fast Blue BB salt, 4-Amino-2,5-diethoxybenzanilide diazotated zinc double salt, was described by Watanabe *et al.*[102] for the determination of cannabinoids in 1979. The authors found stable diazo compounds were produced with cannabinoids in alkaline media (see Figure 1-7). More recently, Dos Santos *et al.*[103] used UV-Vis, TLC and mass spectrometric methods to evaluate the selectivity of Fast Blue BB salt for cannabinoids in street samples and proved the increased selectivity of FBBBS over FBBS. Dos Santos *et al.* undertook studies to determine the structure of the products and thus a better understanding of the chemical reaction taking place. FBBS is present in Clarke's as a visualization reagent in Thin Layer Chromatography (TLC) due to the different colours seen with cannabinoids tetrahydrocannabinol, cannabinol, and cannabidiol[104]. The principal screening test for cannabis used by Brazilian Forensic Police is a Fast Blue B or BB salt[103].

Zwikker[105] first described the use of an aqueous copper sulfate-pyridine solution for detecting barbiturates in 1931. In efforts to determine the mechanism, Levi and Hubley[106] later detailed the enolized barbituric acid ion interacts with a positively charged copper-pyridine complex ion (see Figure 1-7).

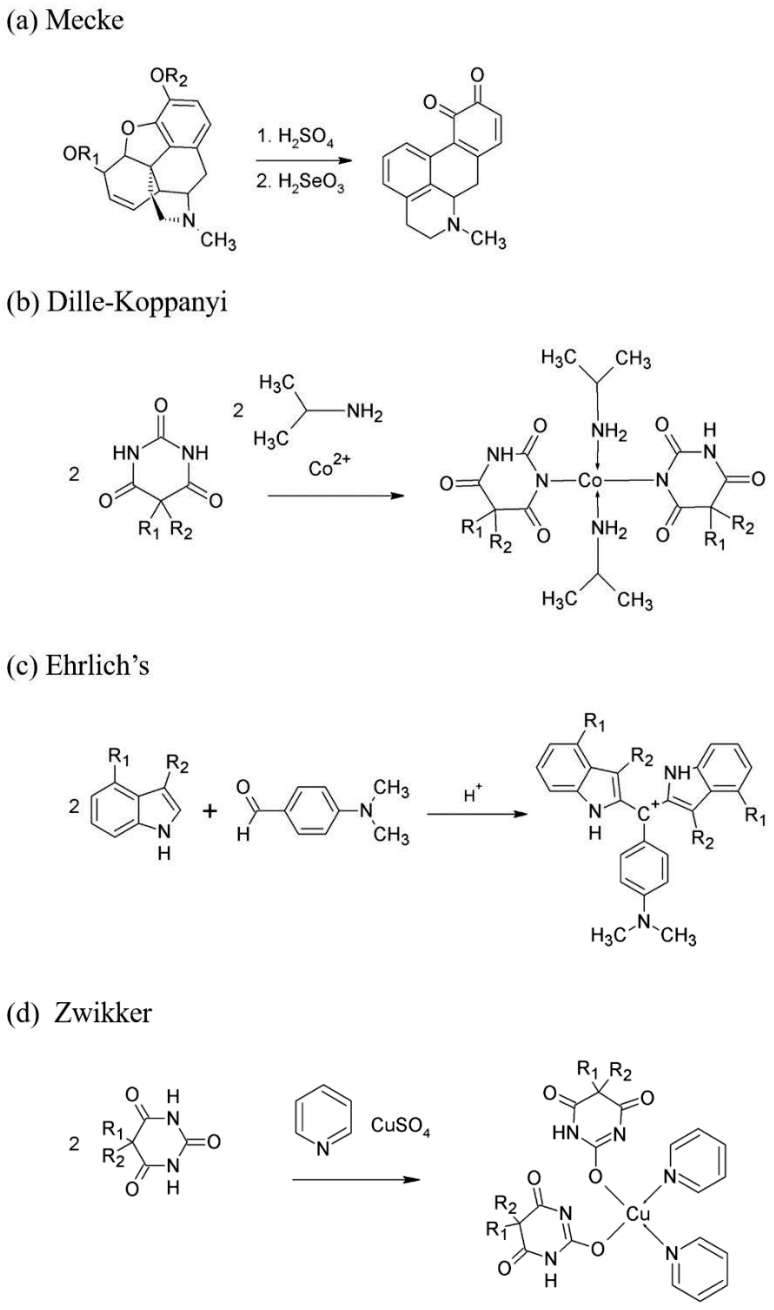

Figure 1-6. Chemical reactions of common colour spot tests that are selective toward a drug class. Duquenois-Levine reagent for cannabinoids (a); Mecke reagent for opium alkaloids (b); Scott's reagent for cocaine (c); Dille-Koppanyi reagent for barbiturates (d).

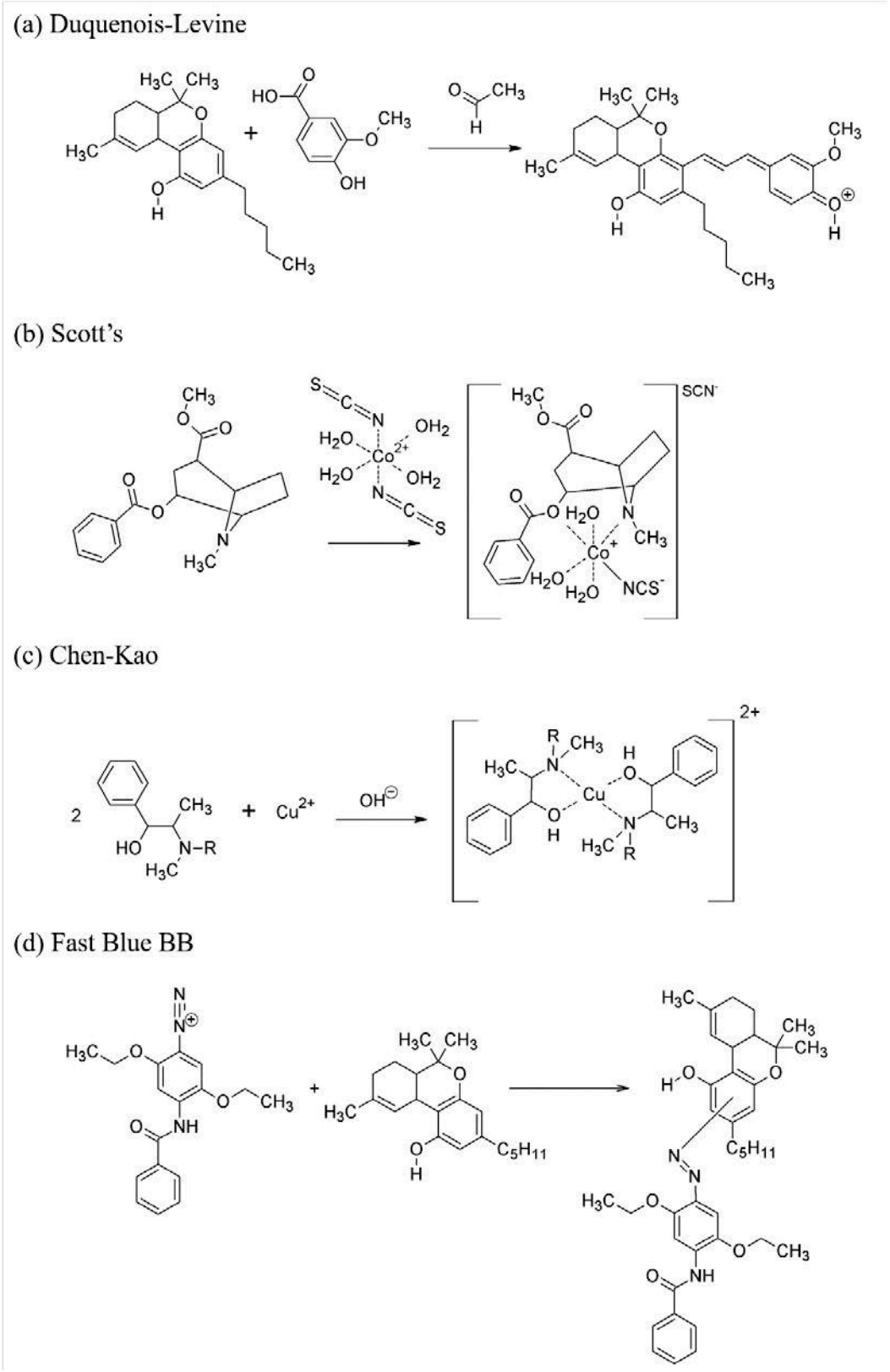

Figure 1-7. Chemical reactions of common colour spot tests that are selective toward a drug class. Chen-Kao reagent for ephedrine/norephedrine (a); Ehrlich's reagent for ergot alkaloids (and LSD) (b); Fast Blue BB reagent for cannabinoids (c); and Zwikker reagent for barbiturates (d).

Today, colour tests are strictly used for the presumptive identification of controlled substances only. A recent International Collaborative Exercise (ICE) by the United Nations Office on Drugs and Crime (UNODC) saw 181 laboratories in 67 countries receive four independent samples for analysis to monitor drug testing performance globally[107]. Colour testing was found to be the most commonly employed screening method in these laboratories for the three most recent studies[107-109] (see Figure 1-8). There are a large number of colour spot tests available; however, typically only a handful of these tests are commonly used in the field by law enforcement.

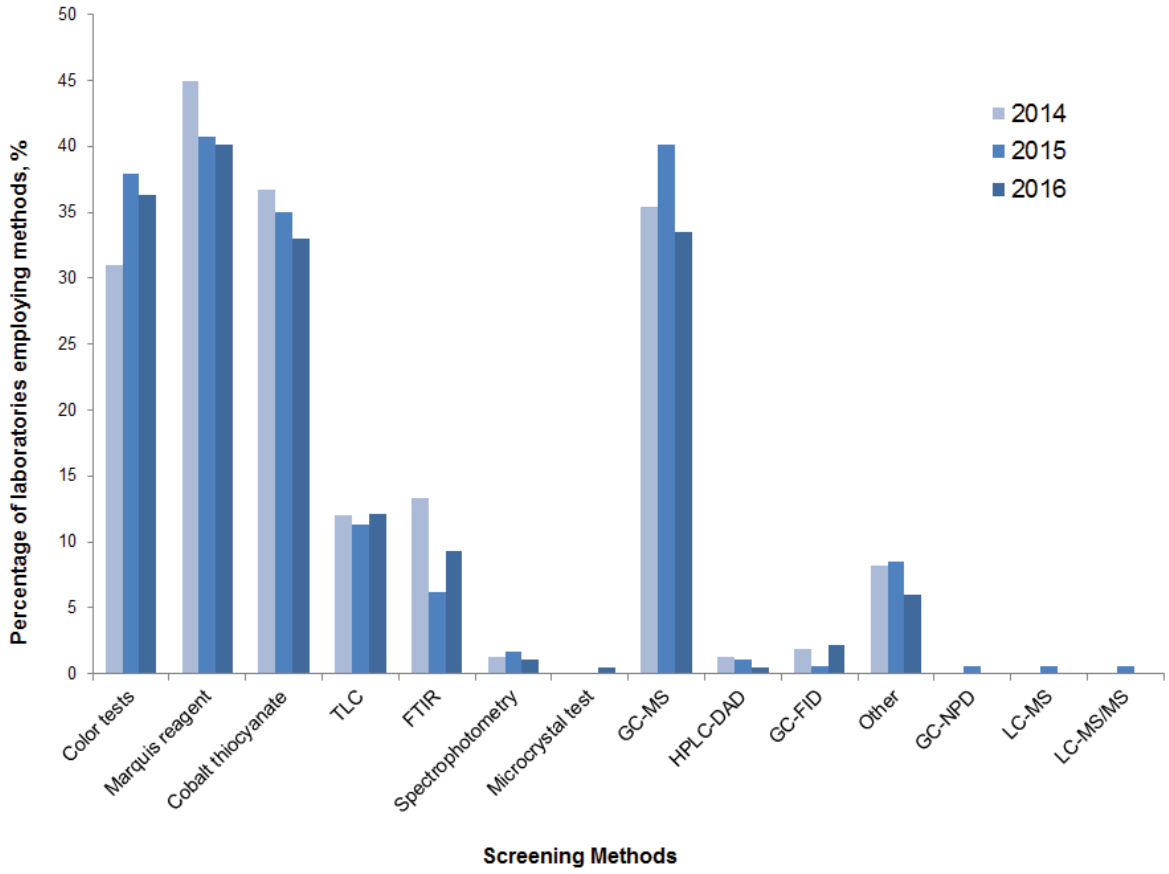

Figure 1-8. Screening methods performed by laboratories taking part in the UNODC's International Collaborative Exercises (ICE) study of seized materials over three separate studies from 2014-2016

1.4.4 Drug test kits

Portable drugs of abuse test kits for law enforcement, other agencies, and even individuals are widely available due to a large number of manufacturers and suppliers of these drug test kits. Purchased test kits are ready to be used in the field and come in a range of designs from reagent tubules to pouches to cartridges (see Table 1-3. Commercial companies producing colour test kits for drugs of abuse and precursor material. In addition to commercial companies, the Laboratory and Scientific Section of the UNODC also develop and produce drug and precursor test kits for law enforcement[110].

Table 1-3. Commercial companies producing colour test kits for drugs of abuse and precursor material.

Company	**Test kits available**	**Target market**	**Reference**
Sirchie (NARK® tests)	27 pouch tests 21 tube tests 1 drug wipe	Law enforcement	[111]
MMC International BV (Narcotic field tests)	55 tube tests 3 purity tests 1 spray 1 drug wipe 1 test strip	Police, customs authorities and forensic laboratories	[112]
NIK® Public Safety (NIK® tests)	20 pouch tests 1 tube test 1 drug wipe	Agencies	[113]
ODV™ Drug Tests (NarcoTest and NarcoPouch)	20 pouch tests 2 tube tests	Investigators	[114]
IDenta Touch&Know	26 test kits	Retail-consumer market and law enforcement	[115]

TestKitPlus	5 Reagent dropper bottles 3 tube tests	Medical centers, harm reduction organizations, government agencies and individuals	[116]
EZ Test	13 test kits 2 purity tests	Professionals and individuals	[117]
Lynn Peavey Company (QuickCheck)	6 tube tests 6 test pouches	Law enforcement and laboratories	[118]

An important feature of companies developing drug test kits is their ability to respond to the current illicit drug situation through the development of new test kits or validation of previous kits. The release of a presumptive test specific for fentanyl in 2016 following an outbreak of fentanyl overdose deaths demonstrated this response[119].

The investigation into spot tests for the determination of anabolic steroids revealed Mandelin's reagent accompanied by the sulphuric acid test provided the best indication[120]. Commercial companies have been established specifically for the identification of anabolic steroids employing colour test reactions that require less than 1 mg of steroid for a visible reaction to occur in typically a few seconds[121, 122].

1.4.5 Harm reduction

In the age of increasing public awareness of drug-facilitated sexual assault, commercial companies developed products suitable for use by those at risk of being drugged. These products are designed to be used discretely in a public club or bar environment. One such test was the "date rape drug detector" coaster that claimed to be able to detect γ-hydroxybutyric acid (GHB) and ketamine[123]. A study by Meyers and Almirall[124] at the time showed this to be true only at high concentrations of the drug in solution, dependent on the beverage matrix, and also stated there are other date rape drugs in circulation that would limit the test's usefulness. Other date-rape drug detection devices that have emerged include beverage containers[125], straws[126], coasters[127], and nail polish[128].

In attempts to reduce harms associated with the use of psychoactive drugs at dance parties, many organizations are providing presumptive colour test kits for users to test their drugs. Murray[129] evaluated screening kits for MDMA testing and concluded they should not be used by the public to give a false sense of security as pure and adulterated forms cannot be distinguished. A recent review in the Harm Reduction Journal compared methods of drug analysis for suitability in point-of-care services and found colour tests to be the best lower technology option due to lower costs, ease of use and rapid results afforded[130]. However, the authors ultimately recommend the use of handheld IR or Raman spectroscopy.

1.4.6 New Psychoactive Substances

A review of presumptive colour testing would be amiss if NPS were not mentioned. Designed to mimic established illicit drugs, the majority of these substances are synthetic cannabinoid receptor agonists, stimulants and classic hallucinogens[1]. The application of common presumptive colour tests to the new compounds revealed a lack of specificity. Among others, researchers at the University of Wisconsin are conducting research into the development of presumptive tests for these new compounds and have patented a colorimetric assay and kit[131]. The drug detection is based on chemical reactions with multiple dyes and claims to be able to detect a range of drugs, including synthetic cannabinoids, piperazines and synthetic cathinones.

Cuypers *et al.*[56] performed a comprehensive investigation into the outcomes of five different current colour test kits on more than 40 NPS. Cuypers proposed a combination of Marquis, Mecke's and Mandelin's reagents to effectively predict the drug class, with Simon's and Scott's reagents used if identification is not ascertained. This study focused on the phenethylamines, with only four cathinones, five cannabinoids, and two piperazine compounds tested. A similar study by a research group in Korea suggested Marquis, D-L, Zwikker, Mandelin and Liebermann's reagents could distinguish synthetic cannabinoids, aminoindanes, phenethylamines and tryptamines[132].

The emergence of synthetic cannabinoids posed significant problems for their presumptive identification by traditional colour tests. Despite being marketed and sold as 'legal high' products, these substances do not contain the active constituent present in marijuana, Δ^9-tetrahydrocannabinol (THC) and therefore the D-L test is inappropriate. The synthetic cannabinoids are a diverse class of NPS that contain several different sub-class structures. The

ketone functional moiety present in many of the structural subclasses was targeted by Isaacs[133] using the well-known reagent, 2,4-dinitrophenylhydrazine (DNP). The proposed test method included vortexing, removal of the supernatant, the addition of DNP and heating for 5-10 minutes if necessary. The structure of the orange-red precipitates that formed was not characterized, however, categories were established based on their reactivity. It is also worth noting that that the synthetic cathinones failed to react with DNP. Isaacs also demonstrated the Van Urk test was ineffective for analysis of the indole ring present in the 'core' of a synthetic cannabinoid structure due to the net electron deficiency as a result of the ketone substructure strongly withdrawing electrons from the indole ring[133].

A commercially available colour test kit has been produced for synthetic cannabinoid presumptive identification. A plastic ampoule containing a reagent and absorbing crystals make up these test kits that are labeled as producing up to six different colours depending on the synthetic cannabinoid present. The specificity of this test is unknown with only concentrated sulphuric acid listed as a reagent and test instructions explaining if the test is shaken more than twice, it will become invalid[134].

The second largest group of NPS, the synthetic cathinones, were the subject of the most recent publication from the UNODC aimed at drug testing laboratories. In this recommendation, the Zimmerman reagent is proposed as the most suitable colour test for synthetic cathinones. Immediate colour changes were seen for 13 of the 16 substances examined, and after 5 minutes, only one cathinone, bupropion, failed to react[80]. An earlier study by Toole *et al.* [84] investigated the suitability of currently available colour test methods to synthetic cathinones and found that the Marquis reagent was able to presumptively identify methylenedioxy substituents, while the Liebermann's reagent was best suited to methcathinone analogs, producing intensely yellow coloured products. Of the 11 synthetic cathinones studied by Toole, 3-fluoromethcathinone failed to react with Marquis or Liebermann's reagents.

The false-positive results shown by pyrrolidine-type cathinones with the Scott's test for cocaine was resolved by Tsujikawa *et al.*[135] who suggested employing Chen-Kao's test to differentiate the cathinones, and cocaine based on the colours produced. The results of this study do not agree with the study by Toole *et al.*[84] that showed cathinone analogs, including one pyrrolidine-type compound, did not react with the Chen-Kao reagent.

Chemical reactions of mephedrone, as an example of a synthetic cathinone, have been studied by research groups for the coloured products that result. Parastekar and Barhate[136] showed

that oxidation with potassium permanganate in an alkaline solution produces a green colour after 10 min, and ferric neocuproine produces a coloured complex after boiling for 30 min. Philp *et al.*[137] also investigated neocuproine complexes and validated a colour test method for synthetic cathinones employing copper-neocuproine. The test requirement of 10 min heating at 80 °C diminished the applicability of the method. Nycz *et al.*[138] recently published work on the synthesis of thiocathinones and the nucleophilic addition of aminoguanidine. These studies may prove useful in developing specific colour test reactions.

The Marquis and Simon's reagents have been recommended for onsite screening of piperazines despite the faint colour changes and low sensitivity[139]. In an attempt to find a more specific colour test, a limited study looked at the reaction of five piperazine analogs with 1,2-naphthoquinone-4-sulfonate (NQS) and validated a successful colour test method based on a nucleophilic substitution reaction to afford an orange-red colour[140]. Chemiluminescent ruthenium complexes with piperazines were described by Waite *et al.*[141], however the test lacked portability with the requirement for a chemiluminescence detector.

Plant-based NPS, kratom, can be differentiated from marijuana using the D-L test, while other colour tests were not especially helpful for its presumptive identification[45]. The intensity of the blue coloured organic layer of Scott's test following the addition of extra chloroform was shown to distinguish crack cocaine from tryptamine substance, 5-methoxy-N,N-diisopropyltryptamione (5-MeO-DIPT, foxy)[142].

Alkaline gold bromide was investigated as a potential colour test reagent for ketamine after it produced a deep purple colour within one minute of interaction and showed no cross-reactivity with compounds often mixed with ketamine[143]. The results also showed that the test reacted with ascorbic acid, mannitol, sucrose, and lactose, however, the colour development over time could be used to distinguish these. Ketamine HCl was also the target analyte in a novel colorimetric kit that produced a purple precipitate with a cobalt complex immobilized onto a nano-SiO_2 support[144].

1.4.7 Limitations

Practitioners are required to have knowledge of the theory and principles behind colour testing, including limitations of the tests[145]. An interesting article published in the New York Times Magazine titled, *How a $2 Roadside Drug Test Sent Innocent People to Jail,* questioned

the selectivity of colour tests. The authors make an example of the failings of chemical colour tests as used by police personnel through the examination of a wrongful conviction due to a false positive result from a presumptive field colour test for cocaine[53]. Online tabloid newspaper articles have published similar individual accounts describing arrests made based on false positive presumptive colour tests for drugs with everyday items such as Krispy Kreme crumbs[146], baking soda[147] and Epsom salts[148].

This is not the first time colour testing has been seen in negative light. In 2008 the Marijuana Policy Project funded an investigation into drug testing aimed at police, prosecutors, and judges which resulted in a 40-page report. Case studies detailing Americans that were wrongfully prosecuted and incarcerated based on false positive test results were presented[149]. Tsumura *et al.*[142] showed Scott's test produced false positives with cutting agents including dibucaine and ketamine when using a test sample of more than one milligram. Presumptive test results may also be affected by the presence of more than one drug or the use of colouring agents usually seen in tablets such as ecstasy and piperazines[30].

The limitation of colour testing was highlighted in a recent case that saw the seizure of unknown heart shaped tablets in Italy which were presumptively identified as amphetamines using the Marquis reagent. However, confirmatory analysis revealed the tablets contained two anabolic androgen steroids (AAS), methanedione and methyltestosterone, and no trace of amphetamine-type substances[150].

The act of performing colour testing in the field also presents problems for those handling the evidence. Extremely potent substances encountered in casework are a threat to law enforcement personnel performing colour tests, as minute amounts are lethal and can be inadvertently inhaled or absorbed through the skin[35]. The handling of colour test reagents themselves also poses significant safety concerns as many are toxic or highly corrosive substances, such as sodium nitroprusside, formaldehyde, and concentrated sulphuric acid.

1.4.8 Spot test regulations

The Laboratory and Scientific Section of the UNODC has produced several useful manuals for drug testing laboratories. These manuals provide method recommendations for the identification and analysis of seized materials such as cocaine[151], cannabis[39], amphetamine-type substances (ATS)[152], and most recently, synthetic cathinones[80].

Practitioners are referred to UNODC manuals that provide procedures for field testing, interpretation of the results and useful practical notes on each test[97].

The development of any scientific method is necessarily accompanied by a thorough and transparent method validation to justify it is fit for purpose. Several groups provide recommendations for such validations. SWGDRUG recommends minimum standards for the forensic examination of seized drugs and includes requirements for method validation studies[37]. Colour test reagents and kits have also been standardised by the USA's National Institute of Justice (NIJ)[68]. The validation parameters pertinent to colour tests are selectivity (and specificity), limit of detection (LOD), precision and stability.

1.4.9 Method validation guidelines

1.4.9.1 *Selectivity (and specificity)*

The selectivity of a colour test toward its target drug class is of paramount importance for method validation. The number of test samples used in this validation should be as broad as possible and include all controlled drugs of interest and their precursors, common diluents and excipients, other controlled drugs and real or simulated seized material samples[70]. For the method to be accepted, there must not be any significant interference from commonly occurring substances.

Independent researchers, companies, and government organizations have published the results of commercially available test kits and commonly used lab reagents against a range of NPS[56, 132], controlled substances and white powder cutting agents[54, 149, 153] in attempts to reveal and report any false positive or negative responses. Philp *et al.* demonstrate the importance of selectivity studies to newly developed presumptive tests for piperazines[140] and synthetic cathinones[137]. Experimental studies on 42 non-marijuana substances with two commercial test kits showed patchouli, spearmint, and eucalyptus all tested positive for marijuana; while lavender, cypress, and oregano gave inconclusive results[149, 154].

An excellent example of a colour test adapting to increase its specificity is that of Scott's test for cocaine. The originally developed cobalt thiocyanate was susceptible to many false positives and was modified in 1973 by Scott to make it more specific to cocaine. In 1986 Fansello and Higgins[155] further developed the test to make it more applicable to the cocaine

free base as well as the cocaine hydrochloride salt. An attempt to simplify this method, increase sensitivity and remove cross-reactivity with lidocaine saw glycerol replaced with other polyhydroxy alcohols and a polyether or silicon derivative of a polyether[156]. Recent studies by Tsujikawa *et al.*[135] have shown the specificity of Scott's test is further improved by the addition of a filtration step.

1.4.9.2 *Limit of detection*

The qualitative nature of the colour spot test often leaves the limit of detection (LOD) neglected in presumptive test studies. Serial dilutions of a pure sample are analyzed until the lowest concentration tests positive in five replicates. This concentration is then multiplied by ten and recorded as the 'operational drug detection limit'[70].

Spot tests have been described as sensitive and specific qualitative analyses. However, few studies have focused on the limit of detection and the factors that may affect this detection cut-off. O'Neal[76] determined the detection limits of 36 combinations of test reagent and illicit drug and showed they were very sensitive, with typical LOD's between 1 and 50 µg. He was also able to show that different colour tests able to detect the same drug had significantly different LOD values. For example, the detection of *d*-methamphetamine HCl had a drug detection limit of 100 µg with the Mandelin's reagent and only 10 µg with Simon's reagent. LOD is of particular importance to substances with high potency and therefore low dosages, such as LSD which produces hallucinogenic effects after 25 µg doses[157].

1.4.9.3 *Precision*

The legal implications of colour tests place significant importance on the results being precise. An analysis of at least ten replicate samples should give no more than 20% false negative results under repeatability and reproducibility conditions[70]. The application of colour test kits in the field requires their performance to be particularly robust by not being susceptible to small changes that may occur during routine analysis. It has been found that the ambient temperature when performing Scott's test affects the resulting colour change due to an excellent example of Le Chatelier's Principle[158]. At much cooler temperatures, the sensitivity of the test is doubled compared to room temperature, while temperatures above 40 °C decreased the sensitivity two-fold. Velapoldi[81] found that performing colour tests at 3 °C

slowed many colour test reactions down significantly. In particular, the Duquenois-Levine test was five times slower. Additionally, reactions carried out at higher temperatures showed rapid colour changes making transition colours difficult to observe.

Another consideration in colour testing is the precision of different people or the same person observing multiple blind colour tests. The subjective nature of the test means the precision is largely determined by the ability of the observer to distinguish colours. A number of factors can affect the perception of colour, including lighting, background colour, viewing angle and surface texture. Furthermore, an individual's colour vision deficiencies of varying degrees could significantly affect a colour test interpretation.

1.4.9.4 *Stability*

The stability of the chemical reagents must be considered. Test reagents requiring fresh preparation and refrigeration when not in use are not suitable for field testing purposes, but may still be useful in drug testing laboratories. Reagent stabilities are widely published and typically require fresh preparation after one month[68]. Velapoldi[81] performed stability studies on ten common colour test reagents: cobalt(II) thiocyanate, Dille-Koppanyi, Duquenois-Levine, Ferric chloride, Froehde's, Mandelin's, Marquis', Mecke's, nitric acid, *para*-dimethylaminobenzaldehyde and Zwikker. The reagent solutions remained stable after ten weeks of being stored in 40 °C water baths.

1.4.10 Advances in colour testing

The chemical colour tests in place today have been used without modifications for decades owing to their simplistic and rapid nature; however, improvements to quality management systems has led to better product quality assurance. The increased portability of technology and understanding of chemical reactions taking place in colour tests has led to advancements in the colour test procedure.

1.4.10.1 *Digital image analysis*

The colour result reported in spot test analysis is a subjective result dependent on the vision of the user and the lighting conditions where the test is performed. Colour reference charts such as Munsell and Centroid are often used to limit this potential subjectivity. However, digital image analysis offers a significantly more objective result without changing the colour spot test method. Information is extracted from digital images and processed by a computer to produce the red, green, blue (RGB) components of the full image for a given colour spot test. Colorimetric analysis products include physical devices such as the Cube®[159], used to accurately capture the colour of a particular surface, to mobile applications such as ColorAssist[160] that employ a device's built-in camera and allow the user to 'point and shoot' at a particular surface to read the RGB values. The Cube® includes an initial calibration step by measuring the RGB value of the white cover. In addition, the unit is designed to eliminate any interfering external light sources when making measurements, unlike point and shoot mobile applications that are largely dependent on lighting conditions and surface texture.

Choodum *et al.* were the first to apply digital image analysis to the coloured products of presumptive colour tests for methamphetamine and amphetamine products[55] and opiates[161] by obtaining RGB values of reactions of Marquis and Simon's reagents, and Marquis and nitric acid reagents, respectively. The results, collected from Adobe Photoshop software, were shown to be semi-quantitative and in good agreement with gas chromatographic data. The group later used the built-in camera of a mobile phone, a mobile application, and a custom built colour detection box to eliminate lighting interferences in their analysis of seized 'Yaba' in Thailand[162]. Importantly, for Amphetamine-type substances (ATS), they were able to demonstrate the ability to subtract a blank colour from the product colour if the seized samples are coloured themselves.

In one study, the performance of Scott's test was evaluated on cut cocaine samples using multivariate image analysis[163]. Principle Component Analysis (PCA) was able to distinguish true negative and true positive samples clearly, and interestingly as the sample weight increased, the false positive results also increased.

Elkins *et al.*[54] compiled a library database of RGB values for colour test results using two mobile applications to make presumptive colour testing more objective. A total of 27 colour tests were used on 39 controlled substances and cutting agents which resulted in over 800

drug-test pairs. The result for forensic laboratories is a significant decrease in the time spent performing the tests and recording the results.

1.4.10.2 *Other colorimetric methods*

In 2010, DETECHIP® (Andrea Holmes; Doane University, Nebraska, USA) was described as a novel sensor for drugs of abuse, employing colorimetric and fluorimetric assays suitable for lab and field use. Different to other spot tests, molecular interactions between the drug of interest and non-toxic dyes produce the observed colour change. The sensor records twenty responses in a single test by using five dyes, two buffer systems and two methods of analysis. The 20-digit identification code produced was able to identify nine illicit drugs from 11 over-the-counter drugs or cutting agents[164]. Significant sample preparation is required, along with the use of a spectrophotometer and plate reader. Lyons *et al.*[165] showed that image analysis could be performed to successfully detect and identify a range of illicit materials using the DETECHIP colorimetric sensor, a camera, and a flatbed scanner.

The inability of current commercial tests to detect γ-hydroxybutyric acid (GHB) at the low levels capable of causing death led Baumes *et al.*[166] to propose a colorimetric sensor array able to detect the colourless liquid, GHB, at sub-millimolar concentrations with the naked eye. The colour changes were based on supramolecular host-guest complexes of fluorescent dyes with organic capsules and even distinguished GHB from γ-butyrolactone (GBL). This differentiation is particularly important in a forensic context as GBL is converted to GHB in the body.

Researchers at the University of Central Florida have identified drugs based on luminescence that appears when the substances react with certain metal classes and have created a low-cost portable handheld spectrometer[167]. This method reportedly has less false positives and false negatives than spot colour tests through its use of a smartphone and online database of fluorescence spectra.

Recently, the first portable upconversion nanoparticle (UCNP) based sensor device for field testing of cocaine was developed in China[168]. Aptamer fragments target cocaine which causes quenching of UCNP luminescence and signals the detection of cocaine. This sensing device is suitable for on-site screening of blood, saliva, and aqueous solutions, despite requiring near infrared (NIR) excitation.

1.4.10.3 *Microfluidic devices*

Microfluidic devices have been applied to four controlled substances to reduce waste, reagent volumes and amount of sample required compared to colour testing[169]. A significantly cheaper alternative has seen paper-based microfluidic devices become popular. Musile *et al.*[170] analyzed seized drugs using paper-based microfluidic devices that employed common colour test reagents. Nine psychotropic substances were detected, with results occurring in five minutes or less. The authors explain that reagents using concentrated sulphuric acid (Marquis and Mandelin), as well as highly volatile reagents are unable to be employed.

Rotation-driven microfluidic (RDM) devices have also been applied to illicit drug seizures and successfully identified 30 unknown samples. This "lab-on-a-disc" device can control rotation speed, direction and time to produce an objective detection method. Authors state this device will be ideal to replace standard colorimetric test kits that require separate test kits for each test[171].

1.4.10.4 *Solid sensors*

The most recent developments have seen the incorporation of wet chemical colour test reagents into different sensor devices. Choodum *et al.*[172] continued their work on presumptive detection of methamphetamine through the creation of a sol-gel colorimetric sensor that contained Simon's reagents trapped within the polymeric network of the sol-gel matrix. This sensor was incorporated into a tube for in-tube detection, affording quantitative results when combined with digital colorimetry even when performed on coloured drug samples and spiked urine samples. Similarly, a solid colorimetric sensor has been developed for the analysis of four amphetamine-type samples by embedding the reagent, 1,2-naphthoquinone-4-sulphonate (NQS), into a polymeric matrix[173]. A colour change is observed following placement of the solid sensor in a buffer solution of the amphetamine samples for 10 minutes. This group is also looking into incorporating cobalt thiocyanate into a matrix for detection of cocaine. The use of solid reagents has been shown to overcome inherent disadvantages of liquid reagents, such as stability.

1.4.11 Future of presumptive colour testing

The successful use of chemical colour test methods developed in previous decades and centuries thus far has been due to their simple, rapid and portable qualities. Historically, these microchemical methods offered the best solution for rapid drug identification; however, in more recent years, serious concerns regarding the use of such tests have been raised. The emergence of over 600 new psychoactive substances put significant pressure onto existing colour tests to be able to detect and differentiate substances. This shortfall came at a time when colour tests had attracted wide attention and comment regarding false positive results with real implications in casework. A common misnomer is that colour tests provide binary outcomes and are easy to interpret. It is important for technicians and officers to be made aware of potential false positives and factors affecting test results.

Advances in technology have led to changes in three key areas surrounding colour testing: the objective analysis of results, the incorporation of the test reagents into a more stable form, and the development of devices capable of multiplexing. Advances in nanotechnology have also provided new methods for reporting the presence of illicit drugs based on luminescence. One thing these methods do not change is the requirement for an officer to physically sample the suspect material. The nature of this procedure presents a real safety concern with the increased prevalence of potent psychoactive substances and drugs absorbed through skin contact, such as fentanyl analogues.

Improvements to current methods would likely see further development of sensor devices that can selectively recognize the drug molecule and report the detection with a visual cue, not based on chemical reactions. These chemosensors and biosensors will provide greater selectivity and specificity with the potential for targeting multiple analytes in one test, thus removing the need to perform a battery of tests.

The future of colour testing can also refer to the existence of such methods at all. As developments in colour testing are made, so too are improvements in the confirmatory analysis to produce devices with increased portability and ease of use. Portable handheld spectroscopic devices with high discriminating power are rapidly becoming popular for forensic drug detection, as they address many limitations of chemical colour testing, such as low discriminating power, handling of potentially dangerous substances, and using harsh, toxic chemicals. However, cost-effectiveness is a key metric in the development of a portable field testing device and will need to be maintained to make it available to the developing world.

The presumptive identification of illicit drugs is a crucial component of forensic drug testing that provides rapid information at points of seizure. In countries with limited resources, colour testing is used to screen all submitted samples, and its low cost will outweigh the benefits provided by replacing them with portable devices. Greater knowledge in the capabilities of current chemical colour tests will significantly improve its successful use in the field.

1.5 Microcrystalline tests

Microcrystalline testing is an interesting presumptive identification method with an extensive history that dates back to work pioneered by Fulton in the 19th century[174] with his book, *Modern Microcrystal Tests for Drugs*[175]. This extremely sensitive technique employs metal salts, mixtures of metal salts, or acidic compounds to react with drug molecules and form crystals of unique shapes and patterns, such as rods, prisms, rosettes, blades, and needles. These tests are limited to use in the laboratory due to the requirement for a microscope. However, they have mostly been replaced by more sophisticated techniques.

The SWGDRUG guidelines classify microcrystalline tests as a category B technique and thus a higher discriminating power than colour tests[37]. The combination of low cost, high selectivity, high sensitivity and ease of use may see microcrystal tests performed in laboratories alongside colour tests. The McCrone Research Institute recently published a detailed summary of microcrystal tests for 19 illicit drugs and diverted pharmaceuticals[176]. This compendium provides coloured photomicrograph images of the resulting crystal formations and also reports the limit of detection values.

Despite microcrystal testing being an antiquated technique, research groups continue to publish results of microcrystal tests with emerging NPS. Elie *et al.*[177] used aqueous mercury dichloride in a reaction with aqueous mephedrone to form crystals with characteristic paddlewheels and rosettes of blades. This research group appears to be at the forefront of new developments in microcrystal testing of illicit drugs with crystal shapes also reported for 1-benzylpiperazine (BZP) and 5,6-methylenedioxy-2-aminoindane (MDAI). The same group has also published improved microcrystalline test methods for γ-hydroxybutyrate (GHB)[178].

One study looked at the changes in crystal morphology of adulterated cocaine samples to identify the adulterant and its concentration, however, the study was limited to samples containing only one adulterant[179]. Microcrystalline testing has been used in combination

with Fourier Transform Infrared (FTIR) spectroscopy to identify drugs in street samples rapidly[118]. The study showed the sensitivity of microcrystal tests can still be of value in today's technology driven laboratories. More recent work saw its combination with Raman micro-spectroscopy for absolute identification of NPS's in the presence of cutting agents and differentiation of constitutional isomers of methylmethcathinone[180]. This combination of techniques would satisfy SWGDRUG requirements for confirmation of drug presence.

1.6 Thin Layer Chromatography (TLC)

1.6.1 History and use

Separations on thin layers were first achieved by Izmailov and Schreiber in 1938 in a quest for a technique requiring less sample and sorbent[181]. This new thin layer method underwent some developments and improvements over the next 16 years until Stahl introduced 'thin layer chromatography' into the literature. During this time, layers had starch binders added, the method of development was made ascending, and the sorbent material became silicic acid[182].

A uniform planar layer of sorbent material on glass or aluminum backing acts as the stationary phase and is immersed in the mobile phase, a mixture of two or more solvents. Separation occurs due to analyte differences in adsorption and partitioning between the two phases. The TLC plate is developed to visualize the compounds. This visualization may occur due to natural fluorescence, colour, quenching of fluorescence or their reaction with chromogenic reagents to produce coloured spots[183].

The identification of drugs by the pharmaceutical industry frequently included TLC. Nowadays, TLC is considered a preliminary identification technique for the screening of drugs of abuse. TLC can afford two points of identification in any one run based on retardation factor (R_f) and reaction with visualization reagents. This extra information offered by TLC is the reason for its classification as a category B technique by SWGDRUG[37].

1.6.2 TLC in drug screening

The open system nature of TLC requires it to be performed under controlled environmental conditions and alongside reference standards. There are a large number of mobile phase and visualisation reagent combinations possible in TLC. Publication of optimal systems for drugs of abuse is necessary for efficient testing by practitioners. *Clarke's Analysis of Drugs and Poisons* is considered the gold standard for TLC solvent system and visualization reagent preparation and use[104]. The Virginia Department of Forensic Science provides freely available procedure manuals with a specific focus on controlled substance analysis, including TLC[184].

Citric acid-acetic anhydride reagent (CAR) was shown to improve detection of tertiary amines in solution with 2.5 to 15 times greater sensitivity than conventional Dragendorff reagent[185]. In an attempt to develop a complete TLC testing strategy for a mixture of heroin, quinine, and maltose, a methanol-chloroform-ammonia mixture was added to the aqueous drug solution and extracted. The TLC plate was spotted with both extracts before development[186].

TLC has also been employed to improve the effectiveness of the cobalt thiocyanate colour test reagent. Haddoub *et al.*[79] pre-coated TLC plates with glycerol/cobalt thiocyanate (1:1) for an *in situ* colour reaction during development. General TLC systems have been established based on the nature of the drug: basic nitrogenous, acidic and neutral[104].

The chemical similarities between traditional amphetamine-type stimulants (ATS) and NPS were demonstrated in one study that could not achieve good separation between 2,5-dimethoxyphenethylamine analogs, methamphetamine and amphetamine[187]. The 16 cathinones examined in one study showed a range of R_f values and varied colours with ninhydrin. However, mephedrone (4-methylmethcathinone) and methcathinone were indistinguishable[80].

1.6.2.1 *Guidelines and Method Validation*

The use of TLC in the preliminary identification of illicit drugs is governed by certain requirements, as described by the UNODC[70]. All controlled drugs in the group of interest, compounds from natural sources or synthetic preparation, substances commonly found in the matrix, other controlled drugs and mixtures of substances with similar retardation factors are to be analysed in selectivity studies. Analysing a selection of drugs from the target drug group in a variety of commonly occurring matrices at a range of dilutions determines the limit of

detection. It is important to note the use of authentic reference standards run in parallel with the test material.

1.6.3 Commercially available TLC

The commercialisation of TLC plates began in 1965 as convenient, pre-coated plates offering efficiency and accuracy to the technique[181]. Aluminum backed plates are easy to cut, lightweight, preferable for field use, and readily available from many chemical companies.

The legalization of cannabis in an increasing number of jurisdictions has led to THC test kits aimed at "breeders, growers, medical cannabis clubs, and consumers." Cannalytics® is a commercially available TLC test kit that provides at-home analysis of cannabis strains in a quick and convenient device. This validated kit screens for THC and five other cannabinoids, with a reference chart to determine results on THC potency and strain[188].

In 2014, Field Forensics introduced a new product, microTLC™, for field analysis of explosives and drugs[189]. The portable test kit is a self-contained, battery operated unit advertised as a perfect complement to colorimetric testing. In under 5 minutes, a built-in digital camera records the TLC plate image with detection limits reportedly reaching nanogram to picogram scale. Spot.On.ID™ from Field Forensics was developed from microTLC, providing disposable tests of greater analytical power than colorimetric tests and also claims to offer a non-destructive analysis[190].

1.6.4 Current developments in TLC

The modern use of TLC has seen a move toward plate scanning and video imaging to provide greater sensitivity and accuracy while still maintaining a permanent record of the result. Tosato *et al.*[191] used a mobile phone and multivariate analysis to provide quantitative and reliable results on cocaine samples.

Comparison of R_f values and visualisation result is not sufficient enough for confirmation of identity. A number of spectroscopic and spectrometric techniques have been applied to the separated substances on the TLC plate to create successful hyphenated techniques. Natural drug materials have been analyzed using TLC/DESI-MS[192] and TLC-MS [193], however, these

techniques are not suitable for field testing. Incorporation of TLC with techniques already well established for field testing of illicit drugs has included TLC-infrared[194] and TLC-Raman[195].

1.7 Portable spectroscopic analysis

The advances made in forensic laboratory instrumentation technology have profoundly impacted the preliminary identification of illicit drugs. Spectroscopic instruments with high discriminating power traditionally bound to laboratory benchtops have been developed into portable; hand held units ideal for field testing. Increasing caseloads experienced by many police departments has resulted in a need for rapid confirmatory analysis of illicit drugs in the field. Portable spectrometers may provide the ability to identify substances in the field and then also present those findings in court without the need for subsequent laboratory analysis.

Fourier Transform-Infrared (FTIR) and Raman spectroscopy are techniques used in the identification of unknown substances through the interaction of energy with the molecular bonds in a sample. FTIR measures the mid-infrared light absorbed by a vibrating molecule, while Raman measures the energy scattered after excitation of a molecule with a single wavelength laser[196]. Both of these techniques are advantageous in a forensic identification due to their non-destructive nature, and thus ability to preserve evidence[197]. SWGDRUG classifies Raman and IR spectroscopy as category A techniques based on their discriminating power[37].

Chemometrics is an important discipline that can be used in the interpretation of data from spectroscopic techniques. Mathematical and statistical methods are used in the selection of experimental procedures and treatment of data. Roggo *et al.*[198] provides a review of chemometrics as applied to near infrared (NIR) spectroscopy. Commonly used chemometric methods include mathematical pre-treatment of data, classification methods to group samples, and regression methods for quantification of samples.

Portable devices currently available on the market are provided in Table 1-4.

1.7.1 Fourier-Transform Infrared (FT-IR) Spectroscopy

Fourier Transform Infrared (FTIR) spectroscopy has been utilized in forensic laboratories as a confirmatory technique for illicit drug analysis for many years. The universal sampling accessory, Attenuated Total Reflection (ATR) is particularly suitable for drug analysis in the field due to its ease of use, minimal sample preparation and fast acquisition. Eliaerts *et al.*[199] presented ATR-FTIR as a rapid classification and quantification tool for cocaine analysis. Importantly, the instrument use was combined with chemometric data (Support Vector Machines (SVM)) to allow end users without FTIR expertise to better interpret the results. Another study developed automated screening methods to determine the probability of cocaine present in a sample based on eight characteristic vibrational bands[200]. Tsujikawa *et al.*[201] applied data treatment methods to 150 substances analyzed using a portable ATR-FTIR spectrometer; however, only 8 out of 11 forensic samples were positively identified.

The ability of mid-IR spectroscopy to differentiate positional isomers is particularly useful considering the emerging NPS analogues. The aromatic out-of-plane deformation region from 600-100 cm^{-1} was shown to be helpful in distinguishing regioisomers of piperazines[139]. In an analysis of an unknown capsule containing isomers of fluoromethcathinone, unused reagent and caffeine, the ATR-FTIR spectrum was still able to distinguish the isomers in the fingerprint region[202]. However, this was following an acetone wash step.

The use of FTIR for confirmatory analysis in forensic laboratories was demonstrated in the study by the UNODC which found it to be the second most common technique used in the identification of samples, behind GC-MS[107].

Portable FTIR instruments have been made available commercially for several years. The instruments themselves vary in their appearance from handheld devices resembling hair dryers or Game Boy consoles, to portable instrumentation that fits into a suitcase (see Table 1-4). TruDefender™ is a rugged, portable ATR-FTIR device that fits in one hand and operates at temperatures between -20 °C and 40 °C[203]. A key feature is the ability to send results wirelessly via email or SMS directly to a mobile phone or computer.

The detection of hallucinogenic NPS, 2,5-dimethoxy-substituted phenethylamines (2C drugs) and their N-2-methoxybenzyl (NBOMe) derivatives was performed using ATR-FTIR with multivariate discriminate analysis successfully, however, the individual NBOMes could not be discriminated[204]. Another study using ATR-FTIR directly on blotter paper without an

extraction step also obtained all positive matches, however, the exact type of NBOMe did not always agree[205].

A common problem encountered with the use of spectroscopic techniques is the overlapping of spectra in the analysis of mixtures of mid to low purity of the particular drug. Monfreda *et al.* [206] showed that cocaine samples in Italy were able to be "fast profiled" using ATR-FTIR and chemometric tools, with prediction errors occurring for purity levels below 50%.

1.7.2 Raman spectroscopy

Raman spectroscopy is gaining widespread use among the forensic community due to its inherent advantages and complementarity with FTIR. A review by Izake[207] demonstrated the usefulness of portable raman spectroscopy to the field of forensic security. The detection of illicit drugs through opaque packaging with Raman spectroscopy is achievable, however, analysis is limited to non-metallic ocntainers and containers that do not excessively fluoresce[208].

Spatially Offset Raman Spectroscopy (SORS) has been shown to be able to detect substances through packaging such as envelopes and plastic bottles with enhanced sensitivity due to a decreased fluorescence[209]. This was further developed by Hargreaves who presented a proof of principle for the analysis of seized drugs in airport environments using portable Raman spectroscopy[210]. The ability to detect potentially illicit substances through packaging is an idyllic situation that would prevent contamination and also sample degradation.

This covert nature of Raman analysis becomes particularly useful when attempting to intercept items suspected to contain illicit materials. One study demonstrated the ease with which the device can detect drugs on fibres and impregnated textiles in 20-25 seconds[211].

Items seized for preliminary testing does not always involve bulk materials, but rather trace amounts. Transparent tapes have been used to collect material from a surface and then folded back over onto itself before analysis using confocal Raman microscopy in a laboratory[212]. Interference from extraneous fibres that are also picked up during the tape lift makes the process of visualising the particles more time consuming for the analyst. This study was not performed using a portable device, however, portable Raman microscopes are now available commercially offering multiple sampling modes and a device resembling a portable sewing machine size[213].

HandyRam™ 785R is a hand-held Raman Spectrometer designed to fit in your pocket and powered by two AA batteries. Point and shoot functions (directly or through plastic or glass) and vial measurements are possible[214]. A recent study that used handheld Raman spectroscopy to analyse NPS samples found the 1064 nm laser improved identification due to the decreased fluorescence seen when compared to the 785 nm. False negatives were due to low NPS amounts or complex chemical composition of the sample[215].

In a study funded by the US Department of Justice, portable Raman technology was investigated for routine use in the field and the laboratory[216]. After enhancements, field testing of methamphetamine was shown to be 100% accurate using the ReporteR, however, testing black tar heroin and marijuana was not feasible. Portable Raman devices have been used in detection of mephedrone[217] and discrimination of cathinone regioisomers[27].

A handheld analyser incorporating dual technologies: FTIR and Raman, has been developed[218]. The Gemini Analyzer is aimed toward the first responders and military personnel for chemical and explosive identification. This combined approach allows for the full capability of the complementary techniques to be realised.

Table 1-4. Selection of companies producing commercial portable spectroscopy instruments for analysis of illicit substances in the field

Company	**Device name**	**Technology**	**Use**	**Reference**
ThermoFisher Scientific	FirstDefender ™ RMX	Raman	Point and shoot	[219]
	TruDefender™ FT and TruDefender FTi	ATR-FTIR	Close contact to sample	[203]
	Gemini™ Analyzer	Raman ATR-FTIR	Raman probe for point and shoot. Automated anvil for close contact ATR-FTIR	[218]

	TruNarc™	Raman	Point and shoot	[220]
Agilent Technologies	4300 Handheld FTIR	FTIR	Close contact to sample	[221]
	4500A Forensics Analyzer	ATR-FTIR	Anvil for close contact with sample	[222]
Rigaku Analytical Devices	Progeny™ ResQ™	Raman	Point and shoot	[223]
Smiths Detection	Target-ID	ATR-FTIR	Anvil for close contact with sample	[224]
	ACE-ID	Raman	Point and shoot	[225]
B&W TEK	TacticID®-N	Raman	Point and shoot	[226]
Innovative Analytical Solutions	ReporteR	Raman	Point and shoot	[227]

1.8 Optical detection methods

The demand for rapid, easy to use, cost effective and reliable presumptive identification tests is still high, particularly with the growing number of NPS samples being received. However, it is clear that traditional chemical colour spot tests are not the only option. Inevitable advances in technology have opened up new areas of detection that are not yet employed for illicit drug screening. Fundamentally, molecular sensing devices require a molecular recognition unit to interact with the target in a highly selective manner and the transformation of a signal from the binding event into a visual or measurable response of a reporter [228]. Fluorescent and colorimetric based sensors are desirable due to their simple detection procedures.

1.9 Molecular recognition

1.9.1 Selective chemical reactions

A chemical colour test is the result of a chemical reaction selective to a drug class of interest resulting in a colour change. Few analytes undergo convenient chromogenic reactions[229], however, by modifying a chemical reaction selective for cathinones via labelling or through multiple reactions, it is possible to create the appearance of a chromogenic reaction. Further, the use of these reactions can be employed in surface functionalization of fluorescent reporting nanoparticles.

The cathinone drug class possesses a chemically distinct functional group that distinguishes it from other compounds, in particular, amphetamines. The carbonyl functional group provides a starting point to consider reactions that can take place. The presence of the keto-functionality has been reported to make cathinones prone to racemisation and dimerization[16]. A number of well-known reactions occur at carbonyl groups of ketones and aldehydes[230] and may provide the selective reaction necessary for incorporation into a screening test.

1.9.1.1 *Imines and Enamines*

Figure 1-9. Reaction equation for the formation of an imine from a ketone

A well-known addition reaction of carbonyl containing compounds with primary and secondary amines forms imines (see Figure 1-9) and enamines, respectively. These products are called Schiff bases, and the conditions for preparation are wide ranging and determinant of the reactants.

The formation of the Schiff base occurs in two steps. The first is the nucleophilic attack on the carbonyl carbon atom forming a carbinol amine. The second step sees the dehydration of the carbinol amine under mild acidic conditions and the formation of the imine [231].

The electron withdrawing group attached to the amine will decrease the electron density of the NH_2 nitrogen atom and decrease its capacity for a nucleophilic attack. Conversely, the presence of an electron donating group attached to the amine will increase Schiff base formation. The electrophilic character of the carbonyl carbon also plays an important role. The more electrophilic the carbon is (increased by electron withdrawing group), the faster the Schiff base formation will occur[231].

Thorat *et al.* describe the condensation of the carbonyl group moiety present in vanillin with various primary and secondary aliphatic and aromatic amines in excess to form the imine with around 80-85% yield [231].

The synthesis of enamines has been shown by the acid catalysed condensation of silylamines with ketones at room temperature[232]. This work was particularly interesting as it allowed for the preparation of dimethylaminoenamines which are inherently difficult due to the high volatility of dimethylamine. This method holds several advantages: water removal no longer necessary and no heating or solvent required. However, the required 24 h at room temperature is far too long when considering developing rapid screening tests.

Early research by Taguchi *et al.* describes the convenient preparation of enamines by a mild reaction in the presence of molecular sieves. It is proposed that the molecular sieves act as a dehydrating agent and catalyst [233]. These claims are refuted by Roelofsen *et al.* who puts the catalytic effect of molecular sieves down to the binding agent present in sieves, and instead propose the combination of molecular sieve powder with an added catalyst of silica-alumina (commercial cracking catalyst) gives far greater yields and faster reaction rates[234].

A Tetrahedron report from 1985 outlines the removal of water from the reaction by a Dean Stark head, molecular sieve or chemically inert drying agent while refluxing in a suitable solvent such as benzene[235]. Solvent free synthesis of enamines is achieved by Varma *et al.* using Montmorillonite K10 clay as a catalyst under microwave irradiation[236].

A recent article by Prashanth[237] describes the spectrophotometric determination of an antimigraine drug, zolmitriptan (ZMT) by the coloured product forming on reaction with vanillin in the presence of sulphuric acid. The authors describe the formation of an enamine due to condensation of the secondary amine group in ZMT and the aldehyde group of vanillin. This simple, cost effective and rapid determination proved superior to existing spectrophotometric methods.

1.9.1.2 *Hydrazones*

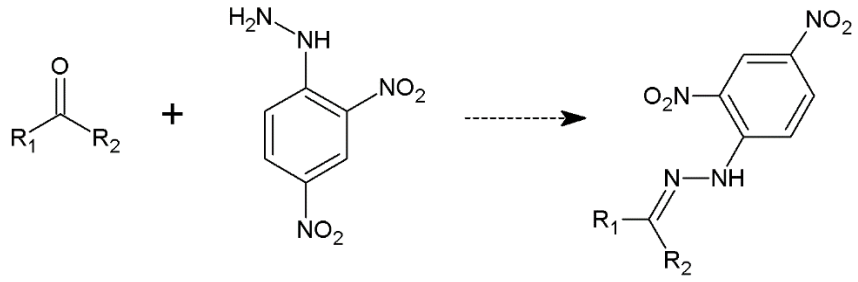

Figure 1-10. Reaction equation for the formation of a hydrazone derivative from a ketone

Hydrazones are the product of a reaction between aldehydes or ketones and a hydrazine (see Figure 1-10). They are a special type of Schiff base employing nucleophilic hydrazine in place of the amine [238].

A popular hydrazine used in the spectrophotometric determination of carbonyl compounds is 2,4-dinitrophenylhydrazine (DNPH), also called Brady's Reagent. In the presence of sulphuric acid, this hydrazine reacts to produce red or yellow crystalline condensation products. The determined melting points of these formed hydrazones can subsequently help in identification of the original carbonyl compound[239]. Thorat *et al.* synthesised 5 different hydrazones from vanillin with 70-80% yield using a range of aromatic hydrazines by dissolving the carbonyl compound in methanol and adding a slight excess of hydrazine with acetic acid catalyst before refluxing[231]. Microwave irradiation and potassium carbonate has also been used in the preparation of hydrazones[240].

1.9.1.3 *Oximes*

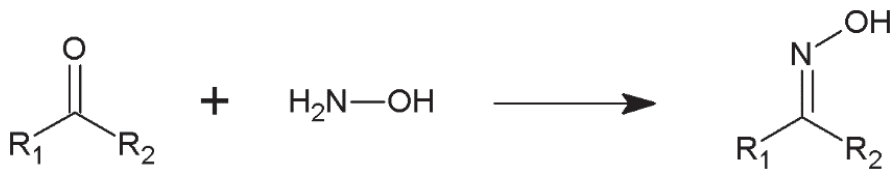

Figure 1-11. Reaction equation for the formation of an oxime from a ketone

The reaction of carbonyl containing compounds with hydroxylamine leads to the formation of oximes (see Figure 1-10). An exhaustive list of reaction conditions have been employed in the formation of oximes.

Common themes in the preparation of these compounds include the use of microwave irradiation [240-242], mechanochemical synthesis routes typically involving simple grinding with a mortar and pestle[243-246], and the use of silica gel as a reagent affording rapid results with high yield[241, 247, 248].

Other typical reagents that accompanied hydroxylamine HCl included bismuth oxide[244], aluminium oxide[242], sodium acetate[249], Amberlyst A-21[250], potassium carbonate[246], calcium oxide[251], zinc oxide[252], and glycine[253].

The use of iron(III) chloride[254] and and Dowex 50x ion exchange resin[255] were also used to show regioselective synthesis.

1.9.1.4 *Semicarbazones*

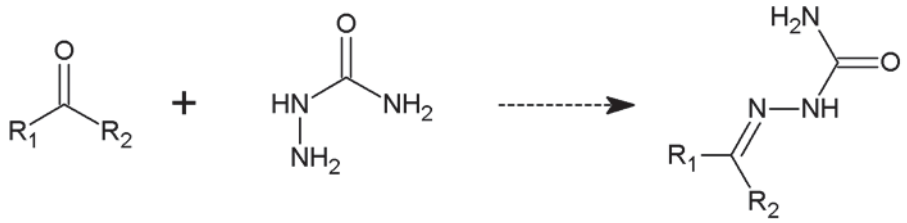

Figure 1-12. Reaction equation for the formation of a semicarbazone from a ketone

Analogous to the formation of oximes, the synthesis of semicarbazones follows the reaction of corresponding semicarbazide with a carbonyl containing compound (see Figure 1-12). Vijayan reports synthesis by dissolving semicarbazide, sodium acetate and the carbonyl compound in ethanol and gently warming the solution[256]. Alternatively, the use of microwave irradiation and potassium carbonate has been described[240].

1.9.1.5 *Chelation in Transition Metal Complexes*

The formation of transition metal complexes can give rise to brilliantly coloured compounds due to the d-d electron transitions. Ligands containing donor atoms in the right orientation are capable of binding to the metal ion centre.

The ligand, 2,9-dimethyl-1,10-phenanthroline (neocuproine) is a conjugated heterocyclic ring system with two nitrogen atoms capable of binding. The chelation of copper(II) ions with neocuproine occurs readily owing to the stability provided by the large, rigid ligands. In the presence of a reductant, the copper(II) ions are reduced to copper(I), forming a yellow-orange coloured complex.

This chemical assay has been used or decades; spectrophotometric determinations of a number of analytes, including reducing sugars in wine [257], hydrazines [258], sulphide and sulphite [259], glutathione [260], explosive residues [261] and ascorbic acid [262] have been described.

This reduction-oxidation process has also been described in several research papers in the measurement of antioxidant capacity of certain compounds or matrices [263, 264]. Apak *et al.* named this the 'cupric reducing antioxidant capacity' (CUPRAC) method [265].

Distinct differences between reported neocuproine reduction conditions include solvent systems, pH range and buffer, source of copper(II) ions and addition of neocuproine following reduction of the copper or beforehand.

An experiment performed by Al-Obaid *et al.* used the copper(II)-neocuproine complex to determine quantitatively, the amount of cathinone in khat leaves [266]. Despite the simplicity, high sensitivity and ease of the reaction, the authors do not describe the reaction occurring, except to say that the copper(II)-neocuproine is reduced to copper(I)-neocuproine. The chemical structure of the product formed after oxidation of the cathinone is not described. This lack of information regarding the reaction mechanism was found in a number of papers using the complex as a spectrophotometric reagent [262, 267-269].

This assay has also been used in the reverse as a method for determining the amount of copper present [270].

An interesting article by Zuhri *et al.* develops a spectrophotometric method for determining ampicillin at pH 5 in an acetate buffer containing copper(II)-neocuproine [269]. The yellow

complex that forms is measured at 446 nm. Again, the reaction mechanism is not explained; however, the proposal suggests the involvement of ampicillin in the complex.

1.9.1.6 *Reduction Reactions*

The reduction of the carbonyl group in an aldehyde or ketone involves two electrons (and two protons) per molecule to produce a primary or secondary alcohol [271]. There are numerous methods for the reduction of organic compounds. The most well-known are the metal hydrides [272], however, a survey of the literature revealed the reduction of carbonyl compounds using transition metal catalysts [273, 274], low valent titanium reagents [275], samarium iodide [276], trichlorosilane [277], diisobutylaluminium hydride [278] and Grignard reagents [279].

The reactions used to replace the carbonyl group in the compound with a hydroxyl group have the potential to be further utilised in a Chen-Kao test, which is currently employed to detect pseudoephedrine, an aminoalcohol, via formation of the coloured copper complex [69].

A reaction that requires the use of a catalyst can be performed using a chemical catalyst or a biocatalyst. The use of biocatalysts affords a number of advantages over typical chemical catalysts. In addition to being environmentally friendly, biocatalysts are selective and easy to handle. They are also particularly of use when stereoselective processes are required [280].

A great number of reactions are catalysed by microorganisms. A report by Borges *et al.* [281] reviewed the use of fungi as biocatalysts in Baeyer-villiger oxidations and ketone reductions. Advantages include: high stereoselectivity and regioselectivity, and the ability to be carried out at ambient temperature and atmospheric pressure. Particular strains of fungi were selected as the most effective for reducing carbonyl compounds. The enzyme availability and stability must be considered.

In the growing literature on biocatalysis aimed at chemists, it is clear there is a potential for exploitation of these natural enzymes in performing organic reactions. An honours thesis from 2011 described the use of pea plants in the biocatalytic reduction of ketones [282]. Substituted acetophenone compounds have also been successfully reduced using Baker's yeast [283].

Alcohol dehydrogenases (ADHs) are a large family of enzymes involved in the reduction of carbonyl groups to their corresponding hydroxyl groups. ADHs can be obtained from a range of

microorganisms; from bacteria to mammals. For example, several species of yeast (Saccharomyces cerevisiae, Sporobolomyces salmonicolor) and bacteria (gluconobacter oxydans and Lactobacillus brevis) contain ADHs [284].

An excellent review of enzyme catalysis reactions is detailed by Laird [285]. The process of reduction via an enzyme catalyst employs a cofactor as a reducing agent (NADH or NADPH). Due to the expensive nature of these reducing agents, the ketone reduction is coupled to a second process to allow for the regeneration of the reducing agent. This is typically the oxidation of a small molecule.

1.9.2 Molecularly Imprinted Polymers (MIPs)

These highly cross-linked porous-rich polymers are regarded as artificial antibodies with highly specific recognition sites situated within the polymer. Their use in the selective enrichment or capture of drug analytes could potentially be employed in the development of an optical screening test.

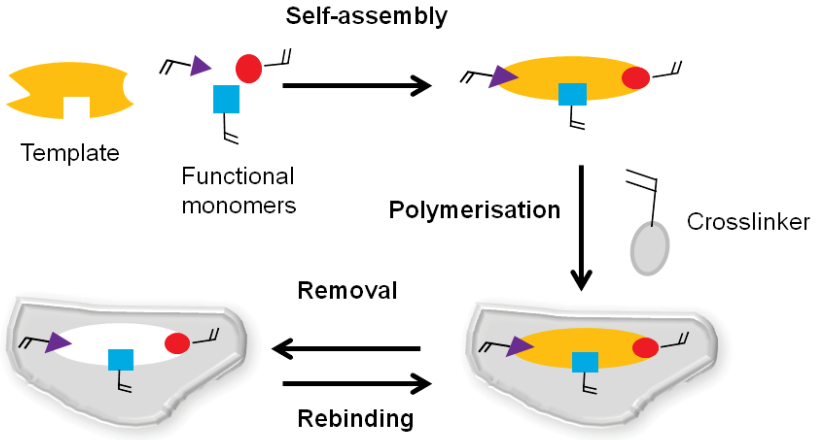

Figure 1-13. Schematic of the preparation process of molecularly imprinted polymers

The process to prepare an imprinted polymer is relatively simple: monomers, crosslinkers, initiator and 'template' or target analyte are dissolved in a suitable solvent and polymerisation via ultraviolet light curing and/or heating fixes the template-monomer reactions inside the crosslinked polymer matrix. The final wash step removes the template species, revealing a 'template' imprint inside the polymer, structurally analogous to the target molecule [286] (see

Figure 1-13). The monomer provides functional groups to form interactions with the template, while the crosslinker fixes the monomers around the template [287].

A number of reviews are available with detailed information regarding most recent uses of MIPHs in small molecule detection [288, 289]. In an extensive review, Li *et al.* describe the balance of cross-linker to monomer required to ensure the imprint is defined, but not too cross-linked so that the template molecules cannot diffuse into the binding sites [286].

Gholivand *et al.* take a sophisticated approach using computationally designed polymers to provide the most effective combination of template, solvent and monomer [290] and MIP sorbent assays have been developed [291]. McCluskey *et al.* identify the advantageous opportunities of MIPs for use in small molecule detection [292] and Poma *et al.* discuss the use of MIP nanoparticles with an inherently larger surface area allowing the cavities to be more accessible by the templates [293].

1.10 Visual signals

Luminescence is the spontaneous emission of radiation from an electronically excited species or from a vibrationally excited species not in thermal equilibrium with its environment [294].

An ideal detection system for screening illicit drugs would see the emission of a specific coloured light when the drug of interest is present. This idea can be realised with the use of luminescent materials.

1.10.1 Types of luminescence

The mode of excitation determines the type of luminescence. There are numerous forms of energy that can cause the electronic states of molecules to be excited, and as such there are a number of types of luminescence. These include: photoluminescence, chemiluminescence, bioluminescence, electroluminescence, cathodoluminescence, sonoluminescence and radioluminescence [294].

Photoluminescence is the phenomenon displayed when a species is excited by the absorption of one or more photons of light. It encompasses fluorescence, phosphorescence and delayed fluorescence.

Chemiluminescence is exhibited when the absorbing species is excited by a chemical reaction and subsequently emits photons. The reaction of luminol and a strong oxidiser in the presence of sensitisers such as iron is a classic example that produces a strong blue emission [295]. Chemiluminescence holds an advantage over fluorescence, as an external light source is not required.

1.10.2 Förster Resonance Energy Transfer (FRET)

FRET is an important phenomenon associated with the transfer of energy from an excited fluorophore (donor) to another molecule (acceptor). The donor and acceptor molecule do not have to be different molecules, termed homoFRET, and the acceptor is not necessarily fluorescent, referred to as a 'dark receptor' [296].

FRET is a useful tool to study reactions in which the basic information obtained is whether or not two molecules are close to each other and whether or not that changes as a result of a process.

The energy level diagram in Figure 1-14 shows how this process occurs. The energy difference for a deactivation process in an excited fluorophore donor (D*) matches an absorption transition in a nearby acceptor molecule (A). With sufficient energetic coupling, both these processes may occur simultaneously, resulting in transfer of excitation from donor to acceptor [296].

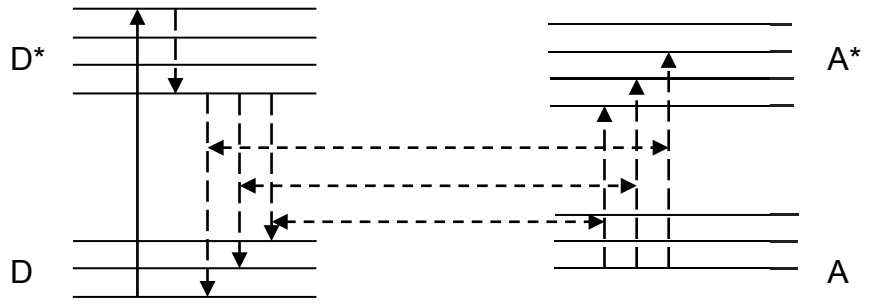

Figure 1-14. Simplified energy level diagram illustrating FRET between an excited donor fluorophore (D*) and an acceptor molecule (A). Horizontal arrows demonstrate coupled transitions

The overlap in donor emission and acceptor absorption provides for an optimal FRET pair able to be used in fluorescence reporting. The spectrum of a FRET pair is given in Figure 1-15.

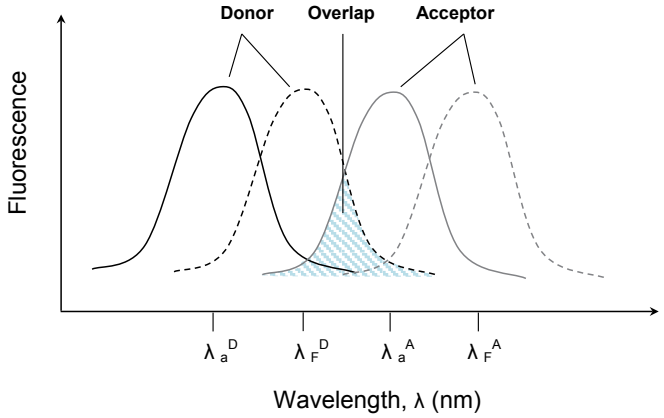

Figure 1-15. Absorption and emission spectra of two fluorophores exhibiting FRET. The shaded area demonstrates the overlap of donor emission and acceptor absorbance

1.10.3 Fluorescence quenching

Quenching is the reduction in fluorescence intensity due to chemical and/or physical processes. This process is particularly useful for probe development, with several types of quenching available, including: contact of fluorophore with another molecule, energy transfer, charge transfer and photochemical [297].

An excited fluorophore making contact with another molecule or atom can facilitate non-radiative transitions to the ground state. This process is termed collisional quenching, and common quenchers include, molecular oxygen, iodide, and acrylamide. Static quenching occurs when a fluorophore non-fluorescent in its ground state, forms a stable complex with another molecule in the ground state [297].

1.10.4 Luminescence reporters

A target compound can be studied directly if it is naturally luminescent; however, most common drugs of abuse are not: in particular, the synthetic cathinones. Therefore, indirect methods for the analysis of such molecules are employed. A great variety of fluorescent and luminescent materials are available to implement as the response units in sensing technologies.

1.10.4.1 *Fluorophores/fluorescent dyes*

Organic dyes are the most commonly used molecules as reporters in fluorescence sensing owing to their availability, low price and versatility [298]. Fluorescence characteristics are dependent on the nature and chemical structure of the fluorescent species.

Core chemical groups on which these organic dyes are based include: xanthene, naphthalene, cyanine, 4,4-difluoro-4-bora-3a,4a-diaza-s-indacene (BODIPY), 4-nitro-2,1,3,-benzoxadiazole (NBD) and coumarin [299].

There is an abundance of information available regarding the use, application and supply of fluorescent dyes. There are a number of factors that need to be considered when selecting a dye: optimal excitation and emission wavelengths, Stokes shift, fluorescence lifetime, photostability and solubility. Dyes can be categorised based on their suitability to a certain function. For instance, fluoresceins, rhodamines, Alexa dyes and BODIPY dyes (see Figure 1-16) are used in labelling experiments in which a responsive function is not needed [298].

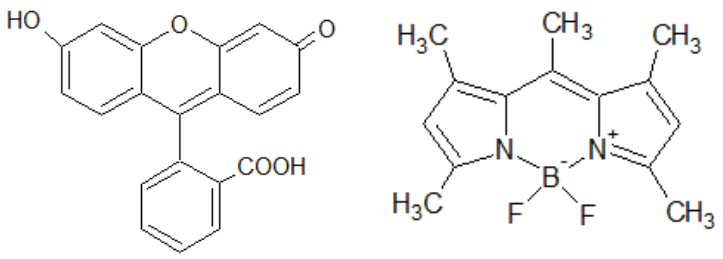

A **B**

Figure 1-16. Structure of organic dyes: fluorescein (A) and BODIPY parent fluorophore (B)

Zhai *et al.* have recently developed a fluorescent sensor for the detection of the date rape drug, GHB. It is based on a fluorescence quenching property using the dye, GHB Orange, a BODIPY compound [300]. This work follows on from previous studies by Zhai *et al.* in the development of a fluorescent sensor for the related date rape drug, GBL, which allows fluorescence of orange light following excitement with a green laser if the drug is present. The GBL disassembles the Green Date fluorescent dye molecules and turns the fluorescence on [301]. Zhai *et al.* initially screened 5120 dyes before arriving at the most responsive and reproducible compound for the detection of GBL by change in fluorescence intensity [301]. These are two straightforward applications of the use of fluorescent dyes in drug detection.

1.10.4.2 *Photonic crystals*

Photonic crystals are periodic dielectric structures possessing a band gap that forbids propagation of a certain light frequency. These engineered optical media have well defined physical properties, superior sensitivity and emission in the visible range of the spectrum which enable their use as sensors [289].

In inverse opals, the regular modulation is imparted by a periodic lattice of voids which are formed by dissolving closely packed PMMA in the last step of the synthesis. MacLeod was able to demonstrate control of the colour of the crystal by varying the spacing of the voids (or size of PMMA spheres) [302].

The controlled growth of spherical silica particles of uniform size was demonstrated by Stober *et al.* in 1967 and has since been the standard method followed for synthesis of the crystal colloids [303].

Walker *et al.* developed a polymerised crystalline colloidal array (PCCA) photonic crystal sensing material able to detect organophophorous compound, parathion, in aqueous solutions using the enzyme acetylcholinesterase as the molecular recognition unit. The irreversible binding of the target compound with the enzyme created a charged species which creates a Donnan potential and leads to the swelling of the hydrogel network [304]. This swelling causes the lattice spacings to shift, and a Bragg diffraction of visible light. A similar study was able to develop a kinase biosensor using a hydrogel network [305].

1.10.4.3 *Quantum dots (QDs)*

Emerging as a new class of fluorescence reporters, quantum dots (QDs) are luminescent nanoparticles with unique properties including efficient absorption and emission of light in the visible region. The small size of these semiconductor particles (core size of 2-10nm) confines the electrons in all spatial directions leading to an effect called ‘quantum confinement’.

The popularity of the quantum dot in imaging and sensor technology is owed to its inherent desirable properties. High quantum yields, excellent photostability, broad absorption wavelength range narrow emission spectrum, and size tunable absorption and emission dependent on particle size and composition. Decreasing the size of the quantum dot leads to a hypsochromic shift [306].

The structure of most quantum dots is based around a crystalline CdSe (or CdTe) core which is coated with a shell of a few atomic layers of a material with a larger band gap, e.g. ZnS, to form the core-shell structure. In addition, coatings can be added to facilitate solubility in aqueous media, e.g. glutathione groups. The core-shell coating improves quantum yield and stability and prevents leaching of metal ions [306].

Surface functionalization of QDs is a technique of particular interest that allows conjugation with other molecules. Particular functional groups are able to be attached onto the surface and used to react with a target analyte, organic dye or other recognition event. Kyeong *et al.* developed a label free and multiplexed detection method for biological molecules by coating QD assembled silica nanoparticles with a polydiacetylene supramolecule [307]. Studies have shown that surface ligand chemistry can have a pronounced effect on particle size [308].

Applications can utilise FRET in the detection of analytes via specific binding that brings the QD in closer proximity to the acceptor. QD bioconjugates have been used in a homogenous assay to determine proteolytic activity [309]

Toxicity is an obstacle for *in vivo* application (bio imaging), while the complex water solubilisation and fluorescence intermittency is a problem for in vitro application. In addition, the availability of materials and instrumentations limits the use of this detection method. In comparison to organic fluorophores, QDs offer greater stability, narrower emission bands and consequently, the potential for use in multiplexing [310].

1.10.4.4 *Upconversion Luminescent Nanoparticles (UCLNP)*

Current imaging and assay technology is based on organic fluorophores and QDs that utilise down-conversion emission. That is, the fluorescent species absorbs light of a particular energy and emits light of a lower energy.

It has been found that solid materials doped with lanthanides show an unconventional anti-stokes emission, meaning that the emission radiation energy is greater than the excitation energy. This photon upconversion process is capable of converting incident NIR energy into visible light [311].

Inherent properties, including weak background fluorescence, long temporal resolution and high resistance to photobleaching that has afforded these upconverting nanocrystals an

advantage over fluorescent dyes and quantum dots. As a result, the past decade has seen a great influx in the coverage of these particles and applications for their wider use. The use of time-gated luminescence has been demonstrated, effectively allowing for a background free condition [312].

The majority of research utilising upconversion nanoparticles is focused on biomedical imaging and drug delivery applications due to advantageous large penetration depth, no autofluorescence from tissues and multimodality imaging [313].

The solid host material is typically an oxide or fluoride nanoparticle (Y2O3 or NaYF4) doped with rare earth elements. These dopant ions are ytterbium (Yb3+) sensitiser ions that absorb energy for transfer to the activator ions such as erbium (Er3+), thulium (Tm3+) or holmium (Ho3+), which subsequently emit the desired energy [310].

A number of processes exist to explain this upconversion. The main three types of upconversion processes are a) excited state absorption, b) energy transfer upconversion on a single type of ion, and c) sensitised energy transfer upconversion where two types of ions are involved: a sensitizer to absorb excitation radiation, and an acceptor ion capable of upconversion following energy transfer [311, 314].

1.11 Molecularly Imprinted Photonic Hydrogels (MIPHs)

The principal governing the use of MIPHs is the swelling of the hydrogel following incorporation of the target analyte into the imprinted binding sites. This swelling is accompanied by a change in colour due to a change in the Bragg diffraction of ordered macropore arrays [315]. This method of detection has been successfully employed as a fast screening method for the detection of ketamine [316] and atropine [317], and also in the chiral recognition of L-Dopa [318].

Zhao *et al.* report the novel use of molecularly imprinted polymer beads (MIPBs) with photonic crystal structure. This technique would provide for multiplexing capabilities able to detect more than 30 kinds of molecules using label free detection [319].

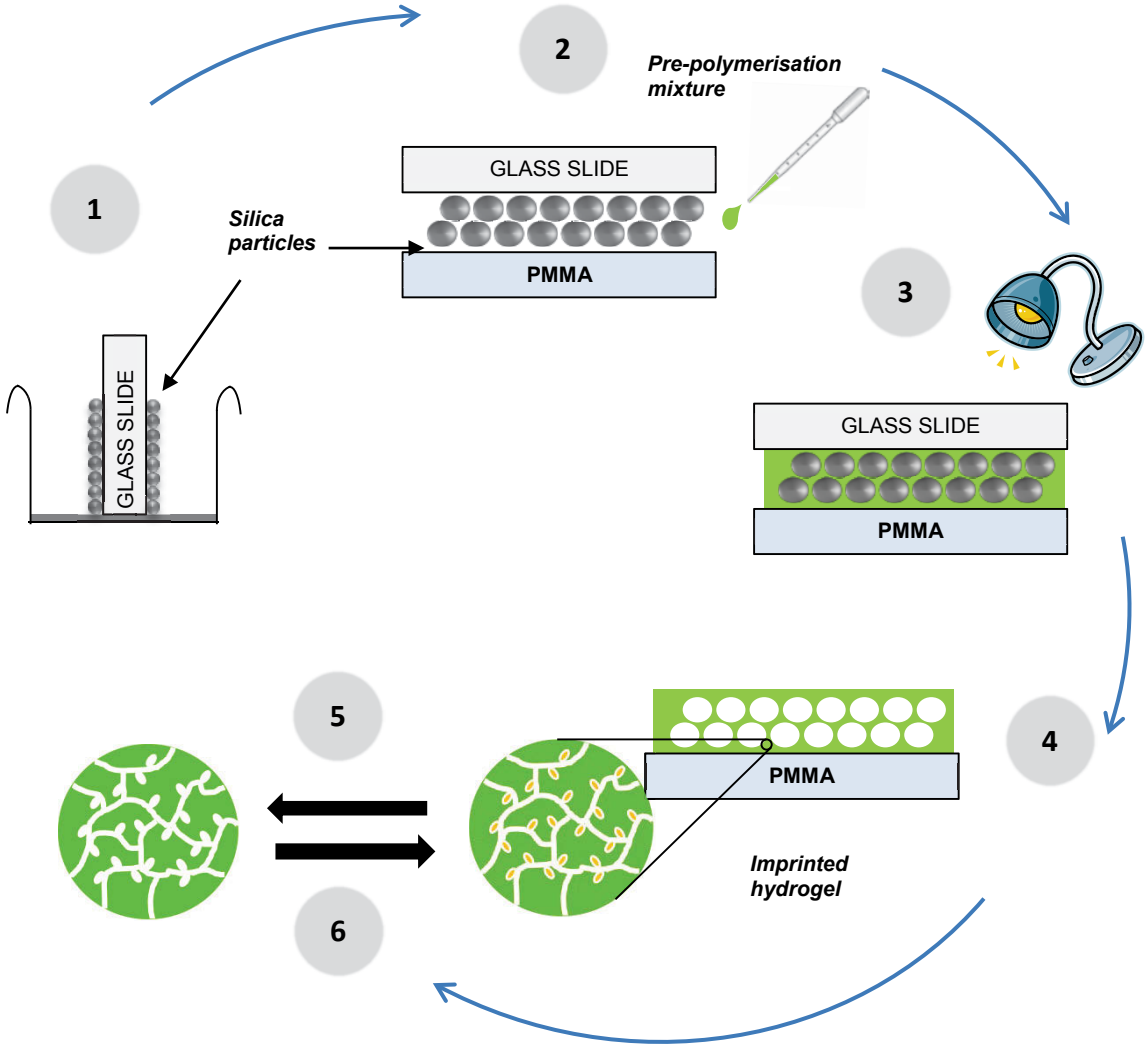

Figure 1-17. Schematic representation of the preparation of molecularly imprinted photonic hydrogels (MIPHs)

1.12 Significance of presumptive screening tests

The preliminary identification of illicit drugs is a crucial component of forensic drug testing that provides rapid information at points of seizure. A positive presumptive test is probable cause for arrest and search warrants. In addition, these preliminary identifications can also impact the judicial system by provoking early pleas from defendants before evidence has been analysed by a forensic laboratory. In September 2013, a presumptive testing trial was started in NSW, Australia which provided that less than trafficable quantities of drugs need to be analysed by FASS only where the drugs are in dispute. The accused can decide to plead based

on the presumptive testing results. In 2016, this trial was codified, and included a new safeguard allowing the accused to seek a second independent drug analysis[320]. Presumptive testing is much less time consuming and can issue a certificate within a four week time frame. The typical turnaround from forensic drug laboratories in Australia is between 3 to 4 weeks.

From commonly employed chemical colour testing to developments in portable spectroscopic instruments and optical screening methods, the ability to analyse substances at the scene is crucial.

1.13 References

1. United Nations Office on Drugs and Crime (UNODC), *NPS: New Psychoactive Substances*, in *Leaflet*. 2016, United Nations.
2. Laboratory and Scientific Section, *The Challenge of new psychoactive substances*. 2013, United Nations Office on Drugs and Crime (UNODC): Vienna, Austria. p. 108.
3. United Nations Office on Drugs and Crime (UNODC), *World Drug Report*. 2017, United Nations publication: Vienna.
4. Commission on Narcotic Drugs, *New psychoactive substances: overview of trends, challenges and legal approaches* 2016, United Nations Office on Drugs and Crime (UNODC): Vienna.
5. Helander, A., *et al.*, *Detection of new psychoactive substance use among emergency room patients: results from the Swedish STRIDA project.* Forensic science international, 2014. **243**: p. 23-29.
6. Elliott, S. and J. Evans, *A 3-year review of new psychoactive substances in casework.* Forensic science international, 2014. **243**: p. 55-60.
7. den Hollander, B., *et al.*, *Long-term cognitive and neurochemical effects of "bath salt" designer drugs methylone and mephedrone.* Pharmacology Biochemistry and Behavior, 2013. **103**(3): p. 501-509.
8. Nic Daeid, N., *et al.*, *Development of gas chromatography–mass spectrometry (GC–MS) and other rapid screening methods for the analysis of 16 'legal high' cathinone derivatives.* Science & Justice, 2014. **54**(1): p. 22-31.
9. United States Drug Enforcement Administration, *Khat*, in *[Fact Sheet]*. December 2011: Springfield.
10. Rosenbaum, C.D., S.P. Carreiro, and K.M. Babu, *Here Today, Gone Tomorrow. and Back Again? A Review of Herbal Marijuana Alternatives (K2, Spice), Synthetic Cathinones (Bath Salts), Kratom, Salvia divinorum, Methoxetamine, and Piperazines.* Journal of Medical Toxicology, 2012. **8**(1): p. 15-32.
11. Palmer, N., *Khat leaves*, in *https://creativecommons.org/licenses/by-sa/4.0/legalcode*, 5366725069_0bfa08d363_b, Editor. 2010, The International Center for Tropical Agriculture (CIAT): Flickr.
12. Expert Advisory Committee on Drugs (EACD), *Methcathinone*. 2002, National New Zealand Drug Policy.
13. Young, A.C., *et al.*, *Two cases of disseminated intravascular coagulation due to "bath salts" resulting in fatalities, with laboratory confirmation.* The American Journal of Emergency Medicine, 2013. **31**(2): p. 445.e3-445.e5.

14. National Drug Intelligence Centre (NDIC), *Synthetic Cathinones (Bath Salts): An Emerging Domestic Threat*. 2011, US Department of Justice.
15. Van Hout, M.C. and R. Brennan, *'Heads held high': An exploratory study of legal highs in pre-legislation Ireland.* Journal of Ethnicity in Substance Abuse, 2011. **10**(3): p. 256-272.
16. Lewin, A.H., *et al.*, *Emergence and properties of spice and bath salts: A medicinal chemistry perspective.* Life Sciences, 2014. **97**(1): p. 9-19.
17. Berrang, B.D., A.H. Lewin, and F.I. Carroll, *Enantiomeric .alpha.-aminopropiophenones (cathinone): preparation and investigation.* The Journal of Organic Chemistry, 1982. **47**(13): p. 2643-2647.
18. Kerrigan, S., *et al.*, *Thermal Degradation of Synthetic Cathinones: Implications for Forensic Toxicology.* Journal of Analytical Toxicology, 2016. **40**(1): p. 1-11.
19. Glicksberg, L. and S. Kerrigan, *Stability of Synthetic Cathinones in Blood.* J Anal Toxicol, 2017. **41**(9): p. 711-719.
20. Glicksberg, L. and S. Kerrigan, *Stability of Synthetic Cathinones in Urine.* J Anal Toxicol, 2017: p. 1-11.
21. Alsenedi, K.A. and C. Morrison, *Comparison of six derivatizing agents for the determination of nine synthetic cathinones using gas chromatography-mass spectrometry.* Analytical Methods, 2017. **9**(18): p. 2732-2743.
22. Smolianitski, E., E. Wolf, and J. Almog, *Proactive forensic science: a novel class of cathinone precursors.* Forensic Sci Int, 2014. **242**: p. 219-227.
23. Paillet-Loilier, M., *et al.*, *Emerging drugs of abuse: current perspectives on substituted cathinones.* Subst Abuse Rehabil, 2014. **5**: p. 37-52.
24. Davies, S. and J. Ramsey, *Drug Monograph: Analytical profiles of the beta keto amphetamines (bkMDMA, bkMDEA, and bkMBDB)*. 2008, London Toxicology Group. p. 1-5.
25. Brandt, S.D., *et al.*, *Analysis of NRG 'legal highs' in the UK: identification and formation of novel cathinones.* Drug Testing and Analysis, 2011. **3**(9): p. 569-575.
26. Lesiak, A.D., *et al.*, *Direct analysis in real time mass spectrometry (DART-MS) of "bath salt" cathinone drug mixtures.* Analyst, 2013. **138**(12): p. 3424-3432.
27. Christie, R., *et al.*, *Discrimination of cathinone regioisomers, sold as 'legal highs', by Raman spectroscopy.* Drug Testing and Analysis, 2014. **6**(7-8): p. 651-657.
28. Zuba, D., P. Adamowicz, and B. Byrska, *Detection of buphedrone in biological and non-biological material – Two case reports.* Forensic Science International, 2013. **227**(1–3): p. 15-20.
29. Concheiro, M., *et al.*, *Simultaneous quantification of 28 synthetic cathinones and metabolites in urine by liquid chromatography-high resolution mass spectrometry.* Analytical and Bioanalytical Chemistry, 2013. **405**(29): p. 9437-9448.
30. Strano Rossi, S., *et al.*, *An analytical approach to the forensic identification of different classes of new psychoactive substances (NPSs) in seized materials.* Rapid Communications in Mass Spectrometry, 2014. **28**(17): p. 1904-1916.
31. Fornal, E., A. Stachniuk, and A. Wojtyla, *LC-Q/TOF mass spectrometry data driven identification and spectroscopic characterisation of a new 3,4-methylenedioxy-N-benzyl cathinone (BMDP).* Journal of Pharmaceutical and Biomedical Analysis, 2013. **72**(0): p. 139-144.
32. Kent, K. and B. Nelson, *Drug Operations*, in *The Practice of Crime Scene Investigation*, J. Robertson, Editor. 2004, CRC Press LLC.
33. United Nations Office on Drugs and Crime (UNODC), *World Drug Report*. 2016, United Nations publication.
34. European Monitoring Centre for Drugs and Drug Addiction (EMCDDA), *European Drug Report 2017: Trends and Developments*. 2017: Luxembourg.

35. Drug Enforcement Administration (DEA), *National Drug Threat Assessment Summary*. 2016, US Department of Justice: USA.
36. Australian Criminal Intelligence Commission (ACIC), *Illicit Drug Data Report 2015-2016*. 2017, Commonwealth of Australia: Canberra.
37. Scientific Working Group for the Analysis of Seized Drugs (SWGDRUG), *SWGDRUG Recommendations Version 7.1*. 2016, United States Department of Justice: USA.
38. Krayem, N., *Presumptive Identification of Commonly Imported Drugs, Precursors and Analogues*, in *Faculty of Science*. 2011, University of Technology Sydney: Sydney. p. 163.
39. United Nations Office on Drugs and Crime (UNODC), *Recommended methods for the identification and analysis of cannabis and cannabis products*. 2009, United Nations: New York.
40. United Nations Office on Drugs and Crime (UNODC), *Recommended Methods for the Identification and Analysis of Cocaine in Seized Materials*. 2012, United Nations: New York.
41. The European Monitoring Centre for Drugs and Drug Addiction (EMCDDA). *Kratom (Mitragyna speciosa) drug profile*. Drug Profiles 2015 [cited 2017 February 1]; Available from: http://www.emcdda.europa.eu/publications/drug-profiles/kratom.
42. The European Monitoring Centre for Drugs and Drug Addiction (EMCDDA). *Salvia divinorum drug profile*. Drug Profiles 2015 [cited 2017 February 1]; Available from: http://www.emcdda.europa.eu/publications/drug-profiles/salvia.
43. The European Monitoring Centre for Drugs and Drug Addiction (EMCDDA). *Khat drug profile*. Drug Profiles 2015 [cited 2017 February 1]; Available from: http://www.emcdda.europa.eu/publications/drug-profiles/khat.
44. The European Monitoring Centre for Drugs and Drug Addiction (EMCDDA). *Hallucinogenic mushrooms drug profile*. Drug Profiles 2015 [cited 2017 February 1]; Available from: http://www.emcdda.europa.eu/publications/drug-profiles/mushrooms.
45. Scott, T.M., J.K. Yeakel, and B.K. Logan, *Identification of mitragynine and O-desmethyltramadol in kratom and legal high products sold online.* Drug Testing and Analysis, 2014. **6**(9): p. 959-963.
46. Zhu, B., L. Meng, and K. Zheng, *Inspection and analysis of mixed drugs recently seized in China.* Forensic Science International, 2014. **242**: p. 44-47.
47. EcstasyData.org. *Test Results*. 2017 [cited 2017 January 4]; Available from: https://www.ecstasydata.org/.
48. Pillreports. *Pillreports Ecstasy Test Results Database*. 2017 [cited 2017 June 7]; Available from: http://www.pillreports.net/index.php.
49. Ornella Corazza, *et al.*, *"Spice," "Kryptonite," "Black Mamba": An Overview of Brand Names and Marketing Strategies of Novel Psychoactive Substances on the Web.* Journal of Psychoactive Drugs, 2014. **46**(4): p. 287-294.
50. Marquis, R., *et al.*, *Drug intelligence based on MDMA tablets data: 2. Physical characteristics profiling.* Forensic Science International, 2008. **178**(1): p. 34-39.
51. Controlled Substances Unit, *Physical Evidence Handbook*, in *Controlled Substances*. 2017, Wisconsin Department of Justice: Wisconsin.
52. Santo, A. *Jolly ranchers, sage and breath mints*. 2015 [cited 2017 July 25]; Available from: https://www.themarshallproject.org/2015/04/02/jolly-ranchers-sage-and-breath-mints#.kbnL7duLZ.
53. Gabrielson, R. and T. Sanders *How a $2 roadside drug test sends innocent people to jail*. The New York Times Magazine, 2016.
54. Elkins, K.M., *et al.*, *Colour quantitation for chemical spot tests for a controlled substances presumptive test database.* Drug Testing and Analysis, 2016. **9**(2): p. 306-310.

55. Choodum, A. and N. Nic Daeid, *Digital image-based colourimetric tests for amphetamine and methylamphetamine.* Drug Testing and Analysis, 2011. **3**(5): p. 277-282.
56. Cuypers, E., A.J. Bonneure, and J. Tytgat, *The use of presumptive color tests for new psychoactive substances.* Drug Testing and Analysis, 2016. **8**(1): p. 136-140.
57. Greenwood, N.N. and A. Earnshaw, *The halogens: Fluorine, chlorine, bromine, iodine and astatine*, in *Chemistry of the Elements*. 1997, Elsevier: University of Leeds, U.K. .
58. Wormley, T.G., *Micro-chemistry of poisons, including their physiological, pathological, and legal relations; with an appendix on the detection and microscopic discrimination of blood: adapted to the use of the medical jurist, physician, and general chemist*. 1885, Philadelphia: J.B. Lippincott Company.
59. Strebinger, *Vorwort.* Mikrochemie, 1923. **1**(1): p. I-IV.
60. Bondi, A., *Editorial.* Israel Journal of Chemistry, 1966. **4**(5-6): p. 166-168.
61. Feigl, F. and V. Anger, *Spot tests in inorganic analysis*. 1972, Amsterdam, The Netherlands: Elsevier Science B.V.
62. Feigl, F. and V. Anger, *Spot tests in organic analysis*. 7th ed. 1966, Amsterdam, The Netherlands: Elsevier Science B.V.
63. Bell, S., *Crime and circumstance: Investigating the history of forensic science*. 2008, Westport: Praeger Publishers.
64. Chen, K.K., *The $CuSO_4$-NaOH test of ephedrine isomers and related compounds.* Journal of the American Pharmaceutical Association, 1929. **18**(2): p. 110-116.
65. Scott, L., *Specific field test for cocaine.* Microgram, 1973. **6**: p. 179-181.
66. Jungreis, E., *Spot test analysis: Clinical, environmental, forensic, and geochemical applications*. 1985: Wiley.
67. Moffat, A.C., *et al.*, *Clarke's analysis of drugs and poisons*. 4th ed. 2011, London, UK: Pharmaceutical Press.
68. National Institute of Standards and Technology (NIST), *Color test reagents/kits for preliminary identification of drugs of abuse*. 2000, National Institute of Justice (NIJ): USA.
69. Kovar, K.-A. and M. Laudszun, *Chemistry and reaction mechanisms of rapid tests for drugs of abuse and precursors chemicals*. 1989, Pharmazeutisches Institut der Universitat Tubingen: Federal Republic of Germany.
70. United Nations Office on Drugs and Crime (UNODC), *Guidance for the validation of analytical methodology and calibration of equipment used for testing of illicit drugs in seized materials and biological specimens*. Laboratory and Scientific Section. 2009, New York: United Nations. 67.
71. Khan, J.I., T.J. Kennedy, and D.R. Christian, *Chemical Screening*, in *Basic Principles of Forensic Chemistry*. 2012, Humana Press: Totowa, NJ. p. 79-90.
72. United Nations International Drug Control Programme, *Rapid testing methods of drugs of abuse*. 1994: New York.
73. B. Widdop, *Colour Tests*, in *Clarke's Analysis of Drugs and Poisons*, A. C. Moffat, *et al.*, Editors. 2011, Pharmaceutical Press: London, U.K.
74. Forrester, D.E., *The duquenois color test for marijuana: Spectroscopic and chemical studies*. 1997: Georgetown University.
75. B. Widdop, *Reagents*, in *Clarke's Analysis of Drugs and Poisons*, A. C. Moffat, *et al.*, Editors. 2011, Pharmaceutical Press: London, U.K.
76. O'Neal, C.L., D.J. Crouch, and A.A. Fatah, *Validation of Twelve Chemical Spot Tests for the Detection of Drugs of Abuse*, in *Encyclopedia of Forensic Sciences*, J.A. Siegel, P.J. Saukko, and M.M. Houck, Editors. 2013, Academic Press: Waltham. p. 380-387.
77. Fraenkl, M., D. Svobodová, and J. Gasparič, *A critical investigation of the liebermann colour test: The formation and behaviour of phenolindophenol in strong acid media.* Microchimica Acta, 1986. **90**(5): p. 367-386.

78. Pavia, D.L., *Introduction to Organic Laboratory Techniques: A Small Scale Approach*. 2005: Thomson Brooks/Cole.
79. Haddoub, R., *et al.*, *Cobalt thiocyanate reagent revisited for cocaine identification on TLC.* New Journal of Chemistry, 2011. **35**(7): p. 1351-1354.
80. United Nations Office on Drugs and Crime (UNODC), *Recommended methods for the identification and analysis of synthetic cathinones in seized materials*. 2015, United Nations: New York.
81. Velapoldi, R.A. and S.A. Wicks, *The use of chemical spot tests kits for the presumptive identification of narcotics and drugs of abuse.* Journal of Forensic Sciences, 1974. **19**(3).
82. Marquis, E., *Über den Verbleib des Morphin im tierischen Organismus*, in *Einer Hochverordnelen Medicinischen Facultat*. 1896, Kaiserlichen Universitat: Jurjew (Dorpat).
83. O'Neal, C.L., D.J. Crouch, and A.A. Fatah, *Validation of twelve chemical spot tests for the detection of drugs of abuse.* Forensic Science International, 2000. **109**(3): p. 189-201.
84. K. E. Toole, *et al. Color Tests for the Preliminary Identification of Methcathinone and Analogues of Methcathinone*. Microgram Journal, 2012. **9**, 27-32.
85. Drug Chemistry Section, *Technical Procedure for Preliminary Color Tests*. 2014, North Carolina Department of Justice (NCDOJ): North Carolina.
86. Wongwiechintana, C., E.M. Holt, and N. Purdie, *Structural identification of a purple product (5,6-dihydro-10-hydroxy-6-methyl-4H-dibenzoquinoline-8,11-dione) of the reaction of Froehde reagent and morphine.* Acta Crystallographica Section C, 1986. **42**(6): p. 685-687.
87. Newton, D.E., *Forensic Chemistry*. 2007: Facts On File, Incorporated.
88. von Bittó, B., *Ueber die Anwendung des Nitroprussidnatriums als Reagens auf Aldehyde und Ketone.* Zeitschrift für analytische Chemie, 1893. **32**(1): p. 347-351.
89. Loach, K.W. and M. Carvalho, *A modified simon-lewin reaction: N-nitrosamines as intermediates in the reaction of secondary amines with nitroprusside and acetaldehyde.* Analytical Letters, 1973. **6**(1): p. 25-29.
90. Allen, W.M., S.J. Hayward, and A. Pinto, *A color test for dehydroisoandrosterone and closely related steroids, of use in the diagnosis of adrenocortical tumors.* The Journal of Clinical Endocrinology, 1950. **10**(1): p. 54-70.
91. Epstein, E., *An aqueous Zimmermann reagent for the determination of 17-ketosteroids.* Clinica Chimica Acta, 1962. **7**(5): p. 735-737.
92. Hasegawa, T. and T. Usui, *Cautionary note regarding the phenol color test by ferric chloride in acidic solution.* Journal of Chemical Education, 1992. **69**(10): p. 840.
93. Soloway, S. and S.H. Wilen, *Improved Ferric Chloride Test for Phenols.* Analytical Chemistry, 1952. **24**(6): p. 979-983.
94. Christian, D., *Forensic Chemistry/Controlled Substances*, in *The Forensic Laboratory Handbook Procedures and Practice*, A. Mozayani and C. Noziglia, Editors. 2011, Humana Press. p. 51-103.
95. Jacobs, A.D. and R.R. Steiner, *Detection of the Duquenois–Levine chromophore in a marijuana sample.* Forensic Science International, 2014. **239**: p. 1-5.
96. Rubiano, C., J. Firmin, and S. Coticone, *The effect of benzene ring substituents on the mechanism of Duquenois Levine (DL) test for cannabinoid detection.* J. Chem. Pharm. Res, 2014. **6**(6): p. 1261-1264.
97. United Nations Office on Drugs and Crime (UNODC), *Rapid testing methods of drugs of abuse*. 1994, United Nations: New York.
98. Levine, B. and S.W. Lewis, *Presumptive Chemical Tests*, in *Encyclopedia of Forensic Sciences*, J.A. Siegel, P.J. Saukko, and M.M. Houck, Editors. 2013, Academic Press: Waltham. p. 616-620.

99. Idaho State Police, *Forensic Laboratory Training Manual*, in *Spot Tests*. 2011: Idaho.
100. Oguri, K., *et al.*, *Specificity and mechanism of the color reaction of cocaine with cobaltous thiocyanate.* Eisei kagaku, 1995. **41**(4): p. 274-279.
101. Lamb, A.C., R.A. Federico-Perez, and Z.-L. Xue, *Product in indole detection by Ehrlich's reagent.* Analytical Biochemistry, 2015. **484**: p. 21-23.
102. Watanabe, K., *et al.*, *A colorimetric method for the determination of cannabinoids with fast blue BB salt.* Eisei kagaku, 1979. **25**(6): p. 321-326.
103. dos Santos, N.A., *et al.*, *Evaluating the selectivity of colorimetric test (Fast Blue BB salt) for the cannabinoids identification in marijuana street samples by UV–Vis, TLC, ESI(+)FT-ICR MS and ESI(+)MS/MS.* Forensic Chemistry, 2016. **1**: p. 13-21.
104. Moffat, A.C., *et al.*, *Thin-Layer Chromatography*, in *Clarke's Analysis of Drugs and Poisons*. 2011 Pharmaceutical Press: London, UK.
105. Zwikker, J., *Het aantonen en het afzonderen van barbitalen bij het toxicologisch onderzoek.* Pharm. Weekbl, 1931. **68**: p. 975.
106. Levi, L. and C.E. Hubley, *Detection and identification of clinically important barbiturates.* Analytical Chemistry, 1956. **28**(10): p. 1591-1605.
107. International Collaborative Exercises (ICE), *Summary Report Seized Materials*. 2016, UNODC: Vienna, Austria.
108. International Collaborative Exercises (ICE), *Summary Report Seized Materials*. 2014, UNODC: Vienna, Austria.
109. International Collaborative Exercises (ICE), *Summary Report Seized Materials*. 2015, UNODC: Vienna, Austria.
110. Laboratory and Scientific Section. *Drug and Precursor Identification Kits*. 2017 [cited 2017 January 10]; Available from: https://www.unodc.org/unodc/en/scientists/druge-kits-new.html.
111. *NARK Presumptive Drug Analysis*. 2016 [cited 2016 November 22]; Available from: http://www.sirchie.com/products/nark-presumptive-drug-analysis.html.
112. MMC International B.V. *Narcotic testing supplies and equipment store*. 2016 [cited 2016 November 22]; Available from: http://shop.narcotictests.com/products/narcotic-field-tests/.
113. *NIK Drug Tests & Kits*. 2016 [cited 2016 November 22]; Available from: http://www.safariland.com/products/forensics/field-drug-tests/nik-drug-tests-and-kits/.
114. *ODV Drug Tests and Kits*. 2016 [cited 2016 November 22]; Available from: http://www.safariland.com/products/forensics/field-drug-tests/odv-drug-tests-and-kits/.
115. *Drug testing kits*. 2016 [cited 2016 November 22]; Available from: http://touchandknowusa.com/products/drug-testing-kits.
116. *Drug Identification Test Kits*. 2016 [cited 2016 November 22]; Available from: http://testkitplus.com/product-category/test-kits/drug-identification-test-kits.
117. *EZ Test kits*. 2016 [cited 2016 November 22]; Available from: http://www.eztestwholesale.com/product-category/ez-test-kits/.
118. *QuickCheck Narcotic Identification (Drug Test) Kits*. 2016 [cited 2016 November 15]; Available from: https://www.lynnpeavey.com/product_info.php?cPath=33_105&products_id=947.
119. Sirchie. *NARK II Fentanyl Reagent*. 2017 [cited 2017 May 5]; Available from: http://www.sirchie.com/nark20033-fentanyl-reagent.html#.WTiijeuGOUk.
120. Chiong, D.M., E. Consuegra-Rodriguez, and J.R. Almirall, *The analysis and identification of steroids.* Journal of Forensic Sciences, 1992. **37**(2): p. 488-502.
121. Colorimetrics. *What's in Your Gear?* 2017 [cited 2017 February 3]; Available from: http://roidtest.com/.

122. LabMax. *Presumptive test for detection and identification of steroids*. 2015 [cited 2017 February 3]; Available from: http://www.labmax.ca/instruction.php.
123. Drink Safe. *Date Rape Test Coaster*. 2015 [cited 2016 November 23]; Available from: http://www.drinksafetech.com/date-rape-test-coaster/.
124. Meyers, J.E. and J.R. Almirall, *A study of the effectiveness of commercially available drink test coasters for the detection of "date rape" drugs in beverages.* J. Anal. Toxicol., 2005. **28**(8): p. 685-688.
125. Abramson, M.T. and J.C. MacDonald, *System and method for detection of a contaminated beverage*, in *Google Patents*. 2015, Drinksavvy Inc.: US.
126. Wade, J.H.C., *et al.*, *Diagnostic testing device for potable liquids*, in *Google Patents*. 2006, Checkmate Organisation Limited: World.
127. Francisco Javier Guerra, Brian Glover, and J.S.T. Mccafferty, *Method for testing a beverage for illicit substances* in *Google Patents*. 2003, Checkmate Organisation Limited: World.
128. Legge, R., *et al.*, *Personal illicit drug detection method*, in *Google Patents*. 2007, Legge, R; Hopson, T; Maracas, G; Bechtel, P: US.
129. Murray, R.A., *et al.*, *Putting an ecstasy test kit to the test: Harm reduction or harm induction?* Pharmacotherapy: The Journal of Human Pharmacology and Drug Therapy, 2003. **23**(10): p. 1238-1244.
130. Harper, L., J. Powell, and E.M. Pijl, *An overview of forensic drug testing methods and their suitability for harm reduction point-of-care services.* Harm Reduction Journal, 2017. **14**(1): p. 52.
131. Pirman, E. *Novel colorimetric drug test for emergent illicit drugs*. 2015; Available from: http://www.wisys.org/news-media/joesph-wu-chuck-cornett.
132. Jaesuk, Y., *et al.*, *A Presumptive Identification of New Psychoactive Substances using Coloring Test.* YAKHAK HOEJI, 2017. **61**(2): p. 65-74.
133. Isaacs, R.C.A., *A structure–reactivity relationship driven approach to the identification of a color test protocol for the presumptive indication of synthetic cannabimimetic drugs of abuse.* Forensic Science International, 2014. **242**: p. 135-141.
134. MMC International B.V. *Narcotic Testing Supplies & Equipment Store*. 2016 [cited 2016 November 22]; Available from: http://shop.narcotictests.com/products/narcotic-field-tests/synthetic-cannabinoids-test-k2-spice/details.
135. Tsujikawa, K., *et al.*, *Development of a new field-test procedure for cocaine.* Forensic Science International, 2017. **270**: p. 267-274.
136. Parastekar, V. and V. Barhate, *Spectrophotometric determination of mephedrone in a bulk form.* International Journal of Current Pharmaceutical Research, 2015. **7**(3): p. 51-55.
137. Philp, M., *et al.*, *Development and validation of a presumptive color spot test method for the detection of synthetic cathinones in seized illicit materials.* Forensic Chemistry, 2016. **1**: p. 39-50.
138. Nycz, J.E., *et al.*, *Identification and derivatization of selected cathinones by spectroscopic studies.* Forensic Science International, 2016. **266**: p. 416-426.
139. Inoue, H., *et al.*, *Analysis of benzylpiperazine-like compounds.* Japanese journal of science and technology for identification, 2004. **9**(2): p. 165-184.
140. Philp, M., *et al.*, *Development and validation of a presumptive colour spot test method for the detection of piperazine analogues in seized illicit materials.* Analytical Methods, 2013. **5**(20): p. 5402-5410.
141. Waite, R.J., *et al.*, *Chemiluminescence detection of piperazine designer drugs and related compounds using tris(2,2'-bipyridine)ruthenium(III).* Talanta, 2013. **116**(0): p. 1067-1072.

142. Tsumura, Y., T. Mitome, and S. Kimoto, *False positives and false negatives with a cocaine-specific field test and modification of test protocol to reduce false decision.* Forensic Science International, 2005. **155**(2–3): p. 158-164.
143. Sarwar, M., *Technical note a new, highly specific color test for ketamine.* Microgram: p. 24.
144. Maddah, B., V. alimardani, and H. moradifard, *A simple colorimetric kit for determination of ketamine hydrochloride in water samples.* Analytical Methods, 2015. **7**(24): p. 10364-10370.
145. ENFSI Drugs Working Group, *Education and training outline for forensic drug practitioners*, in *Other publications*. 2015, European Network of Forensic Science Institutes (ENFSI): Germany.
146. Harris, A. *He was arrested for meth, but the crumbs in his car were Krispy Kreme doughnut glaze*. Miami Herald, 2016.
147. lilley, J. *Baking soda confused for cocaine lands innocent couple behind bars*. KATV, 2016.
148. Augenstein, S. *Man jailed for 4 months until test showed 'meth' was just epsom salt*. Forensic Magazine, 2015.
149. Kelly, J., *False positives equal false justice*. 2008, The Marijuana Policy Project: Washington D.C., USA.
150. Favretto, D., *et al.*, *When color fails: Illicit blue tablets containing anabolic androgen steroids.* Journal of Pharmaceutical and Biomedical Analysis, 2013. **83**: p. 260-264.
151. United Nations Office on Drugs and Crime (UNODC), *Recommended methods for the identification and analysis of cocaine in seized materials*, in *Presumptive Tests*. 2012, United Nations: Vienna.
152. United Nations Office on Drugs and Crime (UNODC), *Recommended methods for the identification and analysis of amphetamine, methamphetamine and their ring-substituted analogues in seized materials*. 2006, United Nations: New York.
153. Cosby, D., *Adulterants and interpretive challenges in forensic science: Effects on colorimetric spot tests for presumptive drug identification and adverse side effects in the body*, in *School of Medicine*. 2014, Boston University.
154. Kelly, J.F., K. Addanki, and O. Bagasra, *The non-specificity of the duquenois-levine field test for marijuana* The Open Forensic Science Journal, 2012. **5**: p. 5.
155. Fasanello, J. and P. Higgins, *Modified Scott test for cocaine base or cocaine hydrochloride.* Microgram, 1986. **19**: p. 137-138.
156. Amisar, S., *Reagent for the identification of cocaine*, in *Google Patents*. 1998, Erez Forensic Technology Ltd: Israel.
157. Campbell, A., *The australian illicit drug guide: Every person's guide to illicit drugs - Their use, effects and history, treatment options and legal penalties*. 2001: Black Incorporated.
158. McGill, J.W., C.A. Dixon, and D. Ritter, *Discovery of an interesting temperature effect on the sensitivity of the cobalt thiocyanate test for cocaine.* Microgram Journal, 2008. **6**(1-2).
159. Palette. *CUBE Portable Color Digitizer*. 2017 [cited 2017 May 5]; Available from: http://palette.com/cube.
160. FTLapps Inc, *ColorAssist*. 2017.
161. Choodum, A. and N. Nic Daeid, *Rapid and semi-quantitative presumptive tests for opiate drugs.* Talanta, 2011. **86**: p. 284-292.
162. Choodum, A., *et al.*, *Real time quantitative colourimetric test for methamphetamine detection using digital and mobile phone technology.* Forensic science international, 2014. **235**: p. 8-13.
163. Marcelo, M.C.A., *et al.*, *Scott test evaluation by multivariate image analysis in cocaine samples.* Microchemical Journal, 2016. **127**: p. 87-93.

164. Burks, R.M., *et al.*, *DETECHIP® - A sensor for drugs of abuse.* Journal of Forensic Sciences, 2010. **55**(3): p. 723-727.
165. Lyon, M., *et al.*, *Image analysis of DETECHIP® – A molecular sensing array*, in *Advances in Computer Science, Engineering & Applications*, D.C. Wyld, J. Zizka, and D. Nagamalai, Editors. 2012, Springer Berlin Heidelberg: Berlin. p. 145-158.
166. Baumes, L.A., *et al.*, *A colorimetric sensor array for the detection of the date-rape drug γ-hydroxybutyric acid (GHB): A supramolecular approach.* Chemistry – A European Journal, 2010. **16**(15): p. 4489-4495.
167. National Institute of Justice (NIJ). *Improving the reliability of drug tests done by officers*. 2016 [cited 2017 March 20]; Available from: https://www.nij.gov/topics/forensics/evidence/controlled-substances/Pages/improving-reliability-of-drug-tests-by-officers.aspx.
168. He, M., *et al.*, *Portable Upconversion Nanoparticles-Based Paper Device for Field Testing of Drug Abuse.* Analytical Chemistry, 2016. **88**(3): p. 1530-1534.
169. Bell, S.C. and R.D. Hanes, *A microfluidic device for presumptive testing of controlled substances.* Journal of Forensic Sciences, 2007. **52**(4): p. 884-888.
170. Musile, G., *et al.*, *The development of paper microfluidic devices for presumptive drug detection.* Analytical Methods, 2015. **7**(19): p. 8025-8033.
171. Krauss, S.T., *et al.*, *Objective method for presumptive field-testing of illicit drug possession using centrifugal microdevices and smartphone analysis.* Analytical Chemistry, 2016. **88**(17): p. 8689-8697.
172. Choodum, A., *et al.*, *A sol–gel colorimetric sensor for methamphetamine detection.* Sensors and Actuators B: Chemical, 2015. **215**(0): p. 553-560.
173. Argente-García, A., *et al.*, *A solid colorimetric sensor for the analysis of amphetamine-like street samples.* Analytica Chimica Acta, 2016. **943**: p. 123-130.
174. Evans, H., *Charles C. Fulton (1900-1992), Microcrystal Test Pioneer.* 1994.
175. Fulton, C.C., *Modern microcrystal tests for drugs: the identification of organic compounds by microcrystalloscopic chemistry*. 1969: Wiley-Interscience.
176. Brinsko, K.M., *et al.*, *A Modern Compendium of Microcrystal Tests for Illicit Drugs and Diverted Pharmaceuticals*. 2016, McCrone Research Institute: Illinois, USA.
177. Elie, L., *et al.*, *Microcrystalline identification of selected designer drugs.* Forensic Science International, 2012. **214**(1–3): p. 182-188.
178. Elie, M.P., M.G. Baron, and J.W. Birkett, *Enhancement of Microcrystalline Identification of γ-Hydroxybutyrate*.* Journal of Forensic Sciences, 2008. **53**(1): p. 147-150.
179. Nelson, H.C., E.A. Gardner, and D. Matteo, *Microcrystal Analysis of Cocaine Hydrochloride and Added Adulterants.* Journal of Forensic Sciences, 2011. **56**(3): p. 736-740.
180. Elie, L., *et al.*, *Microcrystalline testing used in combination with Raman micro-spectroscopy for absolute identification of novel psychoactive substances.* Journal of Raman Spectroscopy, 2016. **47**(11): p. 1343-1350.
181. Merckmillipore. *History of Thin-Layer Chromatography*. Learning Centre 2017 [cited 2017 June 2]; Available from: https://www.merckmillipore.com/AU/en/analytics-sample-preparation/learning-center-thin-layer-chromatography/tlc-history/bSGb.qB.xO4AAAFVQRxDx07D,nav?ReferrerURL=https%3A%2F%2Fwww.google.com.au%2F&bd=1#B.
182. Wall, P.E., *Introduction and History*, in *Thin-Layer Chromatography - A Modern Practical Approach*. 2005, Royal Society of Chemistry.
183. *Theory of Thin Layer Chromatography in Context of Pharmaceutical Analysis*, in *Thin Layer Chromatography in Drug Analysis*. 2013, CRC Press. p. 1-2.
184. *Controlled Substances Procedure Manual*. 2016, Virginia Department of Forensic Science: Virginia, USA.

185. kato, N. and A. Ogamo, *A TLC visualisation reagent for dimethylamphetamine and other abused tertiary amines.* Science & Justice, 2001. **41**(4): p. 239-244.
186. May, L. and C.-l.t. kuo. *Total analysis of an illicit or "street" narcotic sample by thin-layer chromatography*. 1972 [cited 2016 March 10]; Available from: http://www.unodc.org/unodc/en/data-and-analysis/bulletin/bulletin_1972-01-01_3_page007.html.
187. Kanai, K., *et al.*, *Simultaneous analysis of six phenethylamine-type designer drugs by TLC, LC-MS, and GC-MS.* Forensic Toxicology, 2008. **26**(1): p. 6-12.
188. Canalytics Supply. *THC Test Kits*. 2017 [cited 2017 February 18]; Available from: http://www.cannalyticssupply.com/product-category/thc-test-kits/.
189. AZO Materials. *Rapid Analysis of Illegal Narcotics Mixtures Using the MicroTLC*. 2014 [cited 2017 May 4]; Available from: http://www.azom.com/article.aspx?ArticleID=10909.
190. Field Forensics. *Spot.On.ID™ (explosives, narcotics)*. 2017 [cited 2017 February 18]; Available from: http://www.fieldforensics.com/products/by-model/microtlc-explosives-narcotics/.
191. Tosato, F., *et al.*, *Direct quantitative analysis of cocaine by thin layer chromatography plus a mobile phone and multivariate calibration: a cost-effective and rapid method.* Analytical Methods, 2016. **8**(42): p. 7632-7637.
192. Kennedy, J.H. and J.M. Wiseman, *Direct analysis of Salvia divinorum leaves for salvinorin A by thin layer chromatography and desorption electrospray ionization multi-stage tandem mass spectrometry.* Rapid Communications in Mass Spectrometry, 2010. **24**(9): p. 1305-1311.
193. Eikel, D., S.J. Prosser, and J.D. Henion, *Using compact mass spectrometry for detection and quantification of cannabis-related compounds.* LC GC North America, 2015: p. 37-42.
194. Mink, J., *et al.*, *Direct analysis of thin-layer chromatographic spots of narcotics by means of diffuse reflectance Fourier transform infrared spectroscopy.* Microchimica Acta, 1995. **119**(1): p. 129-135.
195. Carter, J.C., W.E. Brewer, and S.M. Angel, *Raman Spectroscopy for the in Situ Identification of Cocaine and Selected Adulterants.* Applied Spectroscopy, 2000. **54**(12): p. 1876-1881.
196. Thermo Fisher Scientific, *Raman and FTIR spectroscopy: Complementary technologies for chemical and explosives identification*. 2015, Thermo Fisher Scientific Inc.: Boston, USA.
197. Hargreaves, M.D., *Drugs of Abuse - Application of Handheld FT-IR and Raman Spectrometers*, in *Infrared and Raman Spectroscopy in Forensic Science*, J.M. Chalmers, H.G.M. Edwards, and M.D. Hargreaves, Editors. 2012, John Wiley & Sons: United Kingdom.
198. Roggo, Y., *et al.*, *A review of near infrared spectroscopy and chemometrics in pharmaceutical technologies.* Journal of Pharmaceutical and Biomedical Analysis, 2007. **44**(3): p. 683-700.
199. Eliaerts, J., *et al.*, *Rapid classification and quantification of cocaine in seized powders with ATR-FTIR and chemometrics.* Drug Testing and Analysis, 2017.
200. Mainali, D. and J. Seelenbinder, *Automated Fast Screening Method for Cocaine Identification in Seized Drug Samples Using a Portable Fourier Transform Infrared (FT-IR) Instrument.* Applied Spectroscopy, 2016. **70**(5): p. 916-922.
201. Tsujikawa, K., *et al.*, *Application of a portable near infrared spectrometer for presumptive identification of psychoactive drugs.* Forensic Science International, 2014(242): p. 162-171.
202. Archer, R.P., *Fluoromethcathinone, a new substance of abuse.* Forensic Science International, 2009. **185**(1–3): p. 10-20.

203. ThermoFisher Scientific. *TruDefender™ FT and TruDefender FTi Handheld Chemical Identification*. 2012 [cited 2017 May 4]; Available from: https://www.thermofisher.com/order/catalog/product/TRUDEFENDERFTCHEM?ICID=search-product.
204. Pereira, L.S.A., *et al.*, *Direct classification of new psychoactive substances in seized blotter papers by ATR-FTIR and multivariate discriminant analysis.* Microchemical Journal, 2017. **133**: p. 96-103.
205. Coelho Neto, J., *Rapid detection of NBOME's and other NPS on blotter papers by direct ATR-FTIR spectrometry.* Forensic Science International, 2015. **252**: p. 87-92.
206. Monfreda, M., *et al.*, *Fast profiling of cocaine seizures by FTIR spectroscopy and GC-MS analysis of minor alkaloids and residual solvents.* Science & Justice, 2015. **55**(6): p. 456-466.
207. Izake, E.L., *Forensic and homeland security applications of modern portable Raman spectroscopy.* Forensic Science International, 2010. **202**(1–3): p. 1-8.
208. Buckley, K. and P. Matousek, *Non-Invasive Detection of Illicit Drugs Using Spatially Offset Raman Spectroscopy*, in *Infrared and Raman Spectroscopy in Forensic Science*, J.M. Chalmers, H.G.M. Edwards, and M.D. Hargreaves, Editors. 2012, John Wiley & Sons: United Kingdom.
209. Olds, W.J., *et al.*, *Spatially offset Raman spectroscopy (SORS) for the analysis and detection of packaged pharmaceuticals and concealed drugs.* Forensic Science International. **212**(1): p. 69-77.
210. Hargreaves, M.D., *et al.*, *Analysis of seized drugs using portable Raman spectroscopy in an airport environment—a proof of principle study.* Journal of Raman Spectroscopy, 2008. **39**(7): p. 873-880.
211. Ali, E.M.A. and H.G.M. Edwards, *Screening of textiles for contraband drugs using portable Raman spectroscopy and chemometrics.* Journal of Raman Spectroscopy, 2014. **45**(3): p. 253-258.
212. Moreno, V.M., *et al.*, *Raman identification of drug of abuse particles collected with colored and transparent tapes.* Science & Justice, 2014. **54**(2): p. 164-169.
213. BioTools. *Mobile µRaman*. 2015 [cited 2017 May 4]; Available from: http://www.btools.com/raman.html.
214. Forensics, F. *HandyRam (explosives, narcotics and chem-bio)*. 2017 [cited 2017 February 18]; Available from: http://www.fieldforensics.com/products/by-model/handyram-explosives-narcotics-and-chem-bio/.
215. Guirguis, A., *et al.*, *Identification of new psychoactive substances (NPS) using handheld Raman spectroscopy employing both 785 and 1064 nm laser sources.* Forensic Science International, 2017. **273**: p. 113-123.
216. Fedchak, S., *Presumptive Field Testing Using Portable Raman Spectroscopy*, in *Research and Development on Instrumental Analysis for Forensic Science*. 2014, Las Vegas Metropolitan Police Department: Las Vegas, USA.
217. Mabbott, S., *et al.*, *Optimization of Parameters for the Quantitative Surface-Enhanced Raman Scattering Detection of Mephedrone Using a Fractional Factorial Design and a Portable Raman Spectrometer.* Analytical Chemistry, 2013. **85**(2): p. 923-931.
218. ThermoFisher Scientific. *Gemini FTIR/Raman Handheld Analyzer*. 2015 [cited 2017 May 4]; Available from: https://www.thermofisher.com/au/en/home/industrial/spectroscopy-elemental-isotope-analysis/portable-analysis-material-id/chemical-explosives-narcotics-identification/gemini-ftir-ftir-raman-handheld-analyzer.html.
219. ThermoFisher Scientific. *FirstDefender™ RMX Handheld Chemical Identification*. 2012 [cited 2017 May 4]; Available from: https://www.thermofisher.com/order/catalog/product/FIRSTDEFENDERRMX?ICID=search-product.

220. ThermoFisher Scientific. *TruNarc™ Handheld Narcotics Analyzer*. 2016 [cited 2017 May 4]; Available from: https://www.thermofisher.com/order/catalog/product/TRUNARC?ICID=search-product.
221. Agilent Technologies, *Agilent 4300 Handheld FTIR with DTGS Detector*. 2014, Agilent Technologies Inc.: USA.
222. Agilent Technologies, *4500A Forensics Analyzer*. 2013, Agilent Technologies Inc.: USA.
223. Rigaku Analytical Devices, *Progeny ResQ*. 2017: Boston, USA.
224. Smiths Detection, *Target-ID*. 2014, Smiths Detection Group Ltd.: USA.
225. Smiths Detection, *ACE-ID*. 2016, Smiths Detection Group Ltd.: USA.
226. B&W Tek, *TacticID®-N*. 2017, B&W Tek: USA.
227. Innovative Analytical Solutions. *Reporter*. 2017; Available from: http://analytik.co.uk/product/handheld-raman-spectroscopy-reporter/.
228. Demchenko, A.P., *Basic Principles*, in *Introduction to Fluorescence Sensing*. 2009, Springer Science: Ukraine. p. 1-36.
229. Flanagan, R.J., *et al.*, *Colour Tests, and Spectrophotometric and Luminescence Techniques*, in *Fundamentals of Analytical Toxicology*. 2007, John Wiley & Sons Inc: West Sussex, England. p. 95-115.
230. Patai, S., *The Chemistry of the Carbonyl Group*. 1966: Interscience Publishers, John Wiley & Sons.
231. Thorat, B.R., *et al.*, *Synthesis of schiff bases of 7-methoxy-2-[4-(methylsulfanyl) phenyl]-1-benzofuran-5-carboxaldehyde and animes and hydrazide.* Heteroletters.org, 2013. **3**(4): p. 461-479.
232. Comi, R., *et al.*, *A preparation of enamines.* Tetrahedron Letters, 1973. **14**(33): p. 3107-3109.
233. Westheimer, F. and K. Taguchi, *Catalysis by molecular sieves in the preparation of ketimines and enamines.* The Journal of Organic Chemistry, 1971. **36**(11): p. 1570-1572.
234. Roelofsen, D. and H. Van Bekkum, *The synthesis of enamines and ketimines using molecular sieves.* Recueil des Travaux Chimiques des Pays-Bas, 1972. **91**(5): p. 605-610.
235. Hickmott, P.W., *Enamines: recent advances in synthetic, spectroscopic, mechanistic, and stereochemical aspects—I.* Tetrahedron, 1982. **38**(14): p. 1975-2050.
236. Varma, R.S., R. Dahiya, and S. Kumar, *Clay catalyzed synthesis of imines and enamines under solvent-free conditions using microwave irradiation.* Tetrahedron Letters, 1997. **38**(12): p. 2039-2042.
237. Prashanth, K.N., K. Basavaiah, and M.S. Raghu, *Spectrophotometric Determination of Zolmitriptan in Bulk Drug and Pharmaceuticals Using Vanillin as a Reagent.* ISRN Analytical Chemistry, 2013. **2013**: p. 7.
238. Newkome, G. and D. Fishel, *Synthesis of simple hydrazones of carbonyl compounds by an exchange reaction.* The Journal of Organic Chemistry, 1966. **31**(3): p. 677-681.
239. Kadam, S.S., *et al.*, *Review article on: Chemical importance of brady's reagent.* International journal of research in pharmacy and chemistry, 2012. **2**(4): p. 1086-1092.
240. Kamakshi, R. and B.S. Reddy, *Solventless rapid synthesis of oxime, semicarbazone, and phenylhydrazone derivatives from carbonyl compounds under microwave conditions.* Australian journal of chemistry, 2005. **58**(8): p. 603-606.
241. Hajipour, A. and S. Mallakpour, *A rapid and convenient synthesis of oximes in dry media under microwave irradiation.* Journal of Chemical Research, Synopses, 1999(3): p. 228-229.
242. Kad, G.L., *et al.*, *Solventless preparation of oximes in the solid state and microwave irradiation.* Green Chemistry, 2001. **3**(6): p. 275-277.
243. Aakeroy, C.B., *et al.*, *A versatile and green mechanochemical route for aldehyde-oxime conversions.* Chemical Communications, 2012. **48**(92): p. 11289-11291.

244. Saikia, L., J. Baruah, and A. Thakur, *A rapid, convenient, solventless green approach for the synthesis of oximes using grindstone chemistry.* Organic and Medicinal Chemistry Letters, 2011. **1**(1): p. 12.
245. Bigdeli, M. and A. Rahmati, *Catalytic effect of wet molecular sieve 3Å in dry media on syntheses of oximes and 1, 3-dioximes.* Journal of Chemical Research, 2005. **2005**(9): p. 605-607.
246. Hajipour, A.R., F. Rafiee, and A. Ruoho, *A rapid and convenient method for the synthesis of aldoximes under microwave irradiation using in situ generated ionic liquids.* Journal of the Iranian Chemical Society, 2010. **7**(1): p. 114-118.
247. Kiasat, A.R., F. Kazemi, and K. Nourbakhsh, *A clean conversion of carbonyl compounds to oximes using silica gel supported hydroxylamine hydrochloride.* Phosphorus, Sulfur, and Silicon and the Related Elements, 2004. **179**(6): p. 1193-1196.
248. Damljanović, I., M. Vukićević, and R.D. Vukićević, *A Simple Synthesis of Oximes.* Monatshefte für Chemie / Chemical Monthly, 2006. **137**(3): p. 301-305.
249. Ley, J.P. and H.-J. Bertram, *Hydroxy-or Methoxy-Substituted Benzaldoximes and Benzaldehyde-alkyloximes as Tyrosinase Inhibitors.* Bioorganic & medicinal chemistry, 2001. **9**(7): p. 1879-1885.
250. Ballini, R., L. Barboni, and p. Filippone, *Amberlyst A-21 an Excellent Heterogenous Catalyst for the Coversion of Carbonyl Compounds to Oximes.* Chemistry Letters, 1997(5): p. 475-476.
251. Sharghi, H. and M. Hosseini Sarvari, *A mild and versatile method for the preparation of oximes by use of calcium oxide.* Journal of Chemical Research-Part S Synopsis, 2000(1): p. 24-25.
252. Sharghi, H. and M. Hosseini, *Solvent-free and one-step Beckmann rearrangement of ketones and aldehydes by zinc oxide.* Synthesis, 2002. **8**(1057): p. 106.
253. Maheswara, M., *et al.*, *A Simple and effective glycine-catalysed procedure for the preparation of oximes.* Journal of Chemical Research, 2006. **2006**(6): p. 362-363.
254. Eshghi, H. and A. Hassankhani, *Regioselective synthesis of e-oximes catalyzed by ferric chloride under solvent-free conditions.* Organic Preparations and Procedures International, 2005. **37**(6): p. 575-579.
255. Setamdideh, D., B. Khezri, and S. Esmaeilzadeh, *Synthesis of Oximes with NH2OH.HCl/DOWEX(R)50WX4 System.* Journal of the Chinese Chemical Society, 2012. **59**(9): p. 1119-1124.
256. Vijayan, N., *et al.*, *Growth of semicarbazone of benzophenone single crystals.* Journal of Crystal Growth, 2002. **236**(1–3): p. 407-412.
257. Araújo, A.N., *et al.*, *Sequential injection system for the spectrophotometric determination of reducing sugars in wines.* Talanta, 2000. **52**(1): p. 59-66.
258. Besada, A., *Analytical Use of Copper (II)-Neocuproine in The Spectrophotometric Determination of Hydrazines.* Analytical Letters, 1988. **21**(10): p. 1917-1925.
259. Bhat, S.R., *et al.*, *Extraction-spectrophotometric determination of sulphide and sulphite in waters based on formation of the bis(2,9-dimethyl-1,10-phenanthroline) copper(I) ion.* Analytica Chimica Acta, 1979. **108**(0): p. 293-296.
260. Byrnes, R.W., W.E. Antholine, and D.H. Petering, *Oxidation-reduction reactions in Ehrlich cells treated with copper-neocuproine.* Free Radical Biology and Medicine, 1992. **13**(5): p. 469-478.
261. Eren, S., *et al.*, *Determination of peroxide-based explosives with copper(II)-neocuproine assay combined with a molecular spectroscopic sensor.* Analyst, 2010. **135**(8): p. 2085-2091.
262. Güçlü, K., *et al.*, *Spectrophotometric determination of ascorbic acid using copper(II)–neocuproine reagent in beverages and pharmaceuticals.* Talanta, 2005. **65**(5): p. 1226-1232.

263. Cárdenas, A., M. Gomez, and C. Frontana, *Relationship between the Chemical Structures of Antioxidants and the differences in their Cupric ion Reducing Antioxidant Capacity (CUPRAC) by Electrochemical Methods.* Journal of Electroanalytical Chemistry.
264. Özyürek, M., K. Güçlü, and R. Apak, *The main and modified CUPRAC methods of antioxidant measurement.* TrAC Trends in Analytical Chemistry, 2011. **30**(4): p. 652-664.
265. Apak, R., *et al.*, *Novel Total Antioxidant Capacity Index for Dietary Polyphenols and Vitamins C and E, Using Their Cupric Ion Reducing Capability in the Presence of Neocuproine: CUPRAC Method.* Journal of Agricultural and Food Chemistry, 2004. **52**(26): p. 7970-7981.
266. Al-Obaid, A.M., *et al.*, *Determination of (S)(−)-cathinone by spectrophotometric detection.* Journal of Pharmaceutical and Biomedical Analysis, 1998. **17**(2): p. 321-326.
267. Ercag, E., A. Ercag, and R. Apak, *Spectrophotometric determination of the soil fumigant: Dazomet with copper(II)-neocuproine reagent.* Analytica Chimica Acta, 2004. **505**(1): p. 95-100.
268. Moreno, A.d.H. and H.R.N. Salgado, *Spectrophotometric Determination of Ceftazidime in Pharmaceutical Preparations Using Neocuproin as a Complexing Agent.* Analytical Letters, 2008. **41**(12): p. 2143-2152.
269. Abuzuhri, A.Z., *et al.*, *Spectrophotometric Determination of Ampicillin by Ternary Complex Formation with 1,10-Phenanthroline and Copper(II).* Microchemical Journal, 1994. **50**(1): p. 111-115.
270. Hoste, J., J. Eeckhout, and J. Gillis, *Spectrophotometric determination of copper with cuproine.* Analytica Chimica Acta, 1953. **9**(0): p. 263-274.
271. Wheeler, O.H., *Reduction of Carbonyl Groups*, in *The Chemistry of the Carbonyl Group*, S. Patai, Editor. 1966, Interscience Publishers, John Wiley & Sons. p. 507-566.
272. McMurry, J., *Alcohols and Phenols*, in *Organic Chemistry*. 2008, Brooks/Cole, Thomson: USA. p. 609-617.
273. Milani, B., C. Crotti, and E. Farnetti, *Hydrogen transfer reduction of polyketones catalyzed by iridium complexes: a novel route towards more biocompatible materials.* Dalton Transactions, 2008(34): p. 4659-4663.
274. Nomura, K., *Transition metal catalyzed hydrogenation or reduction in water.* Journal of Molecular Catalysis A: Chemical, 1998. **130**(1): p. 1-28.
275. Lin, W., *et al.*, *Selective reduction of carbonyl groups in the presence of low-valent titanium reagents.* Tetrahedron Letters, 2014. **55**(14): p. 2238-2242.
276. Szostak, M., M. Spain, and D.J. Procter, *Recent advances in the chemoselective reduction of functional groups mediated by samarium (II) iodide: a single electron transfer approach.* Chemical Society Reviews, 2013. **42**(23): p. 9155-9183.
277. Matsumura, Y., *et al.*, *New Efficient Organic Activators for Highly Enantioselective Reduction of Aromatic Ketones by Trichlorosilane.* Organic Letters, 2006. **8**(17): p. 3789-3792.
278. *Diisobutylaluminium Hydride (DIBAL-H) and other Isobutyl Aluminium Alkyls as Specialty Organic Synthesis Reagents* in *Technical Bulletin*. 2006, AkzoNobel Polymer Chemicals. p. 1-14.
279. Imamoto, T., *et al.*, *Reactions of carbonyl compounds with Grignard reagents in the presence of cerium chloride.* Journal of the American Chemical Society, 1989. **111**(12): p. 4392-4398.
280. Hollmann, F., I.W.C.E. Arends, and D. Holtmann, *Enzymatic reductions for the chemist.* Green Chemistry, 2011. **13**(9): p. 2285-2314.
281. Borges, K.B., *et al.*, *Stereoselective biotransformations using fungi as biocatalysts.* Tetrahedron: Asymmetry, 2009. **20**(4): p. 385-397.
282. Fruchey, E.R., *Asymmetric Reductions of Ketones, Imines, and Oximes Using Biocatalytic Enzymes Found in Pea Plants.* 2011.

283. Patel, R.N., *et al.*, *Enantioselective microbial reduction of substituted acetophenones.* Tetrahedron: Asymmetry, 2004. **15**(8): p. 1247-1258.
284. Groger, H., *et al.*, *Reduction of Ketones and Aldehydes to Alcohols*, in *Enzyme Catalysis in Organic Synthesis*, K. Drauz, H. Groger, and O. May, Editors. 2012, Wiley-VCH Verlag & Co. KGaA: Weinheim, Germany. p. 1037-1110.
285. Laird, T., *Book Review of Enzyme Catalysis in Organic Synthesis.* Organic Process Research & Development, 2013. **17**(4): p. 718.
286. Li, S., *et al.*, *Size matters: Challenges in imprinting macromolecules.* Progress in Polymer Science, 2014. **39**(1): p. 145-163.
287. Chen, L., S. Xu, and J. Li, *Recent advances in molecular imprinting technology: current status, challenges and highlighted applications.* Chemical Society Reviews, 2011. **40**(5): p. 2922-2942.
288. Sharma, P.S., *et al.*, *Surface development of molecularly imprinted polymer films to enhance sensing signals.* TrAC Trends in Analytical Chemistry, 2013. **51**(0): p. 146-157.
289. Nair, R.V. and R. Vijaya, *Photonic crystal sensors: An overview.* Progress in Quantum Electronics, 2010. **34**(3): p. 89-134.
290. Gholivand, M.B., M. Torkashvand, and G. Malekzadeh, *Fabrication of an electrochemical sensor based on computationally designed molecularly imprinted polymers for determination of cyanazine in food samples.* Analytica Chimica Acta, 2012. **713**(0): p. 36-44.
291. Ge, Y. and A.P.F. Turner, *Molecularly Imprinted Sorbent Assays: Recent Developments and Applications.* Chemistry – A European Journal, 2009. **15**(33): p. 8100-8107.
292. McCluskey, A., C.I. Holdsworth, and M.C. Bowyer, *Molecularly imprinted polymers (MIPs): sensing, an explosive new opportunity?* Organic & Biomolecular Chemistry, 2007. **5**(20): p. 3233-3244.
293. Poma, A., A.P.F. Turner, and S.A. Piletsky, *Advances in the manufacture of MIP nanoparticles.* Trends in Biotechnology, 2010. **28**(12): p. 629-637.
294. Valeur, B. and M.N. Berberan-Santos, *Introduction*, in *Molecular Fluorescence*. 2012, Wiley-VCH: Germany. p. 1-25.
295. Demchenko, A.P., *Non-Conventional Generation and transformation of Response*, in *Introduction to Fluorescence Sensing*. 2009, Springer Science: Ukraine. p. 335-370.
296. Jameson, D.M., *Forster Resonance Energy Transfer*, in *Introduction to Fluorescence*. 2014, Taylor & Francis Group: Boca Raton, Florida. p. 145-161.
297. Jameson, D.M., *Quantum Yields and Quenching*, in *Introduction to Fluorescence*. 2014, Taylor & Francis Group: Boca Raton, Florida. p. 131-143.
298. Demchenko, A.P., *Design and Properties of Fluorescence Reporters*, in *Introduction to Fluorescence Sensing*. 2009, Springer Science: Ukraine. p. 119-196.
299. Valeur, B. and M.N. Berberan-Santos, *Effects of the Molecular Structure of Organic Molecules on Their Fluorescence*, in *Molecular Fluorescence*. 2012, Wiley-VCH: Germany. p. 75-107.
300. Zhai, D., *et al.*, *Development of a fluorescent sensor for illicit date rape drug GHB.* Chemical Communications, 2014.
301. Zhai, D., *et al.*, *Development of a fluorescent sensor for an illicit date rape drug - GBL.* Chemical Communications, 2013. **49**(55): p. 6170-6172.
302. MacLeod, J. and F. Rosei, *Photonic crystals: Sustainable sensors from silk.* Nat Mater, 2013. **12**(2): p. 98-100.
303. Stöber, W., A. Fink, and E. Bohn, *Controlled growth of monodisperse silica spheres in the micron size range.* Journal of colloid and interface science, 1968. **26**(1): p. 62-69.
304. Walker, J.P. and S.A. Asher, *Acetylcholinesterase-based organophosphate nerve agent sensing photonic crystal.* Analytical chemistry, 2005. **77**(6): p. 1596-1600.
305. MacConaghy, K.I., *et al.*, *Photonic Crystal Kinase Biosensor.* Journal of the American Chemical Society, 2014. **136**(19): p. 6896-6899.

306. Li, J. and J.-J. Zhu, *Quantum dots for fluorescent biosensing and bio-imaging applications.* Analyst, 2013. **138**(9): p. 2506-2515.
307. Kyeong, S., *et al.*, *Quantum dot-assembled nanoparticles with polydiacetylene supramolecule toward label-free, multiplexed optical detection.* Journal of Colloid and Interface Science, 2013. **394**.
308. Zhang, Y., *Surface functionalization of quantum dots for biotechnological applications*. 2011: Iowa State University.
309. Petryayeva, E. and W.R. Algar, *Multiplexed Homogeneous Assays of Proteolytic Activity Using a Smartphone and Quantum Dots.* Analytical Chemistry, 2014.
310. Ronda, C.R. and T. Justel, *Quantum Dots and Nanophosphors*, in *Luminescence*, C. Ronda, Editor. 2008, WILEY-VCH Germany.
311. Voliani, V. and J. Perez-Prieto, *Fluorescent Probes Based on Upconverting Lanthanide Nanostructures*, in *Fluorophores: Characterization, Synthesis and Applications*, S. Watanabe, Editor. 2013, Nova Science Publishers, Inc.: New York. p. 1-27.
312. Jin, D. and J.A. Piper, *Time-Gated Luminescence Microscopy Allowing Direct Visual Inspection of Lanthanide-Stained Microorganisms in Background-Free Condition.* Analytical Chemistry, 2011. **83**(6): p. 2294-2300.
313. Gu, Z., *et al.*, *Recent advances in design and fabrication of upconversion nanoparticles and their safe theranostic applications.* Advanced Materials, 2013. **25**(28): p. 3758-3779.
314. Suijver, J.F., *Upconversion Phosphors*, in *Luminescence*, C. Ronda, Editor. 2008, WILEY-VCH Germany.
315. Peng, H., *et al.*, *Molecularly imprinted photonic hydrogels as colorimetric sensors for rapid and label-free detection of vanillin.* Journal of agricultural and food chemistry, 2012. **60**(8): p. 1921-1928.
316. Meng, L., *et al.*, *Fast screening of ketamine in biological samples based on molecularly imprinted photonic hydrogels.* Analytica chimica acta, 2013. **771**: p. 86-94.
317. Meng, L., *et al.*, *Molecularly imprinted photonic hydrogels for fast screening of atropine in biological samples with high sensitivity.* Forensic science international, 2013. **231**(1): p. 6-12.
318. Hu, X., *et al.*, *Imprinted photonic polymers for chiral recognition.* Angewandte Chemie International Edition, 2006. **45**(48): p. 8145-8148.
319. Zhao, Y.J., *et al.*, *Multiplex Label-Free Detection of Biomolecules with an Imprinted Suspension Array.* Angewandte Chemie International Edition, 2009. **48**(40): p. 7350-7352.
320. *An Act to amend the Drug Misuse and Trafficking Act 1985 and the Drug Misuse and Trafficking Regulation 2011 with respect to dealing with prohibited plants, prohibited drugs and other substances in police custody; and for other purposes.* 2016, NSW Legislative Assembly: Australia. p. 558.

This page intentionally left blank

Chapter 2: Synthesis of cathinone analogues

This page intentionally left blank

Chapter 2: Synthesis of cathinone analogues

2.1 Introduction

Cathinone is a naturally occurring psychoactive compound found in the leaves of the *Catha edulis* (khat) plant. Analogous to coca leaves in South America and Betel leaves in Asia[321], khat leaves are chewed by locals in many East African countries for the stimulant properties they provide[322]. Synthetic cathinones are a unique class of NPS with a chemical structure based on cathinone. The earliest report of synthetic cathinone synthesis was methcathinone in Germany in 1928[323]. Since then, an increasing number of cathinone analogues have appeared, with recent reports indicating at least 118 different cathinones have been detected[34].

The synthetic methods used to produce these cathinone analogues are often easy to locate in the literature through peer-reviewed publications[324, 325], organic chemistry theses[326], online forums[327], and patents[328, 329]. In addition, the same general procedure can create an array of derivatives from different starting material or by varying carbon chain lengths of reagents.

The objectives behind the synthesis of these compounds were multifaceted: 1) a more economical way to obtain the quantities of material required for subsequent experimental work in this research; 2) it allows for all experimental work to be performed in-house; and 3) to become familiar with the chemistry behind their preparation and common impurities encountered. In this chapter, twenty synthetic cathinone analogues were attempted to be synthesised in order to create a series of compounds with different ring substituents, carbon chain lengths and amine classes that may be encountered in the field. All compounds were characterised using Gas Chromatography-Mass Spectrometry (GC-MS), proton (^{1}H) and carbon (^{13}C) Nuclear Magnetic Resonance (NMR) spectroscopy, Fourier Transform Infrared (FTIR) spectroscopy, Ultraviolet-Visible (UV-Vis) spectroscopy and melting point data.

2.2 Materials and methods

2.2.1 Chemicals

All chemicals used in the synthesis of compounds were of analytical or laboratory grade and were used without prior purification steps. Piperonal, butylmagnesium chloride (2 M solution in tetrahydrofuran (THF)), propylmagnesium chloride (2 M solution in THF), ethylmagnesium chloride (2 M solution in diethyl ether), methylamine hydrochloride, celite® 500 fine, bromine, ethylamine (70% aqueous solution), *p*-tolualdehyde, 4-methylpropiophenone, 4-fluoropropiophenone, pyridinium chlorochromate (PCC), benzonitrile, 4-ethylbenzaldehyde, 4-methoxybenzaldehyde and sodium hydrogen sulphite were obtained from Sigma-Aldrich (Castle Hill, NSW, Australia). Anhydrous sodium sulphate, toluene, diethyl ether, methanol, dichloromethane, acetone, n-hexane, sodium hydroxide (pellets) and potassium carbonate were obtained from Chem-Supply (Port Adelaide, SA, Australia). Glacial acetic acid and anhydrous magnesium sulphate were obtained from Scharlau Chemicals (Sentmenat, Barcelona, Spain). Silicic acid, sodium carbonate and hydrochloric acid were obtained from Mallinckrodt Pharmaceuticals (Surrey, England, UK), Vetec Quimica Fina (Duque de Caxias, RJ, Brazil) and RCI Labscan (Pathum Wan, BNK, Thailand), respectively. Potassium permanganate, ethyl acetate, ammonia solution (28%) and pyrrolidine were obtained from Ajax Finechem (Scoresby, VIC, Australia) and ephedrine hydrochloride and 1-naphthaldehyde were obtained from Aldrich Chemical Company (Castle Hill, NSW, Australia). Deuterated solvents chloroform-d, dimethyl sulfoxide-d_6 and water-d_2 were obtained from Sigma-Aldrich (Castle Hill, NSW, Australia) and methanol-d_4 was obtained from Merck Sharp & Dohme (Granville, NSW, Australia). FTIR grade potassium bromide was obtained from Sigma Aldrich (Castle Hill, NSW, Australia).

2.2.2 Melting point determination

Samples were prepared by packing a small amount of solid material into a glass melting point capillary tube. Melting temperature ranges were determined using a Vernier Melt Station, Go!Link® data-collection interface and Logger Pro® 3 (version 3.8.4) software (Beaverton, OR, USA). In addition to melting temperature ranges, sample decomposition and colour changes were also recorded.

2.2.3 Nuclear Magnetic Resonance (NMR) spectroscopy analysis

Samples were prepared by completely dissolving the solid material in a deuterated solvent before transferring the liquid into an NMR tube. The majority of the samples were dissolved in chloroform-d, dimethyl sulfoxide-d_6 or water-d_2 obtained from Sigma-Aldrich (Castle Hill, NSW, Australia). Methanol-d_4 obtained from Merck Sharp & Dohme (Granville, NSW, Australia) was used in ^{13}C NMR experiments where samples were not soluble in chloroform-d.

^{1}H and ^{13}C NMR spectra were recorded with an Agilent NMR spectrometer (Santa Clara, CA, USA) operating at 500 MHz and 125 MHz, respectively, using standard pulse sequences. The spectra were recorded at 298 K, and chemical shifts (δ) were reported as parts per million (ppm) with respect to the internal standard tetramethylsilane (TMS, 0.00 ppm) or solvent residual signals (HOD, 4.79 ppm (^{1}H); $(CD_3)_2SO$, 39.52 ppm (^{13}C); CD_3OD, 49.00 ppm (^{13}C); $CDCl_3$, 7.26/77.16 ppm ($^{1}H/^{13}C$)).

2.2.4 Gas Chromatography-Mass Spectrometry (GC-MS) analysis

Samples were prepared by dissolving the liquid, oily residue or solid material in analytical grade methanol, dichloromethane or diethyl ether. Samples were analysed for reaction monitoring purposes or compound characterisation.

Samples were injected using an Agilent 7683 series autosampler and analysis was performed using an Agilent 6890 Gas Chromatograph coupled to an Agilent 5973 Mass Spectrometer (Agilent Technologies, Santa Clara, CA, USA). The GC-MS system was equipped with an HP-5MS column with 5% Phenyl 95% dimethylpolysiloxane copolymer phase (30 m x 0.25 mm x 0.25 µm). Unless stated otherwise, injector and interface temperatures were set at 250 °C and 280 °C, respectively, and injections (1.0 µL) were made in split mode with a 25:1 split ratio. The initial oven temperature at 50 °C was held for 2 min before increasing the temperature to 290 °C at a rate of 50 °C/min and holding for a further 4 min. Helium was used as the carrier gas at a constant flow rate of 1.2 mL/min with a 2 min solvent delay. Data was collected using full scan acquisition (40-450 amu) and analysis was carried out using Agilent Enhanced ChemStation software, MSD ChemStation.

2.2.5 Fourier Transform Infrared (FTIR) spectroscopy analysis

Several samples were prepared for FTIR analysis by creating a potassium bromide (KBr) disc of the hydrochloride salt sample. FTIR grade potassium bromide from Sigma Aldrich (Castle Hill, NSW, Australia) was mixed with the solid sample in an agate mortar and pestle from International Crystal Laboratories (Garfield, NJ, USA) to create a 1% w/w mixture. A manual hydraulic press from Specac (Kent, England, UK) and a 13 mm KBr die set was used to create the KBr disc for analysis.

All hydrochloride salt samples were characterised by Attenuated Total Reflection (ATR)-FTIR in which no preparation steps were required.

FTIR spectra were obtained using a Thermo Scientific Nicolet Magna 6700 FTIR spectrometer and associated OMNIC software suite (North Ryde, NSW, Australia). All spectra were collected using 64 scans with a resolution of 4.0 cm^{-1}. For ATR-FTIR analysis, the spectrometer was equipped with a Thermo Scientific Smart iTX ATR accessory.

2.2.6 Ultraviolet-Visible spectroscopy analysis

Samples were prepared by dissolving solid hydrochloride salts in deionised water and diluting to appropriate concentration before transferring the solution to a quartz cuvette for analysis.

Absorption spectra in the ultraviolet region were obtained in the range 200–400 nm using an Agilent Technologies Cary 60 spectrometer (Santa Clara, CA, USA). Spectra were recorded at a rate of 600 nm/min and baseline corrections were performed for all spectral measurements.

2.2.7 Thin Layer Chromatography (TLC)

Reactions were monitored using silica gel 60 F254 TLC plates on aluminium backing from Merck Millipore (Bayswater, VIC, Australia). Samples were spotted onto the plates directly from the reaction mixture or after dilution with methanol. Mobile phases employed during monitoring of Grignard reactions, oxidations and brominations were hexane: methanol (60:40) and methanol: water: acetic acid (70:28:2). Ethyl acetate: methanol: ammonia (85:10:5) was the mobile phase used during the final amination reaction step.

Developed TLC plates were initially viewed using a Spectroline® CM–10A UV viewing cabinet (Spectronics Corporation, Westbury, NY, USA) fitted with a UV lamp (Grace Discovery Sciences, Epping, VIC, Australia). TLC plates were subsequently stained using two visualisation reagents in series. In the first, iodine vapour was allowed to come into contact with the TLC plate by placing the plate into a jar containing a few crystals of iodine. After several min, the plate was removed and the brown coloured spots visualised. The second visualisation reagent, potassium permanganate, was prepared as a solution following literature methods[330]. The TLC plate was dipped into the solution, removed and gently heated using a Bosch heating gun (Clayton, VIC, Australia) before visualising yellow coloured spots on a purple background.

2.2.8 4-Methylmethcathinone (4-MMC, 3)

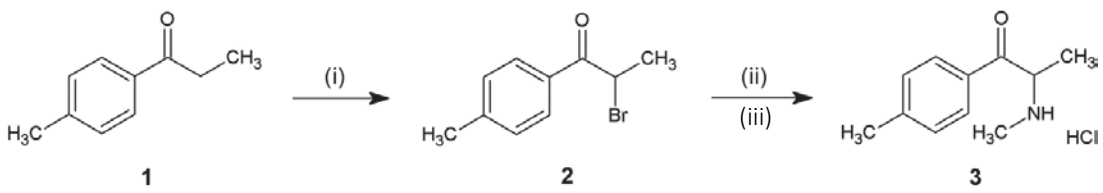

1 2 3

Figure 2-1. Synthesis of 4-methylmethcathinone HCl (**3**) via a two step reaction sequence: α-bromination of **1** followed by nucleophilic substitution of **2** with methylamine. The final product salt was obtained following extraction and HCl work-up.
Reagents and conditions: (i) bromine, glacial acetic acid, RT, 1.5 h; *(ii)* aq. methylamine, toluene, RT, 52 h; *(iii)* HCl work-up.

2.2.8.1 *2-bromo-4-methylpropiophenone (**2**)*

To a round-bottom flask (RBF) containing glacial acetic acid (44 mL) was added 4-methylpropiophenone **1** (4.05 mL, 27.1 mmol) and the mixture stirred. A pressure equalising dropping funnel containing bromine (1.70 mL, 33.0 mmol) was attached and the bromine added dropwise over 1 h. The reaction was then left to stir for 0.5 h. The reaction was quenched by pouring the mixture into 100 mL ice-cold water and the 2-bromo-4-methylpropiophenone product was extracted with dichloromethane (3 x 50 mL). The organic extracts were washed with saturated sodium carbonate solution (2 x 30 mL) and the product rotary evaporated to afford a yellow oil that solidified to form **2** (5.48 g, 24.1 mmol, 89%) as cream coloured, fluffy crystals (Caution! Strong lachrymator): EI (*m/z,* %): 226/228 (M^+, $^{79}Br/^{81}Br$, 1), 120(10), 119(100), 91(34), 65(11).

2.2.8.2 *2-(methylamino)-1-(4-methylphenyl)propan-1-one hydrochloride (4-MMC), (**3**)*

In a RBF, the α-bromoketone **2** (2.285 g, 10.06 mmol) was dissolved in toluene (5 mL) and briefly stirred at room temperature. Separately, in two beakers, sodium hydroxide pellets (1.625 g, 40.63 mmol) were dissolved in cold water (4 mL) and added to a solution of methylamine hydrochloride (2.743 g, 40.64 mmol) in cold water (3 mL). This combined solution was quickly added to the RBF using a Pasteur pipette and the reaction mixture left to stir for 52 h. The reaction was then quenched by pouring into ice-cold water (30 mL), the toluene layer separated and the aqueous layer further extracted with toluene (4 x 10 mL). Combined toluene extracts were washed with water (3 x 10 mL) and acidified with 0.1 M HCl (5 x 10 mL). Acidic extracts were washed with toluene (3 x 10 mL) and evaporated to dryness to afford an off-white coloured crystalline powder **3** (0.9944 g, 4.653 mmol, 46%): mp 219-220 °C (dec.)(lit.[331] 249.6 °C); ^{1}H NMR (500 MHz, D_2O) δ, ppm: 7.946-7.929 (d, $^{3}J_{HH}$= 8.5 Hz, 2H), 7.476-7.460 (d, $^{3}J_{HH}$= 8.0 Hz, 2H), 5.100-5.056 (q, $^{3}J_{HH}$= 7.5 Hz, 1H), 2.806 (s, 3H), 2.460 (s, 3H), 1.620-1.606 (d, $^{3}J_{HH}$= 7.0 Hz, 3H); ^{13}C NMR (125 MHz, $CDCl_3$) δ, ppm: 194.687, 146.087, 130.515, 129.908, 128.952, 59.352, 31.937, 21.840, 16.741; EI (*m/z,* %): 177(M^+, 0), 119(6), 91(17), 65(15), 58(100), 56(15); FTIR (ATR) ν_{max}, cm^{-1}: 2905 (C-H stretch), 2713 and 2455 (asym. and sym. NH_2^+ stretches), 1685 (C=O stretch), 1605 and 1455 (C=C stretch), 1247 (-C-C=O stretch), 832 and 687 (1,4-disubstituted benzene ring); UV (H_2O) λ_{max}, nm: 264.

2.2.9 4-Fluoromethcathinone (4-FMC, 6)

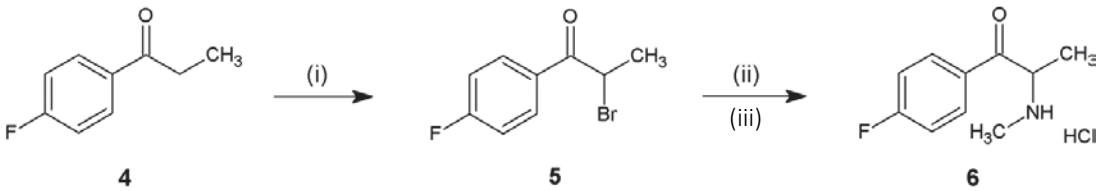

Figure 2-2. Synthesis of 4-fluoromethcathinone HCl (**6**) via a two step reaction sequence: α-bromination of **4** followed by nucleophilic substitution of **5** with methylamine. The final product salt was obtained following extraction and HCl work-up.
Reagents and conditions: (i) bromine, DCM, RT, 10 h; *(ii)* aq. methylamine, toluene, RT, 25 h; *(iii)* HCl work-up.

2.2.9.1 *2-bromo-4-fluoropropiophenone (**5**)*

In a RBF, 4-fluoropropiophenone **4** (1.00 mL, 7.20 mmol) was dissolved in dichloromethane (40 mL) and a pressure equalising dropping funnel containing bromine (0.80 mL, 14 mmol) was attached. One drop of bromine was initially added and the reaction left to stir for 5 min. The remaining bromine was added dropwise over 30 min and the reaction left to stir for 9.5 h. The solvent and excess bromine was removed via rotary evaporation to afford an orange oil **5** (1.75 g, 7.57 mmol, 105%). EI (*m/z,* %): 230/232 (M^+, $^{79}Br/^{81}Br$, 2), 123(100), 95(28), 75(11).

2.2.9.2 *1-(4-fluorophenyl)-2-(methylaminopropan-1-one hydrochloride (4-FMC), (**6**)*

In a RBF, the α-bromoketone **5** (1.75 g, 7.57 mmol) was dissolved in toluene (4 mL) and briefly stirred at room temperature. Separately in two beakers, sodium hydroxide pellets (0.966 g, 24.1 mmol) were dissolved in cold water (2 mL) and added to a solution of methylamine hydrochloride (1.63 g, 24.1 mmol) in cold water (2 mL). This combined solution was quickly added to the RBF using a Pasteur pipette and the reaction mixture left to stir for 25 h. The reaction was then quenched by pouring into ice-cold water (30 mL). The toluene layer was separated and the aqueous layer further extracted with toluene (4 x 10 mL). Combined toluene extracts were washed with water (3 x 10 mL) and acidified with 0.10 M HCl (8 x 10 mL). Acidic extracts were washed with toluene (3 x 20 mL) and evaporated to dryness to afford a crude yellow and white powder (1.08 g, 4.96 mmol, 66%). The crude product was washed with acetone to afford a white powder **6** (0.4822 g, 2.21 mmol, 29.2 %): mp 229-230 °C (dec.)(lit.[332] 230.0 °C); ^{1}H NMR (500 MHz, D_2O) δ, ppm: 8.120-8.079 (dd, $^3J_{HH}$= 8.75 Hz, $^4J_{HF}$= 5.25 Hz, 2H), 7.373-7.325 (dd, $^3J_{HH}$= 9.0 Hz, $^3J_{HF}$= 9.0 Hz, 2H), 5.109-5.065 (q, $^3J_{HH}$= 7.5 Hz, 1H), 2.810 (s, 3H), 1.625-1.610 (d, $^3J_{HH}$= 7.5 Hz, 3H); ^{13}C NMR (125 MHz, $(CD_3)_2SO$) δ, ppm: 195.368, 167.024-165.002 (d, $^1J_{CF}$= 252.75 Hz, 1C), 132.243-132.167(d, $^3J_{CF}$= 9.5 Hz, 2C), 129.804-129.781 (d, $^4J_{CF}$= 2.875 Hz, 1C), 116.694-116.520 (d, $^2J_{CF}$= 21.75 Hz, 2C), 58.547, 30.977, 15.534; EI (*m/z,* %): 181(M^+,1), 123(10), 95(23), 75(15), 58(100); FTIR (ATR) ν_{max}, cm^{-1}: 2905 (C-H stretch), 2707 and 2458 (asym. and sym. NH_2^+ stretches), 1687 (C=O stretch), 1597 and 1461 (C=C stretch), 1236 (C-F stretch), 847 and 684 (1,4-disubstituted benzene ring); UV (H_2O) λ_{max}, nm: 254.

2.2.10 1-(1,3-benzodioxol-5-yl)-2-(methylamino)propan-1-one (methylone, 11)

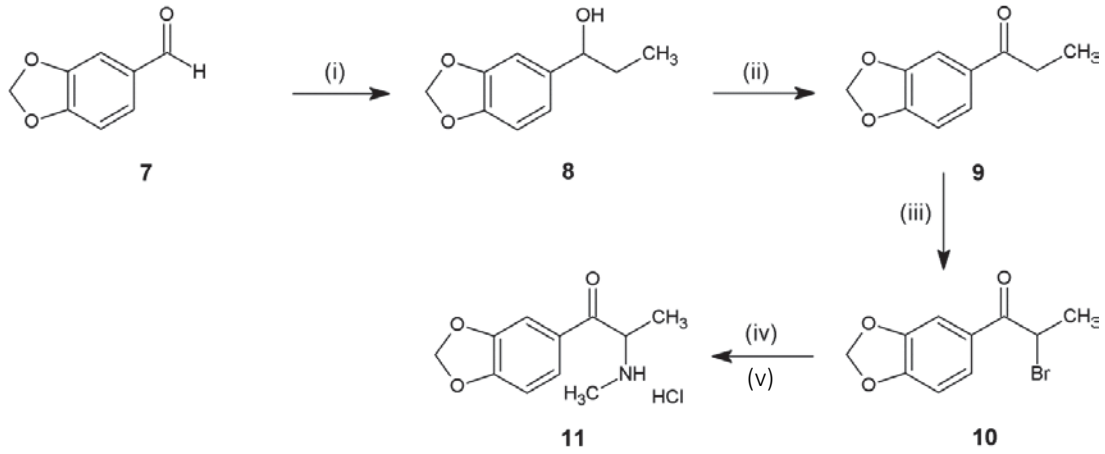

Figure 2-3. Synthesis of methylone HCl (**11**) via a four step reaction sequence: Grignard reaction of **7**, oxidation of **8**, α-bromination of **9**, and nucleophilic substitution of **10** with methylamine. The final product salt was obtained following extraction and HCl work-up.
Reagents and conditions: (i) EthMgCl, Et_2O, N_2 atm., 4 h; *(ii)* PCC/celite, DCM, 25 h; *(iii)* bromine, glacial acetic acid, RT, 6 h; *(iv)* aq. methylamine, toluene, RT, 24 h; *(iii)* HCl work-up.

2.2.10.1 *1-(2H-1,3-benzodioxol-5-yl)propan-1-one (**9**)*

To a RBF maintained under nitrogen atmosphere was added piperonal **7** (1.73 g, 11.5 mmol). Diethyl ether (10 mL) was added via syringe and the solution stirred to dissolve the solid. The flask was kept on an ice bath while ethylmagnesium chloride solution (6.0 mL, 12 mmol) was added via syringe over 3 min. The ice bath was removed after 10 min and the reaction stirred for 4 h. To the RBF was added 1.0 M HCl (10 mL, 10 mmol) and the mixture stirred briefly. The ether layer was separated and washed with water (3 x 5 mL). The ether extract was dried over magnesium sulphate before removing the solvent via rotary evaporation to yield a colourless oil **8** (2.55 g, 14.2 mmol, 123 %). The oily residue **8** was dissolved in dichloromethane (20 mL) in a RBF before adding PCC (3.0 g, 11.5 mmol) and celite (3.0 g) and leaving the reaction to stir for 25 h. Diethyl ether (30 mL) was added to the mixture and the reaction stirred for a further 30 min. The reaction mixture was filtered through a pad of silica in a sintered glass funnel and the filtrate rotary evaporated to afford a green oil that solidified to a strong smelling olive-green crystalline solid **9** (1.59 g, 8.92 mmol, 91%). EI (*m/z,* %): 178(M^+, 27), 149(100), 121(23), 91(6), 65(13).

2.2.10.2 *1-(2H-1,3-benzodioxol-5-yl)-2-bromopropan-1-one (**10**)*

Glacial acetic acid (50 mL) was added to a RBF containing the ketone **9** (1.66 g, 9.32 mmol) and briefly stirred. Bromine (0.62 mL, 12 mmol) was added dropwise over 1 h using a pressure equalising dropping funnel and the reaction mixture left to stir for 5 h. The reaction was quenched by pouring the mixture into 100 mL ice-cold water, and the brominated product **10** was extracted with dichloromethane (4 x 30 mL). The organic extracts were washed with saturated sodium carbonate solution (3 x 30 mL), dried over magnesium sulphate before rotary evaporating to afford an orange oil **10** (2.06 g, 8.01 mmol, 86%). EI (*m/z,* %): 256/258 (M^+, $^{79}Br/^{81}Br$, 8), 149(100), 121(9), 91(9), 65(9).

2.2.10.3 *1-(1,3-benzodioxol-5-yl)-2-(methylamino)propan-1-one hydrochloride (**11**)*

In a RBF, the α-bromoketone **10** (2.06 g, 8.01 mmol) was dissolved in toluene (6 mL) and briefly stirred at room temperature. Separately in two beakers, sodium hydroxide pellets (1.28 g, 32.0 mmol) were dissolved in cold water (1.5 mL) and added to a solution of methylamine hydrochloride (2.16 g, 32.0 mmol) in cold water (1.5 mL). This solution was quickly added to the RBF using a Pasteur pipette and the reaction mixture left to stir for 24 h. The reaction was quenched by pouring into ice-cold water (30 mL). The toluene layer was separated and the aqueous layer further extracted with toluene (3 x 10 mL). The combined toluene extracts were washed with water (3 x 10 mL) and acidified with 1.0 M HCl (4 x 10 mL). Acidic extracts were washed with toluene (3 x 10 mL) and evaporated to dryness to afford a crude mottled white and pink/brown coloured crystalline material **11** (0.810 g, 3.32 mmol, 41%). An acetone wash afforded a bone-white coloured powder **11** (0.575 g, 2.36 mmol, 30%): mp 236-239 °C (dec.)(lit.[333] 248.4 °C); ^{1}H NMR (500 MHz, D_2O) δ, ppm: 7.698-7.678 (dd, $^3J_{HH}$ = 8.25 Hz, $^4J_{HH}$ = 1.75 Hz, 1H), 7.486-7.483 (d, $^4J_{HH}$ = 1.5 Hz, 1H), 7.055-7.038 (d, $^3J_{HH}$= 8.5 Hz, 1H), 6.138-6.134 (d, $^2J_{HH}$= 2.0 Hz, 2H), 4.973-4.930 (q, $^3J_{HH}$= 7.25 Hz, 1H), 2.743 (s, 3H), 1.587-1.573 (d, $^3J_{HH}$= 7.0 Hz, 3H); ^{13}C NMR (125 MHz, CD_3OD) δ, ppm: 194.108, 154.115, 149.412, 127.793, 126.265, 108.592, 108.068, 103.114, 59.540, 30.859, 15.723; EI (*m/z,* %): 207(M^+,1), 149(10), 121(10), 91(5), 65(13), 58(100); FTIR (ATR) ν_{max}, cm^{-1}: 2907 (C-H stretch), 2729 and 2456 (asym. and sym. NH_2^+ stretches), 1676 (C=O stretch), 1602 and 1451 (C=C stretch), 1257 (C-C=O stretch), 1032 (C-O stretch), 883 and 807 (1,2,4-trisubstituted benzene); UV (H_2O) λ_{max}, nm: 235, 281, 319.

2.2.11 Methcathinone (MCAT, 13)

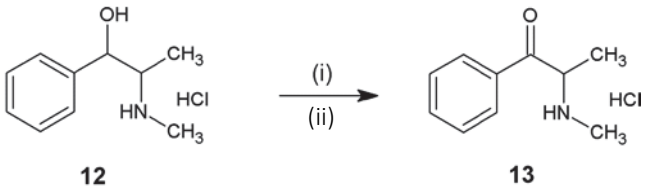

12 13

Figure 2-4. Synthesis of methcathinone HCl (**13**) via oxidation of ephedrine HCl (**12**). The final product salt was obtained following extraction and HCl work-up.
Reagents and conditions: (i) $H^+/KMnO_4$, DCM, RT, 40 min; *(ii)* HCl work-up.

2.2.11.1 *2-(methylamino)-1-phenylpropan-1-one hydrochloride (**13**)*

A 1 L conical flask was charged with ephedrine HCl **12** (2.00 g, 9.92 mmol), potassium permanganate (2.00 g, 12.7 mmol), acetic acid (10 mL) and dichloromethane (200 mL). The solution was stirred at room temperature for 40 min as the solution changed from purple to brown. Solid sodium hydrogen sulphite (approx. 1.20 g, 11.5 mmol) was added to reduce the manganese dioxide formed *in situ*. The aqueous phase was basified with 5 M sodium hydroxide (35 mL) and the dichloromethane layer separated and washed with water (2 x 20 mL). The organic DCM layer was extracted with 1 M HCl (3 x 20 mL) and the combined aqueous extracts washed with dichloromethane (3 x 20 mL). The water was removed via rotary evaporation to afford a white solid **13** (1.53 g, 7.66 mmol, 78%): mp 175-178 °C (dec.)(lit.[334] 176-177 °C); ^{1}H NMR (500 MHz, D_2O) δ, ppm: 7.989-7.974 (d, $^3J_{HH}$= 7.5 Hz, 2H), 7.555-7.726 (t, $^3J_{HH}$= 7.25 Hz, 1H), 7.599-7.569 (t, $^3J_{HH}$= 7.5 Hz, 2H), 5.103-5.062 (q, $^3J_{HH}$= 7.0 Hz, 1H), 2.784 (s, 3H), 1.601-1.566 (d, $^3J_{HH}$= 7.0 Hz, 3H); ^{13}C NMR (125 MHz, CD_3OD) δ, ppm: 196.069, 135.042, 133.194, 129.378, 129.003, 59.676, 30.767, 15.226; EI (*m/z,* %): 163(M^+,0), 132(2), 105(7), 77(19), 58(100), 56(35); FTIR (ATR) ν_{max}, cm^{-1}: 2905 (C-H stretch), 2705 and 2452 (asym. and sym. NH_2^+ stretches), 1688 (C=O stretch), 1596 and 1452 (C=C stretch), 1244 (C-C=O stretch), 697 (mono-substituted benzene); UV (H_2O) λ_{max}, nm: 251.

2.2.12 4-Methylethcathinone (4-MEC, 14)

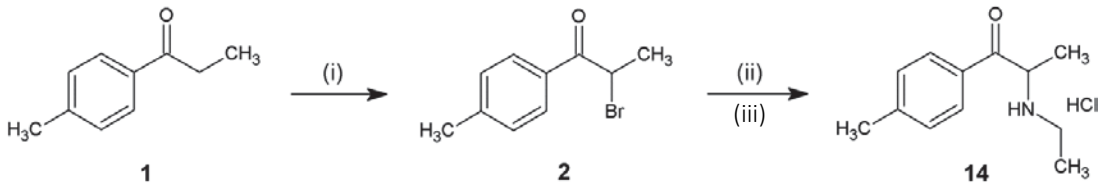

1 2 14

Figure 2-5. Synthesis of 4-methylethcathinone HCl (**14**) via a two step reaction sequence: α-bromination of **1** followed by nucleophilic substitution of **2** with ethylamine. The final product salt was obtained following extraction and HCl work-up.
Reagents and conditions: (i) bromine, glacial acetic acid, RT, 24 h; *(ii)* aq. ethylamine, RT, 18 h; *(iii)* HCl work-up.

2.2.12.1 *2-bromo-4-methylpropiophenone (**2**)*

See section 2.2.8.1 for preparation of **2**.

2.2.12.2 *2-(ethylamino)-1-(4-methylphenyl)propan-1-one hydrochloride (4-MEC) (**14**)*

In a RBF, the α-bromoketone **2** (3.086 g, 13.6 mmol) was dissolved in 5 mL toluene and stirred briefly. Ethylamine solution (0.84 mL, 13.0 mmol) was added to the stirred solution all at once and the reaction left to stir for 18 h. The reaction was quenched by pouring into ice-cold water (100 mL) and subsequently extracted with toluene (3 x 10 mL), washed with water (3 x 10 mL), back-extracted with 1 M HCl (3 x 10 mL) and the aqueous extracts washed with toluene (3 x 10 mL). The water was removed via rotary evaporation to afford a crude mottled tan and white coloured solid **14** (0.722 g, 3.17 mmol, 23%). The crude solid was washed with acetone to afford a fine, white solid **14** (0.488 g, 2.14 mmol, 16%): mp 206-210 °C (dec.)(lit.[335] 210.4 °C); ^{1}H NMR (500 MHz, D_2O) δ, ppm: 7.934-7.918 (d, $^{3}J_{HH}$= 8.0 Hz, 2H), 7.453-7.438 (d, $^{3}J_{HH}$= 7.5 Hz, 2H), 5.120-5.077 (q, $^{3}J_{HH}$= 7.0 Hz, 1H), 3.236-3.167 (dq, $^{2}J_{HH}$= 13.5 Hz, $^{3}J_{HH}$= 7.25 Hz, 1H), 3.145-3.076 (dq, $^{2}J_{HH}$= 13.5 Hz, $^{3}J_{HH}$= 7.25 Hz, 1H), 2.441 (s, 3H), 1.595-1.580 (d, $^{3}J_{HH}$= 7.5 Hz, 3H), 1.360-1.331 (t, $^{3}J_{HH}$= 7.25 Hz, 3H); ^{13}C NMR (125 MHz, $CDCl_3$) δ, ppm: 194.544, 146.171, 130.577, 130.023, 129.101, 57.987, 42.226, 21.950, 16.985, 11.925; EI (*m/z,* %): 191(M^+,0), 146(1), 119(8), 91(14), 72(100), 65(9), 44(21); FTIR (ATR) ν_{max}, cm^{-1}: 2925 (C-H stretch), 2689 and 2476 (asym. and sym. NH_2^+ stretches), 1687 (C=O stretch), 1605 and 1439 (C=C stretch), 1240 (C-C=O stretch), 831 and 686 (1,4-disubstituted benzene); UV (H_2O) λ_{max}, nm: 263.

2.2.13 4-Methylpyrrolidinopropiophenone (4-MPPP, 15)

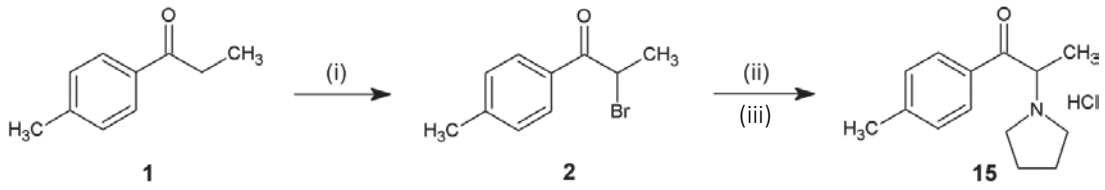

Figure 2-6. Synthesis of 4-methylpyrrolidinopropiophenone HCl (**15**) via a two step reaction sequence: α-bromination of **1** followed by nucleophilic substitution of **2** with pyrrolidine. The final product salt was obtained following extraction and HCl work-up.
Reagents and conditions: (i) bromine, glacial acetic acid, RT, 1.5 h; *(ii)* pyrrolidine, Et_2O, RT, 18 h; *(iii)* HCl work-up.

2.2.13.1 *2-bromo-1-(4-methylphenyl)propan-1-one (**2**)*

See section 2.2.8.1 for preparation of **2**.

2.2.13.2 *1-(4-methylphenyl)-2-(pyrrolidin-1-yl)propan-1-one hydrochloride (**15**)*

In a RBF, the α-bromoketone **2** (2.27 g, 10.0 mmol) was dissolved in diethyl ether (18 mL) and cooled in an ice bath. Pyrrolidine (1.80 mL, 22 mmol) was added at once to the stirred solution and the mixture left to stir at room temperature for 18 h. Water (10 mL) was added to the reaction and the ether layer separated. The aqueous layer was extracted with diethyl ether (2 x 10 mL) and the combined extracts were back-extracted with 1 M HCl (2 x 10 mL). The aqueous extracts were washed with ether (2 x 10 mL) and the water removed via rotary evaporation to afford a crude brown-orange residue with the texture of toffee. The crude substance was washed with small portions of acetone to afford a light brown powder **15** (0.60 g, 2.4 mmol, 24 %): mp 210-213 °C (dec.)(lit.[336] 224.2 °C); ^{1}H NMR (500 MHz, $CDCl_3$) δ, ppm: 7.822-7.805 (d, $^3J_{HH}$= 8.5 Hz, 2H), 7.345-7.329 (d, $^3J_{HH}$= 8.0 Hz, 2H), 5.150-5.106 (q, $^3J_{HH}$= 7.5 Hz, 1H), 3.747-3.728 (m, 2H), 2.451 (s, 3H), 2.227-2.169 (m, 6H), 1.823-1.809 (d, $^3J_{HH}$= 7.0 Hz, 3H); ^{13}C NMR (125 MHz, $CDCl_3$) δ, ppm: 195.156, 146.408, 131.288, 130.043, 128.655, 60.147, 21.831, 16.706; EI (*m/z,* %): 217(M^+,0), 119(4), 98(100), 91(11), 65(9), 56(18); FTIR (ATR) ν_{max}, cm^{-1}: 2956 (C-H stretch), 2568 (NH^+ stretch), 1686 (C=O stretch), 1605 and 1448 (C=C stretch), 1245 (C-C=O stretch), 829 and 687 (1,4-disubstituted benzene); UV (H_2O) λ_{max}, nm: 264.

2.2.14 3,4-Methylenedioxypyrovalerone (MDPV, 19)

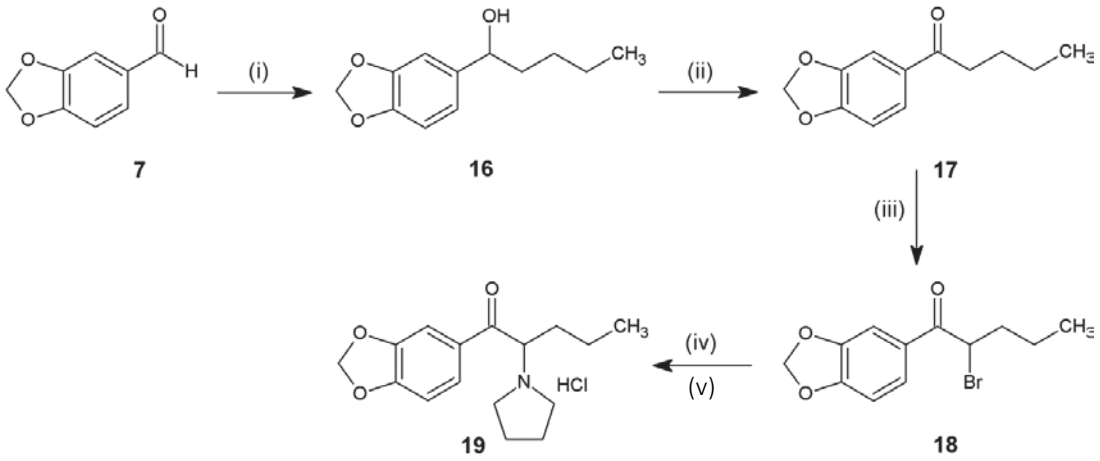

Figure 2-7. Synthesis of MDPV HCl (**19**) via a four step reaction sequence: Grignard reaction of piperonal (**7**), oxidation of **16**, α-bromination of **17** and nucleophilic substitution of **18** with pyrrolidine. The final product salt was obtained following extraction and HCl work-up.
Reagents and conditions: (i) BuMgCl, Et_2O, N_2 atm., RT, 2 h; *(ii)* PCC/celite, DCM, 18 h; *(iii)* bromine, glacial acetic acid, RT, 17.5 h; *(iv)* pyrrolidine, Et_2O, RT, 19 h; *(v)* HCl work-up.

2.2.14.1 *1-(2H-1,3-benzodioxol-5-yl)pentan-1-one (**17**)*

To a RBF maintained under nitrogen atmosphere was added piperonal **7** (1.2013 g, 8.00 mmol). Diethyl ether (10 mL) was added via syringe and the solution stirred to dissolve the solid. The flask was kept on an ice bath while butylmagnesium chloride solution (6.0 mL, 12 mmol) was added dropwise via syringe over 3 min. The ice bath was removed after 10 min and the reaction stirred for 2 h. To the RBF was added 1 M HCl (6 mL, 6 mmol) and the mixture stirred briefly. The ether layer was separated and washed with water (3 x 5 mL). The ether extract was dried over anhydrous sodium sulphate before removing the solvent via rotary evaporation to afford a light yellow oil **16** (1.55 g, 7.42 mmol, 93%). The oil was dissolved in dichloromethane (12 mL) in a RBF before adding pyridinium chlorochromate (PCC) (1.0 g, 4.6 mmol) and celite (1.0 g) sequentially and leaving the mixture to stir for 17 h. Diethyl ether (30 mL) was added to the flask and the reaction stirred for a further 1 h. The reaction mixture was filtered through a pad of silica in a sintered glass funnel and the filtrate rotary evaporated to afford a yellow oil with dark droplets on the surface **17** (1.53 g, 7.42 mmol, 93%). EI (*m/z,* %): 206(M^+,0), 192(24), 164(6), 149(100), 121(16), 91(3), 65(8).

2.2.14.2 *1-(2H-1,3-benzodioxol-5-yl)-2-bromopentan-1-one (**18**)*

In a RBF, the ketone **17** (1.530 g, 7.42 mmol) was dissolved in glacial acetic acid (60 mL) and a pressure equalising dropping funnel containing bromine (0.41 mL, 8.0 mmol) was attached. One drop of bromine was initially added and the mixture stirred for 30 min. The remaining bromine was added dropwise over 10 min and the mixture left to stir for 17.5 h. The reaction was quenched by pouring the mixture into ice-cold water (100 mL). The aqueous mixture was extracted with dichloromethane (3 x 50 mL) and the combined extracts were washed with saturated sodium carbonate solution (3 x 50 mL) before drying over magnesium sulphate. The solvent was removed via rotary evaporation to afford an orange oil **18** (2.02 g, 7.07 mmol, 95%). EI (*m/z,* %): 284/286 (M^+, $^{79}Br/^{81}Br$, 3), 242/244 ($^{79}Br/^{81}Br$, 2), 205(4), 149(100), 121(11), 65(5).

2.2.14.3 *1-(2H-1,3-benzodioxol-5-yl)-2-(pyrrolidin-1-yl)propan-1-one hydrochloride (**19**)*

In an RBF, the α-bromoketone **18** (2.016 g, 7.07 mmol) was dissolved in diethyl ether (15 mL) and cooled on an ice bath. Pyrrolidine (1.5 mL, 18 mmol) was added all at once and the reaction left to stir for 19 h. Diethyl ether (10 mL) and water (10 mL) were added to the RBF before extracting the mixture with diethyl ether (3 x 15 mL) and washing the ethereal extracts with water (3 x 15 mL). The mixture was back-extracted with 1 M HCl (3 x 15 mL) and the aqueous extracts were washed with diethyl ether (3 x 10 mL). The water was removed via rotary evaporation and the residue dried under vacuum overnight to afford a crude brown coloured residue with a toffee-like texture. The crude material was washed with small portions of acetone to afford an off-white, bone coloured powder **19** (0.776 g, 2.49 mmol, 35%): mp 235-238 °C (dec.)(lit.[337] 238-239 °C); ^{1}H NMR (500 MHz, D_2O) δ, ppm: 7.725-7.709 (d, $^3J_{HH}$= 8.0 Hz, 1H), 7.496 (s, 1H), 7.061-7.044 (d, $^3J_{HH}$= 8.5 Hz, 1H), 6.148-6.142 (d, $^4J_{HH}$= 3.0 Hz, 2H), 5.122 (br. s, 1H), 3.455-3.284 (m, 4H), 2.128-1.999 (m, 6H), 1.248-1.147 (m, 2H), 0.850-0.821 (t, $^3J_{HH}$= 7.25 Hz, 3H); ^{13}C NMR (125 MHz, CD_3OD) δ, ppm: 194.334, 153.024, 148.416, 128.728, 126.008, 108.726, 107.979, 102.706, 61.799, 32.142, 31.566, 24.389, 17.295, 13.855; EI (*m/z,* %): 275(M^+,0), 149(5), 126(100), 96(4), 55(5); FTIR (ATR) ν_{max}, cm^{-1}: 2969 (C-H stretch), 2610 (NH^+ stretch), 1684 (C=O stretch), 1609 and 1435 (C=C stretch), 1253 (C-C=O stretch), 1033 (C-O), 867 and 807 (1,2,4-trisubstituted benzene); UV (H_2O) λ_{max}, nm: 237, 285, 324.

2.2.15 1-(1,3-benzodioxol-5-yl)-2-(methylamino)butan-1-one (butylone, 23)

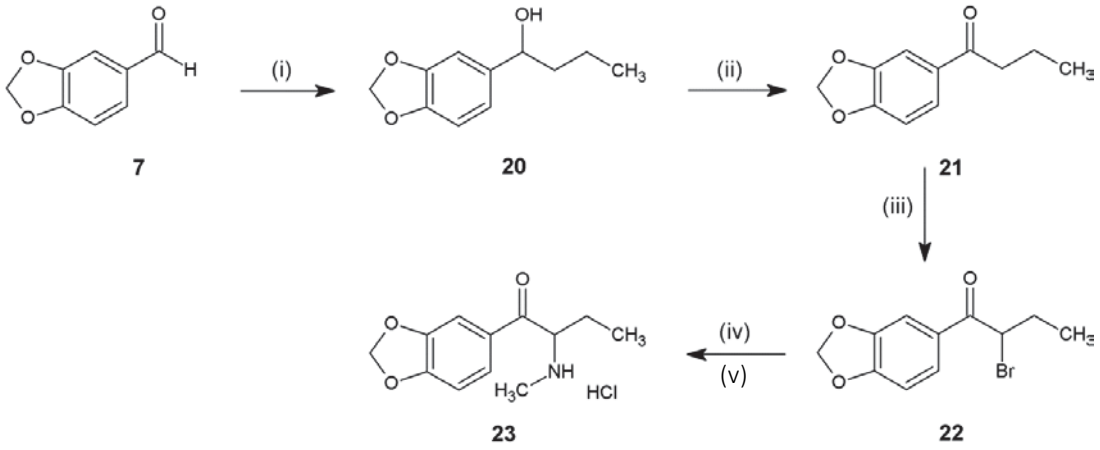

Figure 2-8. Synthesis of butylone HCl (**23**) via a four step reaction sequence: Grignard reaction of piperonal (**7**), oxidation of **20**, α-bromination of **21** and nucleophilic substitution of **22** with methylamine. The final product salt was obtained following extraction and HCl work-up. *Reagents and conditions: (i)* PropMgCl, Et_2O, N_2 atm., RT, 4 h; *(ii)* PCC/celite, DCM, 21 h; *(iii)* bromine, glacial acetic acid, RT, 18 h; *(iv)* pyrrolidine, Et_2O, RT, 20 h; *(v)* HCl work-up.

2.2.15.1 *1-(2H-1,3-benzodioxol-5-yl)butan-1-one (**21**)*

To a RBF maintained under nitrogen atmosphere was added piperonal **7** (1.50 g, 10.0 mmol). Diethyl ether (10 mL) was added via syringe and the solution stirred to dissolve the solid. The flask was kept on ice while propylmagnesium chloride solution (6.0 mL, 12 mmol) was added via syringe over 3 min. The ice bath was removed after 10 min and the reaction stirred for 4 h before carefully adding 1 M HCl (10 mL, 10 mmol). The ether layer was separated, washed with water (3 x 5 mL) and dried over magnesium sulphate before removing the solvent via rotary evaporation to afford a cloudy oil **20** (1.76 g, 9.06 mmol, 91%). The oily residue **20** was dissolved in dichloromethane (20 mL) in a RBF before adding PCC (2.5 g, 11.5 mmol) and celite (2.5 g) and leaving the reaction to stir for 20.5 h. Diethyl ether (30 mL) was added to the mixture and the reaction stirred for a further 30 min. The reaction mixture was filtered through a pad of silica in a sintered glass funnel and the filtrate was rotary evaporated to afford a yellow-brown oil **21** (1.58 g, 8.22 mmol, 82%). EI (*m/z,* %): 192(M^+,0), 177(2), 164(52), 149(100), 121(21), 91(4), 65(20).

2.2.15.2 *1-(2H-1,3-benzodioxol-5-yl)-2-bromobutan-1-one (**22**)*

The ketone **21** (1.58 g, 8.22 mmol) was dissolved in glacial acetic acid (50 mL) in a RBF and a pressure equalising dropping funnel containing bromine (0.50 mL, 9.0 mmol) was attached. A few drops of bromine were added initially and the reaction stirred for 30 min, after which, the remaining bromine was added dropwise. After 18 h of stirring, the reaction was quenched by pouring the mixture into ice-cold water (100 mL). The mixture was extracted with dichloromethane (3 x 40 mL) and carefully washed with sodium carbonate solution (3 x 30 mL). The organic fraction was dried over magnesium sulphate before decanting and removing the solvent via rotary evaporation to afford an orange-brown oil **22** (2.09 g, 7.71 mmol, 94%). EI (*m/z,* %): 270/272 (M^+, $^{79}Br/^{81}Br$, 6), 270(M^+,6), 190(1), 149(100), 121(13), 65(6).

2.2.15.3 *1-(1,3-benzodioxol-5-yl)-2-(methylamino)butan-1-one hydrochloride (**23**)*

In a RBF, the α-bromoketone **22** (2.09 g, 7.71 mmol) was dissolved in toluene (5 mL) and stirred at room temperature briefly. Separately in two beakers, sodium hydroxide pellets (1.28 g, 32.0 mmol) were dissolved in cold water (2.5 mL) and added to a solution of methylamine hydrochloride (2.16 g, 32.0 mmol) in cold water (2 mL). This combined solution was quickly added dropwise to the RBF using a Pasteur pipette and the reaction mixture left to stir for 20 h. The reaction was quenched by pouring the mixture into ice-cold water (30 mL). The toluene layer was separated and the aqueous layer further extracted with toluene (3 x 10 mL). Combined toluene extracts were washed with water (3 x 10 mL) and acidified with 1 M HCl (5 x 10 mL). Acidic extracts were washed with toluene (3 x 10 mL) and evaporated to dryness to afford an off-white coloured crystalline material **23** (1.48 g, 5.74 mmol, 74%): mp 222-227 °C (dec.)(lit.[338] 243.6 °C); ^{1}H NMR (500 MHz, D_2O) δ, ppm: 7.705-7.686 (dd, $^3J_{HH}$= 8.25 Hz, $^4J_{HH}$= 1.25 Hz, 1H), 7.481-7.478 (d, $^4J_{HH}$= 1.5 Hz, 1H), 7.045-7.028 (d, $^3J_{HH}$= 8.5 Hz, 1H), 6.134-6.130 (d, $^2J_{HH}$= 2.0 Hz, 2H), 5.025-5.003 (t, $^3J_{HH}$= 5.5 Hz, 1H), 2.741 (s, 3H), 2.131-2.040 (m, 2H), 0.889-0.859 (t, $^3J_{HH}$= 7.5 Hz, 3H); ^{13}C NMR (125 MHz, CD_3OD) δ, ppm: 194.114, 153.006, 148.401, 128.603, 125.986, 108.719, 107.987, 102.687, 62.641, 31.494, 23.187, 8.385; EI (*m/z,* %): 221(M^+,0), 219(2), 149(11), 121(7), 72(100), 70(30); FTIR (ATR) ν_{max}, cm^{-1}: 2909 (C-H stretch), 2689 and 2475 (asym. and sym. NH_2^+ stretches), 1674 (C=O stretch), 1602 and 1452 (C=C stretch), 1252 (C-C=O stretch), 1035 (C-O stretch), 880 and 802 (1,2,4-trisubstituted benzene); UV (H_2O) λ_{max}, nm: 236, 282, 321.

2.2.16 1-(1,3-benzodioxol-5-yl)-2-(methylamino)pentan-1-one (pentylone, 24)

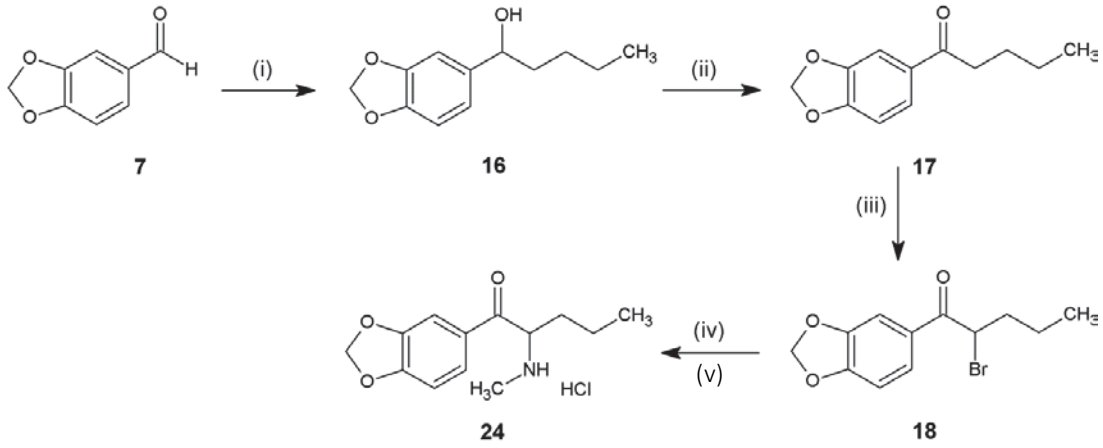

Figure 2-9. Synthesis of pentylone HCl (**24**) via a four step reaction sequence: Grignard reaction of piperonal (**7**), oxidation of **16**, α-bromination of **17** and nucleophilic substitution of **18** with methylamine. The final product salt was obtained following extraction and HCl work-up.
Reagents and conditions: (i) ButMgCl, Et_2O, N_2 atm., RT, 4 h; *(ii)* PCC/celite, DCM, RT, 21 h; *(iii)* bromine, glacial acetic acid, RT, 18 h; *(iv)* pyrrolidine, Et_2O, RT, 19 h; *(v)* HCl work-up.

2.2.16.1 *1-(2H-1,3-benzodioxol-5-yl)pentan-1-one (**17**)*

See section 2.2.14.1 for preparation of **17**.

2.2.16.2 *1-(2H-1,3-benzodioxol-5-yl)-2-bromopentan-1-one (**18**)*

See section 2.2.14.2 for preparation of **18**.

2.2.16.3 *1-(1,3-benzodioxol-5-yl)-2-(methylamino)pentan-1-one hydrochloride (**24**)*

In a RBF, the α-bromoketone **18** (2.30 g, 8.01 mmol) was dissolved in toluene (5 mL) and stirred at room temperature briefly. Separately in two beakers, sodium hydroxide pellets (1.28 g, 32.0 mmol) were dissolved in cold water (2.5 mL) and added to a solution of methylamine hydrochloride (2.16 g, 32.0 mmol) dissolved in cold water (2 mL). The combined solution was quickly added (dropwise) to the RBF using a Pasteur pipette and the reaction mixture left to

stir for 19 h. The reaction was quenched by pouring the mixture into ice-cold water (30 mL). The toluene layer was separated and the aqueous layer further extracted with toluene (3 x 15 mL). Combined toluene extracts were washed with water (3 x 10 mL) and acidified with 1 M HCl (3 x 10 mL). Acidic extracts were washed with toluene (3 x 10 mL) and evaporated to dryness to afford an off-white coloured crystalline material **24** (1.61 g, 5.94 mmol, 74%): mp 216-222 °C (dec.)(lit.[339] 242.0 °C); ^{1}H NMR (500 MHz, D_2O) δ, ppm: 7.696-7.679 (d, $^{3}J_{HH}$= 7.5 Hz, 1H), 7.467 (s, 1H), 7.040-7.023 (d, $^{3}J_{HH}$= 8.5 Hz, 1H), 6.129 (s, 2H), 5.024-5.002 (t, $^{3}J_{HH}$= 5.5 Hz, 1H), 2.734 (s, 3H), 2.031-1.916 (m, 2H), 1.365-1.218 (m, 2H), 0.874-0.845 (t, $^{3}J_{HH}$= 7.25 Hz, 3H); ^{13}C NMR (125 MHz, CD_3OD) δ, ppm: 194.334, 153.024, 148.416, 128.728, 126.008, 108.726, 107.979, 102.706, 61.799, 32.142, 31.566, 17.295, 13.855; EI (*m/z,* %): 235(M^+,0), 192(24), 164(8), 149(100), 121(20), 91(4), 65(9); FTIR (ATR) ν_{max}, cm^{-1}: 2963 (C-H stretch), 2744 and 2481 (asym. and sym. NH_2^+ stretches), 1675 (C=O stretch), 1603 and 1453 (C=C stretch), 1256 (C-C=O stretch), 1033 (C-O stretch), 863 and 806 (1,2,4-trisubstituted benzene); UV (H_2O) λ_{max}, nm: 236, 282, 321.

2.2.17 1-(4-methylphenyl)-2-(pyrrolidin-1-yl)pentan-1-one (pyrovalerone, 29)

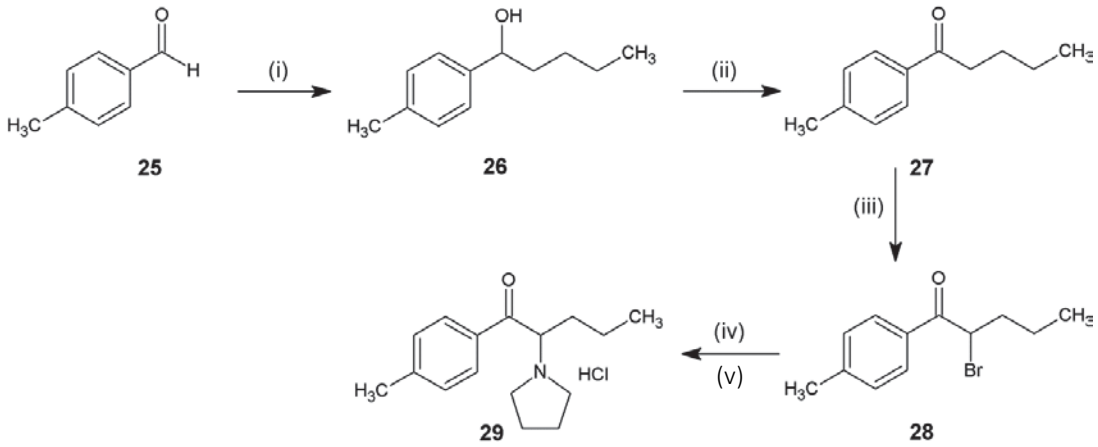

Figure 2-10. Synthesis of pyrovalerone HCl (**29**) via a four step reaction sequence: Grignard reaction of *p*-tolualdehyde (**25**), oxidation of **26**, α-bromination of **27** and nucleophilic substitution of **28** with pyrrolidine. The final product salt was obtained following extraction and HCl work-up.
Reagents and conditions: (i) BuMgCl, Et_2O, N_2 atm., RT, 4 h; *(ii)* PCC/celite, DCM, 26.5 h; *(iii)* bromine, glacial acetic acid, RT, 5 h; *(iv)* pyrrolidine, Et_2O, RT, 5 h; *(v)* HCl work-up.

2.2.17.1 *1-(4-methylphenyl)pentan-1-one (**27**)*

To a RBF maintained under nitrogen atmosphere was added *p*-tolualdehyde **25** (1.18 mL, 10.0 mmol). Dry diethyl ether (15 mL) was added via syringe and the solution stirred. The flask was kept on an ice bath as butylmagnesium chloride solution (6.0 mL, 12 mmol) was added via syringe. The ice bath was removed after 10 min and the reaction stirred for 4 h before carefully adding 1 M HCl (10 mL, 10 mmol). The ether layer was separated and washed with water (3 x 5 mL) before drying over anhydrous sodium sulphate. The solvent was decanted and removed via rotary evaporation to afford a light yellow oil **26** (2.03 g, 11.4 mmol, 114%). The oil was dissolved in dichloromethane (25 mL) in a RBF before adding PCC (3.0 g, 13.9 mmol) and celite (2.5 g) sequentially and leaving the mixture to stir for 26 h. Diethyl ether (30 mL) was added to the flask and the reaction stirred for a further 0.5 h. The reaction mixture was filtered through a pad of silica in a sintered glass funnel and the filtrate rotary evaporated to afford an orange-brown oil **27** (1.89 g, 10.7 mmol, 107%). EI (*m/z,* %): 176(M^+,6), 161(4), 134(43), 119(100), 91(35), 65(11).

2.2.17.2 *2-bromo-1-(4-methylphenyl)pentan-1-one (**28**)*

In a RBF, the ketone **27** (1.89 g, 10.7 mmol) was dissolved in glacial acetic acid (50 mL) and a pressure equalising dropping funnel containing bromine (0.57 mL, 11 mmol) was attached. One drop of bromine was initially added and the mixture stirred for 30 min before adding the remaining bromine dropwise over 10 min and stirring for 5 h. The reaction was quenched by pouring into ice-cold water (100 mL). The mixture was then extracted with dichloromethane (3 x 40 mL, 1 x 20 mL) and carefully washed with saturated sodium carbonate solution (3 x 40 mL). The solvent was removed via rotary evaporation to afford a yellow oil **28** (2.42 g, 9.47 mmol, 89%). EI (*m/z,* %): 254/256 (M^+, $^{79}Br/^{81}Br$, 0), 212/214 ($^{79}Br/^{81}Br$, 1), 175(9), 119(100), 91(19), 65(11).

2.2.17.3 *1-(4-methylphenyl)-2-(pyrrolidin-1-yl)pentan-1-one hydrochloride (**29**)*

In a RBF the α-bromoketone **28** (2.42 g, 9.47 mmol) was dissolved in diethyl ether (10 mL) and cooled in an ice bath. Pyrrolidine (1.72 mL, 21 mmol) was added all at once and the reaction

left to stir for 5 h. Diethyl ether (10 mL) and water (10 mL) were added to the RBF before separating the ether layer and further extracting the aqueous layer with ether (4 x 10 mL). Combined ethereal extracts were washed with water (3 x 15 mL) and acidified with 1 M HCl (3 x 15 mL). Saturated sodium carbonate solution (40 mL) was added to the aqueous extracts and the product extracted with diethyl ether (3 x 20 mL) a second time. Combined ethereal extracts were dried over magnesium sulphate and HCl gas bubbled through the ethereal solution to form the crude hydrochloride salt as a light brown coloured powder (1.639 g, 5.82 mmol, 62%). The crude product was washed with acetone to afford an off-white cream coloured powder **29** (0.324 g, 1.15 mmol, 12%): mp 176-179 °C (dec.)(lit.[340] 180 °C); ^{1}H NMR (500 MHz, $CDCl_3$) δ, ppm: 7.865-7.848 (d, $^{3}J_{HH}$= 8.5 Hz, 2H), 7.357-7.342 (d, $^{3}J_{HH}$= 7.5 Hz, 2H), 5.101-5.073 (dd, $^{3}J_{HH}$= 8.25 Hz, $^{3}J_{HH}$= 5.75 Hz, 1H), 3.877 (s, 1H), 3.778, (s, 1H), 3.650 (s, 1H), 2.794 (s, 1H), 2.459, (s, 3H), 2.268-1.971 (m, 6H), 1.690 (s, 2H), 1.499 -1.304 (m, 2H), 0.929-0.900 (t, $^{3}J_{HH}$= 7.25 Hz, 3H); ^{13}C NMR (125 MHz, $CDCl_3$) δ, ppm: 196.241, 146.719, 133.503, 130.146, 128.648, 61.623, 52.868, 48.624, 33.048, 23.990, 23. 743, 21.843, 19.741, 13.971; EI (*m/z,* %): 245(M^+,0), 127(9), 126(100), 91(5); FTIR (ATR) ν_{max}, cm^{-1}: 2958(C-H stretch), 2612(NH^+ stretch), 1677(C=O stretch), 1604 and 1443(C=C stretch), 1235(C-C=O stretch), 841 (1,4-disubstituted benzene); UV (H_2O) λ_{max}, nm: 266.

2.2.18 α-Pyrrolidinopentiophenone (α-PVP, 34)

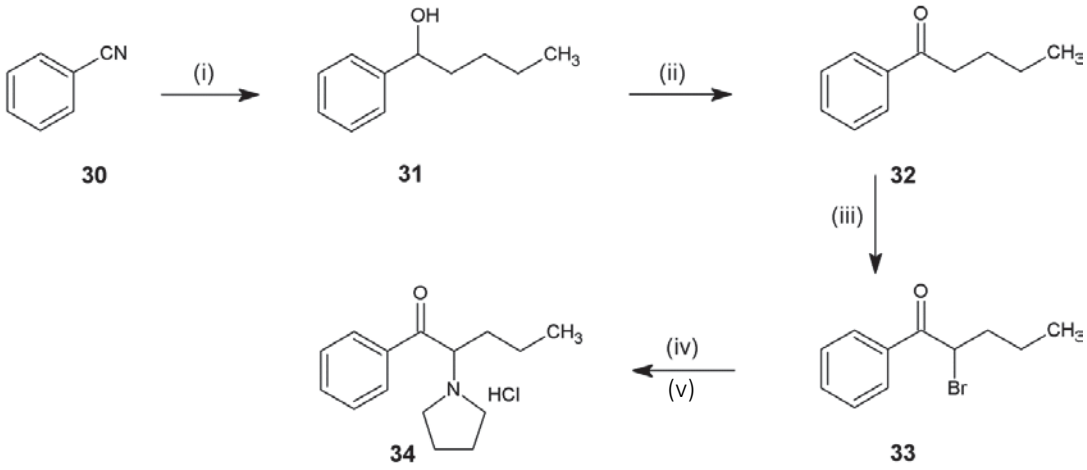

Figure 2-11. Synthesis of α-PVP HCl (**34**) via a four step reaction sequence: Grignard reaction of benzonitrile (**30**), oxidation of **31**, α-bromination of **32**, and nucleophilic substitution of **33** with pyrrolidine. The final product salt was obtained following extraction and HCl work-up.
Reagents and conditions: (i) BuMgCl, Et_2O, N_2 atm., RT, 3 h; *(ii)* PCC/celite, DCM, 10 min; *(iii)* bromine, glacial acetic acid, RT, 40 h; *(iv)* pyrrolidine, Et_2O, RT, 25 h; *(v)* HCl work-up.

2.2.18.1 *1-phenylpentan-1-one (**32**)*

To a RBF containing dried toluene (20 mL) and butylmagnesium chloride solution (6 mL, 12 mmol) was added benzonitrile (1.00 mL, 10.0 mmol) in portions, dropwise over 30 min. This reaction was left to stir at room temperature for 3 h before pouring the mixture onto ice and adding conc. sulphuric acid (2 mL) while stirring. The mixture was extracted with diethyl ether (3 x 20 mL) and dried over magnesium sulphate. The fraction was decanted and the solvent removed via rotary evaporation to afford an orange oil **32** (1.18 g, 7.28 mmol, 73%). EI (*m/z,* %): 162(M^+,7), 133(3), 120(50), 105(100), 77(41), 51(9).

2.2.18.2 *2-bromo-1-phenylpentan-1-one (**33**)*

The ketone **32** (1.180 g, 7.28 mmol) was dissolved in glacial acetic acid (45 mL) in a RBF and a pressure equalising dropping funnel containing bromine (0.80 mL, 16 mmol) was attached. One drop of bromine was initially added and the mixture left to stir for 15 min. The remaining bromine was added dropwise and the reaction stirred for a further 40 h. The reaction was quenched by pouring into cold water (100 mL) and the aqueous layer extracted with dichloromethane (3 x 40 mL). The combined DCM extracts were washed with saturated sodium carbonate solution (3 x 40 mL) and dried over magnesium sulphate. The fraction was decanted and the solvent removed via rotary evaporation to afford a yellow oil **33** (1.68 g, 6.97 mmol, 96%). EI (*m/z,* %): 240/242 (M^+, $^{79}Br/^{81}Br$, 0), 198/200 ($^{79}Br/^{81}Br$, 3), 161(10), 105(100), 77(27), 51(6).

2.2.18.3 *1-phenyl-2-(pyrrolidin-1-yl)pentan-1-one (**34**)*

In a RBF, the α-bromoketone **34** (1.68 g, 6.97 mmol) was dissolved in diethyl ether (10 mL). Pyrrolidine (18 mmol, 1.30 g, 1.47 mL) was added all at once and the reaction mixture stirred for a further 25 h before adding water (10 mL) and extracting the aqueous layer with diethyl ether (4 x 10 mL). The ether layer was then back-extracted with 1M HCl (4 x 10 mL), washed with ether (4 x 10 mL) and the aqueous fraction rotary evaporated to afford a crude, thick, orange-brown oil. The oil was dried under vacuum overnight, dissolved in chloroform and filtered through a layer of silicic acid in a sintered glass funnel. The filtrate was dried over sodium sulphate and rotary evaporated to afford a mixed light brown and white solid **34**

(0.2103 g, 0.785 mmol, 11%): mp 101-104 °C (lit.[341] 161.3 °C); ^{1}H NMR (500 MHz, D_2O) δ, ppm: 8.05-8.04 (d, $^{3}J_{HH}$= 8.0 Hz, 2H), 7.82-7.79 (t, $^{3}J_{HH}$= 7.5 Hz, 1H), 7.65-7.62 (t, $^{3}J_{HH}$= 7.5 Hz, 2H), 5.28-5.26 (t, $^{3}J_{HH}$= 5.0 Hz, 1H), 3.51 (s, 2H), 3.41 (s, 2H), 2.15-2.07 (m, 6H), 1.29-1.11 (m, 2H), 0.82-0.79 (t, $^{3}J_{HH}$= 7.5 Hz, 3H); ^{13}C NMR (125 MHz, $CDCl_3$) δ, ppm: 196.844, 135.794, 135.149, 129.429, 128.571, 62.594, 32.991, 23.879, 19.634, 13.997; EI (*m/z,* %): 231(M^+,0), 229(1), 188(1), 126(100), 105(4), 77(8), 55(4); FTIR (ATR) ν_{max}, cm^{-1}: 2960 (C-H stretch), 2689 (NH^+ stretch), 1681 (C=O stretch), 1595 and 1449 (C=C stretch), 1233 (C-C=O stretch), 719 (monosubstituted benzene); UV (H_2O) λ_{max}, nm: 254.

2.2.19 4-Ethylmethcathinone (4-EMC, 39)

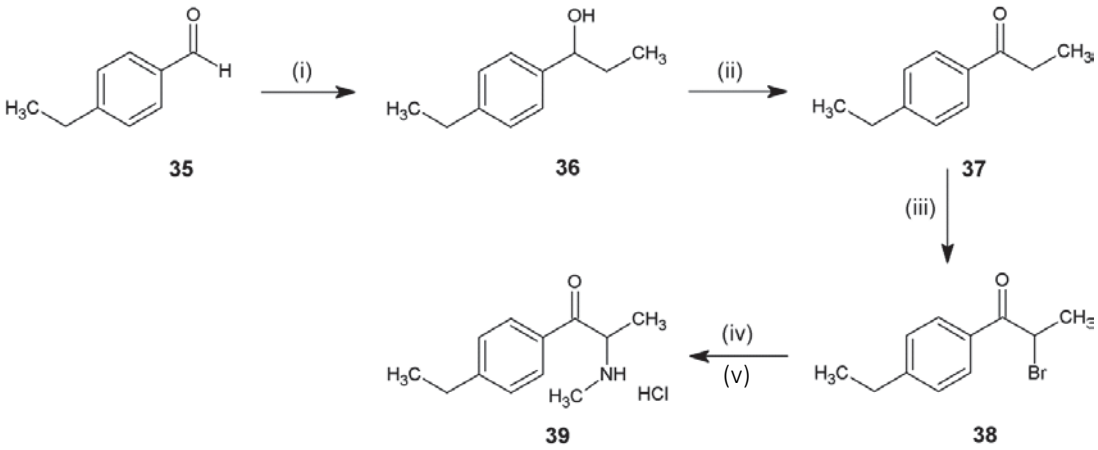

Figure 2-12. Synthesis of 4-EMC HCl (**39**) via a four step reaction sequence: Grignard reaction of p-ethylbenzaldehyde (**35**), oxidation of **36**, α-bromination of **37**, and nucleophilic substitution of **38** with methylamine. The final product salt was obtained following extraction and HCl work-up.
Reagents and conditions: (i) EthMgCl, Et_2O, N_2 atm., RT, 4 h; *(ii)* PCC/celite, DCM, 10 min; *(iii)* bromine, glacial acetic acid, RT, 40 h; *(iv)* aq. methylamine, Et_2O, RT, 25 h; *(v)* HCl work-up.

2.2.19.1 *1-(4-ethylphenyl)propan-1-one (**37**)*

In a RBF maintained under a nitrogen atmosphere, 4-ethylbenzaldehyde **35** (2.05 mL, 15.0 mmol) was dissolved in diethyl ether (10 mL). The flask was kept on an ice bath while ethylmagnesium chloride (8.0 mL, 16 mmol) was added via syringe. The ice bath was removed after 10 min and the reaction stirred for 4 h. To the RBF was added 1.0 M HCl (20 mL) and the mixture stirred briefly. The ether layer was separated and washed with water (3 x 5 mL). The ether extract was dried over magnesium sulphate, decanted and the solvent removed via rotary evaporation to afford a colourless oil **36** (2.32 g, 14.1 mmol). The oil was dissolved in

dichloromethane (25 mL) in a RBF before adding PCC (3.23 g, 15 mmol) and celite (3 g) sequentially. The reaction was stirred at room temperature for 30 h before adding diethyl ether (30 mL) and continuing to stir for 1 h. The reaction mixture was filtered through a pad of silicic acid in a sintered glass funnel and the filtrate was rotary evaporated to afford a green oil **37** (2.02 g, 12.5 mmol, 83%). EI (*m/z,* %): 162(M^+,10), 133(100), 105(16), 79(11), 77(12).

2.2.19.2 *2-bromo-1-(4-ethylphenyl)propan-1-one (**38**)*

In a RBF, the ketone **37** (2.02 g, 12.5 mmol) was dissolved in glacial acetic acid (50 mL) and a dropping funnel containing bromine (0.72 mL, 14 mmol) was attached. One drop of bromine was initially added and the reaction stirred for 30 min. The remaining bromine was then added dropwise and the reaction left to stir for 19.5 h. The reaction was quenched by pouring the mixture into ice-cold water (100 mL). The aqueous mixture was extracted with dichloromethane (3 x 30 mL) and washed with saturated sodium carbonate solution (4 x 30 mL). The dichloromethane extracts were dried over magnesium sulphate, decanted and rotary evaporated to dryness to afford a yellow oil with white precipitates **38** (2.86 g, 11.9 mmol, 95%). EI (*m/z,* %): 240/242 (M^+, $^{79}Br/^{81}Br$, 1), 133(100), 105(14), 79(7), 77(7).

2.2.19.3 *1-(4-ethylphenyl)-2-(methylamino)propan-1-one hydrochloride (**39**)*

In a RBF, the α-bromoketone **38** (2.86 g, 11.9 mmol) was dissolved in toluene (5 mL) and briefly stirred at room temperature. Separately in two beakers, sodium hydroxide pellets (1.92 g, 48 mmol) were dissolved in cold water (2 mL) and added to a solution of methylamine hydrochloride (3.24 g, 48 mmol) in cold water (2 mL). The combined solution was quickly added to the RBF using a Pasteur pipette and the reaction mixture left to stir for 19 h. The reaction was quenched by pouring into ice-cold water (30 mL). The toluene layer was separated and the aqueous layer further extracted with toluene (3 x 10 mL). Combined toluene extracts were washed with water (3 x 10 mL) and back-extracted with 1 M HCl (4 x 10 mL). The combined acidic aqueous extracts were washed with toluene (3 x 10 mL) and rotary evaporated to dryness to afford a crude gold and white coloured solid **39** (2.14 g, 9.40 mmol, 79%). The crude material was then washed with acetone to afford a white powder **39** (1.77 g, 7.78 mmol, 65%). mp 179-181 °C (dec.)(lit.[342] 182.2 °C); ^{1}H NMR (500 MHz, D_2O) δ, ppm:

7.964-7.947 (d, $^3J_{HH}$= 8.5 Hz, 2H), 7.498-7.482 (d, $^3J_{HH}$= 8.0 Hz, 2H), 5.082-5.038 (q, $^3J_{HH}$= 7.5 Hz, 1H), 2.789 (s, 3H), 2.778-2.731 (q, $^3J_{HH}$= 8.0 Hz, 2H), 1.601-1.586 (d, $^3J_{HH}$= 7.5 Hz, 3H), 1.255-1.224 (t, $^3J_{HH}$= 7.75 Hz, 3H); ^{13}C NMR (125 MHz, $CDCl_3$) δ, ppm: 194.551, 152.213, 130.773, 129.252, 128.823, 59.459, 31.801, 29.192, 16.537, 15.137; EI (*m/z,* %): 191(M^+,0), 160(2), 133(5), 103(3), 77(7), 58(100), 56(18); FTIR (ATR) ν_{max}, cm^{-1}: 2969 (C-H stretch), 2681 and 2459 (asym. and sym. NH_2^+ stretches), 1684 (C=O stretch), 1605 and 1470 (C=C stretch), 1242 (C-C=O stretch), 845 and 703 (1,4-disubstituted benzene); UV (H_2O) λ_{max}, nm: 264.

2.2.20 1-(4-methoxyphenyl)-2-(methylamino)pentan-1-one (MOMV, 44)

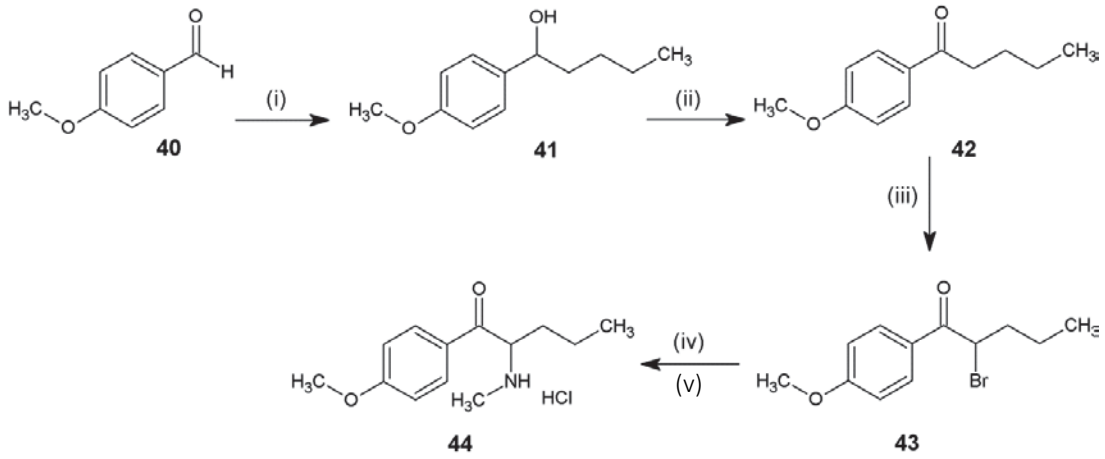

Figure 2-13. Synthesis of MOMV HCl (**44**) via a four step reaction sequence: Grignard reaction of *p*-methoxybenzaldehyde (**40**), oxidation of **41**, α-bromination of **42**, followed by amination of **43** with methylamine. The final product salt was obtained following extraction and HCl work-up.
Reagents and conditions: (i) ButMgCl, Et_2O, N_2 atm., 4.5 h; *(ii)* PCC/celite, DCM, 20.5 h; *(iii)* bromine, glacial acetic acid, RT, 19 h; *(iv)* aq. methylamine, Et_2O, RT, 44 h; *(v)* HCl work-up.

2.2.20.1 *1-(4-methoxyphenyl)pentan-1-one (**42**)*

To a RBF containing *p*-methoxybenzaldehyde **40** (1.55 g, 12.8 mmol) dissolved in diethyl ether (10 mL) was added butylmagnesium chloride solution (8 mL, 16 mmol) via syringe while keeping the flask on ice. The reaction was stirred for 4.5 h before adding 1 M HCl (12 mL, 12 mmol) and stirring for a further 10 min. The ether layer was separated, washed with water (3 x 5 mL) and dried over sodium sulphate before decanting and rotary evaporating to dryness to afford a pale yellow oil **41** (2.235 g, 11.5 mmol, 90%). The oil was dissolved in dichloromethane

(15 mL) in a RBF before adding PCC (2.6 g, 12.1 mmol) and celite (2 g). The reaction was stirred for 19 h before adding diethyl ether (40 mL) and stirring for a further 1.5 h. The reaction mixture was then filtered through a pad of silica in a sintered glass funnel and the filtrate was rotary evaporated to dryness to afford a green-yellow liquid **42** (2.77 g, 14.4 mmol, 113 %). EI (*m/z,* %): 192(M^+,2), 163(2), 150(21), 135(100), 92(8), 77(17).

2.2.20.2 *2-bromo-1-(4-methoxyphenyl)pentan-1-one (**43**)*

In a RBF, the ketone **42** (2.77 g, 14.4 mmol) was dissolved in glacial acetic acid (60 mL) and a pressure equalising dropping funnel containing bromine (0.80 mL, 16 mmol) was attached. One drop of bromine was initially added and the reaction stirred for 30 min. The remaining bromine was subsequently added dropwise and the reaction stirred for 19 h before quenching by pouring the reaction mixture into ice-cold water (100 mL). The aqueous mixture was extracted with dichloromethane (3 x 50 mL), washed with saturated sodium carbonate (3 x 50 mL), dried over magnesium sulphate and rotary evaporated to dryness to afford an orange oil **43** (3.188 g, 11.76 mmol, 82%). EI (*m/z,* %): 272/270 (M^+, $^{79}Br/^{81}Br$, 1), 230/232 ($^{79}Br/^{81}Br$, 1), 191(4), 135(100), 92(11), 77(24).

2.2.20.3 *1-(4-methoxyphenyl)-2-(methylamino)pentan-1-one (**44**)*

In a RBF, the α-bromoketone **43** (3.188 g, 11.76 mmol) was dissolved in toluene (7 mL) and briefly stirred at room temperature. Separately in two beakers, sodium hydroxide pellets (1.955 g, 48 mmol) were dissolved in cold water (4 mL) and added to a solution of methylamine hydrochloride (3.256 g, 48 mmol) in cold water (4 mL). The combined solution was quickly added to the RBF using a Pasteur pipette and the reaction mixture left to stir for 44 h. The reaction was quenched by pouring into ice-cold water (50 mL). The toluene layer was separated and the aqueous layer further extracted with toluene (3 x 20 mL). Combined toluene extracts were washed with water (3 x 20 mL) and back-extracted with 1 M HCl (3 x 20 mL, 25 mL). Acidic aqueous extracts were washed with toluene (3 x 20 mL) and evaporated to dryness to afford a crude pale orange, toffee-like material. The crude material was washed with an acetone, hexane and ethyl acetate mixture to afford a white powder **44** (0.3875 g, 1.50 mmol, 13%): mp 123-126 °C (lit. unk.); ^{1}H NMR (500 MHz, D_2O) δ, ppm: 7.792-7.777 (d, $^3J_{HH}$= 7.5 Hz, 1H), 7.726-7.694 (t, $^3J_{HH}$= 8.0 Hz, 1H), 7.249-7.232 (d, $^3J_{HH}$= 8.5 Hz, 1H), 7.168-7.139 (t, $^3J_{HH}$=

7.75 Hz, 2H), 5.030 (s, 1H), 3.976 (s, 3H), 2.713 (s, 3H), 1.927-1.807 (m, 2H), 1.366-1.211 (m, 2H), 0.847-0.817 (t, $^{3}J_{HH}$= 7.5 Hz, 3H); ^{13}C NMR (125 MHz, $CDCl_3$) δ, ppm: 195.016, 158.775, 135.715, 131.873, 124.024, 121.502, 111.730, 67.466, 55.793, 32.738, 31.751, 18.171, 13.949; EI (*m/z,* %): 221(M^+,0), 178(1), 135(5), 86(100), 77(76), 44(9); FTIR (ATR) ν_{max}, cm^{-1}: 2947 (C-H stretch), 2684 and 2453 (asym. and sym. NH_2^+ stretches), 1682 (C=O stretch), 1598 and 1459 (C=C stretch), 1252 (C-C=O stretch), 1026 (C-O stretch), 827 and 698 (1,4-disubstituted benzene); UV (H_2O) λ_{max}, nm: 319, 256, 211.

2.2.21 1-(2*H*-1,3-benzodioxol-5-yl)-2-(ethylamino)propan-1-one (ethylone, 45)

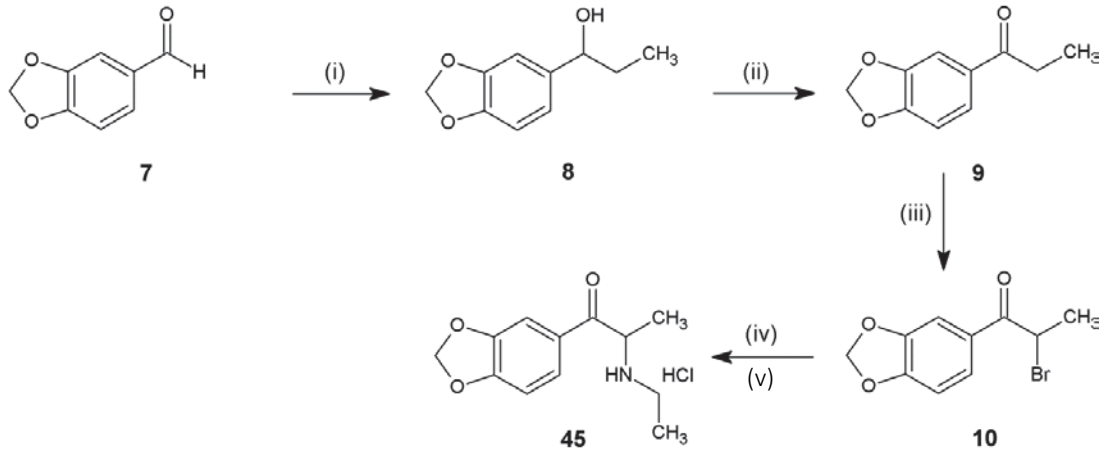

Figure 2-14. Synthesis of ethylone HCl (**45**) via a four step reaction sequence: Grignard reaction of piperonal (**7**), oxidation of **8**, α-bromination of **9**, followed by amination of **10** with ethylamine. The final product salt was obtained following extraction and HCl work-up.
Reagents and conditions: (i) EthMgCl, Et_2O, N_2 atm., 4 h; *(ii)* PCC/celite, DCM, 10 min; *(iii)* bromine, glacial acetic acid, RT, 40 h; *(iv)* aq. ethylamine, Et_2O, RT, 24 h; *(v)* HCl work-up.

2.2.21.1 *1-(2H-1,3-benzodioxol-5-yl)propan-1-one (**9**)*

See Section 2.2.10.1 for preparation of **9**

2.2.21.2 *1-(2H-1,3-benzodioxol-5-yl)-2-bromopropan-1-one (**10**)*

See Section 2.2.10.2 for preparation of **10**

2.2.21.3 *1-(1,3-benzodioxol-5-yl)-2-(ethylamino)propan-1-one hydrochloride (**45**)*

In a RBF, the α-bromoketone **10** (2.70 g, 10.5 mmol) was dissolved in toluene (5 mL) and briefly stirred at room temperature. Aqueous ethylamine (70 % v/v, 1.0 mL, 15 mmol) was added all at once and the reaction stirred for 24 h. The reaction was quenched by pouring into cold water (100 mL) and the toluene layer was separated. The aqueous layer was further extracted with toluene (4 x 25 mL) before combining the toluene extracts and washing with water (3 x 25 mL). The organic fraction was back-extracted with 1 M HCl (3 x 25 mL) and the aqueous extracts washed with toluene (3 x 25 mL) and evaporated to dryness to afford a crude orange crystalline material (1.62 g, 6.29 mmol, 59%). The crude material was washed with acetone to afford an off-white powder **45** (0.428 g, 1.66 mmol, 16%): mp 227-233 °C (dec.)(lit.[343] 235.6-242.6 °C); ^{1}H NMR (500 MHz, D_2O) δ, ppm: 7.696-7.679 (d, $^{3}J_{HH}$= 8.5 Hz, 1H), 7.467 (s, 1H), 7.040-7.023 (d, $^{3}J_{HH}$= 8.0 Hz, 2H), 6.129 (s, 2H), 5.024-5.002 (t, $^{3}J_{HH}$= 7.0 Hz, 1H), 2.734 (s, 3H), 2.031-1.916 (m, 2H), 1.365-1.218 (m, 2H), 0.874-0.845 (t, $^{3}J_{HH}$= 7.25 Hz, 3H); ^{13}C NMR (125 MHz, CD_3OD) δ, ppm: 191.924, 152.067, 147.348, 125.685, 124.167, 106.509, 105.993, 101.039, 55.925, 39.428, 13.929, 8.736; EI (*m/z,* %): 221(M^+,0), 219(1), 149(7), 121(5), 91(2), 72(100), 44(18); FTIR (ATR) ν_{max}, cm^{-1}: 2975 (C-H stretch), 2709 and 2459 (asym. and sym. NH_2^+ stretches), 1673 (C=O stretch), 1604 and 1451 (C=C stretch), 1255 (C-C=O stretch), 1037 (C-O stretch), 867 and 799 (1,2,4-trisubstituted benzene); UV (H_2O) λ_{max}, nm: 235, 281, 319.

2.2.22 2-(methylamino)-1-(naphthalen-1-yl)propan-1-one (α-naphth, 50)

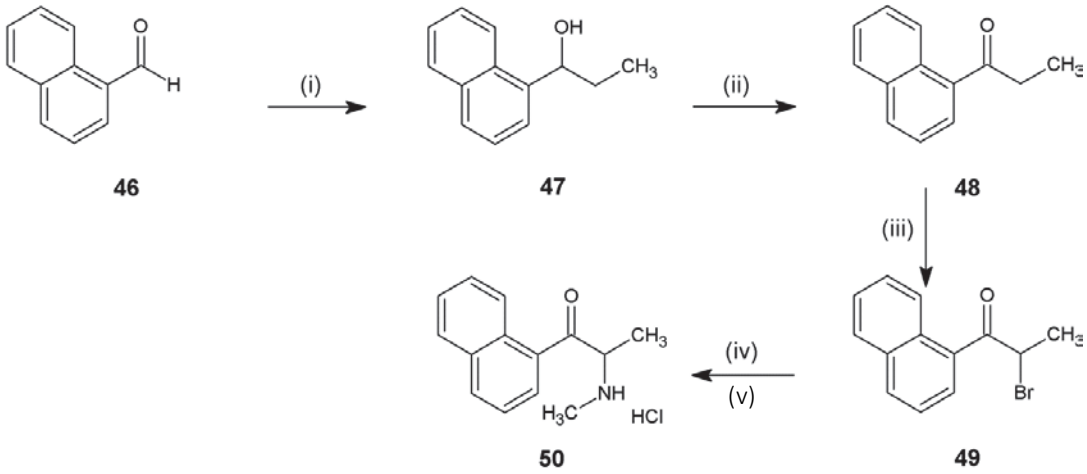

Figure 2-15. Synthesis of α-naphth HCl (**50**) via a four step reaction sequence: Grignard reaction of α-naphthaldehyde (**46**), oxidation of **47**, α-bromination of **48**, amination of **49** with methylamine. The final product salt was obtained following extraction and HCl work-up.
Reagents and conditions: (i) EthMgCl, Et_2O, N_2 atm., 4 h; *(ii)* PCC/celite, DCM, 17 h; *(iii)* bromine, glacial acetic acid, RT, 6 h; *(iv)* aq. methylamine, Et_2O, RT, 22 h. ; *(v)* HCl work-up.

2.2.22.1 *1-(naphthalen-1-yl)propan-1-one (**48**)*

In a two-neck RBF maintained under nitrogen atmosphere, 1-naphthaldehyde **46** (2.34 g, 15.0 mmol) was dissolved in diethyl ether (10 mL). The flask was kept on ice while ethylmagnesium chloride solution (8 mL, 16 mmol) was added via syringe and the reaction left to stir at room temperature for 4 h. To the RBF was added 1.0 M HCl (8 mL, 16 mmol) and the reaction stirred for a further 10 min. The ether layer was separated, washed with water (3 x 5 mL), dried over magnesium sulphate and rotary evaporated to afford a yellow oil **47** (3.21 g, 17.2 mmol, 115%). The crude oil was dissolved in dichloromethane (20 mL) before adding PCC (3.23 g, 15 mmol) and celite (3.0 g). The reaction was stirred for 17 h and the reaction mixture was filtered through a pad of silicic acid in a sintered glass funnel. The filtrate was rotary evaporated to dryness to afford a green-brown oil **48** (2.22 g, 12.1 mmol, 81%): EI (*m/z,* %): 184(M^+,23), 155(100), 127(78), 101(5), 77(8).

2.2.22.2 *2-bromo-1-(naphthalen-1-yl)propan-1-one (**49**)*

In a RBF the ketone **48** (2.22 g, 12.1 mmol) was dissolved in glacial acetic acid (50 mL) and a dropping funnel containing bromine (0.72 mL, 14.0 mmol) was attached. One drop of bromine was initially added and the reaction stirred for 30 min before adding the remaining bromine dropwise and stirring the reaction for a further 6 h. The reaction was quenched by pouring the mixture into ice-cold water (100 mL). The reaction mixture was extracted with dichloromethane (3 x 40 mL) and the combined DCM extracts carefully washed with saturated sodium carbonate (3 x 40 mL). The DCM extracts were dried over magnesium sulphate, decanted and rotary evaporated to dryness to afford a mottled white and brown crystalline material **49** (3.16 g, 12.0 mmol, 99%). EI (*m/z,* %): 262/264 (M^+, $^{79}Br/^{81}Br$, 5), 155(100), 127(46), 77(5), 101(3).

2.2.22.3 *2-(methylamino)-1-(naphthalen-1-yl)propan-1-one hydrochloride (**50**)*

In a RBF, the α-bromoketone **49** (3.16 g, 12.0 mmol) was dissolved in toluene (10 mL) and briefly stirred at room temperature. Separately in two beakers, sodium hydroxide pellets (1.92 g, 48 mmol) were dissolved in cold water (3 mL) and added to a solution of methylamine hydrochloride (3.24 g, 48 mmol) in cold water (2.5 mL). The combined solution was quickly added to the RBF using a Pasteur pipette and the reaction mixture left to stir for 22 h. The reaction was quenched by pouring into ice-cold water (60 mL). The toluene layer was separated and the aqueous fraction further extracted with toluene (4 x 15 mL). The combined toluene extracts were washed with water (3 x 15 mL) and back-extracted with 1.0 M HCl (4 x 15 mL). The combined acidic aqueous extracts were washed with toluene (3 x 15 mL) and evaporated to dryness to afford a crude brown, fluffy solid (1.49 g, 5.97 mmol, 50%). The crude material was washed with acetone to afford a white and brown powder **44** (1.34 g, 5.37 mmol, 45%): mp 179-181 °C (dec.)(no data available); ^{1}H NMR (500 MHz, D_2O) δ, ppm: 8.333-8.316 (d, $^3J_{HH}$= 7.0 Hz, 1H), 8.014-7.997 (d, $^3J_{HH}$= 8.5 Hz, 1H), 7.928-7.914 (d, $^3J_{HH}$= 7.0 Hz, 1H), 7.837-7.820 (d, $^3J_{HH}$= 7.0 Hz, 1H), 7.599-7.470 (m, 3H), 5.102-5.059 (q, $^3J_{HH}$= 7.25 Hz, 1H), 2.855-2.843 (d, $^3J_{HH}$= 6.0 Hz, 3H), 1.433-1.418 (d, $^3J_{HH}$= 7.5 Hz, 3H); ^{13}C NMR (125 MHz, CD_3OD) δ, ppm: 198.774, 135.084, 134.708, 131.006, 130.942, 129.804, 129.064, 128, 916, 127.239, 125.240, 124.868, 61.342, 30.885, 24.527, 14.559; EI (*m/z,* %): 213(M^+,0), 211(1), 170(1), 155(5), 127(18), 58(100); FTIR (ATR) ν_{max}, cm^{-1}: 2905 (C-H stretch), 2712 and 2460 (asym. and sym.

NH_2^+ stretches), 1687 (C=O stretch), 1574 and 1464 (C=C stretch), 1245 (C-C=O stretch), 802 and 774 (α-substituted naphthalene); UV (H_2O) λ_{max}, nm: 212, 244, 313.

2.2.23 1-(2*H*-1,3-benzodioxol-5-yl)-2-(pyrrolidin-1-yl)butan-1-one (MDPBP, 51)

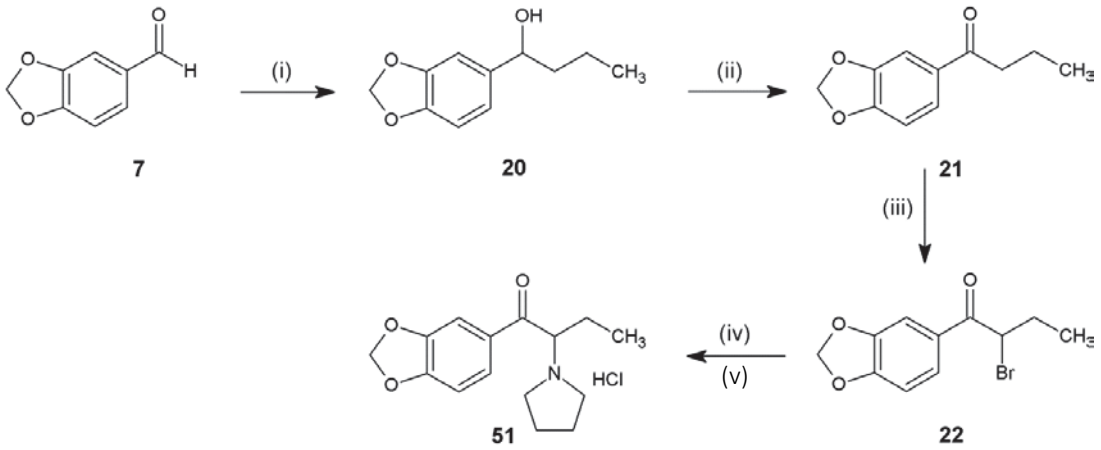

Figure 2-16. Synthesis of MDPBP HCl (**51**) via a four step reaction sequence: Grignard reaction of piperonal (**7**), oxidation of **20**, α-bromination of **21**, followed by amination of **22** with pyrrolidine. The final product salt was obtained following extraction and HCl work-up.
Reagents and conditions: (i) PropMgCl, Et_2O, N_2 atm., 4 h; *(ii)* PCC/celite, DCM, 21 h; *(iii)* bromine, glacial acetic acid, RT, 18 h; *(iv)* pyrrolidine, Et_2O, RT, 25 h; *(v)* HCl work-up.

2.2.23.1 *1-(2H-1,3-benzodioxol-5-yl)butan-1-one (**21**)*

See Section 2.2.15.1 for preparation of **21**

2.2.23.2 *1-(2H-1,3-benzodioxol-5-yl)-2-bromobutan-1-one (**22**)*

See Section 2.2.15.2 for preparation of **22**

2.2.23.3 *1-(2H-1,3-benzodioxol-5-yl)-2-(pyrrolidin-1-yl)butan-1-one—hydrochloride (**51**)*

In a RBF the α-bromoketone **22** (2.18 g, 10.4 mmol) was dissolved in diethyl ether (15 mL). Pyrrolidine (1.30 mL, 15.6 mmol) was added all at once using a Pasteur pipette and the reaction left to stir for 6 h. The reaction was quenched by pouring into ice-cold water (40 mL). The ether layer was separated and the aqueous fraction further extracted with diethyl ether (4 x 10 mL). The combined ethereal extracts were washed with water (3 x 10 mL) and back-extracted into 1.0 M HCl (4 x 10 mL). The combined acidic aqueous extracts were washed with ether (3 x 10 mL) and rotary evaporated to dryness to afford a crude orange-brown substance with a toffee-like appearance **51** (1.48 g, 4.97 mmol, 48%). This crude residue was washed with acetone and ethyl acetate to afford a creamy light brown solid **51** (1.20 g, 4.04 mmol, 39%): mp 220-222 °C (dec.)(lit.[344] 241.9 °C); ^{1}H NMR (500 MHz, D_2O) δ, ppm: 7.722-7.702 (dd, $^{3}J_{HH}$= 8.5 Hz, $^{4}J_{HH}$= 1.5 Hz, 1H), 7.496-7.494 (d, $^{3}J_{HH}$= 2.5 Hz, 1H), 7.057-7.040 (d, $^{3}J_{HH}$= 8.5 Hz, 1H), 6.143-6.140 (d, $^{3}J_{HH}$= 1.5 Hz, 1H), 5.171-5.151 (t, $^{3}J_{HH}$= 5.0 Hz, 1H), 3.752-3.651 (m, 2H), 3.299-3.047 (m, 2H), 2.247-1.933 (m, 6H), 0.879-0.820 (t, $^{3}J_{HH}$= 7.5 Hz, 3H); ^{13}C NMR (125 MHz, CD_3OD) δ, ppm: 193.849, 154.417, 149.516, 129.169, 126.555, 108.628, 107.968, 103.211, 70.001, 55.396, 23.942, 23.290, 23.142, 7.578; EI (*m/z,* %): 232(M^+,1), 149(4), 113(8), 112(100), 70(4); FTIR (ATR) ν_{max}, cm^{-1}: 2914 (C-H stretch), 2614 (NH^+ stretch), 1681 (C=O stretch), 1608 and 1437 (C=C stretch), 1255 (C-C=O stretch), 1031 (C-O stretch), 876 and 805 (1,2,4-trisubstituted benzene); UV (H_2O) λ_{max}, nm: 208, 244, 293.

2.2.24 1-(4-methylphenyl)-2-(pyrrolidin-1-yl)butan-1-one (4-MPBP, 55)

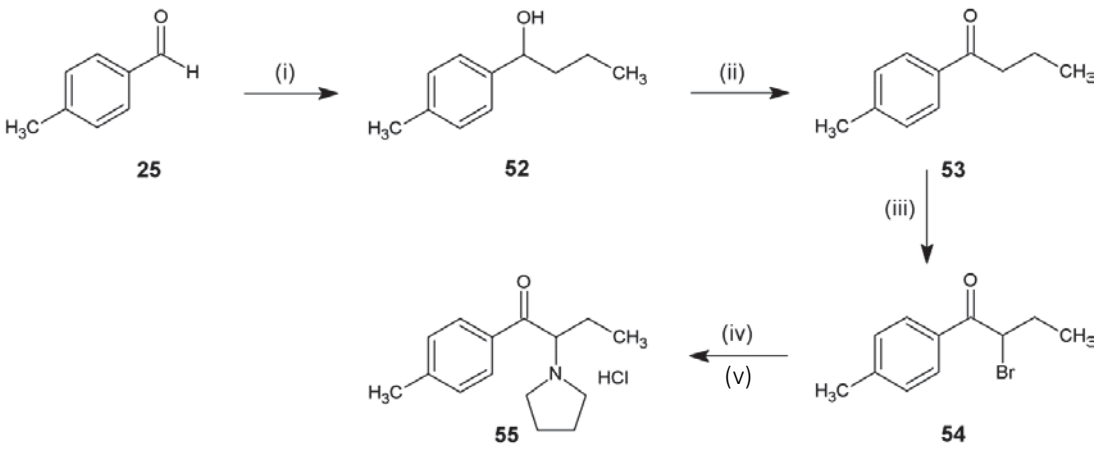

Figure 2-17. Synthesis of 4-MPBP HCl (**55**) via a four step reaction sequence: Grignard reaction of *p*-tolualdehyde (**25**), oxidation of **52**, α-bromination of **53** and nucleophilic substitution of **54** with pyrrolidine. The final product salt was obtained following extraction and HCl work-up.

Reagents and conditions: (i) PropMgCl, Et_2O, N_2 atm., RT, 4 h; *(ii)* PCC/celite, DCM, 26.5 h; *(iii)* bromine, glacial acetic acid, RT, 5 h; *(iv)* pyrrolidine, Et_2O, RT, 5 h; *(v)* HCl work-up.

2.2.24.1 *1-(4-methylphenyl)butan-1-one (**53**)*

In a RBF maintained under a nitrogen atmosphere, *p*-tolualdehyde (1.40 mL, 11.9 mmol) was dissolved in diethyl ether (10 mL). The flask was kept on ice as propylmagnesium chloride solution (6 mL, 12 mmol) was added via syringe. The reaction was stirred for 4 h before adding 1.0 M HCl (15 mL, 15 mmol) and stirring for a further 15 min. The ether layer was separated and the aqueous layer further extracted with diethyl ether (3 x 5 mL). The combined ether extracts were washed with water (3 x 5 mL), dried over magnesium sulphate and rotary evaporated to afford a colourless oil **52** (2.08 g, 17.0 mmol). The oil was dissolved in DCM (30 mL) in a RBF before adding PCC (4.10 g, 19.0 mmol) and celite (4.1 g). The reaction was left to stir for 21 h then filtered through a pad of silicic acid in a sintered glass funnel. The filtrate was rotary evaporated to form a dark orange oil **53** (2.12 g, 13.2 mmol, 111%). EI (*m/z,* %): 162(M^+,7), 147(15), 134(5), 120(8), 91(33), 119(100), 65(10), 41(1).

2.2.24.2 *2-bromo-1-(4-methylphenyl)butan-1-one (**54**)*

In a RBF the oil **53** (2.12 g, 13.2 mmol) was dissolved in glacial acetic acid (50 mL) and a pressure equalising dropping funnel containing bromine (1.00 mL, 19.4 mmol) was attached. One drop of bromine was initially added and the reaction mixture stirred for 15 min. The remainder of the bromine was added dropwise and the reaction stirred for a further 18 h. The reaction was quenched by pouring the mixture into ice-cold water (100 mL). The mixture was extracted with DCM (3 x 40 mL), and the combined extracts were washed with saturated sodium carbonate solution (3 x 40 mL). The DCM fraction was dried over magnesium sulphate and rotary evaporated to afford a yellow oil **54** (2.65 g, 11.0 mmol, 83%). EI (*m/z,* %): 240/242 (M^+, $^{79}Br/^{81}Br$, 1), 120(14), 119(100), 91(40), 65(12).

2.2.24.3 *1-(4-methylphenyl)-2-(pyrrolidin-1-yl)butan-1-one hydrochloride (**55**)*

The α-bromoketone **54** (2.65 g, 11.0 mmol) was dissolved in diethyl ether (15 mL) in a RBF kept on ice and pyrrolidine (1.38 mL, 16.5 mmol) was added all at once using a Pasteur pipette. The reaction was stirred for 5.5 h before quenching by adding ice-cold water (40 mL). The ether layer was separated and the aqueous layer further extracted with ether (4 x 10 mL). The combined ethereal extracts were washed with water (3 x 10 mL) and back-extracted into the aqueous layer using 1.0 M HCl (4 x 10 mL). The acidic aqueous extracts were washed with diethyl ether before rotary evaporating to dryness to afford a crude mottled white and brown solid **55** (1.18 g, 4.41 mmol, 40%). This crude solid was washed with acetone, ethyl acetate and hexane mixtures to afford a light brown and white flaky solid **55** (0.8301, 3.10 mmol, 28%): mp 179-182 °C (dec.)(lit.[345] 178-180 °C); ^{1}H NMR (500 MHz, D_2O) δ, ppm: 7.934-7.917 (d, $^{3}J_{HH}$= 8.5 Hz, 2H), 7.441-7.425 (d, $^{3}J_{HH}$= 8.0 Hz, 2H), 5.237-5.217 (dd, $^{3}J_{HH}$= 6.5 Hz, $^{3}J_{HH}$= 4.5 Hz, 1H), 3.490-3.266 (m, 4H), 2.429 (s, 3H), 2.167-2.053 (m, 6H), 0.819-0.788 (t, $^{3}J_{HH}$= 7.75 Hz, 3H); ^{13}C NMR (125 MHz, $CDCl_3$) δ, ppm: 196.050, 146.691, 133.437, 130.122, 128.745, 63.572, 44.893, 24.436-24.409, 23.897, 21.845, 10.822; EI (*m/z,* %): 231(M^+,0), 202(1), 112(100), 113(9), 91(5); FTIR (ATR) ν_{max}, cm^{-1}: 2961 (C-H stretch), 2672 (NH^+ stretch), 1678 (C=O stretch), 1605 and 1449 (C=C stretch), 1244 (C-C=O stretch), 816 (1,4-disubstituted benzene); UV (H_2O) λ_{max}, nm: 267.

2.2.25 1-(4-hydroxyphenyl)-2-(methylamino)propan-1-one (4-HMC, 60)

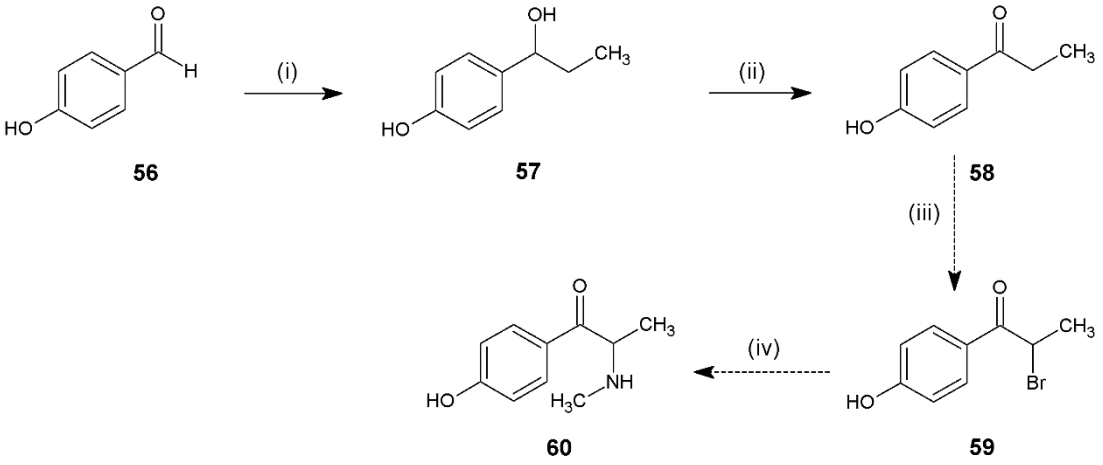

Figure 2-18. Theoretical synthesis of 4-HMC HCl (**60**) via a four step reaction sequence: Grignard reaction of *p*-hydroxybenzaldehyde (**56**), oxidation of **57**, α-bromination of **58** and nucleophilic substitution of **59** with methylamine.
Reagents and conditions: (i) EthMgCl, Et_2O/THF, N_2 atm., RT, 22 h; *(ii)* PCC/celite, DCM, 26.5 h; *(iii)* bromine, glacial acetic acid, RT; *(iv)* aq. methylamine, Et_2O, RT.

2.2.25.1 *1-(4-hydroxyphenyl)propan-1-one (**58**)*

In a RBF maintained under nitrogen atmosphere, *p*-hydroxybenzaldehyde **56** (1.51 g, 12.4 mmol) was dissolved in diethyl ether (10 mL) and THF (5 mL). The flask was kept on ice while ethylmagnesium chloride solution (9 mL, 18 mmol) was addded via syringe. The reaction was left to stir for 22 h before adding 1.0 M HCl (15 mL, 15 mmol) and stirring for a further 35 min. The ether layer was separated, washed with water (3 x 7 mL) and dried over sodium sulphate. The ethereal extracts were filtered through a cotton plug and rotary evaporated to afford a light yellow oil **57** (1.64 g, 10.7 mmol, 86%). The oil was dissolved in DCM (15 mL) in a RBF before adding PCC (2.3 g, 10.7 mmol) and celite (2.3 g) and stirring the reaction mixture for 25 h. Diethyl ether (40 mL) was added to the RBF and the reaction stirred for a further 1.5 h. The reaction mixture was filtered through a pad of silica in a sintered glass funnel. The filtrate was rotary evaporated to afford a light brown oil that solidified on standing **58** (1.4 g, 9.3 mmol, 75%). EI (*m/z,* %): 150(M^+,13), 121(100), 93(18), 65(14).

2.2.25.2 *2-bromo-1-(4-hydroxyphenyl)propan-1-one (**59**)*

The ketone **58** (1.4 g, 9.3 mmol) was dissolved in glacial acetic acid (50 mL) in a RBF. A pressure equalising dropping funnel containing bromine (0.5 mL, 10 mmol) was attached to the flask and one drop was initially added before continuing to add the remaining bromine dropwise. The reaction was left to stir for 30 h before quenching by pouring into ice-cold water (100 mL). The mixture was extracted with DCM (3 x 50 mL) and carefully washed with saturated sodium carbonate solution (3 x 50 mL). The solvent was removed via rotary evaporation to afford an orange oil that solidified on standing (0.43 g, 1.88 mmol, 20%). GC-MS reaction monitoring confirmed the α-bromoketone **60** was not formed in this reaction. As a result, the subsequent amination step was not performed.

2.2.26 2-(methylamino)-1-(naphthalen-2-yl)pentan-1-one (β-naphyrone, 65)

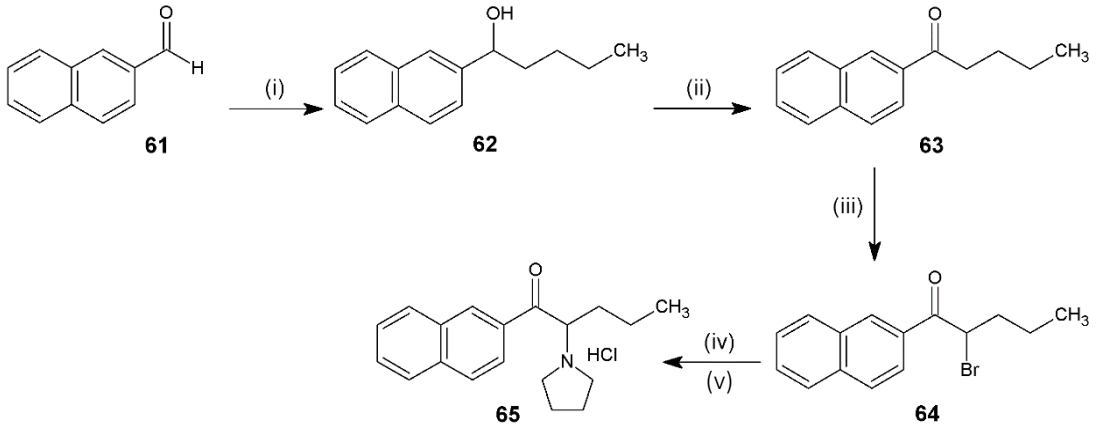

Figure 2-19. Synthesis of β-naphyrone HCl (**65**) via a four step reaction sequence: Grignard reaction of 2-naphthaldehyde (**61**), oxidation of **62**, α-bromination of **63** and nucleophilic substitution of **64** with pyrrolidine. The final product salt was obtained following extraction and HCl work-up.
Reagents and conditions: (i) BuMgCl, toluene, RT, 4 h; *(ii)* RT, 48 h; *(iii)* bromine, $AlCl_3$, Et_2O, RT, 30 h; *(iv)* pyrrolidine, Et_2O, RT, 24.5 h; *(v)* HCl work-up.

2.2.26.1 *1-(naphthalen-2-yl)pentan-1-one (**63**)*

To a RBF containing butylmagnesium chloride solution (6 mL, 12 mmol) and toluene (25 mL) was added, in several portions over 30 min, 2-naphthaldehyde **61**(1.56 g, 10 mmol). The reaction was stirred for 3.5 h before pouring the reaction mixture into a beaker containing ice.

Concentrated sulphuric acid (2 mL, 36.8 mmol) and a stirrer bar were added to the beaker and the solution stirred briefly. The mixture was extracted with diethyl ether (3 x 20 mL), washed with water (3 x 15 mL), dried over magnesium sulphate and rotary evaporated to afford a yellow oil **62** (2.08 g, 9.78 mmol, 98%). EI (*m/z,* %): 212(M^+,0), 197(7), 196(41), 167(100), 165(38), 128(11).

2.2.26.2 *2-bromo-1-(naphthalen-2-yl)pentan-1-one (**64**)*

In a two-neck RBF, the ketone **63** (2.08 g, 9.78 mmol) was dissolved in diethyl ether (30 mL) and placed in an ice bath. Carefully, $AlCl_3$ (2.4 g, 18.0 mmol) was added to the flask and a pressure equalising dropping funnel containing bromine (0.52 mL, 10 mmol) was attached. One drop of bromine was initially added and the reaction stirred for 15 min. The remaining bromine was added dropwise over 40 min and the reaction mixture stirred for 10 h. Diethyl ether (20 mL) was added to the flask and the reaction continued to stir for another 19 h. Saturated sodium carbonate solution (50 mL) was carefully added to the flask and the mixture filtered through a Buchner funnel. The filtrate was extracted with diethyl ether (3 x 20 mL), dried over magnesium sulphate and rotary evaporated to afford an orange-light brown oil **64** (2.41 g, 8.27 mmol, 85%). EI (*m/z,* %): 290(M^+,0), 276/278($^{79}Br/^{81}Br$, 3), 219/221($^{79}Br/^{81}Br$, 4), 196(40), 167(100), 157(40), 141(67).

2.2.26.3 *2-(methylamino)-1-(naphthalen-2-yl)pentan-1-one (**65**)*

The crude α-bromoketone mixture **64** (2.41 g, 8.27 mmol) was dissolved in diethyl ether (10 mL) in a RBF and placed in an ice bath. Pyrrolidine (1.47 mL, 18.0 mmol) was added all at once and the ice bath removed after 10 min. The reaction was stirred for 24.5 h before adding water (10 mL) and diethyl ether (10 mL). The mixture was extracted with diethyl ether (3 x 10 mL) and the ethereal extracts were back-extracted with 1.0 M HCl (3 x 10 mL). The acidic aqueous extracts were washed with diethyl ether (2 x 20 mL) and rotary evaporated to dryness to afford a light orange solid **65** (1.28 g, 4.0 mmol, 48%). EI (*m/z,* %): 291(M^+,0), 210(100), 167(5), 141(27), 115(5), 84(4).

2.2.27 2-Amino-1-phenylpropan-1-one (CAT, 70)

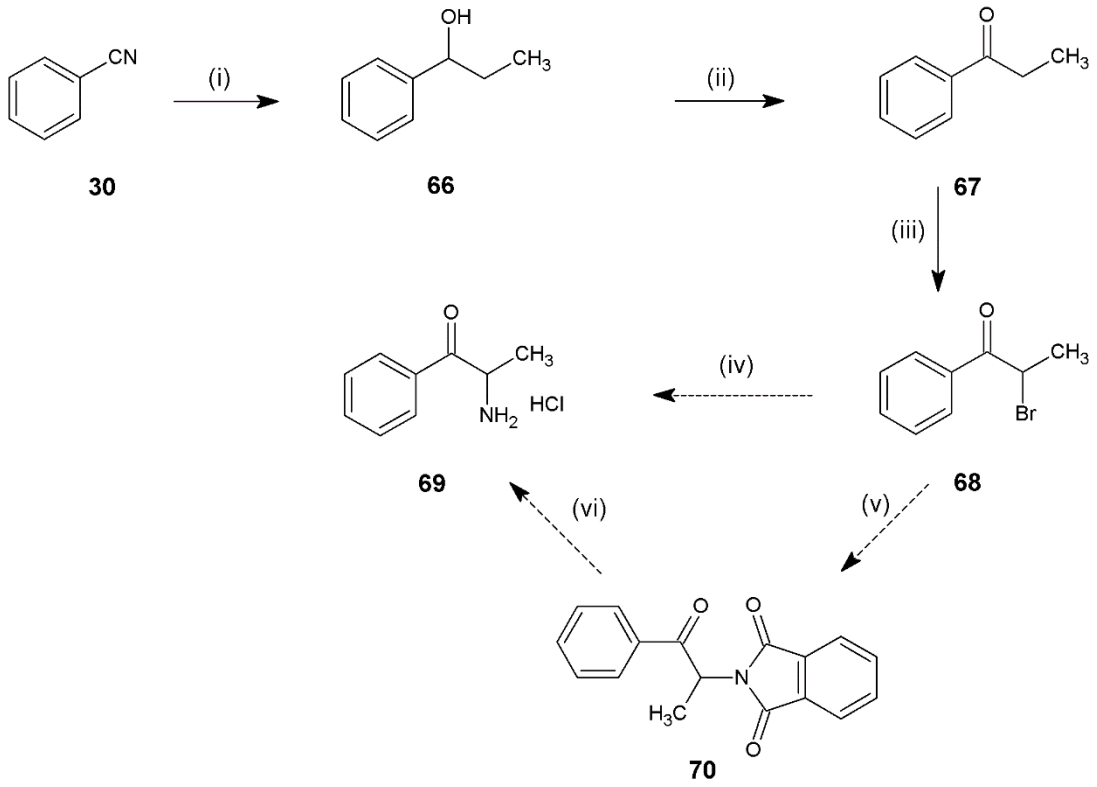

Figure 2-20. Theoretical synthesis of cathinone HCl (**69**) via a four step reaction sequence: Grignard reaction of benzonitrile (**30**), oxidation of **66**, α-bromination of **67** and amination of **68** either directly, or via a phthalimide derivative (**70**).
Reagents and conditions: (i) EthMgCl, toluene, N_2 atm., RT, 3.5 h; *(ii)* RT, 48 h; *(iii)* bromine, glacial acetic acid, RT, 42 h; *(iv)* aq. ammonia, Et_2O, RT; *(v)* phthalimide, DMF, RT; *(vi)* KOH, H_2O, reflux

2.2.27.1 *1-phenylpropan-1-one (**67**)*

To a RBF maintained under nitrogen atmosphere was added dried toluene (20 mL) and ethylmagnesium chloride solution (6 mL, 12 mmol). To this stirred solution was added benzonitrile **30** (1 mL, 10 mmol) in portions, dropwise over 30 min. After stirring at RT for 3 h, the reaction was quenched by pouring onto ice and adding concentrated sulphuric acid (2 mL, 36.8 mmol) with swirling. The mixture was left to stand for 48 h before extracting with diethyl ether (3 x 20 mL), drying over magnesium sulphate, decanting and rotary evaporating to yield a yellow oil **67** (1.08 g, 8.05 mmol, 80.5%). EI (*m/z,* %): 134(M^+,18), 105(100), 45(42), 12(11).

2.2.27.2 *2-bromo-1-phenylpropan-1-one (**68**)*

The ketone **67** (1.08 g, 8.05 mmol) was dissolved in glacial acetic acid (45mL) in a RBF and a pressure equalising dropping funnel containing bromine (0.42 mL, 8.0 mmol) attached. One drop of bromine was initially added and the reaction stirred for 15 min. The remaining bromine was added dropwise over 5 min and the reaction stirred for 28 h before adding more bromine (0.20 mL, 4.0 mmol). The mixture was further stirred for 14 h before pouring into a beaker of ice-cold water (100 mL). The aqueous mixture was extracted with DCM (3 x 40 mL), carefully washed with saturated sodium carbonate solution (3 x 40 mL), dried over magnesium sulphate and rotary evaporated to afford a light yellow oil **68** (1.73 g, 8.12 mmol, 101%). EI (*m/z,* %): 212/214(^{79}Br/^{81}Br, 2), 105(100), 77(35), 51(11).

2.2.27.3 *2-(1-oxo-1-phenylpropan-2-yl)-1H-isoindole-1,3(2H)-dione (**69**)*

Phthalimide (1.85 g, 10 mmol) was dissolved in DMF (30 mL) and added to a RBF containing the α-bromoketone **68** (1.73 g, 8.12 mmol) and left to stir for 7 h. The solution was filtered through a sintered funnel and the filtrate rotary evaporated and washed with acetone to afford beige coloured crystals (0.012 g). GC-MS reaction monitoring confirmed the phthalimide derivative **69** was not formed in this reaction. As a result, the subsequent step was not performed.

2.3 Results and Discussion

2.3.1 Reaction summary

Seventeen synthetic cathinone analogues were successfully synthesised and isolated for use in proceeding work. An overall reaction scheme for the syntheses performed is provided in Figure 2-21 below. The steps include alkylation using a Grignard reagent, α-bromination of a ketone, and nucleophilic substitution with an alkylamine.

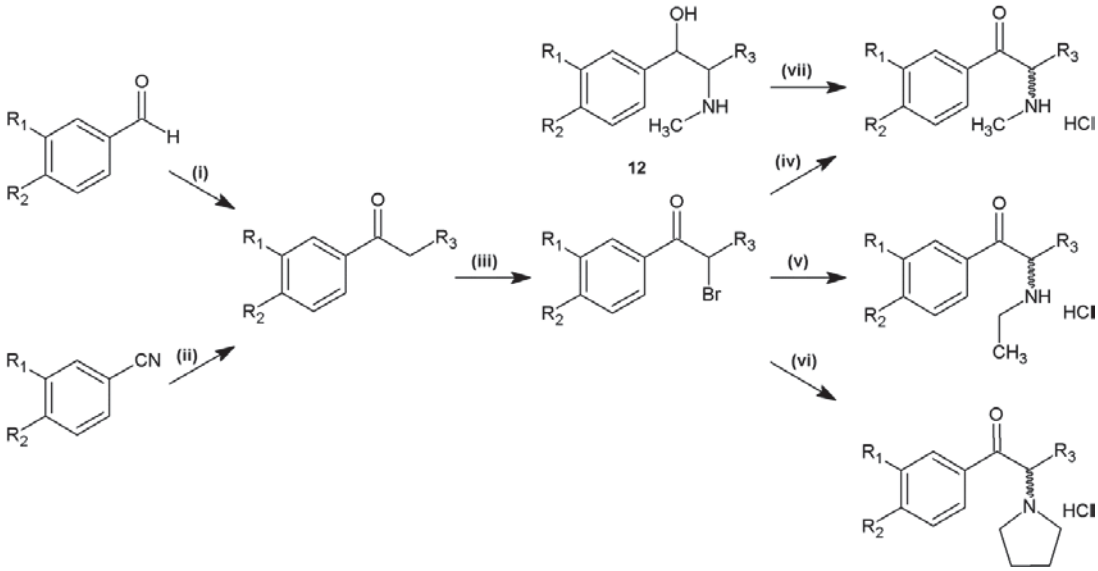

R_1 = -H, -CH_2O, -C_6H_5; **R_2** = -H, -CH_3, -CH_2CH_3, -F, -OH, -OCH_3; **R_3** = -CH_3, -CH_2CH_3, -$CH_2CH_2CH_3$

Figure 2-21. Overall reaction scheme for the preparation of synthetic cathinones. *Reactions: (i) and (ii)* Grignard reaction followed by oxidation; *(iii)* Bromination; *(iv)* Methamination; *(v)* Ethamination; *(vi)* Amination with pyrrolidine; (vii) Oxidation.

The mechanisms for each of the synthetic steps are provided in Figure 2-22 below. The Grignard reactions are used in the first synthetic step to increase the carbon chain length of the analogue dependent on the Grignard reagent selected. The reagents used for brominations performed in this study were glacial acetic acid and a slightly more than equimolar amount of elemental bromine. The glacial acetic acid is required to protonate the carbonyl group and, through resonance, render the alpha carbon more negatively charged. Other methods of bromination that have also been used in the synthesis of synthetic cathinones include hydrobromic acid and bromine[346], cupric bromide[328] and a hydrobromic acid and hydrogen peroxide mixture[347].

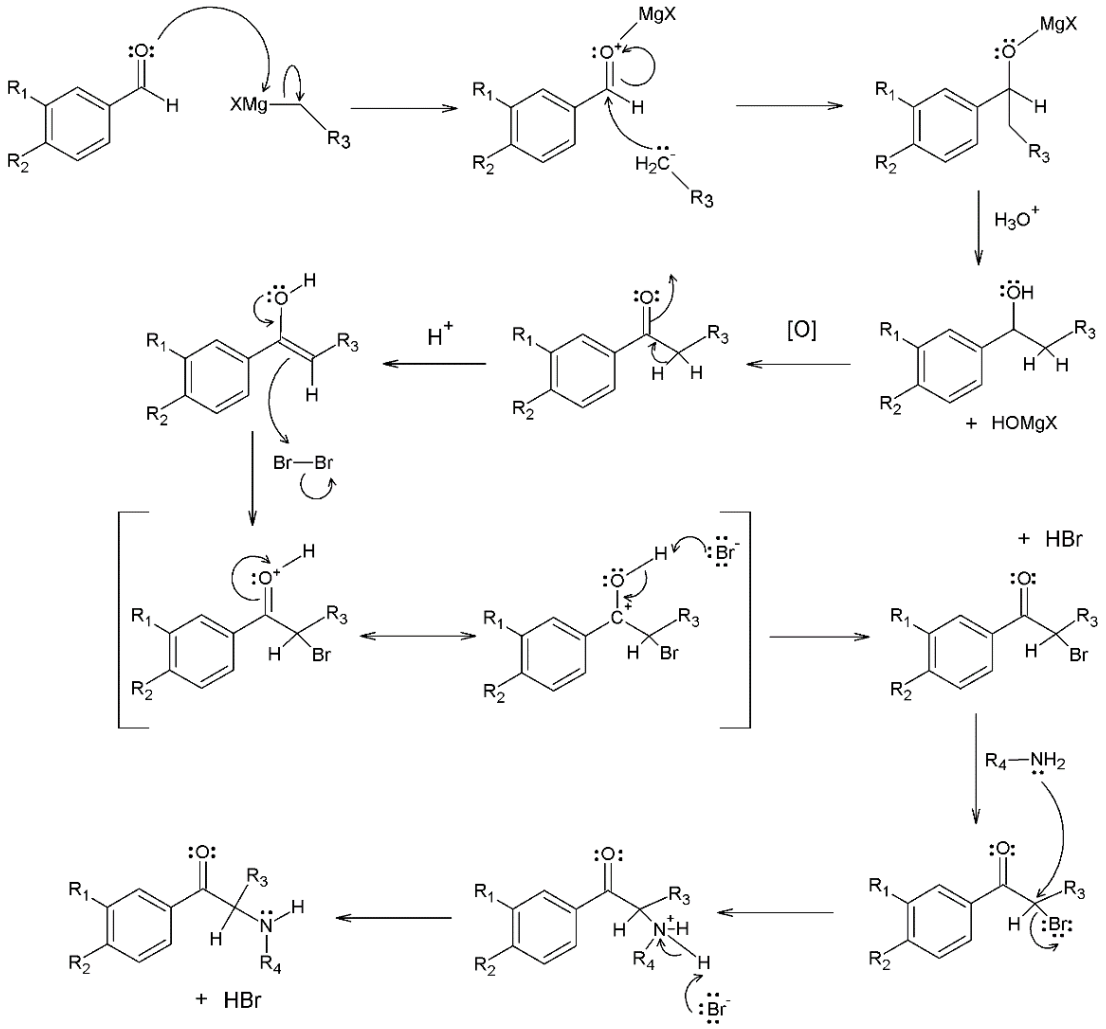

Figure 2-22. Reaction mechanism pathway for the synthesis of a general cathinone analogue.

The final amination step is a nucleophilic substitution with an amine nucleophile and bromine atom leaving group. Experimentally, a large excess of the amine is added to the intermediate to limit unwanted side reactions occurring. In addition, using minimum amounts of water to dissolve the sodium hydroxide and methylamine hydrochloride proved to be beneficial to the reaction. The poor stability of cathinones as a free base led to their conversion into respective hydrochloride salts by passing hydrogen chloride gas through an ethereal solution of the free base cathinone or rotary evaporating pooled aqueous acidic extracts. These hydrochloride salts were typically washed or recrystallised with acetone for purification. It should also be noted that no attempts to purify reaction intermediates were made.

The three analogues that were not isolated and characterised in this study were 4-hydroxymethcathinone (**60**), β-naphyrone (**65**), and cathinone (**70**). A discussion of these reactions is provided in 2.3.2 below.

2.3.2 Yield and melting point

An observable trend appeared following the preparation of all the analogues. The ketone and α-bromoketone intermediates were prepared with relatively high yields and purity, while the amination step saw significant decreases in yield and often purity too. Table 2-1 summarises the yields obtained for intermediates and cathinone analogue hydrochloride salts. The most notable observation is the significant decrease in yield following purification steps. The majority of the analogues afforded percent yields less than 50% following recrystallization or washing with acetone. This is likely due to the volume of acetone used in washing steps and the solubility of cathinones in this solvent. The use of acetone to purify all cathinones is not ideal owing to the differing solubilities of the analogues. Future purification methods should employ different solvents specific to the cathinone. Other solvents and methods that could be employed in purification steps include 2-propanol[348], ethanol/diethyl ether[325, 329], flash chromatography using methanol/DCM[347] and ethanol/acetone[324]. For the purposes of this research, further optimisation of purification methods was not performed.

The melting points obtained for the purified products are also provided in Table 2-1 as an indication of purity. Most of the cathinones decomposed upon heating at higher temperatures, indicated by the significant changes in colour of the crystals before melting. MOMV (**44**) and α-PVP (**34**) were the only two analogues that did not change colour upon heating. The wide melting range recorded for many cathinones may also result from the decomposition of the pure substance prior to reaching its phase transition[349].

A comparison of literature melting point values from different sources showed a significant variability in the data. For example, the melting point for pentylone HCl (**24**) according to Lipomed[350] and SWGDRUG[339] were 230 ±3 °C and 242 °C, respectively. In addition, the literature values for MOMV HCl (**44**) and α-naphth HCl (**50**) could not be found.

2.3.1 Characterisation

The synthesis of these cathinone analogues was followed by characterisations using GC-MS, ^{1}H-NMR, ^{13}C-NMR, FTIR and UV-Vis. The data from these characterisations is summarised here, however, chromatograms and spectra of all intermediate and final products can be found in **Appendix A**.

Table 2-1. Percentage yields obtained for synthetic cathinone analogues and their respective ketone and bromo-ketone intermediates

Cathinone Analogue	**Percent yield (%)[a]**				**Melting point (°C)**
	Ketone	α-Bromoketone	Crude amine HCl	Pure amine HCl	Pure amine HCl
4-MMC (**3**)		89[c]	- [b]	46	219-220
4-FMC (**6**)		105	66	29	229-230
Methylone (**11**)	91	86[c]	41	30	236-239
MCAT (**13**)			- [b]	78	175-178
4-MEC (**14**)		89[c]	23	16	206-210
4-MPPP (**15**)		89[c]	- [d]	24	210-213
MDPV (**19**)	93	95[c]	- [d]	35	235-238
Butylone (**23**)	82	94[c]	- [b]	74	222-227
Pentylone (**24**)	93[c]	95[c]	- [b]	74	216-222
Pyrovalerone (**29**)	107[e]	89[e]	62	12	176-179
α-PVP (**34**)	73	96[e]	- [d]	11	101-104
4-EMC (**39**)	83	95	79	65	179-181
MOMV (**44**)	113	82	- [d]	13	123-126
Ethylone (**45**)	91[c]	86[c]	59	16	227-233
α-Naphth (**50**)	81	99	50	45	179-181
MDPBP (**51**)	82[c]	94[c]	48	39	220-222
4-MPBP (**55**)	111	83[e]	40	28	179-182

[a] Calculated per one step reaction. Intermediates not applicable to synthesis are blank
[b] Amine salt did not require further purification
[c] Repeated procedure from synthesis of different analogue
[d] Yield not calculated
[e] Percentage includes large amount of impurities

2.3.1.1 *GC-MS*

The GC-MS analysis of the intermediate compounds was performed for reaction monitoring purposes while the analysis of the final product was for characterisation. The runtime of the method employed was 10.8 min with the retention times of all cathinone analogues covering a

three minute window during this period. A summary of the GC-MS data for each of the seventeen analogues can be found in Table 2-2 with chromatograms and spectra available in **Appendix A**. The compound earliest to elute is 4-FMC (**6**) at 5.353 min. This is predicted based on the presence of a short carbon chain and fluorine atom not effectively binding to the highly non-polar column. Increasing carbon chain length and the presence of a pyrrolidine ring increased the retention time for all compounds, with MDPV (**19**) possessing a long carbon chain and a pyrrolidine ring displaying the longest retention time at 7.528 min.

Table 2-2. GC-MS data obtained for the isolated and characterised synthetic cathinone analogues

Amino substituent	Cathinone Analogue	TIC	Mass Spectrum	
		Retention time (min)	Base peak (*m/z*)	Molecular ion (*m/z*)
Methyl	4-MMC (**3**)	5.777	58	177
	4-EMC (**39**)	6.105	58	191
	4-FMC (**6**)	5.353	58	181
	MCAT (**13**)	5.543	58	163
	α-Naphth (**50**)	6.929	58	213
	Methylone (**11**)	6.382	58	207
	MOMV (**44**)	6.423	86	221
	Pentylone (**24**)	6.933	86	235
	Butylone (**23**)	6.586	72	221
Ethyl	Ethylone (**45**)	6.724	72	221
	4-MEC (**14**)	5.994	72	191
Pyrrolidine	4-MPPP (**15**)	6.463	98	217
	MDPBP (**51**)	7.392	112	232
	4-MPBP (**55**)	6.774	112	231[a]
	MDPV (**19**)	7.528	126	275
	Pyrovalerone (**29**)	6.962	126	245
	α-PVP (**34**)	6.496	126	231

[a] Molecular ion not present in spectrum

The TIC peak shapes of the cathinones are worth mentioning due to the tailing that was evident in all chromatograms. It is generally well known that amine compounds can produce tailing, however, cathinones have also been shown to undergo thermal degradation during GC-MS analysis to produce artefacts. These artefacts can remain unresolved and appear as tailing in the TIC[18]. An example of this peak tailing seen in MCAT (**13**) and 4-EMC (**39**) is shown in Figure 2-23.

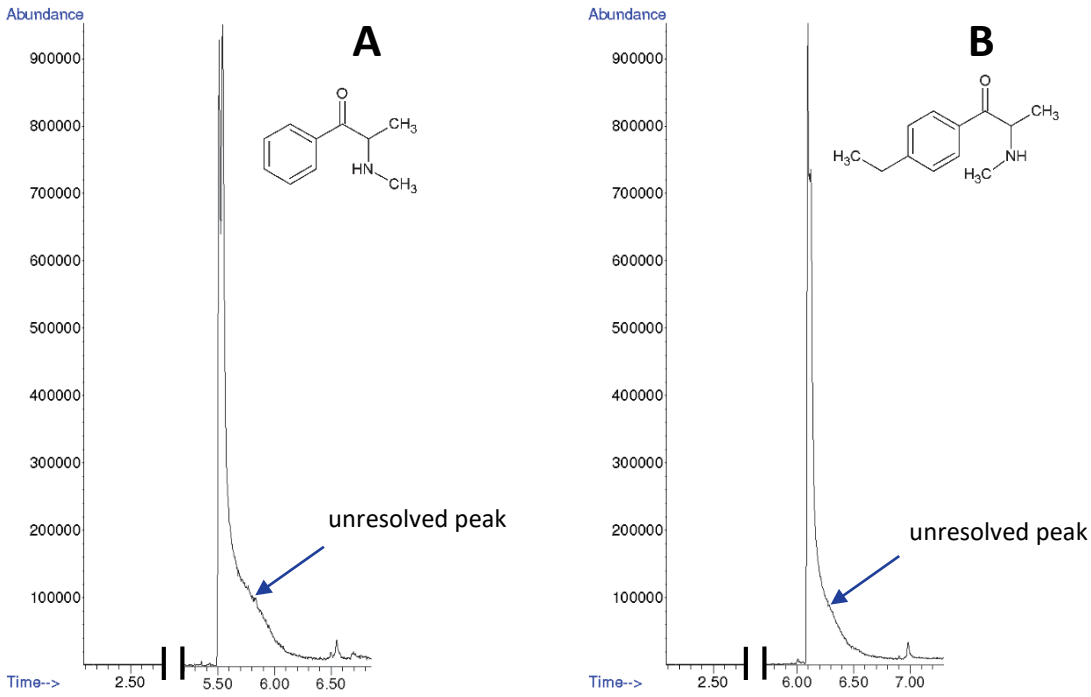

Figure 2-23. Total ion chromatograms showing significant peak tailing potentially due to unresolved artefacts formed during GC-MS analysis. A: MCAT (**13**); B: 4-EMC (**39**).

The EI spectra of cathinone analogues show analogous fragmentation characteristics. Alpha-cleavage of the benzyl bond produces a base peak immonium ion as shown in Figure 2-24. Other major fragmentations include alternative alpha-cleavage reactions to produce immonium ions with a higher *m/z* by the loss of an alkyl radical. Ionisation of the carbonyl oxygen atom and subsequent alpha-cleavage yields a benzoyl cation fragment which is followed by the loss of CO. The EI mass spectrum of MDPV (**19**) with associated fragment ion structures is shown below in Figure 2-24.

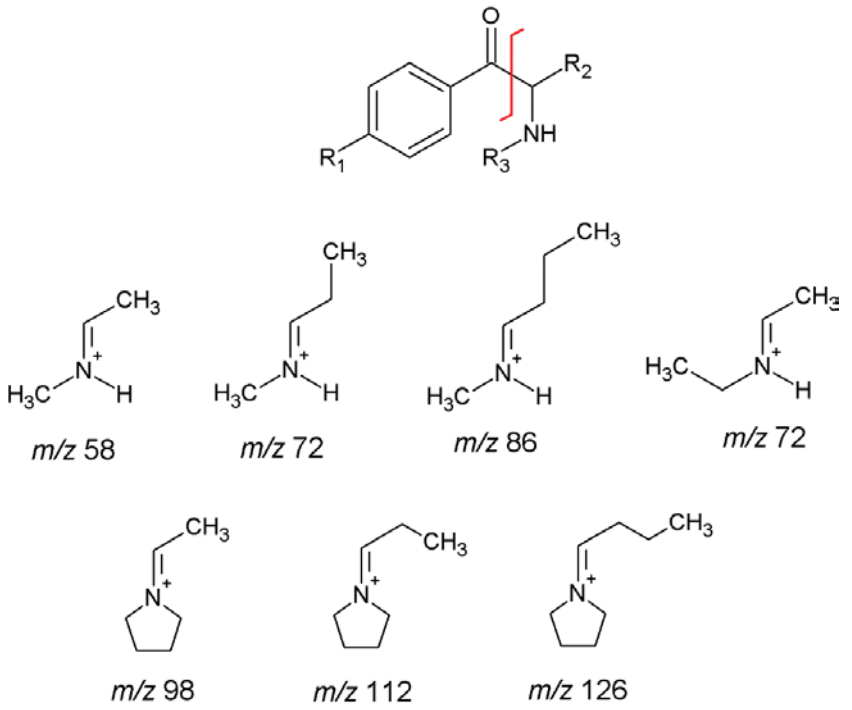

Figure 2-24. Alpha-cleavage reaction of synthetic cathinones to produce the major immonium cation fragments. Alkyl chain length and N-substituent of the cathinone determines the base peak *m/z*.

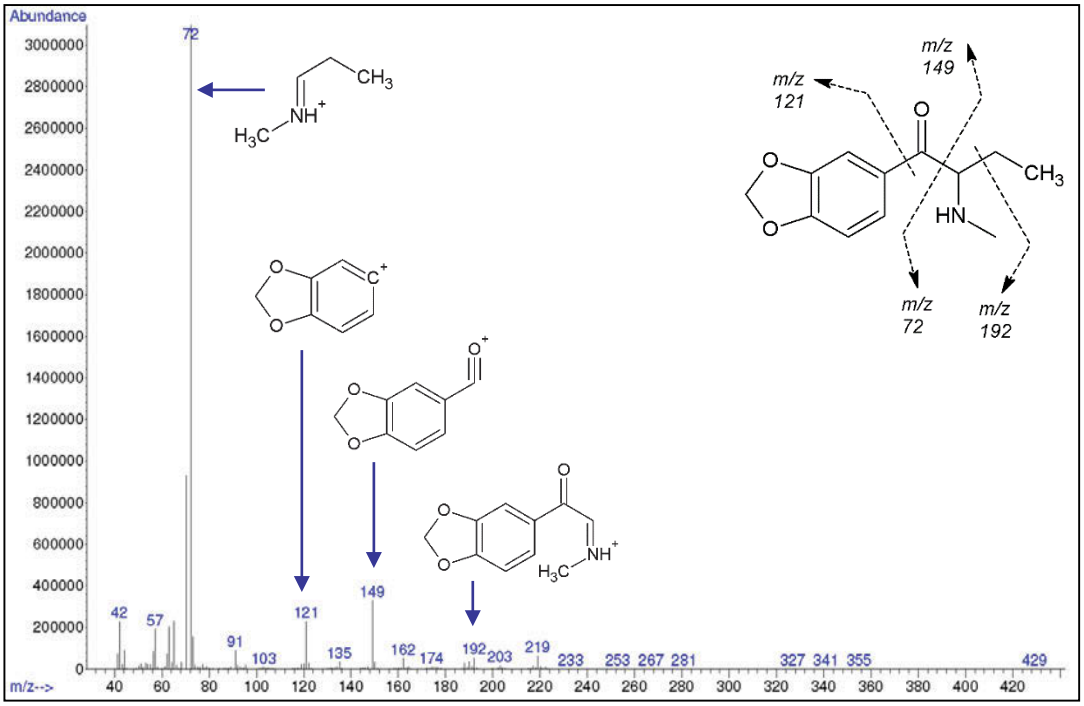

Figure 2-25. EI mass spectrum of butylone HCl (**23**) showing major fragments ions at m/z 72, 121, 149 and 192 due to α-cleavage fragmentation pathways.

2.3.1.2 *FTIR*

The FTIR spectra (see **Appendix A**) were consistent with the molecular structures of the cathinones, with several indicative absorption bands present. The first of which is the intense and sharp carbonyl bond stretching frequency at 1670-1690 cm^{-1} in all spectra. This band appears at a lower frequency than 1700 cm^{-1} of a ketone due to the conjugation that occurs between the carbonyl group and the benzene ring at the alpha position. The frequency is further decreased by the presence of electron donating groups on the benzene ring, e.g. 3,4-methylenedioxy substituted cathinones. The amine N-H stretching bands provided a way of distinguishing the secondary amine salts from the tertiary amine salts. A broad and intense peak at 2770-2380 cm^{-1} is a distinguishing feature of NH^+ in a tertiary amine salt. This differs from the secondary amine salt which appears as two bands at 2860-2770 cm^{-1} and 2560-2380 cm^{-1}[351]. This knowledge is useful when comparing pyrrolidine and alkyl substituted cathinones. Absorption bands present in the fingerprint region of the spectra are indicative of the benzene substitution pattern, e.g. mono-, para- and tri- substitutions. The FTIR spectrum of ethylone HCl (**45**) is provided below in Figure 2-26 showing bonds responsible for selected absorption bands. A summary of major functional group absorption bands across all analogues can be found in Table 2-3.

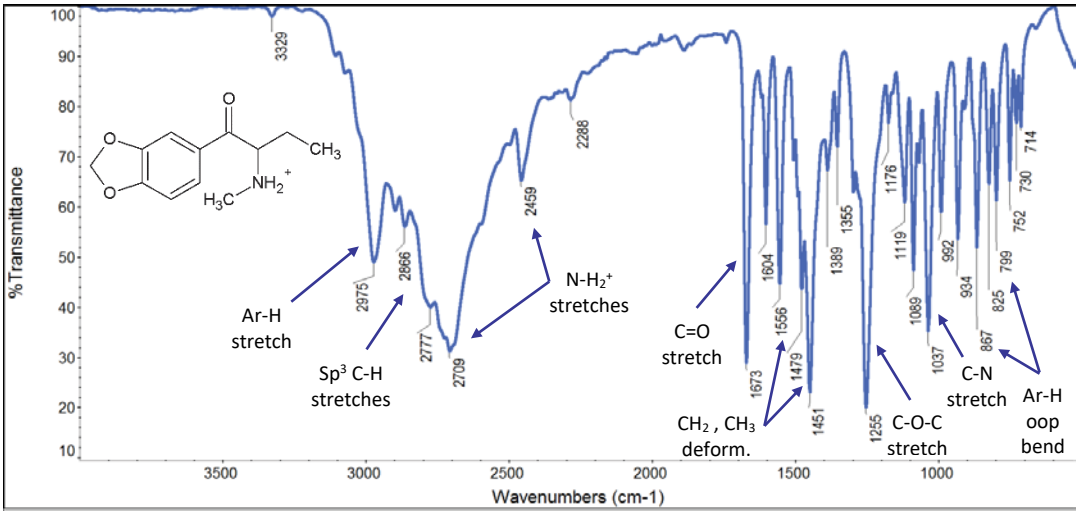

Figure 2-26. Annotated ATR-FTIR spectrum of ethylone HCl (**45**).

Table 2-3. Key FTIR absorption bands for the synthetic cathinone analogues

Benzene ring substituent	**Cathinone Analogue**	**Functional group absorption bands**		
		C=O stretch	**NH^+ / NH_2^+ stretches**	**Sp^2 C-H bend**
4-Methyl	4-MMC (**3**)	1685	2713 and 2455	832 (*p*-disubs.)
	4-MEC (**14**)	1687	2689 and 2476	831 (*p*-disubs.)
	4-MPPP (**15**)	1686	2568	829 (*p*-disubs.)
	Pyrovalerone (**29**)	1677	2612	841 (*p*-disubs.)
	4-MPBP (**55**)	1678	2672	830 (*p*-disubs.)
4-Ethyl	4-EMC (**39**)	1684	2681 and 2459	845 (*p*-disubs.)
4-Fluoro	4-FMC (**6**)	1687	2707 and 2458	847 (*p*-disubs.)
4-Methoxy	MOMV (**44**)	1682	2684 and 2453	827 (*p*-disubs.)
H	α-PVP (**34**)	1681	2689	719 (monosubs.)
	MCAT (**13**)	1688	2705 and 2452	697 (monosubs.)
3,4-Methylenedioxy	Methylone (**11**)	1676	2729 and 2456	883 and 807 (trisubs.)
	Butylone (**23**)	1674	2689 and 2475	880 and 802 (trisubs.)
	Pentylone (**24**)	1675	2744 and 2481	863 and 806 (trisubs.)
	Ethylone (**45**)	1673	2709 and 2459	867 and 799 (trisubs.)
	MDPBP (**51**)	1681	2614	876 and 805 (trisubs.)
	MDPV (**19**)	1684	2610	867 and 832 (trisubs.)
Benzene	α-Naphth (**50**)	1687	2712 and 2460	802 and 774 (α-subs. naphthalene)

2.3.1.3 *NMR*

The NMR studies were performed on the purified cathinone hydrochloride salts to confirm predicted structures. All ^{1}H and ^{13}C NMR spectra are provided in **Appendix A**. The cathinone analogues show characteristic signals in the aromatic region of the spectrum dependent on the substitution pattern at the benzene ring (see Figure 2-27). Monosubstituted cathinones are predicted to show three doublet of doublets due to ortho and meta proton couplings, however, this fine structure is not observed in both MCAT(**13**) and α-PVP (**34**) whose protons only couple over three bonds (^{3}J) to form one doublet and two apparent triplets. The predicted

two doublets splitting pattern was observed in all *p*-disubstituted cathinones analogues with the exception of MOMV (**44**) and 4-FMC (**6**). Despite the symmetry of the disubstituted benzene ring, each aromatic proton in MOMV (**44**) showed its own splitting pattern due to the spatial location of the methoxy group providing chemical inequivalence.

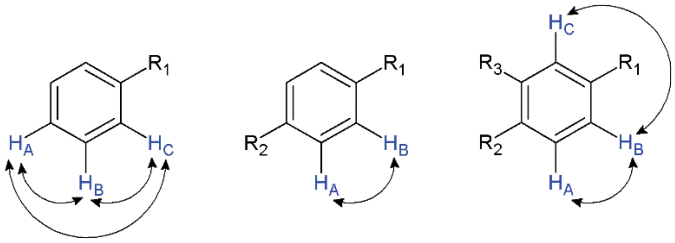

Figure 2-27. Expected proton coupling (^{1}H-^{1}H) on monosubstituted, *p*-disubstituted and trisubstituted benzene rings

The NMR spectra of 4-Fluoromethcathinone (**6**) afforded interesting splitting patterns due to heteronuclear coupling between ^{1}H and ^{19}F. Instead of the two doublets observed in other disubstituted cathinones, two doublet of doublets were observed (see Figure 2-28). This produced diagnostic features that confirmed the fluorine atom was present at the para position on the benzene ring.

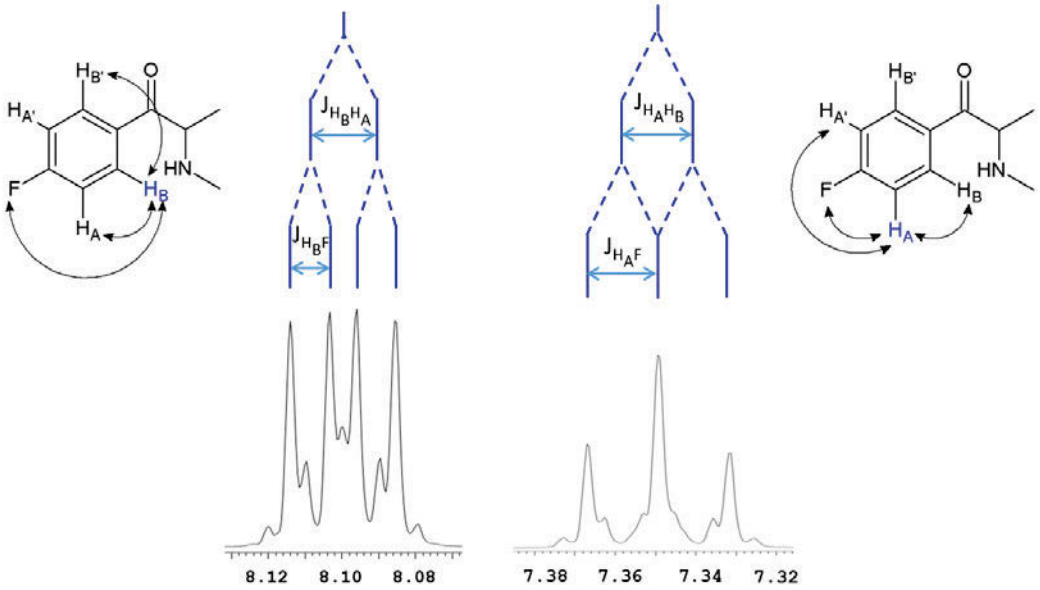

Figure 2-28. Fine structure observed downfield in the ^{1}H NMR spectrum of 4-FMC (**6**) as a result of heteronuclear coupling between ^{1}H and ^{19}F. Extra peaks observed in the spectrum are due to the added complexity of coupling between magnetically nonequivalent H_A and $H_{A'}$ (H_B and $H_{B'}$)

The extra peaks appearing in these splitting patterns is due to the added complexity of the AA'BB'X system in which A and A' (B and B') are not magnetically equivalent and will also couple across four bonds. These splitting patterns for 4-FMC were also observed by Archer [202], however no detailed explanations were provided and they were simply reported as multiplets due to heteronuclear coupling. It should also be mentioned that the ^{13}C NMR spectrum for 4-FMC (**6**) also contained distinct splitting

Trisubstituted cathinones are also easily distinguishable by the two doublets and one doublet of doublet observed in the aromatic region with the exception of MDPV (**19**) and ethylone (**45**) in which only coupling through three bonds (^{3}J) is observed.

Increasing carbon chain length of the cathinones provided interesting couplings in the proton spectra, for example pentylone (**24**) showed splitting of inequivalent methylene protons (see Figure 2-29). Here, the chiral centre at C-9 makes these methylene protons diastereotopic.

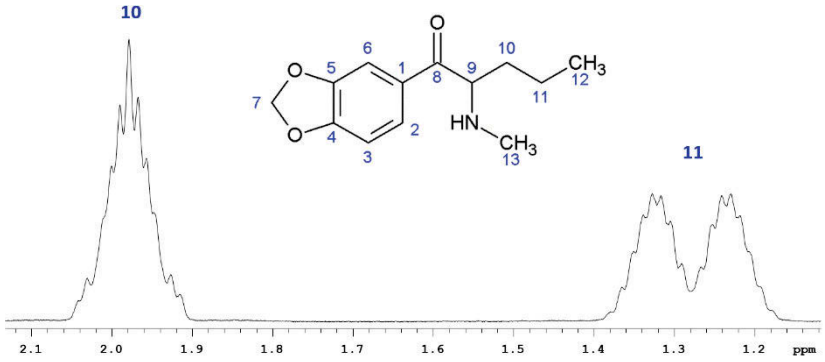

Figure 2-29. Upfield of the pentylone (**24**) ^{1}H NMR spectrum showing methylene proton splitting patterns

The inclusion of the pyrrolidine ring into the cathinone structure showed significant effects upfield in the proton NMR spectrum with overlapping signals and couplings occurring with methylene protons (see Figure 2-30). The pyrrolidine ring contains non-equivalent protons on the same carbon atom due to their 3D spatial arrangement.

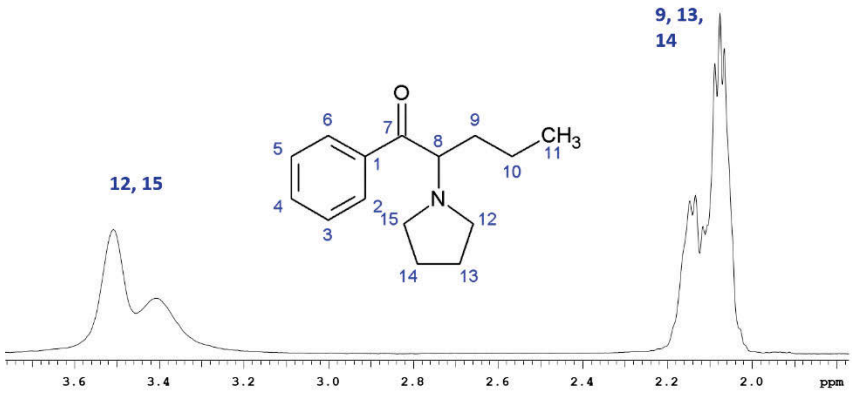

Figure 2-30. Upfield of 1H NMR spectrum of α-PVP (**34**) showing signals due to pyrrolidine ring protons.

2.3.1.4 *UV analysis*

The UV spectra of the cathinones showed characteristic features dependent on the presence of certain benzene ring substituents. The majority of the monosubstituted and disubstituted cathinones showed one clear absorption maximum in the UV region with an absorption shoulder appearing at lower wavelengths. An exception to this was MOMV (**44**) which showed three absorption maxima in the UV region, as did 3,4-methylenedioxy containing analogues due to the additional methoxy group auxochromes. The absorption observed for the naphthalene containing analogue α-naphth (**50**) also showed three absorption bands due to the additional conjugation the extra ring afforded. A tabulated list of the absorption maxima is provided in Table 2-4 below.

Table 2-4. UV-Visible absorption maxima of the synthetic cathinones in this study, recorded in deionised water

Benzene substituent	**Cathinone analogue**	**λ_{max} in water (nm)**
Alkyl group/hydrogen	4-MMC	264
	4-EMC	264
	4-FMC	254
	MCAT	251
	4-MEC	263
	4-MPPP	264
	4-MPBP	267
	Pyrovalerone	266
	α-PVP	254
4-Methoxy	MOMV	211, 256, 319

Benzene	α-Naphth	212, 244, 313
3,4-Methylenedioxy	Methylone	235, 281, 319
	Ethylone	235, 281, 319
	Butylone	236, 282, 321
	Pentylone	236, 282, 321
	MDPBP	237, 285, 323
	MDPV	237, 285, 324

2.3.2 Unsuccessful syntheses

Three reactions failed to effectively produce the desired compound and GC-MS spectra for all intermediate products can be found in **Appendix A**. 4-hydroxymethcathinone (**60**) was not successfully prepared due to competing reactions producing di-brominated products during the bromination step. The large number of side products produced made subsequent reactions difficult. β-naphyrone (**65**) was successfully synthesised, however, several impurities were present in the final product. The analogue was not isolated due to a misfortunate laboratory spill combined with a lack of starting material to repeat the synthesis. Cathinone (**70**) was the final compound that was not successfully isolated. Preparation of this compound proved difficult due to the stability of the primary amine combined with difficulties in performing the amine substitution step.

2.4 Conclusion

Seventeen synthetic cathinone analogues were successfully prepared from commercially available starting material. These compounds differed by the substituents positioned on the benzene ring and nitrogen atom as well as the length of the main carbon chain to provide a good coverage of cathinone analogues that may be encountered in the illicit drug market.

The preparation of these compounds followed typical synthesis procedures whereby the starting material used was easily accessible to the university. For the purposes of this research the yield obtained from the syntheses were not of a high importance due to the relatively small quantities required for most of the compounds. As a result, reactions were not optimised to increase the yield obtained, however, changes to the purification steps would be the first place to start, as acetone washes often proved detrimental to the yield obtained.

Unsuccessful synthesis of 4-hydroxymethcathinone, β-naphyrone and cathinone were not repeated due to limited starting material and the scope of the synthesis portion of my research.

2.5 References

18. Kerrigan, S., *et al.*, *Thermal Degradation of Synthetic Cathinones: Implications for Forensic Toxicology.* Journal of Analytical Toxicology, 2016. **40**(1): p. 1-11.
34. European Monitoring Centre for Drugs and Drug Addiction (EMCDDA), *European Drug Report 2017: Trends and Developments*. 2017: Luxembourg.
202. Archer, R.P., *Fluoromethcathinone, a new substance of abuse.* Forensic Science International, 2009. **185**(1–3): p. 10-20.
321. Bruce-Chwatt, R.M., *Intoxication with Qăat, Catha edulis L.* Journal of Forensic and Legal Medicine, 2010. **17**(5): p. 232-235.
322. Al-Juhaishi, T., S. Al-Kindi, and A. Gehani, *Khat: A widely used drug of abuse in the Horn of Africa and the Arabian Peninsula: Review of literature.* Qatar Medical Journal, 2012. **2012**(2): p. 1-6.
323. Capriola, M., *Synthetic cathinone abuse.* Clinical Pharmacology: Advances and Applications, 2013. **5**: p. 109-115.
324. Kavanagh, P., *et al.*, *The analysis of substituted cathinones. Part 3. Synthesis and characterisation of 2,3-methylenedioxy substituted cathinones.* Forensic Science International, 2012. **216**(1–3): p. 19-28.
325. Meltzer, P.C., *et al.*, *1-(4-Methylphenyl)-2-pyrrolidin-1-yl-pentan-1-one (Pyrovalerone) analogues: a promising class of monoamine uptake inhibitors.* J Med Chem, 2006. **49**(4): p. 1420-32.
326. Carlsson, A., *Synthesis and spectroscopic characterization of emerging synthetic cannabinoids and cathinones*, in *Department of Physics, Chemistry and Biology*. 2016, Linköping University: Linköping, Sweden. p. 62.
327. Anon. *Notes on the Synthesis of Methcathinone*. 2010 [cited 2017 November 1]; Available from: https://erowid.org/archive/rhodium/chemistry/methcathinone.txt.
328. Jacob, P. and A.T. Shulgin, *Novel n-substituted-2-amino-3',4'-methylene-dioxypropiophenones*. 1996, Google Patents.
329. Koppe, H., G. Ludwig, and K. Zeile, *Novel alpha-amino-substituted (3,4-methylenedioxy - phenyl) - alkanones and salts thereof*. 1970, Google Patents.
330. Sigma-Aldrich, *TLC Visualization Laboratory Data Guide*. 2011: St. Louis, MO, USA.
331. Scientific Working Group for the Analysis of Seized Drugs (SWGDRUG), *4-methmethcathinone HCl*, in *Drug Monographs*. 2013, Drug Enforcement Administration (DEA): USA.
332. Scientific Working Group for the Analysis of Seized Drugs (SWGDRUG), *4-fluoromethcathinone HCl*, in *Drug Monographs*. 2013, Drug Enforcement Administration (DEA): USA.
333. Scientific Working Group for the Analysis of Seized Drugs (SWGDRUG), *Methylone*, in *Drug Monographs*. 2013, Drug Enforcement Administration (DEA): USA.
334. Scientific Working Group for the Analysis of Seized Drugs (SWGDRUG), *Methcathinone*, in *Drug Monographs*. 2005, Drug Enforcement Administration (DEA): USA.

335. Scientific Working Group for the Analysis of Seized Drugs (SWGDRUG), *4-methylethcathinone*, in *Drug Monographs*. 2013, Drug Enforcement Administration (DEA): USA.
336. Scientific Working Group for the Analysis of Seized Drugs (SWGDRUG), *4-methyl-a-pyrrolidinopropiophenone*, in *Drug Monographs*. 2013, Drug Enforcement Administration (DEA): USA.
337. Scientific Working Group for the Analysis of Seized Drugs (SWGDRUG), *3,4-MDPV*, in *Drug Monographs*. 2013, Drug Enforcement Administration (DEA): USA.
338. Scientific Working Group for the Analysis of Seized Drugs (SWGDRUG), *Butylone*, in *Drug Monographs*. 2014, Drug Enforcement Administration (DEA): USA.
339. Scientific Working Group for the Analysis of Seized Drugs (SWGDRUG), *Pentylone*, in *Drug Monographs*. 2014, Drug Enforcement Administration (DEA): USA.
340. Scientific Working Group for the Analysis of Seized Drugs (SWGDRUG), *Pyrovalerone*, in *Drug Monographs*. 2016, Drug Enforcement Administration (DEA): USA.
341. Scientific Working Group for the Analysis of Seized Drugs (SWGDRUG), *a-PVP*, in *Drug Monographs*. 2013, Drug Enforcement Administration (DEA): USA.
342. Scientific Working Group for the Analysis of Seized Drugs (SWGDRUG), *4-ethylmethcathinone*, in *Drug Monographs*. 2014, Drug Enforcement Administration (DEA): USA.
343. Scientific Working Group for the Analysis of Seized Drugs (SWGDRUG), *Ethylone*, in *Drug Monographs*. 2013, Drug Enforcement Administration (DEA): USA.
344. Scientific Working Group for the Analysis of Seized Drugs (SWGDRUG), *MDPBP*, in *Drug Monographs*. 2014, Drug Enforcement Administration (DEA): USA.
345. Scientific Working Group for the Analysis of Seized Drugs (SWGDRUG), *4-methyl-a-pyrrolidinobutiophenone*, in *Drug Monographs*. 2013, Drug Enforcement Administration (DEA): USA.
346. Santali, E.Y., *et al.*, *Synthesis, full chemical characterisation and development of validated methods for the quantification of (±)-4'-methylmethcathinone (mephedrone): A new "legal high".* Journal of Pharmaceutical and Biomedical Analysis, 2011. **56**(2): p. 246-255.
347. Power, J.D., *et al.*, *The analysis of substituted cathinones. Part 1: Chemical analysis of 2-, 3- and 4-methylmethcathinone.* Forensic Science International, 2011. **212**(1–3): p. 6-12.
348. Aarde, S.M., *et al.*, *The novel recreational drug 3,4-methylenedioxypyrovalerone (MDPV) is a potent psychomotor stimulant: self-administration and locomotor activity in rats.* Neuropharmacology, 2013. **71**: p. 130-140.
349. Stanford Research Systems (SRS), *Melting Point Determination* in *SRS Application Notes*. Sunnyvale, CA.
350. Lipomed, *Pentylone HCl*, in *Specifications Sheet*. Lipomed AG: Arlesheim, Switzerland.
351. Thompson, W.E., *et al.*, *Identification of primary, secondary, and tertiary pharmaceutical amines by the infrared spectra of their salts.* Journal of Pharmaceutical Sciences, 1965. **54**(12): p. 1819-1821.

This page intentionally left blank

Chapter 3: Chemical colour tests for the colorimetric detection of synthetic cathinones

This page intentionally left blank

This page intentionally left blank

Chapter 3: Chemical colour tests for the colorimetric detection of synthetic cathinones

Summary

This chapter investigates the use of a novel chemical colour test for the detection of synthetic cathinones. The chemical reaction that occurs only in the presence of synthetic cathinones provides the recognition element for the detection method that is transduced to a colorimetric signal. This colour change is visible with the naked eye.

This chapter is taken from a first author publication in the Elsevier journal, Forensic Chemistry (see next page for details).

Development and validation of a presumptive colour spot test method for the detection of synthetic cathinones in seized illicit materials

Morgan Philp[1], Ronald Shimmon[1], Mark Tahtouh[2] and Shanlin Fu[1*]

[1] Centre for Forensic Science, University of Technology Sydney (UTS)
[2] Australian Federal Police (AFP), 110 Goulburn St, Sydney

Forensic Chemistry (2016) **1**: 39-50

Statement of contributions of joint authorship

Morgan Philp: (candidate)
Conception of ideas, conducting experiments and analysing data.
Writing and compilation of manuscript, including tables and figures

Ronald Shimmon: (co-supervisor)
Editing and co-author of manuscript

Mark Tahtouh: (industry supervisor)
Editing and co-author of manuscript

Shanlin Fu: (principal supervisor)
Editing and co-author of manuscript

The majority of this chapter is taken from the above journal paper.

3.1 Introduction

The present-day illicit drug trade continues to be the large, lucrative, global industry of previous decades, with an added degree of complexity owing to technological advances and the ingenuity of rogue chemists and organized crime groups worldwide.

This recreational drug market has seen the increased prevalence and abuse of Drug Analogues and New Psychoactive Substances (DANPS). These are substances structurally similar to a prohibited or scheduled parent compound, or substances intended to have a similar pharmacological effect to prohibited or scheduled drugs[352]. DANPS are causing great concern in the current market due to the large number and diversity of these insufficiently studied substances. In order to circumvent any potential legal barriers, suppliers often label these substances as 'bath salts', 'plant food' or 'not for human consumption'. They are also marketed as 'legal' alternatives to illicit drugs.

Synthetic cathinones are a class of compounds that have accounted for the highest proportion of the number of seizures in the DANPS subset in Australia since 2008. In 2013–14, the number of synthetic cathinone seizures made up 34.8 per cent of those analyzed[352]. In Europe, a similar situation is seen with synthetic cathinones accounting for more than 8000 seizures made in 2014[353]. The general chemical structure of synthetic cathinones is shown in Figure 3-1. Chemical modifications to the general structure result in an almost unlimited number of cathinone-type substances[354].

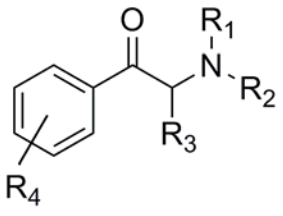

Figure 3-1. General chemical structure of synthetic cathinone substances. R_1 and R_2 can exist as hydrogen, an alkyl moiety, or cyclic structure; R_3 can exist as hydrogen or any alkyl group; and R_4 can exist as hydrogen or a combination of various moieties such as alkyl, alkoxy, alkylenedioxy, haloalkyl, or halide.

Australian Commonwealth legislation has recently been amended to strengthen the response to DANPS. The inclusion of analogue clauses provides wide coverage of drug analogues seized, and emergency temporary scheduling allows for a quick response when full harms of drugs are not yet known[355]. It is now an offence to import psychoactive substances without a legitimate use[356].

The identification and quantification of illicit drugs is most commonly performed using confirmatory techniques such as Gas Chromatography-Mass Spectrometry (GC-MS) and High Performance Liquid Chromatography-Mass Spectrometry (HPLC-MS). These dual function techniques combining separation power with spectroscopic analysis are referred to as the 'gold standard' for routine analysis, achieving identification by comparing to mass spectral libraries and reference standards[152]. Although highly specific and reliable, these instruments are not ideal for high throughput sample analysis owing to their high cost of running, the need for trained personnel, lengthy analysis times, and optimization and maintenance requirements.

The Australian Crime Commission's (ACC) annual Illicit Drug Data Report for the period 2013-14 showed a record 93,086 illicit drug seizures were made by Australian authorities[352]. The significant quantities of potentially illicit samples seized that require identification demonstrates the importance of preliminary testing procedures that are simple, rapid, inexpensive, and able to be used in the field with high selectivity.

Presumptive screening tests are designed to provide an indication of the presence or absence of certain drug classes in a test sample[152]. Colour 'spot' tests are simple and rapid chemical tests that result in a colour change when applied to a sample containing a drug of interest. The chemical reaction occurring between the colour reagent and the drug of interest provides a frequently employed selective screening tool. The increase in prevalence of synthetic cathinones in illicit drug seizures has revealed a lapse in current presumptive testing methodologies. A number of companies have produced commercially available test kits for synthetic cathinones, however, these tests often employ hazardous substances; demonstrate a lack of selectivity toward the cathinone class; or have not been screened on a large number of available synthetic cathinone substances[56, 134, 357].

The principles of reduction-oxidation (redox) reactions have been used to develop simple and sensitive spectrophotometric methods in the detection and quantification of a number of compounds. The Cupric Reducing Antioxidant Capacity (CUPRAC) method, developed by researchers of Istanbul University provides for the measurement of antioxidant compounds via

the reduction of copper(II)-neocuproine reagent to the coloured copper(I)-neocuproine chelate complex[264]. Several antioxidant molecules have been detected via this method, such as ceftazidime[268], ibuprofen[358], reducing sugars[359] and dazomet[267]. Similarly, Al-Obaid *et al.*[266] described a spectrophotometric detection of (S)-(-)-cathinone by treating cathinone with neocuproine and a copper(II) solution to afford a coloured copper(I)-neocuproine complex.

Despite the number and variety of assays employing copper and neocuproine, to the best of our knowledge, the literature contains no reports of its use in the detection of illicit drugs.

This work aims to investigate the use of copper(II)-neocuproine as a colour test reagent and subsequently propose an optimized colour test method for the detection of synthetic cathinones in seized illicit materials.

3.2 Materials and methods

3.2.1 Chemicals

Neocuproine hemihydrate and copper(II) nitrate trihydrate were purchased from Sigma Aldrich (Castle Hill, NSW, Australia); analytical grade anhydrous sodium acetate was from Ajax Finechem (Taren Point, NSW, Australia); sodium hydroxide pellets, sodium hydrogen carbonate ($NaHCO_3$) and analytical grade methanol were from Chem-Supply (Gillman, SA, Australia); and ammonium acetate and analytical grade glacial acetic acid were from BDH Laboratory Chemicals (Poole, England) and LabServ Pronalys (Taren Point, NSW, Australia), respectively. Hydrochloric acid (32% w/w) and reagent grade chloroform were from RCI Labscan (Taren Point, NSW, Australia). Deionized water from a laboratory supply was used throughout the procedure.

3.2.2 Reference materials

The synthetic cathinone, 4-methylmethcathinone hydrochloride (4-MMC HCl), was synthesized in our laboratory with identity and purity confirmed by gas chromatography-mass spectrometry (GC-MS), nuclear magnetic resonance spectroscopy (NMR), Fourier transform infrared spectroscopy (FTIR), and Ultraviolet-Visible spectrophotometry (UV-Vis) (see

Supporting Information). In addition, 88 certified drug reference standards were obtained from the National Measurement Institute (NMI, Sydney, Australia) for a selectivity study. A complete list of these analytes can be found in the results section.

Caffeine, ephedrine hydrochloride, codeine phosphate, starch, glucose, sucrose and a range of powdered substances were obtained from Ajax Finechem, BDH Laboratory Chemicals, Sigma Chemicals, Chem-supply and Sigma-Aldrich. Flour, sugar, protein powder and artificial sweetener were obtained from a local supermarket. A complete list of these substances can be found in the results section.

3.2.3 Preparation of working solutions

A working standard solution of 4-MMC HCl was prepared at a concentration of 500 µg/mL in deionized water. Working standard solutions of starch, glucose, caffeine, sucrose, codeine phosphate and ephedrine HCl were prepared at concentrations of 1000 µg/mL in deionized water.

Working solutions of neocuproine (2.90×10^{-2} mol/L) in 0.100 mol/L hydrochloric acid (HCl), copper(II) nitrate (1.25×10^{-2} mol/L) in deionized water and sodium acetate (2.00 mol/L) in deionized water were prepared. These reagents will be referred to as neocuproine, Cu(II) and acetate buffer, respectively, throughout this paper.

3.2.4 Apparatus and instrumentation

Polypropylene flat bottom 96-well micro plates were obtained from Greiner Bio-One and porcelain spotting well-plates were supplied by UTS. A Simmerstat Plain Top from Industrial Equipment & Control Pty Ltd was used as the hotplate during colour test procedures, set at 80-100°C. All pH measurements were carried out with a pH 211 Microprocessor from HANNA instruments.

All Ultraviolet-Visible (UV-Vis) spectra were produced using a Cary 3E UV-Vis spectrophotometer (Varian Inc., Australia). Nuclear Magnetic Resonance (NMR) spectra were recorded at 298 K using an Agilent 500 MHz spectrometer operating at 499.86 MHz (^{1}H) using standard pulse sequences. Chemical shifts (δ) are reported as parts per million (ppm) with

respect to the internal standard tetramethylsilane (TMS), set at δ 0.00 ppm. Deuterated chloroform and deuterium oxide NMR solvents were from Sigma Aldrich.

3.2.5 Colour test method development

3.2.5.1 *Colour change specifications*

Colour changes were described using the system adopted in Clarke's Analysis of Drugs and Poisons[73]. This system uses ten basic colours (red, orange, yellow, green, blue, violet, together with pink, brown, grey and black) with a variation in hue indicated by combining two colours (e.g. green-blue). Importantly, the second-named colour is considered to be the dominant one.

3.2.5.2 *Preliminary test method*

A method previously described by Al-Obaid *et al.*[266] for detection of cathinone from khat plants was adapted in this study. Reagent working solutions were prepared and testing was performed using 4-MMC HCl working solution.

Briefly, in the order of addition to a small beaker, Cu(II) solution (1.00 mL), 4-MMC HCl solution (1.00 mL), neocuproine solution (1.00 mL) and water (10.0 mL) was added before heating (2 min) on a hotplate set at 80°C, cooling, adding acetate buffer (1.25 mL) and heating a second time (10 min). A control reagent blank test was performed simultaneously by replacing 4-MMC HCl solution with deionized water only. Colour changes were recorded.

3.2.5.3 *Reduction to small scale*

The method was then modified to be performed on a smaller scale in a micro well-plate using Pasteur pipettes to add drop-sized amounts of reagents. Cu(II) (1.25×10^{-2} mol/L, 8 drops) and 4-MMC HCl working solution (100 µg/mL, 8 drops) were added to a well and gently mixed. Neocuproine (2.90×10^{-2} mol/L, 8 drops) and water (5 drops) were added, and the mixture heated on a boiling water bath for 2 minutes. Upon cooling, acetate buffer (2.50 M, 10 drops) was added and the plate heated for a further 10 minutes.

Testing was performed on solutions of 4-MMC HCl, ephedrine HCl, codeine phosphate, caffeine, glucose, sucrose and starch, alongside a control reagent blank. The colour changes were recorded.

3.2.5.4 *Optimisation of reagent concentrations*

Cu(II) solutions at concentrations of 1.25×10^{-2}, 1.25×10^{-3}, 1.25×10^{-4}, 1.25×10^{-5} and 1.25×10^{-6} mol/L were prepared via serial dilution. Each Cu(II) solution (2 drops) was added to two wells of a micro well-plate. An aqueous solution of 4-MMC HCl (100 µg/mL, 5 drops) was added to one of the wells, and water to the second 'blank' well for each Cu(II) concentration. Neocuproine solution (2.90×10^{-2} mol/L, 2 drops) was added to all wells before heating for 2 minutes. The acetate buffer solution (2.50 mol/L, 2 drops) was finally added and the plate heated for a further 10 minutes.

A set of acetate solutions with concentrations of 2.50, 2.00, 1.00, 5.00×10^{-1} and 1.00×10^{-1} mol/L were prepared, affording a pH range of 8.9-9.5. Similarly, a set of neocuproine solutions were prepared at 4.00×10^{-1}, 8.00×10^{-2}, 3.20×10^{-2}, 1.28×10^{-2} and 5.12×10^{-3} mol/L via serial dilution. Cu(II) (1.25×10^{-2} mol/L, 2 drops) was added to 25 wells of two micro well-plates: one containing a water 'blank' and the other charged with 4-MMC HCl solution. Each neocuproine concentration was coupled with each acetate concentration, and the colour testing performed. Colour changes were recorded.

3.2.5.5 *Optimisation of reagent concentrations in solid sample application*

Cu(II) solutions at concentrations of 2.00×10^{-2}, 1.50×10^{-2}, 1.25×10^{-2}, 1.00×10^{-2} and 5.00×10^{-3} mol/L were prepared, along with neocuproine solutions at 8.00×10^{-1}, 3.20×10^{-2}, 1.28×10^{-2} and 5.12×10^{-3} mol/L. Two micro well-plates were prepared: one charged with approximately 0.1-0.2 mg (measured qualitatively as a small pin head sized amount) of 4-MMC HCl in 20 wells, and the other containing empty wells. Testing was performed as follows: add five drops of Cu(II) reagent, followed by two drops of neocuproine reagent and then two drops of acetate buffer. Decreasing Cu(II) concentrations were added to the wells down the plate, and decreasing neocuproine concentrations were added across the plate. A total of 20 unique tests were performed on both the blank and the 4-MMC HCl samples, respectively. The plate was heated on a boiling water bath for 10 minutes and the colour changes recorded.

3.2.5.6 *Optimal buffer conditions*

Solutions of acetic acid, hydrochloric acid, sodium hydroxide, sodium hydrogen carbonate, sodium acetate and ammonium acetate were prepared at 0.100 mol/L. Sodium hydroxide and sodium acetate were also prepared at 2.00 mol/L and 5.00 mol/L, respectively, and a 200 µg/mL methanolic solution of 4-MMC HCl was prepared.

A 200 µL aliquot of 4-MMC was pipetted into twelve wells of a micro well-plate and the methanol left to evaporate in the fume hood. Employing buffer solutions with pH range 1-14 in place of the acetate buffer, the test method described above for solid samples, was applied to the 4-MMC HCl samples and a control blank, in triplicate.

3.2.6 Spectroscopic analysis

The proposed copper-neocuproine test method was applied to a sample of 4-MMC HCl alongside a control reagent blank in glass scintillation vials. The volumes and amount of sample added were increased by a factor of 10. Deionized water (4 mL) was then added to each vial for UV-Vis analysis.

A solution of copper(I) chloride (5.00×10^{-3} M) in 0.100 M HCl was also prepared and substituted for the Cu(II) solution in a neocuproine colour test performed on a 4-MMC HCl sample alongside a control blank. Colour changes and UV-Vis spectra were recorded.

In order to characterize the coloured complex formed in these colour tests, test solutions were left in the wells of porcelain test plates at room temperature for two weeks until the water had slowly evaporated leaving behind fine, orange-red crystals. The metal complex crystals were then washed with diethyl ether; recrystallized using deionized water; and filtered using a cotton-plugged Pasteur pipette. The crystals were then redissolved in organic solvent for collection.

The coloured compound from reaction with 4-MMC HCl as well as that formed using Cu(I) reagent in the absence of 4-MMC HCl were analyzed using ^{1}H-NMR spectroscopy. Deuterated chloroform ($CDCl_3$) and deuterium oxide (D_2O) were used as the solvents, respectively.

3.2.7 Method validation

A set of experiments were performed as specified by the United Nations Office on Drugs and Crime (UNODC) recommendations[70].

3.2.7.1 *Selectivity and specificity*

An extensive range of substances were collected to aid in the investigation of the selectivity and specificity of the neocuproine colour test. These substances included: controlled substances from the synthetic cathinone drug class; controlled substances from other drug classes, common precursors to illicit drugs; common diluents/excipients in the matrix of seized drugs; common pharmaceutical tablets and white powders; and mixtures of synthetic cathinones that are representative of potential case samples.

Drug standards and powders were tested without further processing, and tablets were ground into a fine powder using a mortar and pestle.

A small pin-head sized amount of each substance to be tested was added to a well of a porcelain well-plate. The developed neocuproine colour test procedure was applied and the colour change recorded. Each substance was tested in triplicate.

3.2.7.2 *Limit of detection*

The limit of detection (LOD) was determined using a modified version of that recommended in the National Institute of Justice Colour Test Standard[68] for 4-MMC HCl, as an example cathinone substance.

A 200 µg/mL methanolic solution of 4-MMC HCl was prepared. Five replicate aliquots of this solution at: 0.0, 5.0, 10.0, 15, 20, 25, 30, 50, 100, 150, 200 and 250 µL were pipetted into a micro well-plate and the solvent evaporated in a fume hood. The developed neocuproine colour test procedure was applied to each well and colour changes recorded. The smallest sample size producing a colour change noticeably different to that of the blank and characteristic for the target analyte for all five replicates was used to determine the limit of detection.

3.2.7.3 *Purity testing*

A purity test was undertaken using caffeine and glucose as cutting agents in samples of 4-MMC HCl, before application of the neocuproine test. Methanolic solutions of 4-MMC HCl at a concentration of 200 µg/mL and methanolic solutions of caffeine and glucose at 2000 µg/mL were prepared.

Aliquots of 100 µL of the drug standard solution were pipetted into eleven consecutive wells of a micro well-plate and the solvent left to evaporate in a fume hood. To each of these wells was added, a unique aliquot of the methanolic caffeine solution: 0.0, 2.5, 5.0, 10.0, 15, 20, 25, 32.5, 50, 65, 100 and 200 µL (0-95 % g/g impurity). The solvent was again left to evaporate. The developed neocuproine colour test procedure was applied to each well. This was performed in triplicate and colour changes recorded. The procedure was repeated using glucose as the cutting agent.

3.2.7.4 *Precision analysis*

The developed neocuproine colour test procedure was applied to known samples of 4-MMC HCl. The test was performed on five replicate samples at the same time. Further testing was completed in triplicate on the same day with the same reagents in the same laboratory. The developed test method was also performed in triplicate on different days, using different reagents and in different laboratories.

Certified reference samples were tested in triplicate at the AFP laboratory on both the same day and on different days, representing an inter-laboratory analysis.

The developed colour test was also performed on two samples of 4-MMC HCl that were synthesized at different times using the same synthetic procedures, representing potential drug samples from different sources.

3.2.7.5 *Stability*

A neocuproine reagent solution, prepared at a concentration of 2.00×10^{-3} M, was divided into four separate vials and allocated a different storage environment, including: laboratory bench top, laboratory cupboard, refrigerator (7 ^{o}C), and a water bath (35 ^{o}C).

Each reagent solution was employed in the developed colour test method by applying to triplicate samples of the target analyte, 4-MMC HCl, alongside a blank reagent weekly for up to three months. The colours produced in each test were recorded.

3.3 Results and discussion

3.3.1 Colour test method development

3.3.1.1 *Preliminary test method*

As recommended in the UNODC's Guidance for the Validation of Analytical Methodology[70], a candidate method was chosen upon which to develop a novel colour test method. The original method reported by Al-Obaid *et al.*[266] was preliminarily investigated to confirm that a chemical reaction occurs in the presence of 4-MMC HCl, and results in a distinct colour change. The 4-MMC HCl reacted with the reagents to produce a yellow-orange coloured solution as seen in Figure 3-2. A number of important factors were determined: the addition of acetate buffer leads to a colour change from blue to green; the reaction requires heat to occur; and the yellow-orange colour produced in the presence of 4-MMC HCl is stable at room temperature.

Figure 3-2. Preliminary copper-neocuproine test results. Method performed on control reagent blank *(a)* and aqueous 4-MMC HCl solution *(b)*. Coloured solutions were pipetted from beakers into white well-plates after heating to improve the colour contrast.

3.3.1.2 *Reduction to small scale*

The first step in the evolution of a new method involves an identification of its requirements. 'Colour testing' for the purposes of preliminary identification of illicit drugs must be performed on a small scale using both: a small amount of the illicit powdered substance and a limited amount of each reagent.

The test reduction to small scale still displayed a colour change for 4-MMC HCl; demonstrating the reaction is scalable. The 4-MMC HCl sample produced a bright orange colour, contrasting to the light green-blue colour afforded by starch, glucose, caffeine, sucrose, ephedrine HCl and the control reagent blank. Codeine phosphate, however, did produce a yellow colour.

The aqueous samples were tested as a preliminary means of determining the selectivity, and to establish whether further investigation into this reagent would be of benefit. As 4-MMC HCl produced the most intense colour change; and common cutting agents, caffeine and glucose, did not show a reaction, the method was further developed and optimized.

3.3.1.3 *Reagent concentrations*

At copper(II) concentrations below 1.25×10^{-5} M, no observable colour change was produced. Light yellow and bright yellow colours were produced with 1.25×10^{-4} M and 1.25×10^{-3} M Cu(II), respectively. A further ten-fold increase in Cu(II) concentration saw the control blank appear blue and the test for 4-MMC HCl, orange. It was decided to continue further colour testing using 1.25×10^{-2} M Cu(II) as the preliminary Cu(II) concentration due to the most intense colour change it afforded.

The different neocuproine concentrations tested against a blank control solution afforded interesting results, as shown in Figure 3-3. At concentrations of 4.0×10^{-1} M and 8.0×10^{-2} M, intense, bright orange coloured solutions were observed. This showed that the coloured product formed here was not due to a reaction with the drug molecule, but rather an excess of the neocuproine reagent. It was determined that the neocuproine test reagent will need to be less than 3.20×10^{-2} M for reliable results to be produced. The test plate containing 4-MMC HCl produced yellow to orange coloured solutions for each neocuproine and acetate concentration combination, including tests below 3.20×10^{-2} M neocuproine, which appear light green to blue in the control blank tests.

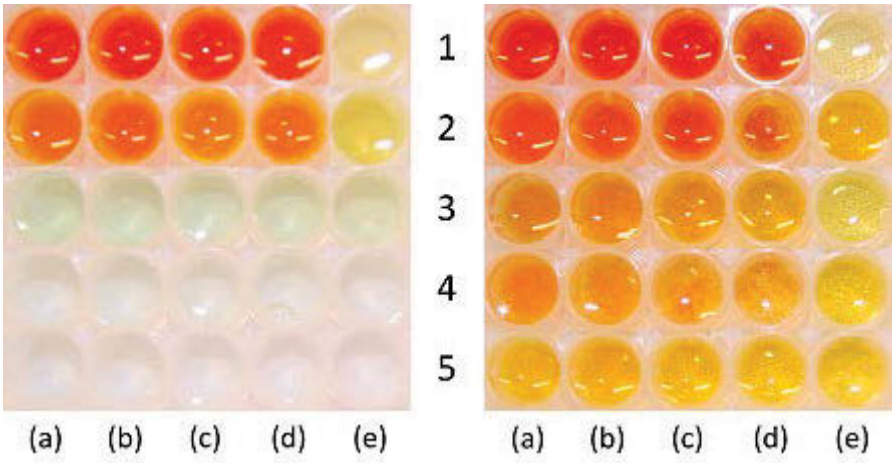

Figure 3-3. Reagent concentration optimization study results. Colour testing performed using decreasing neocuproine concentrations *(1-5)* and decreasing acetate concentrations *(a-e)* with Cu(II) concentration kept at 1.25×10^{-2} M for control reagent blank *(left)* and aqueous 4-MMC HCl *(right)*. The well at 5b in the control blank and 4-MMC HCl charged plate was chosen to have the optimal concentrations for testing: 1.25×10^{-2} M Cu(II); 5.12×10^{-3} M neocuproine; and 2.00 M acetate buffer.

The results in Figure 3 demonstrate that varying the acetate concentration does not adversely affect the colours produced. However, it was determined that in order for the 4-MMC HCl to afford the most intense coloured product, a concentration above 1.00 M would be ideal. The optimal reagent concentrations for use on aqueous sample solutions were decided: 1.25×10^{-2} M Cu(II); 5.12×10^{-3} M neocuproine; and 2.00 M acetate buffer.

3.3.1.4 *Effect of Heating Temperature*

In order to determine the effect of the heating temperature, two separate experiments were performed. The first one involving reducing the temperature of the water bath to 80 °C had a significant effect on the colour test results. The test results show no reaction occurred with the 4-MMC HCl solution under these conditions. It is likely the heating period would need to be increased to see a colour change.

The second experiment saw the removal of the first heating step, and showed no difference to the preliminary test involving two heating steps. This confirmed that the two minute heating period could effectively be removed without jeopardizing the results. Considering the intended

purpose of the test would be in rapid screening methods, possibly in the field, limiting the number of steps required is of prime importance.

Future research into developing this test as a field screening method for cathinone substances could focus on finding a suitable catalyst to substitute the heating step. Commercial drug testing company, MMC International B.V., employ the use of catalysts in several of their narcotic field test kits as a sphere, grain or pellet in the lid of the test ampoule[134].

3.3.1.5 *Reagent concentrations to solid sample*

The number of drops of Cu(II) reagent was increased due to the absence of water in the solid powder sample. The colour test results show there is a significant decrease in colour intensity for the 4-MMC HCl sample. Optimal reagent concentrations would need to be adjusted.

3.3.1.6 *Optimal Reagent Concentrations*

The need for established test conditions when performing a colour test on solid powder samples is essential: seized drugs are likely to be found in solid salt form, so this allows testing to be performed immediately.

The control blank reactions with each neocuproine and Cu(II) combination were analysed and then compared to the reactions with 4-MMC under the same conditions. There was a general observable trend in the blank reagent testing: as the neocuproine concentration increased, the resulting colours transitioned from light blue, to green and finally, orange. The 4-MMC HCl test plate displayed a general trend with increasing neocuproine concentration: yellow to orange to red.

Based on the coloured results obtained for 4-MMC HCl samples compared to blank samples using each concentration of Cu(II) and neocuproine, optimal concentrations were determined to be 5.00×10^{-3} M Cu(II) and 5.12×10^{-3} M neocuproine. These conditions provided the most significant colour change using the lowest reagent concentrations possible in order to avoid inherent reactions occurring. An example of a blank reagent control and positive control are shown in Figure 3-4. It should also be noted that the reagent concentrations were determined with respect to 4-MMC as an example cathinone, and therefore may not necessarily be optimal for other cathinone substances.

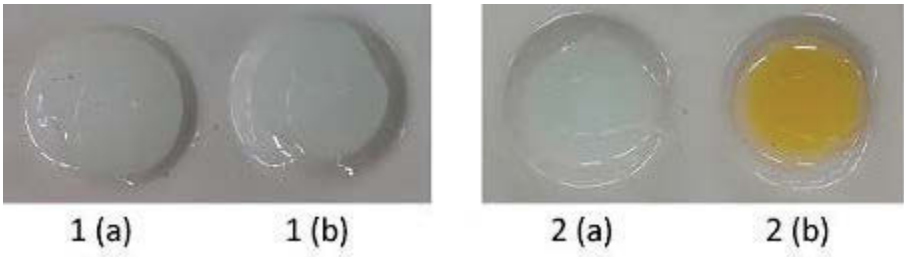

Figure 3-4. Final copper-neocuproine test results. Method performed on control blank *(1)* and solid 4-MMC HCl *(2)* at two different stages: before heating *(a)* and after heating *(b)*.

3.3.1.7 *Optimal buffer conditions*

Testing performed using the prepared buffer solutions did not afford a colour change in their respective reactions with 4-MMC HCl, with the exception of 2.00 M sodium acetate and 5.00 M NaOH. The 5.00 M NaOH solution produced an intense blue/black control blank and a dark yellow with the 4-MMC HCl. As predicted, the 2.00 M acetate produced a characteristic light blue control blank and bright yellow-orange with 4-MMC, while the other buffer solutions afforded a colourless reagent blank and 4-MMC HCl test sample.

The characteristic light blue control blank and yellow-orange 4-MMC colour test results were only apparent with 2.00 M acetate buffer. The concentrated NaOH solution produced coloured reactions of a far greater intensity than the 2.00 M acetate. This demonstrated that under harsh, highly basic conditions, coloured products will result, possibly due to the electron donation occurring between the hydroxide ion Lewis base and the Cu(II) ion. Acetate ions are weak bases due to resonance stabilization and are therefore a better buffer choice so as to minimize this electron donating to Cu(II) ion.

3.3.2 General recommended procedure

A presumptive colour test methodology to identify synthetic cathinones encountered in seizures was developed. The developed methodology is designed for use by non-scientists such as police officers and customs inspectors. Two testing procedures employing a porcelain

well-plate and hotplate or a plastic micro well-plate and water bath were studied, which provides the methodology with a greater versatility.

To a small pin-head sized amount of seized material (approximately 0.1-0.2 mg) placed in the well of a test plate:

1. Add five drops of 5.00×10^{-3} M copper(II) nitrate solution
2. Add two drops of 5.12×10^{-3} M neocuproine solution
3. Add two drops of 2.00 M sodium acetate buffer
4. Heat the plate on a boiling water bath (plastic well-plate) or a hot plate set at 100 °C (porcelain well-plate)
5. Record the colour change before 10 minutes

In accordance with general operational procedures, a negative control standard and positive control standard would be tested alongside the seized material sample.

3.3.3 Spectroscopic analysis

The UV-Vis absorbance spectra of the blank reagent control and coloured product formed in the presence of 4-MMC HCl show distinct differences in the visible region with a maximum absorption seen at 453 nm for the coloured complex where there is no absorbance in the control blank, as shown in Figure 3-5. This wavelength of maximum absorbance corroborates with similar values seen in the literature for Cu(I)-neocuproine coloured complexes formed following a redox reaction[267, 360, 361].

The testing performed employing Cu(I) as a reagent in the absence of 4-MMC HCl produced a yellow-orange colour change indistinguishable to the colour change of Cu(II) reagent in the presence of 4-MMC HCl. This colour change also occurred in the absence of 4-MMC HCl. This test demonstrated two things: the copper(I) ion is responsible for the colour change; and the presence of the 4-MMC leads to the reduction of Cu(II) to Cu(I). The UV-Vis absorbance spectrum for the coloured Cu(I) reagent (data not shown) revealed significant peak shape similarities and identical maximum absorbance wavelength to that of the Cu(II) reagent in the presence of 4-MMC HCl (Figure 3-5).

The UV region of the spectrum showed two major absorption peaks at 217 nm and 273 nm in all tests performed. These intense bands are due to the presence and absorption of the

neocuproine molecule. This was confirmed through a UV-Vis analysis of the neocuproine reagent only.

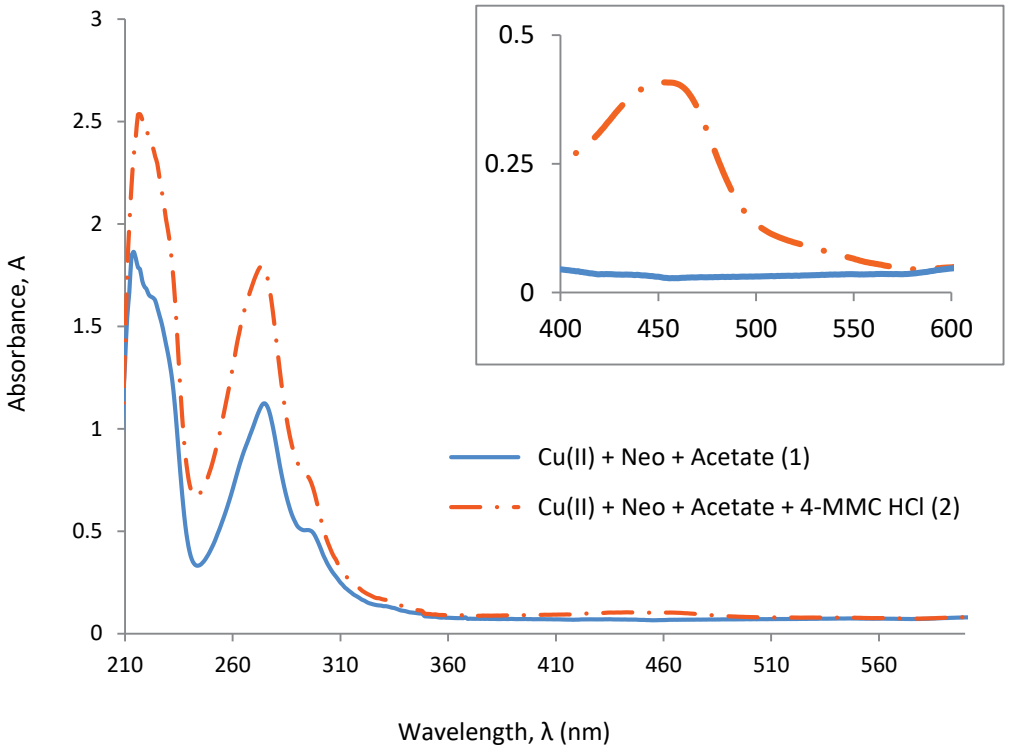

Figure 3-5. Overlaid Ultraviolet-Visible absorbance spectra of colour test results. Cu(II)-neocuproine colour test control reagent blank *(1)* and Cu(II)-neocuproine colour test on 4-MMC HCl *(2)*. Inset: Zoomed region of the absorption band centered at 453 nm.

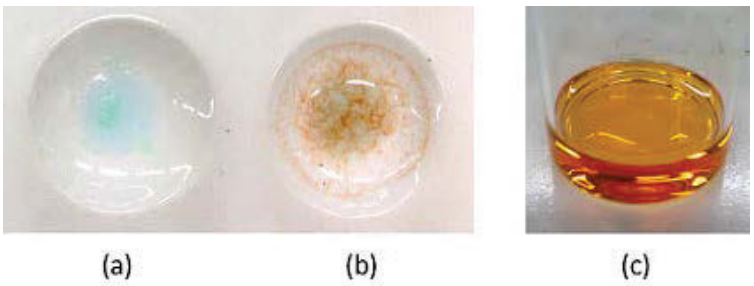

Figure 3-6. The residue/crystalline material remaining in the well-plate 48 hours after testing of control blank *(a)* and 4-MMC HCl sample *(b)*. The combined crystalline materials were washed with diethyl ether and cold water; filtered through a cotton-plugged pipette; and collected by redissolving in organic solvent *(c)*.

The coloured complex was successfully extracted as a very fine, bright red, needle-like, crystalline material as shown in Figure 3-6, and characterized using instrumental techniques available.

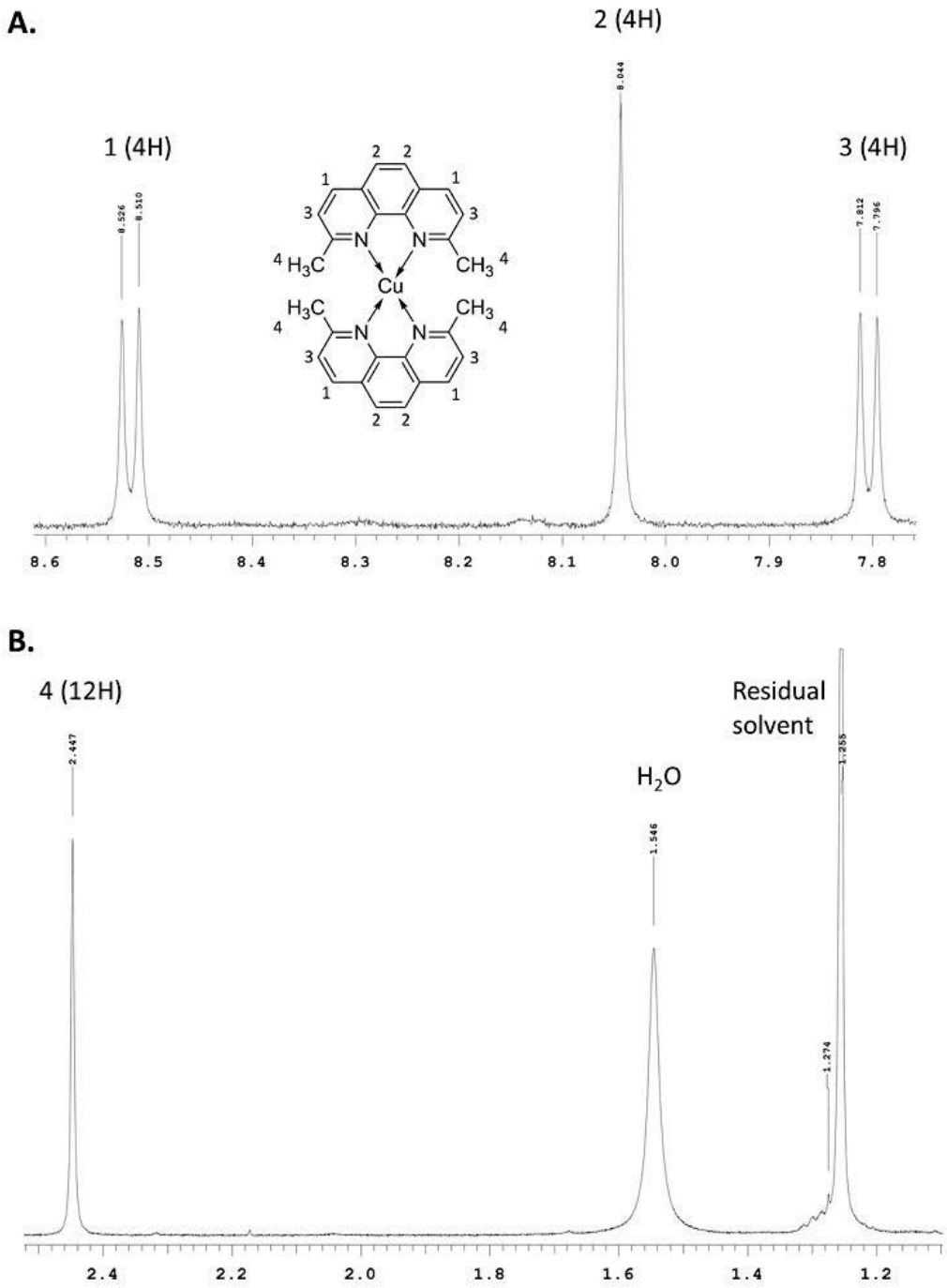

Figure 3-7. ^{1}H-NMR spectrum of extracted yellow-orange coloured product, Cu(I)(neocuproine)$_2$, recorded in deuterated chloroform. Downfield *(A)* and upfield spectral regions *(B)* are defined. Proton environments have been assigned, with labeled peaks corresponding to the protons on the complex structure. Integration values are provided in brackets for each relevant chemical shift.

The ^{1}H-NMR spectrum of the coloured complex and proton assignments are presented in Figure 3-7. The presence of only 3 signals downfield confirms that the coloured complex contains only one type of chelating ligand, i.e. neocuproine. The aromatic protons of the neocuproine chelate appear as two doublets and one singlet in this region. The two methyl substituents of the ligand resonate at 2.45 ppm upfield of the spectrum. The chemical shift values of these signals were compared to the appropriate signals of neocuproine as a free ligand as well as the broad signals of the paramagnetic Cu(II) complex. The aromatic protons of the copper-chelate complex had values shifted further downfield due to the electron withdrawing effect of coordinating to the copper atom. Structural differences exist between Cu(I) and Cu(II) oxidation states, with preference for four coordinate and nearly tetrahedral geometry in Cu(I), and a Jahn-Teller distorted 5- or 6-coordinate geometry adopted by Cu(II)[362]. The upfield shifting of methyl substituents in the complex compared to the free ligand further confirm the tetrahedral geometry due to their position in the pi system shielding cone of neighbouring neocuproine ligand. The reaction equation for the formation of the coloured complex and 3D molecular structures are shown in Figure 3-8.

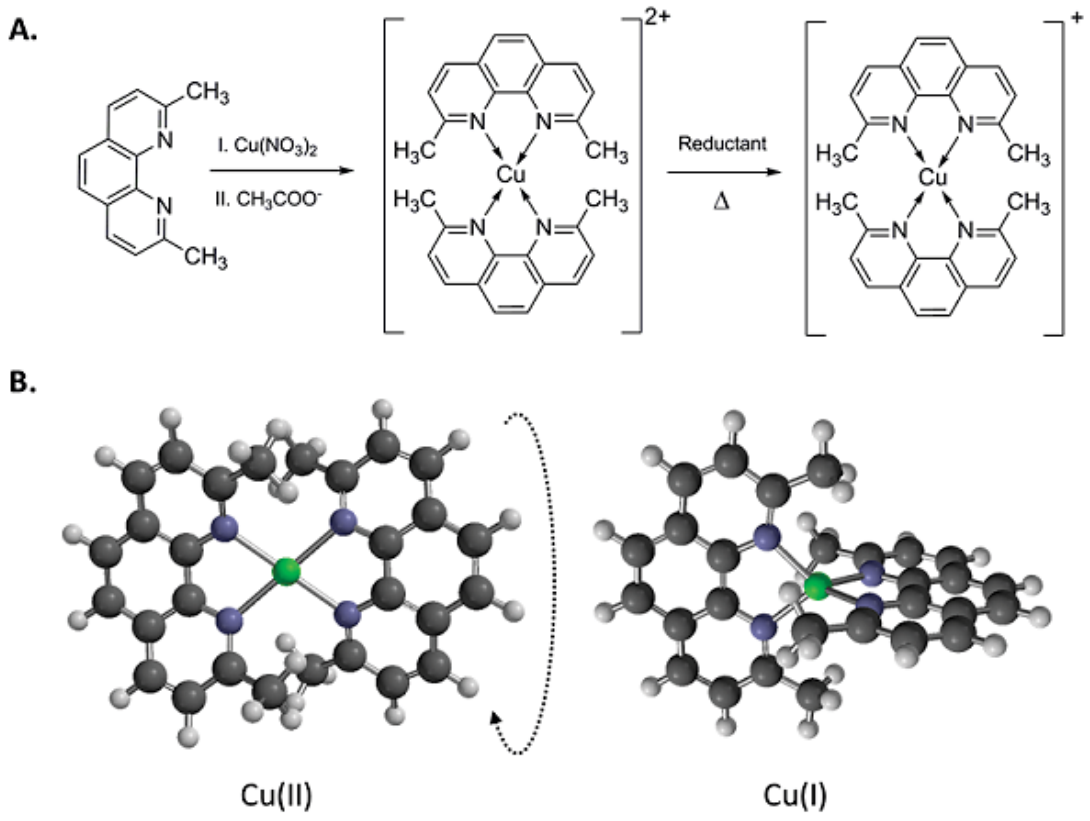

Figure 3-8. Reaction equation for the formation of the yellow-orange coloured complex. The copper metal center in Cu(II)(neocuproine)$_2$ is reduced in the presence of a reductant to form

Cu(I)(neocuproine)$_2$ *(A)*. 3-Dimensional molecular structures of Cu(II)(neocuproine)$_2$ (drawn without potential acetate or water ligands) and Cu(I)(neocuproine)$_2$ are proposed to demonstrate the difference in geometry and arrangement of the neocuproine chelating ligands *(B)*.

3.3.4 Method validation

Qualitative methods for drug testing rely on the determination of validation parameters. This method validation study ensures the proposed test is valid and suitable for its intended purpose.

3.3.4.1 *Selectivity and specificity*

The UNODC recommend a minimum of 20 test samples in selectivity analyses. In this study over 120 test samples were examined. A complete list of colour changes observed for each substance subjected to the neocuproine test can be found in Table 3-1, Table 3-2 and Table 3-3 below.

The selectivity of a colour test used in the preliminary identification of drugs is particularly important, as interferences from substances other than the analyte of interest may lead to false positives. Ideally, the copper-neocuproine test would be selective for cathinone analogues only. The testing of 44 cathinone analogues using the neocuproine colour test resulted in 39 of these compounds providing a definitive positive result, i.e. a yellow-orange colour change (see Table 3-1). In accordance with colour test development procedures, all drugs in the target group with negative test results must be identified. In an attempt to determine the mechanism of the reaction, the five cathinone substances that failed to react were able to be grouped together based on a calculated value called the carbon bond saturation, as defined by fraction sp^3 (Fsp^3). This value is equal to the number of sp^3 hybridized carbons/total number of carbons in the molecule. The result is a measure of complexity for the molecule. It was found that cathinone substances with an Fsp^3 value greater than 0.50 did not produce a yellow-orange colour change with the neocuproine spot test. The complex nature of these compounds led to the inability to reduce the copper(II) ion, and therefore produce a colour change.

Table 3-1. Selectivity study results of proposed neocuproine colour test method with pure synthetic cathinone substances and in mixtures with other analytes

Compound	**Spot test colour [a]**	**Test result [c]**	**Fsp^3 [f]**
1-(4-methoxyphenyl)-2-(1-pyrrolidinyl)-1-propanone HCl (MOPPP)	Lt yellow-orange [d]	+	0.50
1-phenyl-2-methylamino-pentan-1-one HCl	yellow-orange	+	0.42
2,3-dimethylmethcathinone HCl (2,3-DMMC)	yellow-orange [b]	+	0.42
2,4,5-trimethylmethcathinone HCl (2,4,5-TMMC)	Lt orange [b, d, e]	+	0.46
2,4-dimethylmethcathinone HCl (2,4-DMMC)	yellow-orange [b]	+	0.42
2-benzylamino-1-(3,4-methylenedioxyphenyl)-1-butanone HCl (BMDB)	yellow-orange	+	0.24
2-fluoromethcathinone HCl (2-FMC)	yellow-orange [b]	+	0.30
2-methylmethcathinone HCl (2-MMC)	Lt yellow-orange [b]	+	0.36
3,4-methylenedioxy-α-pyrrolidinobutiophenone HCl	Lt green	-	0.53*
3,4-dimethylmethcathinone HCl (DMMC)	Lt yellow-orange	+	0.42
3,4-methylenedioxymethcathinone HCl (MDMC)	Lt yellow-orange	+	0.36
3,4-methylenedioxy-*N,N*-dimethylcathinone HCl	Lt yellow-orange	+	0.42
3,4-methylenedioxypyrovalerone HCl (MDPV)	Wk yellow	-	0.56*
3-bromomethcathinone HCl (3-BMC)	yellow-orange [b]	+	0.30
3-fluoromethcathinone HCl (3-FMC)	yellow-orange	+	0.30
3-methylmethcathinone HCl (3-MMC)	yellow-orange	+	0.36
4-bromomethcathinone HCl (4-BMC)	yellow-orange [b]	+	0.30

4-fluoromethcathinone HCl	yellow-orange	+	0.30
4-methoxymethcathinone HCl	Lt yellow-orange	+	0.36
4-methylethylcathinone HCl	yellow-orange	+	0.42
4-methylmethcathinone HCl (4-MMC)	Lt yellow-orange	+	0.36
4-methyl-*N*-benzylcathinone HCl (4-MBC)	yellow-orange	+	0.24
4-methyl-pyrrolidinopropiophenone HCl	Lt yellow-orange	+	0.50
4-methyl-α-pyrrolidinobutiophenone HCl	Wk yellow	-	0.53*
cathinone HCl (bk-amphetamine)	yellow-orange [b]	+	0.22
dibutylone HCl (bk-DMBDB)	Lt yellow-orange [d]	+	0.46
iso-ethcathinone HCl	Lt orange [b, d, e]	+	0.36
methcathinone HCl	Lt yellow-orange	+	0.30
methylenedioxy-α-pyrrolidinopropiophenone HCl	Lt yellow-orange	+	0.50
N,N-diethylcathinone HCl	yellow-orange [b]	+	0.46
N,N-dimethylcathinone HCl	yellow-orange [b]	+	0.36
naphthylpyrovalerone HCl (naphyrone)	yellow-orange	+	0.42
N-ethyl-3,4-methylenedioxycathinone HCl	Lt yellow-orange [d]	+	0.42
N-ethylbuphedrone HCl	yellow-orange	+	0.42
N-ethylcathinone HCl	yellow-orange	+	0.36
pentylone HCl	Lt yellow-orange [d]	+	0.46
pyrovalerone HCl	Lt green	-	0.56*
α-dimethylaminobutyrophenone HCl	yellow-orange	+	0.42
α-dimethylaminopentiophenone HCl	yellow-orange	+	0.46
α-ethylaminopentiophenone HCl	yellow-orange	+	0.46
α-pyrrolidinobutiophenone HCl (α-PBP)	Lt yellow-orange	+	0.50
α-pyrrolidinopentiophenone HCl	green-yellow	-	0.53*
α-pyrrolidinopropiophenone HCl	yellow-orange	+	0.46

β-keto-*N*-methyl-3,4-benzodioxyolylbutanamine HCl (bk-MBDB)	Lt yellow-orange	+	0.42
Methylone + 4-FMC	yellow-orange	+	N/A
MMC + benzocaine	yellow-orange	+	N/A
MMC + caffeine	yellow-orange	+	N/A
MMC + codeine phosphate	yellow-orange	+	N/A
MMC + ephedrine	yellow-orange	+	N/A
MMC + 4-FMC	yellow-orange	+	N/A
MMC + lactose	yellow-orange	+	N/A
MMC + methylone	yellow-orange	+	N/A

[a] NC = no colour change; Lt = light
[b] Colour changes were seen before heating step
[c] Test result indicated as positive (+) or negative (-)
[d] Spot test result was slow to occur, however, still within 10 minutes
[e] Formed a mottled orange solution with a dark green ring in spotting well during heating step
[f] Calculated fractional sp^3 value. (*) indicates a value > 0.50

It was discovered that of the 82 non-cathinone analogue substances tested, eight substances afforded a yellow colour that could be classed as a positive reaction; however, only one managed to produce the characteristic yellow-orange obtained for the majority of the target cathinone analogues. A weak or light yellow colour change was observed for three of the 15 amphetamines, one of the piperazine analogues, and four of the precursor or other illicit substances tested. The remaining substances that resulted in a colour change either turned an easily distinguishable orange, or a blue/green colour that more closely resembled the control reagent blank. These colour test results can be seen in Table 3-2 and Table 3-3.

This selectivity study has shown that the neocuproine colour test displays good selectivity toward cathinone analogues. The majority of the amphetamine-type substances and other illicit compounds showed no signs of a coloured reaction. A colour test is accepted if commonly occurring substances do not interfere, and these tests showed that common pharmaceutical tablets and other white powders failed to react.

The application of the spot test to mixtures of cathinone substances with other cathinones, adulterants and diluents, showed that there was no effect on the expected positive colour

change result. This is as predicted because the coloured product that forms is the same in all positive drug samples, and therefore other positive reaction colours should not interfere with the colour observed.

Table 3-2. Selectivity study results of proposed neocuproine colour test method with amphetamines, common precursor chemicals and other recreational drugs

Compound	**Spot test colour** [a]	**Test result** [c]
(-)-ephedrine HCl	NC	-
(-)-methylephedrine HCl	NC	-
(+)-cathine HCl	NC	-
(+/-)- 3,4-methylenedioxyamphetamine (MDA) HCl	Wk yellow	-
(+/-)- *N*-methyl-3,4-methylenedioxyamphetamine (MDMA) HCl	NC	-
(+/-)-methamphetamine HCl	NC	-
(+/-)-*N*-ethyl-3,4-methylenedioxyamphetamine (MDEA) HCl	NC	-
(+/-)-*N*-methyl-1-(3,4-methylenedioxyphenyl)-2-butylamine HCl	NC	-
(+/-)-phenylpropanolamine	NC	-
(2S*,3R*)-2-methyl-3-[3,4-(methylenedioxy)phenyl]glycidic acid methyl ester	NC	-
1-(3-chlorophenyl)piperazine (mCPP) HCl	Wk, Lt green	-
1-[3-(trifluoromethyl)phenyl]piperazine (TFMPP) HCl	Lt yellow	+
1-benzylpiperazine (BZP) HCl	NC	-
2,5-dimethoxy-4-iodophenylethylamine HCl	Wk yellow	-
2,5-dimethoxy-4-methylamphetamine	NC	-
2,5-dimethoxy-4-propylthio-phenylethylamine	NC	-
2,5-dimethoxyamphetamine	NC	-
2-bromo-4-methylpropiophenone	Wk, Lt green	-

2-fluoroamphetamine	NC	-
2-fluoromethamphetamine	NC	-
3,4-dimethoxyamphetamine	NC	-
3,4-methylenedioxyphenyl-2-propanone (MDP2P)	orange [b]	-
4-bromo-2,5-dimethoxyamphetamine HCl	NC	-
4-bromo-2,5-dimethoxyphenethylamine HCl	NC	-
4-fluoroamphetamine	NC	-
4-fluorococaine HCl	NC	-
4-fluoromethamphetamine	NC	-
4-hydroxyamphetamine	Wk yellow	-
4-methoxyamphetamine (PMA)	Wk yellow	-
4-methoxymethamphetamine (PMMA)	NC	-
4-methylmethamphetamine	NC	-
4-methylpropiophenone	yellow	+
5-methoxy-*N,N*-diallyltryptamine	Lt yellow	+
amphetamine sulphate	NC	-
cocaine HCl	NC	-
dimethamphetamine (DMA)	NC	-
gamma-hydroxy butyrate	NC	-
heroin HCl	Wk yellow	-
ketamine	NC	-
methoxetamine HCl	NC	-
methylamine HCl	NC	-
phencyclidine HCl	NC	-
phentermine	NC	-
triethylamine	orange	-

[a] NC = no colour change; Lt = light; Wk = weak

[b] Colour change occurred before heating step

[c] Test result indicated as positive (+) or negative (-)

The current recommended presumptive colour test for synthetic cathinones by the United Nations Office on Drugs and Crime (UNODC) is the Zimmerman reagent which employs hazardous, corrosive and irritating chemicals[363]. In addition to providing a negative result with several cathinone type substances, there were a limited number of cathinone substances studied, and a lack of information on false positive results given. This reagent is also known to react with benzodiazepines and phenyl-2-propanone analogues[69]. The widely used Marquis reagent is only applicable as a single test for methylenedioxy substituted cathinones where it affords a bright yellow colour. The remaining cathinone analogues afford no reaction with Marquis and must be subject to a sequence of colour reagents in order to appropriately identify the compound[84]. In addition, several synthetic cathinone substances, such as 3-fluoromethcathinone, are unaccounted for by these commonly used colour test reagents.

Table 3-3. Selectivity study results of proposed neocuproine colour test method with a range of common adulterants, excipients and powdered substances

Compound	**Spot test colour** [a]	**Test result** [c]
artificial sweetener	NC	-
ascorbic acid	Lt orange [b]	+
benzocaine [d]	green-yellow	-
benzoic acid	NC	-
boric acid	NC	-
brown sugar	green-yellow	-
caffeine [d]	NC	-
calcium chloride	NC	-
caster sugar/ icing sugar	NC	-
citric acid	NC	-
codeine phosphate	Lt orange	+
dimethylsulfone	NC	-
ephedrine HCl	NC	-
glucose	NC	-
glycine	blue	-
Lactose [d]	NC	-

L-cysteine	Lt orange [b]	+
levamisole	NC	-
L-glutathione	yellow-orange [b]	+
magnesium sulphate	NC	-
maltose	NC	-
mannitol	NC	-
O-acetylsalicylic Acid	NC	-
paracetamol	yellow	+
phenethylamine	NC	-
phenolphthalein	NC	-
potassium carbonate	blue	-
protein powder	brown-yellow	-
self-raising/plain flour	blue-yellow	-
sodium carbonate	blue	-
sodium chloride	NC	-
starch/cellulose	NC	-
stearic acid	NC	-
sucrose	NC	-
tartaric acid	NC	-

[a] NC = No colour change; Lt = light

[b] Colour change occurred before heating step

[c] Test result indicated as positive (+) or negative (-)

[d] Commonly used adulterants/excipients with cathinone substances

3.3.4.2 *Limit of detection*

The LOD was determined by approaching the sample concentration, of 4-MMC HCl as an example, in which no change in colour could easily be determined in reference to a control blank. The Seized Drugs Subcommittee of the Organization of Scientific Area Committees (OSAC), and more specifically, the Scientific Working Group for the Analysis of Seized Drugs (SWGDRUG) recommends a cut-off value be set at the lowest concentration tested which results in an observable colour change[37]. The amounts of target compound, 4-MMC HCl,

were 1.0, 2.0, 3.00, 4.0, 5.0, 6.0, 10, 20, 30, 40 and 50 µg, alongside a control blank containing 0 µg for direct comparison. The results of these colour tests with 4-MMC HCl can be found in Figure 3-9.

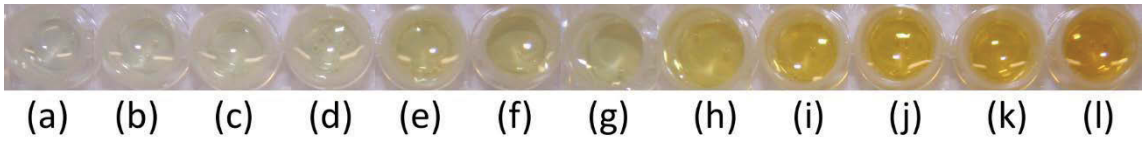

Figure 3-9. Limit of detection method validation test results for 4-MMC HCl using the proposed neocuproine colour test method. Amounts of 4-MMC HCl subjected to testing are 0, 1, 2, 3, 4, 5, 6, 10, 20, 30, 40, 50 µg (a-l).

It was determined that with 4.0 µg of sample present, the colour change could just be visualized, and therefore the 'operational detection limit' was subsequently calculated to be 40 µg[37]. Colour changes remained for approximately four hours following LOD testing, with significant fading of positive controls to the blue colour of the reagent blank occurring after 24 hours. It should be noted that LOD is not a particularly robust parameter and may be affected by minor changes in operational conditions. In addition, the determination of LOD is highly subjective and dependent on the particular cathinone substance being tested.

It was also observed that at higher concentrations of the drug sample (more than the recommended 0.1-0.2 mg) the desired colour change occurred much faster.

3.3.4.3 *Purity testing*

The presence of glucose or caffeine impurities in a sample at concentrations ranging from 0 to 95 % g/g, showed no obvious effect on the coloured product forming under visual examination. The sample cut with 95% g/g impurities still reacted with the copper-neocuproine reagent to produce the characteristic yellow-orange colour. Given a common sample matrix may contain endogenous or exogenous interfering substances, purity testing is carried out to determine the effects these interfering substances have on the colour produced.

Synthetic cathinones are typically advertised as being 95%-99% pure on internet websites and analysis has generally confirmed this high purity[364, 365]. The European Monitoring Centre for Drugs and Drug Addiction (EMCDDA) reported that samples of 3,4-methylenedioxypyrovalerone (MDPV) and mephedrone are commonly found in combination with other synthetic cathinones, for example, methylone, ethcathinone, methoxymethcathinone and flephedrone. Pharmaceutical agents including benzocaine, lidocaine, caffeine and paracetamol have been detected in small proportions of seizures, while controlled drugs cocaine, ketamine, amphetamines and piperazines have been encountered in some submissions[366, 367].

3.3.4.4 *Precision analysis*

Precision measures the closeness in hue, saturation and value of coloured spot tests from a series of replicate measurements performed on the same sample using the proposed test method. The visual examination of five replicate 4-MMC HCl samples afforded indistinguishable yellow-orange products with neocuproine, demonstrating a high level of precision.

Repeatability of the method was determined by testing samples on the same day with the same reagents in the same laboratory. The colour results of these analyses confirm the repeatability of the proposed methods.

Reproducibility was determined by varying the conditions of testing. Discrepancies were shown in testing performed at the AFP laboratory using different equipment. The different type of well-plate used, and thus heating conditions experienced by the samples are the likely reason for the lack of reproducibility. A hotplate and porcelain well-plate were employed at the AFP laboratory, while plastic micro well-plates on a boiling water bath were used at the UTS laboratory. It has been demonstrated that neocuproine is affected by temperature of reaction, and therefore, any differences in heating will affect the end result.

3.3.4.5 *Stability*

The extent to which the neocuproine reagent, specifically, is stable is demonstrated in this validation by comparing freshly prepared reagents with those of equal concentration that have been retained over a 3 month period under various storage conditions.

The neocuproine reagent demonstrated great stability in regards to both the storage environment, and length of storage. After three months of being kept under each of the specified storage conditions, the reagents were tested and found to produce colour changes in accordance with freshly prepared reagents.

3.4 Conclusion

The investigation into the use of copper-neocuproine as a presumptive colour test reagent has shown significant potential for further development and exploitation. The proposed colour test method affords a yellow-orange complex in the presence of the target compound, 4-MMC HCl, as well as a number of other cathinone analogues. The test requires only a small amount of the solid substance for a positive reaction to be recorded, and in addition, the reagents used are in aqueous solutions, non-corrosive and safer to handle than other commonly used colour test reagents. The procedure requires the addition of three separate reagents, followed by a heating period of up to 10 minutes. This test condition may be considered cumbersome and time consuming for application to field testing, however, its application in a forensic laboratory would be beneficial. In light of the increasing prevalence and awareness of synthetic cathinones in Australia, the development of a suitable preliminary detection method or sequence of appropriate chemical colour tests is highly desirable.

3.5 References

37. Scientific Working Group for the Analysis of Seized Drugs (SWGDRUG), *SWGDRUG Recommendations Version 7.1*. 2016, United States Department of Justice: USA.
56. Cuypers, E., A.J. Bonneure, and J. Tytgat, *The use of presumptive color tests for new psychoactive substances.* Drug Testing and Analysis, 2016. **8**(1): p. 136-140.
68. National Institute of Standards and Technology (NIST), *Color test reagents/kits for preliminary identification of drugs of abuse*. 2000, National Institute of Justice (NIJ): USA.

69. Kovar, K.-A. and M. Laudszun, *Chemistry and reaction mechanisms of rapid tests for drugs of abuse and precursors chemicals*. 1989, Pharmazeutisches Institut der Universitat Tubingen: Federal Republic of Germany.
70. United Nations Office on Drugs and Crime (UNODC), *Guidance for the validation of analytical methodology and calibration of equipment used for testing of illicit drugs in seized materials and biological specimens*. Laboratory and Scientific Section. 2009, New York: United Nations. 67.
73. B. Widdop, *Colour Tests*, in *Clarke's Analysis of Drugs and Poisons*, A. C. Moffat, *et al.*, Editors. 2011, Pharmaceutical Press: London, U.K.
84. K. E. Toole, *et al. Color Tests for the Preliminary Identification of Methcathinone and Analogues of Methcathinone*. Microgram Journal, 2012. **9**, 27-32.
134. MMC International B.V. *Narcotic Testing Supplies & Equipment Store*. 2016 [cited 2016 November 22]; Available from: http://shop.narcotictests.com/products/narcotic-field-tests/synthetic-cannabinoids-test-k2-spice/details.
152. United Nations Office on Drugs and Crime (UNODC), *Recommended methods for the identification and analysis of amphetamine, methamphetamine and their ring-substituted analogues in seized materials*. 2006, United Nations: New York.
264. Özyürek, M., K. Güçlü, and R. Apak, *The main and modified CUPRAC methods of antioxidant measurement.* TrAC Trends in Analytical Chemistry, 2011. **30**(4): p. 652-664.
266. Al-Obaid, A.M., *et al.*, *Determination of (S)(−)-cathinone by spectrophotometric detection.* Journal of Pharmaceutical and Biomedical Analysis, 1998. **17**(2): p. 321-326.
267. Ercag, E., A. Ercag, and R. Apak, *Spectrophotometric determination of the soil fumigant: Dazomet with copper(II)-neocuproine reagent.* Analytica Chimica Acta, 2004. **505**(1): p. 95-100.
268. Moreno, A.d.H. and H.R.N. Salgado, *Spectrophotometric Determination of Ceftazidime in Pharmaceutical Preparations Using Neocuproin as a Complexing Agent.* Analytical Letters, 2008. **41**(12): p. 2143-2152.
352. Australian Crime Commission (ACC), *Illicit Drug Data Report 2013-2014*. Other Drugs. 2015, Canberra: Commonwealth of Australia. 109-154.
353. European Monitoring Centre for Drugs and Drug Addiction (EMCDDA) and Europol, *EU Drug Markets Report: In-Depth Analysis*. 2016: Publications Office of the European Union, Luxembourg.
354. The European Monitoring Centre for Drugs and Drug Addiction (EMCDDA). *Synthetic Cathinones Drug Profile*. Drug Profiles 2015 [cited 2015 21st February]; Available from: http://www.emcdda.europa.eu/publications/drug-profiles/synthetic-cathinones.
355. Intergovernmental Committee on Drugs (IGCD), *Framework for a national response to new psychoactive substances*. 2014, Australia: National Drug Strategy. 1-36.
356. *Crimes Legislation Amendment (Psychoactive Substances and Other Measures) Act*. 2015, Cth: Australia.
357. NarcoCheck. *Identification Test: Synthetic Cathinones*. Tests for solid substances 2015 [cited 2016 9 April]; Available from: http://www.narcocheck.com/en/identification-tests-for-drugs-of-abuse/identification-id-test-mephedrone-mdpv-methylone-cathinones-bath-salts.html?search_query=cathinone&results=2.
358. Ragehy, N.A.E., M. Abdelkawy, and A.E. Bayoumy, *Spectrophotometric Determination of Ibuprofen via its Copper (II) Complex.* Analytical Letters, 1994. **27**(11): p. 2127-2139.
359. Lee, G., *et al.*, *The reduction of Cu(II)/neocuproine complexes by some polyphenols: Total polyphenols determination in wine samples.* Food Chemistry, 2011. **126**(2): p. 679-686.
360. Cárdenas, A., M. Gómez, and C. Frontana, *Relationship between the chemical structures of antioxidants and the differences in their Cupric Ion Reducing Antioxidant*

Capacity (CUPRAC) by electrochemical methods. Journal of Electroanalytical Chemistry, 2014. **729**: p. 116-120.
361. Nakamura, T., N. Coichev, and H.D. Moya, *Modified CUPRAC spectrophotometric quantification of total polyphenol content in beer samples using Cu(II)/neocuproine complexes.* Journal of Food Composition and Analysis, 2012. **28**(2): p. 126-134.
362. Scaltrito, D.V., *et al.*, *MLCT excited states of cuprous bis-phenanthroline coordination compounds.* Coordination Chemistry Reviews, 2000. **208**(1): p. 243-266.
363. United Nations Office on Drugs and Crime (UNODC), *Recommended Methods for the Identification and Analysis of Synthetic Cathinones in Seized Materials*. 2015, United Nations: New York. p. 16.
364. Gibbons, S. and M. Zloh, *An analysis of the 'legal high' mephedrone.* Bioorganic & Medicinal Chemistry Letters, 2010. **20**(14): p. 4135-4139.
365. German, C.L., A.E. Fleckenstein, and G.R. Hanson, *Bath salts and synthetic cathinones: An emerging designer drug phenomenon.* Life Sciences, 2014. **97**(1): p. 2-8.
366. European Monitoring Centre for Drugs and Drug Addiction (EMCDDA), *Risk assessment report of a new psychoactive substance: 4-methylmethcathinone (mephedrone)*. 2010: Lisbon, Portugal. p. 16.
367. European Monitoring Centre for Drugs and Drug Addiction (EMCDDA) - Europol, *Joint Report on a New Substance: MDPV (3,4-methylenedioxypyrovalerone)*. 2014: Lisbon, Portugal.

This page intentionally left blank

Chapter 4: Investigation into a chemical colour test device

This page intentionally left blank

Chapter 4: Investigation into a chemical colour test device

4.1 Introduction

Chemical colour tests for illicit drugs are designed to be simple, rapid and easy to use. To better provide for detection in the field, the chemical reactions occurring in porcelain spot plates have been moved into commercially available portable test kits. These colour test kits differ in design across brands from single glass ampoules[117] to ampoules encased in sealable polyethylene pouches[368] and plastic cartridges[369]. Furthermore, the incorporation of the drug into the test has been achieved using customised spatulas[370] and adhesive probe tips[369].

The drug kits described so far are marketed to detect one class of illicit drug per kit and thus a battery of colour test kits are required to screen an unknown seized material. Attempts to overcome this drawback have employed microfluidic devices incorporating more than one colour test reagent. Bell *et al.*[169] showed that a device the size of a microscope slide was able to incorporate three colour test reagents and one microcrystal test while using less sample and reagents than a spot test plate. Musile *et al.*[170] further improved the translation of the microfluidic colour test device by using significantly cheaper chromatographic paper and wax printing.

Improvements to the chemical colour test device have looked at incorporating a semi-quantitative element that also reduces the subjective nature of visually inspecting a colour test result. This has been achieved using smart phone applications[162], however, portable colour digitizers have not been employed for this purpose.

The previous chapter described the development of a chemical colour test for the detection of synthetic cathinones. The high selectivity and simplicity of the test is overshadowed by two major drawbacks to using this chemical colour test in the field: the 80 °C temperature and 10 minute test period. The aim of this chapter is to optimise the currently developed colour test so it is not limited to being performed near an AC power outlet of a forensic laboratory benchtop. Several methods are explored to provide a rapid colour test applicable at room temperature that also uses small volumes and limited hazardous chemicals.

4.2 Materials and methods

4.2.1 Chemicals

Copper(II) nitrate hemi(pentahydrate), copper(II) chloride dihydrate, copper(I) chloride, neocuproine hemihydrate, sodium chloride and potassium chloride were obtained from Sigma Aldrich (Castle Hill, NSW, Australia); analytical grade anhydrous sodium acetate and lithium fluoride was from Ajax Finechem (Taren Point, NSW, Australia); Amberlyst A-21 and silica gel 60 were from BDH Laboratory Chemicals (Poole, England); potassium fluoride was obtained from Merck KGaA (Darmstadt, Germany); molecular sieves were obtained from Prolabo (Paris, France); and sodium hydroxide pellets, chloroform, dichloromethane and diethyl ether were from Chem-Supply (Port Adelaide, SA, Australia).

4.2.2 Reference material

Synthetic cathinones, 4-methylmethcathinone (4-MMC), 4-ethylmethcathinone (4-EMC), 4-fluoromethcathinone (4-FMC), 4-methylethcathinone, methcathinone, methylone, butylone, pentylone, 3,4-methylenedioxypyrovalerone (MDPV), ethylone, 4-methylpyrrolidinopropiophenone (4-MPPP), pyrovalerone and α-pyrrolidinovalerophenone (α-PVP) were synthesised in-house as their hydrochloride salts (see Chapter 2 for details) for use as reference material in this investigation.

4.2.3 Apparatus and materials

Polyethylene (PE) zip-lock bags and hand warmers were obtained from Daiso Australia (Abbotsford, VIC, Australia); and glass beads (ø = 1 mm) were obtained from Sigma Aldrich. Polypropylene flat bottom 96-well micro plates were obtained from Greiner Bio-One and porcelain spotting well-plates were supplied by UTS. A Simmerstat Plain Top was from Industrial Equipment & Control Pty Ltd (Thornbury, VIC, Australia), polyvinyl acetate (PVAc) solid resins, polyethylene pellets and glass beads (ø = 2 mm, 3 mm) were obtained from the university (unknown source). A USB-powered mug warmer and electric cigarette lighter were purchased online through eBay from Malaysia (‘goodgadgetsa’) and Australia (‘2012huifen’), respectively.

4.2.4 Investigation of friction and heat generating mechanisms

4.2.4.1 *Polyethylene bag method (Experiment 1)*

To a PE bag was added a sample of 4-MMC (approx. 100 µg), followed by the colour test reagents developed in the previous chapter: copper nitrate (5 mM, 5 drops), neocuproine (5 mM, 2 drops) and sodium acetate (2 M, 2 drops). The solution was mixed in the PE bag using the thumb and forefingers until a yellow-orange colour was observed or 10 minutes had elapsed. In a second trial, the method was repeated with the inclusion of four glass beads (ø = 3 mm) prior to mixing. The third trial used a hand warmer as a source of heat surrounding the PE bag while mixing, and the fourth trial combined both the hand warmer and the glass beads. All trials were performed in triplicate and alongside a control reagent blank for comparison purposes.

4.2.4.2 *Glass vial method (Experiment 2)*

To a 5 mL glass vial was added a sample of 4-MMC (approx. 100 µg), followed by the colour test reagents developed in the previous chapter: copper nitrate (5 mM, 5 drops), neocuproine (5 mM, 2 drops) and sodium acetate (2 M, 2 drops). The tube was capped and shaken until a colour change was observed or 10 minutes had elapsed. The method was repeated in the second trial, with the addition of two glass beads (ø = 3 mm). All trials were performed in triplicate and alongside a control reagent blank for comparison purposes.

4.2.4.3 *Microbead method (Experiment 3)*

To a PE bag containing 16 PE pellets was added a sample of 4-MMC (approx. 100 µg), followed by the colour test reagents developed in the previous chapter: copper nitrate (5 mM, 5 drops), neocuproine (5 mM, 2 drops) and sodium acetate (2 M, 2 drops). The solution was mixed in the PE bag using the thumb and forefingers until a yellow-orange colour was observed or 10 minutes had elapsed. Three more trials were performed by repeating the method using 16 glass beads (ø = 2 mm), 32 glass microbeads (ø = 1 mm) and a spatula of PVAc solid resins. All trials were performed in triplicate and alongside a control reagent blank for comparison purposes.

4.2.4.4 *External heat source (Experiment 4)*

To a 20 mL glass scintillation vial was added a sample of 4-MMC (approx. 100 µg), followed by the colour test reagents developed in the previous chapter: copper nitrate (5 mM, 5 drops), neocuproine (5 mM, 2 drops) and sodium acetate (2 M, 2 drops). The vial was placed on a USB-powered mug warmer (see Figure 4-1A) until a yellow-orange colour was observed or 10 minutes had elapsed. All trials were performed in triplicate and alongside a control reagent blank for comparison purposes. A second trial employed the use of a 5 mL glass vial and an electric cigarette lighter (see Figure 4-1B) as the source of heat. All trials were performed in triplicate alongside a control reagent blank for comparison purposes.

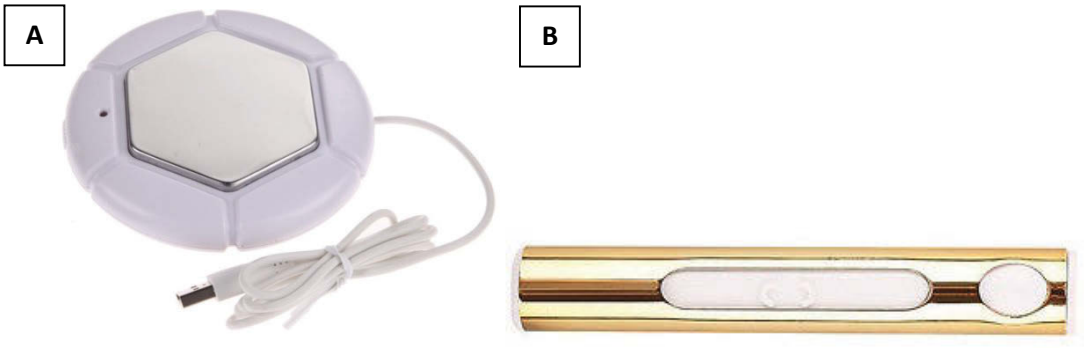

Figure 4-1. Alternative heating devices used in Experiment 4 in replacement of the AC powered hot plate. A) USB-powered mug warmer and B) rechargeable electric cigarette lighter

In a third trial, the 5 mL vial was placed inside an open 20 mL glass scintillation vial containing three sodium hydroxide pellets. Once the 4-MMC and reagents were added to the small vial, water (2 mL) was added to the scintillation vial to surround the colour test reaction. The vials were left to stand and the time taken for a colour change to occur was recorded. All trials were performed in triplicate and alongside a control reagent blank for comparison purposes.

4.2.5 Investigation of catalysts and heat activators

4.2.5.1 *Preliminary methods employing catalysts (Experiment 5)*

To wells of a porcelain spot plate containing a small amount of solid catalyst salt or other heat activator was added a sample of 4-MMC (approx. 100 μg), followed by the colour test reagents developed in the previous chapter: copper nitrate (5 mM, 5 drops), neocuproine (5 mM, 2 drops) and sodium acetate (2 M, 2 drops). Catalyst salts included LiF and KF; heat activators included silica gel, Amberlyst A-21 and unactivated and activated molecular sieves (3A, 4A and 5A). The time taken to observe a colour change was recorded. All trials were performed in triplicate and alongside a control reagent blank for comparison purposes. The tests were also repeated with the addition of the catalyst/activator *after* the addition of the three test reagents.

4.2.5.2 *Optimal amounts of catalyst (Experiment 6)*

To wells of a porcelain spot plate containing three different amounts of solid catalyst salt or other heat activator was added a sample of 4-MMC (approx. 100 μg), followed by the colour test reagents developed in the previous chapter: copper nitrate (5 mM, 5 drops), neocuproine (5 mM, 2 drops) and sodium acetate (2 M, 2 drops). The time taken to observe colour changes were recorded. The catalysts employed and their amounts are shown in Table 4-1. All tests were performed in triplicate alongside a control reagent bank.

Table 4-1. Amounts of catalyst/activator employed in test trials

Catalyst/Activator	**Insoluble**			**Soluble**	
	Molecular sieve 3A	Amberlyst A-21	Silica gel	LiF	KF
Trial 1	0.10 g	0.005 g	0.01 g	0.01 g	0.01 g
Trial 2	0.15 g	0.010 g	0.02 g	0.02 g	0.02 g
Trial 3	0.20 g	0.015 g	0.06 g	0.03 g	0.04 g

4.2.6 Combination of friction/heating mechanism and catalyst

4.2.6.1 *Microbeads with catalyst method (Experiment 7)*

To a PE bag containing microbeads was added a heat activator/catalyst, followed by a sample of 4-MMC (approx. 100 µg) and the colour test reagents developed in the previous chapter: copper nitrate (5 mM, 5 drops), neocuproine (5 mM, 2 drops) and sodium acetate (2 M, 2 drops). The solution was mixed in the PE bag using the thumb and forefingers until a yellow-orange colour was observed. Catalysts employed were: KF (0.05 g), LiF (0.005 g), silica gel (0.1 g), molecular sieve 3A (0.05 g) and Amberlyst A-21 (0.02 g). Microbeads employed were PE pellets (15 pellets), glass beads (20 beads) and PVAc solid resins (0.12 g). The time taken to observe a weak yellow, yellow and yellow-orange colour change was recorded. All trials were performed in triplicate alongside a control reagent blank for comparison purposes.

4.2.6.2 *Simple heating mechanism with catalyst method (Experiment 8)*

To a 5 mL glass vial containing 4-MMC (approx. 100 µg) and KCl (0.01 g) as catalyst was added colour test reagents developed in the previous chapter: copper nitrate (5 mM, 5 drops), neocuproine (5 mM, 2 drops) and sodium acetate (2 M, 2 drops). This vial was placed inside a 20 mL vial containing three NaOH pellets. Water (2 mL) was added to the larger vial and the time taken to observe a colour change was recorded. The test was performed in triplicate alongside a reagent blank.

4.2.7 Preliminary investigation of paper test strips (Experiment 9)

Filter paper (Whatman no. 1) was cut into rectangular strips (5.0 cm x 0.70 cm) with a tapered end. The strips were then spotted with the three reagents in the correct ratio and sequence as shown in the schematic in Figure 4-2 and left to air dry.

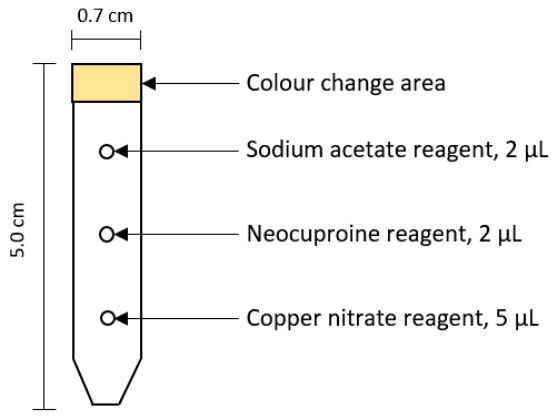

Figure 4-2. Schematic of the paper test strip used in preliminary work on a paper-based device

The dried paper strip was dipped into a single well of a 96-well plate containing an aqueous solution of 4-MMC. The strip was left in solution until capillary action allowed the solution to reach the top of the paper strip. The strip was then placed on a hotplate set at 60 ℃ and heated for several minutes to dry the test strip. The test was performed alongside a control blank deionised water solution and colour changes were recorded.

4.2.8 Investigation into test simplicity and adaptability

4.2.8.1 *Robustness of test protocol*

Copper(II) nitrate hemi(pentahydrate) (0.1163 g), copper(II) chloride dehydrate (0.0852 g) and copper(I) chloride (0.0495 g) were each dissolved in deionised water (100 mL) to create three copper salt solutions at a concentration of 5.0 mM.

The protocol described in chapter 3 was applied to a sample of 4-MMC, 4-FMC and methylone alongside a blank well in a porcelain spot plate in triplicate using the above prepared copper(II) nitrate solution. In a second plate, the copper(II) chloride solution replaced the copper nitrate solution described in the protocol and was performed on the same samples. In a third plate, copper(I) chloride solution replaced the copper(II) nitrate solution and the test was performed on blank wells only. Colour changes were recorded with the naked eye.

4.2.8.2 *Mixed reagent stability*

The three test reagents described in the test protocol of the previous chapter were combined in the ratio: 5 parts copper(II), 2 parts neocuproine and 2 parts sodium acetate. This combined solution was stored in a glass vial on a benchtop and used in a test protocol alongside freshly prepared and individually applied test reagents after: 20 days, 3 months, 1 year and 1.5 years of storage. Colour changes were recorded for 4-MMC alongside a reagent blank in triplicate.

4.2.8.3 *Extraction with organic solvent*

To a semi-micro test tube containing a sample of 4-MMC (approx. 100 µg) was added colour test reagents developed in the previous chapter: copper nitrate (5 mM, 5 drops), neocuproine (5 mM, 2 drops) and sodium acetate (2 M, 2 drops) followed by organic solvent (5 drops). The tube was lightly tapped to mix the solution and the time taken to afford colour changes was recorded. Organic solvents employed included: diethyl ether, dichloromethane, and chloroform. Testing was performed in triplicate alongside a control reagent blank.

In a second trial, the test was repeated using a tapered glass tube made by melting the tip of a Pasteur pipette.

4.2.9 Creation of a simple colour test method

4.2.9.1 *Test method protocol*

To a semi-micro test tube containing a drug sample (approx. 100 µg) was added the mixed reagent (7 drops) from section 4.3.1.2 followed by NaCl solution (1 M, 2 drops) and dichloromethane (5 drops). The tube was tapped to lightly mix the solution and colour changes were recorded. The test was performed in triplicate alongside a control reagent blank.

4.2.9.2 *Selectivity*

The protocol described in section 4.2.9.1 was applied to 100 µg samples of 4-ethylmethcathinone (EMC), 4-fluoromethcathinone (4-FMC), methylone, butylone, pentylone,

pyrovalerone, ethylone, 4-methylpyrrolidinopropiophenone (4-MPPP), 3,4-methylenedioxypyrovalerone (MDPV), methcathinone (MCAT) and α-pyrrolidinovalerophenone (α-PVP). The time taken to visualise a colour change was recorded.

4.2.9.3 *Limit of detection (LOD)*

4-MMC HCl (10 mg) was dissolved in methanol (25 mL) to create a solution with concentration 400 µg/mL. Aliquots of this solution (1, 2, 4, 6, 8, 10, 20, 30, 40, 50, 60, 100, 200, 300, 400 and 500 µL) were pipette into semi-micro test tubes and placed in a dry heating block set at 60 ℃ under nitrogen flow to evaporate. The residual 4-MMC present in the tubes at 0.1, 0.2, 0.4, 0.8, 1, 2, 3, 4, 5, 6, 10, 20, 30, 40 and 50 µg was treated with the colour test protocol described in 4.2.9.1 and the colour changes recorded.

4.3 Results

4.3.1 Investigation of friction and heat generating mechanisms

Initial device trials performed using PE bags and glass beads were able to produce a colour change at room temperature (see Figure 4-3). Further tests performed using different beads smaller in size were able to produce a colour change within 5 minutes at room temperature (see Figure 4-4). The results of all friction generating mechanisms are provided in Table 4-2 below.

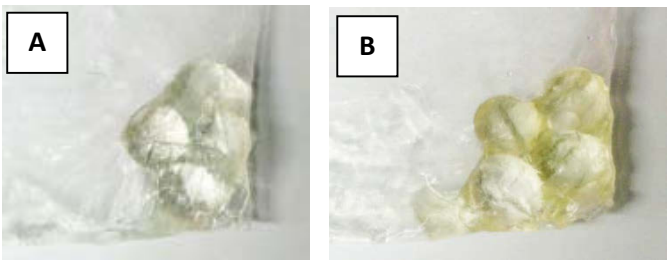

Figure 4-3. Test results using a combination of PE bag and glass beads (Exp 1-2) performed with A) reagents only as a control reagent blank and B) 4-MMC as a positive control

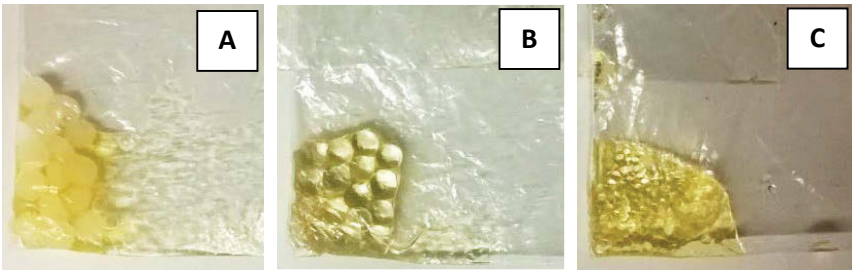

Figure 4-4. Test results using a combination of PE bag and microbeads performed with addition of 4-MMC after 5 min using A) PE pellets (Exp 3-1), B) glass beads (Exp 3-2) and C) PVAc solid resins (Exp 3-3)

Table 4-2. Results of colour test device trials that employed friction generating mechanisms as an alternative to the hotplate

Exp. No.	Test components	Test method	Result with 4-MMC
1-1	• PE zip-lock bag	Rub contents of bag between thumb and forefingers	10 min: No reaction
1-2	• PE zip-lock bag • Four glass beads (ø = 3 mm)		5 min: Very light yellow 10 min: Light yellow-orange
1-3	• PE zip-lock bag • Hand warmer		10 min: No reaction
1-4	• PE zip-lock bag • Four glass beads (ø = 3 mm) • Hand warmer		6 min: Light yellow
2-1	• Glass vial	Shake contents of sealed vial	10 min: No reaction
2-2	• Glass vial • Two glass beads		10 min: No reaction
3-1	• PE zip-lock bag • 16 PE pellets	Rub contents of bag between thumb and forefingers	5 min: Light yellow-orange
3-2	• PE zip-lock bag • 16 glass beads (ø = 2 mm)		
3-3	• PE zip-lock bag • Spatula of PVAc solid resins		

3-4	• PE zip-lock bag • 16 glass beads • (ø = 1 mm)		

The use of a simple external heating mechanism as an alternative to the hotplate was able to produce a colour change (see Table 4-3). Figure 4-5 shows the result of using the mug warmer and Figure 4-6 shows the result of using the electronic cigarette lighter. The light yellow colour result of the surrounding exothermic reaction of Experiment 4-3 is shown in Figure 4-7.

Table 4-3. Results of colour test device trials that employed heat generating methods alternative to the hotplate

Exp. No.	**Test components**	**Test method**	**Result with 4-MMC**
4-1	• Glass vial • Mug warmer	Vials placed onto warmer	4 min: Yellow-orange
4-2	• Small glass vial • Electronic cigarette lighter	Vial is placed onto the heating coil intermittently	4 min: Yellow
4-3	• Small glass vial • Glass vial • NaOH pellets • Water	Water added to glass vial that contains NaOH pellets and the smaller glass vial	8 min: Light yellow 1 h: Yellow-orange

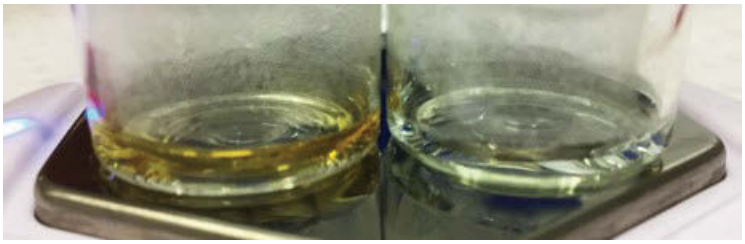

Figure 4-5. Result of colour test (Exp 4-1) performed on 4-MMC as a positive control (*left*) and control reagent blank (*right*) using USB-powered mug warmer after 10 minutes of heating

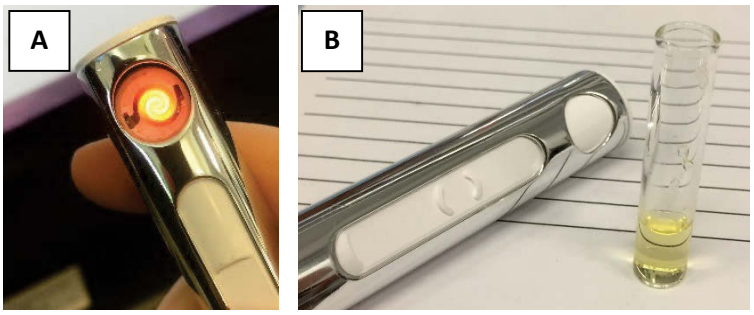

Figure 4-6. The use of the electronic cigarette lighter in colour test methods (Exp 4-2). A) The coil heating element on which the glass vial was intermittently placed and B) result of colour test performed on 4-MMC as positive control

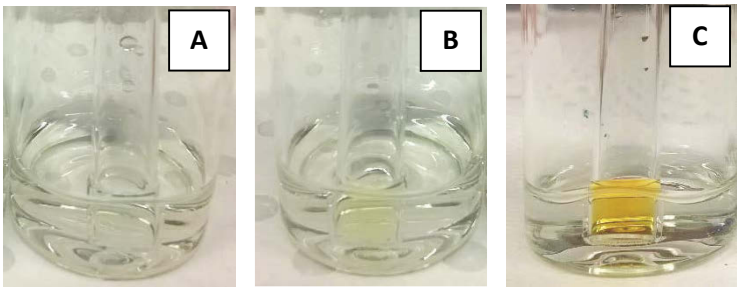

Figure 4-7. Test results using small glass vial and surrounding exothermic reaction (Exp 4-3). A) control reagent blank after 8 min, B) 4-MMC positive control after 8 min, and C) 4-MMC after 1 h

4.3.2 Investigation of catalysts and heat activators

The presence of a catalyst or heat activator allowed the test to be performed at room temperature within 5 minutes. The addition of the catalyst before or after the drug and reagents had no significant effect. The results of preliminary tests are presented below in Table 4-4.

Table 4-4. Results of colour test trials using catalysts and "heat activators" at room temperature

Exp. No.	Activator	Time for colour change to begin	Colour after 5 min
5-1	Lithium fluoride	3 min	
5-2	Potassium fluoride	1 min	
5-3	Silica gel	1 min	
5-4	Molecular sieve 4A	2 min	
5-5	Amberlyst A-21	3 min	

The molecular sieve that provided the most visual colour change was the unactivated molecular sieve 3A. The results of all colour tests employing molecular sieves are provided below in Table 4-5.

Table 4-5. Results of colour test trials using three different sized molecular sieves at room temperature

Exp. No.	Molecular sieve	Unactivated		Activated	
		Reagent blank	4-MMC	Reagent blank	4-MMC
5-6	3A				
5-7	4A				
5-8	5A				

Experiment 6 looked at the relative optimal amounts of catalyst that provided a faster rate of colour change. The results varied for each catalyst, with small amounts of catalyst providing better results with LiF and molecular sieves and greater amounts proving optimal for Amberlyst A-21, silica and KF.

4.3.1 Combination of friction/heating mechanism and catalyst

The combination of a friction mechanism for portability and a catalyst to speed up the reaction at room temperature proved successful (Experiment 7). The results of possible combinations are provided in Table 4-6 below. Optimal results were observed with glass beads and PE pellets employing silica gel or potassium fluoride as catalyst (see Figure 4-8).

Table 4-6. Results of colour test trials combining a heat activator with a friction mechanism[a]

	PE pellets	**Glass beads**	**PVAc solid resins**
KF (0.05 g)	W: 1 min Y: 5 min Y-O: N/A	W: 30 sec Y: 2 min Y-O: 5 min	W: 1 min Y: 5 min Y-O: N/A
LiF (0.005 g)	W: 3 min Y: 6 min Y-O: N/A	W: 3 min Y: 4.5 min Y-O: N/A	W: 4 min Y: 7 min Y-O: N/A
Silica gel (0.1 g)	W: 1 min Y: 2 min Y-O: 3 min	W: 1.5 min Y: 3 min Y-O: 5 min	W: 2 min Y: 4 min Y-O: 7 min
Molecular sieve 3A (0.05 g)	W: 7 min Y: N/A Y-O: N/A	W: 3 min Y: 5 min Y-O: 7 min	W: 5 min Y: N/A Y-O: N/A
Amberlyst 21 (0.02 g)	W: 2 min Y: 4 min Y-O: N/A	W: 4 min Y: N/A Y-O: N/A	W: 4 min Y: N/A Y-O: N/A

[a] W: Weak yellow, Y: Yellow, Y-O: Yellow-orange

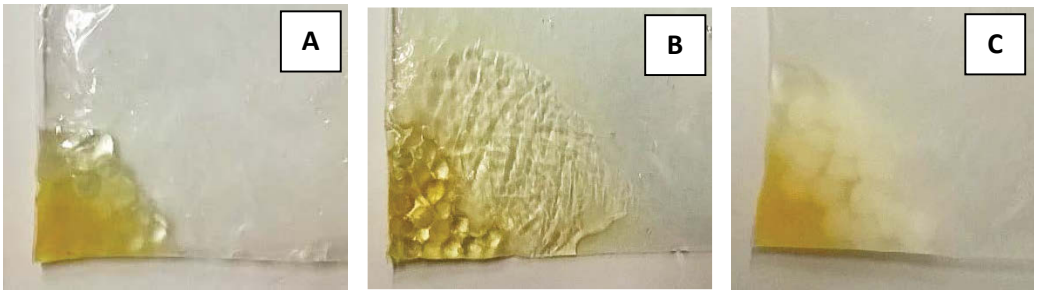

Figure 4-8. Results of the most optimal combinations of heat activator and friction mechanism after 5 min (Exp 7). A) silica gel and glass beads, B) KF and glass beads, and C) silica gel and PE pellets

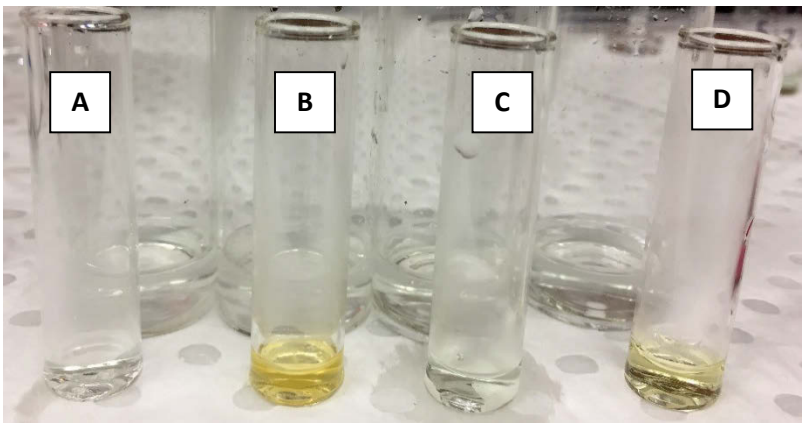

Figure 4-9. Colour test result after 4 minutes by combining the use of a catalyst with an external exothermic reaction as a simple heating mechanism (Exp 8). A) control blank with KCl, B) 4-MMC with KCl, C) control blank without KCl, D) 4-MMC without KCl

4.3.2 Preliminary investigation of paper test strips (Experiment 9)

The preliminary investigation of a paper-based test device showed potential when the strip dipped in 4-MMC solution produced a yellow colour change, noticeably different from the control reagent blank (see Figure 4-10).

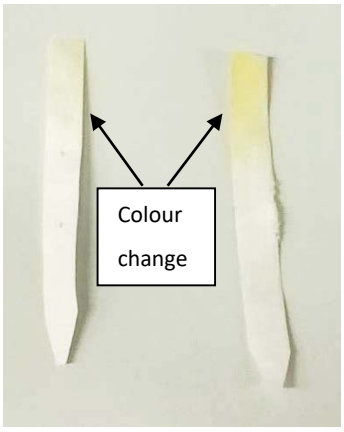

Figure 4-10. Result of preliminary paper test strip method (Exp 9) performed on a blank control (*left*) and 4-MMC (*right*).

4.3.1 Investigation into test simplicity and adaptability

4.3.1.1 *Robustness of test protocol*

Testing performed using copper(II) nitrate and copper(II) chloride produced a light blue reagent blank and yellow-orange for 4-MMC, 4-FMC and methylone HCl after 8 minutes of heating. Testing with Cu(I) chloride produced a yellow-orange colour in the control reagent blank.

4.3.1.2 *Mixed reagent stability*

The mixed reagent solution initially appeared as a very light blue colour, and changed to a green colour after storage. Colour test results with 4-MMC showed the mixed solutions behaved the same as if applied as individual reagents, sequentially. In addition, the mixed reagent produced identical colour changes and remained stable after 1.5 years being stored at room temperature.

4.3.1.3 *Extraction with organic solvent*

The trials employing organic solvent successfully concentrated the coloured complex and appeared to increase the rate of the colour change. The chlorinated solvents concentrated the

coloured product at the bottom of the tube and were easier to visualise than the diethyl ether on the top layer. The use of the tapered tube improved the visualisation of a colour change significantly (see Figure 4-11).

Figure 4-11. Colour test result employing chloroform as an organic extraction solvent to concentrate the coloured product performed in A) a semi-micro test tube and B) a sealed Pasteur pipette

4.3.1 Creation of a simple colour test method

4.3.1.1 *Test method protocol*

The test protocol combining the extraction solvent, mixed reagent solution and catalyst showed successful yellow-orange colour changes at room temperature in under 1 minute. The sodium chloride salt also provided indistinguishable results to those of KCl.

4.3.1.2 *Selectivity*

To confirm the selectivity for other cathinones was also improved the test was performed on other cathinone analogues (listed in methods section), all of which also produced the yellow-orange colour change in under 1 minute.

4.3.1.3 *Limit of detection (LOD)*

The results of the LOD study showed the limit of detection of the colour test was also improved. The smallest amount of 4-MMC that was able to produce an observable colour

change was 2 µg (see Figure 4-12). In addition, lower LOD's were achieved with longer reaction times.

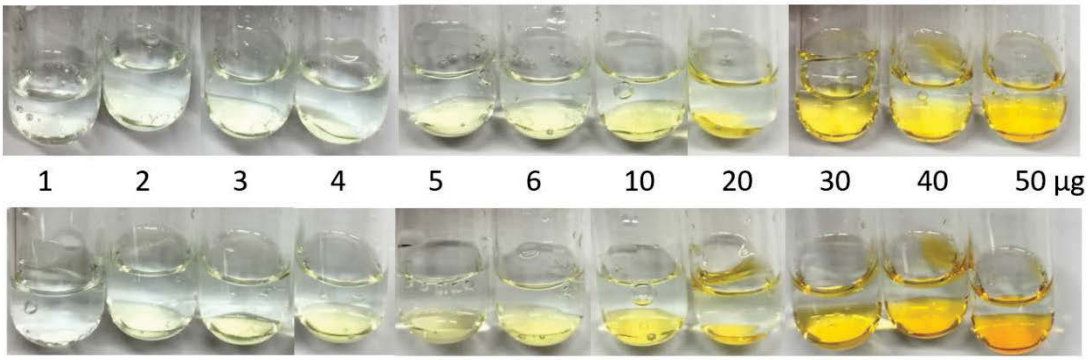

Figure 4-12. Results of limit of detection (LOD) study performed on 4-MMC after 2 minutes (*top*) and 5 minutes (*bottom*). Amounts between 0.1 µg and 0.8 µg are not shown here due to no colour change being observed.

4.4 Discussion

The successful use of microbeads in PE bags provided great insight into the development of a useful test device able to be performed at room temperature. The friction generated through the act of massaging the beads provides heat to the reaction and removes the necessity for an AC powered hotplate. A number of issues arose while using this method and are provided in Table 4-7 below along with possible solutions.

Table 4-7. Issues arising from the use of microbeads in a PE bag and possible solutions to these problems

Issue	**Possible solution**
Beads breaking through PE bag	Use a thicker plastic bag or one without seams
PE bag scrunching	Use a thicker plastic bag or alternative to plastic
Difficulty getting drug to bag corner	Reduce size of PE bag or change shape of bag to a tube

Difficulty seeing colour change	Use white coloured beads and reduce size of PE bag
Tiresome and painful to massage beads for at least 2 min with fingers	Remove need to directly handle the microbeads by using a barrier of sandpaper or glass slides.
Difficulty rolling beads while using hand warmer to heat PE bag contents.	Use an alternative heat generating method

The poor PE bag performance was a common theme of all issues described, and resulted in an idea for a colour test device that used beads sandwiched between two rotating glass discs (see Figure 4-13). This device would make the grinding mechanism easier on the fingers and would eliminate the bag scrunching issues. The use of colourless glass discs in the device would also allow the colour change to be visualised through the discs. The device design was altered to include a well wherein the reagent, beads and drug would be added before attaching the top glass disc and rotating (see Figure 4-14).

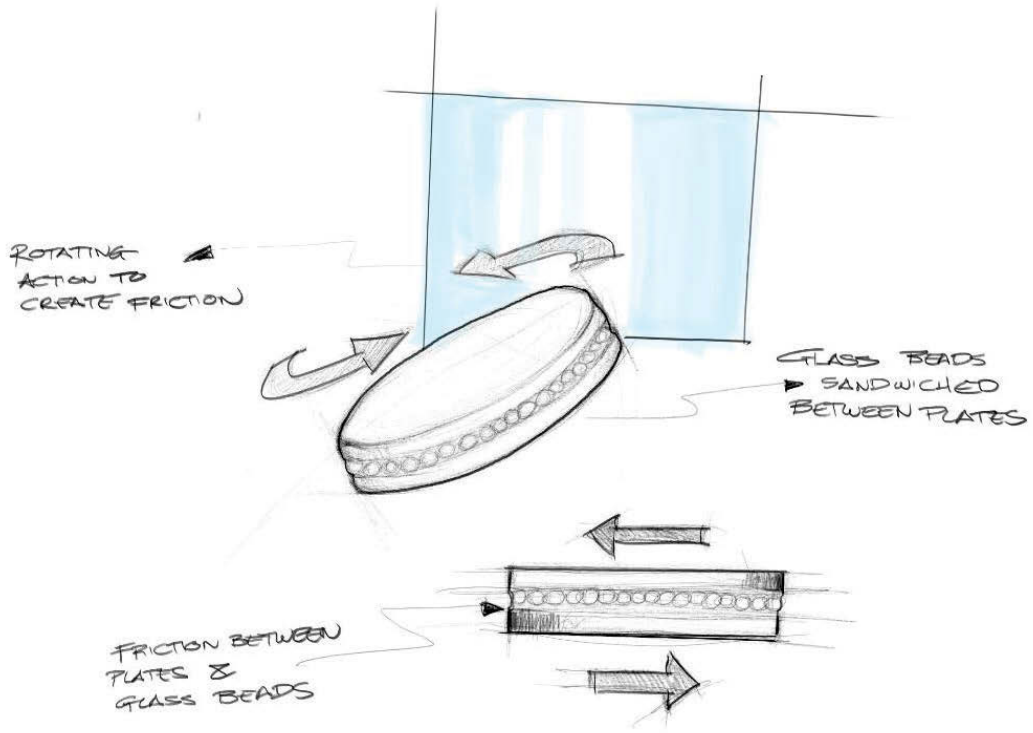

Figure 4-13. Colour test device design employing glass beads sandwiched between two rotating glass discs

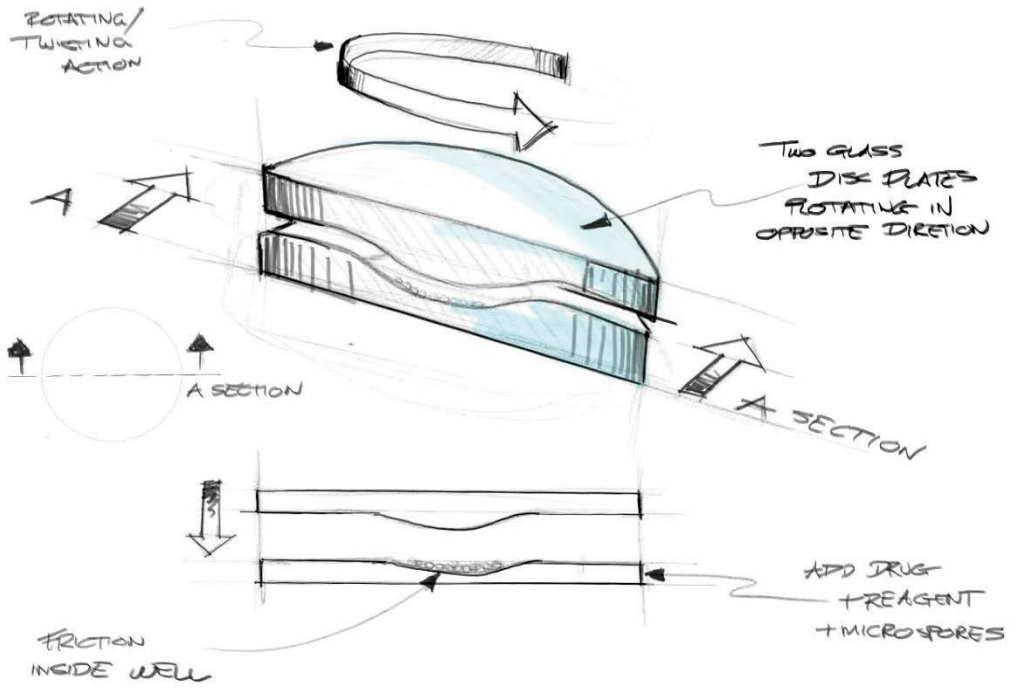

Figure 4-14. Colour test device design employing glass beads sandwiched between one concave and one convex shaped glass discs that rotate to generate friction

Glass bead success led to trials using other microbeads, including smaller glass beads with a diameter of 2 mm which proved to be the easiest to see the colour change with. The smallest glass beads (diameter 1 mm) did not afford any improvements in the colour change rate and were actually more difficult to manoeuvre in the PE bags. PE moulds were trialled due to the opaque colour which may help the colour change of the reaction become easier to visualise. The PVAc solid resins were also trialled however, the irregular and often sharp shape of the resins proved difficult to use in the PE bags due to punctures occurring easily.

The heat generating methods that were trialled were chosen based on their simple and inexpensive nature. The mug warmer is very lightweight and conveniently USB-powered, and the electronic cigarette lighter is completely portable and rechargeable. Although both tests were successful, the colour test would be better improved by the removal of any electric heating devices for both simplicity and cost effectiveness. The final heat generating method employed the exothermic reaction of the dissolution of solid sodium hydroxide surrounding a vial containing the colour test. Although effective in producing a colour change at room temperature, this method is not particularly ideal due to the corrosive nature of the

concentrated sodium hydroxide employed and the long reaction time required for full development of colour.

The notion behind the use of a catalyst for this reaction was based on the fact that the colour test when performed at room temperature will undergo a colour change if left overnight. The addition of heat only speeds up the reaction and therefore, a catalyst could be employed to increase the reaction rate. Preliminary trials employed fluoride salts, silica gel, molecular sieves and Amberlyst A-21. The soluble fluoride salts noticeably increased the rate of colour change in the presence of a cathinone drug. Further testing showed inexpensive halide salt alternatives also behaved as catalysts in the reaction, e.g. KCl and NaCl. These metal halide salts are thought to play a role in the stabilisation of the copper complex or the radical intermediates resulting from the electron transfer process.

Insoluble 'heat activators' also showed catalyst potential. The small pore sizes of the molecular sieves indicate the coloured complex would not be adsorbed inside the material, however, after longer reaction times the adsorption of the complex to the outside of the sieves was observed. It is likely that the sieves adsorb water molecules and thus effectively concentrate the coloured product. The improved reaction rate using activated sieves over unactivated ones can be explained by the greater porosity in activated sieves due to the prior removal of water molecules. The greater surface area of the smaller 3A sieve led to its preference over the other sieve sizes. Silica gel performed the best of the insoluble activators due to the adsorption of the coloured complex within several minutes. Amberlyst A-21 is an anionic exchange resin with larger pore sizes and thus likely has a more active role in catalysing the reaction. The effective adsorption of the coloured complex potentially be translated into a solid sensor test method, however, no further work on these insoluble catalysts was undertaken.

Combining a friction mechanism with a catalyst was the obvious next step and produced good results. The silica gel concentrated the coloured complex which allowed for it to be more easily visualised, however, it was gritty to work with in the PE bag. Similarly, Amberlyst-A21 was a static material and difficult to control in the PE bag, while the old source of KF had absorbed a lot of water, making amounts used unknown.

The preliminary work performed to develop a paper-based test device demonstrated showed potential. Attempts to simplify the device were unsuccessful and also led to false positives when using a mixed reagent solutions. Testing confirmed the reagent volumes need to be small, reagents must be applied individually, and the test still requires heat to develop a colour change.

Looking at the chemical reaction taking place, it was shown that the test is able to be performed using any source of Cu(II) ions as a reagent. This can come from copper(II) nitrate as described in the published protocol, however can also be from copper(II) chloride. The investigation showed the anions have no effect on the coloured product at such low concentrations. Furthermore, testing using copper(I) chloride confirmed that the Cu(I) ion is involved in the coloured complex.

A significant finding in this investigation was the ability to combine the three reagents into one solution to create a one-step test sequence. The high stability of the reagent was also demonstrated in studies performed. The second significant find of the study was the successful coloured complex extraction by the addition of organic solvent. The use of dichloromethane was preferred due to its lesser toxicity compared to chloroform as well as its high density which leads to the bottom layer of the test tube containing the coloured portion.

A colour test device was proposed that employed the combined use of the mixed reagent solution, a catalyst solution and dichloromethane based on current polyethylene pouches that are available (see Figure 4-15). Although good results for 4-MMC were achieved with the addition of dichloromethane only, other synthetic cathinone analogues such as MDPV and α-PVP benefited from the combination of catalyst solution and organic extraction solvent.

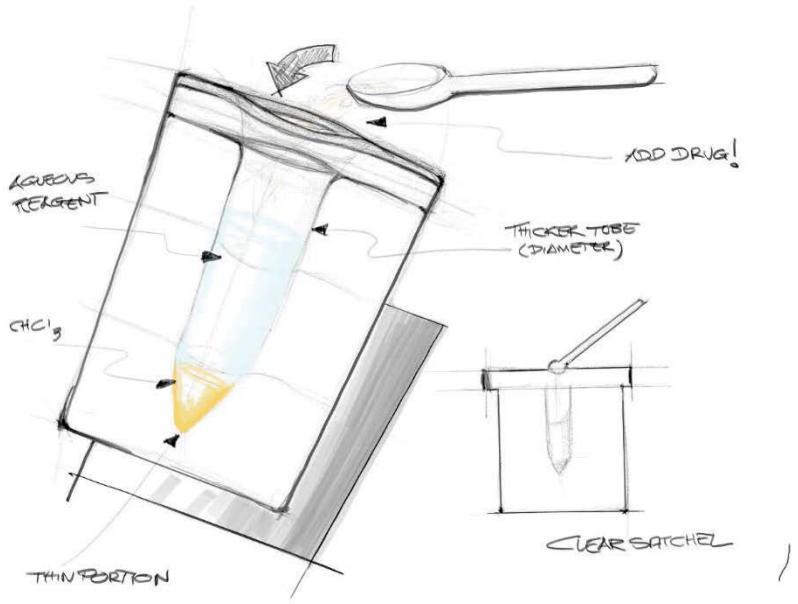

Figure 4-15. Colour test device design that employs a polyethylene pouch that contains a glass ampoule with organic solvent and colour test reagents

A second colour test device was also designed that contained a collection swab that could be used to collect the drug material. This swab also acted as a lid to a tube that contained the aqueous reagent mix as well as dichloromethane. Once the swab lid is screwed on, the tube is shaken and the lower portion of the tapered tube is observed for a yellow-orange colour change (see Figure 4-16).

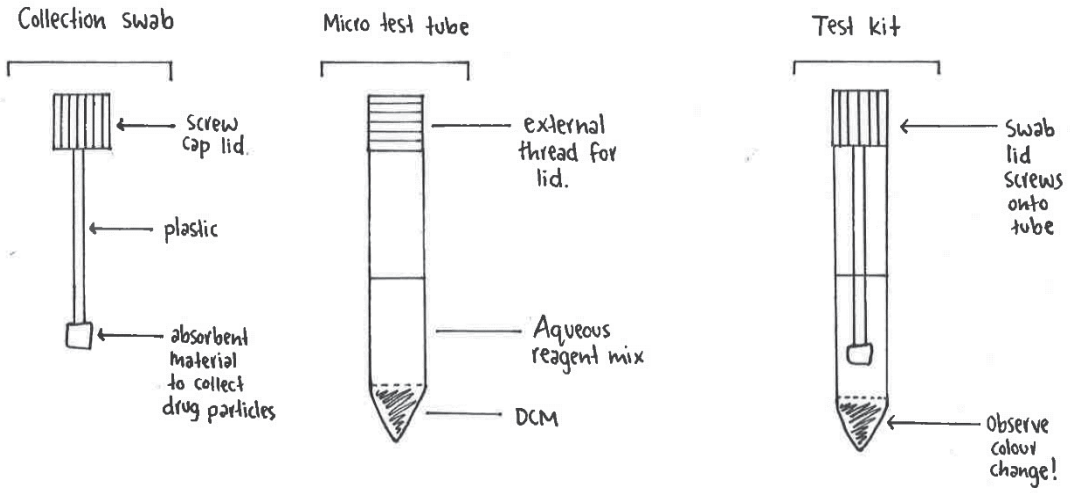

Figure 4-16. Colour test device design employing a collection swab that screws into a sealed tube containing the reagent mix and dichloromethane

The colour test device can also be employed in semi-quantitative analysis through the employment of a light controlled box and attachment of a colour digitiser or smart phone with colour reading applications installed (see Figure 4-17).

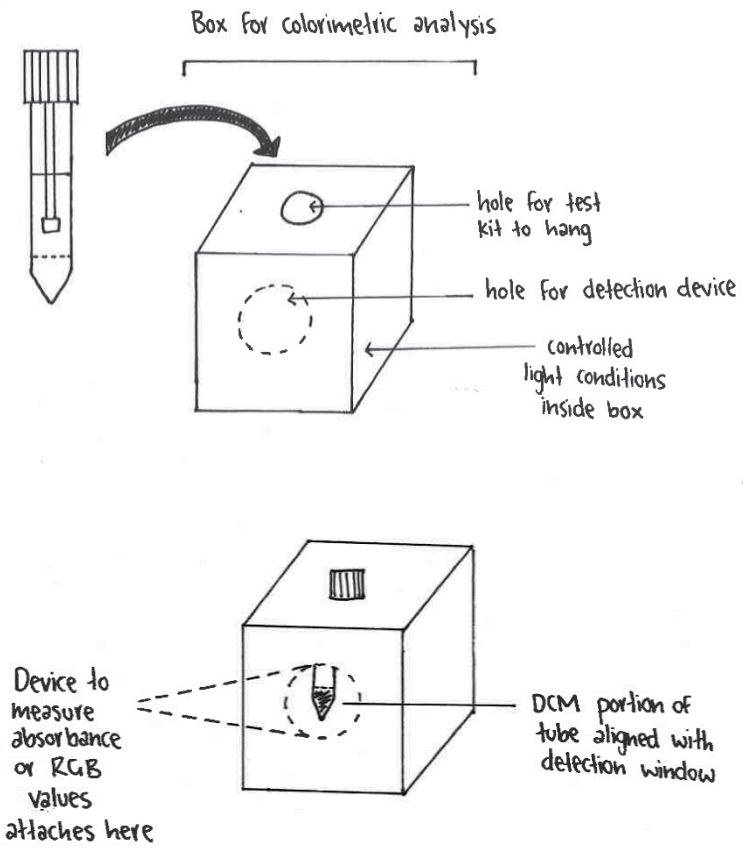

Figure 4-17. Colour test device accessory that allows the coloured portion of the tapered tube to be recorded using a portable colour digitiser or smart phone application

The selectivity toward synthetic cathinones was improved in the updated test method described here. Synthetic cathinones that showed sluggish reactions in the previous protocol were able to develop colour changes within minutes at room temperature. In addition, the operational limit of detection[37] value for 4-MMC was decreased by 50% to 20 µg.

4.5 Conclusion

The previously developed chemical colour test protocol for the detection of synthetic cathinones was transformed into a test method that can be easily incorporated into a simple and portable colour test device applicable at room temperature. A number of methods were trialled in this study, including friction and heat generating mechanisms in order to eliminate the heating requirement of the test. The simplest device amalgamated several methods

producing fast and easily visualised colour changes, from addition of organic extraction solvent and use of a tapered micro tube to combining reagent solutions and the addition of a metal halide salt catalyst. The work in this chapter culminated into a patent application.

4.6 References

37. Scientific Working Group for the Analysis of Seized Drugs (SWGDRUG), *SWGDRUG Recommendations Version 7.1*. 2016, United States Department of Justice: USA.
117. *EZ Test kits*. 2016 [cited 2016 November 22]; Available from: http://www.eztestwholesale.com/product-category/ez-test-kits/.
162. Choodum, A., *et al.*, *Real time quantitative colourimetric test for methamphetamine detection using digital and mobile phone technology.* Forensic science international, 2014. **235**: p. 8-13.
169. Bell, S.C. and R.D. Hanes, *A microfluidic device for presumptive testing of controlled substances.* Journal of Forensic Sciences, 2007. **52**(4): p. 884-888.
170. Musile, G., *et al.*, *The development of paper microfluidic devices for presumptive drug detection.* Analytical Methods, 2015. **7**(19): p. 8025-8033.
368. SIRCHIE. *Pouches*. Narcotics Investigation 2017 [cited 2017 10th September]; Available from: http://www.sirchie.com/forensics/narcotics-investigation/pouches.html.
369. *Products - Drug testing kits*. 2016 [cited 2016 22nd November]; Available from: http://www.identa-corp.com/products/drug-testing-kits.
370. Self-Diagnostics. *Substance Test Amphetamines / Opiates (AMP/OPI)*. 2017 [cited 2018 January 4]; Available from: https://www.self-diagnostics.com/en/substance-test-amphetamines-opiates-amp-opi.html.

This page intentionally left blank

Chapter 5: Chemical reactions of synthetic cathinones: A potential recognition element?

This page intentionally left blank

Chapter 5: Chemical reactions of synthetic cathinones: A potential recognition element?

5.1 Introduction

Chemical reactions have been shown to be effective in the presumptive detection and identification of illicit drugs through the unique formation of a chromophoric compound in colour tests. However, there are many selective chemical reactions that do not elicit a coloured product and therefore success of the reaction cannot be established with the naked eye.

To overcome this problem in the development of an optical detection method, the chemical reaction can be linked to an alternative luminescent reporting signal (chemical tagging) to indicate when the reaction takes place. Fluorescent molecules[301] and upconversion nanoparticles[371, 372] have been employed as optical reporters for the detection of illicit drugs and other small molecules using chemical reactions. In both instances, the chemical reaction provides the selectivity and target molecule recognition, while the optical reporter provides a visual signal through the enhancement or quenching of luminescence.

The development of detection methods for more recently available compounds such as the synthetic cathinones requires an investigation into their chemical behaviour, and identification of simple chemical reactions in which they are involved. Limited research into cathinone derivatisation includes thionation and elimination reactions by Nycz *et al.*[138] and chemical derivatisation methods by Kerrigan[373] for GC-MS analysis.

In addition to the usefulness of chemical derivatisation in optical detection, it has also been employed as a means to get cathinones across borders[22], or alternatively taken as 'pro-drugs' that metabolise in the body to produce the initial compound[374].

This chapter aims to investigate potential chemical tagging methods appropriate to the synthetic cathinone class of compounds by targeting the electrophilic carbonyl group. In addition, the stabilities of the compounds are investigated to determine what conditions will produce degradation products.

5.2 Materials and methods

5.2.1 Chemicals

Hydroxylamine hydrochloride, sodium borohydride, *p*-tolualdehyde, 4-methylpropiophenone, copper(II) chloride dihydrate, 2,9-dimethyl-1,10-phenanthroline hemihydrate, d-(+)-glucose, iron(III) chloride, trifluoroacetic acid, potassium chloride, K10 montmorollinite clay and piperonal were obtained from Sigma Aldrich (Castle Hill, NSW, Australia). Methanol, ethanol, hexane, dichloromethane, chloroform, sodium sulfate and sodium hydroxide were obtained from Chem-Supply (Gillman, SA, Australia). Bismuth oxychloride, sodium acetate, aniline, piperidine, Amberlyst A-21, and 2,4-dinitrophenylhydrazine were obtained from BDH Laboratory chemicals (Poole, England). Sulphuric acid and hydrochloric acid were obtained from RCI Labscan (Pathum Wan, BNK, Thailand). Benzophenone, semicarbazide hydrochloride, bismuth oxide, ammonium acetate, ascorbic acid, potassium ferricyanide, sodum tetraborate decahydrate, potassium dihydrogen phosphate, sodium phosphate and ethyl acetate were obtained from Ajax Finechem (Scoresby, VIC, Australia). Ammonium molybdate was obtained from JT Baker Chemical Company (Phillipsburg, NJ, USA). Glacial acetic acid and anhydrous magnesium sulphate were obtained from Scharlau Chemicals (Sentmenat, Barcelona, Spain). Molecular sieves were obtained from Prolabo (Paris, France).

5.2.2 Reference material

Synthetic cathinone reference materials and brominated cathinone reaction intermediates were obtained from syntheses described in Chapter 2 and included: 4-methylmethcathinone (4-MMC), 4-fluoromethcathinone (4-FMC), 4-methylethcathinone (4-MEC), methcathinone (MCAT), methylone, butylone, pentylone, pyrovalerone, α-pyrrolidinovalerophenone (α-PVP), 2-bromo-4-methylpropiophenone and 1-(2*H*-1,3-benzodioxol-5-yl)-2-bromopropan-1-one.

5.2.3 Instrumentation

Irradiation with microwaves was achieved using a Palsonic 1330 W domestic microwave oven (Waterloo, NSW, Australia). Irradiation with ultraviolet light was achieved using a purpose-built

UV light box (22.5 x 21.0 x 13.3 cm) containing two 16 W fluorescent UV (365 nm) light bulbs (UTS Science Workshop).

5.2.4 Ultraviolet-Visible spectroscopy analysis

Absorption spectra in the ultraviolet region were obtained in the range 200–400 nm using an Agilent Technologies Cary 60 spectrometer (Santa Clara, CA, USA). Spectra were recorded at a rate of 600 nm/min using a quartz cuvette. Baseline corrections were performed for all spectral measurements.

5.2.5 Thin Layer Chromatography (TLC)

Reactions were monitored using silica gel 60 F254 TLC plates on aluminium backing from Merck Millipore (Bayswater, VIC, Australia). Samples were spotted onto the plates directly from the reaction mixture or after dilution with methanol. Ethyl acetate: methanol: ammonia (85:10:5) was used as the mobile phase in TLC monitoring.

Developed TLC plates were initially viewed using a Spectroline® CM–10A UV viewing cabinet (Spectronics Corporation, Westbury, NY, USA) fitted with a UV lamp (Grace Discovery Sciences, Epping, VIC, Australia). TLC plates were subsequently stained using iodine vapour as a visualisation reagent.

5.2.6 Gas Chromatography-Mass Spectrometry (GC-MS) analysis

Samples were injected using an Agilent 7683 series autosampler and analysis was performed using an Agilent 6890 Gas Chromatograph coupled to an Agilent 5973 Mass Spectrometer (Agilent Technologies, Santa Clara, CA, USA). The GC-MS system was equipped with an HP-5MS column with 5% Phenyl 95% dimethylpolysiloxane copolymer phase (30 m x 0.25 mm x 0.25 µm). Injector and interface temperatures were set at 250 °C and 280 °C, respectively, and injections (1.0 µL) were made in split mode with a 25:1 split ratio. The initial oven temperature at 50 °C was held for 2 min before increasing the temperature to 290 °C at a rate of 50 °C/min and holding for a further 4 min. Helium was used as the carrier gas at a constant flow rate of 1.2 mL/min with a 2 min solvent delay. Data was collected using full scan acquisition (40-450

amu) and analysis was carried out using Agilent Enhanced ChemStation software, MSD ChemStation.

5.2.7 Preparation of cathinone stock solutions

In a 20 mL glass scintillation vial, the synthetic cathinone (0.0060 g) was dissolved in methanol (15 mL) to make a 400 μg/mL solution. Synthetic cathinones in this study included: 4-methylmethcathinone (4-MMC), 4-fluoromethcathinone (4-FMC), 4-methylethcathinone (4-MEC), 3,4-methylenedioxypyrovalerone (MDPV), α-pyrrolidinovalerophenone (α-PVP), methylone, butylone, pentylone, pyrovalerone and methcathinone (MCAT).

5.2.8 Imine (and enamine) formation

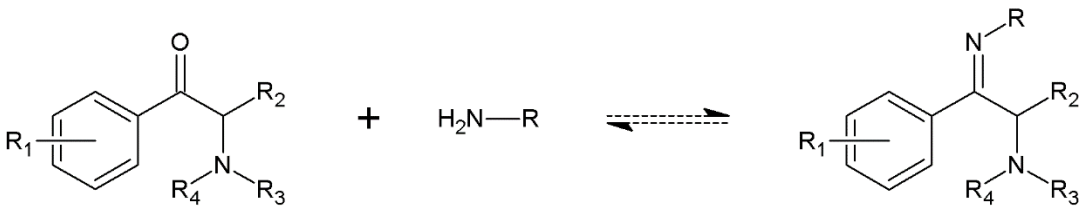

Figure 5-1. Synthetic preparation of an imine from a synthetic cathinone and a primary amine

5.2.8.1 *Imine formation method 1*

The method described in Thorat *et al.*[231] was modified for application in this study. To a RBF was added 4-MMC HCl (0.0053 g, 0.025 mmol), methanol (5.00 mL), aniline (2.5 μL, 0.027 mmol) and acetic acid solution (0.10 M, 2.00 mL). The reaction mixture was refluxed for 30 min and monitored by TLC. The remaining mixture was poured into cold water (5 mL), basified with sodium hydroxide (100 μL, 1 M), extracted with dichloromethane (1 mL), dried over sodium sulphate and subjected to direct GC-MS analysis.

5.2.8.2 *Enamine formation method 1*

The method described by Varma *et al.*[236] was modified for application in this study. To a glass scintillation vial was added 4-MMC HCl (0.0050 g, 0.023 mmol), piperidine (2.3 µL, 0.023 mmol), K10 montmorillonite clay (20 mg) and DI water (200 µL). The vial was irradiated in a domestic microwave oven (1100 W) using 10 s pulses for a total of 2 min before monitoring the reaction by TLC. The remaining mixture was filtered, extracted with dichloromethane (1 mL), dried over sodium sulphate and subjected to direct GC-MS analysis.

5.2.8.3 *Enamine formation method 2*

The method described by Taguchi and Westheimer[233] was modified for application in this study. To a glass scintillation vial was added 4-MMC HCl (0.0050 g, 0.023 mmol), piperidine (2.3 µL, 0.023 mmol), and molecular sieves 4A (100 mg) followed by diethyl ether (1 mL) and sodium hydroxide solution (6.0 µL, 2.0 M). The vial was placed on the roller mixer for 1 hr at room temperature before monitoring the reaction mixture by TLC. Water (2 mL) was added to the vial, the solution separated from the molecular sieves, extracted with diethyl ether (1 mL), dried over sodium sulphate and subjected to direct GC-MS analysis.

5.2.9 Hydrazone formation

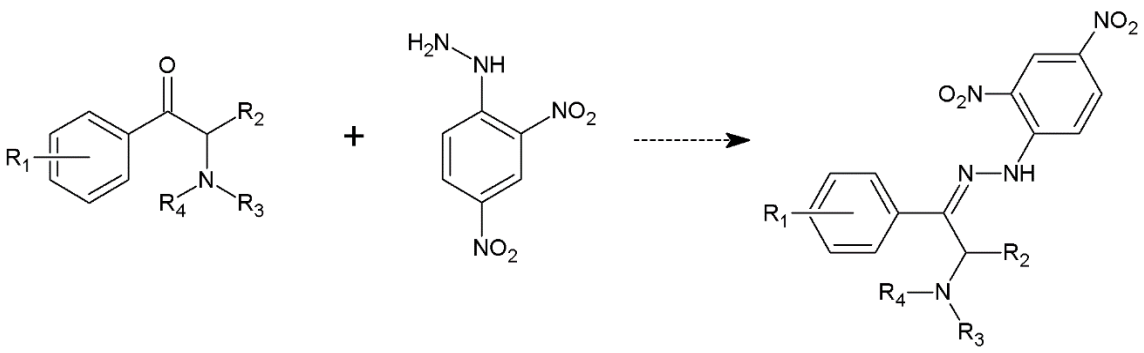

Figure 5-2. Synthetic preparation of 2,4-dinitrophenylhydrazone derivative from a synthetic cathinone and 2,4-dinitrophenylhydrazine (DNP)

5.2.9.1 *DNP Method 1*

The method outlined in Martin and Gilbert[375] was modified for application in this study. In a glass scintillation vial, 2,4-dinitrophenylhydrazine (DNP) (0.200 g, 1.01 mol) was dissolved in concentrated sulphuric acid (1.00 mL) and added to a mixture of water (1.50 mL) and ethanol (5.00 mL, 96% w/w). In a test tube, a pin-head sized amount of solid sample was dissolved in ethanol (2.00 mL) and added to a second test tube containing the DNP solution (2.00 mL) prepared above. The tube was shaken to mix contents and precipitate formation was recorded immediately, after standing at room temperature for 24 h, and after heating in a water bath at 80 °C for 1 h. Solid samples tested included 4-MMC free base, 4-MMC HCl, piperonal and 1-(2*H*-1,3-benzodioxol-5-yl)-2-bromopropan-1-one. The test was performed in triplicate alongside a reagent blank.

5.2.9.2 *DNP method 2*

The method outlined in Kadam *et al.*[239] was modified for application in this study. In a glass scintillation vial, DNP (0.250, 1.26 mol) was dissolved in methanol (5.00 mL) and concentrated sulphuric acid (0.50 mL) added cautiously. In a small test tube, a pin-head sized amount of solid (or drop of liquid) sample was dissolved in methanol (0.50 mL), followed by 10 drops of DNP reagent prepared above. The tube was shaken to mix contents and precipitate formation was recorded immediately. Samples tested included piperonal, 4-methylpropiophenone, p-tolualdehyde, 2-bromo-4-methylpropiophenone, methylone HCl, pyrovalerone HCl, 4-FMC HCl, MDPV HCl and α-PVP HCl. The test was performed in triplicate alongside a reagent blank.

5.2.10 Semicarbazone formation

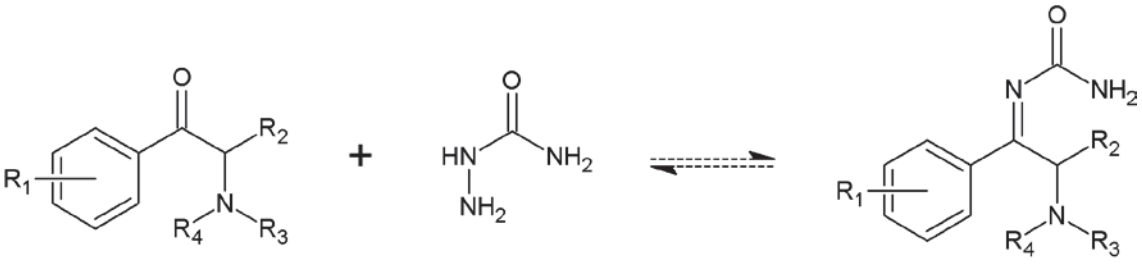

Figure 5-3. Synthetic preparation of a semicarbazone derivative from a synthetic cathinone and semicarbazide hydrochloride

5.2.10.1 *Semicarbazone Method 1*

The method described in Jafri *et al.*[376] was modified and applied in this study. To a glass scintillation vial was added semicarbazide HCl (0.0057 g, 0.051 mmol), ethanol (1 mL) and glacial acetic acid (3 drops). This mixture was subsequently added to a solution of 4-MMC HCl (0.0050 g, 0.023 mmol) in ethanol (3 mL). The vial was irradiated in a domestic microwave oven (1100 W) using 10 s pulses for a total of 1 min before monitoring the reaction by TLC. The remaining mixture was rotary evaporated, dissolved in water (2 mL), extracted with dichloromethane (1 mL), dried over sodium sulphate and subjected to direct GC-MS analysis.

5.2.10.2 *Semicarbazone Method 2*

The method described in Vijayan et al[256] was modified and applied in this study. To a glass scintillation vial was added 4-MMC HCl (0.0050 g, 0.023 mmol), semicarbazide HCl (0.0057g, 0.051 mmol) and sodium acetate (0.0082 g, 0.100 mmol). The vial was placed in a warm water bath and swirled while adding ethanol (2.5 mL) until a clear solution was obtained. The vial was then capped and stored in an incubator oven at 35 °C for 1 h. The reaction was monitored by TLC and the remaining mixture was rotary evaporated, dissolved in water (2 mL), extracted with dichloromethane (1 mL), dried over sodium sulphate and subjected to direct GC-MS analysis.

5.2.11 Oxime formation

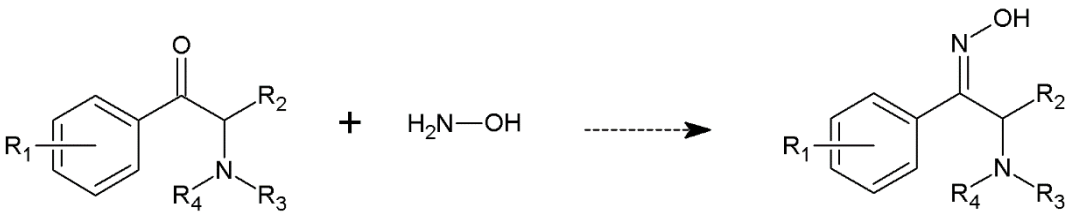

Figure 5-4. Synthetic preparation of an oxime derivative from a synthetic cathinone and hydroxylamine

5.2.11.1 *Oximation method 1*

The method described in Aakeroy *et al.*[243] was modified and applied in this study. In a mortar and pestle, 4-MMC HCl (0.177 g, 0.828 mmol) and hydroxylamine HCl (0.083 g, 1.20 mmol) were ground for 30 s. Sodium hydroxide (0.048 g, 1.20 mmol) and methanol (4 drops) were added and the mixture ground for 2 min. After 5 min standing, methanol (4 drops) was added and the mixture ground for a further 2 min. Following TLC analysis, the mixture was extracted with dichloromethane (1 mL), dried over sodium sulphate and subjected to direct GC-MS analysis.

5.2.11.2 *Oximation method 2*

The method described in Ballini *et al.*[250] was modified and applied in this study. In a glass scintillation vial, 4-MMC HCl (0.021 g, 0.098 mmol) and hydroxylamine HCl (0.014g, 0.200 mmol) were dissolved in ethanol (15 mL) before adding Amberlyst A-21 and leaving the mixture to stand for 1 h. Following TLC analysis, the reaction mixture was filtered, extracted with dichloromethane (1 mL), dried over sodium sulphate and subjected to direct GC-MS analysis.

5.2.11.3 *Oximation method 3*

The method described by Kerrigan[373] was modified and applied in this study. To a test tube was added an aliquot of prepared methanolic cathinone solutions from section 5.2.7 (1 mL, 400 µg/mL) and the methanol evaporated in a dry heating block at 50 °C under a gentle stream of nitrogen. An aliquot of aqueous hydroxylamine HCl (500 µl, 1.6 M) was added to the tube. The tubes were subsequently capped and heated for 80 min at 80 °C before cooling to room temperature and adding chloroform (1 mL) and sodium hydroxide solution (2 mL, 1.0 M). The tubes were shaken and roller mixed for 5 min. The chloroform layer was extracted with a Pasteur pipette and dried over magnesium sulphate before filtering into a high recovery GC-vial for direct analysis by GC-MS. The solvent was subsequently evaporated and the residue reconstituted in methanol for GC-MS analysis and the UV spectra were recorded after 4 days standing at room temperature. The experiment was repeated using greater amounts of starting material (800 µg) and heating for longer periods of time (2 h) at 80 °C.

5.2.12 Reduction reactions

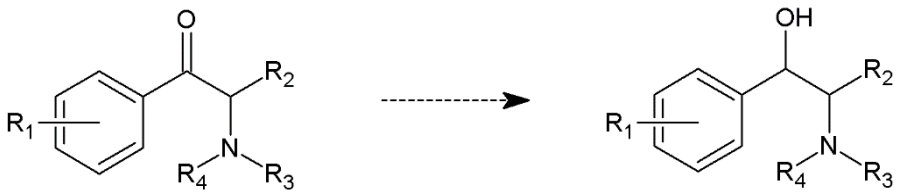

Figure 5-5. The synthetic preparation of secondary alcohol of synthetic cathinones via a reduction reaction

5.2.12.1 *Reduction method 1*

A method from Kerrigan[373] was modified in the following procedure. To a test tube was added an aliquot of methanolic cathinone solution prepared in section 5.2.7 (1 mL, 400 µg/mL) and the methanol evaporated. Ethanolic sodium borohydride solution (100 µL, 0.17 M) was then added and the tubes were capped and heated at 70 °C for 15 min. The solvent was removed and the residue washed with hexane (2 mL) before reconstituting in ethyl acetate (1 mL) and subjecting the sample to direct GC-MS analysis.

5.2.13 Antioxidant activity

5.2.13.1 *Cupric ion reducing antioxidant capacity (CUPRAC)*

The method described by Apak *et al.*[265] for CUPRAC determination was performed using the prepared solutions: copper chloride solution (10 mM), ammonium acetate buffer (pH 7) and ethanolic neocuproine solution (7.5 mM). Ten cathinone sample solutions were prepared at a concentration of 1 mM in methanol using the stock solutions prepared in section 5.2.7. Ascorbic acid and glucose sample solutions at 1 mM were also prepared.

To a test tube was added, copper chloride solution (1 mL), neocuproine (1 mL), buffer solution (1 mL) and methanolic sample solution (1.1 mL). The solution was left to stand for 1 h before recording the absorbance at 450 nm after 1 h.

5.2.13.2 *Ferric ion reducing antioxidant power (FRAP)*

The method described by Vijayalakshmi and Ruckmani[377] for FRAP determination was slightly modified for use in this study. The following reagent solutions were prepared: potassium ferricyanide solution (0.03 M), iron(III) chloride solution (6 mM), phosphate buffer solution (0.2 M, pH 6.6), and trifluoroacetic acid solution (0.9 M). Ten cathinone analogue solutions were also prepared at concentrations of 20 µg/mL using the stock solutions prepared in section 5.2.7. Ascorbic acid and glucose sample solutions at 20 µg/mL and 400 µg/mL were also prepared.

The method was followed according to the literature with slight modifications. To a test tube was added sample solution (1 mL), buffer (2.5 mL), potassium ferricyanide (2.5 mL) and the tube was vortexed for 1 minute. The tube was then incubated at 50 °C for 20 minutes before adding trifluoroacetic acid (2.5 mL) and centrifuging for 10 min at 3000 rpm. The supernatant (2.5 mL) was collected and added to DI water (2.5 mL) and ferric chloride solution (0.5 mL). The tube contents were mixed and the tubes left to stand at room temperature for 20 minutes before recording the absorbance at 700 nm. The test was performed in duplicate alongside a control reagent blank sample containing water, and a positive control solution containing ascorbic acid.

5.2.13.3 *Total antioxidant capacity*

The method described by Prieto *et al.*[378] was modified for application in this study. The reagent was prepared by mixing sulphuric acid (0.61 M, 100 mL), sodium phosphate (28 mM, 100 mL) and ammonium molybdenate (4 mM, 100 mL). Ten cathinone analogue solutions were also prepared at concentrations of 0.5 mM using the stock solutions prepared in section 5.2.7. Ascorbic acid and glucose sample solutions at 0.5 mM were also prepared.

To a test tube was added test sample solution (1 mL, 0.5 mM) followed by water (1 mL) and reagent solution (2 mL). The test tubes were sealed with screw caps and heated in a water bath at 95 °C for 60 min before recording the absorbance at 695 nm. Testing was performed in duplicate alongside a control reagent blank.

5.2.14 Cathinone stability studies

5.2.14.1 *Preparation of buffer solutions*

- pH 2 buffer: Potassium chloride (0.2 M, 125 mL) and hydrochloric acid (0.20 M, 32.5 mL) were combined in a 500 mL volumetric flask and made up to the mark with deionised water.
- pH 6 buffer: Potassium dihydrogen phosphate (0.1 M, 250 mL) and sodium hydroxide (0.10 M, 28 mL) were combined in a 500 mL volumetric flask and made up to the mark with deionised water.
- pH 8 buffer: Sodium tetraborate decahydrate (0.025 M, 250 mL) and hydrochloric acid (0.10 M, 102.5 mL) were combined in a 500 mL volumetric flask and made up to the mark with deionised water.
- pH 10 buffer: Sodium tetraborate decahydrate (0.025 M, 250 mL) and sodium hydroxide (0.10 M, 91.5 mL) were combined in a 500 mL volumetric flask and made up to the mark with deionised water.

5.2.14.2 *Preparation of stability study solutions*

For each cathinone stock solution prepared in section 5.2.7, an aliquot (1.00 mL) was added to 14 glass scintillation vials. The methanol was allowed to evaporate in the fumehood overnight before reconstituting with 20 mL of storage solution to make a 20 µg/mL solution and storing in an environment condition as shown in Table 5-1 below.

Table 5-1. Storage solutions and environment conditions examined in stability studies performed on 10 synthetic cathinone analogues

Vial no.	**Solution**[a]	**Storage environment**
1	pH 2 buffer	Benchtop
2		Refrigerator (7 °C)
3	pH 6 buffer	Benchtop
4		Refrigerator (7 °C)
5	pH 8 buffer	Benchtop
6		Refrigerator (7 °C)

7	pH 10 buffer	Benchtop
8		Refrigerator (7 °C)
9	DI water	Benchtop
10		Refrigerator (7 °C)
11		UV light box
12		- [b]
13	Methanol	Benchtop
14		Refrigerator (7 °C)

[a] Synthetic cathinone concentration of 20 µg/mL
[b] This solution used to create UV calibration curve immediately

5.2.14.3 *Creation of UV calibration curve*

Vial 12 (see Table 5-1) of each cathinone analogue was used to prepare the calibration standards via direct dilution. Into a 5 mL volumetric flask was added 4.00, 3.00, 2.00, 1.00 and 0.500 mL of the 20 µg/mL standard and the solutions were made up to the mark with deionised water to create 16.0, 12.0, 8.0, 4.0 and 2.0 µg/mL concentrations, respectively. These solutions were analysed by UV spectrophotometry and the absorbance at selected wavelength maxima was plotted against concentration to create a calibration curve for each cathinone.

5.2.14.4 *Analysis of solutions for stability*

At certain time periods, an aliquot (2 mL) of each stored solution was added to a 5 mL volumetric flask and filled to the mark with deionised water (or methanol for vial 13 and 14). This solution was analysed by UV-Vis spectrophotometry and the absorption maximum and peak shape were recorded. The time periods of analysis were 1, 7, 14, 21 and 28 days. After 28 days of storage, the solutions in vial 7 were extracted with ethyl acetate (1 mL), dried over sodium sulphate, and analysed directly by GC-MS.

5.3 Results

5.3.1 Imine (and enamine) formation

Imine method 1 failed to produce the desired imine product with aniline in all experiments trialled. Enamine method 2 and 3 also failed to produce the enamine with piperidine in all experiments performed. Apart from major peaks in the TIC belonging to the starting materials, a third peak was observed, 4-methylpropiophenone, due to N-demethylation of the starting material, 4-methylmethcathinone (see Figure 5-6).

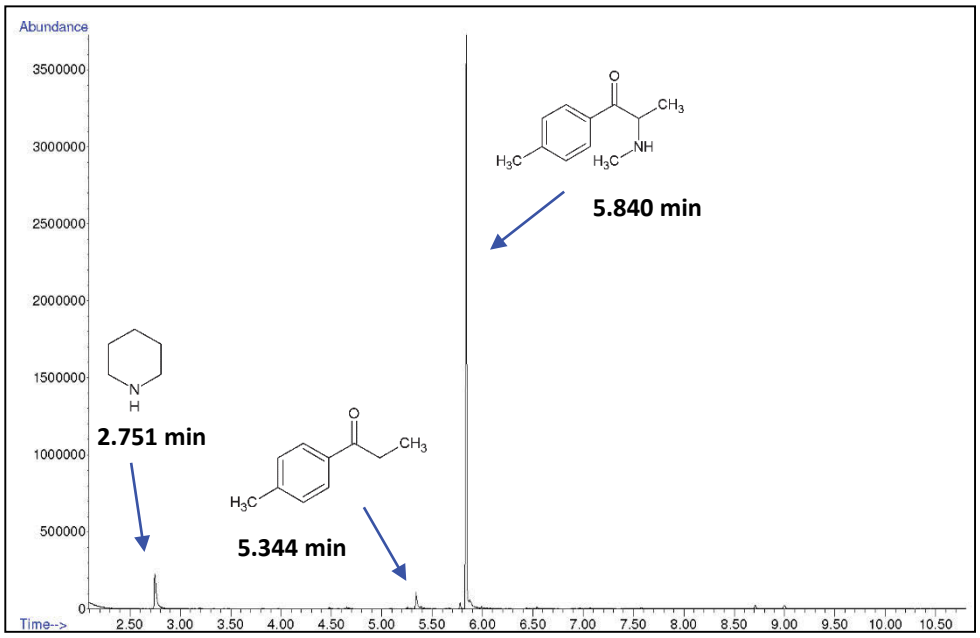

Figure 5-6. Representative TIC of enamine formation method 2 product mixture using 4-MMC as starting material.

5.3.2 Hydrazone formation

DNP method 1 and DNP method 2 failed to produce the red or orange precipitate indicative of formation of a DNP hydrazone derivative with the synthetic cathinones tested. In addition, the α-bromoketone intermediate compounds also failed to react (see Table 5-2). Increasing reaction time and reaction temperature did not change this negative result. The substituted benzaldehydes and 4-methylpropiophenone successfully reacted with the DNP reagent to produce red precipitates.

Table 5-2. Results of the hydrazone derivative preparation performed on selected cathinones and intermediates containing carbonyl functional groups

Compound tested	**Result** [a]
Blank	Yellow solution
Piperonal	Red ppt
4-methylpropiophenone	Red ppt
p-tolualdehyde	Red ppt
1-(2*H*-1,3-benzodioxol-5-yl)-2-bromopropan-1-one.	Yellow-brown solution
2-bromo-4-methylpropiophenone	Yellow solution
methylone HCl	Yellow solution
pyrovalerone HCl	Yellow solution
4-FMC HCl	Yellow solution
MDPV HCl	Yellow solution
α-PVP HCl	Yellow solution
4-MMC free base	Yellow solution
4-MMC HCl	Yellow solution

[a] ppt = precipitate

5.3.3 Semicarbazone formation

The semicarbazone reactions that were attempted in this study failed to produce any products, with GC-MS monitoring confirming no reaction was taking place.

5.3.4 Oxime formations

Oximation method 1 employing the grinding mechanism failed to react in all experiment trials with GC-MS monitoring showing the cathinone starting material remained. The successful derivatisation of 4-MMC in oximation method 2 was demonstrated through GC-MS analysis, however, a large amount of unreacted 4-MMC remained in the product mixture (see Figure 5-7). In addition, benzonitrile degradation impurity was also present.

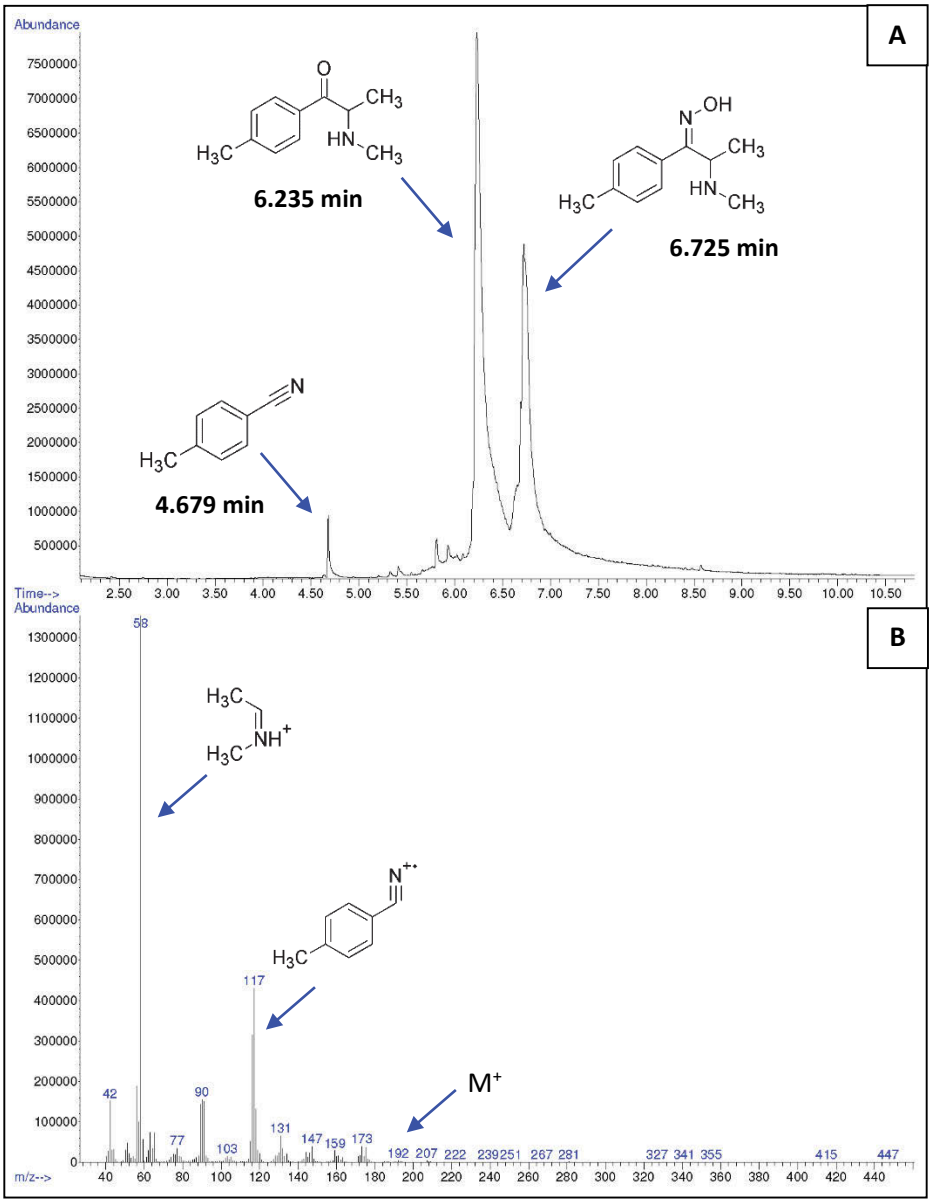

Figure 5-7. GC-MS analysis of the product of *oximation method 2* performed on 4-MMC. A) Representative TIC showing two major components are unreacted 4-MMC and the 4-MMC oxime derivative, B) Mass spectrum obtained for the peak at 6.725 min in the TIC trace

Oximation method 3 was performed on ten cathinone analogues and produced varying results mostly dependent on carbon chain length (see Table 5-3). Increasing reaction time and drug concentration increased the amount of oxime derivative that was seen in the product mixture. The UV spectra obtained for each analogue after sitting for 4 days at room temperature are provided in **Appendix B**.

Table 5-3. Results of oximation method 3 performed on 10 cathinone analogues

Carbon chain length	**Cathinone analogue**	**Oximation method 3 result**[a]
3 carbon chain	4-MMC	Large amount of oxime; 4-methylbenzonitrile also present
	4-FMC	Small amount of oxime present
	4-MEC	Small amount of oxime and 4-methylbenzonitrile present
	MCAT	Small amount of oxime present
	Methylone	Small amount of degradation to benzaldehyde
4 carbon chain	Butylone	NR
5 carbon chain	Pentylone	NR
	MDPV	NR
	α-PVP	NR

[a] NR = No Reaction

5.3.5 Reduction reactions

Initial reaction monitoring via TLC showed a new product was formed as a result of the reduction reaction.

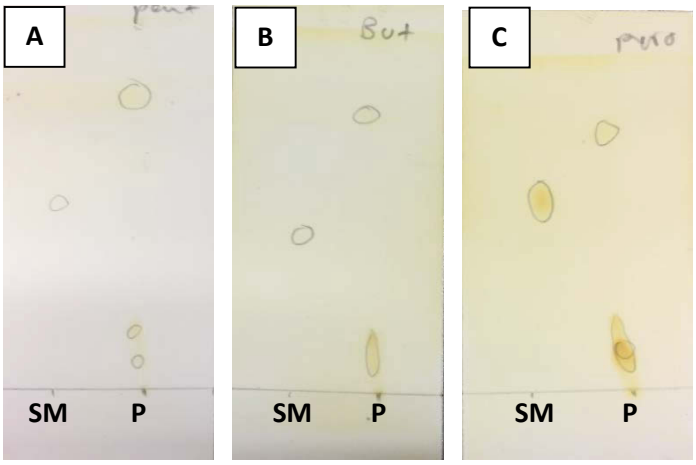

Figure 5-8. Developed and iodine stained TLC plates used in reduction reaction monitoring of A) pentylone, B) butylone, and C) pyrovalerone showing formation of new compounds

GC-MS analysis of the reduction reaction products showed new compounds were present in all analogues. Analogues containing a pyrrolidine ring and 4-methylethcathinone showed split peaks eluting in the TIC trace. The shorter chain cathinones producing short chain aminoalcohols following reduction proved difficult to detect using the same GC-MS method without derivatisation; MCAT and 4-FMC reduction products were undetectable.

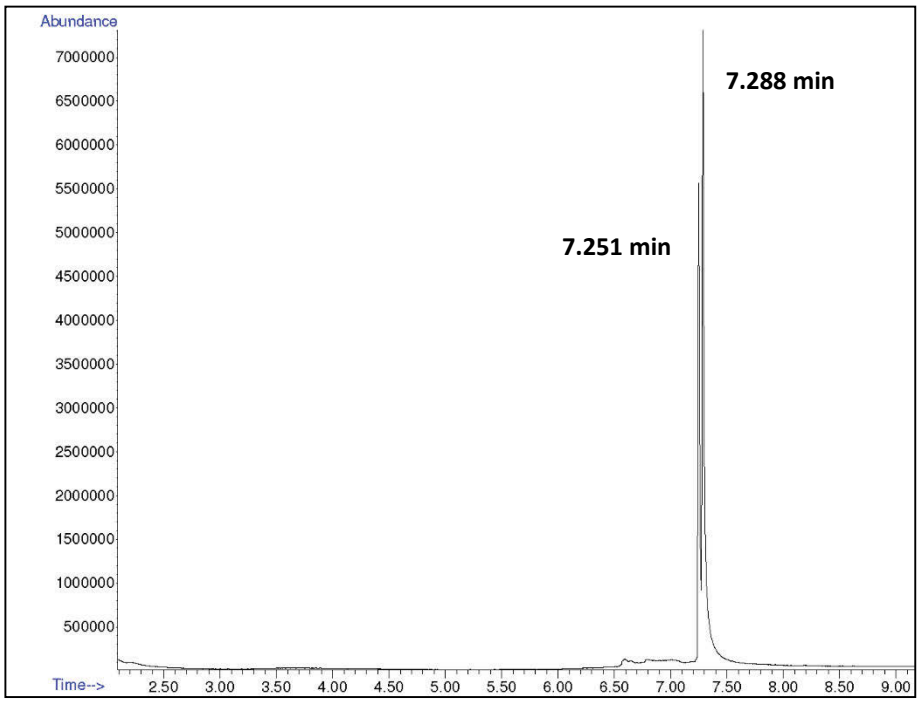

Figure 5-9.TIC trace of MDPV reduction product mixture showing the split peak observed in all pyrrolidine containing analogues

5.3.6 Antioxidant activity

The FRAP assay showed negligible absorbance with the ten cathinones in this study and appeared similar in colour to the control reagent blank, yellow. The ascorbic acid solution produced an immediate turquoise colour with 1000 ug and green-blue and lime green colours with 100 ug and 20 ug sample, respectively.

The CUPRAC assay produced positive results for all 10 cathinones, however the antioxidant capacity was much lower than the ascorbic acid reference (see Figure 5-10).

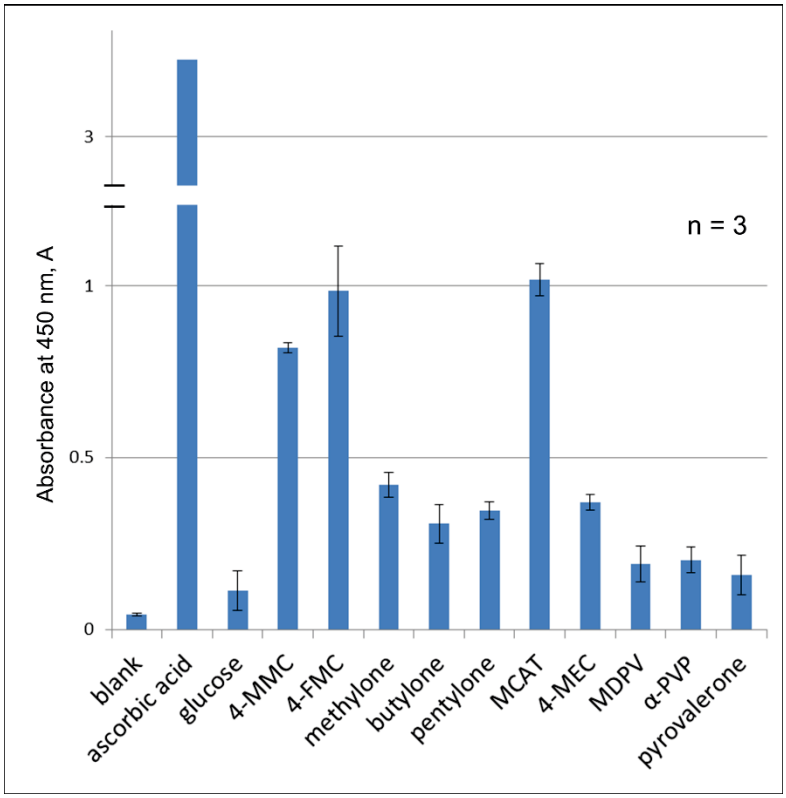

Figure 5-10. The absorbance of control blank, ascorbic acid, glucose and 10 cathinone analogues at 450 nm following the CUPRAC assay

The total antioxidant capacity measurements performed on selected cathinones showed a very small absorbance at the specified 695 nm wavelength. In comparison to the ascorbic acid reference, these absorbances were negligible, however they were still higher than the blank (see Figure 5-11). In terms of visual colour changes, the ascorbic acid solution instantly turned a turquoise-green colour, the cathinone and glucose solutions were a light yellow and the blank remained colourless.

The pyrrolidine containing analogues formed a precipitate in all experiments and were therefore not analysed by UV spectrophotometry.

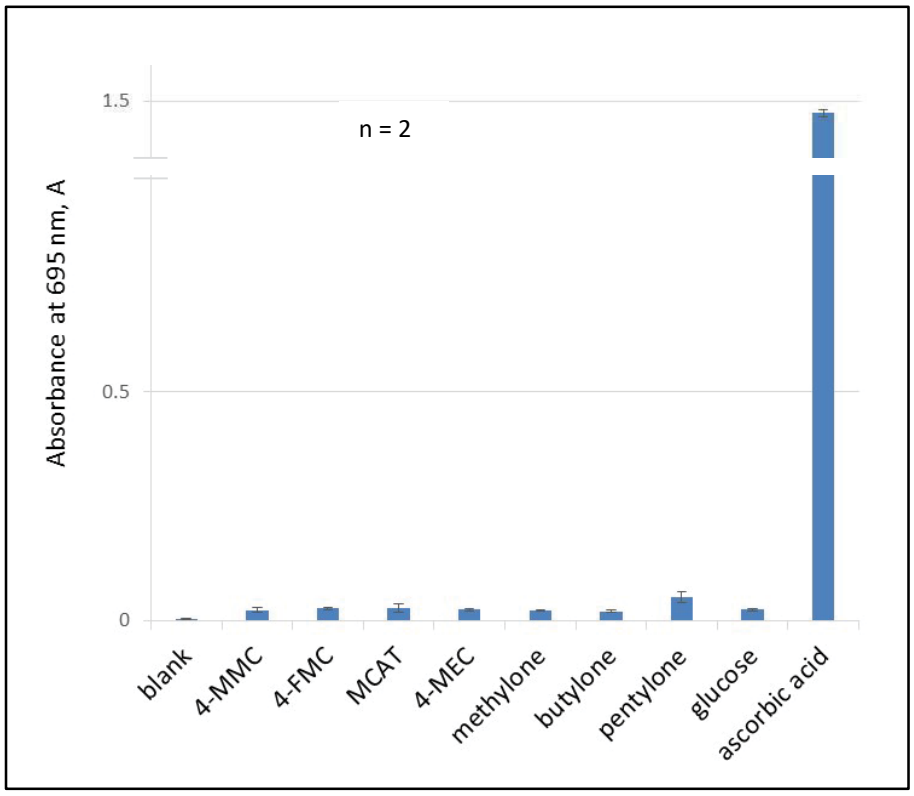

Figure 5-11. The absorbance of control blank, ascorbic acid, glucose and 7 cathinone analogues at 695 nm following a total antioxidant capacity measurement

5.3.7 Cathinone stability studies

UV calibration curves for all cathinone analogues in this study are provided in **Appendix C**. All cathinone analogues in this study predictably showed greater stability in acidic solutions when stored for any amount of time due to the stability afforded by the protonated amine salt form. In addition, solutions stored in the refrigerator showed a slowed rate of degradation compared to those at room temperature. More interestingly, the study revealed that different analogues showed significantly different stabilities in alkaline solutions at pH 10. These differences were able to be grouped based on the cathinone structure (see Table 5-4 for analogue classifications).

Table 5-4. Three cathinone analogue classifications based on substituents and structure

Group	**'Propiophenones'**	**'Methylenedioxy'**	**'Pyrrolidines'**
Structure	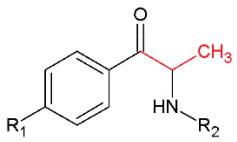	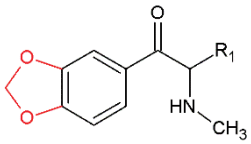	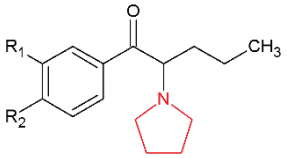
Description	Contains a 3-carbon chain without pyrrolidine ring or methylenedioxy substituent	Contains a 3,4-methylenedioxy substituted benzene ring without pyrrolidine ring	Contains a pyrrolidine ring
Cathinone analogues	• 4-MMC • 4-FMC • 4-MEC • MCAT	• methylone • butylone • pentylone	• MDPV • α-PVP • pyrovalerone

The changes in the UV spectra of the stored solutions were used as an indication of the degradation occurring to the cathinone molecule. The 'propiophenone' group of cathinones showed the most instability at pH 10 compared to the two other groups. This degradation is demonstrated by the significant decrease in absorbance at λ_{max} as well as significant changes in spectrum shape (see Figure 5-12). The two most unstable analogues in this study were 4-FMC and MCAT which showed significant change in the UV spectrum absorbance and peak shape after just one week of storage at pH 10.

Methylone also showed significant spectral changes over the 28 days in pH 10 buffer, while the three analogues of the 'pyrrolidine' group showed very little spectral changes. Figure 5-13 shows the changing spectra of methylone and pyrovalerone as examples of methylenedioxy and pyrrolidine cathinone groups.

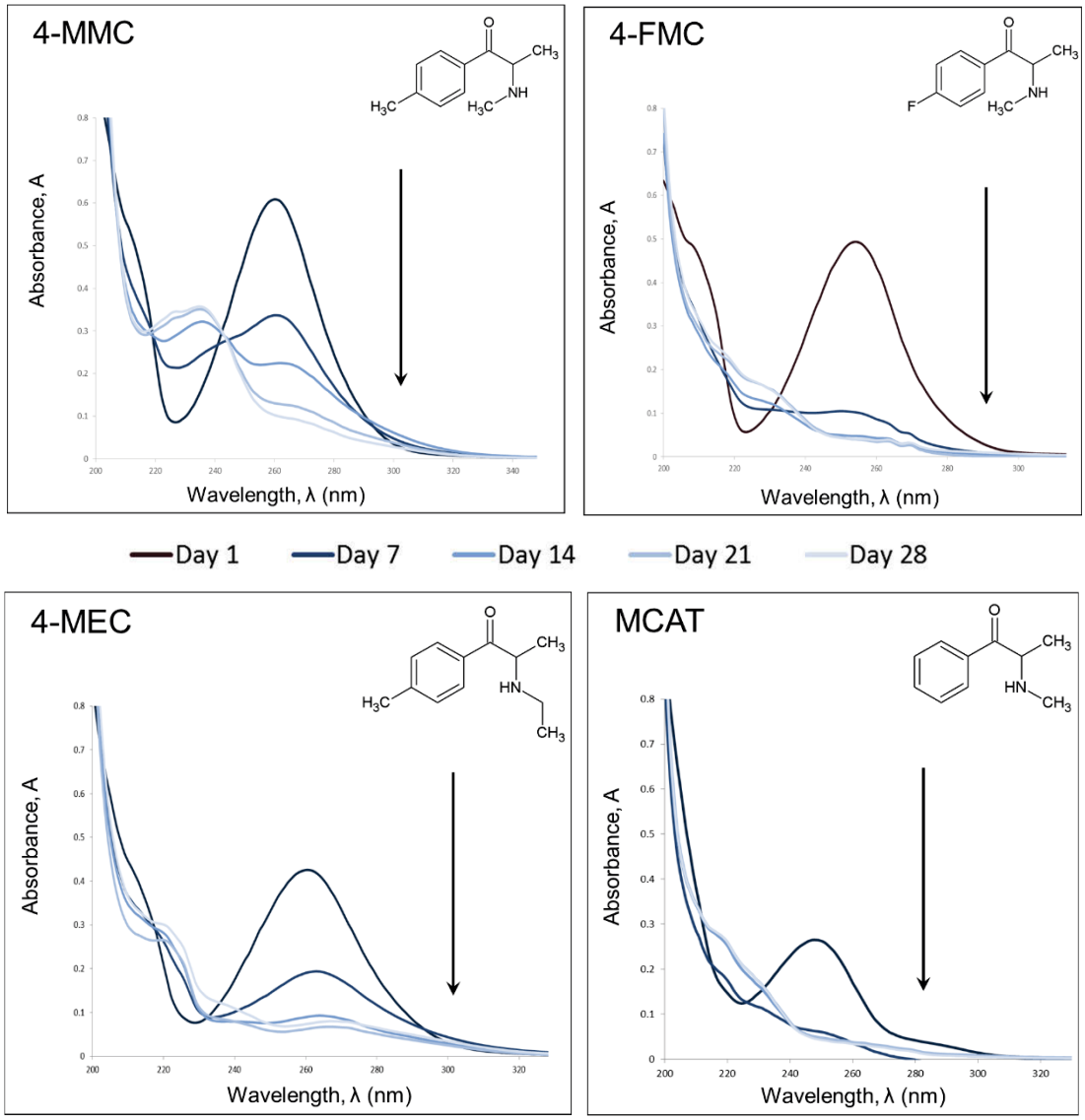

Figure 5-12. UV spectra of 'propiophenone' analogues stored in pH 10 buffer at room temperature over a one month period. 4-FMC and MCAT showed significant degradation after one week storage.

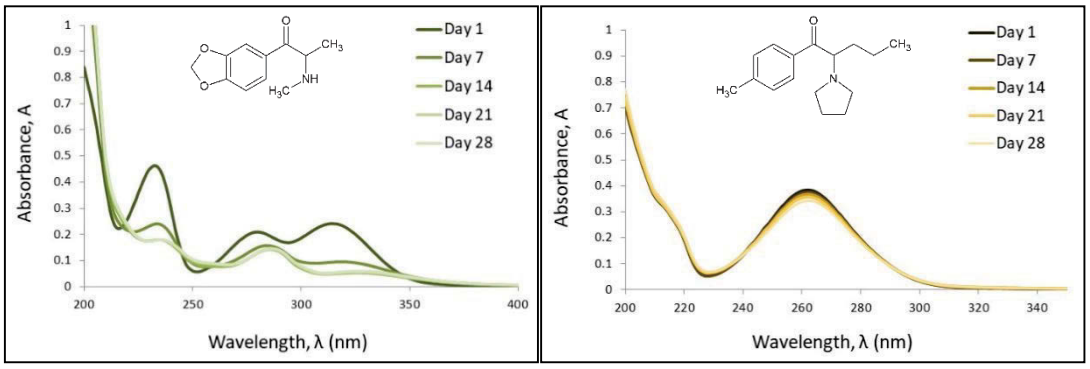

A **B**

Figure 5-13. UV spectra of A) methylone HCl and B) pyrovalerone HCl stored in pH 10 buffer at room temperature over a one month period

GC-MS analysis of the pH 10 room temperature solutions extracted into ethyl acetate was able to show the degradation of the cathinones to form respective benzaldehydes. Table 5-5 shows the extent of degradation observed using GC-MS analysis for all 10 cathinones.

Table 5-5. Results of GC-MS analysis of pH 10 cathinone solutions after 28 days storage at room temperature

Cathinone group	**Analogue**	**Extent of degradation**	**Number of degradation products**	**Impurity TIC peak area%** [a]
'Propiophenone'	MMC	Large	1	91
	MEC	Complete	1	100
	MCAT	Complete	1	100
	FMC	Complete	1	100
'Methylenedioxy'	methylone	Complete	1	100
	butylone	Small	1	17
	pentylone	Small	1	44
'Pyrrolidino'	α-PVP	Small	3	4
	pyrovalerone	Nil	3	0
	MDPV	Small	2	7

[a] Relative to the sum of cathinone and impurity TIC peak areas

Pyrovalerone was shown to be the most stable of the analogues with no impurities detectable via GC-MS analysis. Other analogues, such as 4-MEC showed complete degradation to the respective benzaldehyde (see Figure 5-14) while longer carbon chain analogues showed small amounts of degradation (see Figure 5-15).

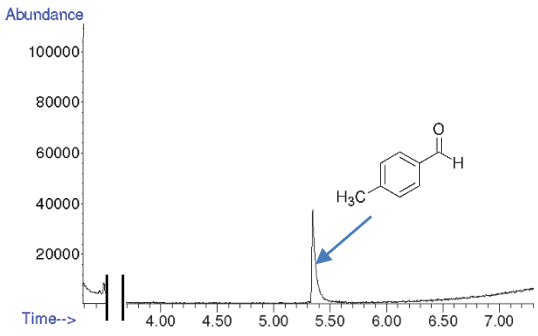

Figure 5-14. TIC of extracted sample of 4-MEC stored in pH 10 buffer after 28 days showing all 4-MEC had degraded to 4-methylbenzaldehyde

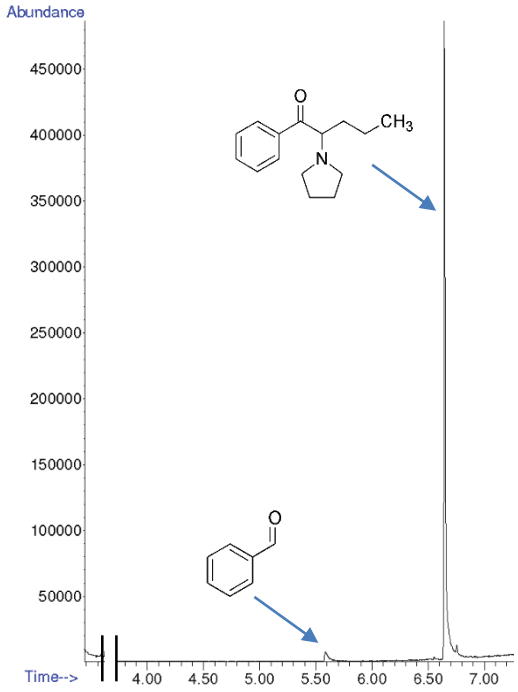

Figure 5-15. TIC of extracted sample of α-PVP stored in pH 10 buffer after 28 days showing small presence of degradation product, benzaldehyde

The stability of the cathinones in deionised water and methanol did not show signs of degradation, particularly when stored in the refrigerator. The rate of degradation of cathinones in water was increased under UV light, with α-PVP the analogue most susceptible to this degradation (see Figure 5-16).

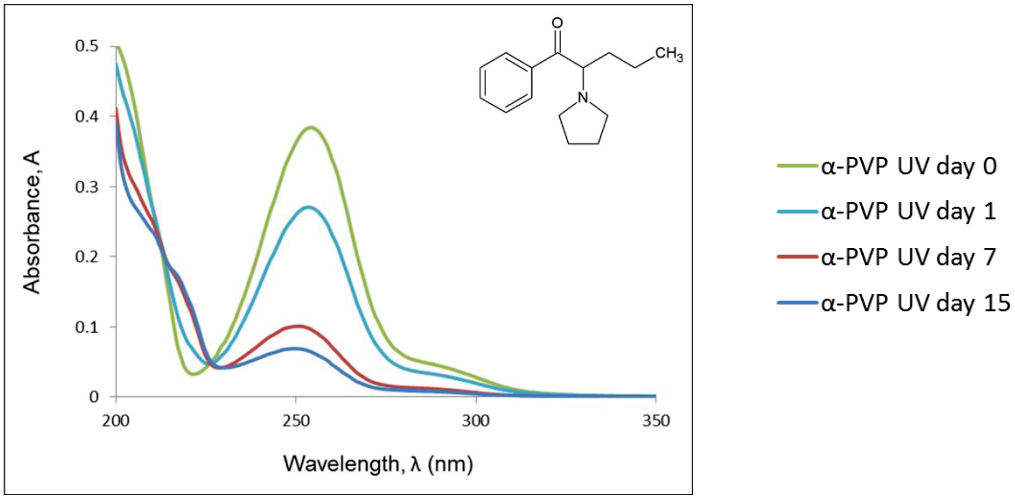

Figure 5-16. UV spectra of aqueous α-PVP HCl solution stored under UV light over a one month period

5.4 Discussion

The substituents on the carbonyl group of a synthetic cathinone molecule are electron donating and therefore reduce the electrophilicity of the carbonyl carbon (see Figure 5-17). This reduced electrophilicity explains the decreased carbonyl reactivity of the reactions performed in this chapter. In addition to the electrophilicity, steric hindrance at the carbonyl group may also prevent nucleophilic attacks in the larger cathinone compounds.

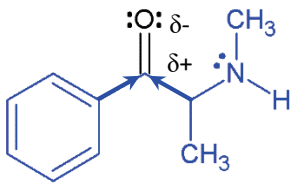

Figure 5-17. The electron donating substituents on the carbonyl group of a cathinone that effectively reduce the nucleophilicity of the C atom and reactivity of the carbonyl group

The inability to form imines, enamines and semicarbazones demonstrated the effect the nitrogen atom of the cathinone has on the electrophilicity of the carbonyl carbon. This reduced electrophilicity prevents nucleophilic attack by amines to form the respective Schiff base. Preparation of the well-known hydrazone derivatives was attempted with ketones, α-

bromoketones and α-aminoketones using cathinone analogues and intermediate reaction products to determine what effect the substituent on the alpha carbon had on the carbonyl reactivity. 2,4-Dinitrophenylhydrazine has been used in the preparation of derivatives of aldehydes and ketones for decades due to the stable, crystalline structures that result. The DNP test failed to react not only with the synthetic cathinones, but also the brominated intermediates. Analogous tests performed on the ketone intermediates showed successful conversion to the coloured derivative. The ketones are unhindered and contain alkyl group substituents so electrophilic character is retained.

Oximation reactions are one of the most published derivatisation methods for carbonyl groups in the literature and the methods vary significantly from grinding mechanisms[243, 244, 247, 248, 254] to microwave irradiation[242, 379] and refluxing in oil baths[252]. In this study, oximation methods were initially chosen based on simplicity with the final application in mind. The use of 4-MMC in trial studies was particularly helpful in determining if reaction conditions would be successful. 4-MMC is one the more reactive analogues in this study and if an oxime could not be produced, then those reaction conditions were aborted. The grinding methods attempted with 4-MMC failed to produce the relevant oximes, however, the simple method employing Amberlyst A-21 and leaving the mixtures to stand at room temperature successfully derivatised half of the 4-MMC. Amberlyst A-21 is a weakly basic anion exchange resin that acts as a catalyst in this reaction. Further oximation methods employing higher temperatures showed analogues containing a carbon chain length above three carbon atoms or containing a pyrrolidine ring failed to react. The reason for this is likely due to a combination of steric hindrance from the pyrrolidine ring and reduction of electrophilicity due to a longer carbon chain. The shorter cathinone analogues reacted incompletely to produce the oximes, with the reaction time period determining the amount of derivatisation.

The carbonyl group derivatisation methods showed limited success and additionally required long reaction time periods for partial reaction completion to take place. This is not an ideal result when looking to find reaction mechanisms that can be performed for field testing purposes.

Other reactions that may be useful in devising a field test for synthetic cathinones could potentially employ a reduction reaction, followed by a method to detect the α-aminoalcohol such as the Chen-Kao chemical colour test method for ephedrine. The reduction was successful and required a short period of heating, however, combined with the use of a harsh chemical reagent like sodium borohydride, it would not be suitable for everyday use in the field. More

importantly, the generic reactive nature of this reagent would likely also effect the optical reporters employed in any test method.

The antioxidant activity measurements were performed for the purpose of investigating the chemical behaviour of the synthetic cathinone class which would allow for further predictions in the development of a suitable detection method. The unsuccessful FRAP assay with the synthetic cathinones indicates the compounds do not easily reduce the ferric ion, however, the CUPRAC assay demonstrated the ability for cathinones to donate an electron to the cupric ion. Further, the results of the assay allow the analogues to be ordered based on this capacity to reduce cupric ions. MCAT, 4-FMC and 4-MMC displayed a significantly greater antioxidant capacity than the other analogues in this study due to their short chain length combined with secondary amine and lack of strong electron donating substituents

The stability studies performed also provided insight into the chemical behaviour of cathinone analogues stored in solutions over time. The purpose of this study was to investigate the dissolution and storage of cathinones from seized materials to determine if any chemical changes were taking place and to select appropriate collection solutions that would limit this degradation. The instability of MCAT and 4-FMC can be explained by the lack of electron donation and provided by the benzene ring and nitrogen atom substituents. The stability observed in pyrovalerone is likely due to the electron donating methyl group benzene substituent and the tertiary amine stability preventing dealkylation at the carbonyl group.

Although monitoring via UV spectrophotometry provides a quick snapshot of the level of degradation, it does not afford a great deal of information regarding what the degradation product is or percentage of degradation. In addition to monitoring with UV spectrophotometry, GC-MS analysis was performed on the room temperature pH 10 solutions after 28 days storage. This analysis confirmed the unstable nature of the propiophenone analogues by the absence of the cathinone peak in the TIC and appearance of the degraded benzaldehyde derivative.

The photodegradation of cathinones under UV light was a separate inclusion into the stability studies due to work in the proceeding chapter on Molecular Imprinted Polymers (MIPs) that requires incubation under UV light for the radical polymerisation of the polymers. These studies were able to show that the UV light exposure did increase the rate of cathinone degradation. This information may also be useful to others interested in the synthetic cathinone class of illicit drugs and their photodegradation in hair[380], or in waste water treatment plants that consist of a UV treatment phase[381]. Other factors that may influence

the rate of photodegradation that were not investigated in this study include pH of solution, choice of organic solvent and drug concentration[382].

Several cathinone stability studies have been published, however most of which focus on the stability in the biological matrices: blood[19], urine[20] and oral fluid[383]. These studies also showed that the presence of the tertiary amine pyrrolidine ring provided stability to the cathinone molecule.

5.5 Conclusion

The cathinone class of compounds possess a distinguishing feature, a benzylic carbonyl functional group that was targeted in the reactions performed in this chapter. The formation of imines (and enamines), hydrazones and semicarbazones proved unsuccessful, while oximes and reduction products were obtained. The success of these reactions provides insight into a potential mechanism for chemical binding of cathinone analogues to a receptor in an optical detection device. Ultimately this would be achieved through incorporation onto the functionalised surface of a luminescent nanoparticle or through labelling of a luminescent dye. These combinations would fulfil the receptor and reporter roles of a detection method. As demonstrated in this study, the production of the oxime derivative is highly dependent on the cathinone analogue and requires a long period of time for reaction to occur. The reduction of cathinone analogues could potentially be used in detection methods, however, the presence of reducing agents such as sodium borohydride in situ would also affect the optical reporter selected.

The stability of individual cathinone analogues differs and in the development of detection methods it is important to consider these stabilities under operating conditions, such as alkaline buffers and organic solvents. The analogues possessing the shortest three carbon chain showed the most degradation with 4-FMC and MCAT the most unstable.

5.6 References

19. Glicksberg, L. and S. Kerrigan, *Stability of Synthetic Cathinones in Blood.* J Anal Toxicol, 2017. **41**(9): p. 711-719.
20. Glicksberg, L. and S. Kerrigan, *Stability of Synthetic Cathinones in Urine.* J Anal Toxicol, 2017: p. 1-11.

22. Smolianitski, E., E. Wolf, and J. Almog, *Proactive forensic science: a novel class of cathinone precursors.* Forensic Sci Int, 2014. **242**: p. 219-227.
138. Nycz, J.E., *et al.*, *Identification and derivatization of selected cathinones by spectroscopic studies.* Forensic Science International, 2016. **266**: p. 416-426.
231. Thorat, B.R., *et al.*, *Synthesis of schiff bases of 7-methoxy-2-[4-(methylsulfanyl) phenyl]-1-benzofuran-5-carboxaldehyde and animes and hydrazide.* Heteroletters.org, 2013. **3**(4): p. 461-479.
233. Westheimer, F. and K. Taguchi, *Catalysis by molecular sieves in the preparation of ketimines and enamines.* The Journal of Organic Chemistry, 1971. **36**(11): p. 1570-1572.
236. Varma, R.S., R. Dahiya, and S. Kumar, *Clay catalyzed synthesis of imines and enamines under solvent-free conditions using microwave irradiation.* Tetrahedron Letters, 1997. **38**(12): p. 2039-2042.
239. Kadam, S.S., *et al.*, *Review article on: Chemical importance of brady's reagent.* International journal of research in pharmacy and chemistry, 2012. **2**(4): p. 1086-1092.
242. Kad, G.L., *et al.*, *Solventless preparation of oximes in the solid state and microwave irradiation.* Green Chemistry, 2001. **3**(6): p. 275-277.
243. Aakeroy, C.B., *et al.*, *A versatile and green mechanochemical route for aldehyde-oxime conversions.* Chemical Communications, 2012. **48**(92): p. 11289-11291.
244. Saikia, L., J. Baruah, and A. Thakur, *A rapid, convenient, solventless green approach for the synthesis of oximes using grindstone chemistry.* Organic and Medicinal Chemistry Letters, 2011. **1**(1): p. 12.
247. Kiasat, A.R., F. Kazemi, and K. Nourbakhsh, *A clean conversion of carbonyl compounds to oximes using silica gel supported hydroxylamine hydrochloride.* Phosphorus, Sulfur, and Silicon and the Related Elements, 2004. **179**(6): p. 1193-1196.
248. Damljanović, I., M. Vukićević, and R.D. Vukićević, *A Simple Synthesis of Oximes.* Monatshefte für Chemie / Chemical Monthly, 2006. **137**(3): p. 301-305.
250. Ballini, R., L. Barboni, and p. Filippone, *Amberlyst A-21 an Excellent Heterogenous Catalyst for the Coversion of Carbonyl Compounds to Oximes.* Chemistry Letters, 1997(5): p. 475-476.
252. Sharghi, H. and M. Hosseini, *Solvent-free and one-step Beckmann rearrangement of ketones and aldehydes by zinc oxide.* Synthesis, 2002. **8**(1057): p. 106.
254. Eshghi, H. and A. Hassankhani, *Regioselective synthesis of e-oximes catalyzed by ferric chloride under solvent-free conditions.* Organic Preparations and Procedures International, 2005. **37**(6): p. 575-579.
256. Vijayan, N., *et al.*, *Growth of semicarbazone of benzophenone single crystals.* Journal of Crystal Growth, 2002. **236**(1–3): p. 407-412.
265. Apak, R., *et al.*, *Novel Total Antioxidant Capacity Index for Dietary Polyphenols and Vitamins C and E, Using Their Cupric Ion Reducing Capability in the Presence of Neocuproine: CUPRAC Method.* Journal of Agricultural and Food Chemistry, 2004. **52**(26): p. 7970-7981.
301. Zhai, D., *et al.*, *Development of a fluorescent sensor for an illicit date rape drug - GBL.* Chemical Communications, 2013. **49**(55): p. 6170-6172.
371. Zhou, H.-P., *et al.*, *Clean and Flexible Modification Strategy for Carboxyl/Aldehyde-Functionalized Upconversion Nanoparticles and Their Optical Applications.* Advanced Functional Materials, 2009. **19**(24): p. 3892-3900.
372. Wang, W., *et al.*, *Highly selective and sensitive sensing of 2,4,6-trinitrophenol in beverages based on guanidine functionalized upconversion fluorescent nanoparticles.* Sensors and Actuators B: Chemical, 2018. **255**: p. 1422-1429.
373. Kerrigan, S., *Improved Detection of Synthetic Cathinones in Forensic Toxicology Samples: Thermal Degradation and Analytical Considerations*. 2015, US Department of Justice.

374. PM, O.B., *et al.*, *Synthesis, screening and pharmacokinetic evaluation of potential prodrugs of bupropion. Part one: in vitro development.* Pharmaceuticals (Basel), 2014. **7**(5): p. 595-620.
375. Martin, S.F. and J.C. Gilbert, *2,4-dinitrophenylhydrazine test for aldehydes and ketones*, in *Organic chemistry lab experiments: Miniscale and MIcroscale*, M. Finch, Editor. 2011, Brooks/Cole Cengage Learning: Boston, MA, USA. p. 813-814.
376. Jafri, L., *et al.*, *Microwave-assisted Synthesis and Bioevaluation of Some Semicarbazones.* Chemical Biology & Drug Design, 2012. **79**(6): p. 950-959.
377. Vijayalakshmi, M. and K. Ruckmani, *Ferric reducing anti-oxidant power assay in plant extract.* Bangladesh Journal of Pharmacology, 2016. **11**(3): p. 3.
378. Prieto, P., M. Pineda, and M. Aguilar, *Spectrophotometric Quantitation of Antioxidant Capacity through the Formation of a Phosphomolybdenum Complex: Specific Application to the Determination of Vitamin E.* Analytical Biochemistry, 1999. **269**(2): p. 337-341.
379. Elmakssoudi, A., *et al.*, *Efficient conversion of aldehydes and ketones into oximes using a nanostructured pyrophosphate catalyst in a solvent-free process.* Catalysis Communications, 2012. **29**: p. 53-57.
380. Favretto, D., *et al.*, *A study on photodegradation of methadone, EDDP, and other drugs of abuse in hair exposed to controlled UVB radiation.* Drug Test Anal, 2014. **6 Suppl 1**: p. 78-84.
381. Trawinski, J. and R. Skibinski, *Studies on photodegradation process of psychotropic drugs: a review.* Environ Sci Pollut Res Int, 2017. **24**(2): p. 1152-1199.
382. Kumar, A. and G. Pandey, *A Review on the factors affecting the photocatalytic degradation of hazardous materials* Material Science & Engineering International Journal, 2017. **1**(3): p. 1-10.
383. Miller, B., J. Kim, and M. Concheiro, *Stability of synthetic cathinones in oral fluid samples.* Forensic science international, 2017. **274**: p. 13-21.

Chapter 6: Preparation and application of Molecularly Imprinted Polymers (MIPs)

This page intentionally left blank

Chapter 6: Preparation and Application of Molecularly Imprinted Polymers (MIPs)

6.1 Introduction

The selective enrichment or capture of target molecules is a technique employed in routine laboratory sample preparation through the use of solid phase extraction (SPE) sorbents. These sorbents are made from chromatographic material that has been chemically modified with hydrophobic or hydrophilic functional groups to separate compounds of interest from impurities.

Molecularly imprinted polymers (MIPs) are selective, adsorbent materials designed to be behave as 'Artificial antibodies'. The application of these polymers is diverse and wide ranging, from selective enrichment of drug molecules in waste water through Molecularly Imprinted Solid Phase Extraction (MISPE) [384] to selective adsorption of drugs in body fluids using a purpose-built MIP stirrer bar[385]. In all applications of these materials, the imprinted polymer acts as a receptor that can recognise target molecules based on molecular structure and arrangement of particular functional groups.

In the development of a detection method for the synthetic cathinone class of new psychoactive substances, molecularly imprinted polymers were investigated for their potential use as the recognition element in a detection method.

Although the majority of work performed using MIPs has seen them used for selective extraction, enrichment and collection of target analytes, relatively few have seen the combination of an MIP receptor with an optical reporting signal. Meng *et al.* have reported successful detection of ketamine[316] and atropine[317] using molecularly imprinted photonic hydrogels (MIPHs), while more recent research has focused on the incorporation of the selective polymer to the surface of luminescent nanomaterials[386].

This chapter investigates the development of a molecularly imprinted polymer selective toward synthetic cathinones that could be utilised as the molecular recognition element in the overall development of a complete optical screening test.

6.2 Materials and methods

6.2.1 Chemicals

Methacrylic acid, ethylene glycol dimethacrylate, theophylline, vanillin and chloroform-d were obtained from Sigma Aldrich (Castle Hill, NSW, Australia). Chloroform, methanol, sodium sulphate and sodium hydroxide were obtained from Chem-Supply (Gillman, SA, Australia). Paraformaldehyde, acetonitrile and urea and were obtained from Ajax Finechem (Scoresby, VIC, Australia). Melamine and 2,2'-Azobis(2-methylpropionitrile) (AIBN) were obtained from BDH Laboratory Chemicals (Poole, England). Ephedrine hydrochloride was obtained from Aldrich Chemical Company (Castle Hill, NSW, Australia). Glacial acetic acid was obtained from Scharlau Chemicals (Sentmenat, Barcelona, Spain).

6.2.2 Reference material

Synthetic cathinone reference material, 4-methylmethcathinone (4-MMC) was obtained from syntheses described in Chapter 2.

6.2.3 Instrumentation

Sonication of solutions was achieved using Unisonics ultrasonic Cleaner (Sydney, Australia) and centrifugation was achieved using an Eppendorf centrifuge 5702 (North Ryde, NSW, Australia). Polymerisation with ultraviolet light was achieved using a purpose-built UV light box (22.5 x 21.0 x 13.3 cm) containing two 16 W fluorescent UV (365 nm) light bulbs (UTS Science Workshop).

6.2.4 Ultraviolet-visible (UV-Vis) spectroscopy analysis

Absorption spectra in the ultraviolet region were obtained in the range 200–400 nm using an Agilent Technologies Cary 60 spectrometer (Santa Clara, CA, USA). Spectra were recorded at a rate of 600 nm/min and baseline corrections were performed for all spectral measurements.

6.2.5 Gas Chromatography-Mass Spectrometry (GC-MS) analysis

Samples were injected using an Agilent 7683 series autosampler and analysis was performed using an Agilent 6890 Gas Chromatograph coupled to an Agilent 5973 Mass Spectrometer (Agilent Technologies, Santa Clara, CA, USA). The GC-MS system was equipped with an HP-5MS column with 5% Phenyl 95% dimethylpolysiloxane copolymer phase (30 m x 0.25 mm x 0.25 µm). Unless stated otherwise, injector and interface temperatures were set at 250 °C and 280 °C, respectively, and injections (1.0 µL) were made in split mode with a 25:1 split ratio. The initial oven temperature at 50 °C was held for 2 min before increasing the temperature to 290 °C at a rate of 50 °C/min and holding for a further 4 min. Helium was used as the carrier gas at a constant flow rate of 1.2 mL/min with a 2 min solvent delay. Data was collected using full scan acquisition (40-450 amu) and analysis was carried out using Agilent Enhanced ChemStation software, MSD ChemStation.

6.2.6 Nuclear Magnetic Resonance (NMR) spectroscopy study

^{1}H and ^{13}C NMR spectra were recorded with an Agilent NMR spectrometer (Santa Clara, CA, USA) operating at 500 MHz and 125 MHz, respectively, using standard pulse sequences. The spectra were recorded at 298 K, and chemical shifts (δ) were reported as parts per million (ppm) with respect to the internal standard tetramethylsilane (TMS, 0.00 ppm) or solvent residual signals ($CDCl_3$, 7.26/77.16 ppm ($^{1}H/^{13}C$)).

6.2.7 Preparation of Molecularly Imprinted Polymers (MIPs)

6.2.7.1 *Preliminary preparation: Literature methods*

A number of methods described in the literature for the preparation of molecularly imprinted polymers were replicated to verify their selective adsorption of nominated molecules and thus provide a starting point for the development of selective polymers for synthetic cathinones.

The general method of preparation of the imprinted polymers is described here, with specific details provided in Table 6-1 below. In a small conical vial was dissolved the template molecule, methacrylic acid (MAA) and ethylene glycol dimethacrylate (EGDMA) in the selected porogen. The vials were covered with Parafilm® M Film and the solutions pre-polymerised. To

the vial was added 2,2'-Azobis(2-methylpropionitrile) (AIBN), and the solution was sonicated (10 min), degassed with nitrogen (10 min) and dropped onto PMMA slides. The slides were placed on ice under UV light for 2 h to polymerise. Non-imprinted polymers were prepared alongside without the inclusion of the template molecule.

Table 6-1. Experiment parameters for methods adapted from the literature

Experiment No.	**1-1**	**1-2**	**1-3**
Template molecule	Vanillin (2 mmol)	Ephedrine HCl (1.5 mmol)	Theophylline (2.5 mmol)
Ratio of MAA : EGDMA	MAA (8 mmol): EGMDA (2.4 mmol)	MAA (47 mmol): EGDMA (11 mmol)	MAA (59 mmol): EGDMA (11 mmol)
Porogen	Methanol (15 mL)	Dichloromethane (2 mL)	Dichloromethane (2 mL)
Pre-polymerisation method	Fridge at 8 °C 16 h	Room temperature 48 h	Room temperature 24 h
AIBN	0.020 g	0.010 g	0.010 g
Reference	Peng *et al.*[387]	Hu *et al.*[388]	Hu *et al.*[388]

6.2.7.2 *Preliminary preparation: bulk monolith polymer*

The pre-polymerisation mixtures prepared in section 6.2.7.1 were transferred into Pasteur pipettes that were sealed at the tip using a Bunsen burner. The open end of the pipette was plugged with cotton wool and the tubes were carefully heated in a water bath at 80 °C until the polymer set. Once polymerised, the glass pipettes were carefully broken open to collect the hardened polymer. The polymer was then ground using a mortar and pestle, sieved (106 μm) and washed with methanol (200 mL) using a sintered glass crucible (Grade 4). The polymers were dried overnight in an oven set at 110 °C. Adsorption testing was performed by adding template solution (7 mL, 0.05 mM) to the polymer (80 mg) in a falcon tube. The tubes were roller mixed for 12 h, centrifuged for 10 min at 4400 rpm and the supernatant directly analysed by UV-Vis spectroscopy.

6.2.7.3 *Preliminary preparation: Ephedrine trials*

To a glass scintillation vial was added, MAA (0.3444 g, 4.0 mmol) and ephedrine (0.5 mmol) (free base extracted from ephedrine HCl) in chloroform (2 mL). The vial was then sealed and roller mixed for 5 h before adding EGDMA (3.172 g, 16 mmol) and sonicating the mixture for 10 min. AIBN (0.057 g, 0.35 mmol) was added to the vial and the solution purged with nitrogen for 10 min. The vial was sealed again and polymerised on ice in the UV light box for 24 h. The mixtures were then heated at 40 °C for 24 h before drying in an oven at 110 °C for 1 h and grinding the particles in a mortar and pestle. The polymer particles were then dry sieved (106 µm) and filtered (16-40 µm) before being washed using a Soxhlet extractor for 24 h using methanol: acetic acid (9:1) solution with UV monitoring of the eluate. The resulting polymers (pol-3) were dried in the oven at 50 °C for 5 h before collection. The preparation was repeated without the addition of ephedrine (non-imprinted polymer).

The polymers were then subjected to binding studies using aqueous solutions of ephedrine HCl according to the conditions listed in Table 6-2 below. Following incubation periods in falcon tubes, the solutions were centrifuged for 20 min (4400 rpm) and the supernatant removed and filtered into a quartz cuvette for UV-Vis analysis.

Table 6-2. Binding studies performed on the ephedrine imprinted (and non-imprinted) polymer (pol-3)

Experiment No.	**Mass of polymer (mg)**	**Volume of ephedrine solution (mL)**	**Ephedrine concentration (mM)**	**Length of time roller mixed (h)**
3-1	40	5	1	18
3-2	40	10	0.5 (basic buffer)	0.5, 1, 2, 3
3-3	40	10	1, 0.5, 0.1, 0.05, 0.01	0.2
3-4	10, 20, 40, 80	10	0.1	0.2

6.2.8 Cathinone imprinted polymers

To a test tube was added 4-MMC (0.0214 g, 0.1 mmol), chloroform (7.5 mL) and NaOH solution (0.5 mL, 5 M). After thoroughly shaking the contents of the tube, the chloroform layer was removed and added to a glass scintillation vial. To this vial was added MAA (34 µL, 0.4 mmol), followed by EGDMA (396 µL, 2 mmol). The scintillation vials were sealed with a septum and placed in an ice bath for 30 min. AIBN (100 mg) was then added to the vial before degassing with nitrogen and placing in water bath at 60 °C for 20 h. Following this the vials were placed in the oven at 70 °C to dry overnight. Polymers were ground with a mortar and pestle, sieved (106 m) and Soxhlet extracted with methanol: acetic acid (9: 1) overnight. The polymers were washed with methanol (100 mL) and left to air dry.

The non-imprinted MIP and imprinted MIP (0.15 g) were packed into empty makeshift SPE cartridges (cotton-plugged syringes) and attached to the SPE vacuum manifold system. The 'cartridges' were conditioned with methanol (1 mL), water (1 mL), and phosphate buffer solution (1 mL) before loading with a sample solution of 4-MMC (1 mL, 200 mg/mL). The cartridges were washed with buffer solution (1 mL) and air dried before eluting with methanol (1.5 mL). The eluents from the non-imprinted and imprinted cartridge were analysed by GC-MS.

6.2.8.1 *Optimisation of cathinone imprinted polymers*

The general method of preparation of the imprinted polymers is described here, with specific details provided in Table 6-3 below. In a glass scintillation vial the free base template molecule was dissolved in the porogen before adding methacrylic acid (MAA) and allowing the solutions to pre-polymerise. Following this, ethylene glycol dimethacrylate (EGDMA) was added, the sample sonicated (10 min), purged with nitrogen (10 min) and the AIBN initiator was added. The solutions were polymerised, ground, sieved, filtered and washed with methanol: acetic acid (9:1) solution. Non-imprinted polymers were prepared alongside without the inclusion of the template molecule.

Binding studies were performed on successfully prepared polymers.

Table 6-3. Cathinone imprinted polymer preparation conditions

Polymer code	4-MMC moles	Ratio (T:M:XL)	porogen	Pre-polymerisation	polymerisation	AIBN
1A	0.030	1:2:20	$CHCl_3$ (7 mL)	Roller mixer 1h	55 °C oven 16 h (lid off)	20 mg
1B	0.105	1:2:20	$CHCl_3$ (7 mL)	Roller mixer 1h	55 °C oven 16 h	20 mg
1C	0.105	1:2:20	$CHCl_3$ (7 mL)	Roller mixer 1h	55 °C oven 16 h	60 mg
1D	0.105	1:2:20	$CHCl_3$ (7 mL)	Fridge at 14 °C 20 h	55 °C oven 16 h	60 mg
1E	0.105	1:2:20	$CHCl_3$ (7 mL)	Roller mixer 1h	UV light 30 h	60 mg
1F	0.105	1:2:20	$CHCl_3$ (7 mL)	Roller mixer 1h	60 °C oil bath 24 h	60 mg
1G	0.105	1:2:20	$CHCl_3$ (15 mL)	Roller mixer 1h	60 °C oil bath 24 h	60 mg
1H	0.105	1:2:20	DCM (7 mL)	Roller mixer 1h	UV light 48 h	60 mg
1I	0.105	1:2:20	ACN: MeOH (10 mL)	Roller mixer 1h	UV light 48 h	60 mg
2F	0.105	1:4:20	$CHCl_3$ (7 mL)	Roller mixer 1h	60 °C oil bath 24 h	60 mg
2D	0.105	1:2:20	$CHCl_3$ (7 mL)	Fridge at 14 °C 72 h	55 °C oven 16 h	60 mg

6.2.9 Melamine-Urea-Formaldehyde (MUF) resins

6.2.9.1 *Preparation MUF resins*

The method described in Guo *et al.*[389] was modified for application in this study. To a beaker was added melamine (6.3 g, 50 mmol), urea (6.8 g, 110 mmol) and formaldehyde (12.9 g, 430 mmol) and the contents stirred on a hotplate set to 45 °C for 1 h before increasing the temperature to 85 °C for 2 h. A second portion of urea (2.3 g, 38 mmol) was added and the reaction stirred for a further 30 min before cooling to 45 °C and adding methanol (10 mL). After 1 h, the mixture was cooled to room temperature. The mixture was divided into two ceramic mortars and 4-MMC HCl solution (2 mL, 10 mg/mL) was added to one of the mortars. Hydrochloric acid (1 mL, 6 M) was added to both mortars with stirring and the resins incubated at 60 °C for 36 h. The resins were ground using a mortar and pestle and sieved (106 μm) and washed in a Soxhlet apparatus with water, methanol and acetone, sequentially, for 15 h periods per solvent. The Soxhlet washings were analysed by UV-Vis to confirm the elution of 4-MMC template molecule.

6.2.9.2 *MUF adsorption testing: static binding*

The non-imprinted MUF and imprinted MUF resins (0.15 g) was placed into 15 mL falcon tubes, followed by addition of 4-MMC HCl solution (2 mL, 200 mg/mL). Tubes were sonicated for 10 min, left to stand for 2 h and centrifuged for 4.5 min at 2000 rpm. An aliquot (0.5 mL) of the supernatant was removed from each tube and added to NaOH solution (250 μL, 5 M) before extracting with dichloromethane (3 x 5 mL). The organic fractions were combined and evaporated under a stream of nitrogen. The residues were reconstituted in methanol (1.5 mL) and filtered into GC vials for direct GC-MS analysis.

6.2.9.3 *MUF adsorption testing: dynamic binding*

The non-imprinted MUF and imprinted MUF resins (0.15 g) were packed into empty makeshift SPE cartridges (cotton-plugged syringes) and attached to the SPE vacuum manifold system. The ‘cartridges’ were conditioned with methanol (1 mL), water (1 mL), and phosphate buffer solution (1 mL) before loading with a sample solution of 4-MMC (1 mL, 200 mg/mL). The cartridges were washed with buffer solution (1 mL) and air dried before eluting with methanol

(1.5 mL). The eluents from the non-imprinted and imprinted cartridge were analysed by UV spectrophotometry.

6.2.10 Molecular interaction studies

6.2.10.1 *Monomer selection*

To a vial containing 4-MMC HCl (0.0038 g, 0.018 mmol) was added distilled water (0.5 mL) and NaOH solution (5 µL, 5 M). The 4-MMC free base was extracted with deuterated chloroform (1 mL) and the extract analysed by ^{1}H and ^{13}C NMR experiments. Following this, the contents of the NMR tube were emptied into a scintillation vial and an aliquot of methacrylic acid (MAA) was added (1.53 µL, 0.018 mmol). The solution was mixed and transferred back into the NMR tube for re-analysis by NMR. The addition of MAA (1.53 µL, 0.018 mmol) followed by NMR analysis and was repeated a total of 10 times as outlined in Table 6-4.

Table 6-4. Solution preparation for NMR interaction study of 4-MMC with monomer, MAA

Ratio of 4-MMC : MAA	**4-MMC**	**MAA**
1:0	0.018 mmol	0.00 µL
1:1	0.018 mmol	1.53 µL
1:2	0.018 mmol	3.06 µL
1:3	0.018 mmol	4.59 µL
1:4	0.018 mmol	6.12 µL
1:6	0.018 mmol	9.18 µL
1:8	0.018 mmol	12.24 µL
1:10	0.018 mmol	15.30 µL
1:12	0.018 mmol	18.36 µL
1:14	0.018 mmol	21.42 µL
1:16	0.018 mmol	24.48 µL

6.2.10.2 *Cross-linker selection*

To a vial containing 4-MMC HCl (0.0032 g, 0.015 mmol) was added distilled water (0.5 mL) and NaOH solution (5 µL, 5 M). The 4-MMC free base was extracted with deuterated chloroform (1 mL) and the extract analysed by ^{1}H and ^{13}C NMR experiments. Following this, the contents of the NMR tube were emptied into a scintillation vial and an aliquot of ethylene glycol dimethacrylate (EGDMA) was added (2.83 µL, 0.015 mmol). The solution was mixed and transferred back into the NMR tube for re-analysis by NMR. The addition of EGDMA (2.83 µL, 0.015 mmol) followed by NMR analysis and was repeated a total of 7 times as outlined in Table 6-5.

Table 6-5. Solution preparation for NMR interaction study of 4-MMC with cross-linker, EGDMA

Ratio of 4-MMC : EGDMA	**4-MMC**	**EGDMA**
1:0	0.015 mmol	0.00 µL
1:1	0.015 mmol	2.83 µL
1:2	0.015 mmol	5.66 µL
1:4	0.015 mmol	11.32 µL
1:8	0.015 mmol	22.64 µL
1:10	0.015 mmol	28.30 µL
1:20	0.015 mmol	56.60 µL

6.3 Results and discussion

6.3.1 Preparation of MIPs

6.3.1.1 *Preliminary preparation: Literature methods*

The methods taken from the literature proved very difficult to replicate even when employing the same template molecule. Experiment 1-1 failed to polymerise and experiment 1-3 had

difficulty getting the template molecule to dissolve. Experiment 1-2 was able to polymerise on the PMMA slides only if very small amounts were used. These methods were taken from published articles on the preparation of molecularly imprinted photonic hydrogels (MIPH). Following these results it was decided to investigate the imprinted polymers themselves with greater scrutiny before preparing complete MIPHs.

6.3.1.2 *Preliminary preparation: bulk monolith polymer*

The thermal polymerisation method was successful in producing hardened bulk polymer monoliths (see Figure 6-1) compared to the UV polymerisation. This is likely due to the smaller diameter of the Pasteur pipette vessel and therefore greater surface area, as well as a smaller amount of solution mixture. Adsorption testing of experiment 1-1 showed differences between the non-imprinted and imprinted polymer adsorption (see Figure 6-2). These differences indicated successful adsorption of the vanillin molecule by the imprinted polymer and not the non-imprinted polymer. The ephedrine and theophylline imprinted polymers did not show any selective adsorption. Further research into MIP preparation by a number of other research groups showed the large majority of bulk monolith preparation methods used a relatively high molar ratio amount of cross-linker compared to the monomer and target analyte. Further preparation methods took this into consideration. It was also noted that the polymers from each study physically appeared significantly different.

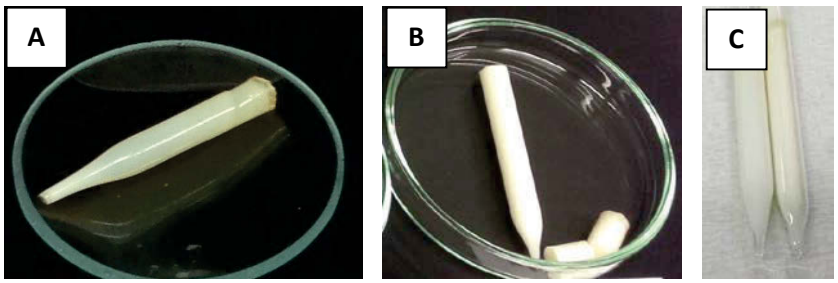

Figure 6-1. Bulk monolith polymers prepared from pre-polymerisation solutions of A) Experiment 1-1 (non-imprinted), B) Experiment 1-3 (imprinted), and C) Experiment 1-3 (imprinted and non-imprinted still in glass pipette)

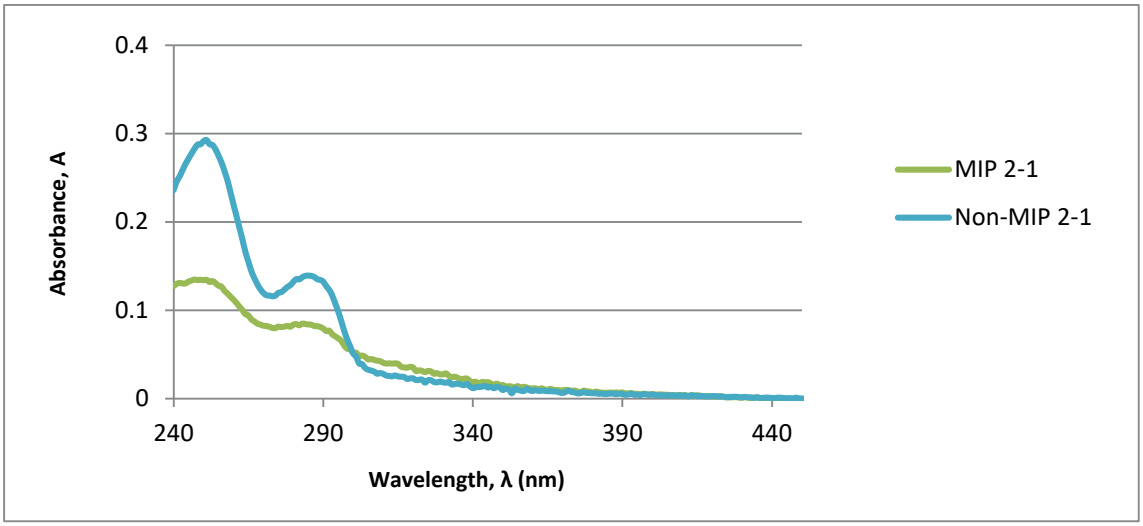

Figure 6-2.UV-Vis spectra of resulting binding solutions after incubation of polymer 1-1 (80 mg) and vanillin solution (0.05 mM) for 12 h.

6.3.1.3 *Preliminary preparation: ephedrine trials*

The initial UV polymerisation failed to completely polymerise the mixture after 24 h, and so the vial was heated to encourage thermal polymerisation instead. Figure 6-3 shows the appearance of the opaque polymers following polymerisation. UV analysis of the Soxhlet eluate showed a clear presence of ephedrine HCl in the imprinted polymer washings. This demonstrated that ephedrine was successfully being removed from inside the polymer. Continual analysis of the eluate by UV-Vis provides an easy means of determining if the Soxhlet extraction can be stopped due to no more template elution.

Figure 6-3. The polymerised solutions of ephedrine imprinted (left) and non-imprinted (right) polymers (pol-3)

The binding studies performed on the ephedrine imprinted polymer showed selective adsorption of ephedrine may be occurring to some extent, however, the non-imprinted polymer was also capturing ephedrine molecules to a lesser extent (Experiment 3-1). Improvements to this method would need to see a reduction in non-selective binding. Experiment 3-2 showed that the adsorption of ephedrine to the imprinted polymer increased with a longer incubation period. In this study, all non-MIP solutions showed higher UV absorbance than the respective MIP solution.

The ephedrine binding solution concentration study (Experiment 3-3) showed that the greatest difference between non-imprinted polymer and imprinted polymer adsorption occurred at 0.1 mM (see Figure 6-4). This appears as though it could be an outlier in this study, however, the same results were seen with repeated testing. This could be the result of a binding equilibrium occurring. The amount of polymer used in binding study (Experiment 3-4) was also shown to have an effect on adsorption, as predicted. The greater the amount of polymer used, the more non-selective binding occurs.

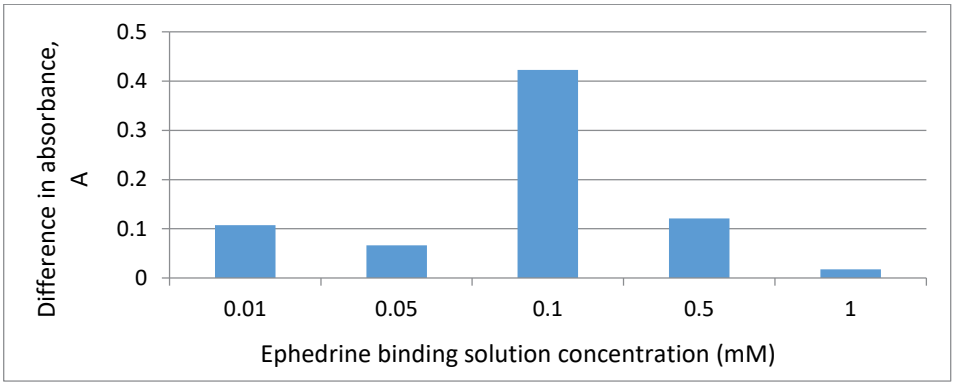

Figure 6-4. Difference in absorbance of ephedrine at 207 nm between non-imprinted polymer binding solutions and imprinted polymer binding solutions at different concentrations after 12 min

The studies performed using ephedrine as a template were particularly useful in this research as it provided insight into what parameters need optimising and what difficulties will be encountered. The preparation of MIPs requires around 100 mg for just one type of polymer preparation. For this reason, it was ideal to save precious cathinone compound until knowledge of MIP preparation was gained.

6.3.2 Cathinone imprinted polymers

The preparation of cathinone imprinted polymers produced a rubbery polymer that was dried in the oven to produce a smaller, shrunken, hard polymer. The analysis of the polymers was performed in a slightly different way to previous times and involved the use of a makeshift SPE cartridge packed with the imprinted polymer. The results of the GC-MS analysis of methanolic elution solvents showed there was a small difference in adsorption (see Figure 6-5) between the imprinted and non-imprinted polymer with every analysis performed.

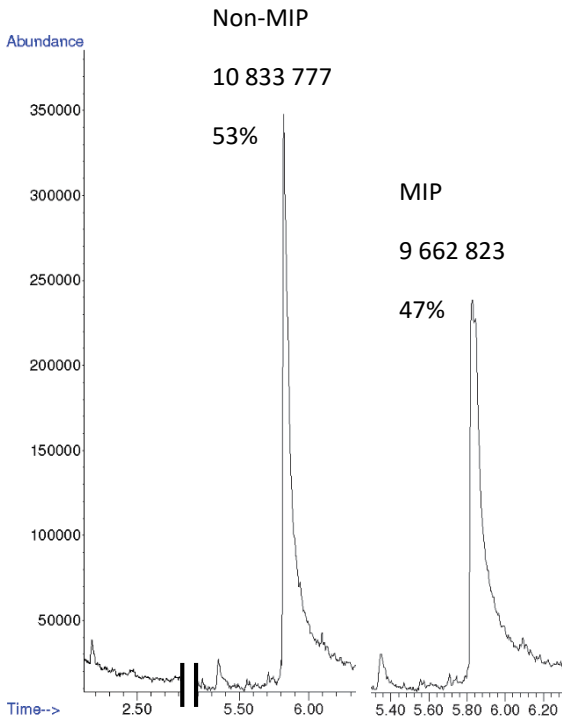

Figure 6-5. TIC from the analysis of methanol elution solvent of makeshift SPE tube from 4-MMC loading solution. Non-imprinted and imprinted polymers were examined.

It is important to note here that despite the small differences between the non-imprinted polymer and the imprinted polymer in adsorption experiments, the polymers may still be able to be used for detection based on this difference.

The large number of experiments performed to determine optimal parameters with cathinone MIP preparation produced a range of interesting results. Polymer 1A failed to polymerise at all, likely due to the reaction being open to the atmosphere which allows oxygen to enter reaction and prevent polymerisation. Following this result, the remaining polymers were polymerised in sealed vessels. The remaining polymers produced hard brittle and shrivelled solid fragments

that were ground with a mortar and pestle. The imprinted polymer was often obvious at this point as it had a slight yellow colouration.

Binding studies were performed extensively on these prepared polymers employing different incubation time periods, polymer masses and also analyte solutions in order to test for selectivity toward a particular molecule.

The results showed all the polymers prepared, except one, failed to produce repeated selective adsorption of the template molecule, 4-MMC. The polymer 1D showed good selective adsorption when compared to the non-imprinted polymer, but also when exposed to an aqueous solution of ephedrine HCl in which the non-MIP and MIP binding solutions had similar absorbances in the UV spectrum.

These results are considered very preliminary and were used as an investigation into this method of molecular recognition that has received a lot of attention recently. A considerable amount of laborious optimisation work is necessary to prepare the desired polymers.

6.3.3 MUF resins

The MUF mixtures were a thick, sticky, transparent gel prior to heating, and solidified to a solid, white resin after heating (see Figure 6-6). The solid resins formed in the oven reduced in mass following Soxhlet extraction to afford an imprinted MUF and non-imprinted MUF resin

Figure 6-6. Preparation of MUF resins for selective adsorption: A) MUF gel mixture prior to incubation, B) imprinted and non-imprinted MUF resins after incubation, C) grinding MUF resins in mortar and pestle

UV-Vis analysis was able to confirm that 4-MMC was eluted during the Soxhlet extraction of the imprinted polymer until no more analyte remained in the resin.

GC-MS analysis of the supernatant following static binding was unable to detect the presence of any 4-MMC in either the imprinted or non-imprinted solutions. This could indicate a number of problems: 1) MUF resins did not capture any 4-MMC during the binding period (selectively or non-selectively), 2) the static method of binding the template 4-MMC molecule was not adequate, or 3) errors in the extraction, reconstitution and analysis of the supernatant.

Dynamic binding of the 4-MMC template to the MUF resin showed some success in selective adsorption of 4-MMC by the imprinted MUF resin only. The UV spectrum of the MMC HCl loading solution eluent showed there was greater adsorption of 4-MMC by the imprinted resin. The decreased concentration of 4-MMC after passing though the imprinted resin cartridge was demonstrated by the lower absorbance in the UV spectrum by the non-imprinted resin (see Figure 6-7). The final methanol eluate showed negligible differences in the UV spectra of the non-imprinted and imprinted MUF resins. This could be due to the 4-MMC molecules remaining bound to the resin despite the methanol wash.

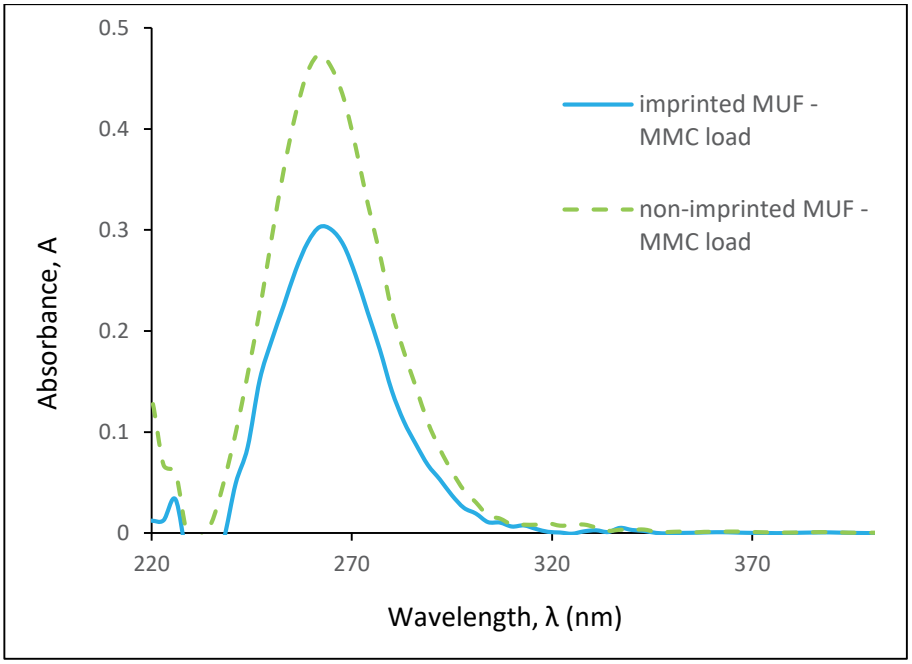

Figure 6-7. UV spectrum of 4-MMC loading solution eluate after passing through a cartridge containing imprinted and non-imprinted MUF resins. The imprinted resin adsorbs more 4-MMC molecules, and decreases the 4-MMC concentration

The MUF resins were not investigated any further and focus was put into just one type of molecular recognition polymer.

6.3.4 Molecular interaction studies

Molecular interaction studies are typically performed using expensive molecular modelling software. In this work, NMR titration was performed as an alternative to computer-aided molecular modelling. The results of which were able to indicate the optimal molar ratios of monomer and cross-linker to use in the preparation of polymers. Increasing the amount of MAA relative to the concentration of template molecule, 4-MMC resulted in a chemical shift of the carbonyl group carbon, and to a lesser extent, the N-methyl carbon (see Figure 6-8). This chemical shift indicates that the MAA is effectively interacting with the template molecule. This interaction is necessary and is what is used to determine the selectivity of the cavities that are created. However, too much interaction can make the removal of the template molecule during washing steps difficult. A greater degree of selectivity would potentially be observed if the template molecule was able to interact with the monomer in more than one location.

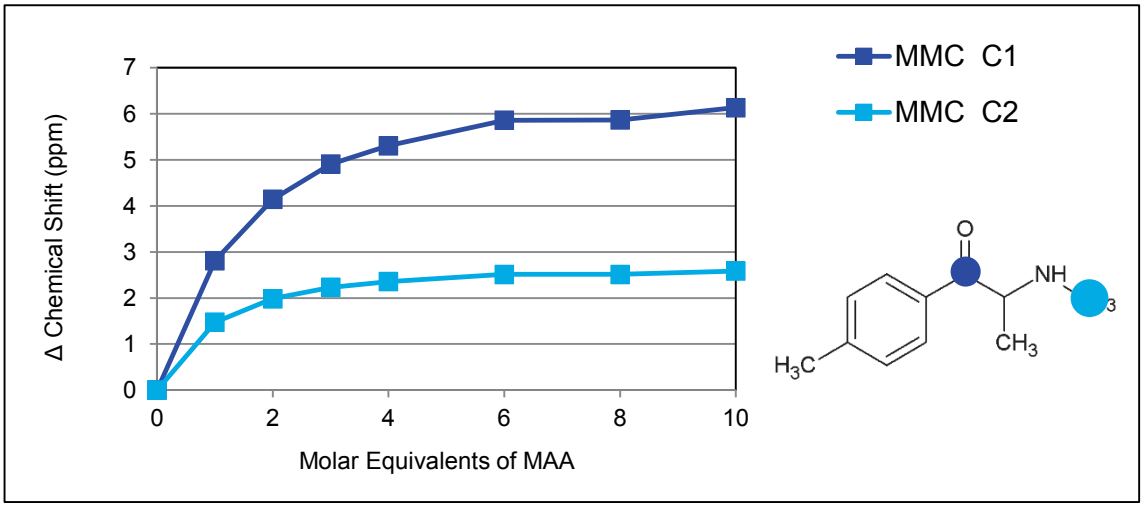

Figure 6-8. NMR titration plot showing the change in chemical shift values of two key carbon signals as a function of molar equivalents of MAA added

The analogous study performed using the cross-linker, EGDMA showed that very little binding is occurring with the template molecule (see Figure 6-9). This is an ideal situation as the cross-linker is responsible for creating the polymer structure around the cavities and should not be involved in interacting with the template. These unwanted interactions would lead to non-selective binding.

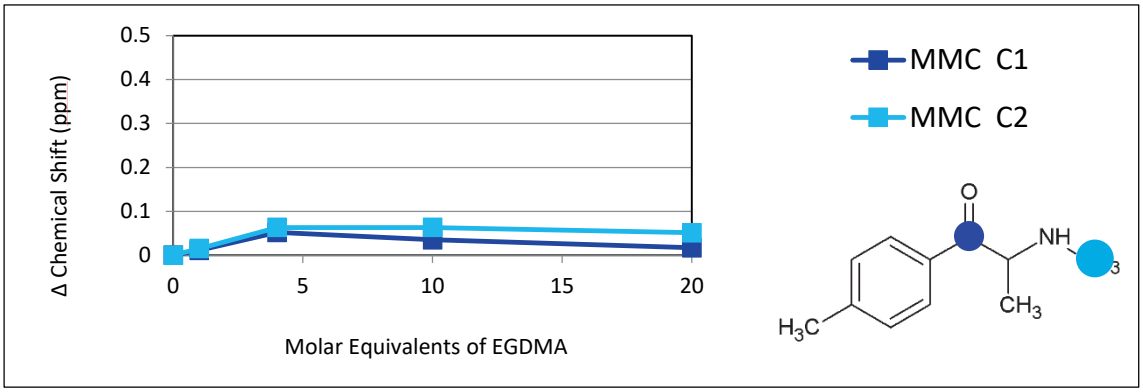

Figure 6-9. NMR titration plot showing the change in chemical shift values of two key carbon signals as a function of molar equivalents of EGDMA are added

6.4 Conclusion

The preparation of molecularly imprinted polymers is a tedious and cumbersome task, especially when using the bulk monolith preparation method. In addition, the large number of variable parameters that must be considered in order to optimise the polymers results in a lengthy process to determine suitable conditions.

In this research, the polymer preparation was optimised to allow the synthetic cathinone to selectively adsorb to the imprinted polymer in a series of testing methods employed. This adsorption was measured as the difference between the imprinted and non-imprinted polymer binding solutions.

Molecularly imprinted polymers have gained popularity as selective enrichment materials typically used for in the extraction of analytes from dilute samples. Although this study employed bulk polymers in methods similar to solid phase extraction, the end-purpose of the pre-polymerisation mixture was intended to coat a potential optical reporter such as a photonic hydrogel or luminescent nanoparticle. Future work in this area would look further into the optimisation of the pre-polymer mixture employed as the receptor in an optical detection device.

6.5 References

316. Meng, L., *et al.*, *Fast screening of ketamine in biological samples based on molecularly imprinted photonic hydrogels.* Analytica chimica acta, 2013. **771**: p. 86-94.
317. Meng, L., *et al.*, *Molecularly imprinted photonic hydrogels for fast screening of atropine in biological samples with high sensitivity.* Forensic science international, 2013. **231**(1): p. 6-12.
384. Zunngu, S.S., *et al.*, *Synthesis and application of a molecularly imprinted polymer in the solid-phase extraction of ketoprofen from wastewater.* Comptes Rendus Chimie, 2017. **20**(5): p. 585-591.
385. Peng, J., *et al.*, *Molecularly imprinted polymeric stir bar: Preparation and application for the determination of naftopidil in plasma and urine samples.* J Sep Sci, 2016. **39**(2): p. 383-90.
386. Canfarotta, F., *et al.*, *Solid-phase synthesis of molecularly imprinted nanoparticles.* Nat. Protocols, 2016. **11**(3): p. 443-455.
387. Peng, J., *et al.*, *Molecularly imprinted polymeric stir bar: preparation and application for the determination of Naftopidil in Plasma and Urine samples.* Journal of Separation Science, 2015: p. n/a-n/a.
388. Hu, X., *et al.*, *Ultrasensitive specific stimulant assay based on molecularly imprinted photonic hydrogels.* Advanced Functional Materials, 2008. **18**(4): p. 575-583.
389. Guo, Z.-F., T.-T. Guo, and M. Guo, *Preparation of molecularly imprinted adsorptive resin for trapping of ligustrazine from the traditional Chinese herb Ligusticum chuanxiong Hort.* Analytica chimica acta, 2008. **612**(2): p. 136-143.

This page intentionally left blank

Chapter 7: Conclusions and Future Work

This page intentionally left blank

Chapter 7: Conclusions and Future Work

7.1 Concluding remarks

The demand for accurate and sensitive presumptive illicit drug identification methods has increased with the increasing number of drugs being seized by law enforcement and other security personnel. The aims of this research were to investigate the potential avenues for creating and developing new optical screening methods for the class of NPS, the synthetic cathinones. Current presumptive methods of detection are limited to non-selective, general screening chemical colour tests that often result in false negative colour changes when applied to many of the new psychoactive substances.

The synthesis of eighteen synthetic cathinone analogues in-house was crucial to this research in order to obtain the required amount of each different compound for testing. Chapter 2 details synthetic procedures used to obtain the compounds. The in-house preparation of materials also provided insight into the likely contaminants present in street samples of the drug, and thus anticipation of the effects on presumptive testing methods. This was performed in this study through the testing of crude samples of the compounds prior to purification.

Initial investigations were focused on developing chemical reactions to produce coloured products with the target drug class, and thus create a chemical colour spot test. This became a focus due to its inherent simplicity, cost-effectiveness and ability to be incorporated into current testing protocols easily. Chapter 3 details the development of a chemical colour spot test using the reaction between synthetic cathinones and the neocuproine reagent to produce a chromophoric compound.

The chemical colour test was further improved in chapter 4 to eliminate the potential limitations of the protocol. This included the requirement for heating, and the false negative results observed with several cathinone analogues. The improved chemical colour test protocol was successfully achieved through the use of a small amount of organic solvent to extract the coloured product and metal halide salts that behaved as a catalyst. Additional mechanisms were investigated for their potential use and application in a colour test device.

The translation of the test method developed in the laboratory into a suitable commercially available device proved difficult. A number of device designs were conceptualised through the use of sketches. A provisional patent was obtained for the chemical colour test method and device design from this research.

Chemical colour tests can be seen as an optical detection method that incorporates a molecular recognition event with a reporting signal. The reaction between synthetic cathinones and the neocuproine reagent produced a chromophoric compound that behaved as the reporting signal in this detection. Chapter 5 examined other potential chemical reactions that the synthetic cathinone class of compounds can undergo. Despite the obvious lack of colour change that occurs in many chemical reactions, it is still possible to incorporate these reactions into an optical detection method through the use of taggant materials, such as nanoparticles and fluorescent dyes.

The carbonyl group targeted reactions showed limited reactivity with the cathinone analogues. Ideally, these reactions would occur simply and easily at room temperature in order to bind with the cathinone molecule in a sample solution. The reduced electrophilicity of the cathinone carbonyl group has made these reactions difficult to achieve and thus eliminates their detection through surface functionalisation of nanoparticles with these reagents.

An alternative to selective chemical reactions in the field of molecular recognition is the use of molecularly imprinted polymers (MIPs) in which the presence of the target analyte, the cathinone molecule, is detected by the polymer through its adsorption in pre-made cavities.

The work performed in chapter 6 using MIPs showed great promise for the enrichment and collection of the targeted cathinone, 4-methylmethcathinone. However, there are several limitations in this study, including the tedious and time-consuming preparation process. In addition, the polymer is only one component to the screening test, and an optical reporting signal must be incorporated. This can be achieved using molecularly imprinted polymer hydrogels (MIPHs) or MIP coated nanoparticles, however, the success of such combinations is yet to be seen.

A thorough evaluation of a developed test procedure must include testing of real samples in order to ensure its success in real world applications. This study had limited access to case samples, however, testing was performed on simulated case samples through testing mixtures of cathinone analogues and also cathinones cut with inert substances.

The research contained in this thesis is not intended to be a conclusive optical detection product, but rather a source of information to the reader on the chemical characteristics of synthetic cathinones. The future of presumptive drug detection methods will emphasise the combination of a molecular recognition event with an optical reporting signal.

The outputs from each chapter in this thesis are varied in their fields of chemistry but are all facing the same direction, and that is toward developing optical detection methods for NPS, such as the synthetic cathinones.

7.2 Future work

Screening tests employed for the analysis and identification of controlled substances is a static list of techniques that has not changed in over a decade. This list includes colour tests, UV spectroscopy, microscopic examinations and immunoassays. TLC, infrared spectroscopy and microcrystalline tests are also able to be used for screening purposes.

The subjective nature of chemical colour testing presents a number of inherent problems as these tests rely on the interpretation of colour changes by the user in the field. The degree of colour-blindness of the user as well as environmental lighting conditions are not taken into consideration. Future work in this area would need to objectify the results of optical detection methods in order to eliminate these issues. This does not necessarily mean that more expensive instrumentation will need to replace simple colour spot test procedures, as the increased use of mobile phone applications may become more viable in the future.

Future work in the field of optical screening test development will see the incorporation of a new technique into regular use by law enforcement personnel and other interested parties. The synthetic cathinone class of illicit drugs may not be amenable to the selective chemical reaction trialled in this research, however, other controlled substances may be more suitable. It is hoped that the detection of illicit drugs in the field will be as simple as shining a light onto a solution of the suspicious material. The fluorescence that is returned will indicate the presence or absence of an illicit substance.

Future screening tests will also ideally be performed with the ability for multiplexing. This highly desirable quality of detecting the presence of more than one compound with one test is also easily achievable using upconversion nanoparticles. Multiplexing not only performs simultaneous identification, but also removes the limitations that a negative result affords. A negative result in colour testing for example does not provide any value toward determining the identification of the drug, apart from ruling out one particular class. This has obvious benefits in terms of cost and time.

The research performed in this study culminated into a provisional patent on a chemical spot test device that has received interest from a commercial drug screening company. Future work in this field would see the evolution from chemical spot tests to more sophisticated optical screening devices that incorporate more than one drug molecule into a molecular recognition screening device.

This study mostly focused on the NPS class of compounds, the synthetic cathinones, however, future work in this area should focus on other NPS classes that are of concern to the general public and law enforcement. In addition, traditional drugs of abuse should also be incorporated into new detection methods. This will not be achieved until the proposed methods demonstrate an enhanced detection over current presumptive methods.

Appendices

Appendix A: Characterisation data for synthetic cathinones

A.1 4-Methylmethcathinone (4-MMC, 3)

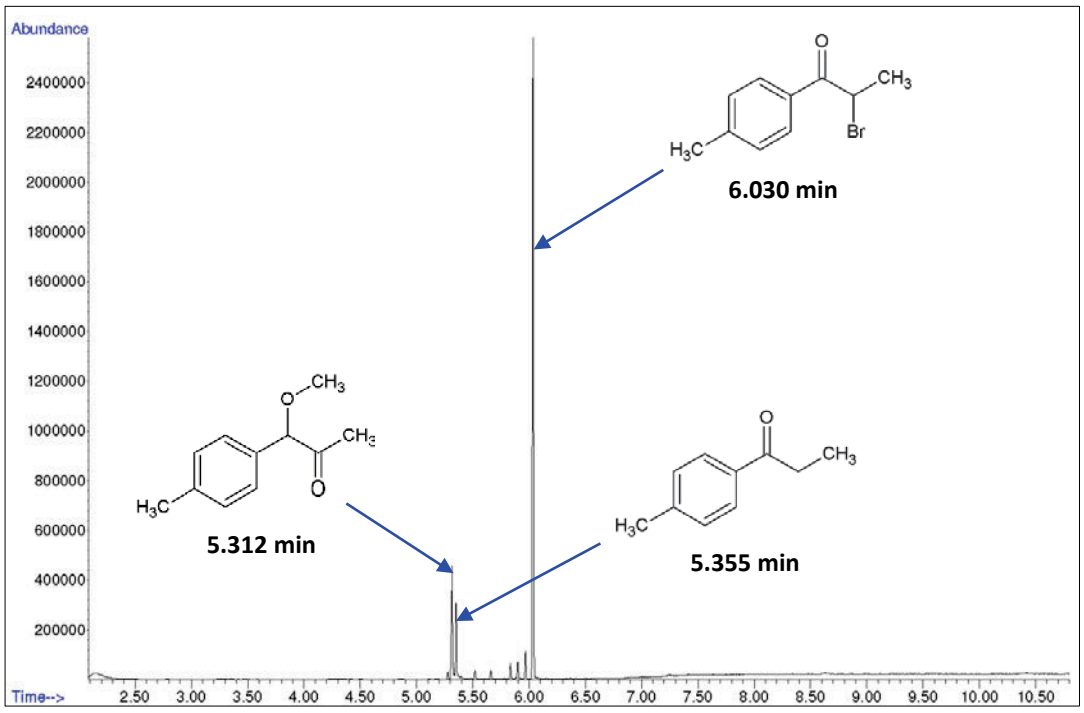

Figure A-1. Representative TIC of crude 2-bromo-4-methylpropiophenone (2) showing unreacted starting material and impurities

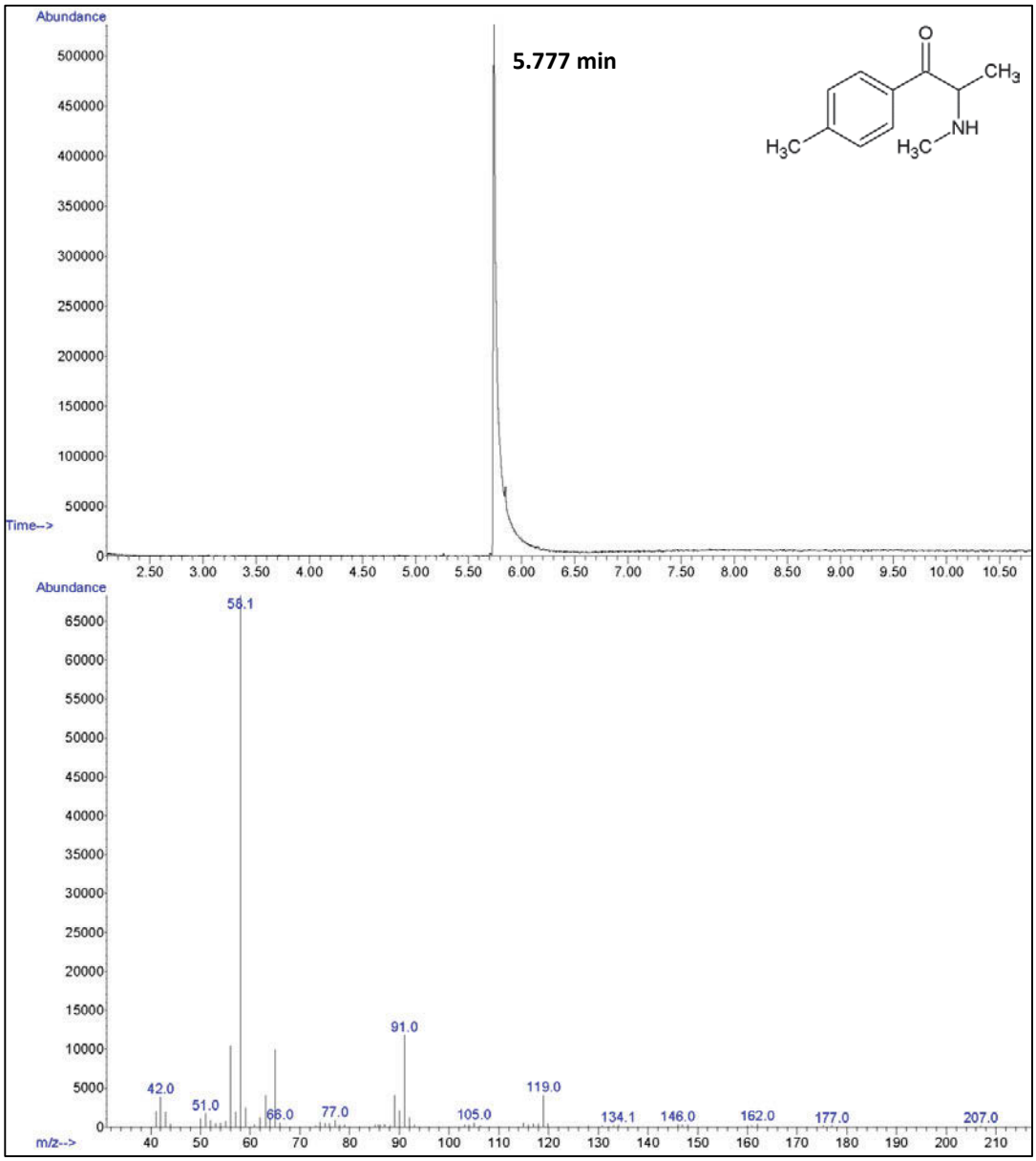

Figure A-2. TIC of 4-MMC HCl (**3**) (above) and associated mass spectrum (below)

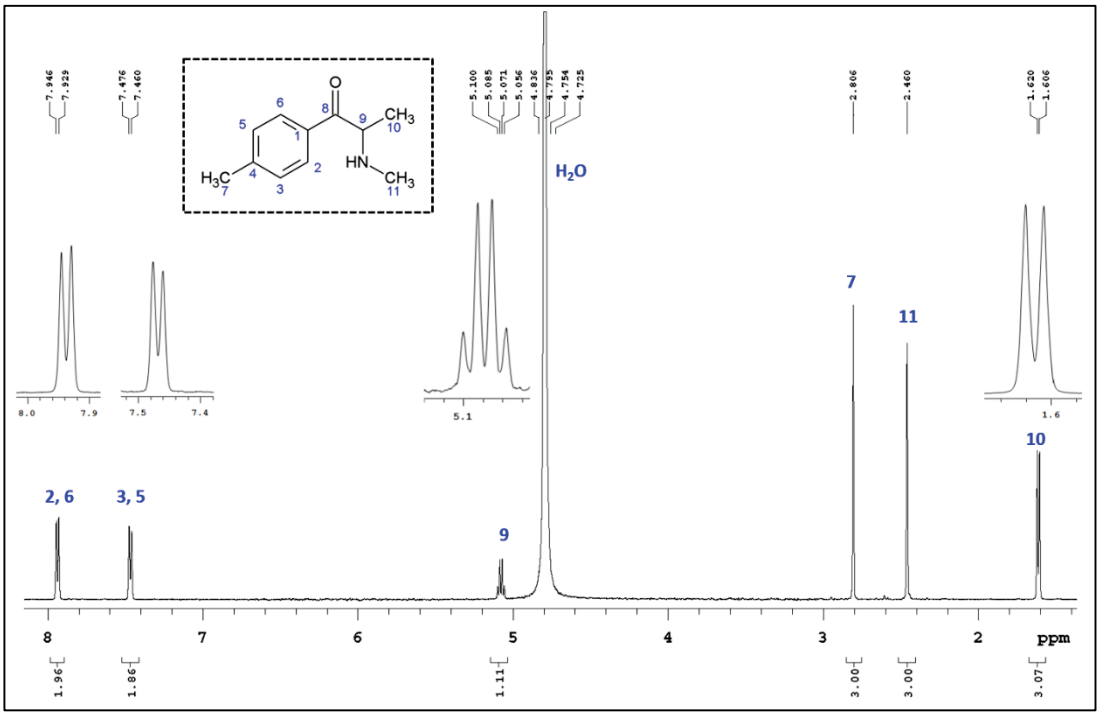

Figure A-3. Annotated ^{1}H-NMR spectrum of 4-MMC HCl (**3**) measured in deuterated water (δ 4.79 ppm). Inset: zoomed regions containing splitting patterns

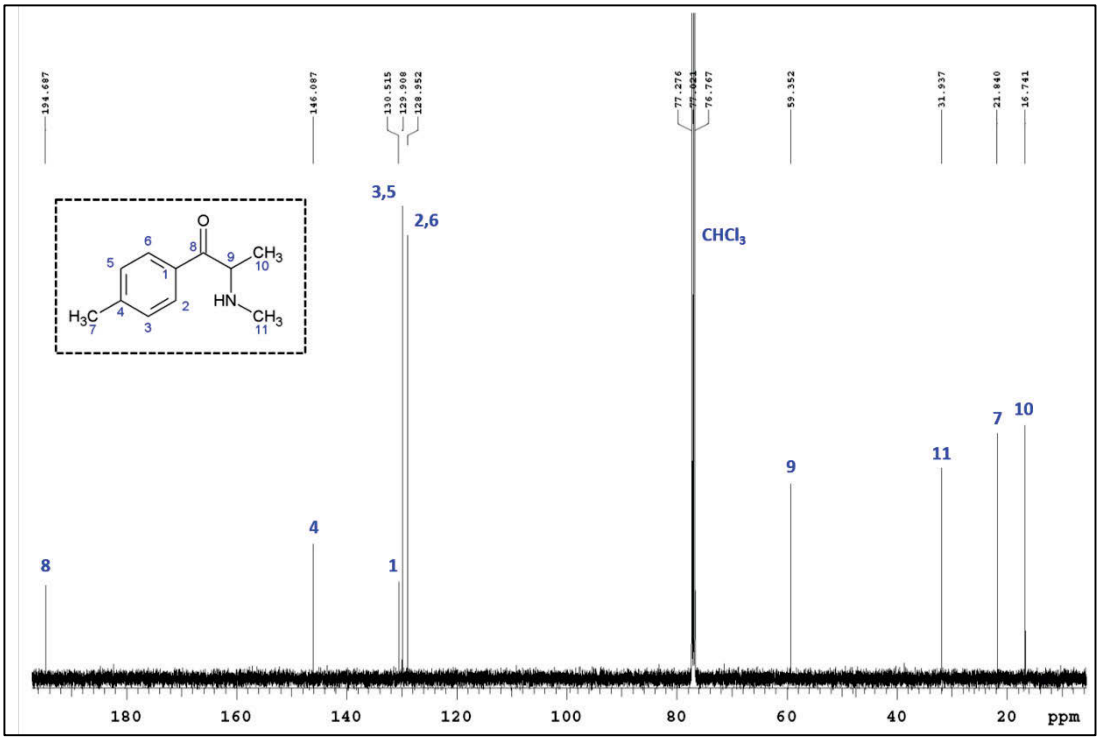

Figure A-4. Annotated ^{13}C-NMR spectrum of 4-MMC HCl (**3**) measured in deuterated chloroform (δ 77.16 ppm)

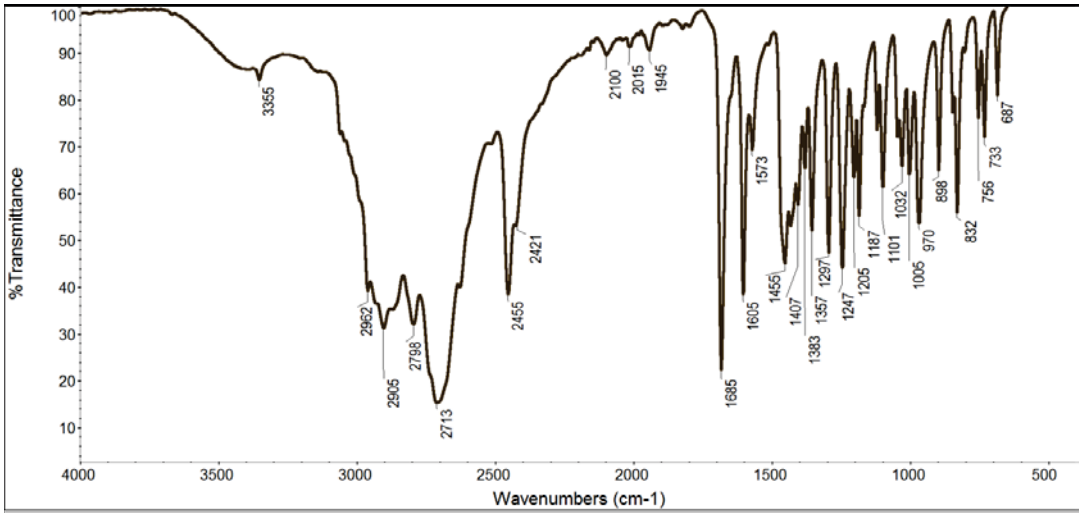

Figure A-5. ATR-FTIR spectrum of 4-MMC HCl (**3**)

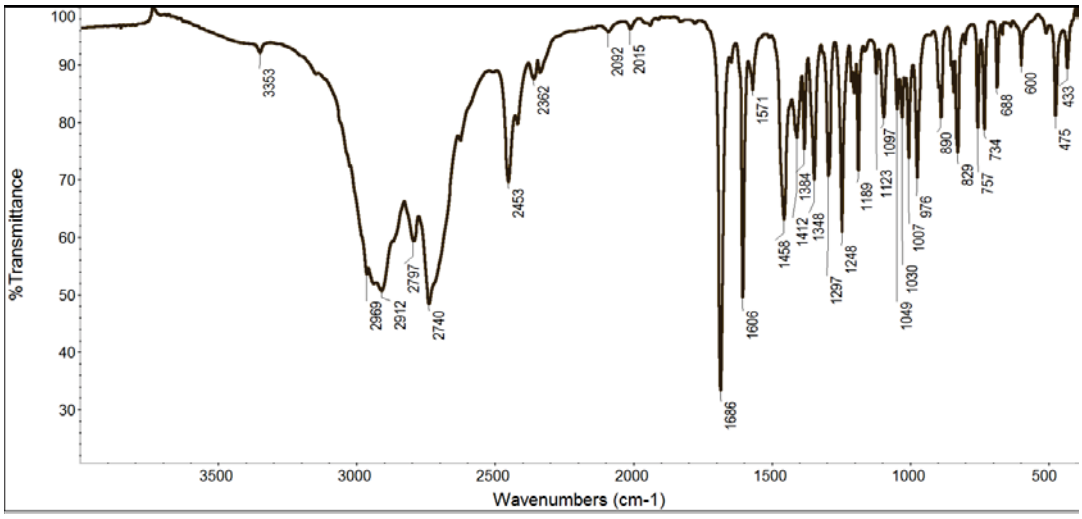

Figure A-6. FTIR spectrum (KBr pressed pellet) of 4-MMC HCl (**3**)

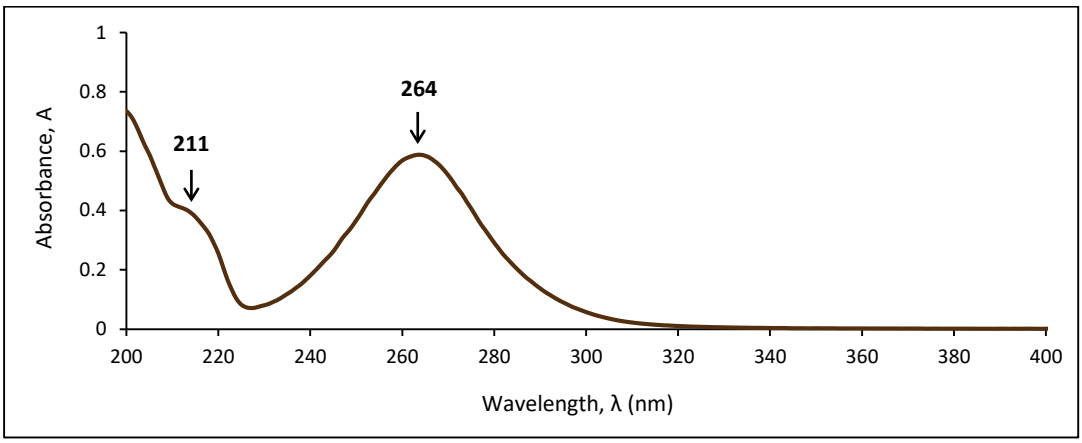

Figure A-7. UV spectrum of 4-MMC HCl (**3**) in deionised water

A.2 4-Fluoromethcathinone (4-FMC, 6)

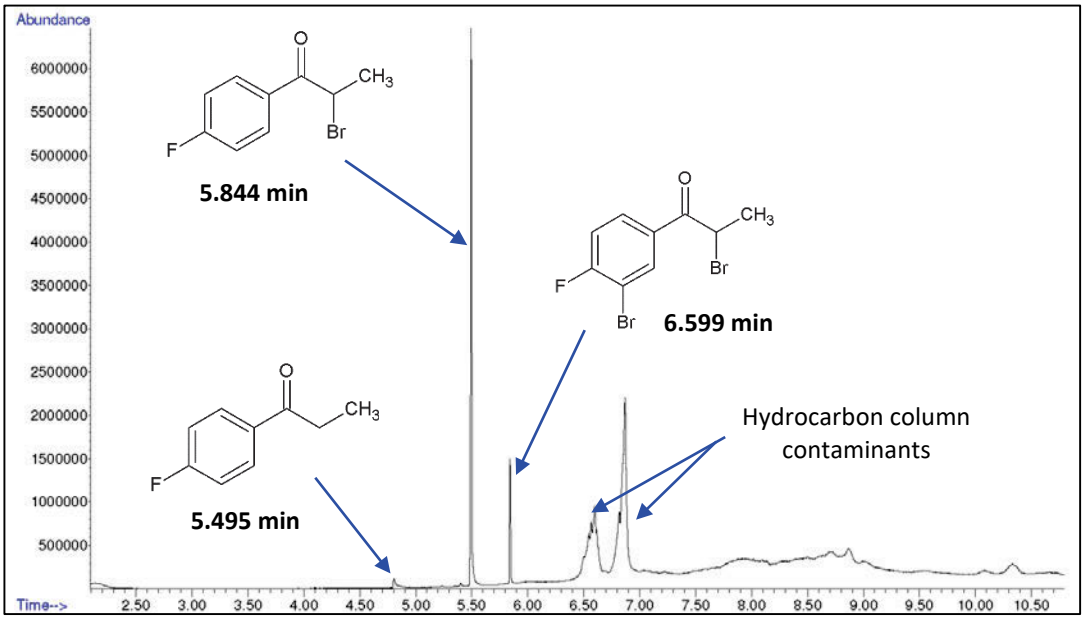

Figure A-8. Representative TIC of crude 2-bromo-4-fluoropropiophenone (**5**)

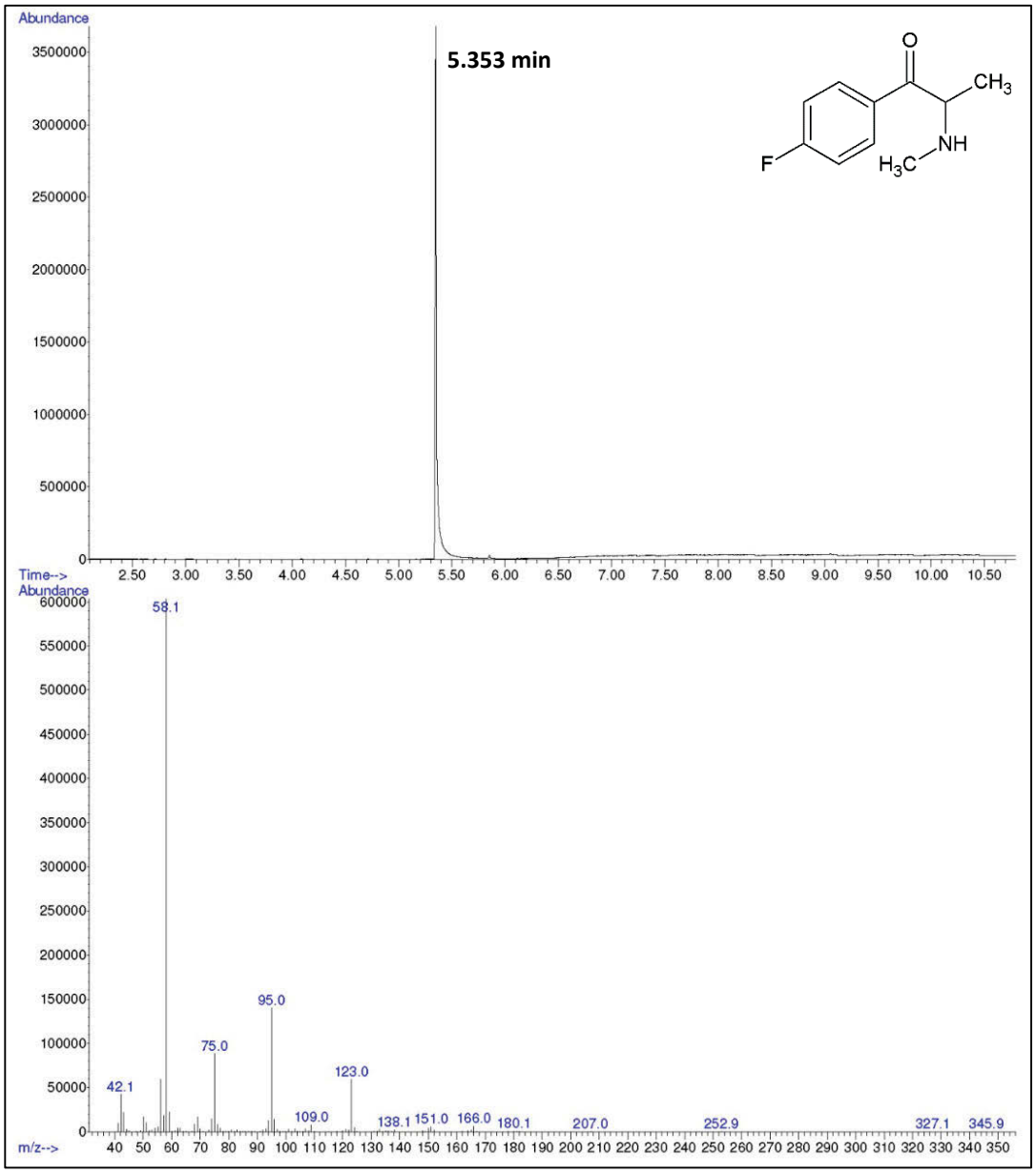

Figure A-9. Representative TIC of 4-FMC HCl (**6**) (above) and associated mass spectrum (below).

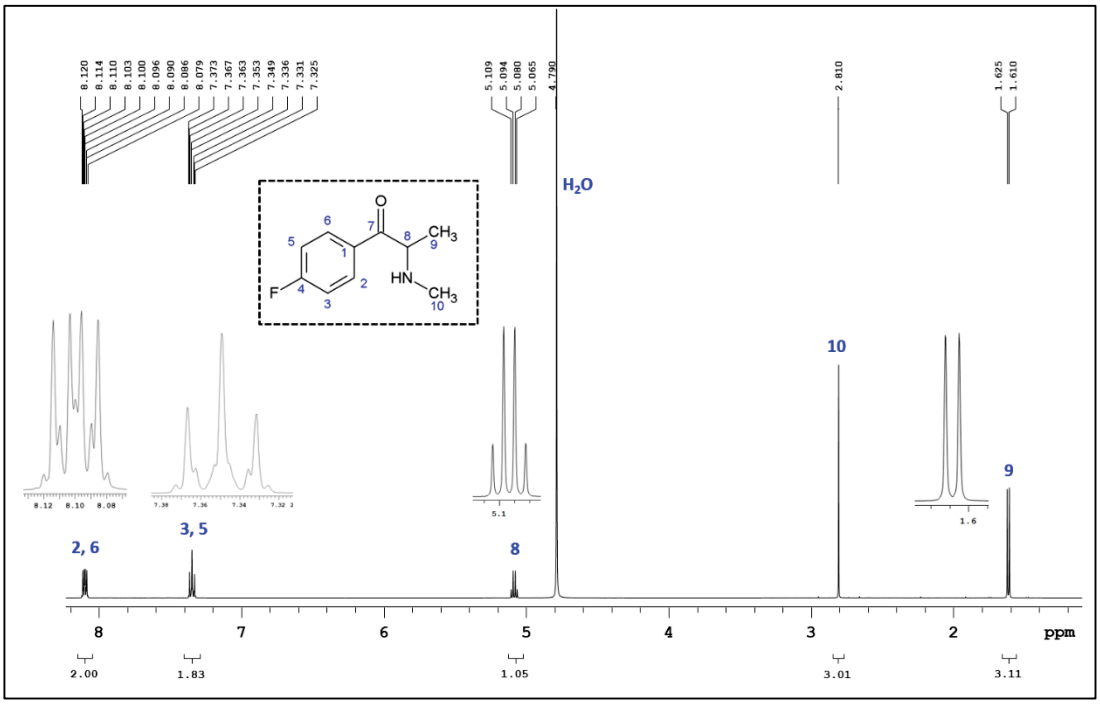

Figure A-10. Annotated ^{1}H-NMR spectrum of 4-FMC HCl (**6**) measured in deuterated water (δ 4.79 ppm). Inset: zoomed regions containing splitting patterns

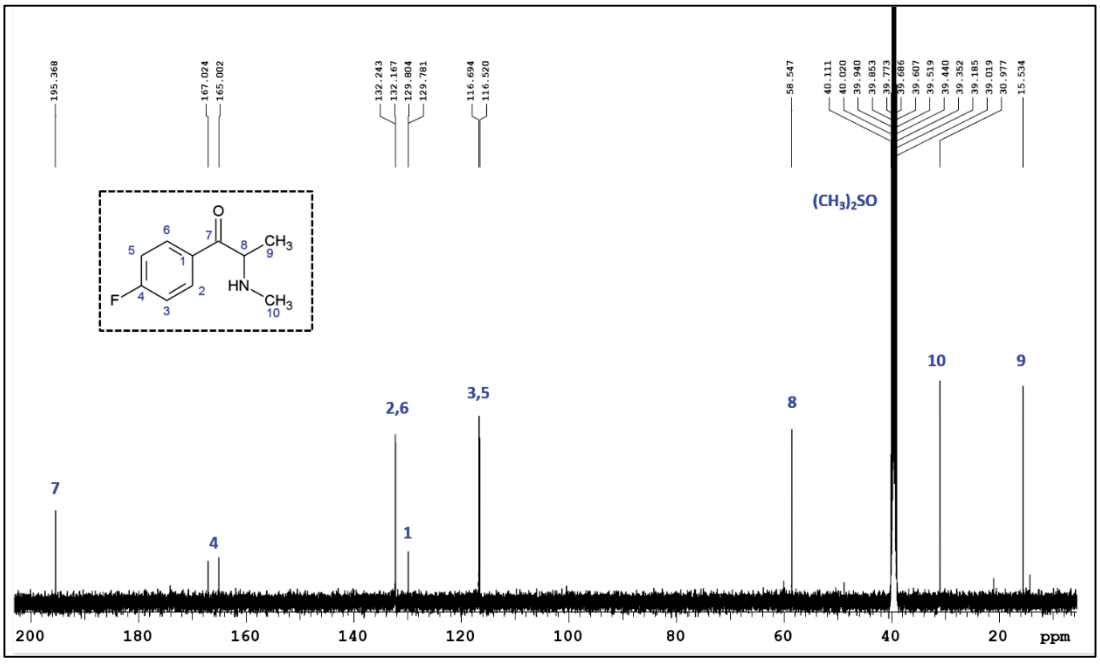

Figure A-11. Annotated ^{13}C-NMR spectrum of 4-FMC HCl (**6**) measured in deuterated dimethyl sulfoxide (δ 39.52 ppm)

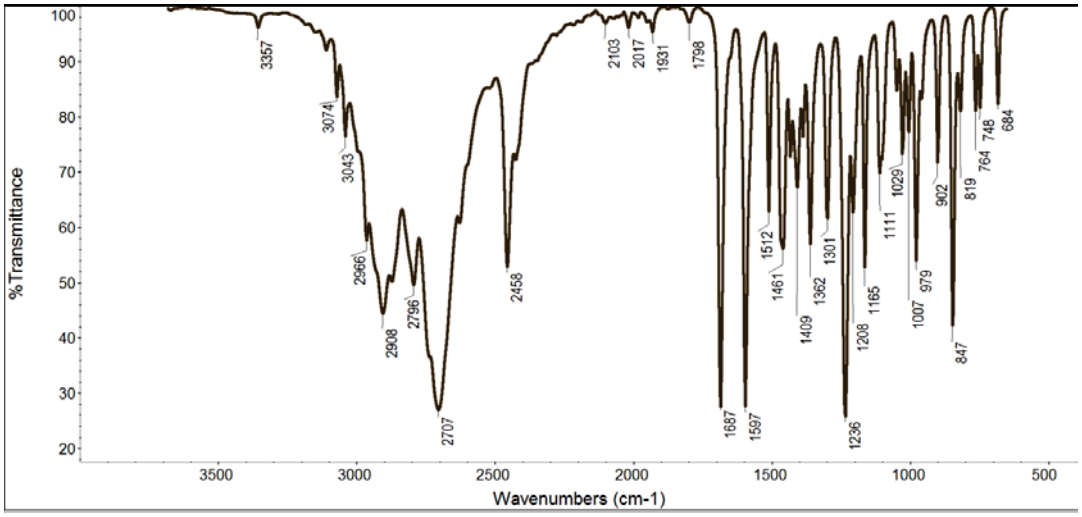

Figure A-12. ATR-FTIR spectrum of 4-FMC HCl (**6**)

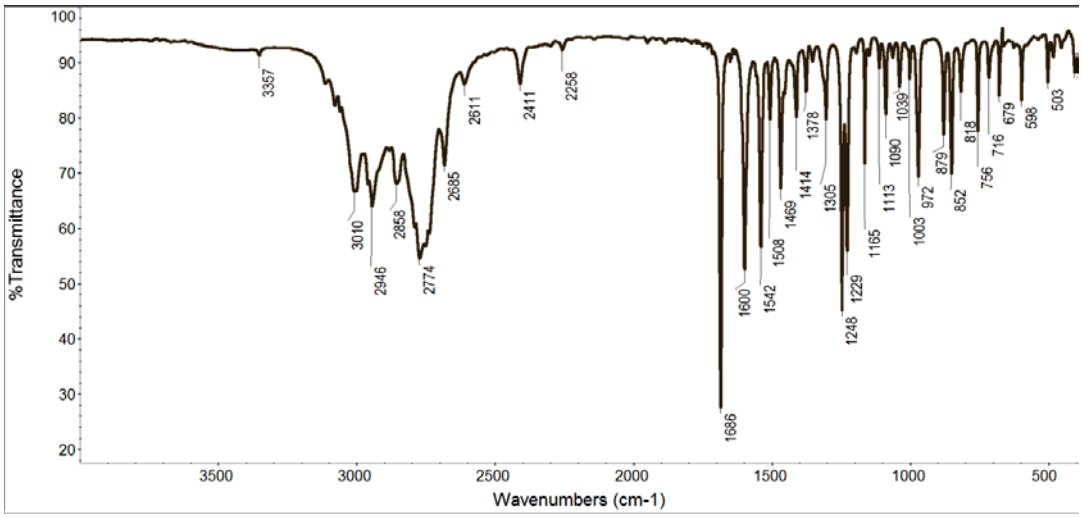

Figure A-13. FTIR spectrum (KBr pressed pellet) of 4-FMC HCl (**6**)

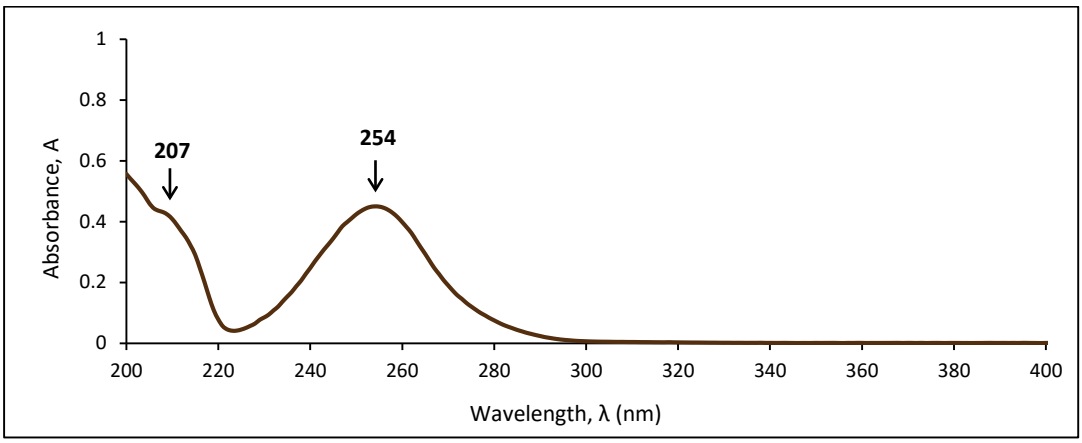

Figure A-14.UV spectrum of 4-FMC HCl (**6**) in deionised water

A.3 Methylone (11)

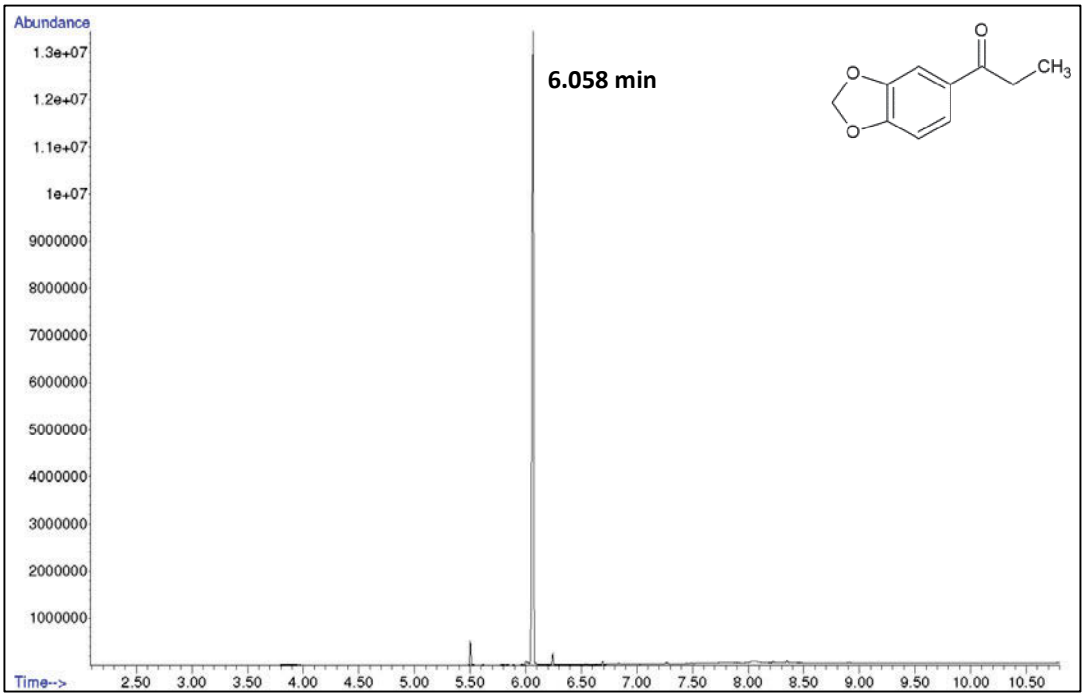

Figure A-15. Representative TIC of crude 1-(2H-1,3-benzodioxol-5-yl)propan-1-one (**9**)

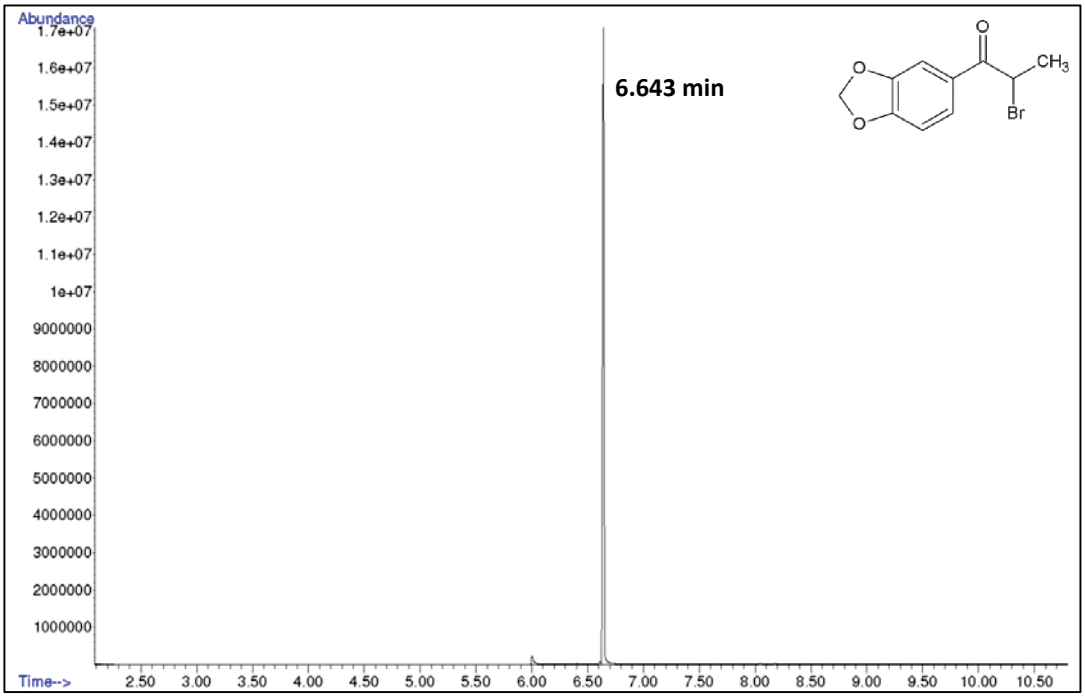

Figure A-16. Representative TIC of crude 1-(2H-1,3-benzodioxol-5-yl)-2-bromopropan-1-one (**10**)

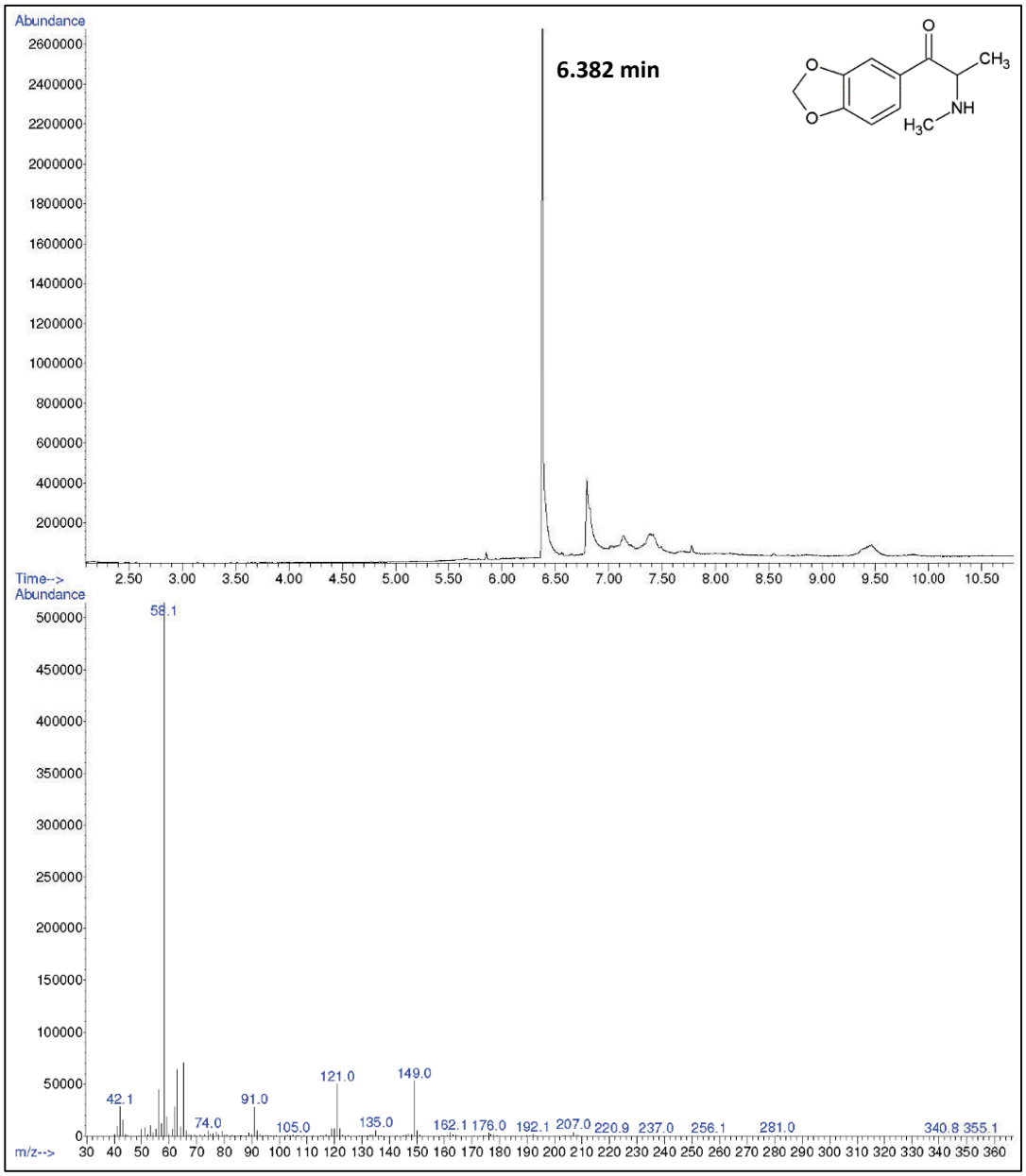

Figure A-17. Representative TIC of methylone HCl (**11**) (above) and associated mass spectrum (below).

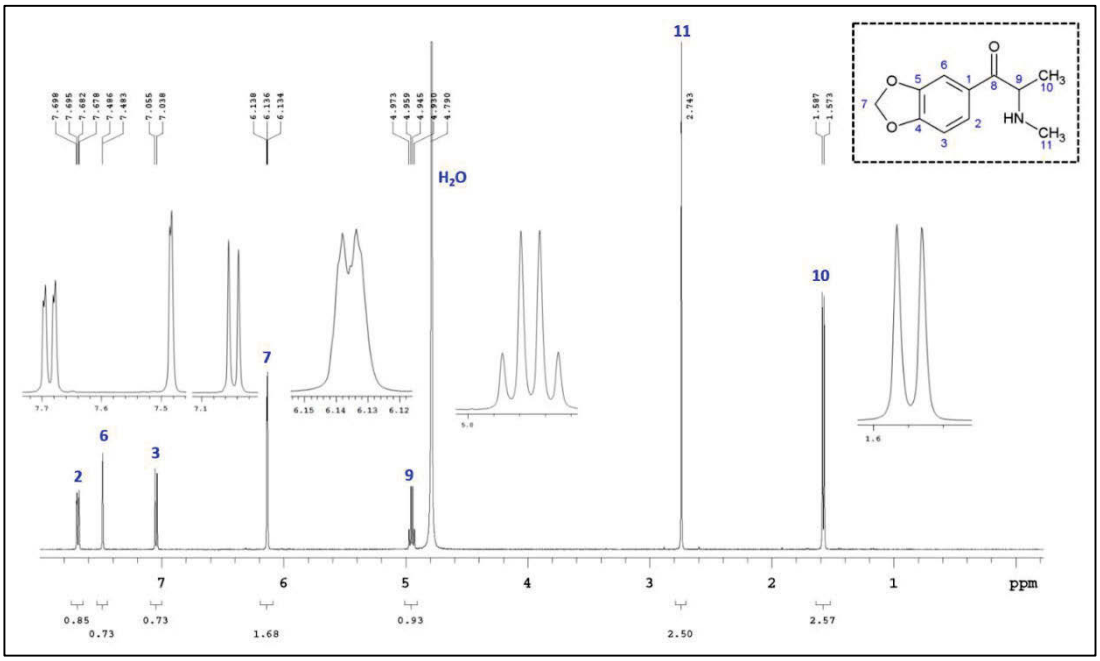

Figure A-18. Annotated 1D ^{1}H-NMR spectrum of methylone HCl (**11**) measured in deuterated water (δ 4.79 ppm). Inset: zoomed regions containing splitting patterns

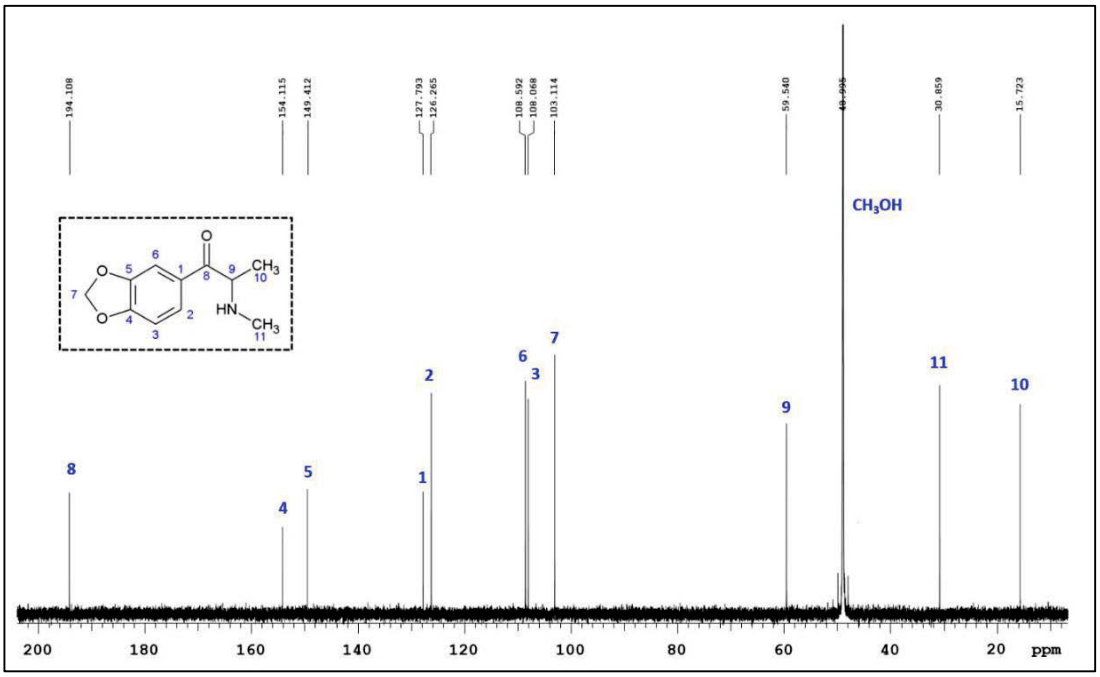

Figure A-19. Annotated ^{13}C-NMR spectrum of methylone HCl (**11**) measured in deuterated methanol (δ 49.00 ppm)

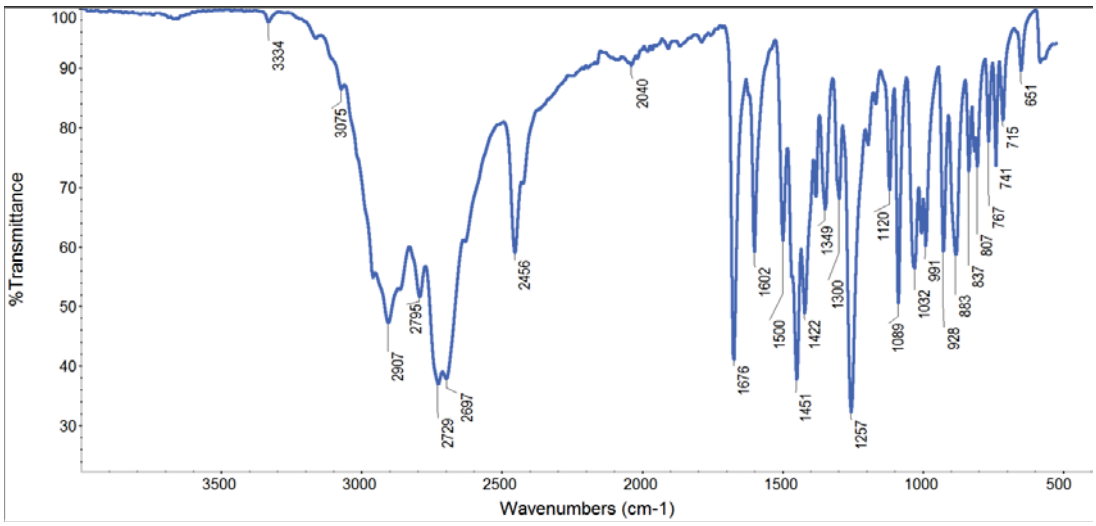

Figure A-20. ATR-FTIR spectrum of methylone HCl (**11**)

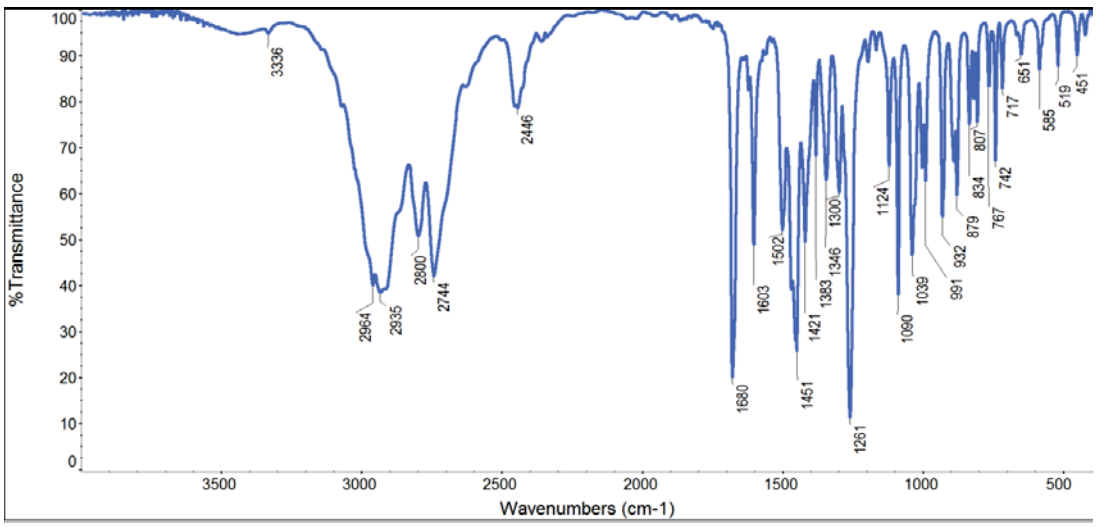

Figure A-21. FTIR spectrum (KBr pressed pellet) of methylone HCl (**11**)

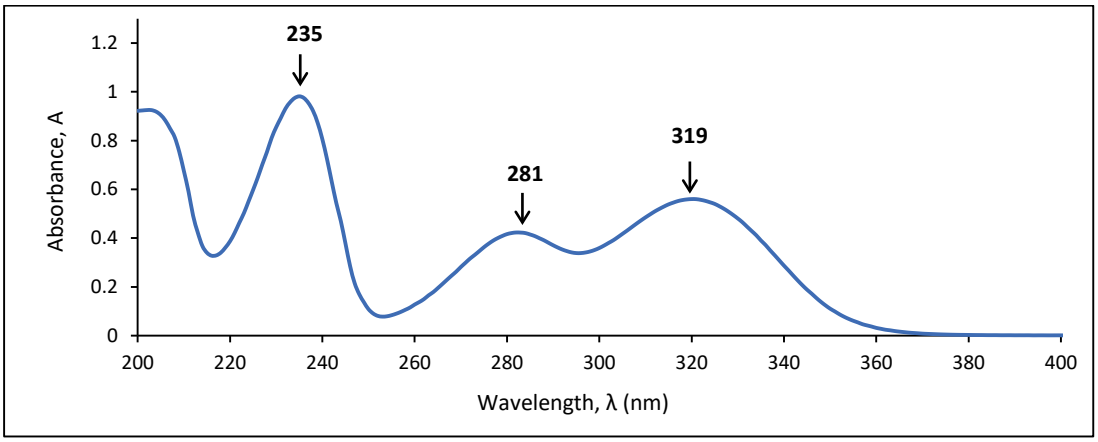

Figure A-22. UV spectrum of methylone HCl (**11**) in deionised water

A.4 Methcathinone (MCAT, 13)

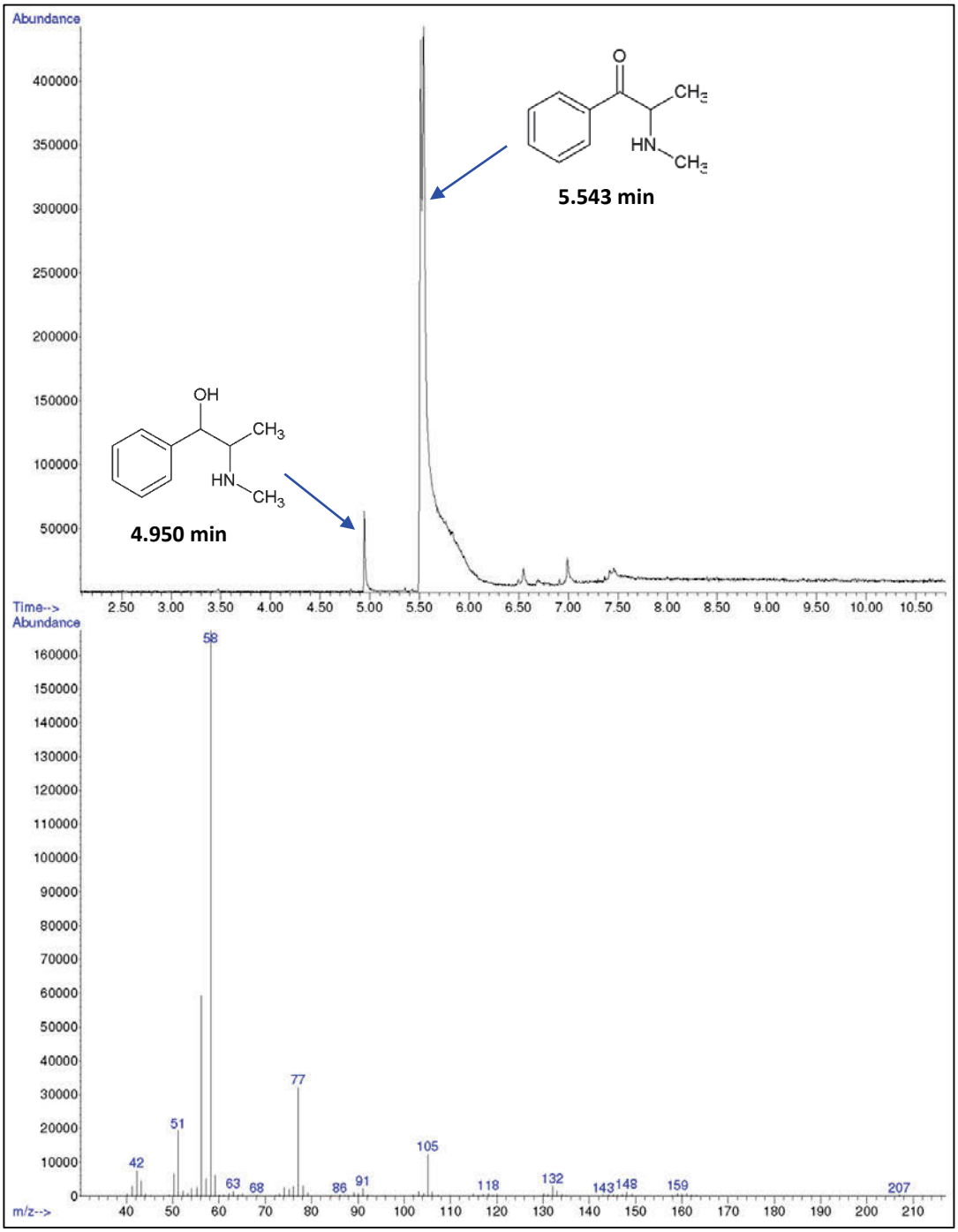

Figure A-23. Representative TIC of MCAT HCl (**13**) (above) and associated mass spectrum (below).

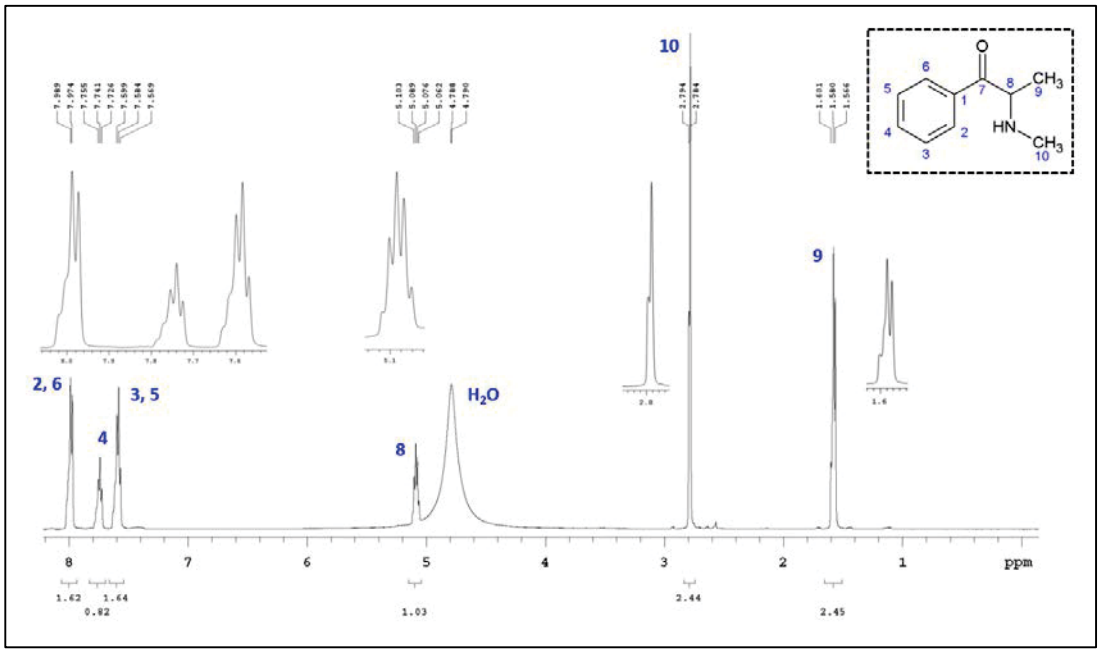

Figure A-24. Annotated ^{1}H-NMR spectrum of MCAT HCl (**13**) measured in deuterated water (δ 4.79 ppm). Inset: zoomed regions containing splitting patterns

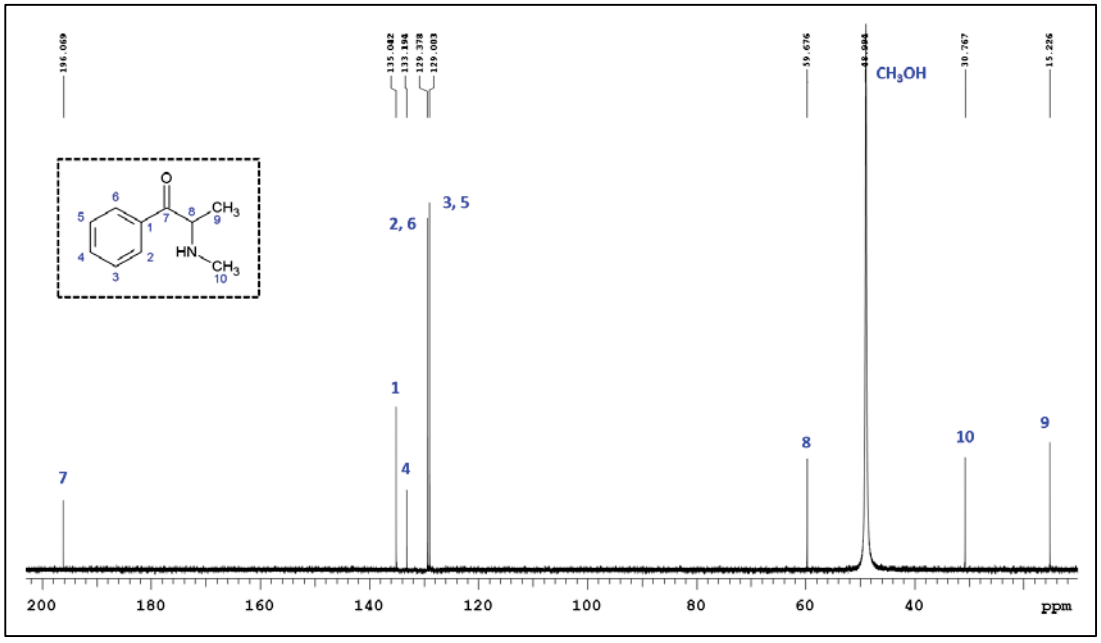

Figure A-25. Annotated ^{13}C-NMR spectrum of MCAT HCl (**13**) measured in deuterated methanol (δ 49.00 ppm)

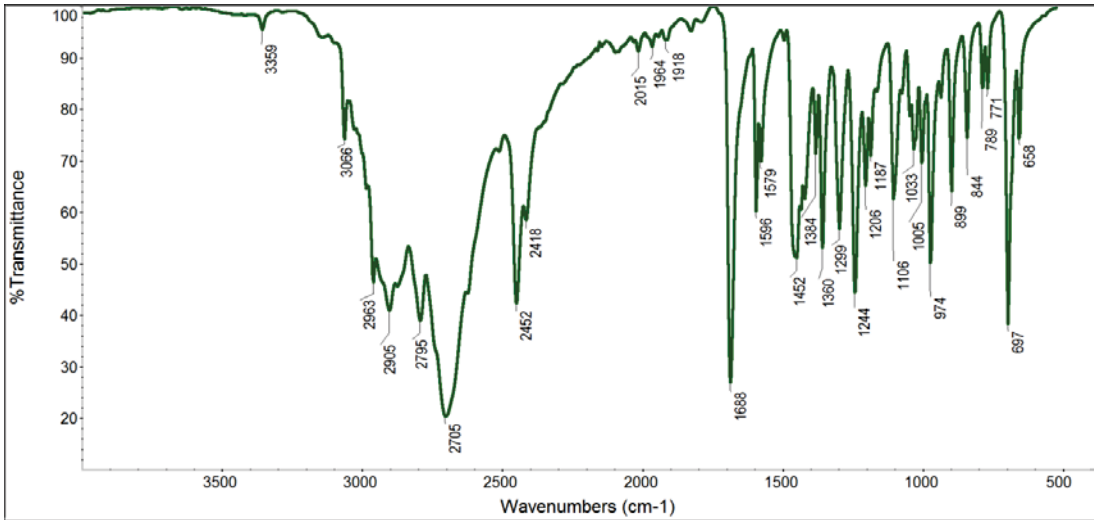

Figure A-26. ATR-FTIR spectrum of MCAT HCl (**13**)

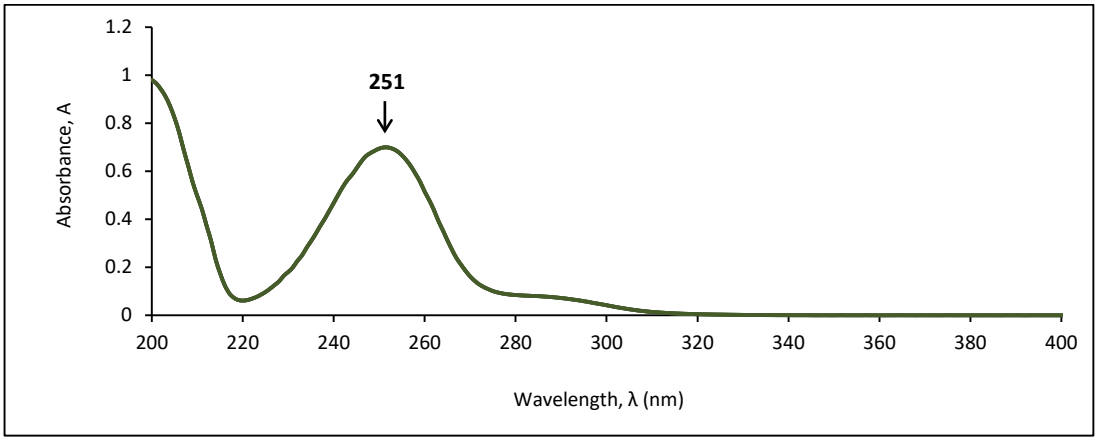

Figure A-27. UV spectrum of MCAT HCl (**13**) in deionised water

A.5 4-Methylethcathinone (4-MEC, 14)

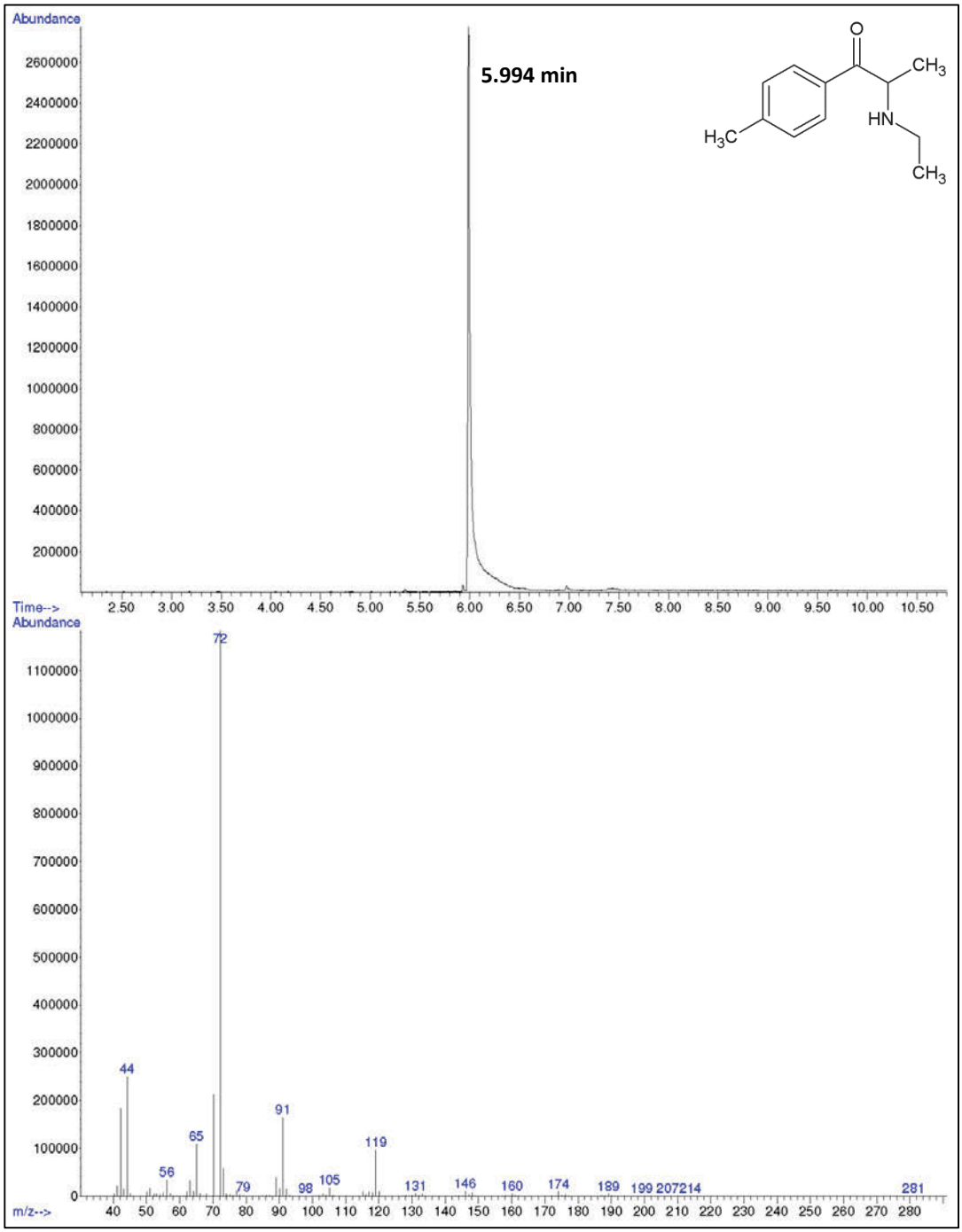

Figure A-28. Representative TIC of 4-MEC HCl (**14**) (above) and associated mass spectrum (below).

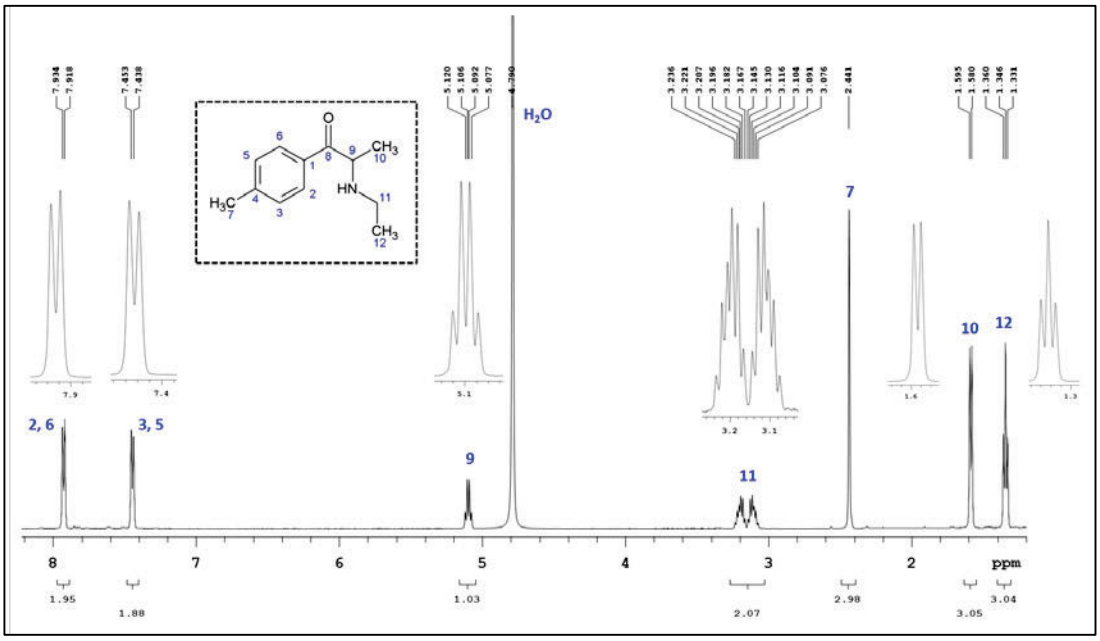

Figure A-29. Annotated ^{1}H-NMR spectrum of 4-MEC HCl (**14**) measured in deuterated water (δ 4.79 ppm). Inset: zoomed regions containing splitting patterns

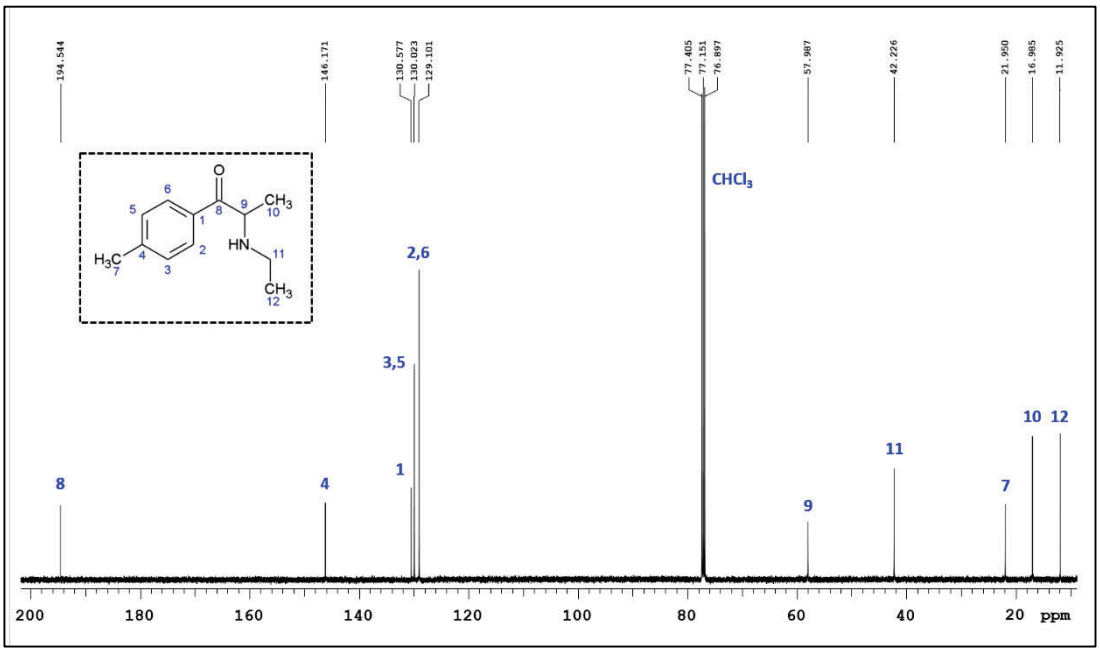

Figure A-30. Annotated ^{13}C-NMR spectrum of 4-MEC HCl (**14**) measured in deuterated chloroform (δ 77.16 ppm)

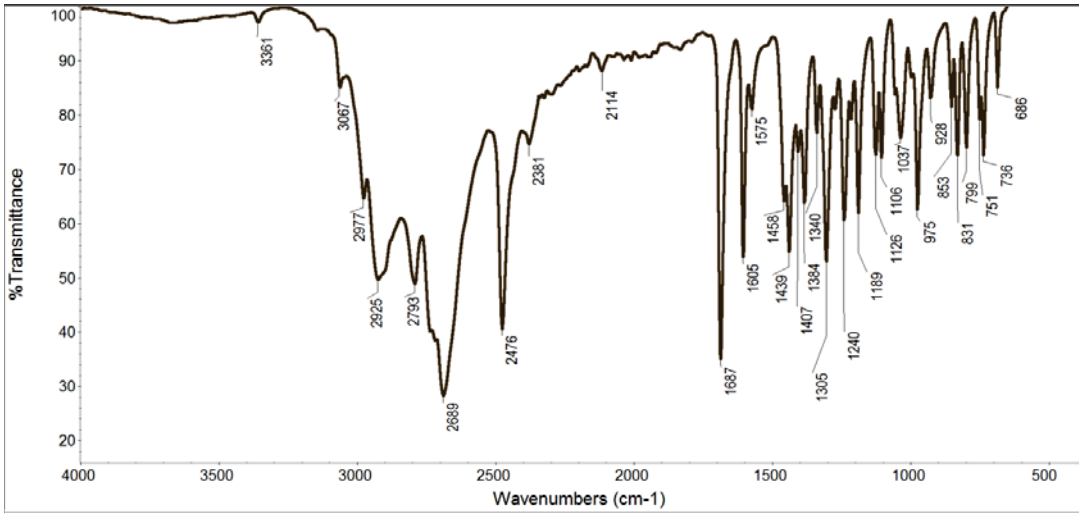

Figure A-31. ATR-FTIR spectrum of 4-MEC HCl (**14**)

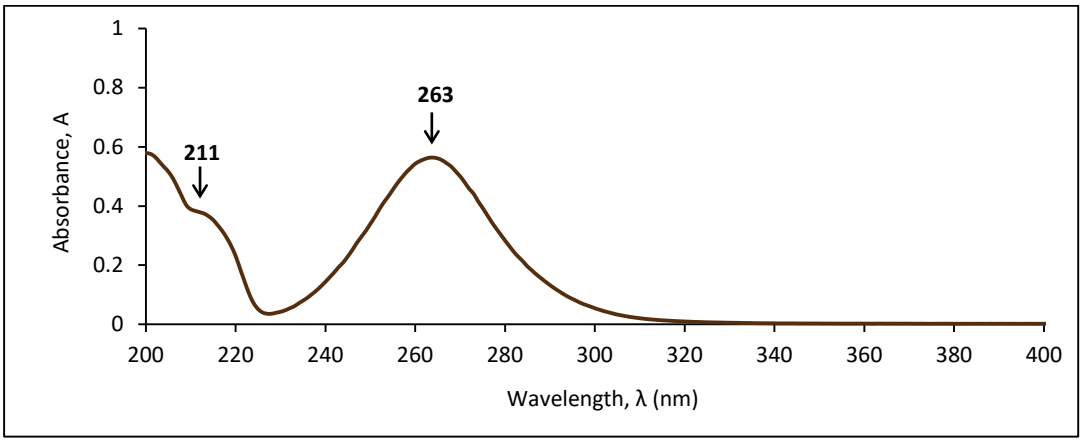

Figure A-32. UV spectrum of 4-MEC HCl (**14**) in deionised water

A.6 4-Methylpyrrolidinopropiophenone (4-MPPP, 15)

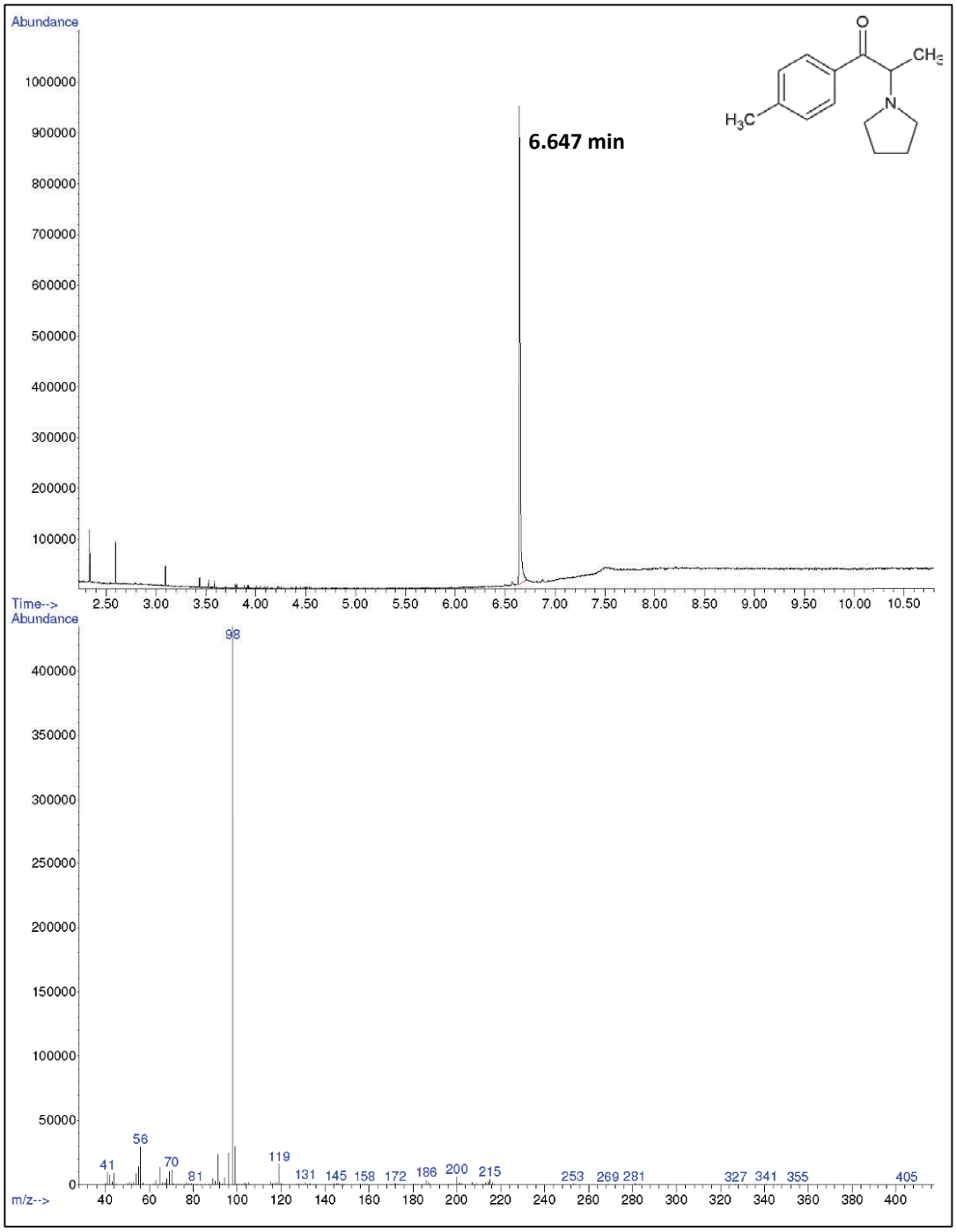

Figure A-33. Representative TIC of 4-MPPP HCl (**15**) (above) and associated mass spectrum (below).

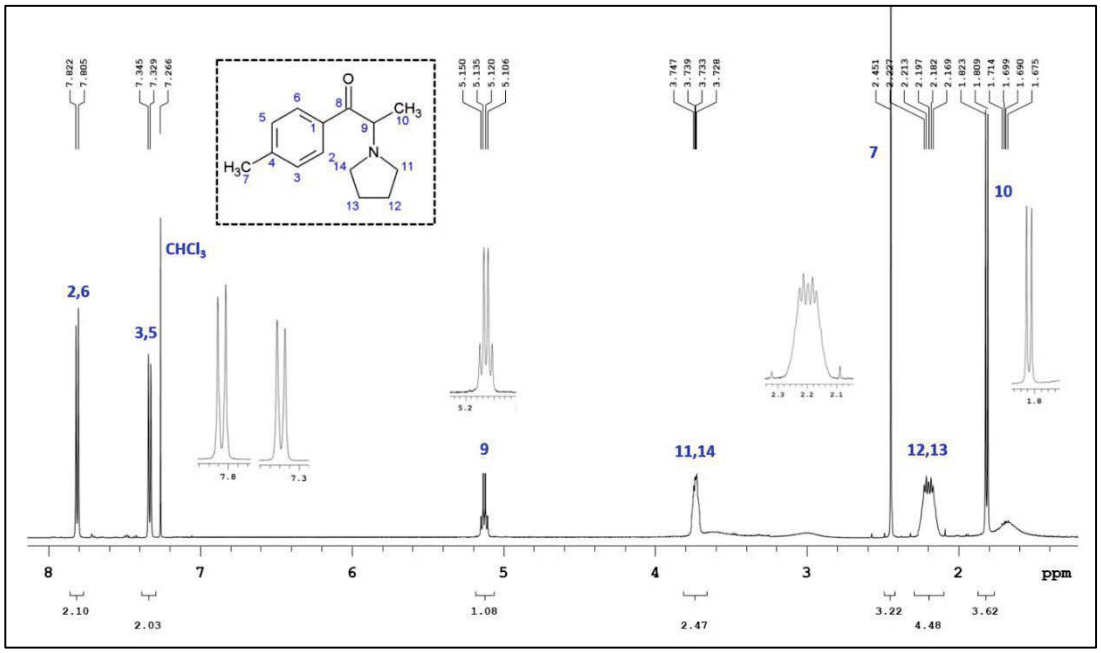

Figure A-34. Annotated ^{1}H-NMR spectrum of 4-MPPP HCl (**15**) measured in deuterated chloroform (δ 7.26 ppm). Inset: zoomed regions containing splitting patterns

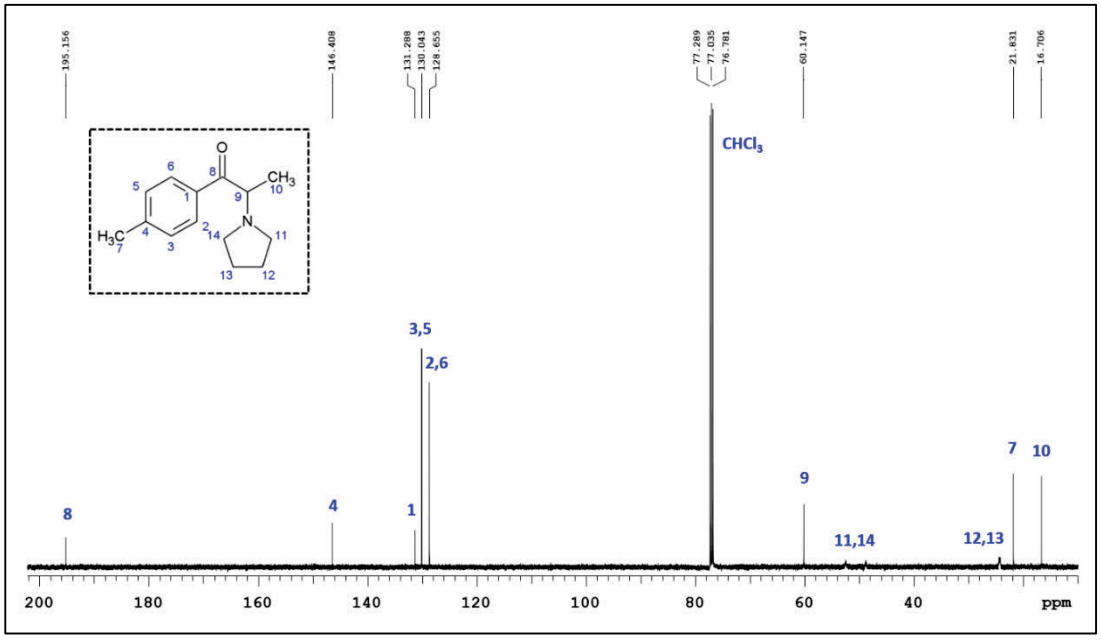

Figure A-35. Annotated ^{13}C-NMR spectrum of 4-MPPP HCl (**15**) measured in deuterated chloroform (δ 77.16 ppm)

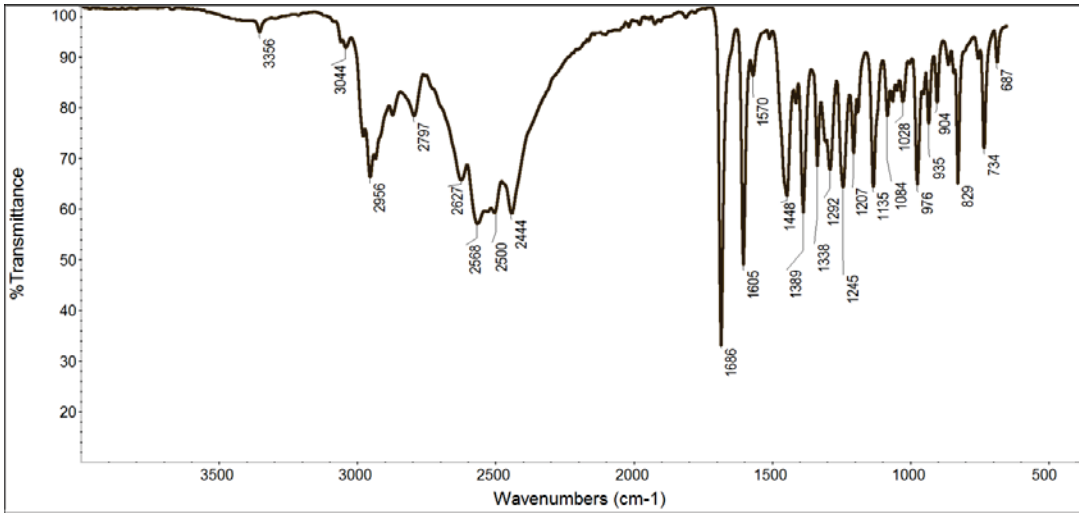

Figure A-36. ATR-FTIR spectrum of 4-MPPP HCl (**15**)

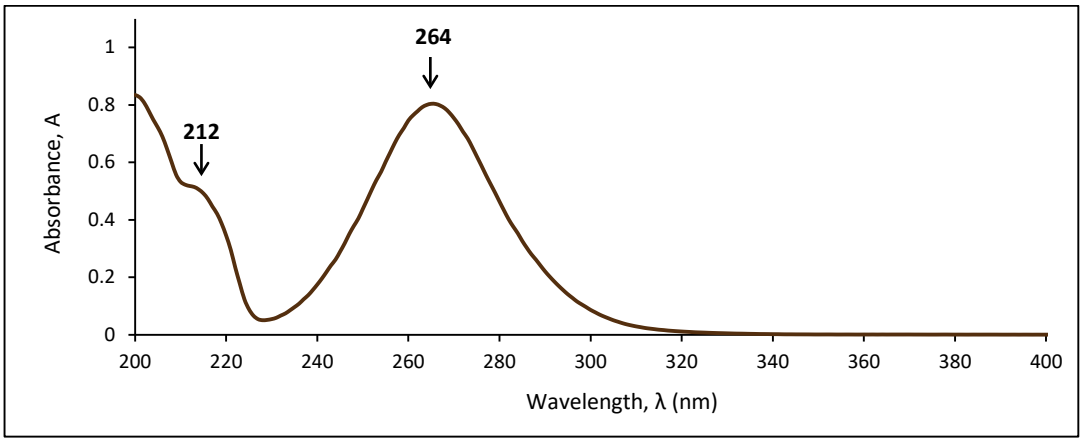

Figure A-37. UV spectrum of 4-MPPP HCl (**15**) in deionised water

A.7 3,4-Methylenedioxypyrovalerone (MDPV, 19)

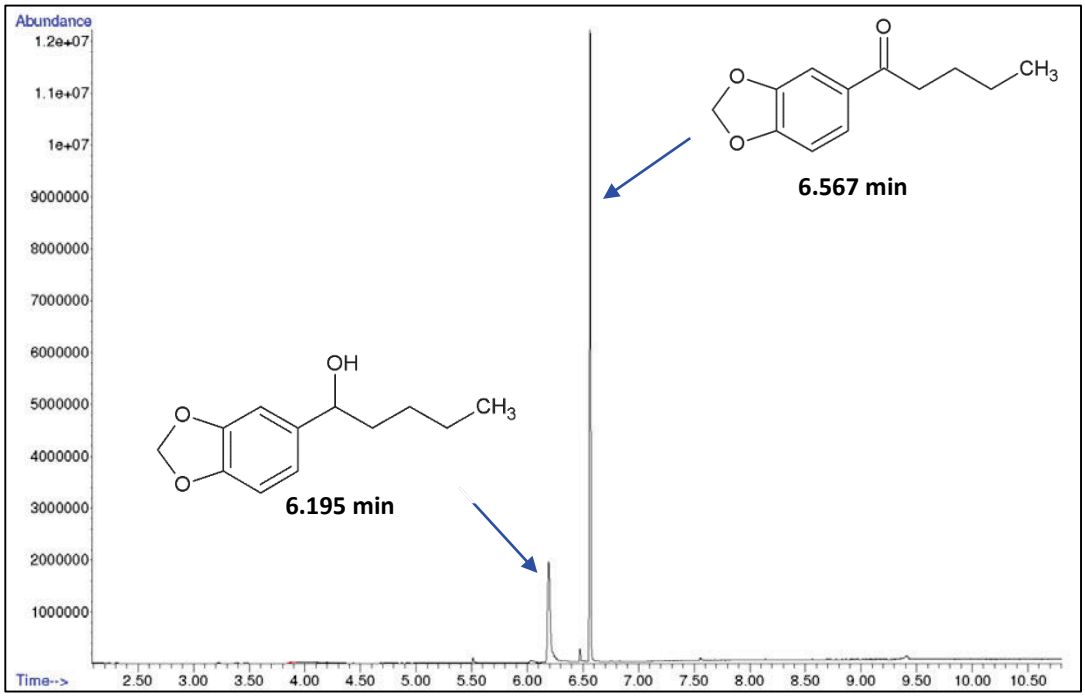

Figure A-38. Representative TIC of crude 1-(2H-1,3-benzodioxol-5-yl)pentan-1-one (**17**)

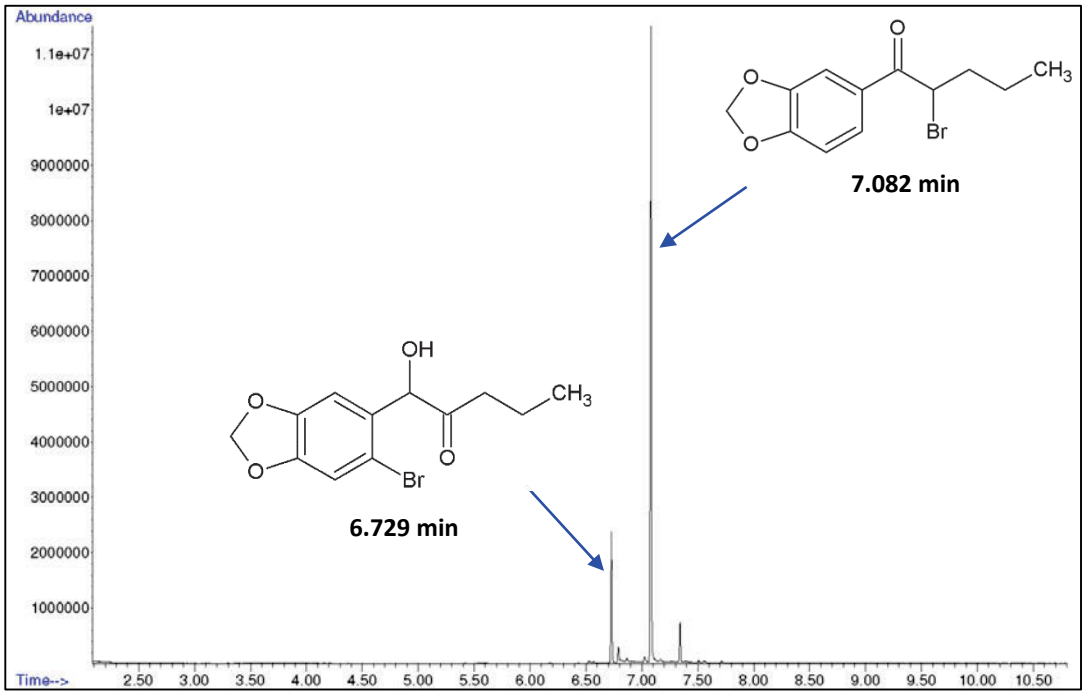

Figure A-39. Representative TIC of crude 1-(2H-1,3-benzodioxol-5-yl)-2-bromopentan-1-one (**18**)

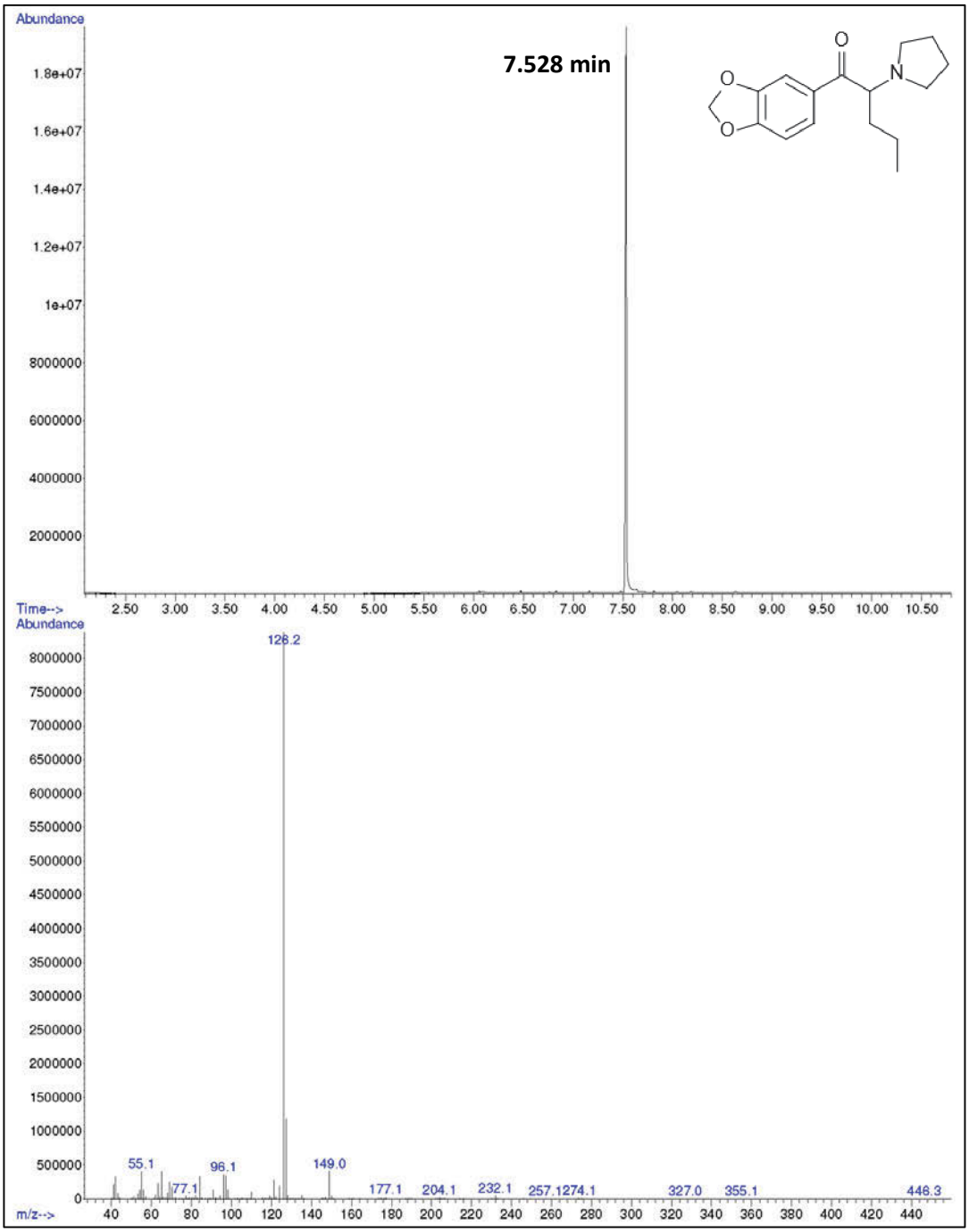

Figure A-40. Representative TIC of MDPV HCl (**19**) (above) and associated mass spectrum (below).

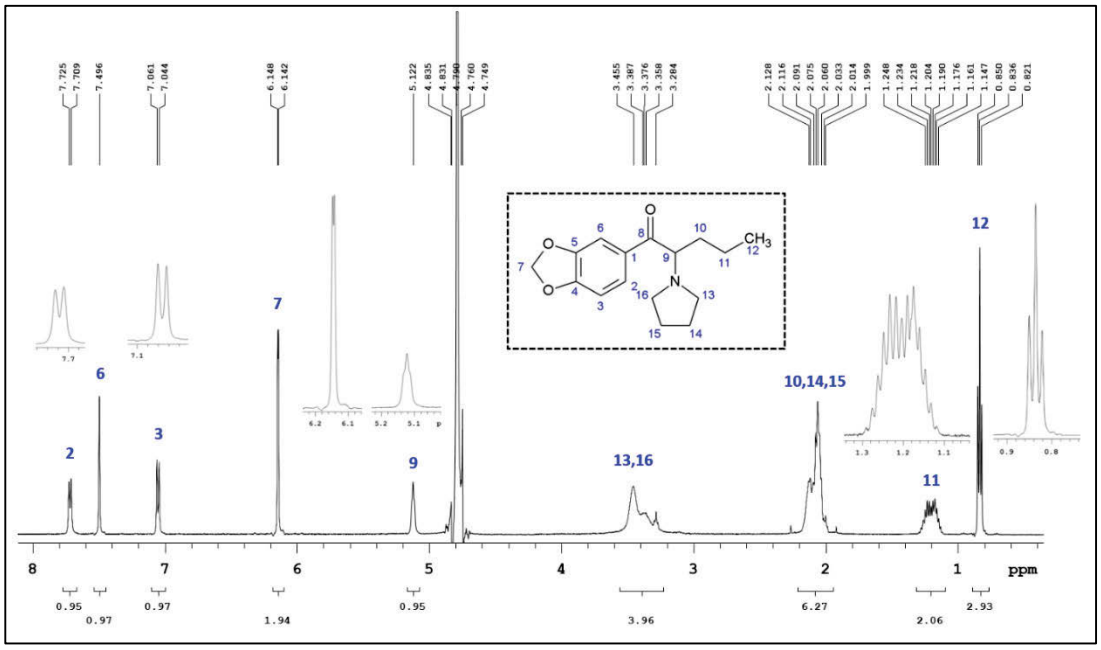

Figure A-41. Annotated ^{1}H-NMR spectrum of MDPV HCl (**19**) measured in deuterated water (δ 4.79 ppm). Inset: zoomed regions containing splitting patterns

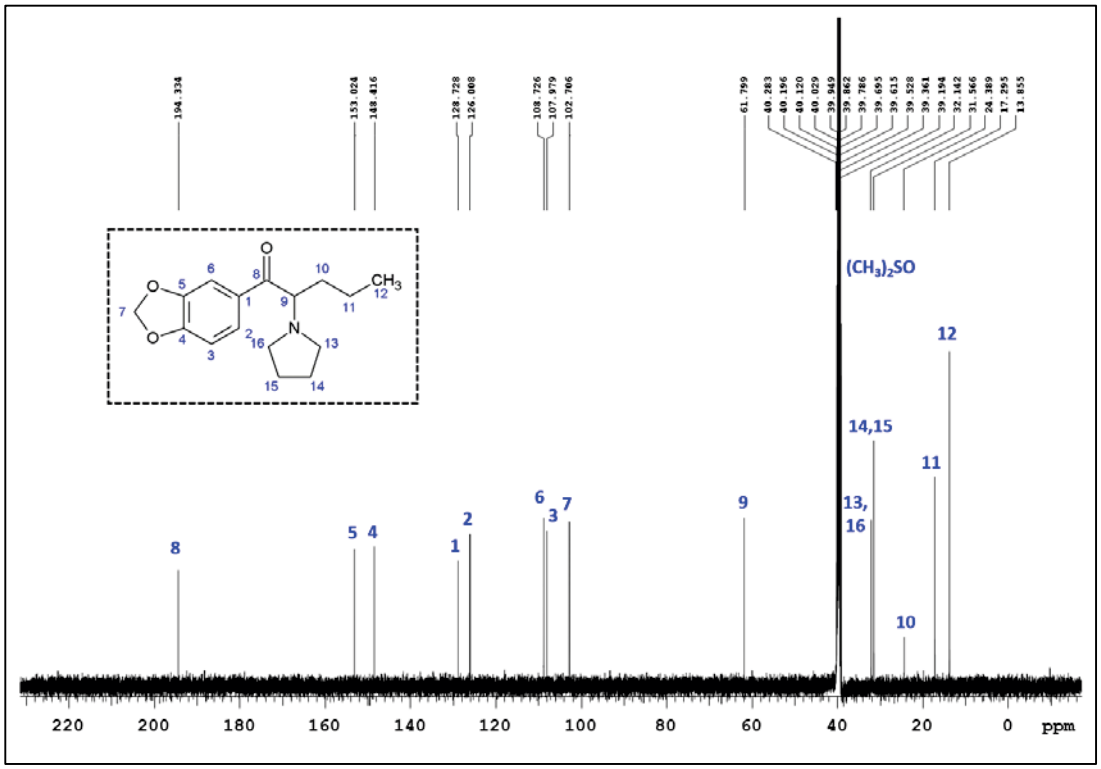

Figure A-42. Annotated ^{13}C-NMR spectrum of MDPV HCl (**19**) measured in deuterated dimethyl sulfoxide (δ 39.52 ppm)

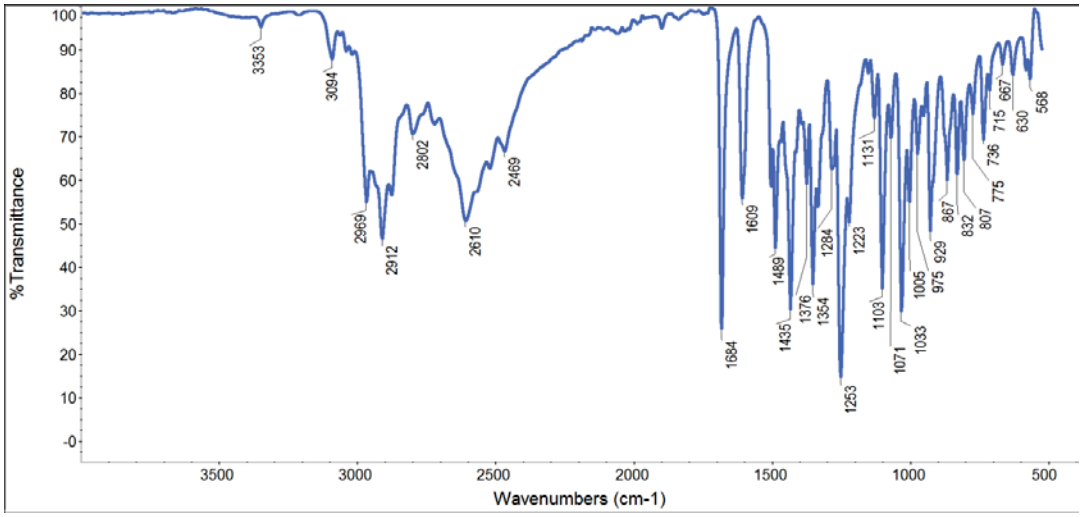

Figure A-43. ATR-FTIR spectrum of MDPV HCl (**19**)

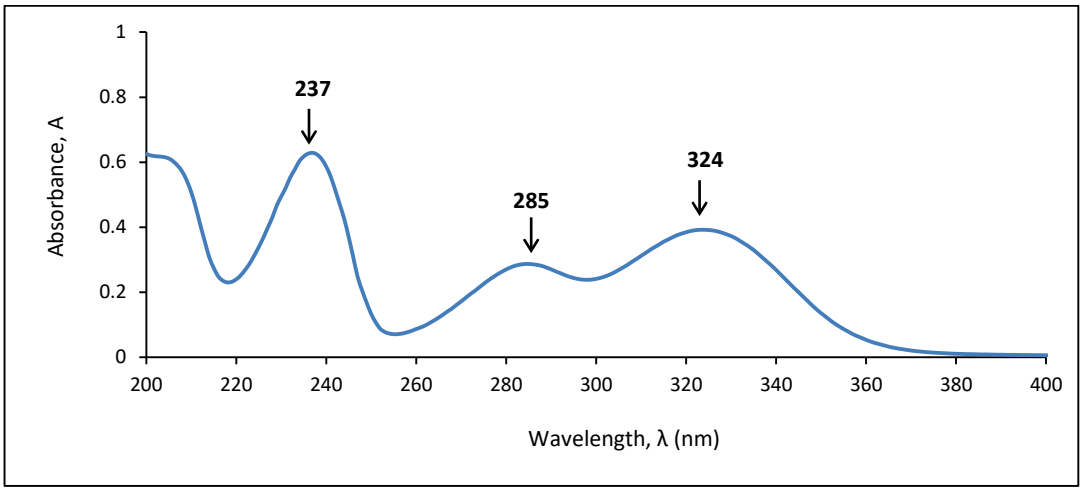

Figure A-44. UV spectrum of MDPV HCl (**19**) in deionised water

A.8 Butylone (23)

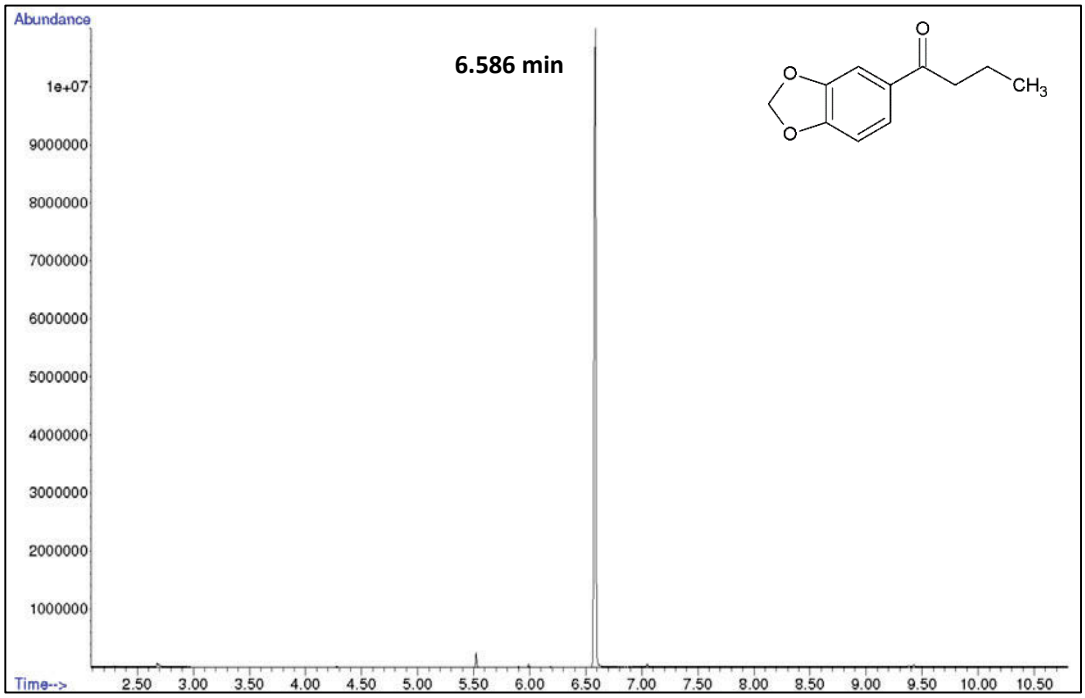

Figure A-45. Representative TIC of crude 1-(2H-1,3-benzodioxol-5-yl)butan-1-one (**21**)

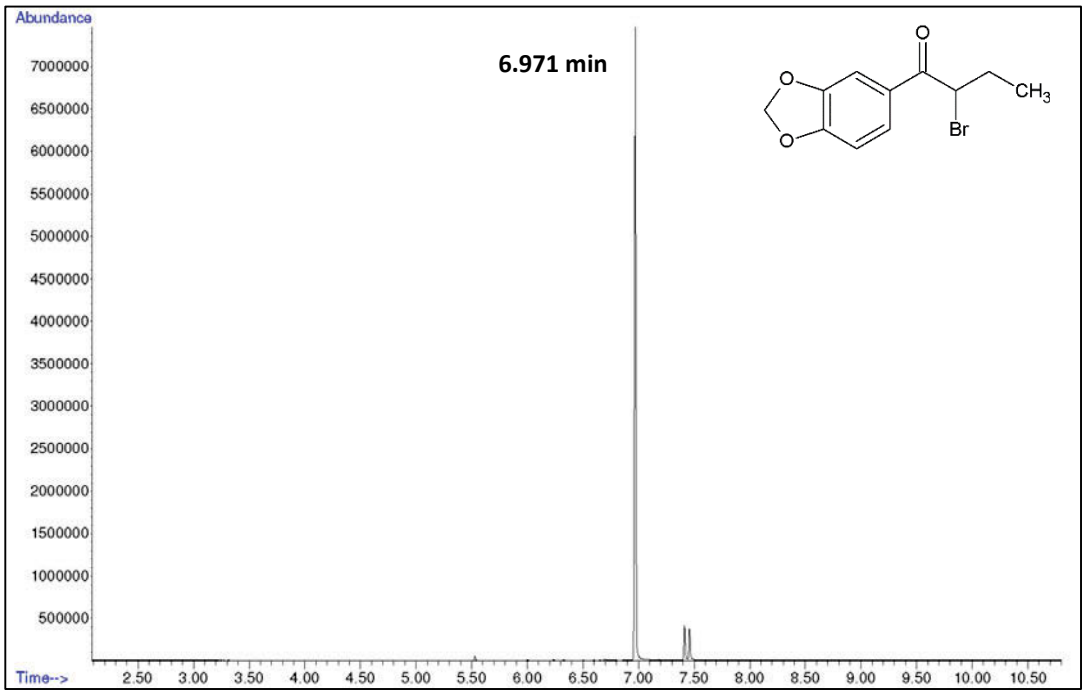

Figure A-46. Representative TIC of crude 1-(2H-1,3-benzodioxol-5-yl)-2-bromobutan-1-one (**22**)

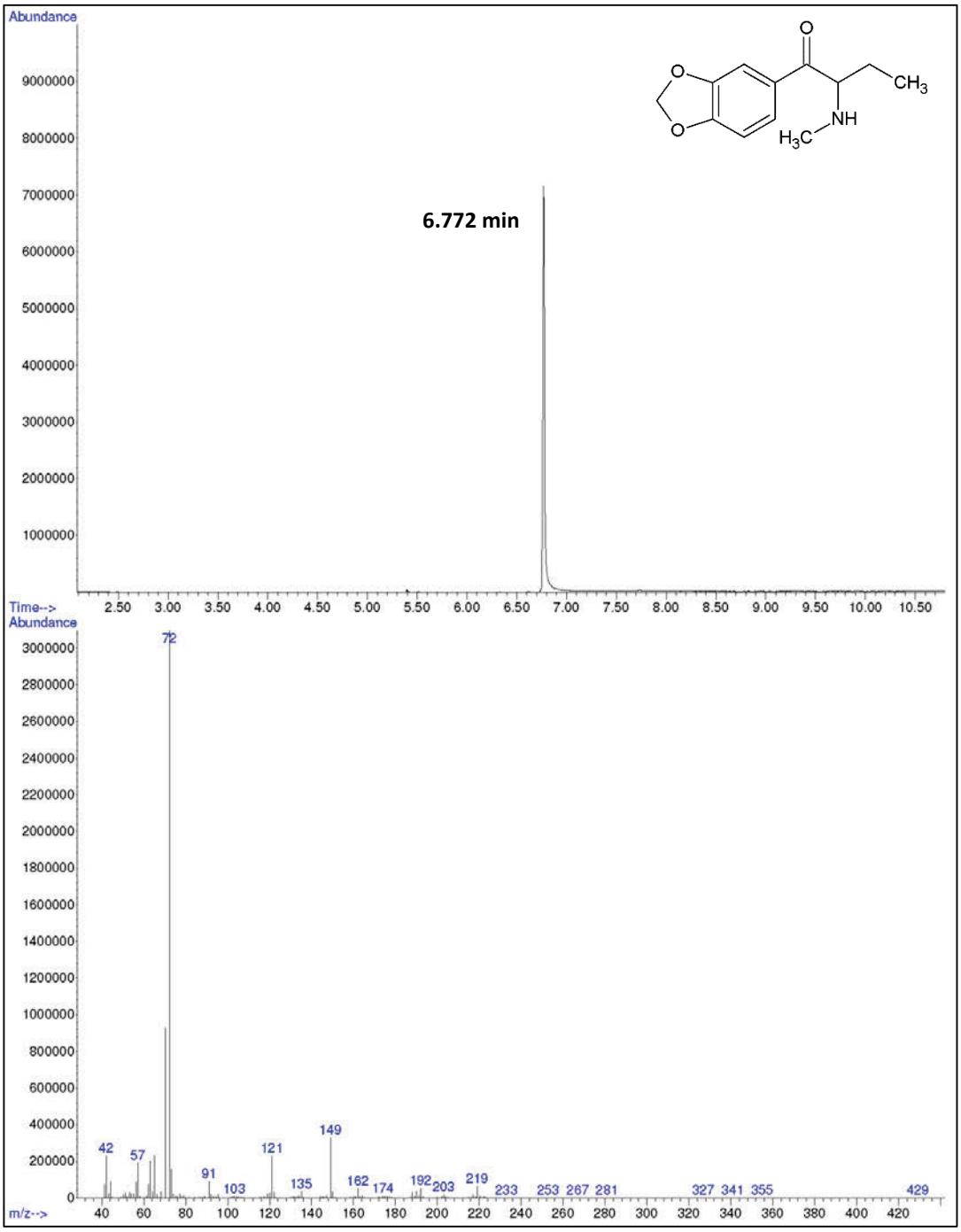

Figure A-47. Representative TIC of butylone HCl (**23**) (above) and associated mass spectrum (below).

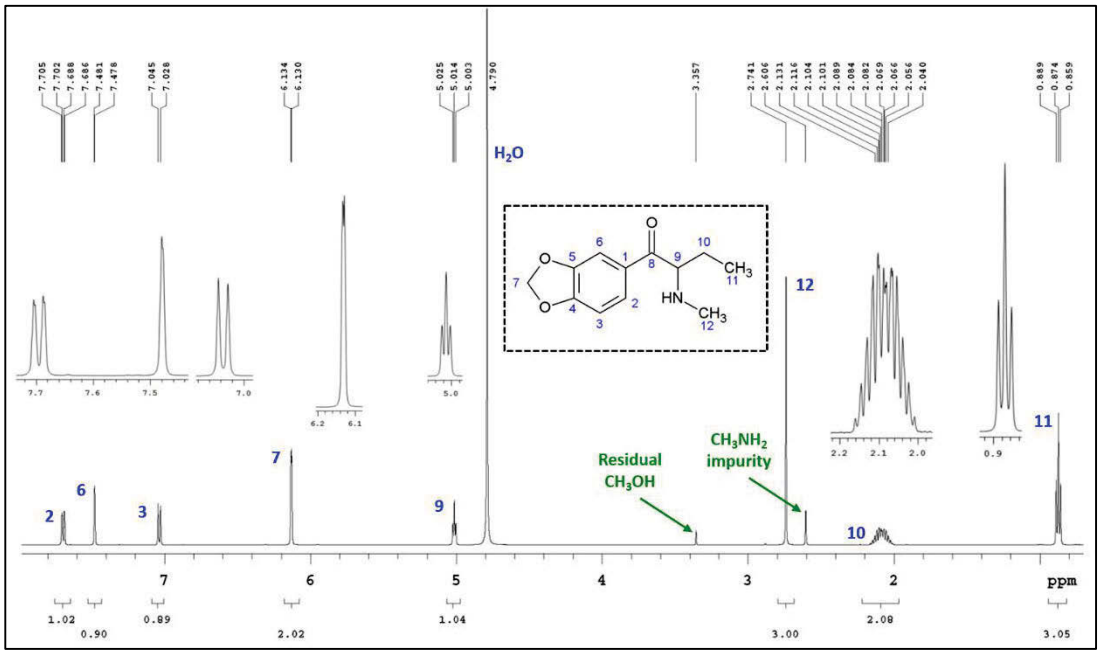

Figure A-48. Annotated ^{1}H-NMR spectrum of butylone HCl (**23**) measured in deuterated water (δ 4.79 ppm). Inset: zoomed regions containing splitting patterns

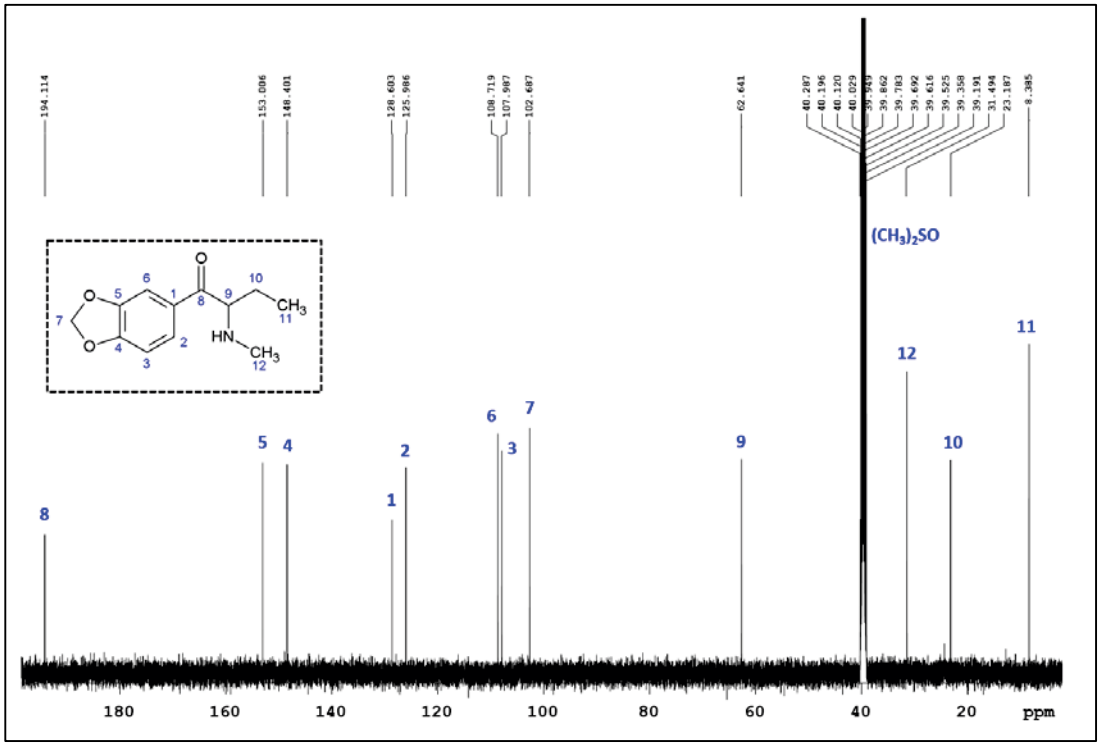

Figure A-49. Annotated ^{13}C-NMR spectrum of butylone HCl (**23**) measured in deuterated dimethyl sulfoxide (δ 39.52 ppm)

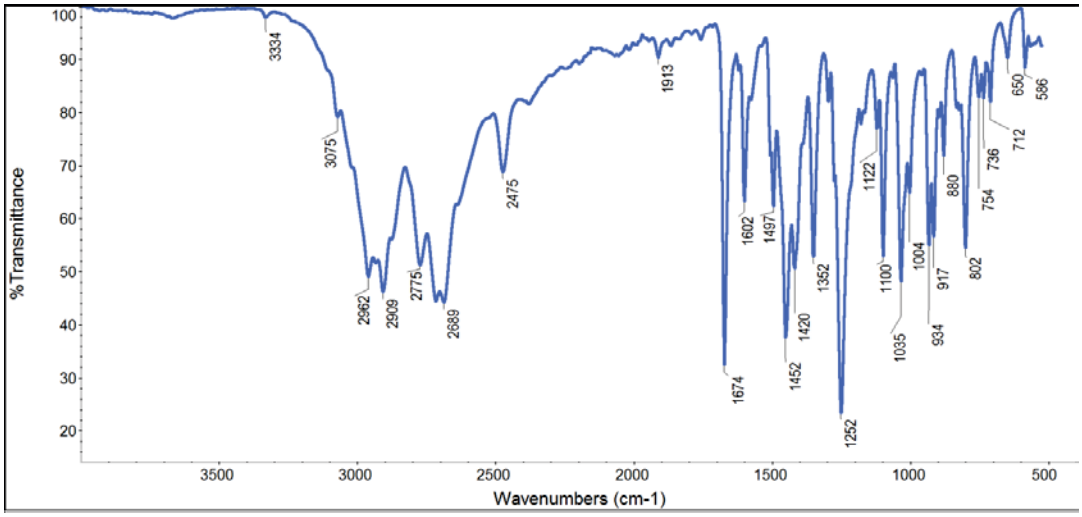

Figure A-50. ATR-FTIR spectrum of butylone HCl

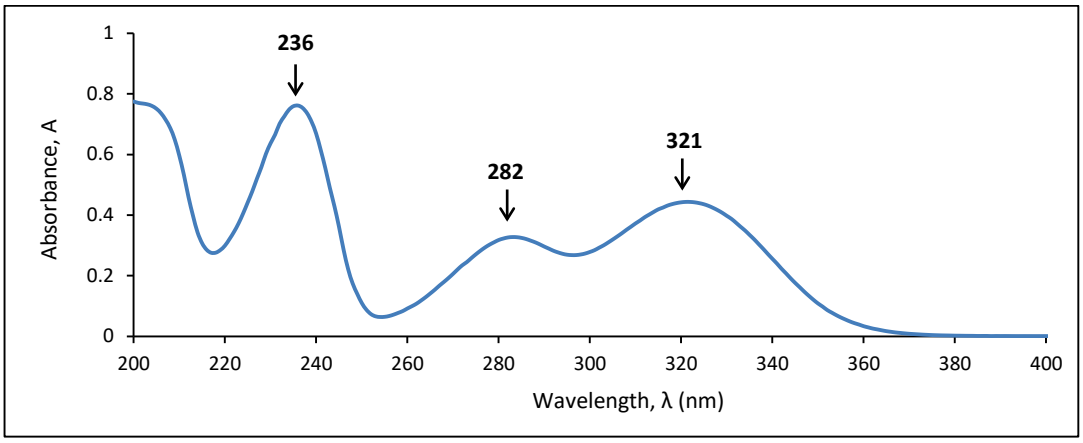

Figure A-51. UV spectrum of butylone HCl (**23**) in deionised water

A.9 Pentylone (24)

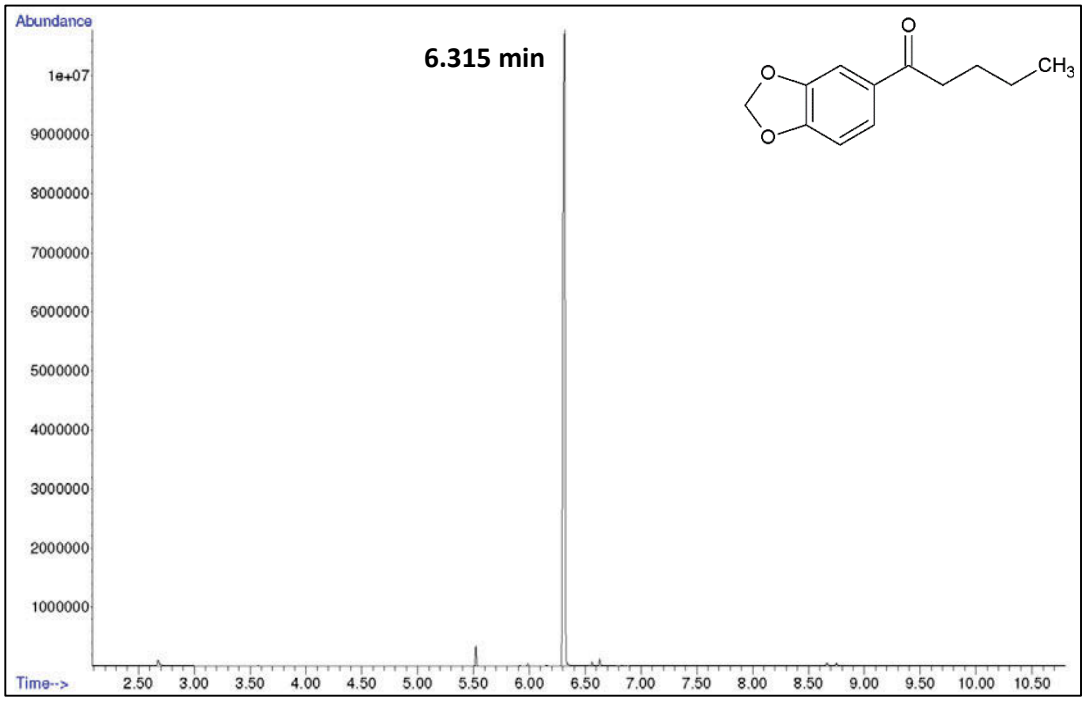

Figure A-52. Representative TIC of crude 1-(2H-1,3-benzodioxol-5-yl)pentan-1-one (**17**)

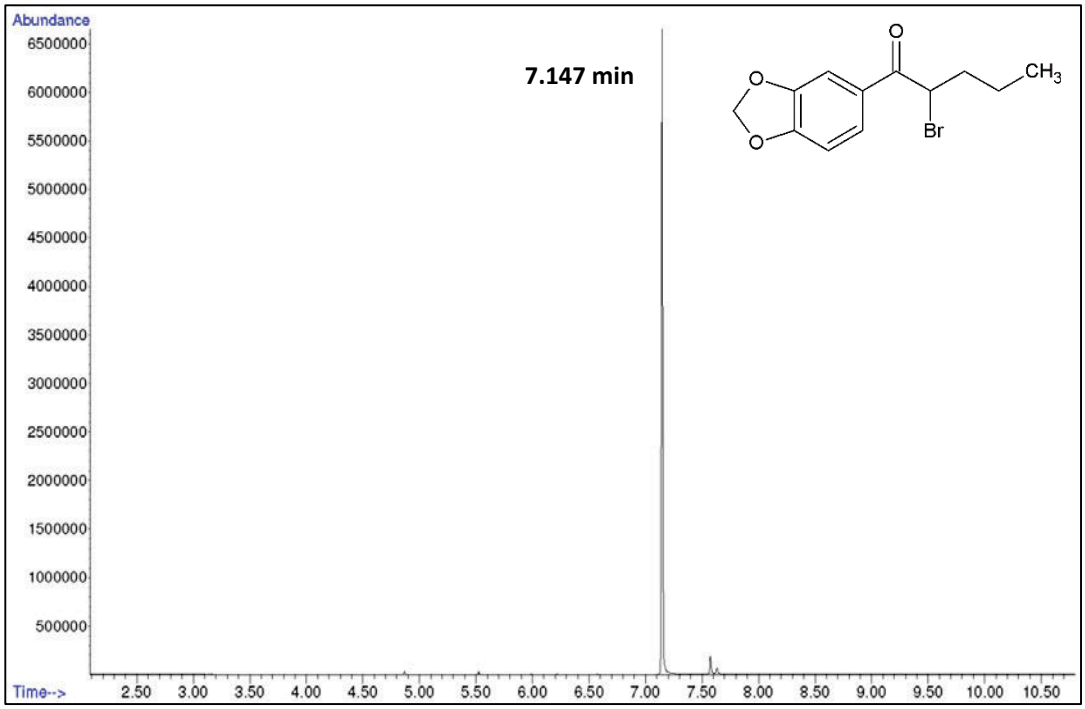

Figure A-53. Representative TIC of crude 1-(2H-1,3-benzodioxol-5-yl)-2-bromopentan-1-one (**18**)

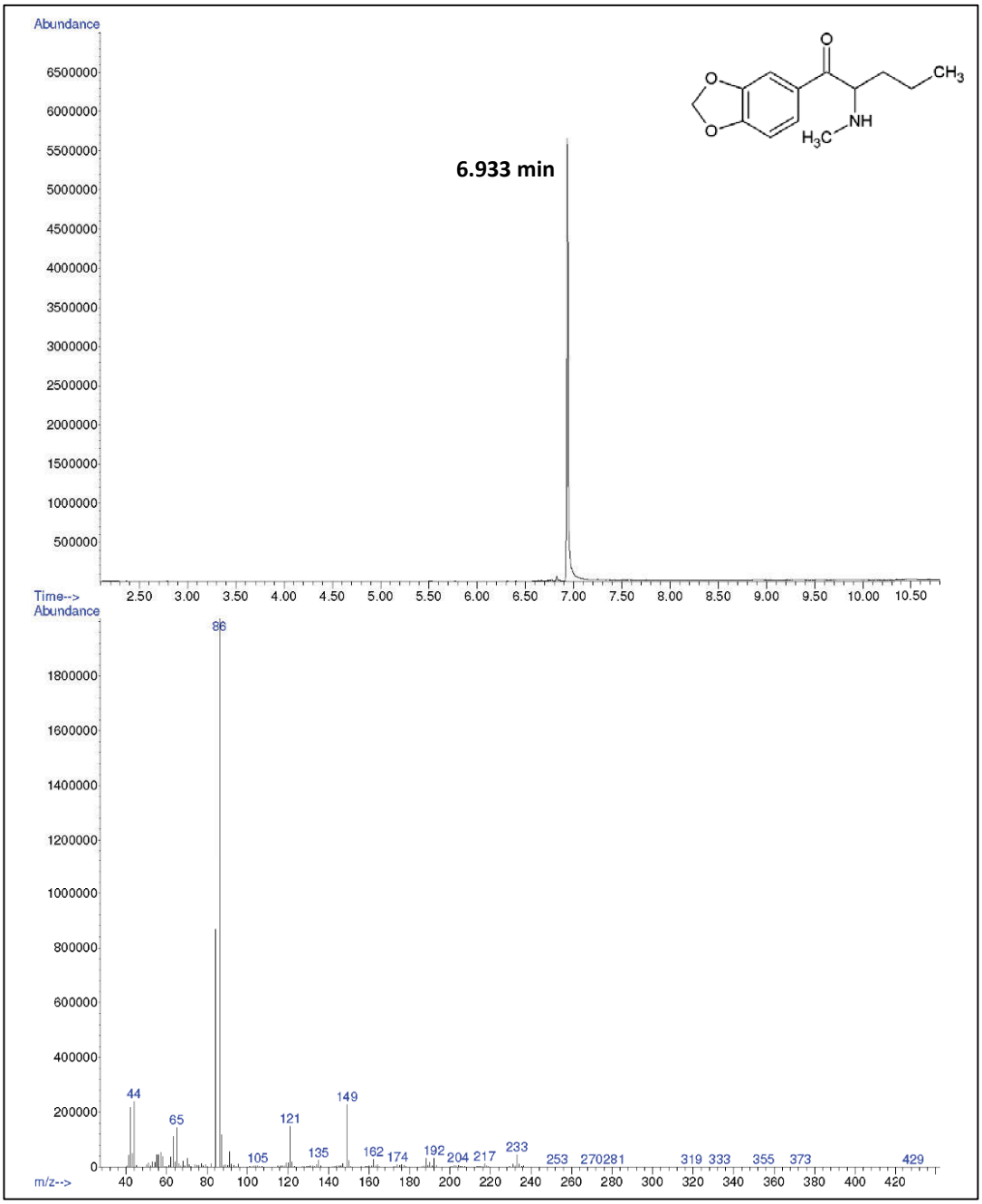

Figure A-54. Representative TIC of pentylone HCl (**24**) (above) and associated mass spectrum (below).

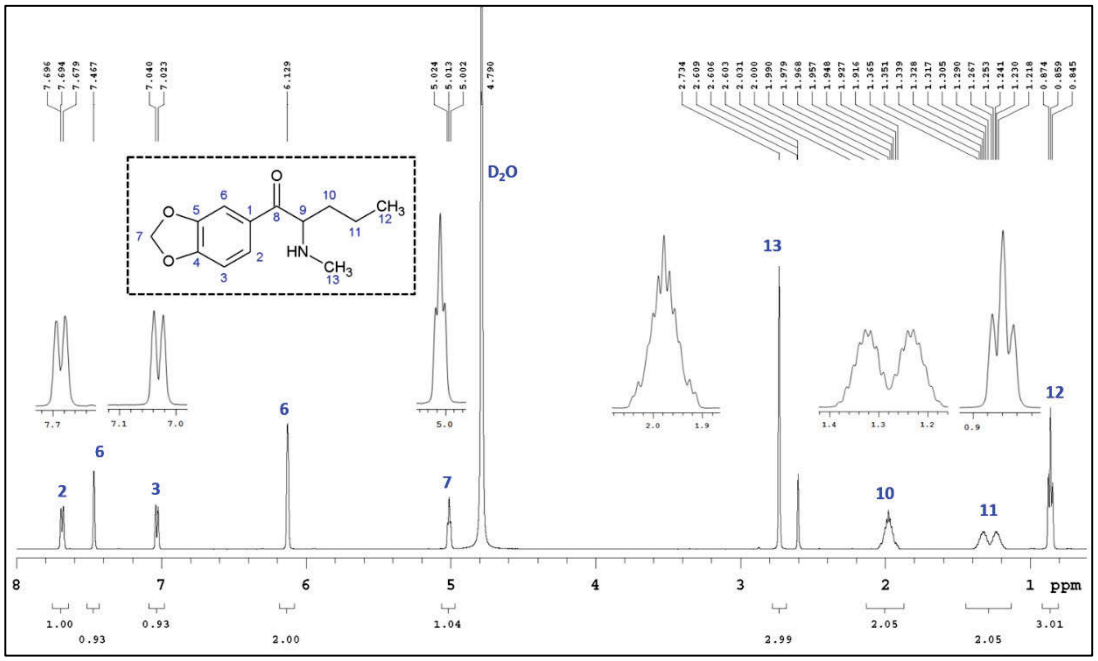

Figure A-55. Annotated ^{1}H-NMR spectrum of pentylone HCl (**24**) measured in deuterated water (δ 4.79 ppm). Inset: zoomed regions containing splitting patterns

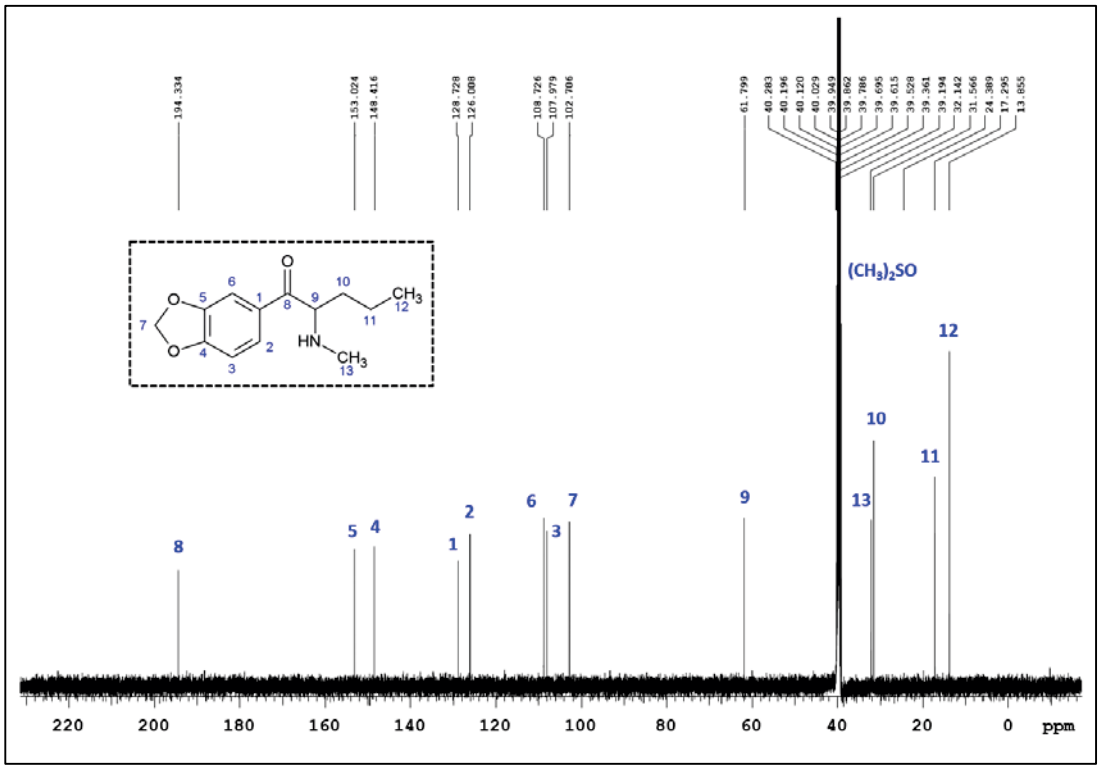

Figure A-56. Annotated ^{13}C-NMR spectrum of pentylone HCl (**24**) measured in deuterated dimethyl sulfoxide (δ 39.52 ppm)

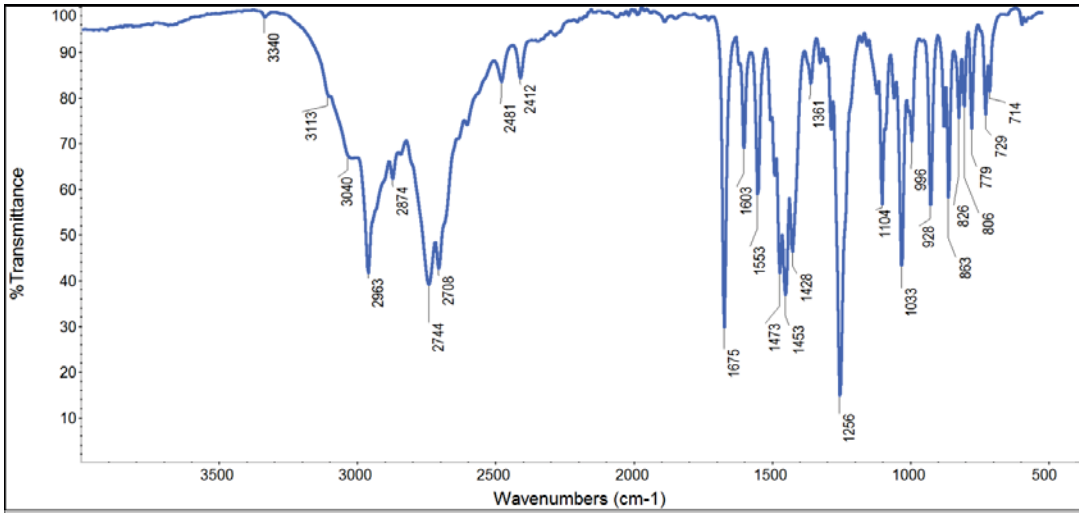

Figure A-57. ATR-FTIR spectrum of pentylone HCl (**24**)

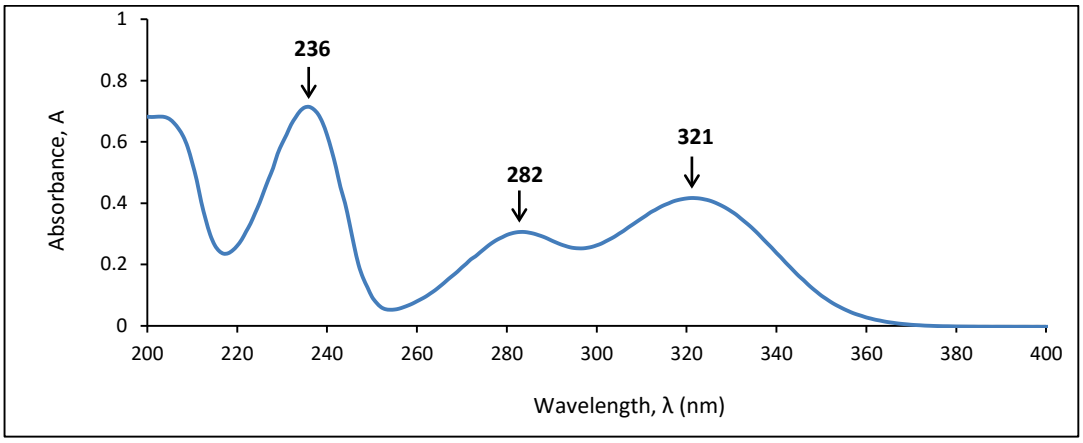

Figure A-58. UV spectrum of pentylone HCl (**24**) in deionised water

A.10 Pyrovalerone (29)

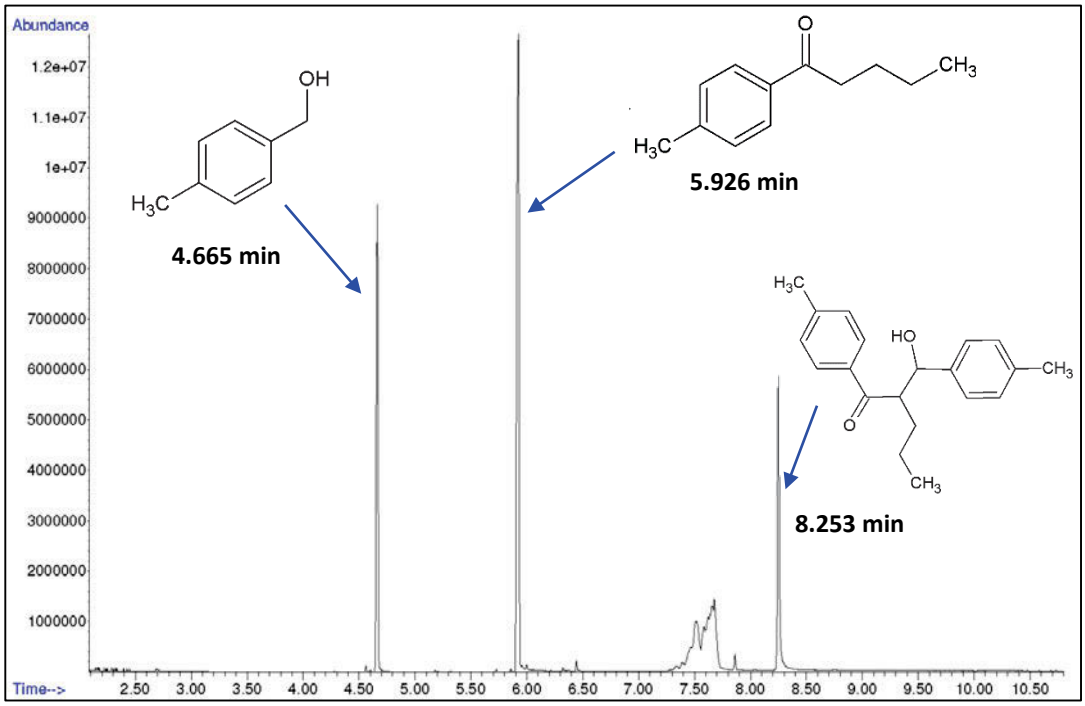

Figure A-59. Representative TIC of crude 1-(4-methylphenyl)pentan-1-one (**27**)

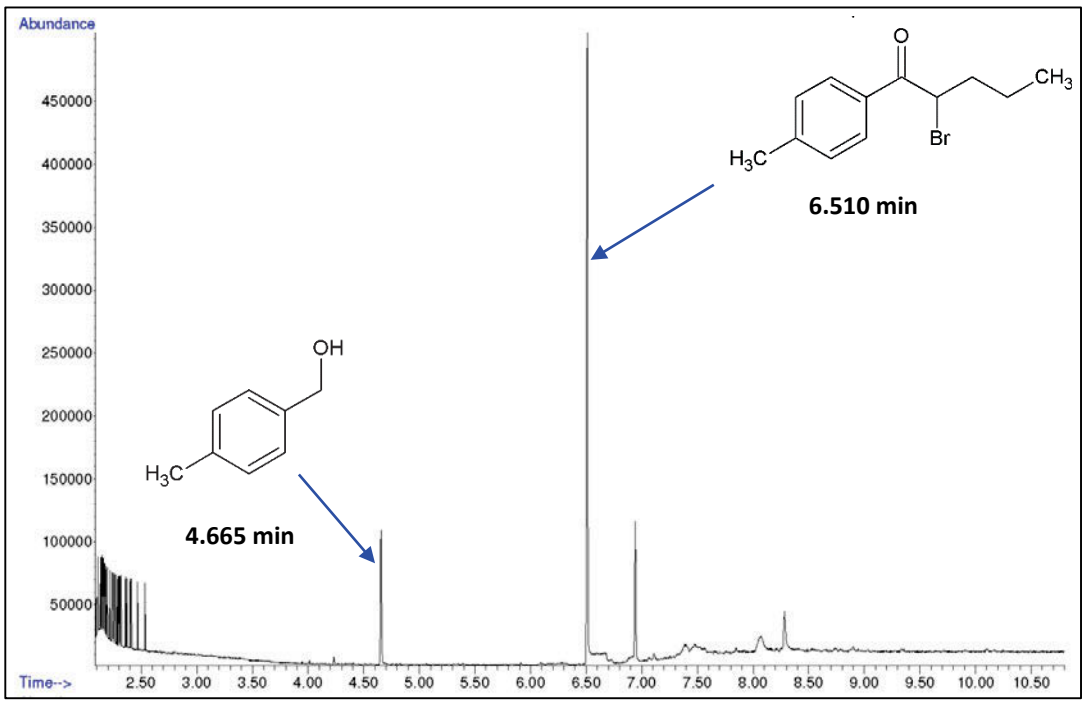

Figure A-60. Representative TIC of crude 2-bromo-1-(4-methylphenyl)pentan-1-one (**28**)

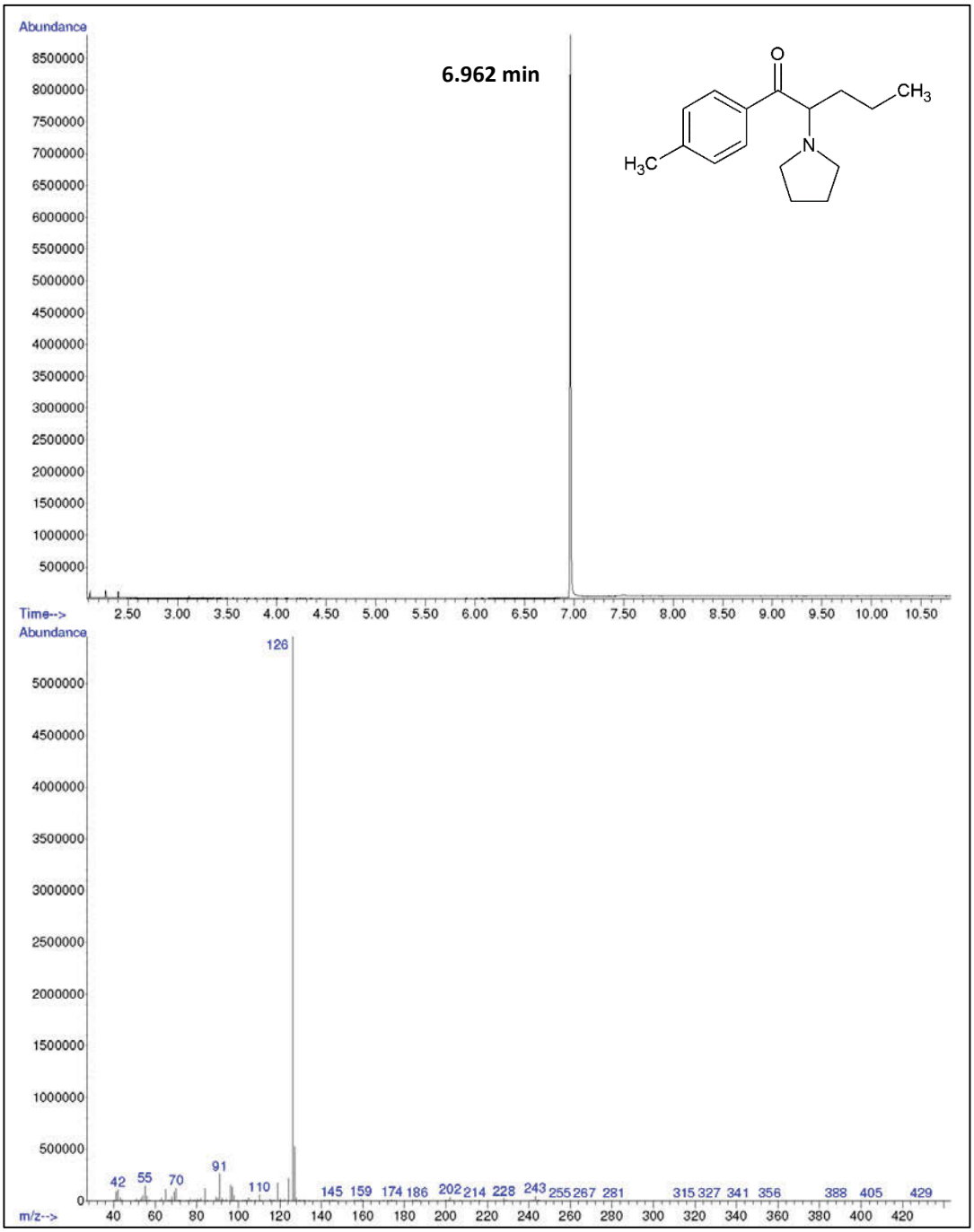

Figure A-61. Representative TIC of pyrovalerone HCl (**29**) (above) and associated mass spectrum (below).

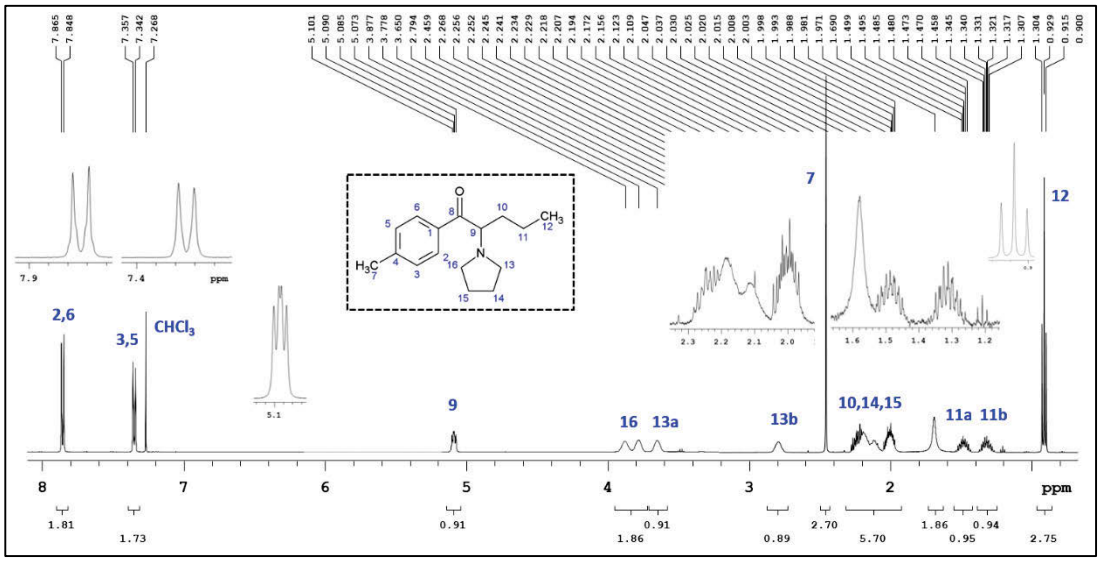

Figure A-62. Annotated ^{1}H-NMR spectrum of pyrovalerone HCl (**29**) measured in deuterated chloroform (δ 7.26 ppm). Inset: zoomed regions containing splitting patterns

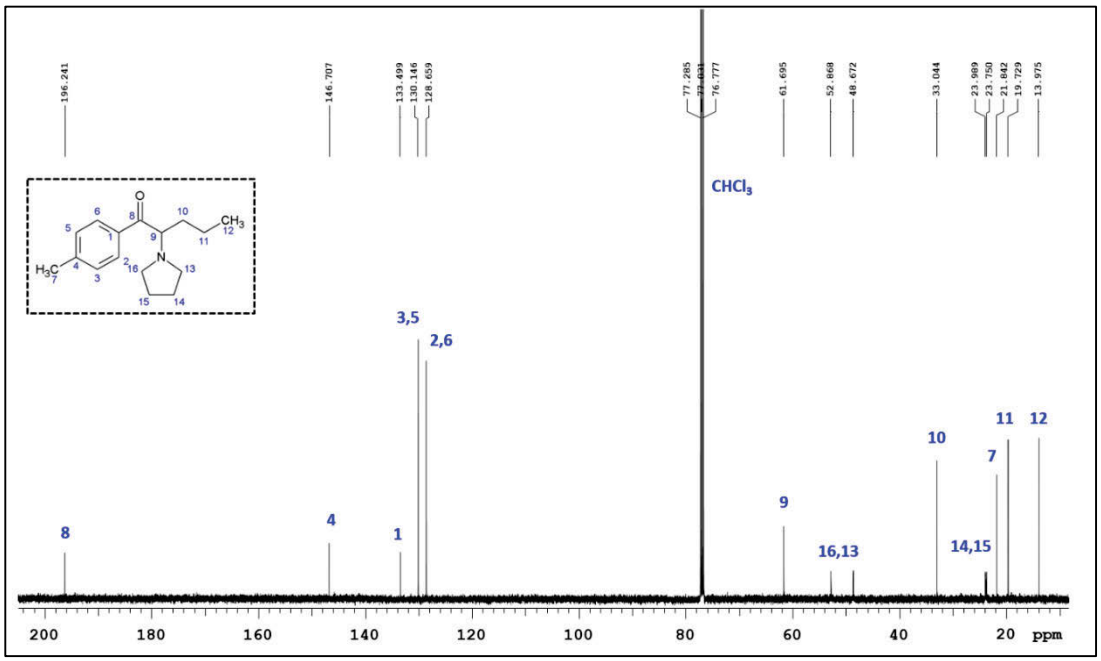

Figure A-63. Annotated ^{13}C-NMR spectrum of pyrovalerone HCl (**29**) measured in deuterated chloroform (δ 77.16 ppm)

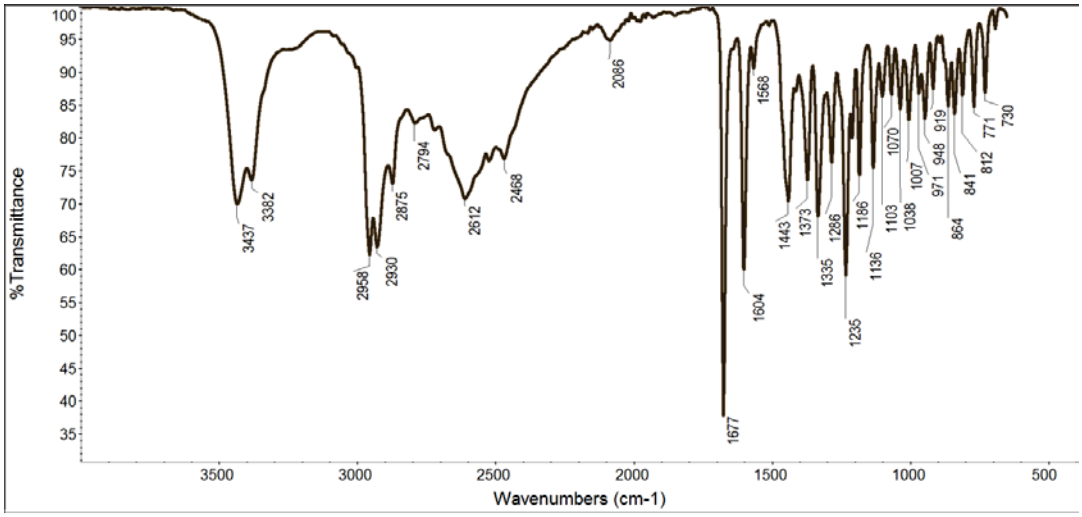

Figure A-64. ATR-FTIR spectrum of pyrovalerone HCl (**29**)

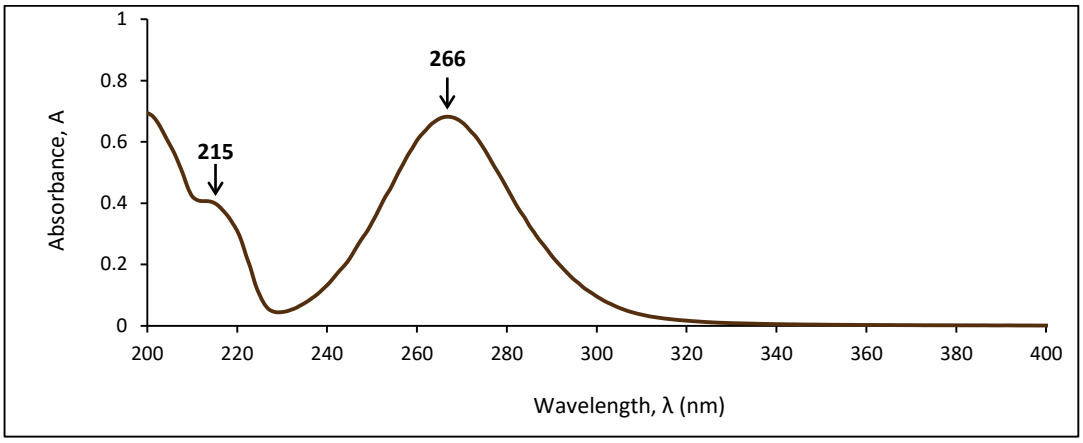

Figure A-65. UV spectrum of pyrovalerone HCl (**29**) in deionised water

A.11 α-Pyrrolidinovalerophenone (α-PVP, 34)

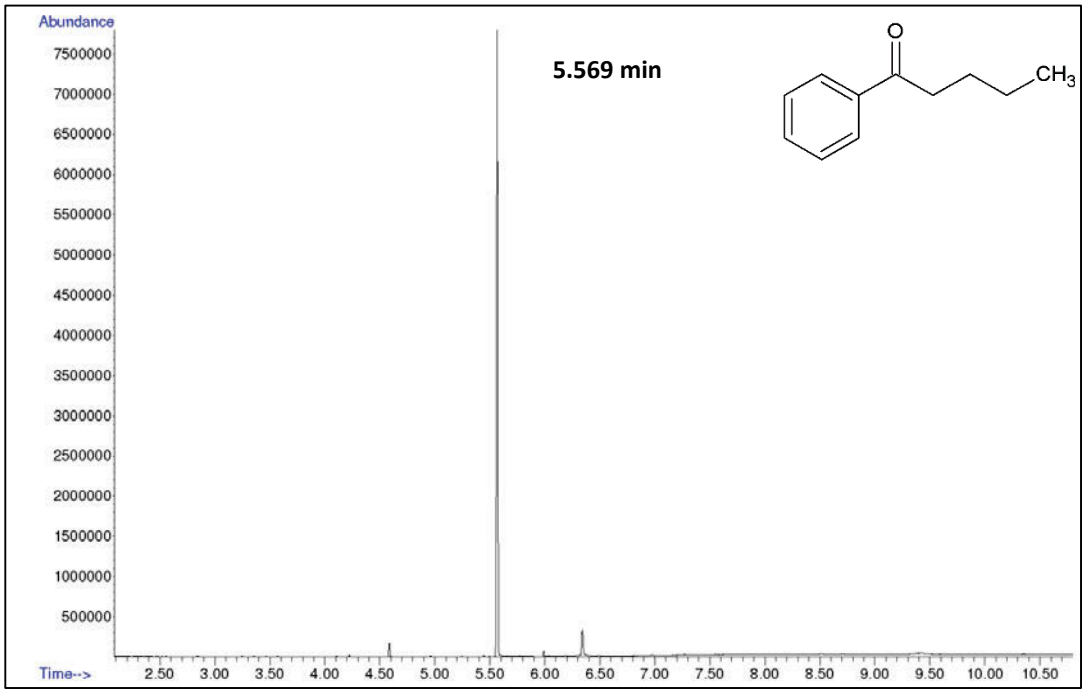

Figure A-66. Representative TIC of crude 1-phenylpentan-1-one (**32**)

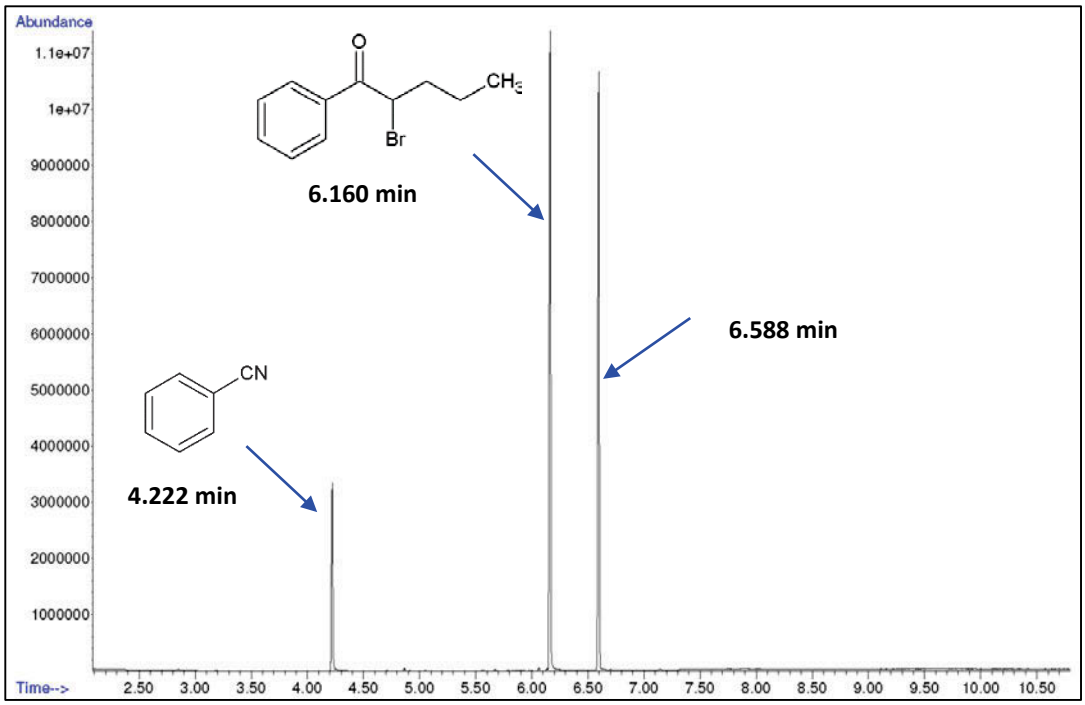

Figure A-67. Representative TIC of crude 2-bromo-1-phenylpentan-1-one (**33**)

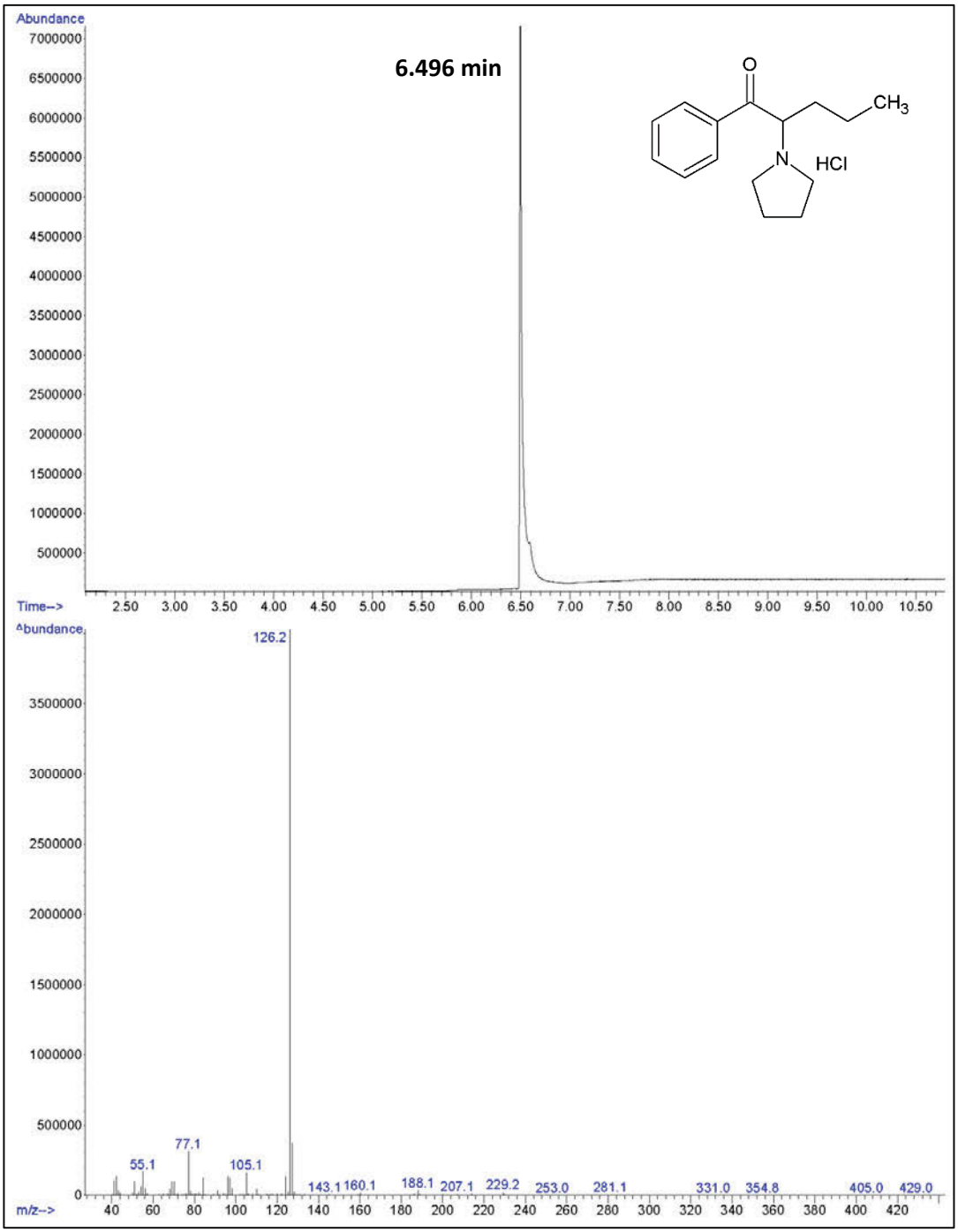

Figure A-68. Representative TIC of α-PVP HCl (**34**) (above) and associated mass spectrum (below)

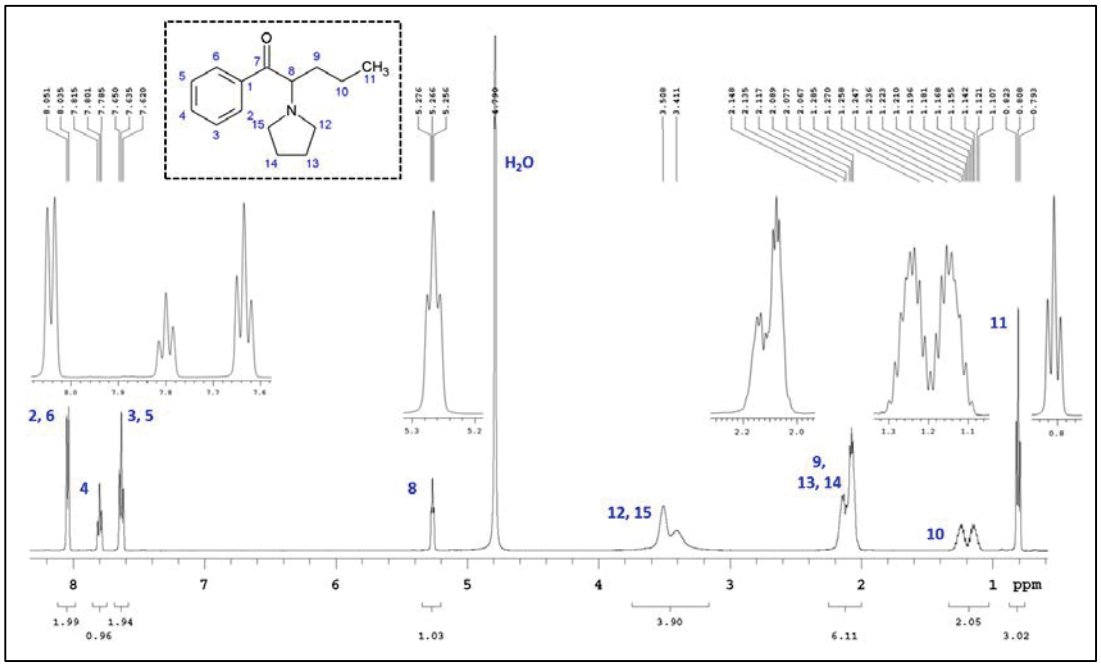

Figure A-69. Annotated ^{1}H-NMR spectrum of α-PVP HCl (**34**) measured in deuterated water (δ 4.79 ppm). Inset: zoomed regions containing splitting patterns

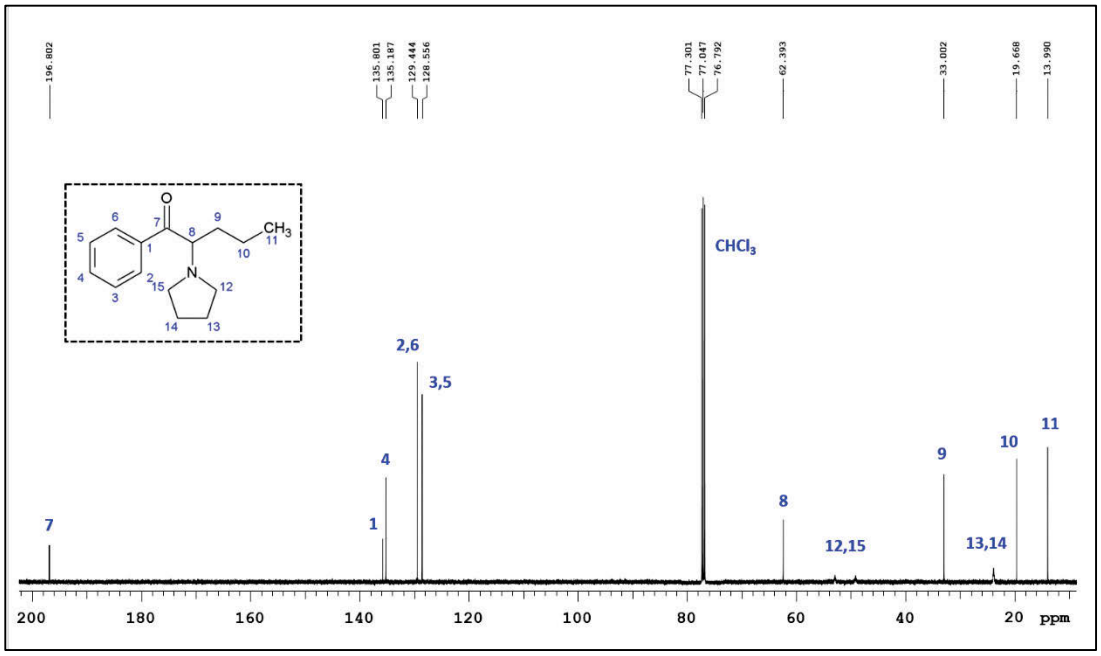

Figure A-70. Annotated ^{13}C-NMR spectrum of α-PVP HCl (**34**) measured in deuterated chloroform (δ 77.16 ppm)

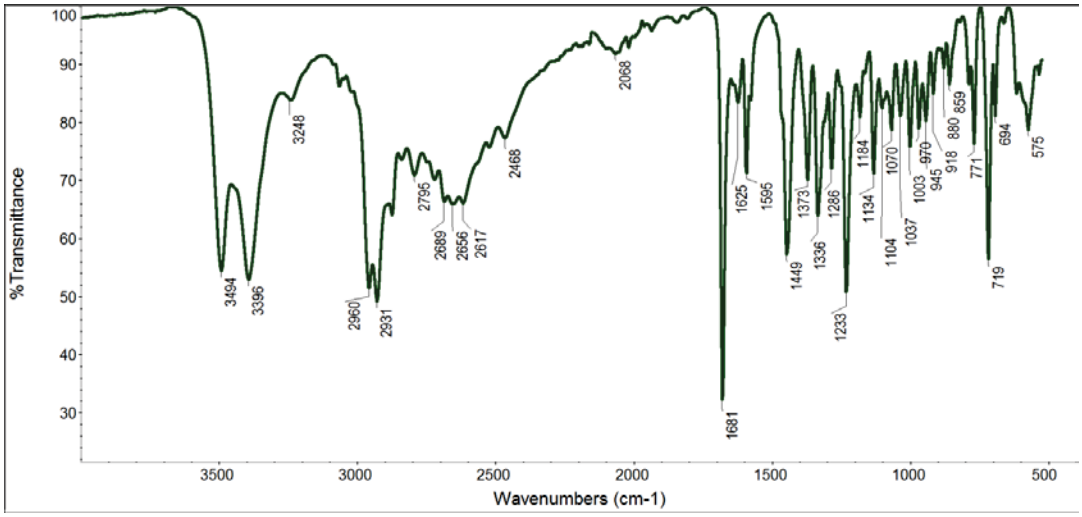

Figure A-71. ATR-FTIR spectrum of a-PVP HCl (**34**)

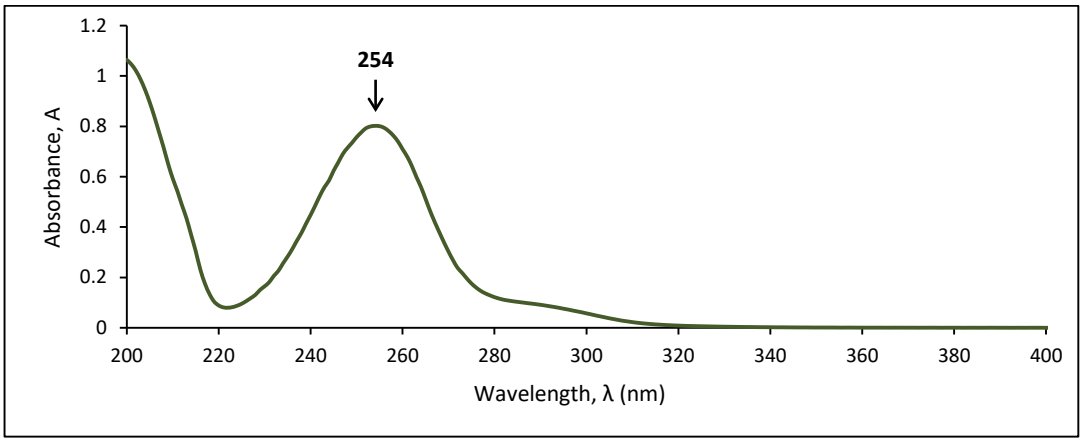

Figure A-72. UV spectrum of a-PVP HCl (**34**) in deionised water

A.12 4-Ethylmethcathinone (4-EMC, 39)

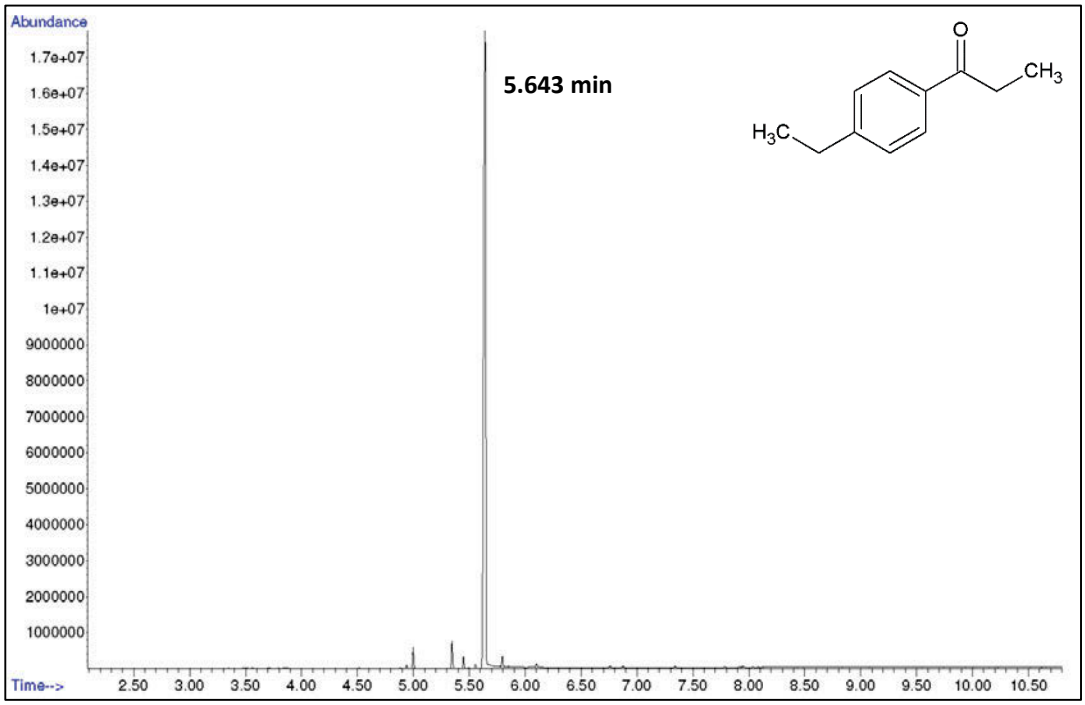

Figure A-73. Representative TIC of crude 1-(4-ethylphenyl)propan-1-one (**37**)

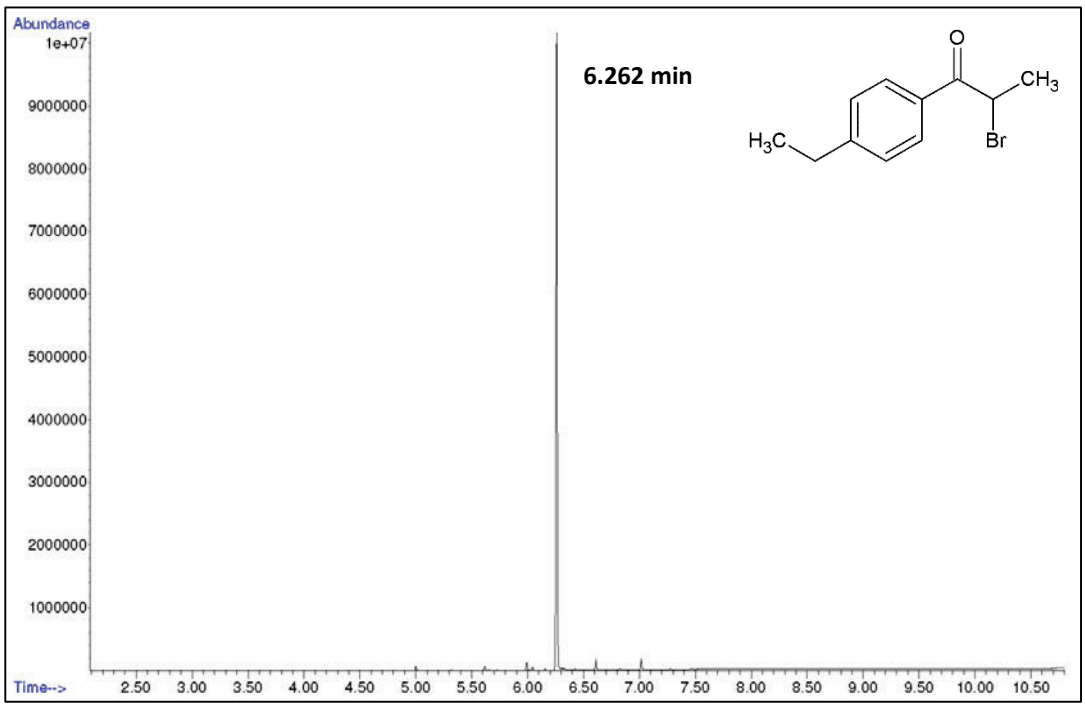

Figure A-74. Representative TIC of crude 2-bromo-1-(4-ethylphenyl)propan-1-one (**38**)

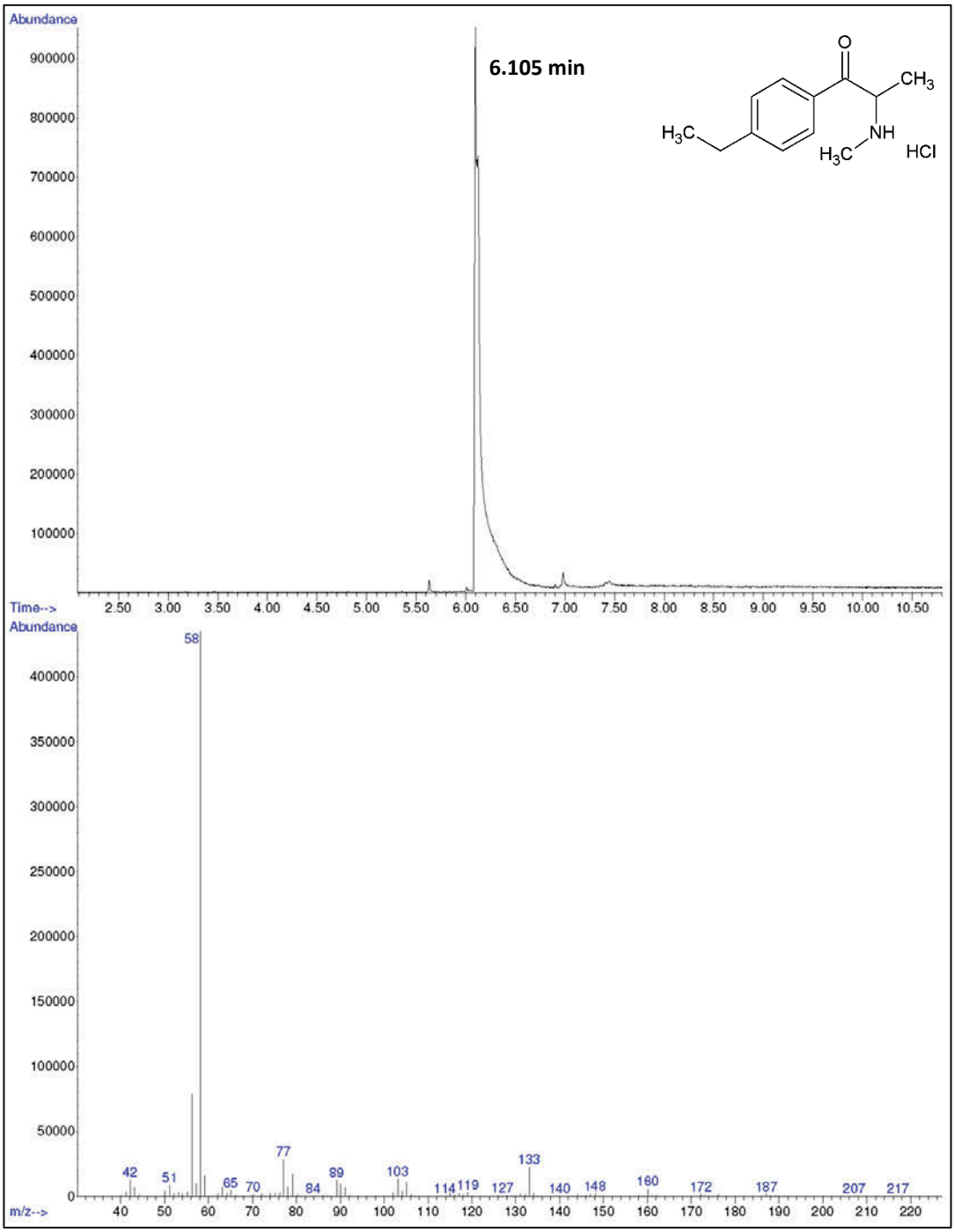

Figure A-75. Representative TIC of 4-EMC HCl (**39**) (above) and associated mass spectrum (below).

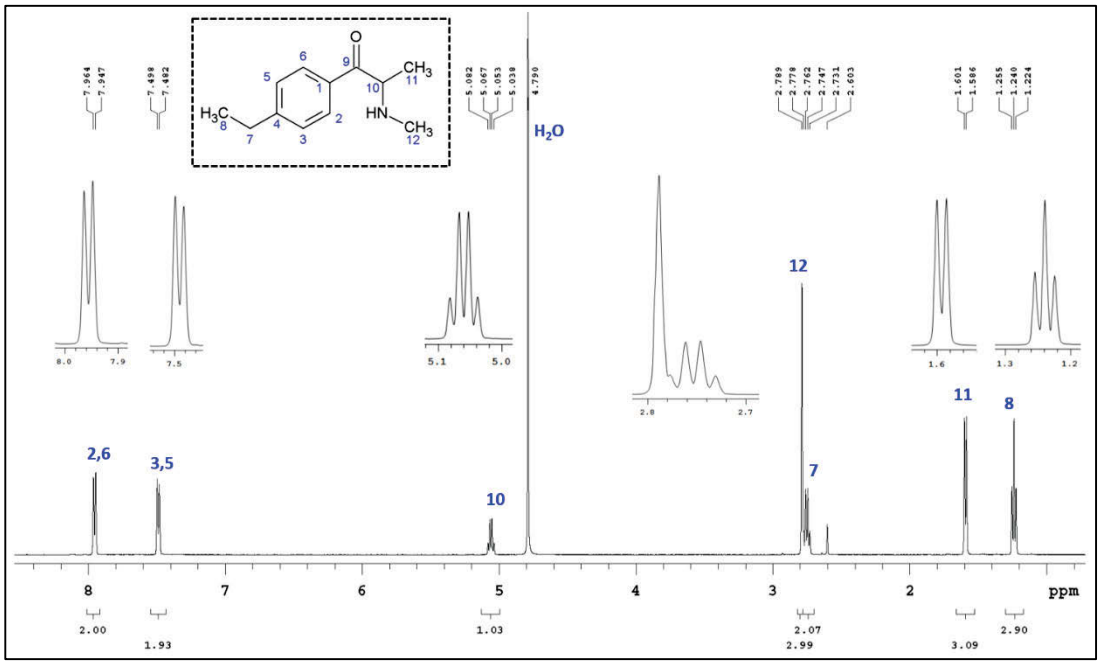

Figure A-76. Annotated ^{1}H-NMR spectrum of 4-EMC HCl (**39**) measured in deuterated water (δ 4.79 ppm). Inset: zoomed regions containing splitting patterns

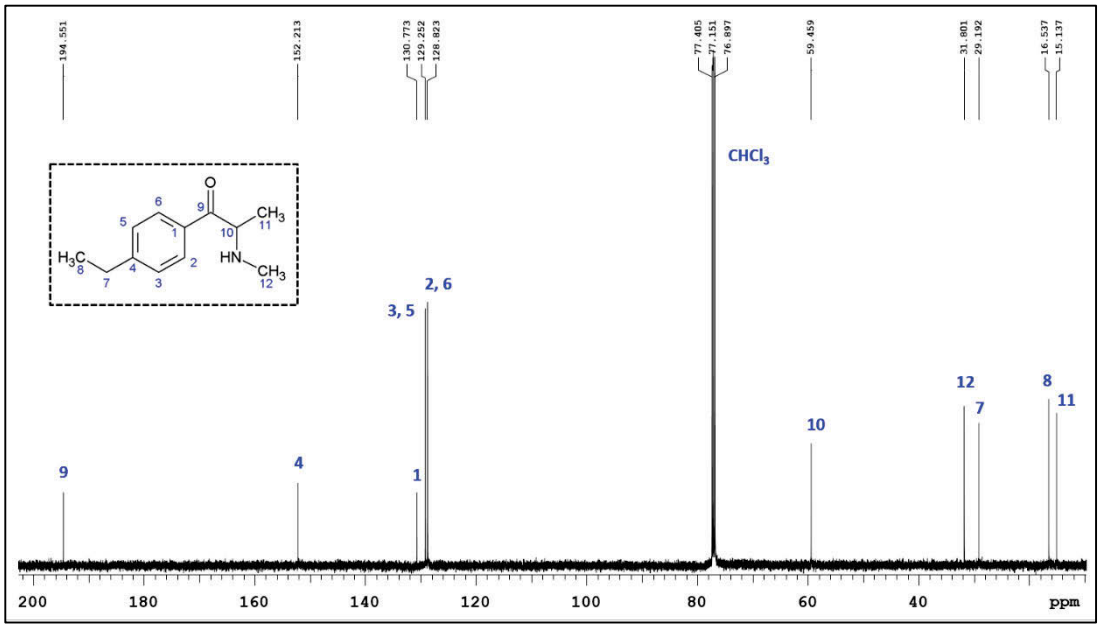

Figure A-77. Annotated ^{13}C-NMR spectrum of 4-EMC HCl (**39**) measured in deuterated chloroform (δ 77.16 ppm)

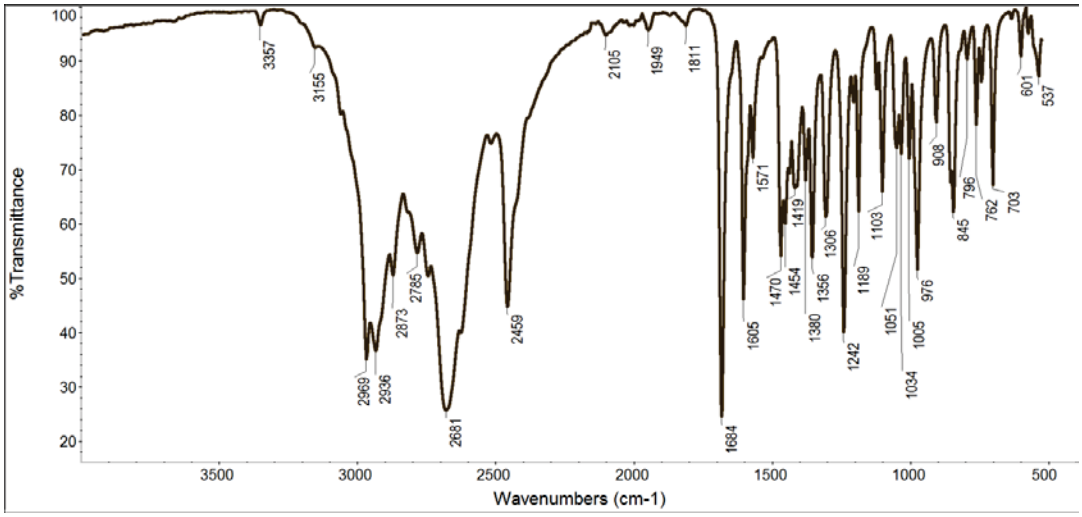

Figure A-78. ATR-FTIR spectrum of 4-EMC HCl (**39**)

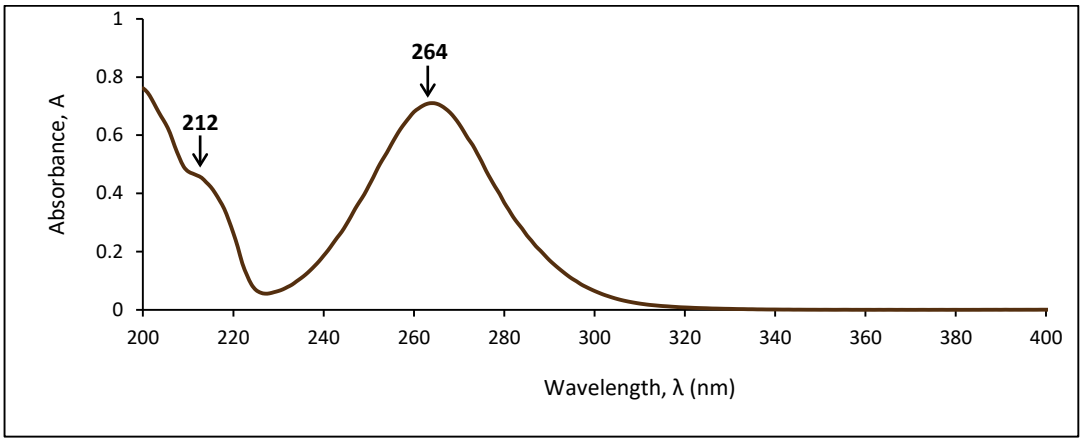

Figure A-79. UV spectrum of 4-EMC HCl (**39**) in deionised water

A.13 4-Methoxymethvalerone (4-MOMV, 44)

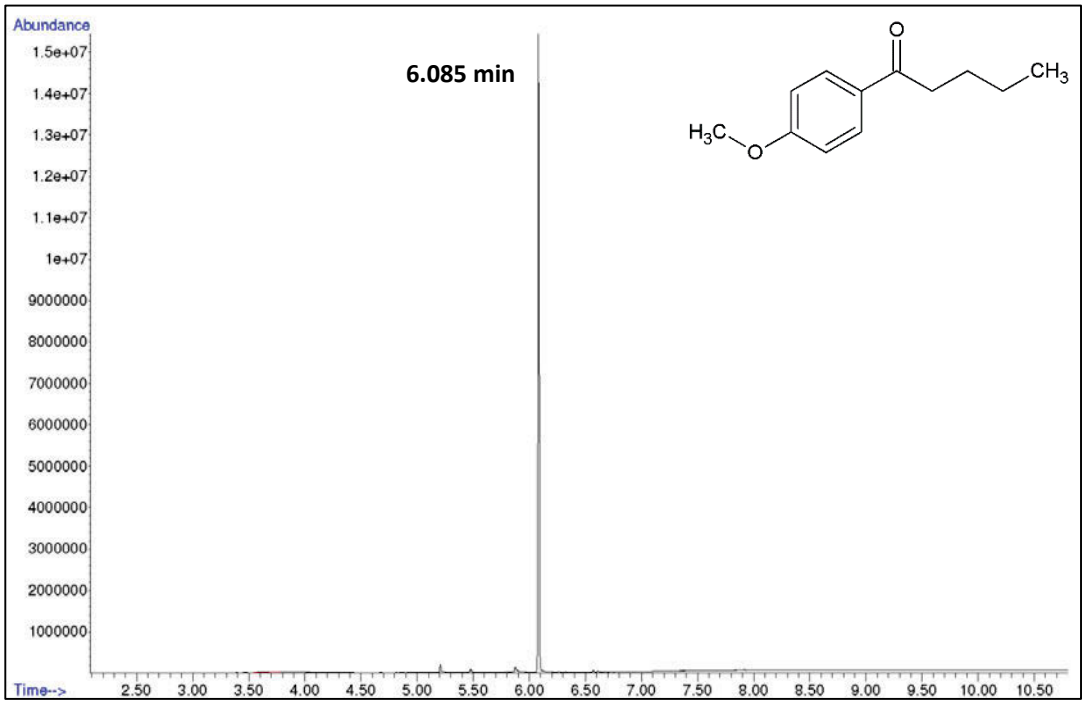

Figure A-80. Representative TIC of crude 1-(4-methoxyphenyl)propan-1-one (**42**)

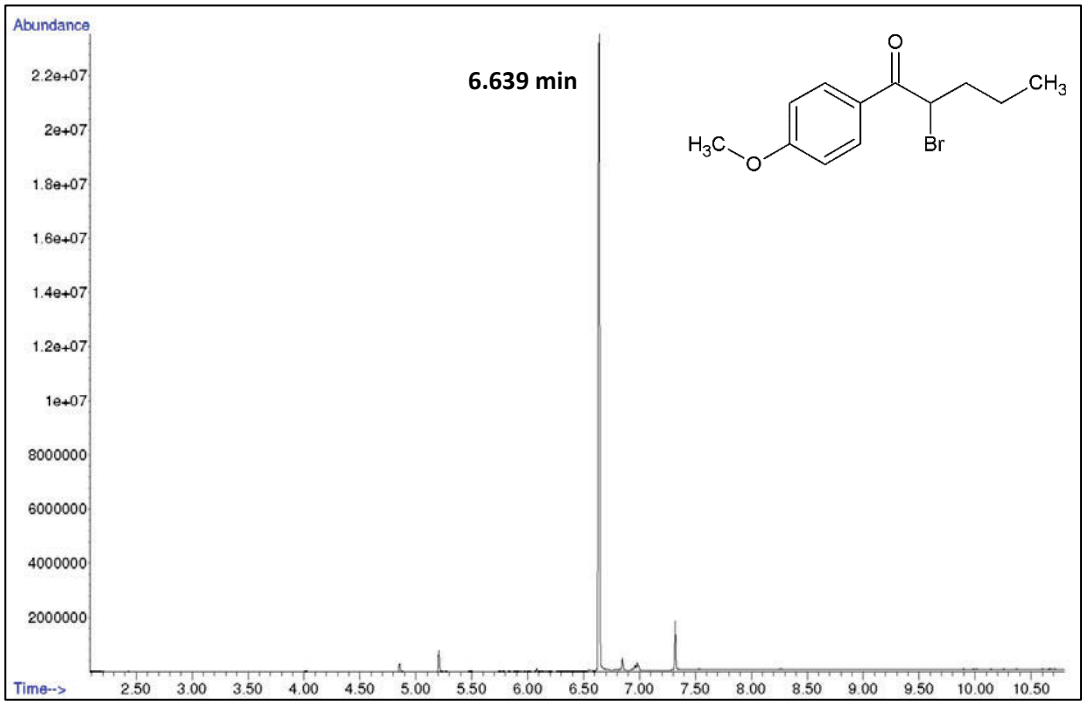

Figure A-81. Representative TIC of crude 2-bromo-1-(4-methoxyphenyl)propan-1-one (**43**)

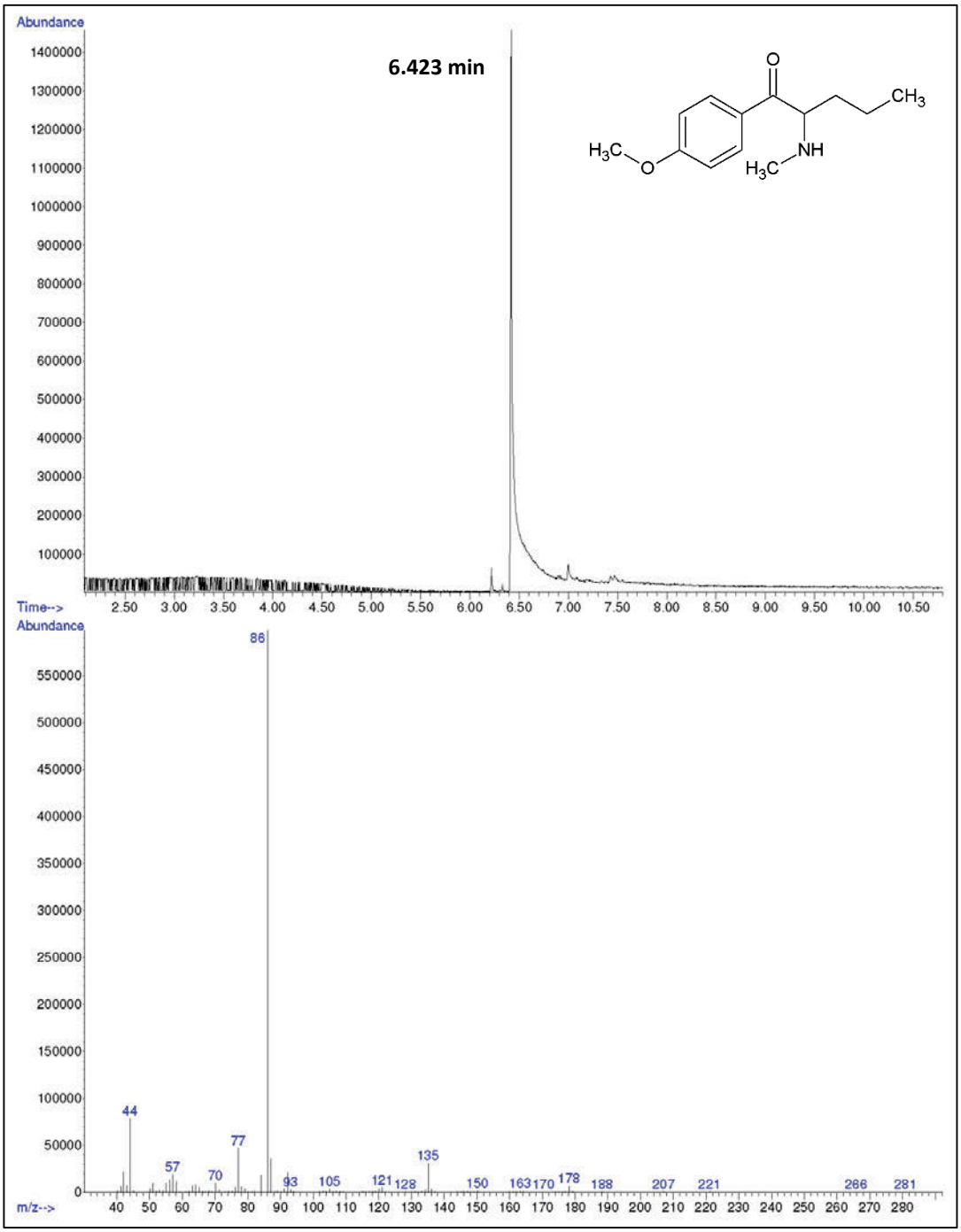

Figure A-82. Representative TIC of 4-MOMV HCl (**44**) (above) and associated mass spectrum (below).

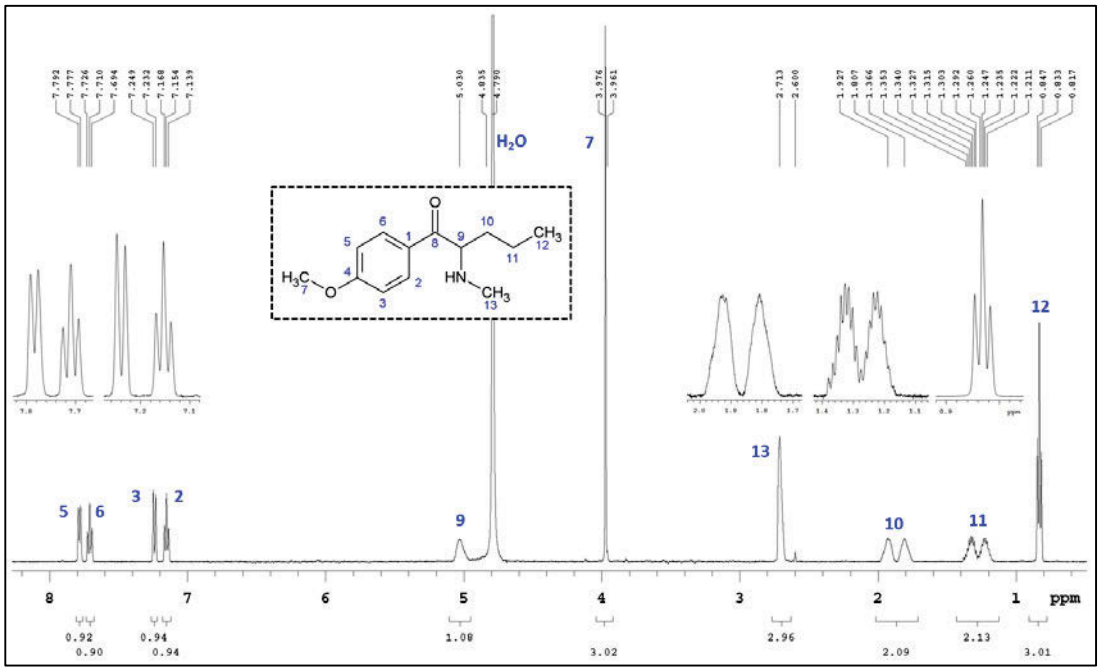

Figure A-83. Annotated ^{1}H-NMR spectrum of 4-MOMV HCl (**44**) measured in deuterated water (δ 4.79 ppm). Inset: zoomed regions containing splitting patterns

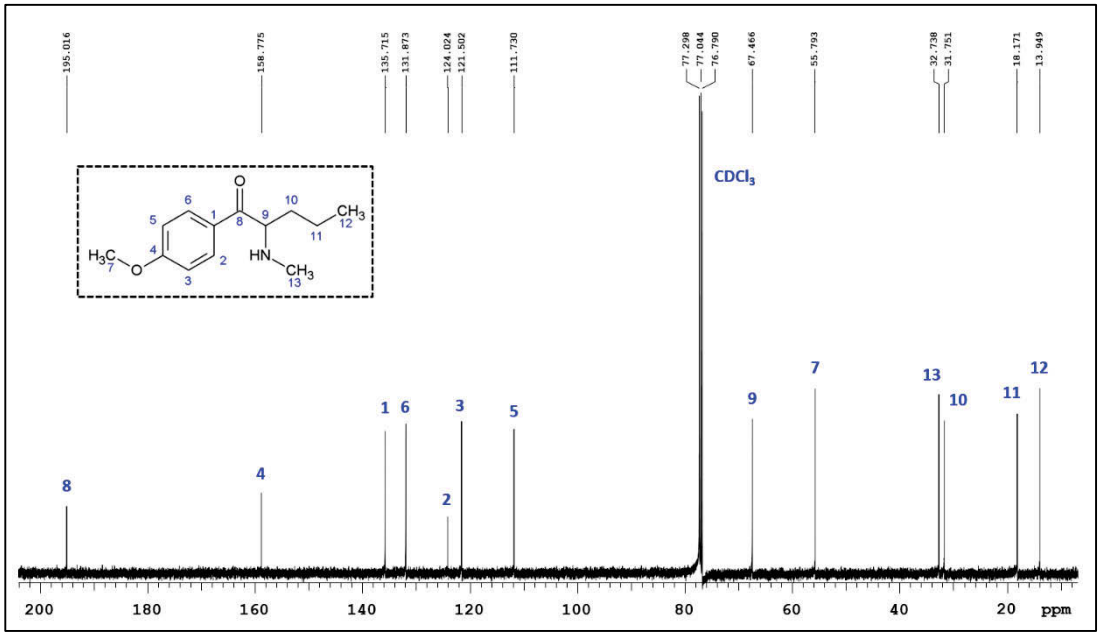

Figure A-84. Annotated ^{13}C-NMR spectrum of 4-MOMV HCl (**44**) measured in deuterated chloroform (δ 77.16 ppm)

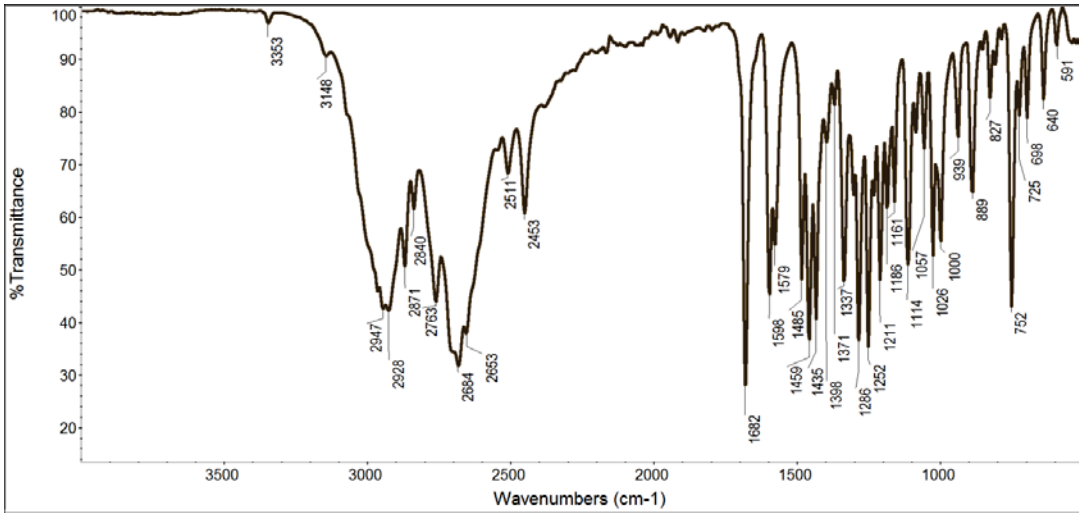

Figure A-85. ATR-FTIR spectrum of 4-MOMV HCl (**44**)

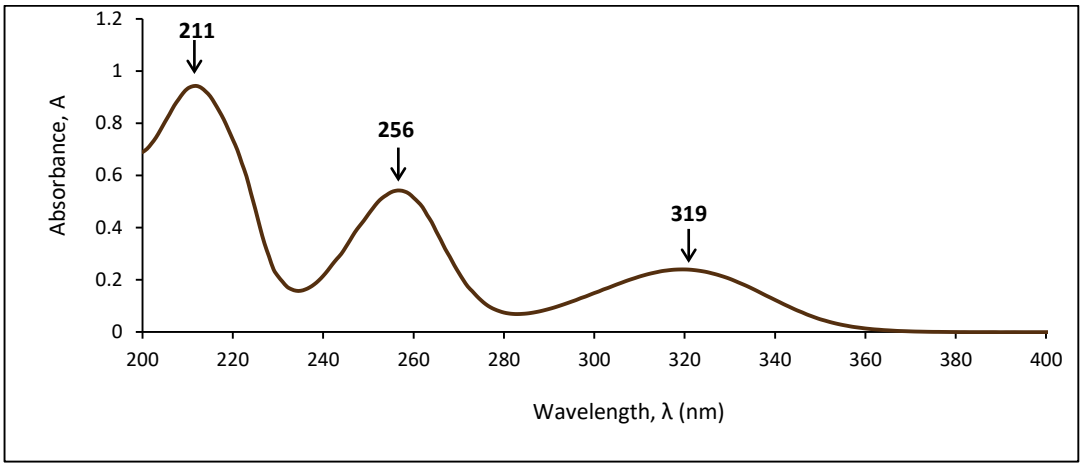

Figure A-86. UV spectrum of 4-MOMV HCl (**44**) in deionised water

A.14 Ethylone (45)

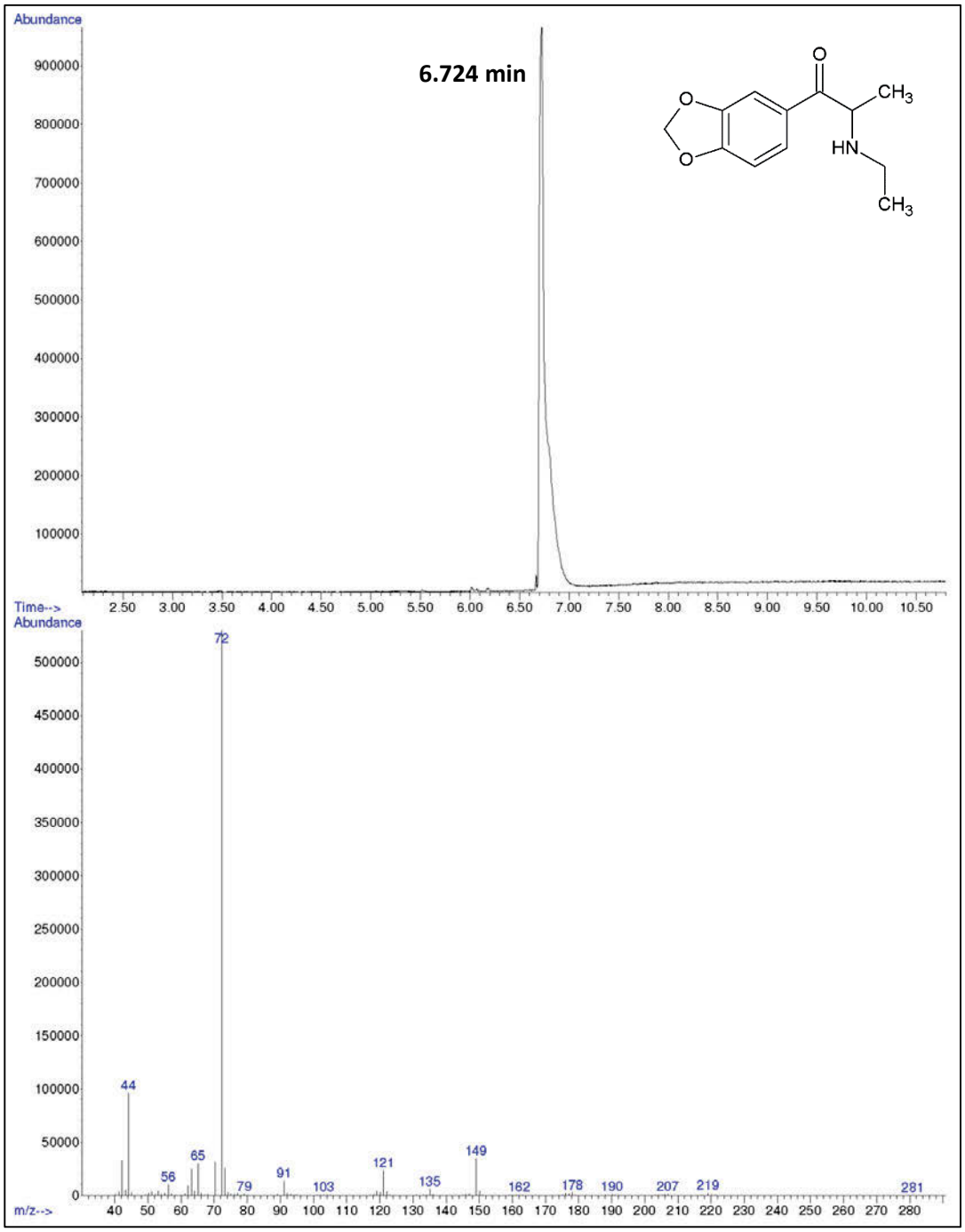

Figure A-87. Representative TIC of ethylone HCl (**45**) (above) and associated mass spectrum (below).

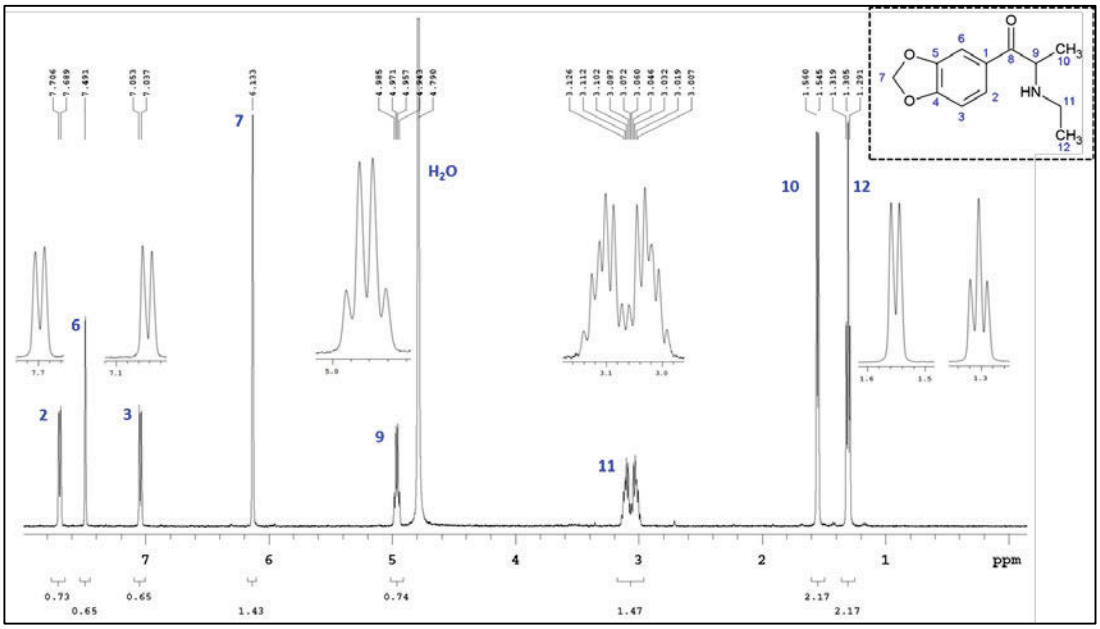

Figure A-88. Annotated ^{1}H-NMR spectrum of ethylone HCl (**45**) measured in deuterated water (δ 4.79 ppm). Inset: zoomed regions containing splitting patterns

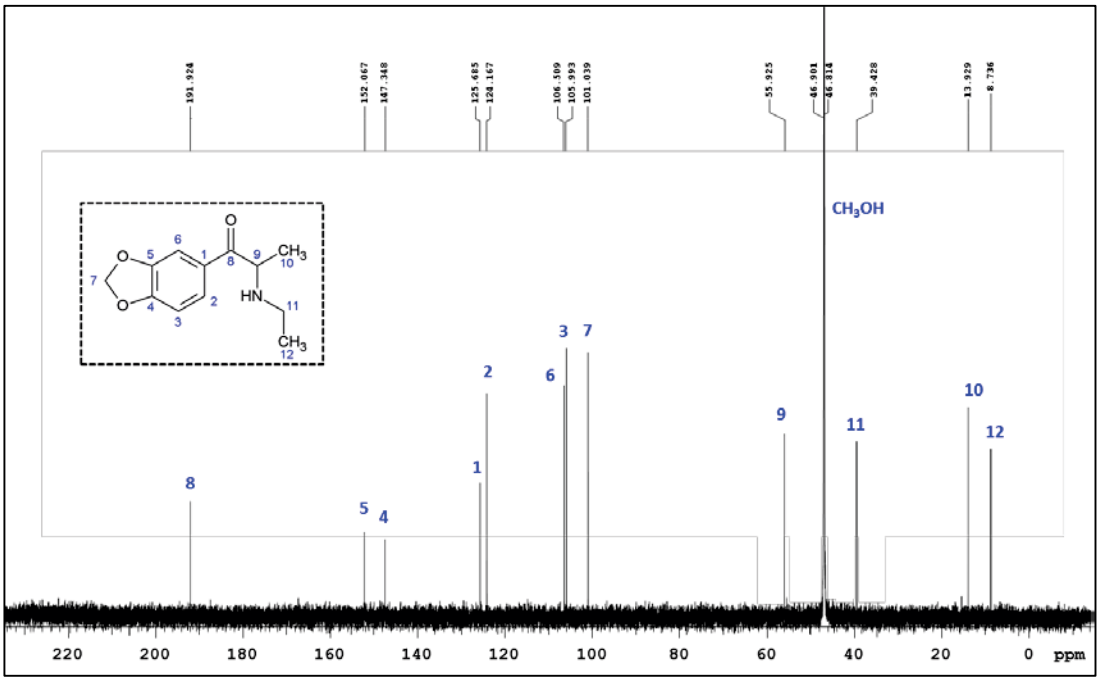

Figure A-89. Annotated ^{13}C-NMR spectrum of ethylone HCl (**45**) measured in deuterated methanol (δ 49.00 ppm)

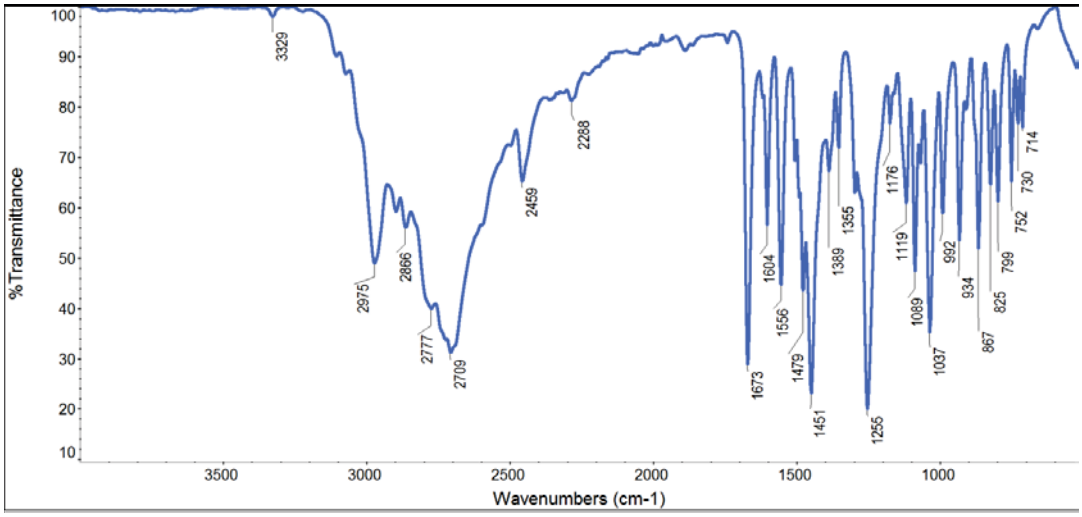

Figure A-90. ATR-FTIR spectrum of ethylone HCl (**45**)

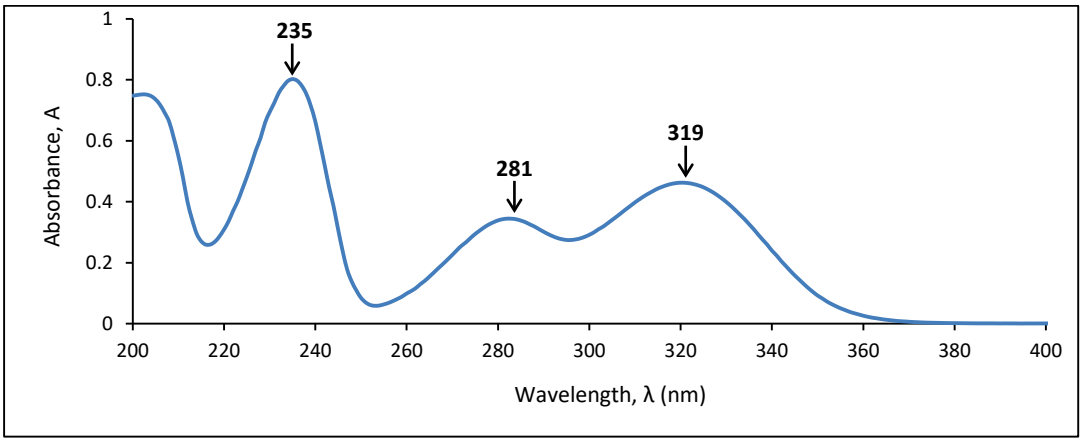

Figure A-91. UV spectrum of ethylone HCl (**45**) in deionised water

A.15 2-(Methylamino)-1-(naphthalen-1-yl)propan-1-one (α-naphth, 50)

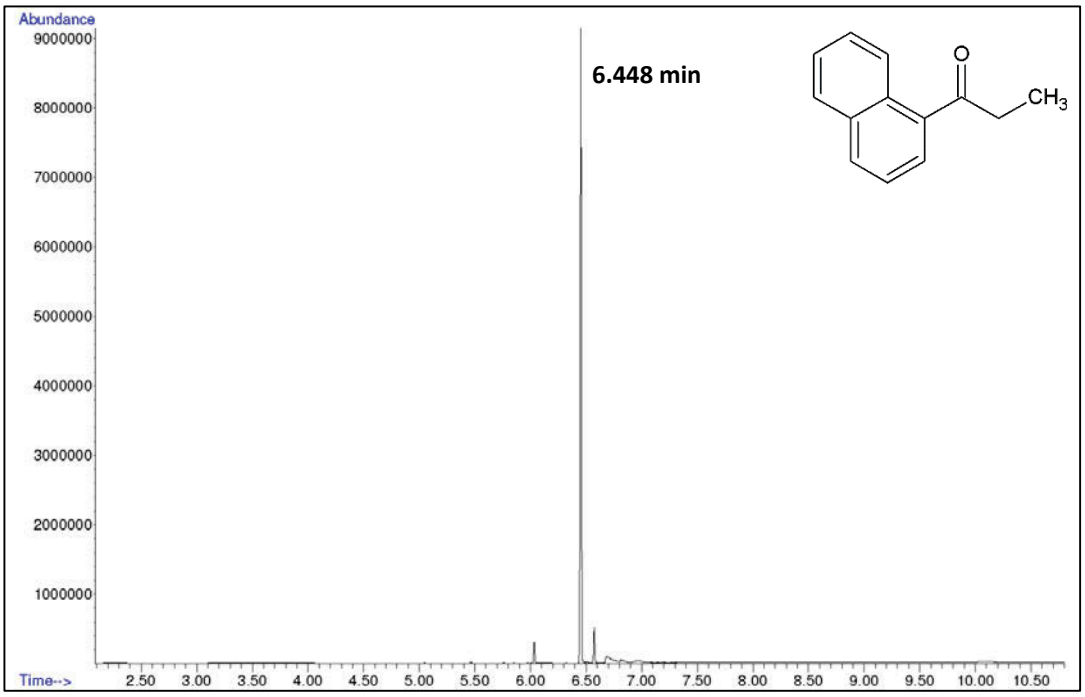

Figure A-92. Representative TIC of crude 1-(naphthalen-1-yl)propan-1-one (**48**)

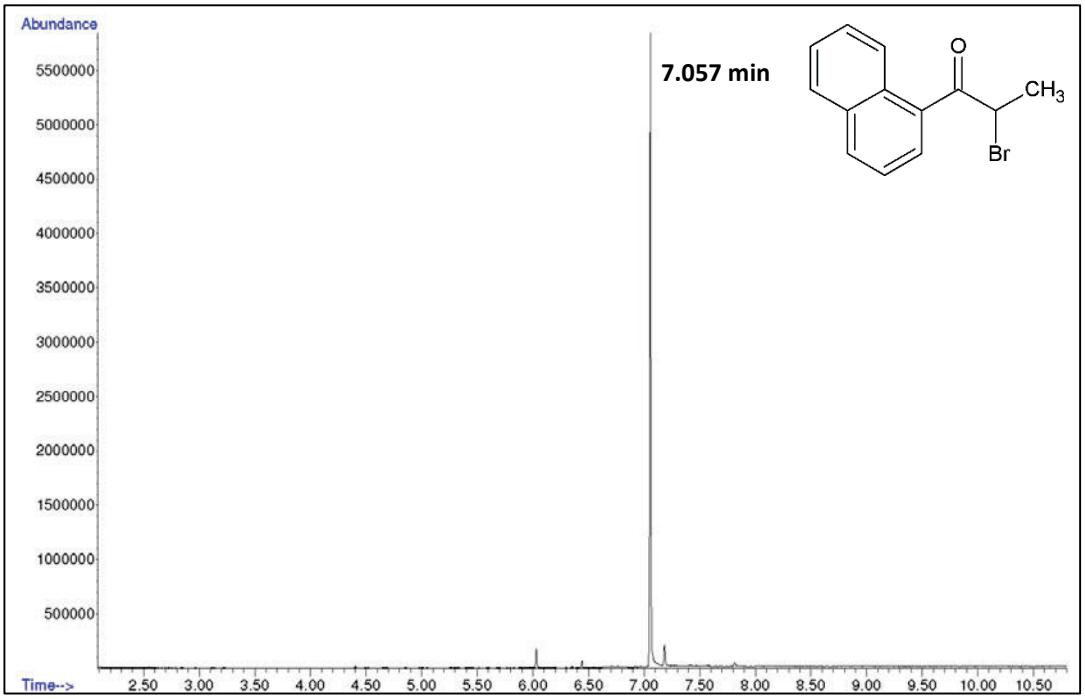

Figure A-93. Representative TIC of crude 2-bromo-1-(naphthalen-1-yl)propan-1-one (**49**)

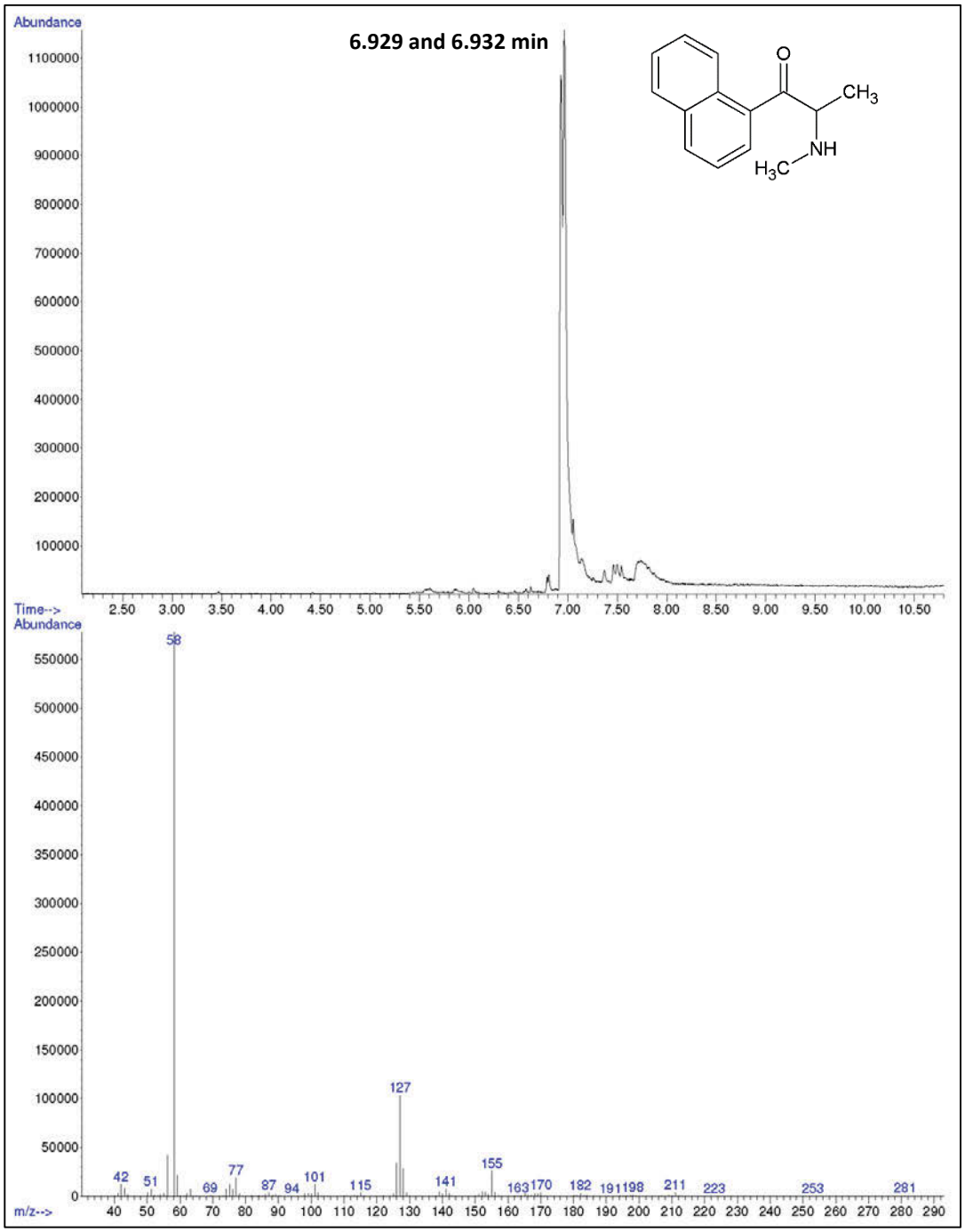

Figure A-94. Representative TIC of α-naphth HCl (**50**) (above) and associated mass spectrum (below).

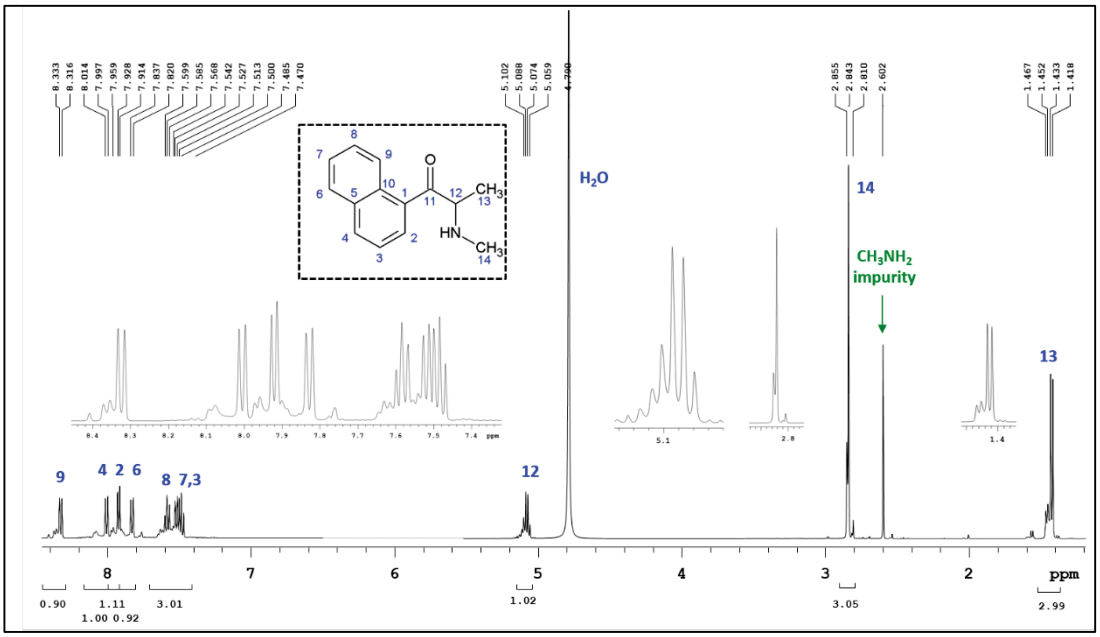

Figure A-95. Annotated ^{1}H-NMR spectrum of α-naphth HCl (**50**) measured in deuterated water (δ 4.79 ppm). Signal at δ 2.602 ppm determined to be residual methylamine. Inset: zoomed regions containing splitting patterns

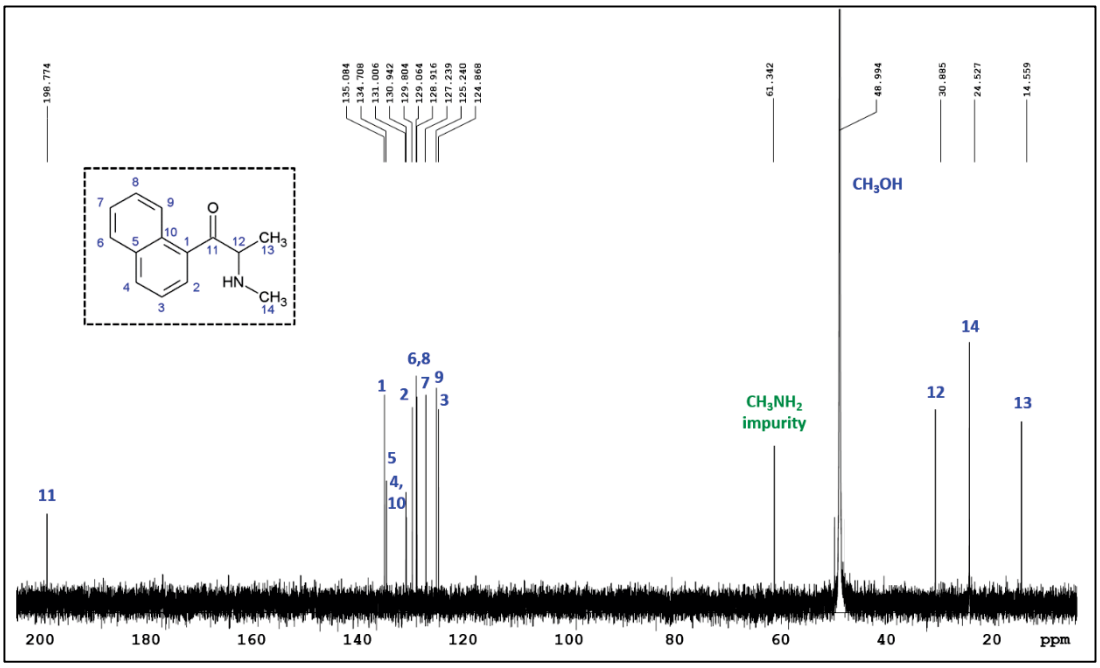

Figure A-96. Annotated ^{13}C-NMR spectrum of α-naphth HCl (**50**) measured in deuterated methanol (δ 49.00 ppm). Signal at δ 61.342 ppm determined to be residual methylamine.

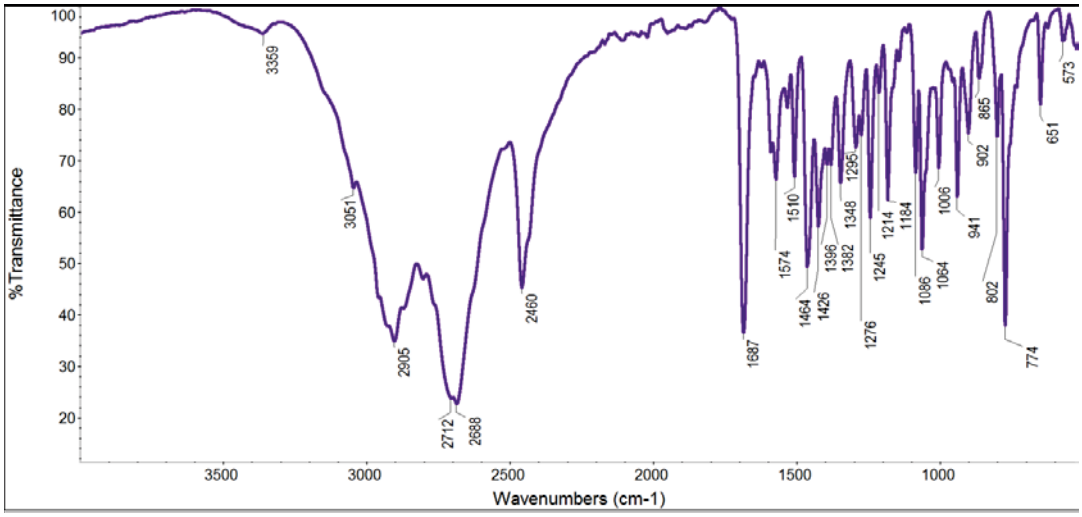

Figure A-97. ATR-FTIR spectrum of α-naphth HCl (**50**)

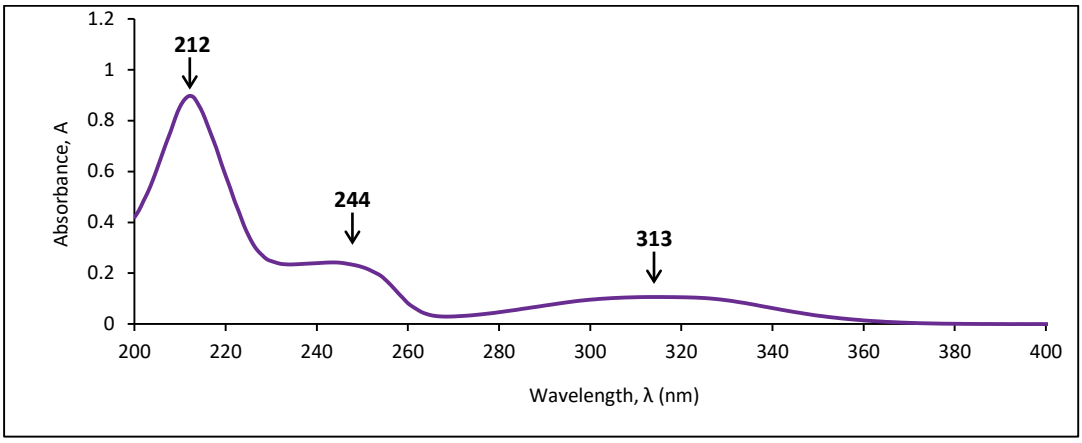

Figure A-98. UV spectrum of α-naphth HCl (**50**) in deionised water

A.16 3,4-Methylenedioxypyrrolidinobutiophenone (MDPBP, 51)

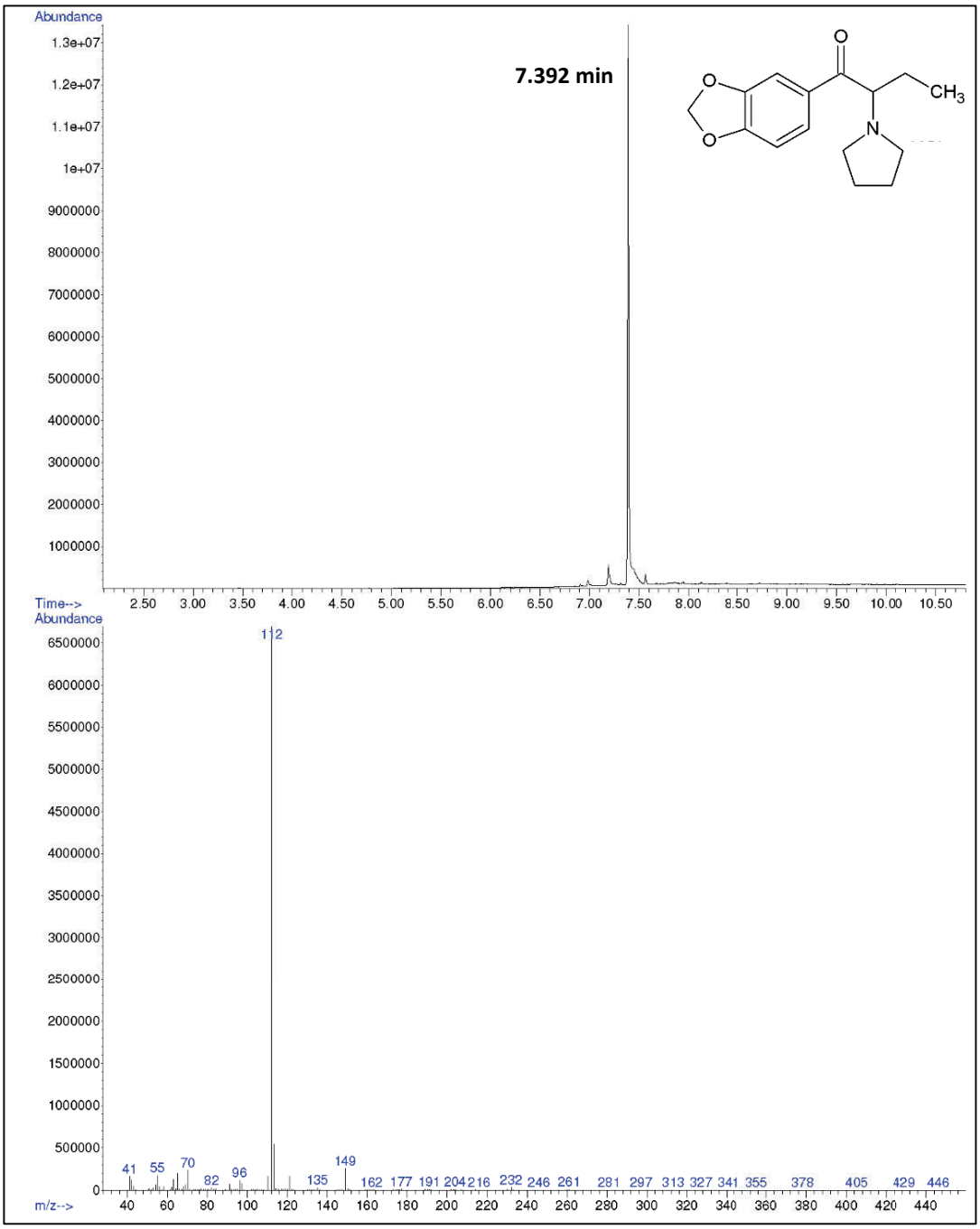

Figure A-99. Representative TIC of MDPBP HCl (**51**) (above) and associated mass spectrum (below).

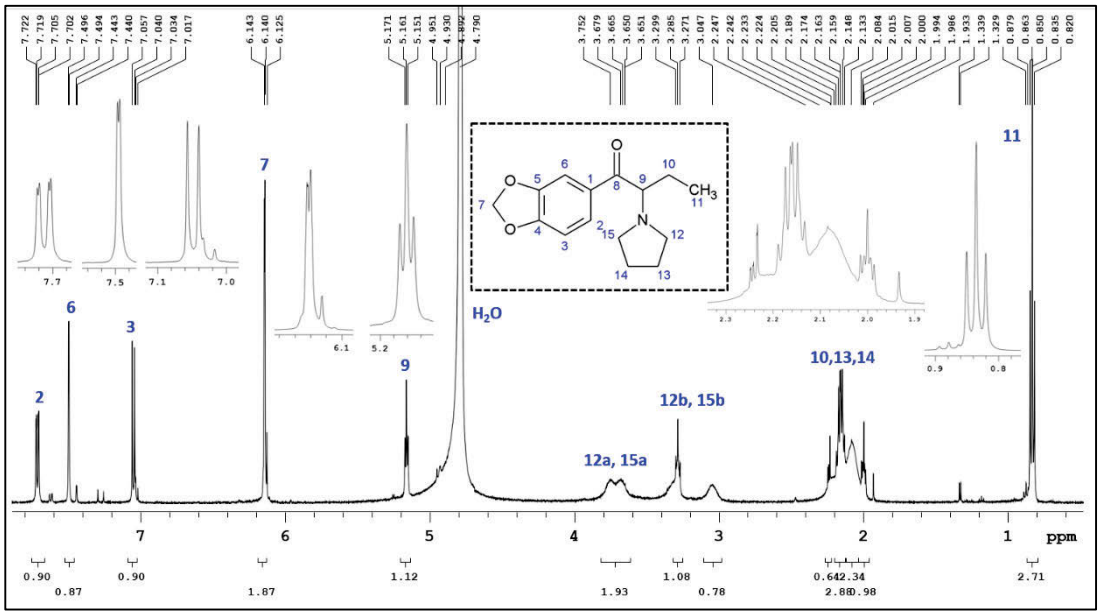

Figure A-100. Annotated ^{1}H-NMR spectrum of MDPBP HCl (**51**) measured in deuterated water (δ 4.79 ppm). Inset: zoomed regions containing splitting patterns

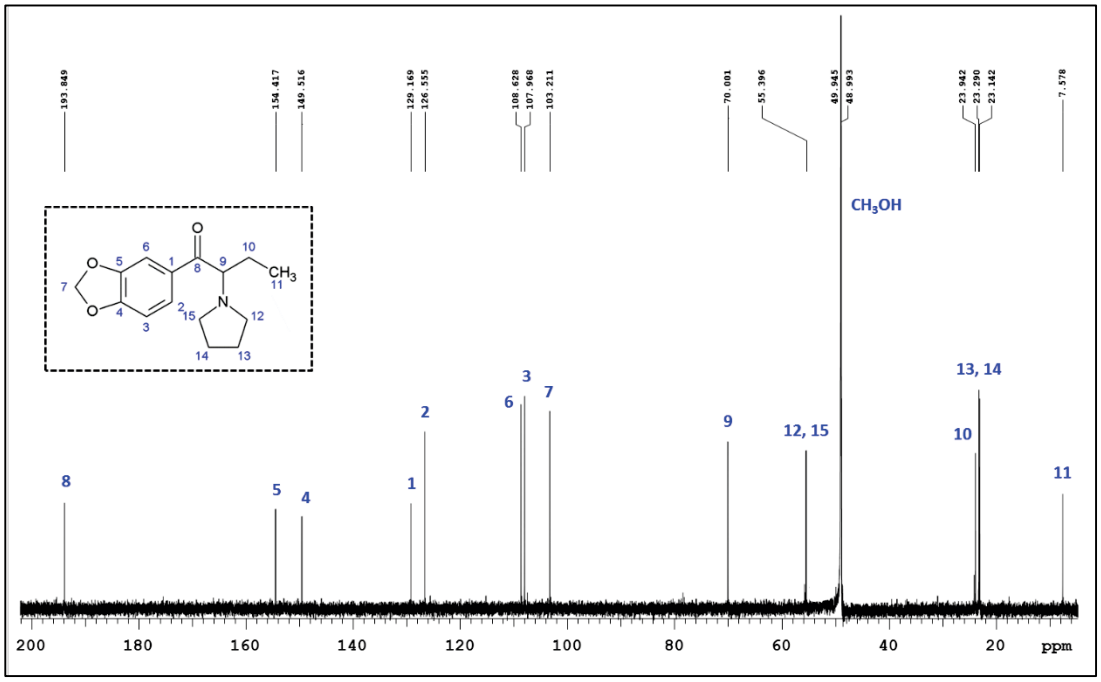

Figure A-101. Annotated ^{13}C-NMR spectrum of MDPBP HCl (**51**) measured in deuterated methanol (δ 49.00 ppm)

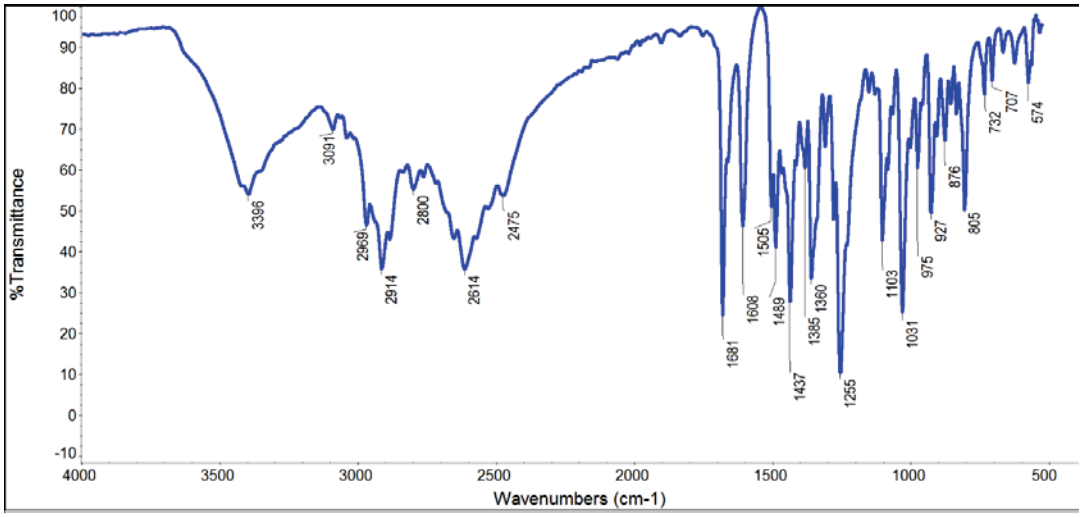

Figure A-102. ATR-FTIR spectrum of MDPBP HCl (**51**)

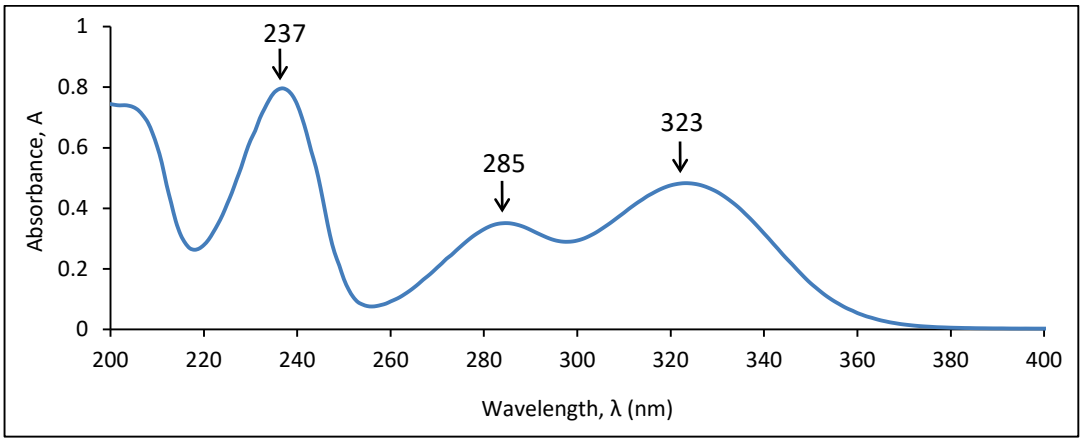

Figure A-103. UV spectrum of MDPBP HCl (**51**) in deionised water

A.17 4-Methylpyrrolidinobutiophenone (4-MPBP, 55)

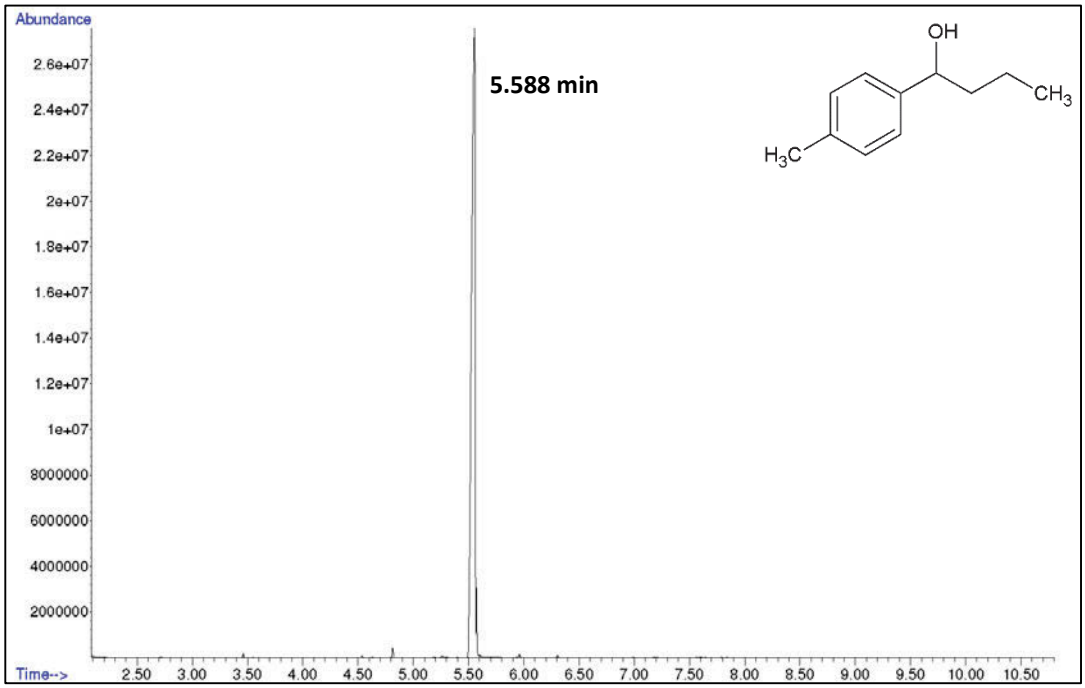

Figure A-104. Representative TIC of crude 1-(4-methylphenyl)butan-1-ol (**52**)

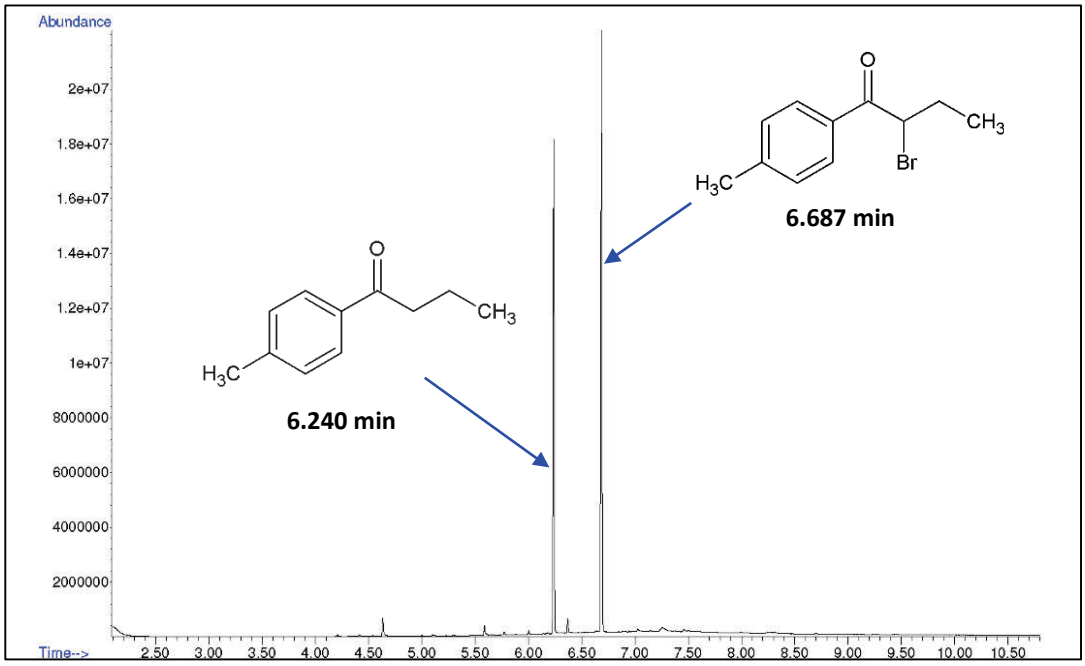

Figure A-105. Representative TIC of crude 2-bromo-1-(4-methylphenyl)butan-1-one (**54**)

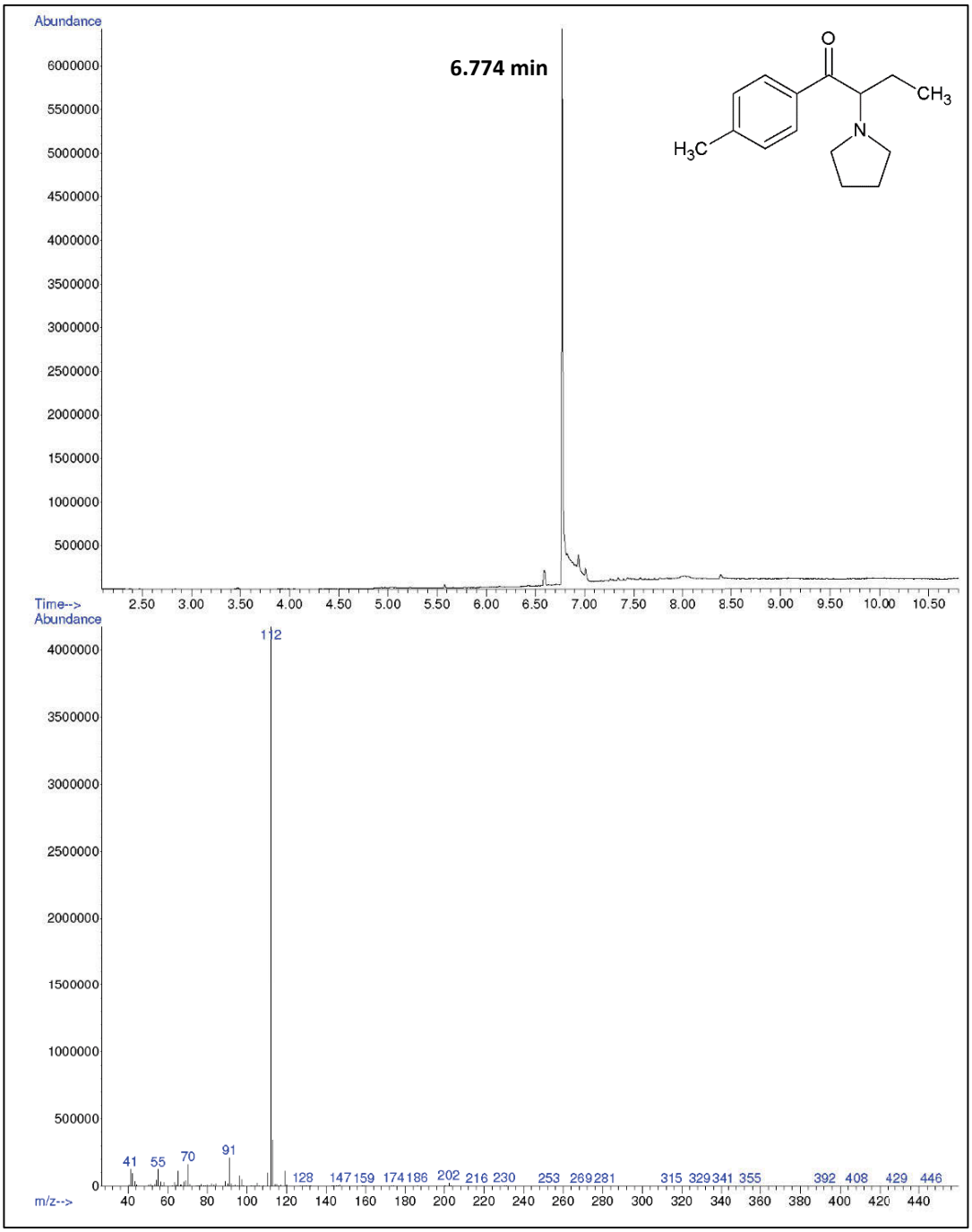

Figure A-106. Representative TIC of 4-MPBP HCl (**55**) (above) and associated mass spectrum (below).

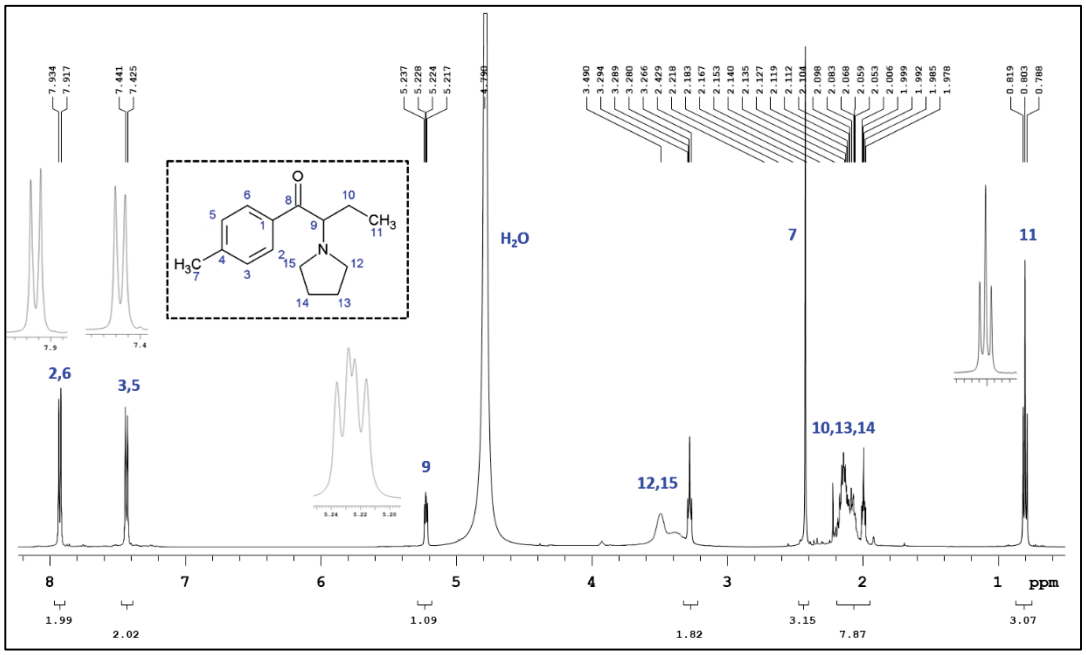

Figure A-107. Annotated ^{1}H-NMR spectrum of 4-MPBP HCl (**55**) measured in deuterated water (δ 4.79 ppm). Inset: zoomed regions containing splitting patterns

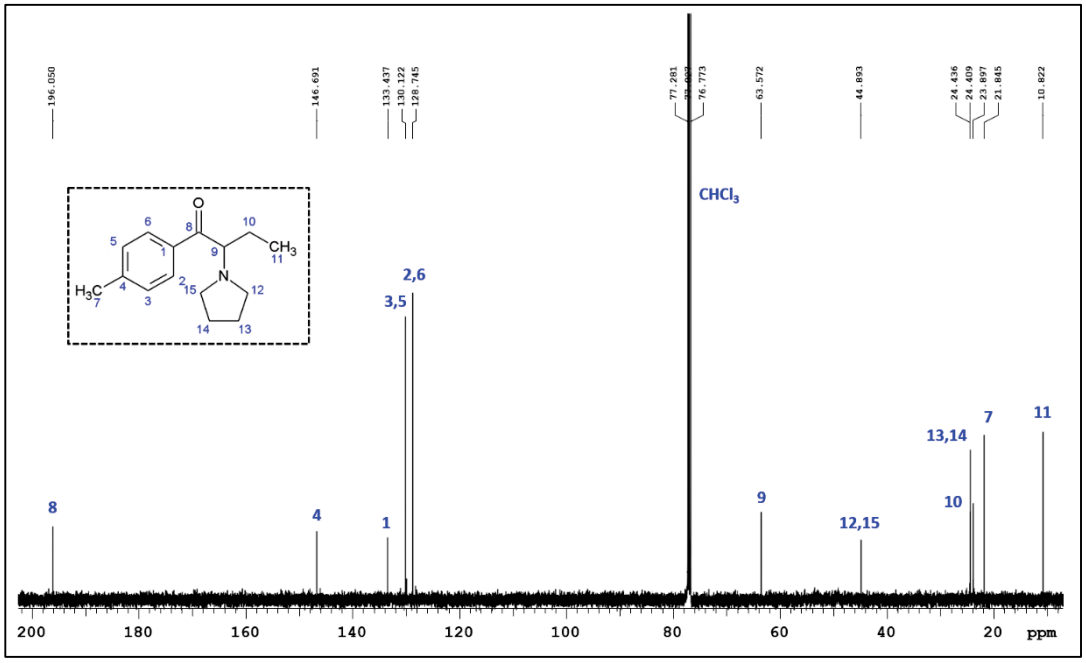

Figure A-108. Annotated ^{13}C-NMR spectrum of 4-MPBP HCl (**55**) measured in deuterated chloroform (δ 77.16 ppm)

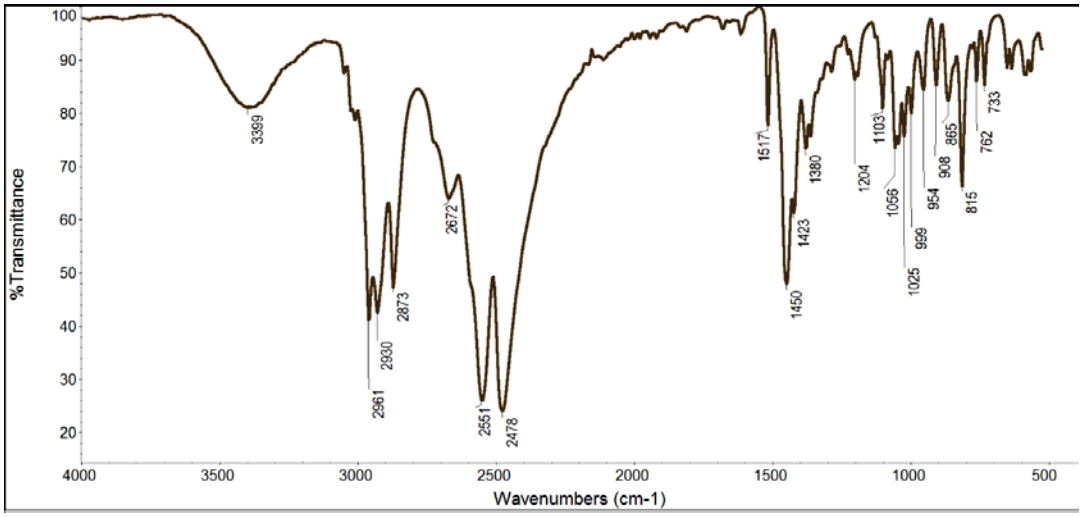

Figure A-109. ATR-FTIR spectrum of 4-MPBP HCl (**55**)

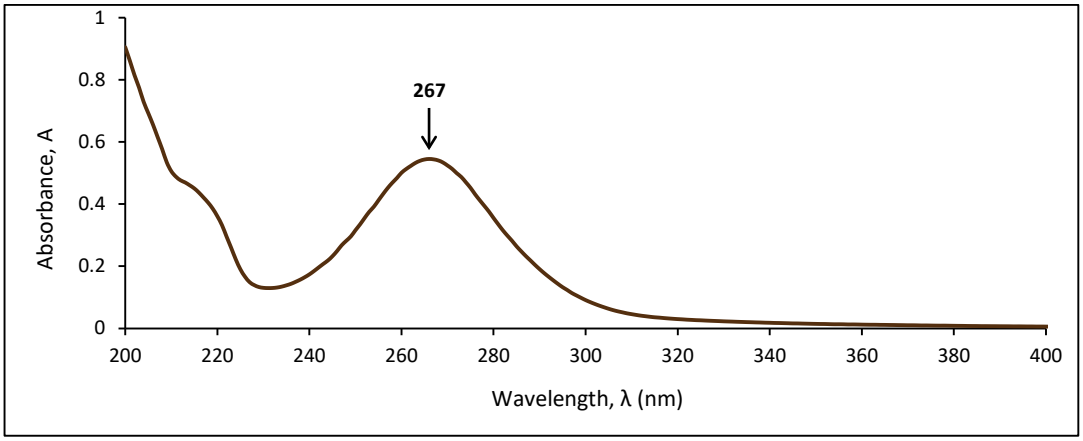

Figure A-110. UV spectrum of 4-MPBP HCl (**55**) in deionised water

A.18 4-Hydroxymethcathinone (4-HMC, 60)

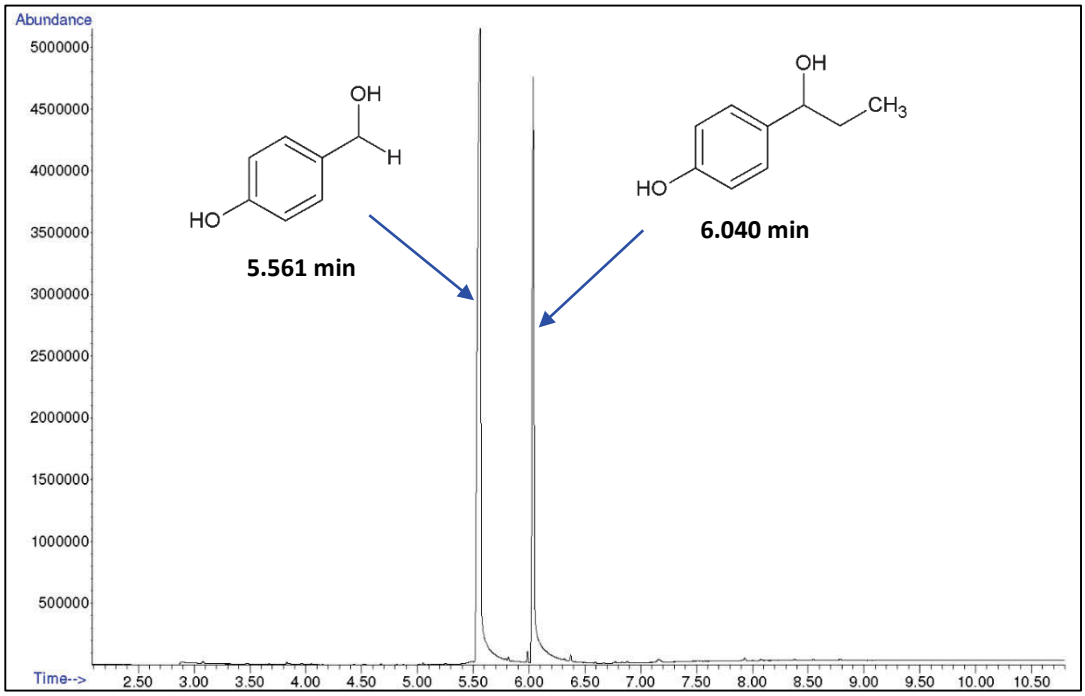

Figure A-111. Representative TIC of crude reaction mixture during the preparation of 1-(4-hydroxyphenyl)propan-1-one (**58**)

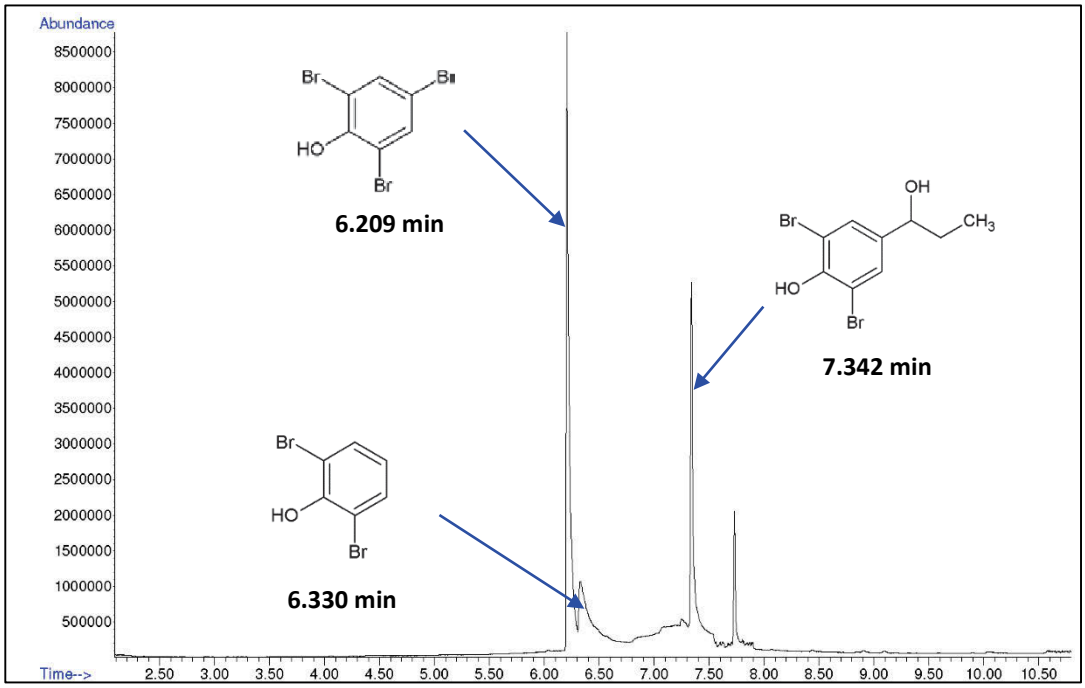

Figure A-112. Representative TIC of crude 2-bromo-1-(4-hydroxyphenyl)propan-1-one (**59**) showing di- and tri-brominated impurities

A.19 β-naphyrone (65)

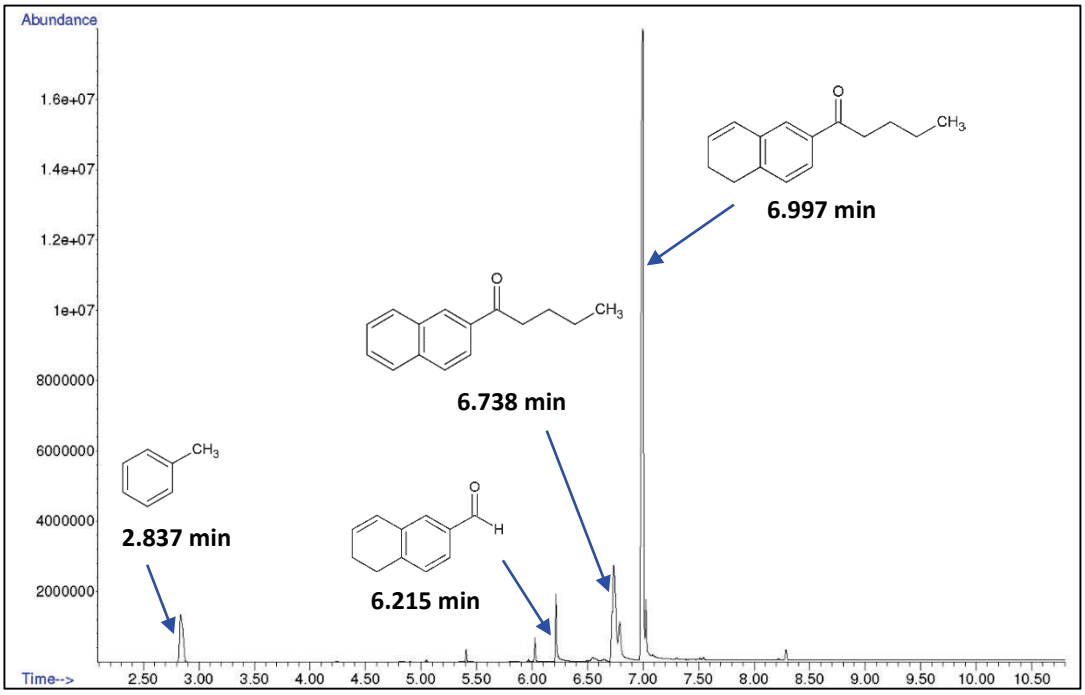

Figure A-113. Representative TIC of crude 1-(naphthalen-2-yl)pentan-1-one (**63**) showing the major impurities present

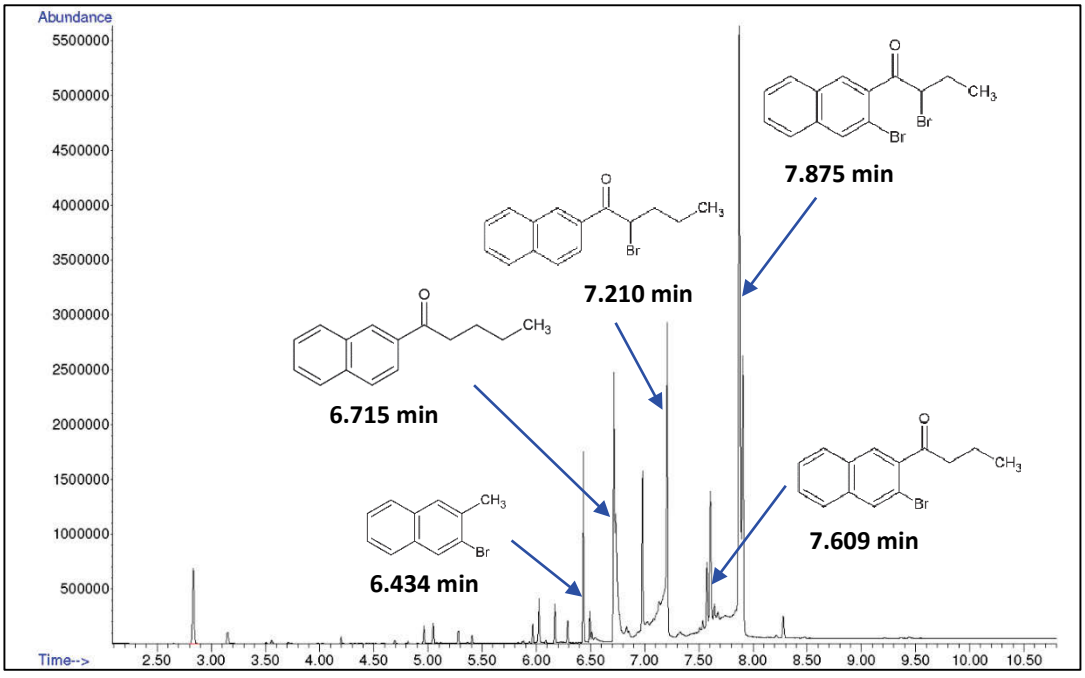

Figure A-114. Representative TIC of crude 2-bromo-1-(naphthalen-2-yl)pentan-1-one (**64**) showing the major impurities present

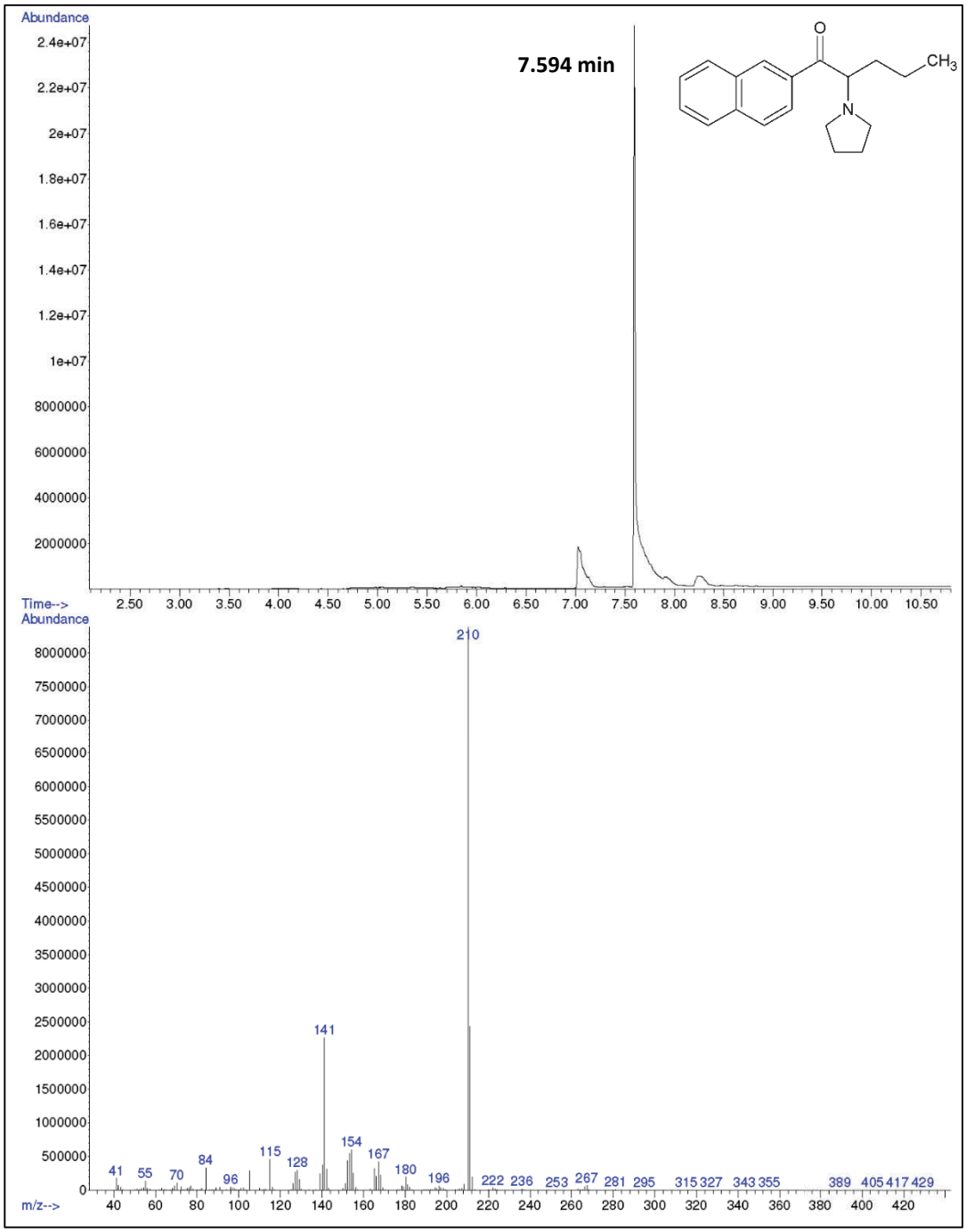

Figure A-115. Representative TIC of β-naphyrone (**65**)

A.20 Cathinone (CAT, 70)

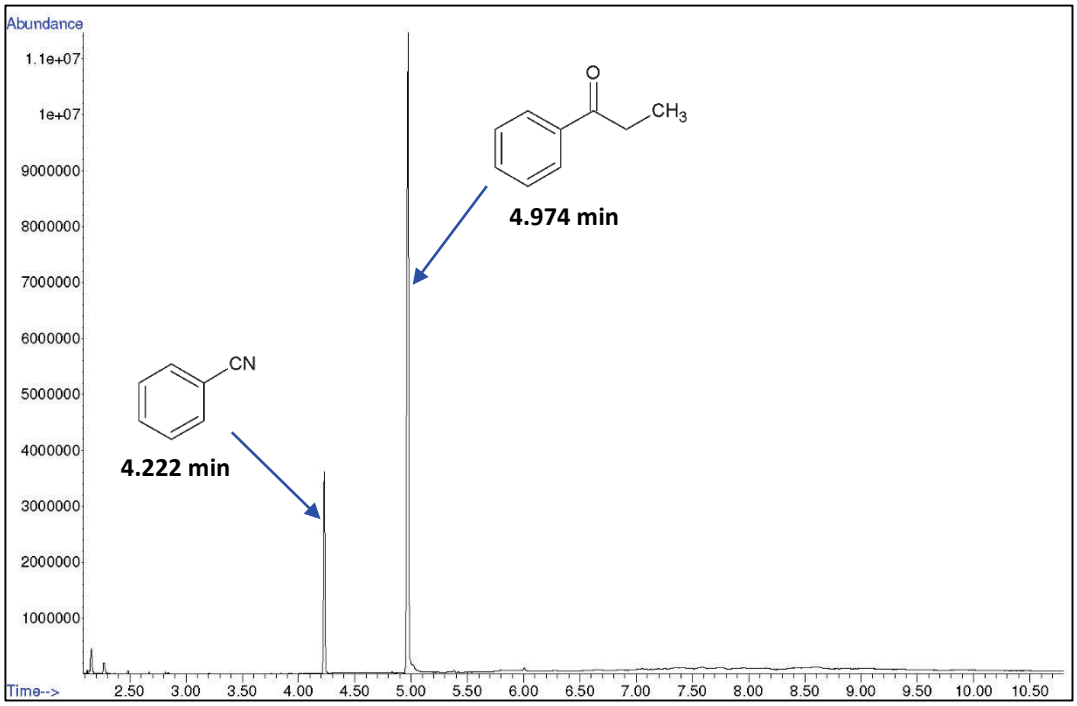

Figure A-116. Representative TIC of crude 1-phenylpropan-1-one (67)

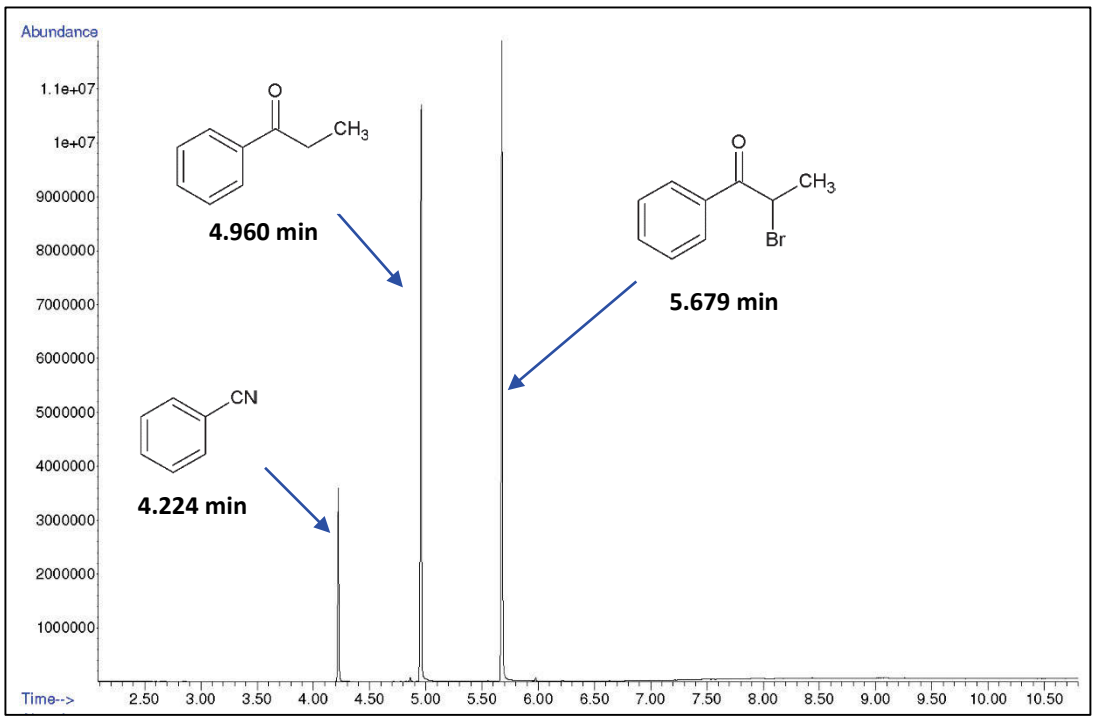

Figure A-117. Representative TIC of 2-bromo-1-phenylpropan-1-one (68)

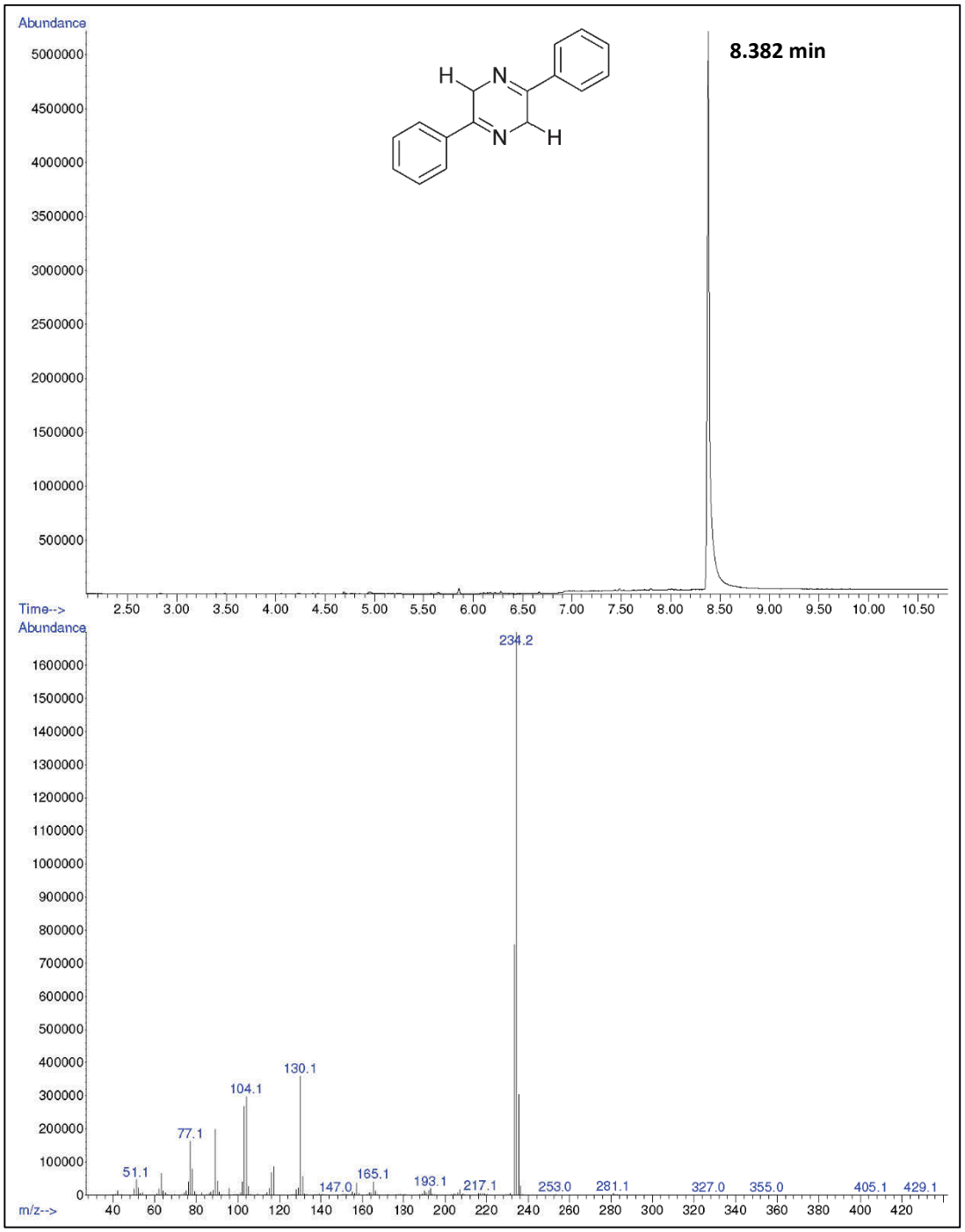

Figure A-118. Representative TIC of 2-(1-oxo-1-phenylpropan-2-yl)-1H-isoindole-1,3(2H)-dione (69)

Appendix B: Cathinone oximation data

B.1 4-methylmethcathinone (4-MMC)

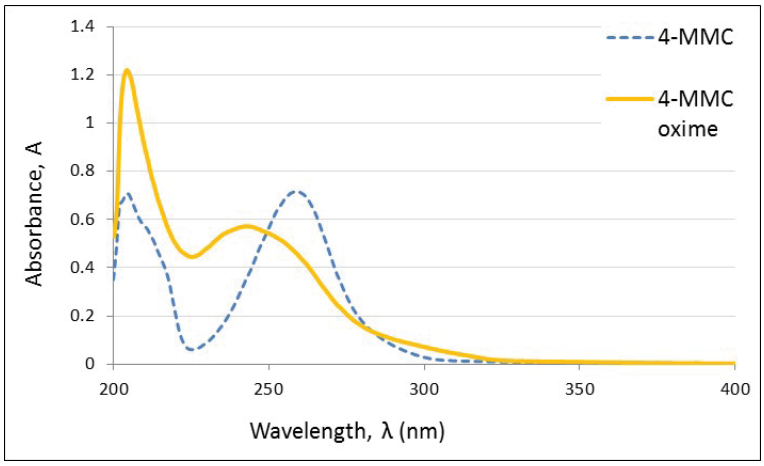

Figure B-1. UV spectrum of 4-MMC (- - -) and 4-MMC oxime reaction solution (——) reconstituted in methanol after 4 days

B.2 4-fluoromethcathinone (4-FMC)

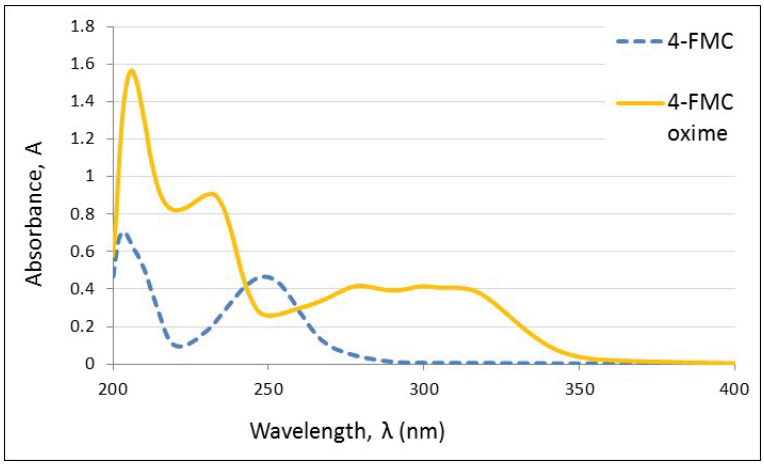

Figure B-2. UV spectrum of 4-FMC (- - -) and 4-FMC oxime reaction solution (——) reconstituted in methanol after 4 days

B.3 4-Methylethcathinone (4-MEC)

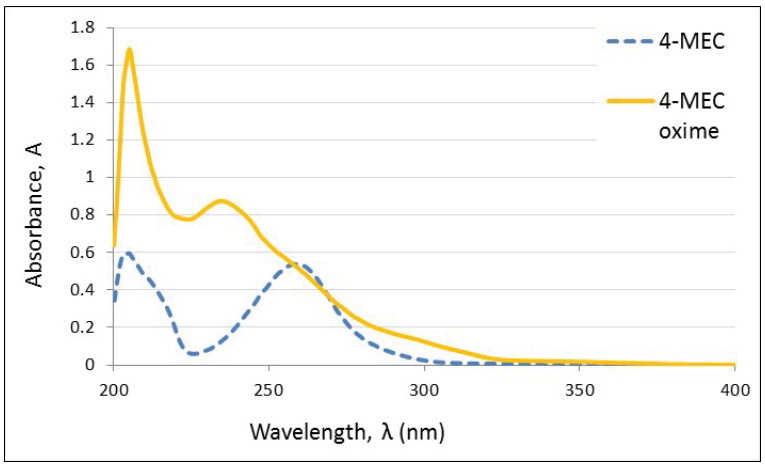

Figure B-3. UV spectrum of 4-MEC (- - -) and 4-MEC oxime reaction solution (——) reconstituted in methanol after 4 days

B.4 Methcathinone (MCAT)

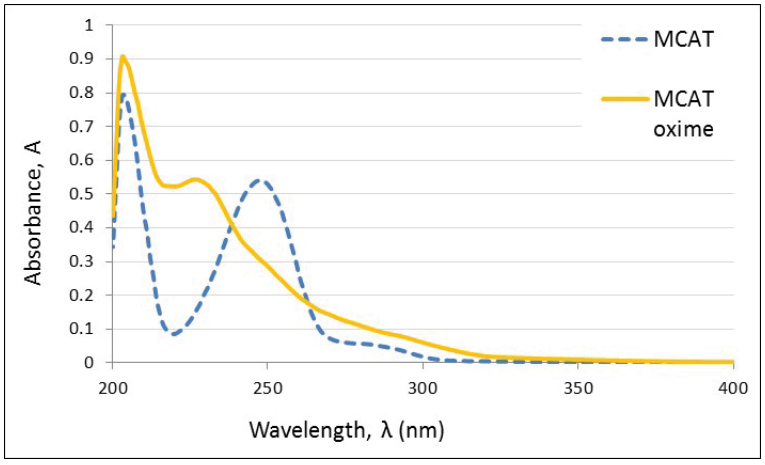

Figure B-4. UV spectrum of MCAT (- - -) and MCAT oxime reaction solution (——) reconstituted in methanol after 4 days

B.5 Methylone

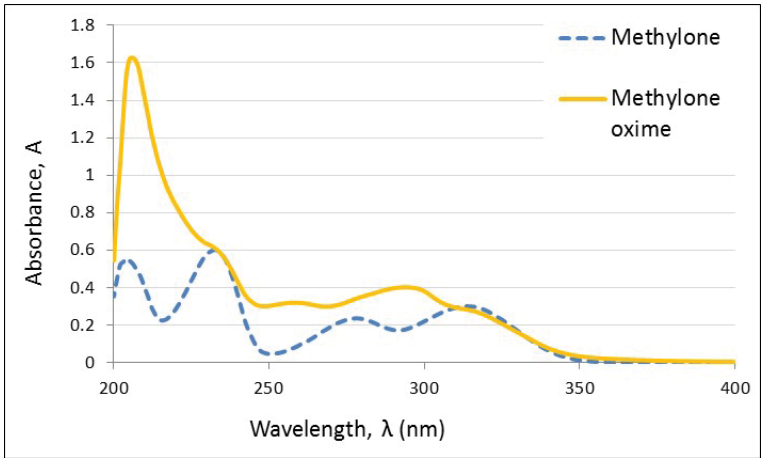

Figure B-5. UV spectrum of methylone (- - -) and methylone oxime reaction solution (——) reconstituted in methanol after 4 days

B.6 Butylone

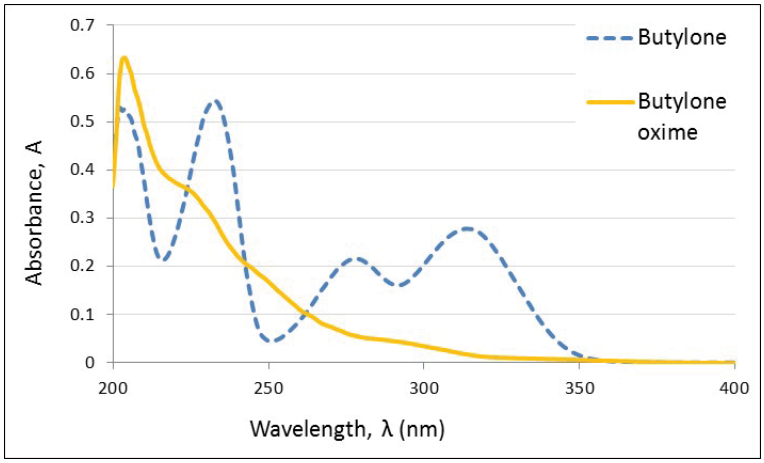

Figure B-6. UV spectrum of butylone (- - -) and butylone oxime reaction solution (——) reconstituted in methanol after 4 days

B.7 Pentylone

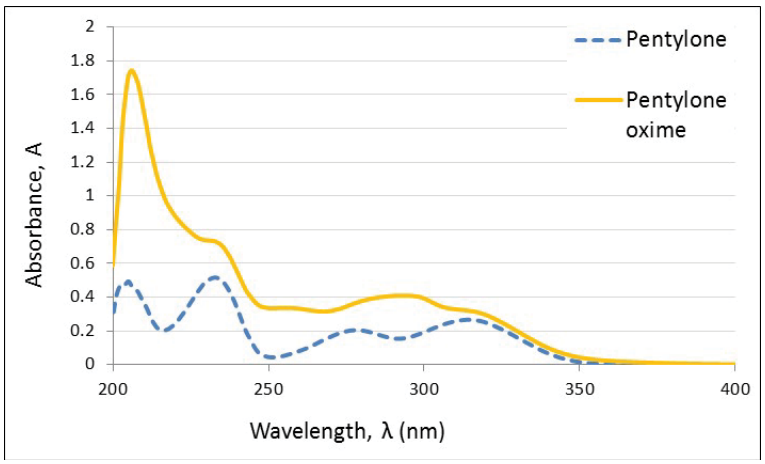

Figure B-7. UV spectrum of pentylone (- - -) and pentylone oxime reaction solution (——) reconstituted in methanol after 4 days

B.8 3,4-methylenedioxypyrovalerone (MDPV)

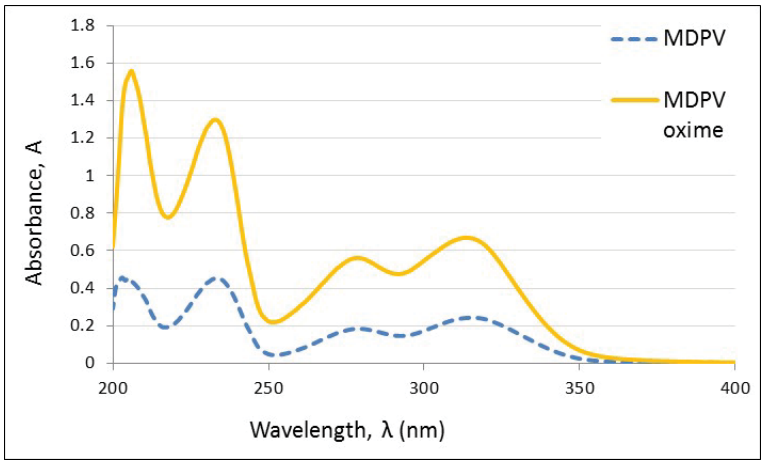

Figure B-8. UV spectrum of MDPV (- - -) and MDPV oxime reaction solution (——) reconstituted in methanol after 4 days

B.9 Pyrovalerone

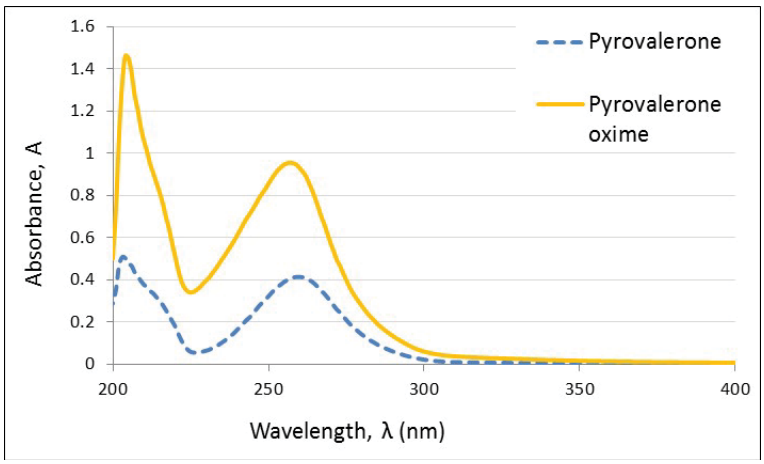

Figure B-9. UV spectrum of pyrovalerone (- - -) and pyrovalerone oxime reaction solution (——) reconstituted in methanol after 4 days

B.10 α-pyrrolidinovalerophenone (α-PVP)

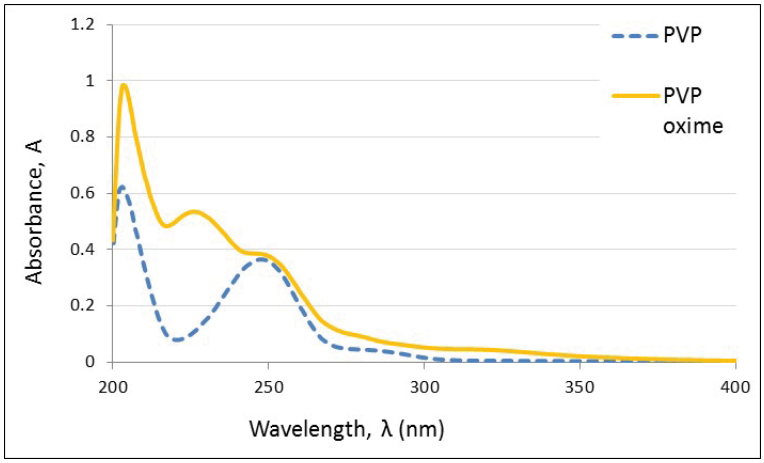

Figure B-10. UV spectrum of α-PVP (- - -) and α-PVP oxime reaction solution (——) reconstituted in methanol after 4 days

Appendix C: UV calibration curves

C.1 4-methylmethcathinone (4-MMC)

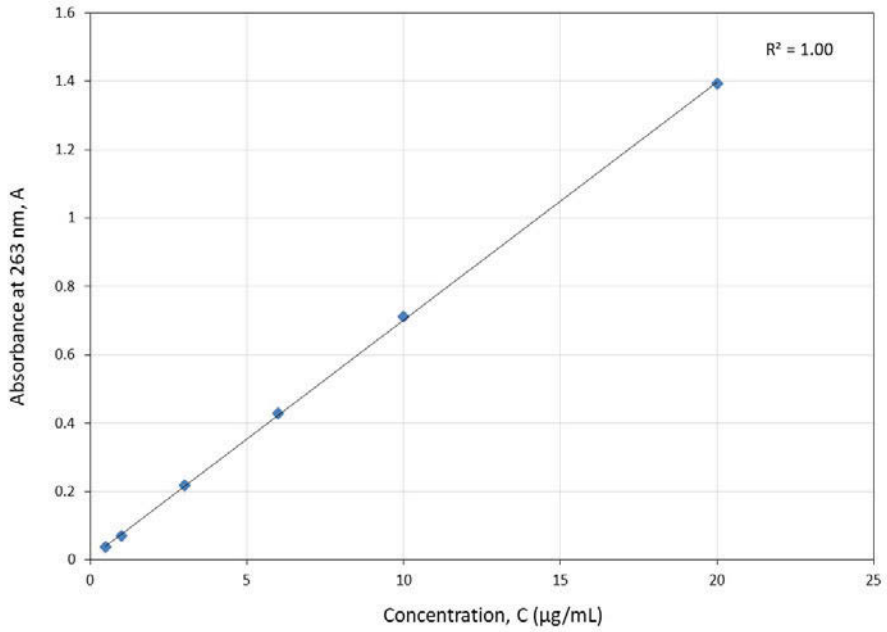

Figure C-1. Spectrophotometer calibration curve of 4-MMC in water at 263 nm in the 2-20 µg/mL concentration range

C.2 4-fluoromethcathinone (4-FMC)

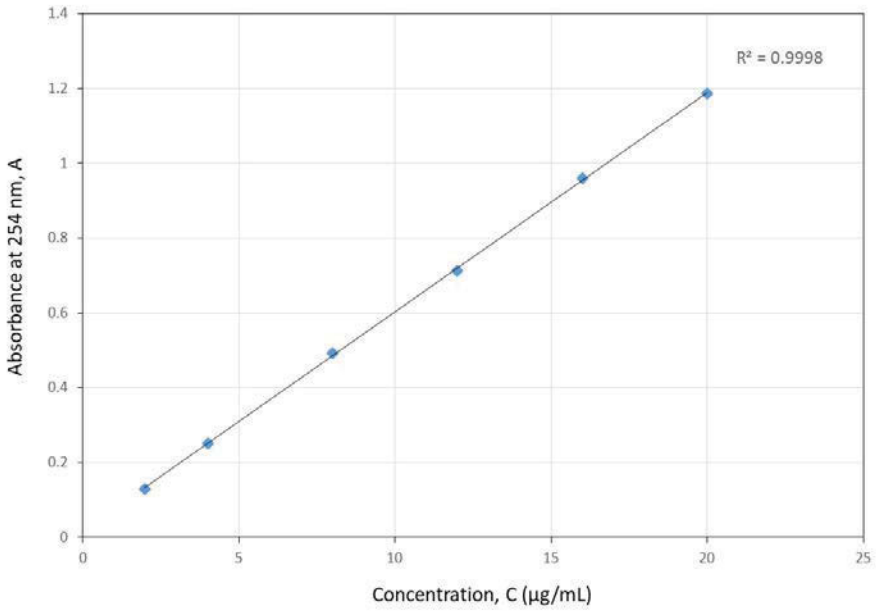

Figure C-2. Spectrophotometer calibration curve of 4-FMC in water at 254 nm in the 2-20 µg/mL concentration range

C.3 4-methylethcathinone (4-MEC)

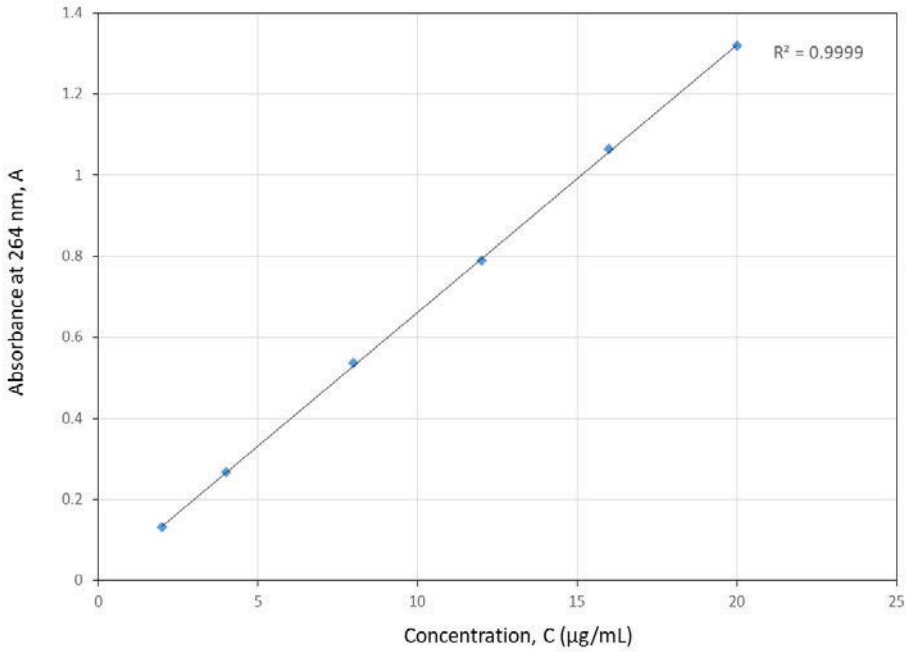

Figure C-3. Spectrophotometer calibration curve of 4-MEC in water at 264 nm in the 2-20 µg/mL concentration range

C.4 Methcathinone (MCAT)

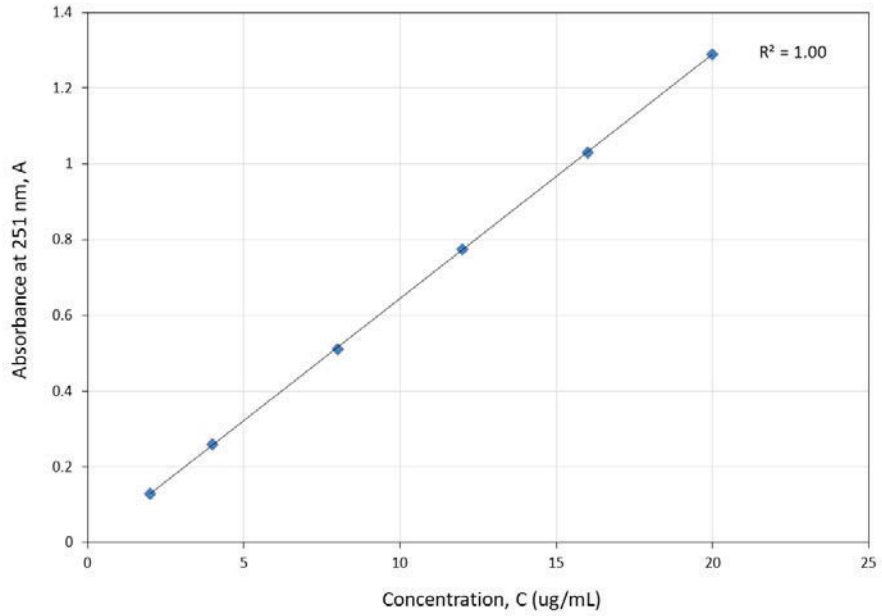

Figure C-4. Spectrophotometer calibration curve of MCAT in water at 251 nm in the 2-20 µg/mL concentration range

C.5 Methylone

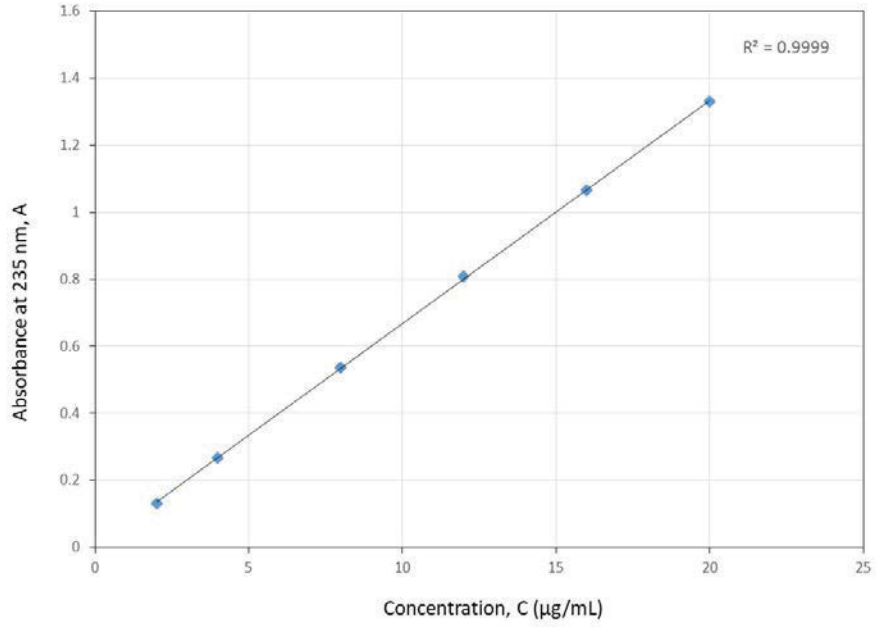

Figure C-5. Spectrophotometer calibration curve of methylone in water at 235 nm in the 2-20 µg/mL concentration range

C.6 Butylone

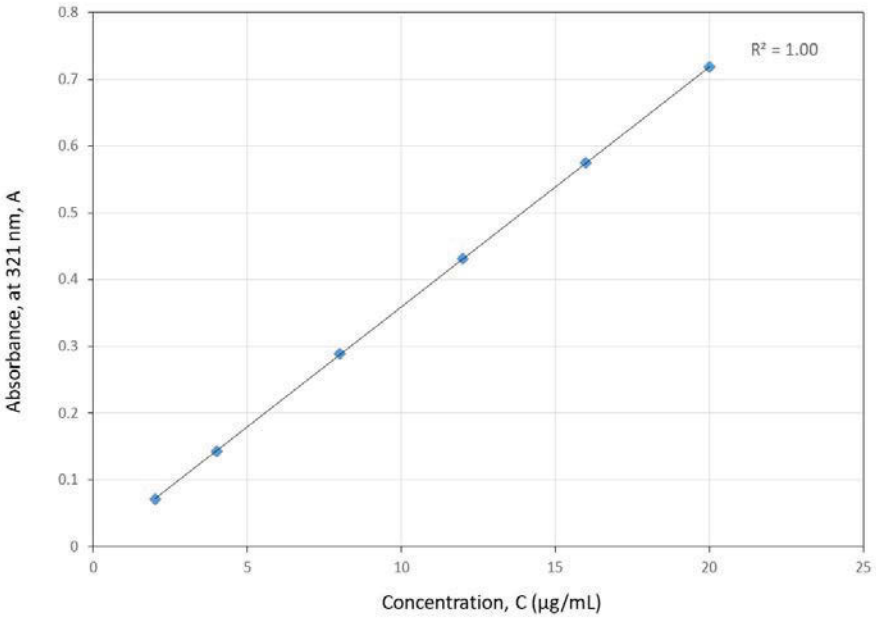

Figure C-6. Spectrophotometer calibration curve of butylone in water at 321 nm in the 2-20 µg/mL concentration range

C.7 Pentylone

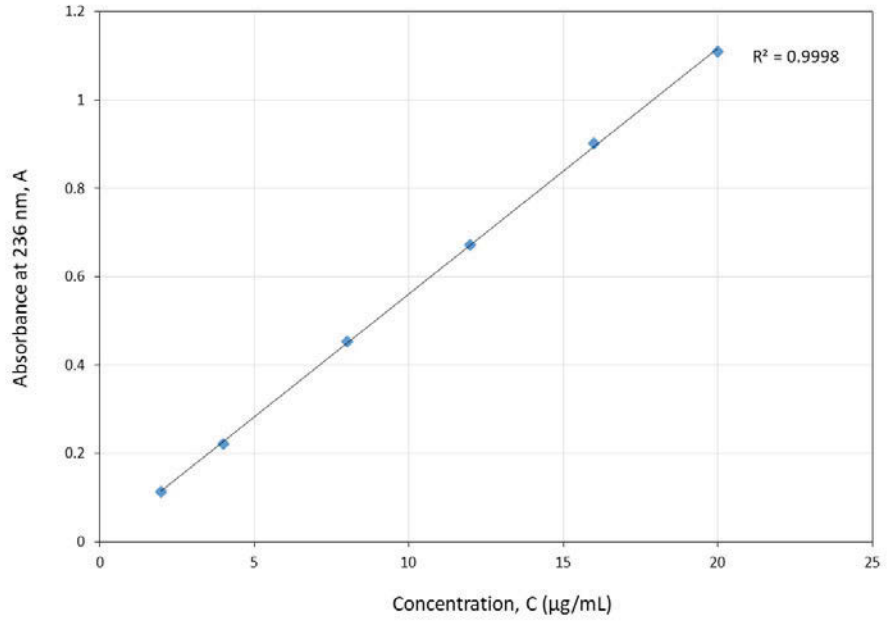

Figure C-7. Spectrophotometer calibration curve of pentylone in water at 236 nm in the 2-20 µg/mL concentration range

C.8 3,4-methylenedioxypyrovalerone (MDPV)

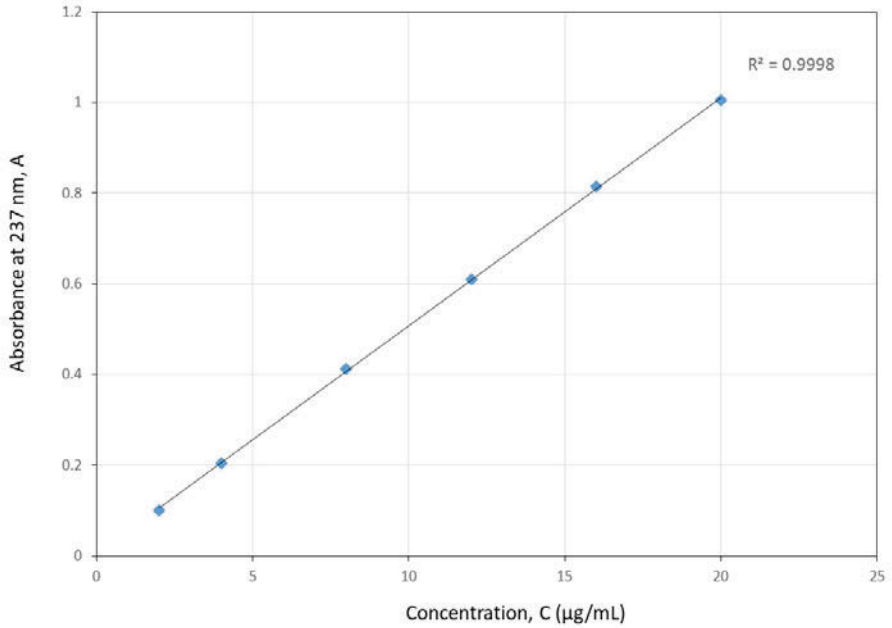

Figure C-8. Spectrophotometer calibration curve of MDPV in water at 237 nm in the 2-20 µg/mL concentration range

C.9 Pyrovalerone

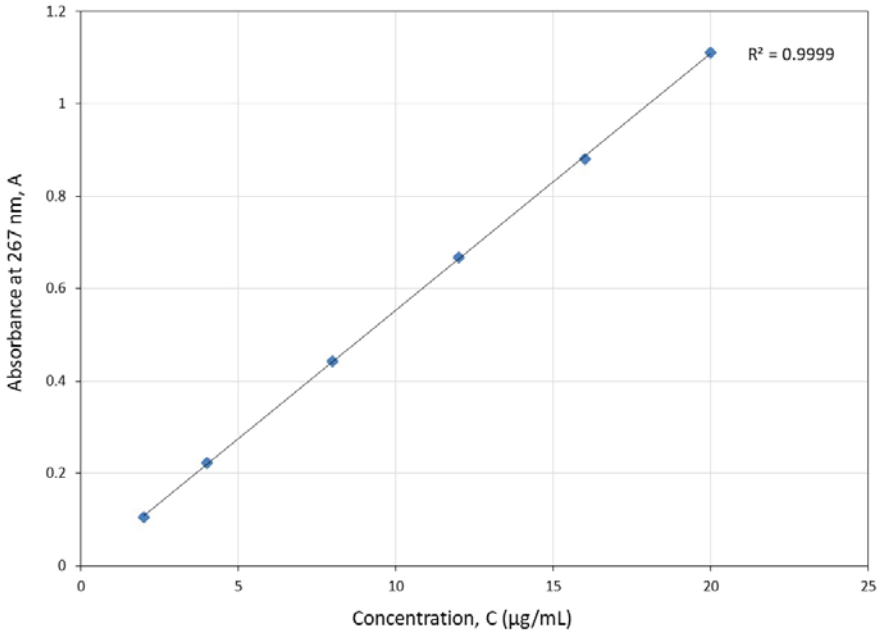

Figure C-9. Spectrophotometer calibration curve of pyrovalerone in water at 267 nm in the 2-20 µg/mL concentration range

C.10 α-Pyrrolidinovalerophenone (α-PVP)

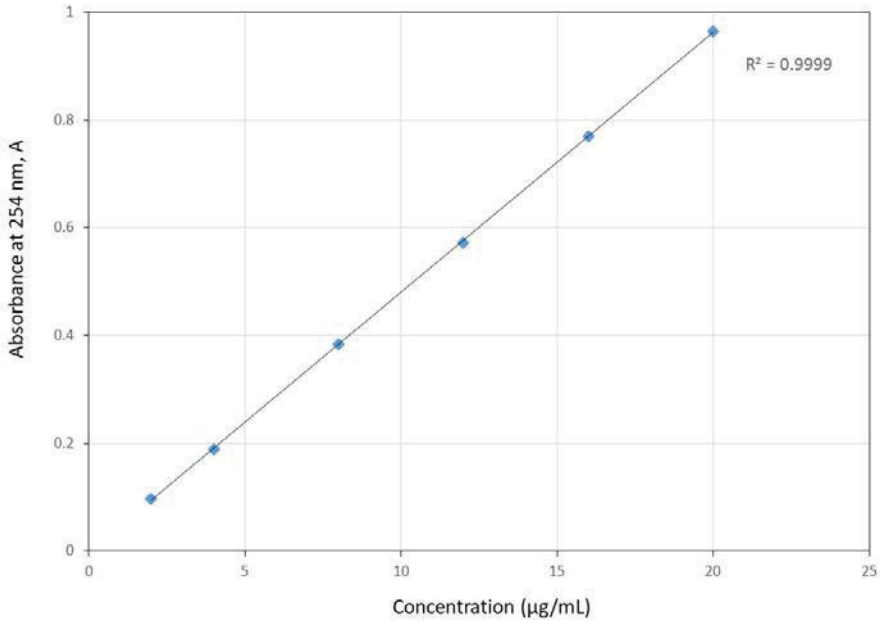

Figure C-10. Spectrophotometer calibration curve of α-PVP in water at 254 nm in the 2-20 µg/mL concentration range